

2012-01-01

Calibration of Concrete Pavement Performance Models

Alejandra Gallegos

University of Texas at El Paso, agallegos4@miners.utep.edu

Follow this and additional works at: https://digitalcommons.utep.edu/open_etd



Part of the [Civil Engineering Commons](#)

Recommended Citation

Gallegos, Alejandra, "Calibration of Concrete Pavement Performance Models" (2012). *Open Access Theses & Dissertations*. 2088.
https://digitalcommons.utep.edu/open_etd/2088

This is brought to you for free and open access by DigitalCommons@UTEP. It has been accepted for inclusion in Open Access Theses & Dissertations by an authorized administrator of DigitalCommons@UTEP. For more information, please contact lweber@utep.edu.

CALIBRATION OF CONCRETE PAVEMENT PERFORMANCE MODELS

ALEJANDRA GALLEGOS

Department of Civil Engineering

APPROVED:

Carlos M. Chang-Albitres, Ph.D., Chair

Soheil Nazarian, Ph.D.

Otakar Vacin, Ph.D.

Benjamin Flores, Ph.D.
Interim Dean of the Graduate School

Copyright ©

by

Alejandra Gallegos

2012

CALIBRATRON OF CONCRETE PAVEMENT PERFORMANCE MODELS

by

ALEJANDRA GALLEGOS, Bachelor of Science

THESIS

Presented to the Faculty of the Graduate School of

The University of Texas at El Paso

in Partial Fulfillment

of the Requirements

for the Degree of

MASTER OF SCIENCE

Department of Civil Engineering

THE UNIVERSITY OF TEXAS AT EL PASO

May 2012

Acknowledgments

I would like to express my most sincere gratitude to my advisor Dr. Carlos M. Chang for his guidance and support. His significant contribution to the research is deeply appreciated. The successful completion of this project was also possible thanks to Dr. Imad Abdallah who provided me countless hours of his time and rendered his unconditional guidance. I would also like to thank Dr. Soheil Nazarian for his valuable input and assistance throughout the development of this project. Special thanks to Dr. Otakar Vacin for his support and encouragement in this research during my stay in Prague.

This project would not have been possible without the expertise provided by TxDOT personnel. Their contribution is greatly appreciated.

Last, but not least, I would like to thank my family for their unconditional support throughout my studies. Without their help and encouragement, my achievements would not be possible. I am blessed to have them in my life.

Preface

This research is focused on the creation of a methodology for pavement performance model development in the network management level. Ultimately, pavement performance models for CRC pavement will be developed for TxDOT's PMIS. Through the development of these models, a reliable tool for predicting pavement performance will be provided which can result in better pavement treatment strategies and cost savings. This study is part of research project number 0-6386 titled "Evaluation and Development of Pavement Scores, Performance Models and Needs Estimates for the TxDOT Pavement Management Information System" (Gharaibeh et al. 2012). This research was undertaken by the University of Texas at El Paso, the University of Texas at San Antonio and the Texas Transportation Institute. This research was performed in cooperation with the Texas Department of Transportation who was the sponsoring agency.

Abstract

Pavement performance models exist in various forms to cater to the pavement management agencies' needs and resources. Well-calibrated models are needed to accurately predict future pavement conditions, and to forecast and prioritize confidently the future rehabilitation and maintenance expenditures. Statistical tools are commonly used to develop the performance models. These statistical models may be impractical or misleading if not constrained with experts' opinions. This paper presents a hybrid technique where statistical tools and expert knowledge are combined for the calibration of pavement performance models. This technique was validated using historical pavement condition data for continuously-reinforced-concrete pavements (CRCP) from the Texas Department of Transportation's Pavement Management Information System (TxDOT-PMIS). The recalibrated CRCP performance models obtained with the hybrid technique represent an improvement when compared to the current models since they merge expert opinion and statistical analysis which allow to better reflect field observations regarding distress initiation, distress evolution rate, and maximum allowable amount of distress growth. Furthermore, this paper also discusses the application of this technique for the calibration of the Highway Development and Management Model (HDM-4) and Mechanistic-Empirical Pavement Design (MEPD) performance models.

| Table of Contents | Page |
|---|-------------|
| Acknowledgments..... | iv |
| Preface..... | v |
| Abstract..... | vi |
| Table of Contents..... | vii |
| List of Tables..... | xiv |
| List of Figures..... | xvii |
| Chapter 1: Introduction..... | 1 |
| 1.1 Continuously Reinforced Concrete Pavement..... | 2 |
| 1.2 Pavement Management Systems and Management Levels..... | 2 |
| 1.3 Pavement Performance Models for PMS..... | 4 |
| 1.4 Research Objective and Project Scope..... | 5 |
| 1.5 Thesis Organization..... | 6 |
| 2. Literature Review..... | 8 |
| 2.1 Overview of Types of Pavement Performance Models..... | 8 |
| 2.2 TxDOT's Pavement Management Information System (PMIS): Overview of PMIS CRCP Performance Curves..... | 13 |
| 2.2.1 Pavement Distresses Evaluated In Texas..... | 15 |
| 2.2.1.1 Spalled Cracks..... | 17 |
| 2.2.1.2 Punchouts..... | 17 |

| | |
|--|----|
| 2.2.1.3 ACP Patches..... | 18 |
| 2.2.1.4 PCC Patches..... | 18 |
| 2.2.1.5 Failed Joints and Transverse Cracks..... | 19 |
| 2.2.1.6 Failures..... | 19 |
| 2.2.1.7 Shattered Slabs..... | 20 |
| 2.2.1.8 Slabs with Longitudinal Cracks..... | 21 |
| 2.2.1.9 Concrete Patches..... | 21 |
| 2.2.2 Pavement Performance Models for CRCP and JCP..... | 22 |
| 2.2.2.1 Distress Pavement Performance Models for CRCP and JCP..... | 25 |
| 2.2.2.2 Ride Quality Pavement Performance Models for CRCP and JCP..... | 31 |
| 2.3 HDM-4: Overview of Concrete Pavement Performance Models..... | 34 |
| 2.3.1 HDM-4 Road Deterioration Models..... | 36 |
| 2.3.2 Rigid Pavement distresses modeled in HDM-4..... | 38 |
| 2.3.2.1 Transverse Cracking..... | 41 |
| 2.3.2.2 Faulting..... | 42 |
| 2.3.2.3 Spalling..... | 42 |
| 2.3.2.4 Failures..... | 43 |
| 2.3.2.5 Present Serviceability Rating..... | 43 |
| 2.3.2.6 Roughness..... | 43 |

| | |
|---|----|
| 2.4 Mechanistic-Empirical Pavement Design Guide: Overview of Concrete Pavement Performance Models..... | 44 |
| 2.4.1 MEPD Concrete Pavement Distress Performance Models..... | 45 |
| 2.4.1.1 MEPD Jointed Plain Concrete Pavement Performance Models..... | 47 |
| 2.4.1.1.1 Transverse Slab Cracking..... | 47 |
| 2.4.1.1.2 Mean Transverse Joint Faulting..... | 48 |
| 2.4.1.2 MEPD Continuously Reinforced Concrete Pavement Performance Model for Punchouts..... | 49 |
| 2.4.2 MEPD Concrete Pavement Roughness Performance Models..... | 49 |
| 2.5 Summary..... | 50 |
| Chapter 3: Overview of Hybrid Technique for the Calibration of CRC Pavement Performance Network Level Models..... | |
| 3.1 Challenges when Calibrating CRCP Performance Network Level Models..... | 54 |
| 3.2 Overcoming the Challenges through a Proposed Hybrid Technique..... | 55 |
| 3.3 Step by Step Methodology of the Hybrid technique..... | 56 |
| 3.4 Validation of the Hybrid technique through the Calibration of CRCP Performance Network Level Models..... | 58 |
| 3.5 Conclusion..... | 59 |
| Chapter 4- PMIS Data Collection and Statistical Analysis..... | |
| 4.1 Introduction..... | 61 |

| | |
|---|----|
| 4.2 Overview of the PMIS Database..... | 62 |
| 4.3 Statistical Analysis..... | 67 |
| 4.3.1 Spalled Cracks..... | 69 |
| 4.3.2 Punchouts..... | 70 |
| 4.3.3 ACP Patches..... | 72 |
| 4.3.4 PCC Patches..... | 74 |
| 4.3.5 Summary of CRCP Distresses by District..... | 76 |
| 4.3.6 Percent of Ride Quality Lost (Li)..... | 79 |
| 4.4 Conclusions..... | 80 |
| 4.5 Recommendations..... | 82 |
| Chapter 5- Data Compilation and Synthesis..... | 84 |
| 5.1 Introduction..... | 84 |
| 5.2 Methodology for Pavement Age Estimation..... | 84 |
| 5.2.1 Assumption 1..... | 86 |
| 5.2.2 Assumption 2..... | 86 |
| 5.2.3 Assumption 3..... | 87 |
| 5.3 “Windows” Method Datasets..... | 89 |
| 5.4 Data Filters and Li Quartile and Li Median Subsets..... | 92 |
| 5.4.1 Li Quartile Subset..... | 93 |
| 5.4.2 Li Median Subset..... | 94 |

| | |
|--|-----|
| 5.5 Conclusion..... | 94 |
| Chapter 6: Calibration of CRC Pavement Performance Models..... | 97 |
| 6.1 Introduction..... | 97 |
| 6.2 CRC Pavement Performance Models' Calibration Methodology..... | 97 |
| 6.2.1 Selection of CRC Pavement Performance Model for Calibration..... | 97 |
| 6.2.2 Non-linear Regression Analysis..... | 98 |
| 6.2.3 Validation of Calibrated Models..... | 100 |
| 6.2.4 Calibrations with Constrained Alpha (α) Parameter..... | 101 |
| 6.3 CRCP Distress Performance Model..... | 101 |
| 6.3.1 Districts..... | 102 |
| 6.3.1.1 Unconstrained Calibrations..... | 102 |
| 6.3.1.2 Constrained Calibrations..... | 105 |
| 6.3.2 Climate and Subgrade Zones..... | 110 |
| 6.3.2.1 Unconstrained Calibrations..... | 110 |
| 6.3.2.2 Constrained Calibrations..... | 111 |
| 6.3.3 Statewide..... | 111 |
| 6.3.3.1 Unconstrained Calibrations..... | 111 |
| 6.3.3.2 Constrained Calibrations..... | 114 |
| 6.3.4 Recommended CRC Pavement Performance Models..... | 117 |
| 6.4 CRCP Ride Quality Performance Models..... | 124 |

| | |
|--|-----|
| 6.4.1 Ride Quality Performance Model Calibration Process..... | 125 |
| 6.4.2 Districts..... | 125 |
| 6.4.3 Climate and Subgrade Zones..... | 127 |
| 6.4.4 Statewide..... | 128 |
| 6.4.5 Recommended CRCP Ride Quality Pavement Performance Curves..... | 129 |
| 6.6 Summary, Conclusions and Recommendations..... | 131 |
| Chapter 7. Adapting the Hybrid Technique for the Calibration of HDM-4 and MEPD | |
| Concrete Pavement Performance Models..... | 135 |
| 7.1 Introduction..... | 135 |
| 7.2 Calibration of HDM-4 and MEPD Rigid Pavement Performance Models | |
| Overview..... | 135 |
| 7.2.1Challenges Encountered in the Calibration of HDM-4 and MEPD Models.... | 135 |
| 7.2.2 Recommendations for Adapting Hybrid Technique for the Calibration of HDM-4 | |
| and MEPD Performance Models..... | 137 |
| 7.3 Case Study: Recommendations for the Calibration of HDM-4 and MEPD Transverse | |
| Cracking Performance Models using the Hybrid Technique..... | 139 |
| 7.3.1 JPCP Transverse Cracking Models..... | 139 |
| 7.3.2 Adapting Hybrid Technique to HDM-4 Model..... | 147 |
| 7.3.3 Adapting Hybrid Technique to MEPD Model..... | 148 |
| 7.4 Conclusion..... | 151 |

| | |
|---|-----|
| Chapter 8: Summary, Conclusions and Recommendations..... | 153 |
| 8.1 Summary..... | 153 |
| 8.2 Conclusions..... | 155 |
| 8.3 Recommendations..... | 158 |
| References..... | 161 |
| Appendix A:HDM-4 and MEPD Pavement Performance Models for Rigid Pavement..... | 166 |
| Appendix B:Microsoft Visual Basic Excel File for the Calibration of CRCP Performance Models..... | 194 |
| Appendix C: Calibrated CRCP Distress Performance Models for Texas Districts..... | 202 |
| Appendix D: Calibrated CRCP Distress Performance Models for Climate and Subgrade Zones..... | 321 |
| Appendix E: Calibrated CRCP Ride Quality Performance Models for Texas Districts... | 352 |
| Appendix F: Calibrated CRCP Ride Quality Performance Models for Climate and Subgrade Zones..... | 389 |
| Vita..... | 398 |

List of Tables

| | |
|--|----|
| Table 2. 1. Performance Models used in Pavement Management Levels (Adapted from Lytton 1987). | 12 |
| Table 2.2. PMIS Pavement Types (Adapted from TxDOT 2010)..... | 16 |
| Table 2. 3. Distresses Modeled in PMIS Performance Models (Adapted from TxDOT 2010). .. | 16 |
| Table 2.4. Distresses Classified as Failures. | 20 |
| Table 2.5. PMIS Rating for CRCP Distress Types | 25 |
| Table 2.6. PMIS Rating for JCP Distress Types..... | 25 |
| Table 2.7. PMIS Pavement Performance Coefficients for CRCP, JPCP, and JRCP (Adapted from TxDOT 2010)..... | 27 |
| Table 2.8. RSmin Value for Calculating Ride Quality Li (Adapted from TxDOT 2010)..... | 33 |
| Table 2.9. Pavement Performance PMIS Coefficients for CRCP and JCP Ride Quality Performance Models (JPCP and JRCP) (Adapted from TxDOT 2010). | 33 |
| Table 2.10. Pavement Distresses Modeled in HDM-4 | 38 |
| Table 2. 11. Pavement Types and Distresses Modeled in HDM-4..... | 39 |
| Table 2.12. Pavement Data Required for HDM-4. | 40 |
| Table 2.13. HDM-4 Default Calibration Factors (Adapted from Kerali and Odoki 2000). | 41 |
| Table 2.14. Input parameters for Rigid Pavement Distress Performance Models (Adapted from NCHRP b,c,d). | 46 |
| Table 2.15. Overview of PMIS, MEPDG and HDM-4 Pavement Management Tools (continued). | 53 |
| Table 4. 1. Texas Districts (TxDOT 2012)..... | 64 |
| Table 4. 3. Inventory Data Collected for Calibration of PMIS Pavement Performance Models. | 66 |

| | |
|---|-----|
| Table 4.4. Parameters Evaluated for Statistical Analysis. | 68 |
| Table 4.5. Li Statistical Parameters for Spalled Cracks..... | 70 |
| Table 4.6. Statistical Parameters for Li for Punchouts. | 72 |
| Table 4. 7. Li Statistical Parameters for ACP Patches..... | 74 |
| Table 4.8. Li Statistical Parameters for PCC Patches. | 76 |
| Table 4. 9. Number of Sections with Level of Distress (Li) Greater than Zero. | 78 |
| Table 4. 10. Li Statistical Parameters for CRCP Ride Quality. | 80 |
| Table 5. 1. Climate and Subgrade Characteristics for Zones..... | 91 |
| Table 6. 1. Calibrated CRCP Distress Performance Models for Texas Districts (Li Median Subset)..... | 103 |
| Table 6.2. Constrained Calibration of CRCP Distress Performance Models for Texas Districts (Li Median Subset). | 107 |
| Table 6.3. Calibrated CRCP Distress Performance Models for Climate and Subgrade Zones (Li Median Subset). | 110 |
| Table 6.4. Constrained Calibration of CRCP Distress Performance Models for Climate and Subgrade Zones (Li Median Subset)..... | 111 |
| Table 6.5. Calibrated Statewide CRCP Distress Performance Models (Li Median Subset). | 112 |
| Table 6.6. Constrained Calibration of Statewide CRCP Distress Performance Models (Li Median Subset)..... | 114 |
| Table 6.7. Recommended Statewide CRCP Performance Curve Coefficients..... | 120 |
| Table 6.8. Calibrated CRCP Ride Quality Performance Models for Texas Districts (Li Median Subset)..... | 126 |

| | |
|---|-----|
| Table 6.9. Calibrated CRCP Ride Quality Performance Models for Climate and Subgrade Zones (Li Median Subset). | 128 |
| Table 6.10. Calibrated Statewide CRCP Ride Quality Performance Models (Li Median Subset). | 128 |
| Table 6. 11.Recommended Statewide CRCP Ride Quality Performance Curve Coefficients. .. | 130 |
| Table 6.12. Final Recommended Statewide CRCP Distress and Ride Quality Performance Model Coefficients. | 134 |
| Table 6. A.13. Model Coefficient for Temperature Correction (adapted from Volume 4 of HDM-4 Manual). | 172 |

List of Figures

| | |
|---|----|
| Figure 2. 1. PMIS Performance Curve for Spalled Cracks..... | 27 |
| Figure 2.2. PMIS Performance Curve for Punchouts. | 28 |
| Figure 2.3. PMIS Performance Curve for ACP Patches..... | 28 |
| Figure 2.4. PMIS Performance Curve for PCC Patches. | 28 |
| Figure 2.5. PMIS Performance Curve for Failed Joints and Transverse Cracks. | 29 |
| Figure 2.6. PMIS Performance Curve for Failures. | 29 |
| Figure 2.7. PMIS Performance Curve for Shattered Slabs. | 30 |
| Figure 2.8. PMIS Performance Curve for Slabs with Longitudinal Cracks. | 30 |
| Figure 2.9. PMIS Performance Curve for Concrete Patches. | 31 |
| Figure 2.10. PMIS Ride Quality Performance Curve for CRCP. | 34 |
| Figure 2.11. PMIS Ride Quality Performance Curve for JCP (JPCP and JRCP)..... | 34 |
| Figure 3. 1. Hybrid technique For The Calibration Of Network Level Pavement Performance Models..... | 56 |
| Figure 4. 1. Texas District Divisions (TxDOT 2012)..... | 65 |
| Figure 4. 2. Box Plot Structure. | 68 |
| Figure 4. 3. Histogram of Observed Li for Spalled Cracks. | 69 |
| Figure 4. 4. Relative Frequency Histogram of Observed Li for Spalled Cracks. | 69 |
| Figure 4.5. Box Plot of Observed Li for Spalled Cracks. | 70 |
| Figure 4. 6. Histogram of Li for Punchouts. | 71 |
| Figure 4.7. Relative Frequency Histogram of Li for Punchouts..... | 71 |
| Figure 4.8. Box Plot of Li for Punchouts..... | 72 |
| Figure 4.9. Histogram of Observed Li for ACP Patches. | 73 |

| | |
|---|-----|
| Figure 4.10. Relative Frequency Histogram of Observed Li for ACP Patches. | 73 |
| Figure 4.11. Box Plot of Observed Li for ACP Patches. | 74 |
| Figure 4. 12. Histogram of Li for PCC Patches..... | 75 |
| Figure 4.13. Relative Frequency Histogram of Li for PCC Patches..... | 75 |
| Figure 4. 14. Box Plot of Observed Li for PCC Patches. | 76 |
| Figure 4. 15. Histogram of Li for CRCP Ride Quality..... | 79 |
| Figure 4. 16. Relative Frequency Histogram of Li for CRCP Ride Quality..... | 79 |
| Figure 4. 17. Box Plot of Li for CRCP Ride Quality..... | 80 |
| Figure 5. 1. Pavement Age Estimation Process for Li Records..... | 85 |
| Figure 5.2. Example of Pavement Age Estimation: Assumption 1. | 86 |
| Figure 5. 3. Example of Pavement Age Estimation: Assumption 2. | 87 |
| Figure 5. 4. Example of Pavement Age Estimation: Assumption 3. | 88 |
| Figure 5. 5.Example of Pavement Age Estimation Using Assumptions 1, 2 and 3..... | 89 |
| Figure 5. 6. Calibration of Pavement Performance Curves using the “Windows” Technique (Bustos et al. 1998). | 90 |
| Figure 5.7. Climate and Subgrade Zones utilized for Calibration of CRCP Performance Curves (Gharaibeh et al. 2012). | 92 |
| Figure 5. 8. Example of Li Quartile Filter Technique. | 93 |
| Figure 5.9. Example of Li Median Technique..... | 94 |
| Figure 5. 10. Sets of Data Prepared for the Calibration: Spalled Crack Example..... | 96 |
| Figure 6. 1. Least Squares Method for Non-linear Regression Analysis..... | 100 |
| Figure 6.2. Calibrated CRCP Spalled Cracks Performance Model, Statewide, Li Median Subset (Unconstrained)..... | 112 |

| | |
|---|-----|
| Figure 6.3. Calibrated CRCP Punchouts Performance Model, Statewide, Li Median Subset (Unconstrained)..... | 113 |
| Figure 6.4. Calibrated CRCP ACP Patches Performance Model, Statewide, Li Median Subset (Unconstrained)..... | 113 |
| Figure 6.5. Calibrated CRCP PCC Patches Performance Model, Statewide, Li Median Subset (Unconstrained)..... | 114 |
| Figure 6.6. Calibrated CRCP Spalled Cracks Performance Model, Statewide, Li Median Subset (Constrained)..... | 115 |
| Figure 6.7. Calibrated CRCP Punchouts Performance Model, Statewide, Li Median Subset (Constrained)..... | 115 |
| Figure 6.8. Calibrated CRCP ACP Patches Performance Model, Statewide, Li Median Subset (Constrained)..... | 116 |
| Figure 6.9. Calibrated CRCP PCC Patches Performance Model, Statewide, Li Median Subset (Constrained)..... | 116 |
| Figure 6. 10. Recommended Statewide CRCP Spalled Cracks Performance Curve, Median Method. | 121 |
| Figure 6.11. Recommended Statewide CRCP Punchouts Performance Curve, Median Method. | 122 |
| Figure 6. 12.Recommended Statewide CRCP ACP Patches Performance Curve, Median Method. | 123 |
| Figure 6. 13.Recommended Statewide CRCP PCC Patches Performance Curve, Median Method. | 124 |

| | |
|---|-----|
| Figure 6.14. Calibrated CRCP Ride Quality Performance Model, Statewide, Li Median Subset (Unconstrained)..... | 129 |
| Figure 6.15. Calibrated CRCP Ride Quality Performance Model, Statewide, Li Median Subset (Constrained)..... | 129 |
| Figure 6. 16. Calibrated CRCP Ride Quality Performance Model, Statewide, Li Median Subset (Constrained)..... | 131 |
| Figure 7.1. PMIS Failed Joints and Transverse Cracks Model with Varying Coefficient α (α)..... | 140 |
| Figure 7. 2. PMIS Failed Joints and Transverse Cracks Model with Varying Coefficient β (β)..... | 141 |
| Figure 7. 3. PMIS Failed Joints and Transverse Cracks Model with Varying Coefficient ρ (ρ)..... | 141 |
| Figure 7. 4 HDM-4 Transverse Cracking Model with Varying Coefficient K_{jpc} | 143 |
| Figure 7. 5. MEPD Transverse Cracking Model with Varying Coefficient C_4 | 145 |
| Figure 7. 6. MEPD Transverse Cracking Model with Varying Coefficient C_5 | 146 |
| Figure 7. 7. MEPD Transverse Cracking Model with Varying Coefficient C_1 | 146 |
| Figure 7. 8.MEPD Transverse Cracking Model with Varying Coefficient C_2 | 147 |

Chapter 1: Introduction

Continuously reinforced concrete pavements (CRCP) have become a popular choice for highway networks due to CRCP's durability, reduced maintenance, and high traffic volume capacity. CRCP was first introduced in the United States in 1921 and started to gain popularity in the 1960s with the construction of the U.S. Interstate Highway System (Liebertz 2010). CRCP is particularly adequate for roads with heavy traffic since closing lanes for repairs is expensive and causes major inconveniences to users and the agency. CRC pavements are a cost-effective investment that should be preserved.

Pavement performance models are a key tool used in pavement management systems (PMS) to maintain a CRC pavement network in good condition. Through the model's pavement performance predictions, an understanding of future pavement deterioration can be obtained and adequate preventive actions taken to maintain the pavement in a desirable state. Effective pavement management yields healthy road networks, cost savings and a satisfied driving public. In order for the models to perform their function in PMS and yield these benefits, they must reliably predict pavement performance. Reliable pavement performance predictions can be obtained if the models are representative of the deterioration patterns in the pavements studied. Performance models can be developed through mechanistic, empirical, or mechanistic empirical methods. The type of model and its prediction capabilities are dependent on the PMS management level the model is catered for. For example, complex detailed models or general models can be developed for the PMS project and network levels, respectively. Ultimately, the needs of the PMS management level dictate the model characteristics and their development.

1.1 Continuously Reinforced Concrete Pavement

Continuously reinforced concrete pavement is a portland cement concrete (PCC) pavement that is continuously reinforced with longitudinal steel bars. The need of transverse joints is eliminated in CRCP; therefore, allowing the pavement to expand several miles with required breaks only at structures. Transverse cracks at relatively close intervals can be commonly observed in CRCP. Nonetheless, these cracks should not be a major concern if they are uniformly spaced and the amount of longitudinal steel is properly designed. The longitudinal reinforcing steel controls the crack width and provides high load transfer across cracks. CRCP also demonstrates good riding quality if the structural continuity of the cracks is maintained. (Shiraz et al. 2001). Common distresses in CRC pavements are punchouts, spalling along transverse cracks, pumping and faulting across transverse cracks (Choi and Chen 2005). Punchouts, which are developed by two closely spaced transverse cracks and a longitudinal crack, is a major concern for CRCP. It can significantly affect the structural and riding quality of the pavement. Distress development is inevitable as the pavement ages, but can be mitigated if the proper maintenance strategies are implemented by the pavement management system.

1.2 Pavement Management Systems and Management Levels

According to the American Association of State Highway and Transportation Officials (AASHTO), a pavement management system is a set of tools or methods that assists decision-makers in finding the optimum strategies for providing, evaluating, and maintaining pavements in a serviceable condition over a period of time (Huang 2004). Pavement management systems are designed to provide the necessary information and treatment needs analysis for the development of cost effective strategies. In general, the components of PMS

can be broadly categorized into five categories: inventory data, pavement condition surveys, analysis scheme, decision criteria, and implementation procedures (Muench et al. 2003). The inventory data consists of basic descriptive information of the pavement sections in the network. The pavement condition surveys consist of pavement performance data collected of the pavement sections (e.g. observed distress, ride quality, skid resistance). This type of data allows for pavement management agencies to monitor the condition of the sections in their roads and measure the effectiveness of their management activities. The analysis scheme mainly consists of algorithms used to interpret the data in more significant ways. For example, this can include pavement performance prediction, cost analysis, optimization algorithms and impact analysis of treatment strategies. Furthermore, the decision criteria consist of rules developed to guide pavement management decisions. This can include decision trees and decision matrices for treatment selection for the pavement sections under study. Finally, PMS is composed of implementation procedures which are methods used to apply management decisions to roadway sections (Muench et al. 2003). In order for PMS to effectively accomplish its objectives, it is important that each component adequately satisfies its duties.

The structure of PMS and its activities can be adapted to satisfy two general management levels: network level and project level. The network level deals with the pavement network as a whole. It mainly concentrates in the following areas: maintenance and rehabilitation needs; funding needs; forecasting future impacts for various funding options; and prioritizing treatment lists of candidate sections. The responsibilities of this management level may include: identifying pavement maintenance, reconstruction, and rehabilitation needs; determining funds needed to address these needs; selecting feasible funding options and

strategies to be tested; determining the impact of the funding options on the pavement performance as well as the overall safety of the driving public; and developing optimum pavement budget recommendations (Huang 2004). In the network management level, PMS offers support in the planning, programming, budgeting and analysis phases. On the other hand, the project management level deals with the individual pavement sections. The responsibilities at this management level may include: assessment of the need for construction or cause of deterioration; identifying feasible design, maintenance, rehabilitation and reconstruction strategies; analysis of the cost-effectiveness of various alternatives; definition of imposed constraints; and the selection of the most cost-effective strategy within imposed constraints. In the project management level, PMS primarily provides support for identifying the optimal maintenance or rehabilitation activity for one given section under the budget constraints and policies set by the network level. Regardless of the management level in which it is employed, PMS can provide the tools necessary to perform the levels' responsibilities and goals.

1.3 Pavement Performance Models for PMS

A common and valuable tool used in Pavement Management Systems is the pavement performance model which forecasts pavement condition. The function of these models is an important foundation to PMS and its goal of providing the necessary information for effective pavement management. The complexity of these models varies according to the level of management catered. For example, project level models are more detailed than network level models. Project level models need to provide more accurate predictions since they are needed for establishing and designing necessary corrective actions for a given pavement section. On the other hand, the network level models' predictions are more general and representative of

the usual behavior of a pavement group. Through network level pavement condition predictions, pavement managers are able to determine future treatment needs and adequately develop multi-year treatments strategies. Therefore, network level models are mainly used in the selection of maintenance and rehabilitation treatments that are refined later at the project level. These models may be based on mechanistic principles or field observations. A combination of both is common to develop more realistic performance models.

Models for predicting pavement performance have adopted different types of equations. Network models are simple and usually follow a sigmoidal form; project models are more complex and are usually mechanistic empirical models that take various forms (e.g. logarithmic and power functions). For example, the AASHTO Mechanistic Empirical Design Guide (MEPDG) and Highway Development and Management Model (HDM-4) may model one distress through a collaboration of multiple functions with various forms. Furthermore, the amount and type of data used for the development of network and project management level performance models also differ. Due to the complexity of project level models, more detailed performance and core data of the pavements under study is required than in network models. In order to properly fulfill the function of pavement performance models in PMS, performance models must be updated regularly to continue to reflect deterioration patterns.

1.4 Research Objective and Project Scope

The aim of this research is to develop a methodology for the development of reliable network level concrete pavement performance models. Through the integration of various methods, it is expected to develop a calibration process for pavement performance models that could be easily adapted by network level road management agencies. The integration of various modeling approaches is expected to develop well rounded models which account for various

factors affecting deterioration. Ultimately, it is desired to provide a tool for pavement management systems to develop reliable concrete pavement performance prediction models and ultimately maintain healthy road networks.

This research consists of the presentation of the hybrid technique developed for the calibration of network level pavement performance models. This method will be validated with historical pavement performance data obtained for CRC pavements from the Pavement Management Information System (PMIS) of the Texas Department of Transportation (TxDOT). Recommendations for the application of this technique for the calibration of HDM-4 and MEPD models will also be presented.

1.5 Thesis Organization

The thesis will present the findings and results of this research in eight chapters. An overview of the existing pavement performance modeling methods and models will be presented in Chapter 2. Chapter 3 will then introduce and describe the hybrid technique developed. Chapters 4, 5 and 6 will describe the implementation of the method for the calibration of PMIS's CRCP performance models. Chapter 4 will describe the CRC pavement performance data collection process and statistical analysis. Chapter 5 will outline the data compilation and synthesis process performed on the collected CRCP data. Chapter 6 will describe the calibration process of the prepared data and the results. It will also outline the model selection process and present the final recommended CRCP performance models for TxDOT's PMIS. Chapter 7 will present general recommendations for using the hybrid technique when calibrating HDM-4 and MEPD models. A case study of the application of this technique for the calibration of the jointed plain concrete pavement (JPCP) transverse cracking performance model for HDM-4 and MEPD will also be presented in this chapter.

Chapter 8 will end this report with a summary of the results, conclusions and recommendations for future research.

2. Literature Review

A pavement management system can be described as a programming tool that collects and monitors information of existing pavements, forecasts future pavement condition, and evaluates and prioritizes pavement preservation and reconstruction strategies to successfully maintain a level of performance (Saba 2007). Accurate prediction of pavement performance is essential for an effective pavement management system. Through accurate prediction, agencies can effectively strategize activities to maintain pavements and extend their serviceable life in the most cost effective manner. Several types of pavement performance models are available to satisfy the needs of the different pavement management levels. In this chapter, a brief overview of the existing types of pavement performance models will be presented. Pavement management tools used in Texas and countries around the world will be introduced. These tools include the Pavement Management Information System (PMIS) used in the Texas Department of Transportation in the United States (U.S.), the Highway Development and Management Model (HDM-4) used worldwide, and the Mechanistic-Empirical Design Guide (MEPDG) mainly adapted by many U.S. highway agencies. The models for pavement performance prediction used in each will be presented and discussed.

2.1 Overview of Types of Pavement Performance Models

Different types of pavement performance models are used by agencies according to their specific management needs and available resources. There are two main categories into which pavement performance models can be grouped: deterministic and probabilistic models. Deterministic models are those that predict the pavement's level of distress or other pavement condition measures. Probabilistic models predict the distribution of the pavement condition throughout its life. These models can be further classified into more detailed categories

which are presented in Table 2.1. This table presents four detailed management levels and the performance models that may be used in each.

Deterministic models can be further classified as primary response, structural performance, functional performance, and damage models. Primary response models predict the primary responses of the pavement when imposed to different loads and climatic conditions. Primary responses include deflection, stress, strain, thermal stress, water content and temperature. Structural performance models predict pavement distress and measures of pavement condition (e.g. Pavement Condition Index [PCI]). Furthermore, functional performance models predict measures used to describe the pavement's serviceability (e.g. pavement's ability to provide comfort and safety). Measures of functional performance may include: present serviceability index (PSI), pavement surface friction, and wet-weather safety index. Finally, damage models are equations representing the normalized distress or loss of serviceability index of a pavement. These can be derived from structural or functional models by dividing these models by the acceptable values of distress or serviceability index, respectively. These models are important since they can be used to derive load equivalence factors used in pavement design (Lytton 1987).

On the other hand, probabilistic models address the stochastic characteristics of the pavement deterioration process. They can be further classified into survivor curves and transition process models. Survivor curves express the percentage of pavement sections that remain in service after a number of years or passes of a standard load without requiring any corrective action. Transition process models include Markov and Semi-Markov models. Markov models, which are the basis for most proposed probabilistic models, describe the probability that a group of pavements of similar age or traffic level will transition from one condition

state to another within a period of time. The state of the system depends on the previous state, but not on how the previous state was obtained. The transition from one state to another is independent of time which is not realistic and is considered a major limitation of this type of model performance (Saba 2007). On the other hand, Semi-Markov models are more realistic transition process models. These models are very similar to Markov models except that they recognize that the condition of the pavement, changing weather and changing traffic conditions have an effect on the transition process from one state to another.

Deterministic and probabilistic models can be further described as empirical, mechanistic or mechanistic-empirical models according to the data used in their development. Empirical models are developed from data based on experiments, experience and observations. These models do not represent the theoretical mechanisms of pavement response. Empirical models can be used to relate estimated or measured variables such as deflection or accumulated traffic loads to loss of serviceability or measures of deterioration (i.e., pavement distresses). On the other hand, mechanistic models are developed from theoretical knowledge of pavement responses. Purely mechanistic models exist for pavement responses such as stress, strain and deflection. Furthermore, mechanistic-empirical models are developed by combining mechanistic models with empirical data. The form and variables of the model may be developed from theory, but the coefficients are determined from regression analysis with measured or observed data. For example, these models may relate pavement responses with loss of serviceability or measures of deterioration (Rauhut and Gendel 1987).

Careful attention must be given when selecting the type of model to represent the performance of pavements. Limitations and advantages of the models should be considered during the selection process. For example, empirical models are only applicable to pavements

under the same material and environmental conditions considered during their development. Mechanistic and mechanistic-empirical models have the advantage that they are capable of extrapolating beyond the data from which they were calibrated (Lytton 1987). Nevertheless, empirical models can usually be developed with data collected in pavement management systems while mechanistic-empirical models require more detailed material data which is not usually available in pavement management databases. Furthermore, probabilistic models are adequate for higher levels of management. They require historical data or subjective opinions of experienced engineers which can be a limitation to some agencies. Other limitations include the amount of data needed to develop the models. When selecting the model to represent pavement condition behavior, these factors must be taken into consideration to select the most adequate model for the agency and its needs.

Table 2. 1. Performance Models used in Pavement Management Levels (Adapted from Lytton 1987).

| Levels of Management | Description of Management Level | Types of Performance Model | | | | | | |
|----------------------------------|---|---|-----------------------------------|--|---|----------------------|---------------------------|-------------|
| | | Deterministic Models | | | | Probabilistic Models | | |
| | | Primary Response | Structural | Functional | Damage | Survival Curves | Transition Process Models | |
| | | Deflection ,Stress, Strain, Temperature, Thermal Stress, Moisture, Energy Frozen and Unfrozen Water Content | Distress Pavement Condition Index | Serviceability , Index Skid Loss, Wet Weather Safety Index | Load Equivalence, Marginal Load Equivalence | | Markov | Semi-Markov |
| National Network | The performance at this level is mainly concerned with matters of policy and economics (i.e. cost allocation, fund apportionment, and equity in taxation). It is affected by the needs of individual States or Provinces. | | | | X | X | X | X |
| State/ Providence Network | At this level, there is less concern with the conditions and trends of individual projects. It concentrates in measures of the overall condition of the pavement networks in each geographical subdivision. | | X | X | X | X | X | X |
| District Network | Performance is defined by the condition and trends of individual projects, the overall condition of the network and the level of performance provided by the different road types and functional classes. | | X | X | X | X | X | X |
| Project | This level is concerned with the distress, loss of serviceability, index and skid resistance, loss of overall condition, and damage done by the traffic. | X | X | X | X | | | |

2.2 TxDOT's Pavement Management Information System (PMIS): Overview of PMIS CRCP Performance Curves

The Pavement Management Information System (PMIS) is an automated system used by the Texas Department of Transportation (TxDOT) as a decision tool for the effective management of Texas' pavements. This system stores, retrieves, analyzes and reports pavement inventory and condition data. It was first implemented in May of 1993 to satisfy a pavement management and design policy set by the Federal Highway Administration. This policy required each State Highway Agency (SHA) to have a pavement management system. PMIS is an upgraded version of the Pavement Evaluation System which was part of a statewide management information system developed in the early 1980's (Dossey et al. 1998). PMIS provides a better understanding of pavement rehabilitation and reconstruction needs that in turn guide decision makers to a more appropriate allocation of funds. Through the support provided by PMIS, the transportation infrastructure is maintained in good condition.

PMIS can be used at all management levels within TxDOT: at the central Division offices, District offices, Area offices and at the Maintenance Section offices. The central Division offices use PMIS to help TxDOT monitor statewide trends in pavement condition. Through PMIS, statewide pavement condition and needs can be analyzed to help formulate and justify funding and resource allocation to Texas districts. In the District offices, PMIS can be used to monitor, select, and set priorities for preventive maintenance and rehabilitation works, and to estimate pavement needs. PMIS may also be used in the Area and Maintenance Section offices. It can provide pavement information for a single location that can be used to diagnose causes of premature failure and gather information for pavement design. PMIS has the information needed

by all management levels to work together and ultimately support and strengthen TxDOT's overall pavement management process (TxDOT 2010).

Currently, PMIS is composed of a series of analysis programs that incorporate the analysis of pavement inventory and condition data to support pavement management decisions. The analysis programs can be categorized into the following: Needs Estimate, Optimization, and Impact Analysis. These programs serve as tools that help pavement managers estimate pavement needs and select preventive maintenance and rehabilitation works. The first analysis program is the Needs Estimate process which determines treatment needs (in terms of lane miles and total treatment costs) without budget constraints. The purpose of this program is to inform pavement managers about the total present and future treatment needs of the pavements in their jurisdiction. Knowing future treatment needs provides districts justification for pavement rehabilitation decisions and strategies. This program also provides an understanding of the adequacy of current funding by allowing the comparison between existing funds and the costs of needed treatments. In the Needs Estimate process, performance models are used to predict future pavement condition with and without treatment (TxDOT 2010).

The second analysis program is the Optimization process which helps determine the most cost effective treatment strategies. The optimization program estimates the benefit of applying the recommended Needs Estimate treatment and compares it with available funding. It also calculates and compares the benefit and effective life of different treatment levels in different periods of the pavement section's life. The benefit provided by the treatment is estimated by the area between the performance model that represents the pavement condition behavior after the application of a treatment and the performance model that represents the pavement condition behavior of an untreated pavement section. Ultimately, the Optimization process calculates

treatment benefit, treatment effective life, and the estimated cost of treatment to determine a cost-effectiveness ratio. This ratio is then used to select the sections to receive treatment (TxDOT 2010).

The third analysis program is the Impact analysis which is used to estimate the effects of pavement decisions, policies and external factors on overall pavement condition. In this analysis, the impact of funding, section limits, section treatments, truck traffic, and preventive maintenance policies are studied. The impacts can be assessed in three points in time: current, after the imaginary application of needs estimate treatments and after the imaginary application optimization treatments. These help to determine the condition of the pavement network in the “current case”, “best case” where no funding restrictions are present, and the “expected case” where funding restrictions are implemented. With the consideration of all these factors in different periods of time, this analysis can help pavement managers make informed policies and decisions that can help bring the pavement network to optimal conditions (TxDOT 2010).

2.2.1 Pavement Distresses Evaluated In Texas

PMIS evaluates pavement performance for three major broad types of pavement in Texas: Asphalt Concrete Pavement (ACP), Jointed Concrete Pavement (JCP) and Continuously Reinforced Concrete Pavement (CRCP). These pavement types are subdivided into ten detailed pavement types (TxDOT 2010) which are displayed in Table 2.2. Performance models predicting pavement distress are used to represent pavement deterioration in each of the pavement types. The distresses modeled for each pavement type are presented in Table 2.3. To monitor the pavement deterioration, TxDOT conducts pavement evaluation surveys every year. The annual PMIS TxDOT pavement survey is composed of three separate surveys: a visual evaluation survey, a ride quality survey and a skid resistance survey. For the first survey,

TxDOT uses visual methods to identify existing distresses in pavements. The proper methods for conducting a visual pavement evaluation survey are described in a rater's manual developed by TxDOT. The second survey, which evaluates the riding quality of pavements, uses the Profiler/Rut Bars to collect the ride data and the automated rutting data (TxDOT 2010).

Table 2.2. PMIS Pavement Types (Adapted from TxDOT 2010).

| Pavement Type | | Description |
|----------------------|---------------|---|
| Broad | Detail | |
| CRCP | 1 | Continuously Reinforced Concrete Pavement |
| JCP | 2 | Jointed Concrete Pavement, reinforced (JRCP) |
| | 3 | Jointed Concrete Pavement, unreinforced ("plain") (JPCP) |
| ACP | 4 | Thick Asphalt Concrete Pavement (greater than 5.5" thick; 14.0 cm) |
| | 5 | Intermediate Asphalt Concrete Pavement (2.5-5.5" thick; 6.4-14.0 cm) |
| | 6 | Thin Asphalt Concrete Pavement (less than 2.5" thick; 6.4 cm) |
| | 7 | Composite Pavement (heavily-stabilized asphalt-surfaced pavement) |
| | 8 | Overlaid or Widened Old Concrete Pavement |
| | 9 | Overlaid or Widened Old Flexible Pavement |
| | 10 | Thin-surfaced Flexible Base Pavement (surface treatment or seal coat) |

Table 2. 3. Distresses Modeled in PMIS Performance Models (Adapted from TxDOT 2010).

| Pavement Type | Distresses Modeled |
|----------------------|---|
| ACP | Shallow Rutting, Deep Rutting, Patching, Failures, Block Cracking, Alligator Cracking, Longitudinal Cracking, Transverse Cracking |
| JCP | Failed Joints and Transverse Cracks, JCP Failures, Slabs with Longitudinal Cracks, Concrete Patches, Shattered Slabs |
| CRCP | Spalled Cracks, Punchouts, ACP Patches, Portland Cement Concrete (PCC) Patches |

Due to the focus of this research, only the distresses evaluated in CRCP and JCP as well as their evaluation methods will be described in the following sections.

2.2.1.1 Spalled Cracks

According to PMIS Rater's Manual, a spalled crack can be described as a crack that shows signs of chipping on either side, either along some or all of its width (TxDOT 2009). Spalled cracks usually occur due to excessive stresses at the joint or cracks that are caused by infiltration of incompressible materials and by subsequent expansion or traffic loading. The occurrence of spalled cracks can also be attributed to the disintegration of concrete (Huang 2004). TxDOT evaluates cracks as spalled cracks in CRCP if they display spalling (i.e. edge chipping or secondary cracking) of greater than 3.0 inches (76 mm) long (on either side of the crack) that covers one foot (0.3 m) or more of the cracks total width across the lane (TxDOT 2009). Only transverse cracks that have spalled should be rated. Spalled cracks are measured by counting the number of existing spalled cracks.

2.2.1.2 Punchouts

A punchout can be defined as a full depth block of pavement formed when one longitudinal crack intersects two transverse cracks. Punchouts in CRCP can be caused by steel corrosion, inadequate amount of steel, repeated heavy loads, free moisture beneath the pavement, erosion along the supporting base or subgrade material, loss of load transfer efficiency (LTE) between two closely spaced transverse cracks, and negative slab curling and moisture warping (drying shrinkage) (Huang 2004). TxDOT recognizes the existence of a punchout if each of the edges (except the slab edge) of the punchout has either severe faulting or spalling. Faulting occurs when one edge of the crack is one-quarter-inch or more higher than the other edge. A crack can be considered to be severely spalled if it can be observed that the slab is not supporting any of the traffic loads. The punchout should be greater than 12 inches (305 mm) long or wide in order to be considered in the rating process. It is evaluated by counting the number of existing

punchouts. Punchouts are rated as one punchout for every 10 feet of length if its length is greater than 10 feet (3 meters) (TxDOT 2009).

2.2.1.3 ACP Patches

TxDOT also evaluates ACP patches as a type of CRCP distress. This distress can be described as a localized area of asphalt concrete that has been placed to the full depth of the concrete slab surrounding it. ACP patches should be used as temporary solutions for the correction of surface or structural defects. Given that the visual survey is not enough to determine the depth of the patch, a full depth patch can be identified by its shape. Full-depth patches are usually shaped into a square or rectangle since the patch is usually cut into the slab. Another criterion that must be met to consider the existence of an ACP patch is that the patch must be greater than 12 inches (305 mm) long. ACP patches are measured by counting the number of existing ACP patches. Long patches are rated as one patch for every 10 feet if the patch length is greater than 10 feet (3 meters) (TxDOT 2009).

2.2.1.4 PCC Patches

PMIS's Rater's Manual identifies PCC patches as an area of newer concrete which has been placed to the full depth of the existing slab to correct surface or structural defects. The criteria for determining the existence of a PCC patch is the same as that used for ACP patches. These patches can also be identified by their shape. PCC patches are measured by counting the number of existing PCC patches. Level-ups, overlays and repaired spalls in good condition should not be classified as PCC patches (TxDOT 2009).

2.2.1.5 Failed Joints and Transverse Cracks

For JCP, PMIS uses this distress category to account for spalled joints and transverse cracks, and the asphalt patches of spalled joints and transverse cracks. Besides the causes of spalling that were already mentioned, spalling can occur in JCP due to weak concrete at the joint that is caused by overworking or by poorly designed or constructed load transfer devices. In order to be classified as a spalled crack, it is stated in the manual that the crack must display spalling (i.e., edge chipping or secondary cracking) greater than 1.0 inch (25mm) long which covers greater than 1 foot (0.3 meters) of the crack's total width across the lane (TxDOT 2009). On the other hand, transverse cracks can usually be triggered by a combination of heavy load repetitions and temperature gradient, moisture gradient and drying shrinkage stresses (Huang 2004). Only the transverse cracks or joints that have spalled should be rated. Failed joints and cracks are measured by counting the number of failed joints and cracks observed (TxDOT 2009).

2.2.1.6 Failures

According to the PMIS's Rater's Manual, failures can be described as localized areas in which traffic loads do not seem to be transferred across reinforcing bars. These localized areas typically display surface distortion or disintegration. The following distresses can be rated as failures in JCP: corner breaks, punchouts, asphalt patches, failed concrete patches, d-cracking, spalls, and popouts (TxDOT 2009). Table 2.4 lists the distresses rated as failures.

Table 2.4. Distresses Classified as Failures.

| Distress | Description | Criteria to be rated as a failure |
|--------------------------------|--|--|
| Corner Break | A corner break is a crack (which may or may not be spalled or faulted) that travels from a joint to a slab edge. | Crack must intersect between 1 foot (0.3 meter) and halfway across each edge. |
| Punchouts | A punchout is a block of pavement formed when two transverse cracks are crossed by a longitudinal crack. | The boundaries of a punchout (except the slab edge) must show either spalling or faulting. If a punchout is longer than 10 feet (3 meters), then one punchout is rated for each 10 feet of length. |
| Asphalt Patches | An asphalt patch is a localized area of asphalt concrete that has been placed to the full depth of the concrete slab surrounding it. Shallow depth patches are also rated as failures. | An asphalt patch must be greater than 10 inches (254 mm) long. Long patches are rated as one failure for every 10 feet (3 meters). |
| Failed Concrete Patches | A concrete patch is an area of newer concrete which has been placed to the full depth of the existing slab to correct surface or structural defects. | Failed concrete patches that are spalled and/or faulted around all edges are rated as failures. |
| D-cracking | D-cracking is a series of closely spaced crescent shaped hairline cracks which usually cluster together along joints, slab edges and larger transverse/longitudinal cracks. | |
| Spalls | Spalls filled or not filled with asphalt. | Spalls greater than 10 inches long and greater than 12 inches wide. |
| Popouts | A popout is a piece of pavement missing which forms a hole in the concrete pavement's surface. | Popouts greater than 12 inches wide or long and greater than 3 inches deep are rated as failures. |

2.2.1.7 Shattered Slabs

For JCP, PMIS also considers shattered slabs as a distress. Shattered slabs are slabs that are severely cracked to the point that complete replacement of the slab is needed. A shattered slab can be identified if the slab has 5 or more failures or if the slab has one or more failures covering more than half of the slab's area. Shattered slabs are measured by counting the number of shattered slabs observed (TxDOT 2009).

2.2.1.8 Slabs with Longitudinal Cracks

In jointed concrete pavements, slabs with longitudinal cracks are rated as a distress. Longitudinal cracks can be described as cracks that run somewhat parallel to the roadbed centerline. Longitudinal cracks are caused by a combination of repeated heavy loads, loss of foundation support, and curling and warping stresses. Longitudinal cracks can also be attributed to improper construction of longitudinal joints (Huang 2004). In order to be rated as a longitudinal crack, a longitudinal crack must be severely spalled or faulted and must travel from one transverse joint to the next transverse joint, or it must travel from one transverse joint to an edge joint (this crack must be over half the slabs length). To be considered a severely spalled crack, the crack must be chipped or cracked in areas greater than 1.0 inch (254 mm) wide for more than half of its length. On the other hand, a faulted crack means one edge of the crack must be $\frac{1}{4}$ of an inch (6 mm) or greater higher than the other edge. Slabs with longitudinal cracks are measured by counting the number of slabs with longitudinal cracking (TxDOT 2009).

2.2.1.9 Concrete Patches

Concrete patches that have been placed as a method of correcting surface or structural defects, and have not failed are rated as concrete patches as opposed to failures. A concrete patch can be described as a localized area of newer concrete placed to full slab depth in order to correct defects. Concrete patches that are cleanly-shaped into a square or rectangle must be rated as concrete patches. Level ups, overlays, repaired spalls in good condition and patched corner breaks in good condition should not be rated as concrete patches. The patch must be greater than 10 inches (254 mm) long to be rated as a concrete patch. Longer patches than 10 feet (3 meters) should be rated as one patch for every 10 feet. Concrete patches are measured by counting the number of existing concrete patches (TxDOT 2009).

2.2.2 Pavement Performance Models for CRCP and JCP

Performance models are used to predict future pavement condition of Texas highways by projecting distress development and ride quality loss throughout the pavement's life. As was stated, they are used in all PMIS analysis programs as a tool to monitor pavement condition under various maintenance and rehabilitation strategies. Given the role they play in PMIS, it is important for these models to be accurate so they can remain a valuable tool.

The performance models used in PMIS are sigmoidal curves. A sigmoidal curve, also known as an S-shaped model, is a curve that has an inflection point and upper and lower asymptotes. Due to these characteristics, this type of model is good for modeling pavement condition indices. Condition indices are usually bounded by upper values that are set according to acceptable pavement conditions. These upper limits can be represented by the upper asymptotes of the sigmoidal curve. Furthermore, the inflection point of the model can effectively represent the different deterioration rate stages present during the service life of the pavement (Sadek et al. 1996).

Pavement Performance is evaluated as the level of distress (L_i) in TxDOT's PMIS. PMIS performance models depend on pavement age to predict L_i . Equation 2.1 displays the general format of the performance model used to represent the behavior of pavement in PMIS. The coefficients change according to the distress modeled and pavement type (TxDOT 2010).

$$L_i = \alpha e^{-\left(\frac{\rho \chi \sigma \epsilon}{\text{Age}}\right)^\beta}$$

Equation 2.1

where:

L_i = level of distress in a pavement section or percent of ride quality lost for the distress and ride quality performance models, respectively.

Alpha (α) = horizontal asymptote factor that represents the maximum range of distress growth. This coefficient varies according to the type of pavement and distress modeled.

Beta (β) = a slope factor that controls how steeply utility is lost in the middle of the model. This coefficient varies according to the type of pavement and distress modeled.

Rho (ρ) = prolongation factor that controls the time it takes before significant increases in distress occur. This coefficient varies according to the type of pavement and distress modeled.

Chi (χ) = the traffic weighting factor that controls the effect of an 18-k ESAL on performance. In PMIS, traffic is only accounted for load associated distresses in asphalt pavement (e.g. shallow rutting, deep rutting, alligator cracking). The chi value for all other distress types and pavement types is set to one as suggested by Research 1908 conducted by the Center for Transportation Research in the University of Texas at Austin (Robinson et al. 1995)

Epsilon (ϵ) = climate weighting factor that controls the effect of rainfall and freeze-thaw cycles on performance. PMIS uses a value of one for epsilon for all distress types and pavements. This value is used given that there are many uncertainties of the effects of climate on Texas' pavements. The uncertainties are due to the fact that most TxDOT-

sponsored research studies are focused on the effects of traffic on performance rather than climate.

Sigma (σ) = sub grade weighting support factor that controls the effect of sub grade strength on performance. As was the case for the traffic factor, X , the sigma factor was only defined for some ACP distress types (such as Shallow Rutting, Deep Rutting, Alligator Cracking and Block Cracking), and ACP Ride Quality. For other distress types, Sigma is defined as one. For rigid pavements (CRCP and JCP), a value of one is also used for sigma as was suggested by the Research Study 1908 (Robinson et al. 1995).

Age=pavement age of section in years. In the absence of consistent accumulated traffic load data, PMIS defines pavement age as the number of years since the last resurface or reconstruction.

There are two existing special cases of the Li calculation that need to be addressed differently. First, when age is equal to zero the Li is set equal to 0 since there should be no distresses in a new pavement. Second, if the calculated Li is less than or equal to zero, then Li should be set equal to 0.0001 to prevent errors in other calculations.

Given that this report will only be discussing rigid pavement, the criteria used for computing Li (level of distress) values for JCP and CRCP will be presented. Table 2.5 and Table 2.6 display the criteria used for computing Li values for CRCP and JCP distress types, respectively. For CRCP, the level of distress is obtained by “normalizing” the PMIS rating with the length of the pavement section (Equation 2.2). In JCP, Equation 2.2 and Equation 2.3 are used to calculate the Li values.

**Table 2.5. PMIS Rating for CRCP Distress Types
(adapted from (TxDOT 2010)).**

| CRCP Distress Type | PMIS Rating | Computing L_i Value |
|---------------------------|-------------------------|--|
| Spalled Cracks | Total number (0 to 999) | L_i =number of spalled cracks per mile (Equation 2. 2) |
| Punchouts | Total number (0 to 999) | L_i =number of punchouts per mile (Equation 2. 2) |
| ACP Patches | Total number (0 to 999) | L_i =number of asphalt patches per mile (Equation 2. 2) |
| PCC Patches | Total number (0 to 999) | L_i =number of concrete patches per mile (Equation 2. 2) |

$$L_i = \frac{\text{Rating}}{\text{Length}} \quad \text{Equation 2. 2}$$

**Table 2.6. PMIS Rating for JCP Distress Types
(adapted from (TxDOT 2010)).**

| CRCP Distress Type | PMIS Rating | Computing L_i Value |
|---------------------------|-------------------------|---|
| Failed Joints and Cracks | Total number (0 to 999) | L_i =percent of joints and cracks that have failed (Equation 2. 3) |
| Failures | Total number (0 to 999) | L_i =number of failures per mile (Equation 2. 2) |
| Shattered (Failed) Slabs | Total number (0 to 999) | L_i =percent of slabs that are shattered (Equation 2. 3) |
| Longitudinal Cracks | Total number (0 to 999) | L_i =percent of slabs that have longitudinal cracks (Equation 2. 3) |
| Concrete Patches | Total number (0 to 999) | L_i =number of concrete patches per mile (Equation 2. 2) |

$$L_i = 100 \times \left[\frac{\text{Rating}}{\left(\frac{5280 \times \text{Length}}{\text{Average Joint Spacing}} \right)} \right] \quad \text{Equation 2. 3}$$

2.2.2.1 Distress Pavement Performance Models for CRCP and JCP

In general, the factors α , β and ρ are the main determinants of the shape and behavior of the sigmoidal curve. The ϵ , σ and X factors are curve modifiers. If they are greater than one, the pavement life is increased. If they are less than one, the pavement life is decreased. In the first

rigid pavement models developed in 1993, only α , β and ρ were determined. The climate (ϵ), the pavement's subgrade (σ), and traffic (X) were not investigated in that study. A second study which was conducted in 1994 attempted to calibrate the models by also considering σ and X . A test of significance of the modifying coefficients (σ and X) was conducted to determine if the inclusion of these coefficients provided more representative models than the previously calibrated curves. It was concluded that the new models considering σ and X did not show significant improvements when compared to the models developed in 1993. This finding along with the need for more detailed data led to the conclusion that ϵ , σ and X should be set to a value of one for the concrete pavement models (Robinson et al. 1995).

The performance model for each distress in the different pavement type categories is described by a set of coefficients. Table 2.7 lists the coefficients currently used in PMIS to describe the distresses in CRCP, JPCP and JRCP. Even though PMIS has different treatment level categories (Preventive Maintenance, Light Rehabilitation, Medium Rehabilitation and Heavy Rehabilitation), only one performance model is used to represent the deterioration of a given type of pavement regardless of the treatment received. This practice is used for both CRCP and JCP. The improvement in pavement condition that should be experienced by the application of a treatment is only considered with recommended values in utility increase. In PMIS, utility is described as the usefulness of a pavement. Given that this research paper's focus is on pavement performance models, pavement utility will not be discussed. More about this topic can be found in the *PMIS Technical Manual* of 2010 (TxDOT 2010).

**Table 2.7. PMIS Pavement Performance Coefficients for CRCP, JPCP, and JRCP
(Adapted from TxDOT 2010).**

| Pavement Type | Distress Type | Alpha (α) | Beta (β) | Rho (ρ) |
|----------------------|---------------------------------------|--------------------|------------------|----------------|
| CRCP | Spalled Cracks | 1.690 | 22.090 | 10.270 |
| | Punchouts | 101.517 | 0.438 | 538.126 |
| | ACP Patches | 96.476 | 0.375 | 824.139 |
| | PCC Patches | 146.000 | 1.234 | 40.320 |
| JPCP and JRCP | Failed Joints and Cracks | 37.020 | 5.210 | 7.950 |
| | JCP Failures | 47.670 | 0.360 | 47.890 |
| | Slabs with Longitudinal Cracks | 34.470 | 0.520 | 240.750 |
| | Shattered Slabs | 80.000 | 1.000 | 30.000 |
| | Concrete Patching | 478.600 | 0.370 | 504.570 |

The current CRCP PMIS performance models for spalled cracks, punchouts, ACP patches, and PCC patches are shown in Figure 2.1 through Figure 2.4 respectively.

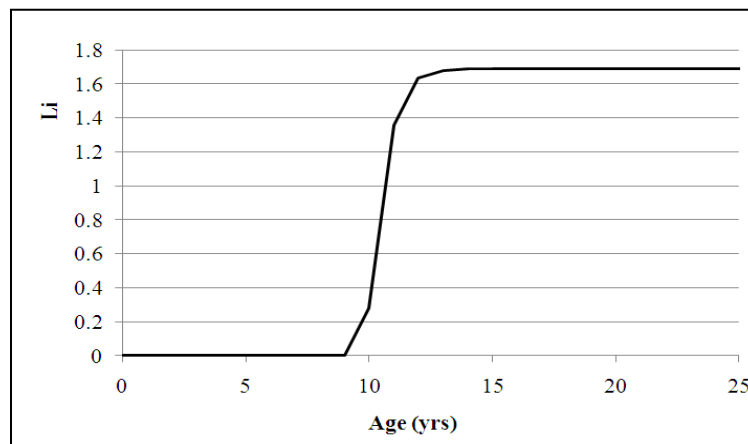


Figure 2. 1. PMIS Performance Curve for Spalled Cracks.

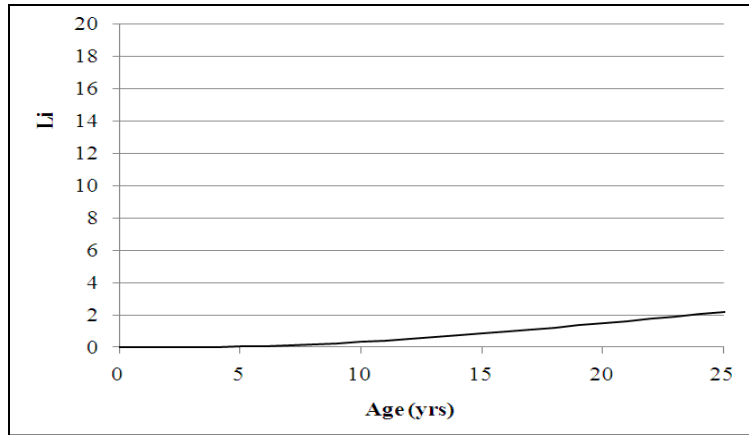


Figure 2.2. PMIS Performance Curve for Punchouts.

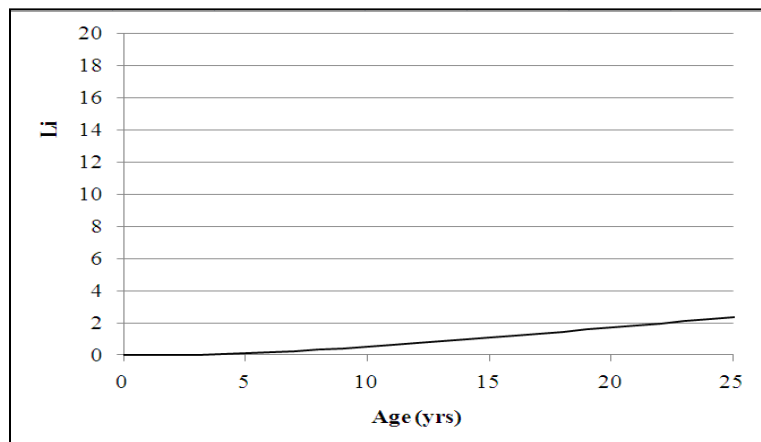


Figure 2.3. PMIS Performance Curve for ACP Patches.

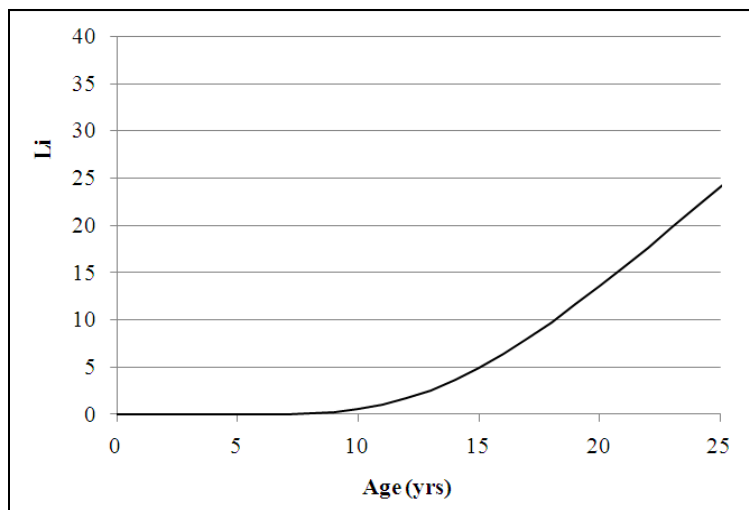


Figure 2.4. PMIS Performance Curve for PCC Patches.

The current JCP PMIS performance models for failed joints and transverse cracks, failures, shattered slabs, slabs with longitudinal cracks and concrete patches are shown in Figure 2.5 through Figure 2.9, respectively.



Figure 2.5. PMIS Performance Curve for Failed Joints and Transverse Cracks.



Figure 2.6. PMIS Performance Curve for Failures.

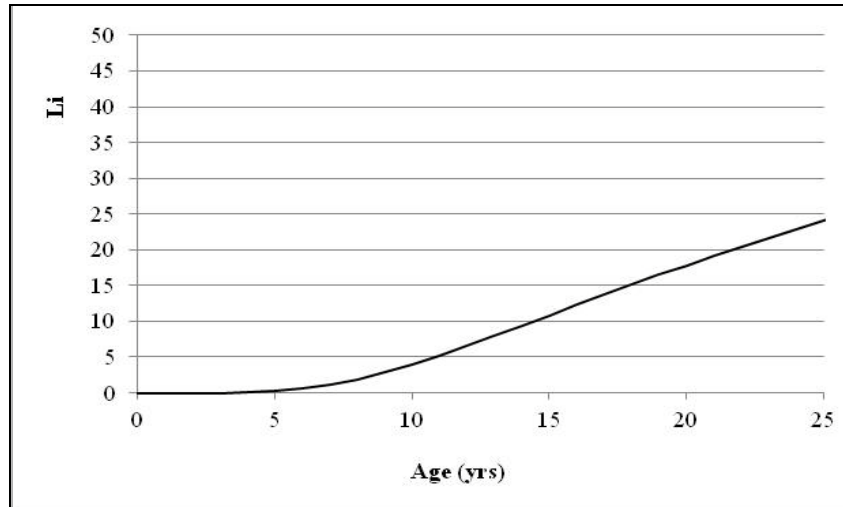


Figure 2.7. PMIS Performance Curve for Shattered Slabs.

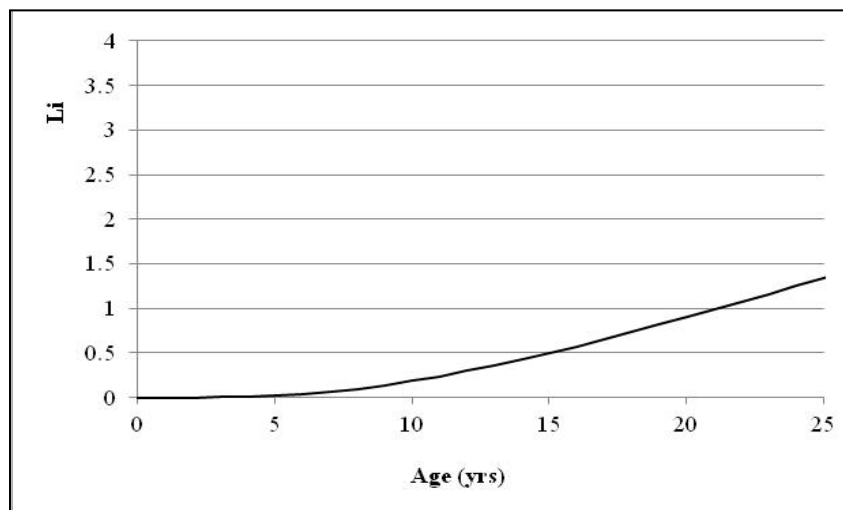


Figure 2.8. PMIS Performance Curve for Slabs with Longitudinal Cracks.

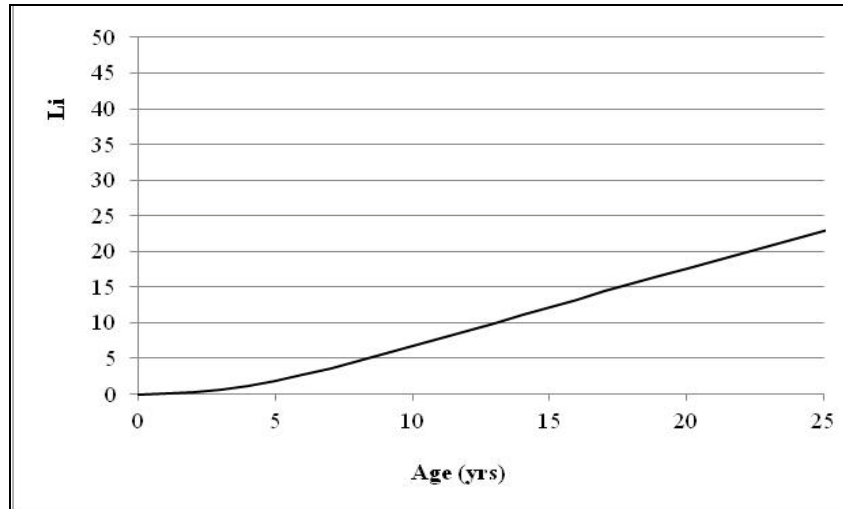


Figure 2.9. PMIS Performance Curve for Concrete Patches.

2.2.2.2 Ride Quality Pavement Performance Models for CRCP and JCP

PMIS defines the ride quality of a pavement through a Ride Score. Ride Score is a length-weighted arithmetic mean of all Serviceability Index (SI) values of a pavement section. Ride Score ranges from 0.1 (very poor quality) to 5.0 (very good ride quality). Ride Score is calculated through Equation 2. 4 (TxDOT 2010).

$$RS = \frac{\sum_{i=1}^n d_i SI_i}{\sum_{i=1}^n d_i} \quad \text{Equation 2. 4}$$

Where:

N=number of SI values collected for the pavement section

d=length of pavement, in miles, covered by the SI value

SI=Serviceability Index from Profiler. Given that SI is not measured directly by TxDOT profilers, SI is calculated from the International Roughness Index (IRI) measured by the Profiler and Equation 2.5. The coefficients L_{IRI} and R_{IRI} represent the measured IRI for the left and right wheel path, respectively.

$$SI = 8.8532704 - 4.425873 \times \left[\frac{(L_{IRI} + R_{IRI})/2}{63.36} \right]^{0.35} \quad \text{Equation 2.5}$$

The ride quality of a pavement is predicted through performance models. Equation 2.1 is also used to model the ride quality of a pavement as a function of pavement age. The coefficients of this equation retain the same meaning as previously described. Nevertheless, the definition of Li changes between the distress and ride quality performance equations due to the contrasting progression of each with time. The level of distress (Li) in the distress performance model describes an increasing distress with pavement age; therefore, the performance model has a positive slope. The ride quality of a pavement does not increase with pavement age; on the contrary, it decreases. In order to model ride quality adequately, a negative slope in the sigmoidal curve would be needed. This situation makes the use of the same definition for Li inadequate. Given to this situation and that it was desired to maintain the same pavement performance equation for simplicity purposes, a different approach had to be taken with the ride quality performance equation. For the ride quality performance model, Li was redefined as the percent of ride quality lost. Li is calculated through Equation 2.6. In this equation, it is assumed that the best Ride Score possible is 4.8 since no pavement can be built with a perfect ride of 5.0.

$$Li = \frac{4.8 - RS}{4.8 - RS_{min}} \quad \text{Equation 2.6}$$

Where:

RS= Ride Score

RS_{min}= value at which all ride quality has been lost. This value is determined according to the traffic level experienced in the pavement section. PMIS has three traffic level classifications (Low, Medium and High) which are described by the product of the

Average Daily Traffic (ADT) and the Speed Limit of the section. The RS_{min} values for each traffic level are displayed in Table 2.8.

Table 2.8. RSmin Value for Calculating Ride Quality Li (Adapted from TxDOT 2010).

| PMIS Traffic Class | Product of ADT and Speed Limit | RS_{min} Value |
|--------------------|--------------------------------|------------------|
| Low | 1-27,500 | 0.5 |
| Medium | 27,501-165,000 | 1.0 |
| High | 165,001-999,999 | 1.5 |

There are two existing special cases of the Li calculation that need to be addressed differently. First, if the calculated Li is greater than or equal to one (or in other words, Ride Score is less than or equal to RS_{min}), then Li is set equal to one. Second, if the calculated Li is less than or equal to zero (or in other words, the Ride Score is greater than or equal to 4.8), then Li is set equal to zero.

There is one ride quality performance model for each pavement type. Table 2.9 displays the set of coefficients currently used in PMIS that describe the ride quality of CRCP, JPCP and JRCP. Figure 2.10 and Figure 2.11 display the ride quality performance models for CRCP and JCP (JPCP and JRCP), respectively.

Table 2.9. Pavement Performance PMIS Coefficients for CRCP and JCP Ride Quality Performance Models (JPCP and JRCP) (Adapted from TxDOT 2010).

| Pavement Type | Alpha (α) | Beta (β) | Rho (ρ) |
|---------------|--------------------|------------------|----------------|
| CRCP | 1.000 | 1.000 | 25.000 |
| JPCP and JRCP | 1.000 | 1.500 | 10.000 |



Figure 2.10. PMIS Ride Quality Performance Curve for CRCP.

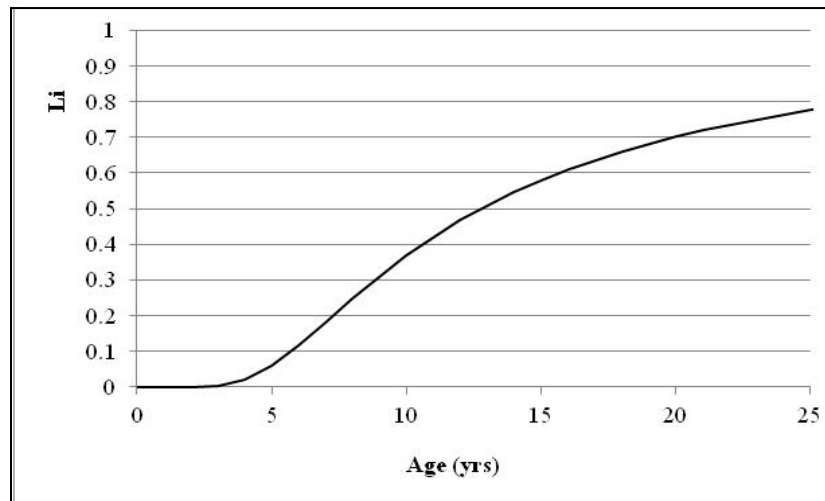


Figure 2.11. PMIS Ride Quality Performance Curve for JCP (JPCP and JRCP).

2.3 HDM-4: Overview of Concrete Pavement Performance Models

The Highway Development and Management Model (HDM-4) is a pavement management tool used for the planning, budgeting, monitoring and management of road networks. It incorporates road user effects, road work effects, social effects, road deterioration, and environmental effects to estimate the costs and benefits of treatment implementation. HDM-4 was developed by the

University of Birmingham in the United Kingdom through the International Study of Highway Development and Management Tools (ISOHDM) carried out between 1994 and 2000. Two main versions of HDM-4 have been released: Version 1 in 2000 and Version 2 in 2005. The latest version available is Version 2.08. Besides updating the World Bank's Highway Design and Maintenance Standards Model (HDM-III), HDM-4 provides an enhanced set of new tools that provide a powerful system for the analysis of road management and investment alternatives. It introduced new technical relationships to model concrete pavement deterioration, accident costs, traffic congestion, energy consumption and environmental effects (Kerali et al. 1988). Ultimately, HDM-4 is a decision support tool developed to facilitate the selection of cost-effective maintenance and rehabilitation plans for a road network.

The HDM-4 software can perform three types of analyses: strategy analysis, programmed analysis and project analysis. These can be applied by the national and state networks, district network, and project management levels, respectively. The strategy analysis may be used to analyze a whole road network or a road network matrix. A road network matrix can be categorized according to traffic level, pavement type, environmental or climatic zone and road functional class. In this analysis, medium to long term planning estimates of treatment needs and maintenance and rehabilitation activities can be prepared for periods of usually 5 to 40 years. The strategy analysis can also be used to forecast medium to long term funding requirements for specific target road maintenance standards, forecast long term road network performance under different funding levels, optimize fund allocation for different budget heads (e.g. routine maintenance, reconstruction), and study the impact of policies on the road network (e.g. impact of changes to the axle load limit). On the other hand, the programmed analysis deals with a defined long list of candidate road projects that are analyzed in a one-year or multi-year work

program. These candidate road projects are selected depending on maintenance, improvement or development standards defined by a road administration. The programmed analysis of HDM-4 can be used to compare the life-cycle costs of a base case (no work applied) against a treatment or development alternative. This can help estimate the cost-effectiveness of implementing the alternative. In this analysis, the sections that will be receiving treatment and the treatment type are determined. Furthermore, the project analysis is concerned with the evaluation of one or more road projects or investment options. The most cost effective project for each candidate section is determined for a specified list of pavement sections. These three levels of analysis differ in the amount of detail needed and provided. For example, in the project level analysis, road roughness data is analyzed in terms of measured defects. On the other hand, for the programmed and strategic analyses, road roughness data can be analyzed in terms of IRI value and quality level (good, fair and poor), respectively (Kerali et al. 1988).

2.3.1 HDM-4 Road Deterioration Models

The prediction of road deterioration is an important factor in every effective pavement management system. Reliable pavement performance prediction models are needed for proper determination of future treatment needs and optimal selection of treatment strategies. HDM-4 classifies its pavement deterioration models as structured empirical models. The structured empirical approach for developing models was first adopted in HDM-III to minimize problems arising from mechanistic and empirical models. This approach uses the functional form and primary variables from external sources, and then through various statistical techniques it quantifies their impacts. Using structured empirical models can give the advantage that the models combine the theoretical and experimental bases of mechanistic models with the behavior observed in empirical studies (Kerali and Odoki 2000).

The road deterioration models used can be further divided into two categories according to their predictive purposes: incremental and absolute models. Incremental models describe the change in pavement condition from an initial state while absolute models predict the pavement condition at a given time. Nevertheless, both of these models predict the pavement condition as a function of independent variables. In HDM-4, bituminous, unsealed and block pavement performance models are incremental models, while models representing concrete pavement performance are absolute models.

HDM-4 models account for various key variables that affect the deterioration of pavements. The key variables accounted for in the models include: climate, environment, traffic, pavement history, pavement geometry, drainage conditions, load transfer efficiency, pavement age, dowel properties, reinforcing steel properties, and PCC slab, base and subgrade properties. The climate and environment have a very significant impact on the rate of road deterioration. The climatic and environmental factors taken into consideration in HDM-4 models are related to: temperature, precipitation and winter conditions. The factors considered include: mean monthly and annual average precipitation, Thornthwaite moisture index, freezing index, mean monthly ambient temperature range, and days with temperatures greater than 32°C. Traffic parameters like the traffic composition, traffic volume, and axle loading are also major factors influencing road deterioration. The pavement history, which is also considered in HDM-4 pavement deterioration models, is represented by pavement age and previous maintenance, rehabilitation and construction works. These variables are also very important when modeling pavement condition (Kerali and Odoki 2000).

The HDM-4 road deterioration models are used to model different distresses for bituminous, concrete, block and unsealed pavements. Table 2.10. lists the distresses modeled for each of the distresses.

**Table 2.10. Pavement Distresses Modeled in HDM-4
(adapted from (Kerali and Odoki 2000)).**

| Bituminous | Concrete | Block | Unsealed |
|---|--|---|--|
| <ul style="list-style-type: none"> • Cracking • Raveling • Potholing • Edge break • Rutting • Surface texture • Skid resistance • Roughness | <ul style="list-style-type: none"> • Cracking • Joint spalling • Faulting • Failures • Serviceability loss • Roughness | <ul style="list-style-type: none"> • Rutting • Surface texture • Roughness | <ul style="list-style-type: none"> • Gravel loss • Roughness |

2.3.2 Rigid Pavement distresses modeled in HDM-4

Due to the nature of this report, concrete pavement performance models used in HDM-4 will be the main focus of this discussion. The concrete pavement deterioration models used in HDM-4 are based on research performed by the Latin American Study Team in Chile (Bustos et al. 1998). Efforts of this research were aimed at choosing the most adequate concrete pavement performance models. Models were determined for JPCP without load transfer dowels, JPCP with load transfer dowels, JRCP and CRCP. Table 2.11 provides a brief description of each concrete pavement type. The distresses modeled for each pavement type are also presented in Table 2.11. Table 2.12 provides a more detailed description of the pavement data required for the pavement performance models.

The modeling of pavements is considered in two phases: phase 1 which refers to the time before any major work, and phase 2 which refers to the time after a major work has been performed

(Kerali and Odoki 2000). Only models from phase 1 will be discussed in this report. The calibration factors for the first phase before any major work is performed are displayed in Table 2.13. As can be noted, all the calibration factors are recommended to a default value of 1.

Table 2. 11. Pavement Types and Distresses Modeled in HDM-4.

| Pavement Type | Description | Distresses Modeled |
|---|--|--|
| Jointed plain concrete pavement without load transfer dowels | This pavement consists of short slabs without reinforcement steel. Transverse load transfer between slabs is achieved through aggregate interlock. | Cracking (% of slabs cracked), Faulting, Spalling, Roughness |
| Jointed plain concrete pavements with load transfer dowels. | This pavement consists of short slabs without reinforcement steel. Transverse load transfer between slabs is achieved through dowel bars. | Cracking (% of slabs cracked), Faulting, Spalling, Roughness |
| Jointed reinforced concrete pavement | This pavement consists of slabs with a quantity of longitudinal reinforcement that allow longer slab lengths. Transverse load transfer between slabs is achieved through dowel bars. | Cracking (number per mile), Faulting, Spalling, Serviceability Loss, Roughness |
| Continuously reinforced concrete pavement | This pavement has longitudinal reinforcement throughout its length. It has no transverse joints; therefore, there is no need for any type of load transfer. | Failures, Serviceability loss, Roughness |

Table 2.12. Pavement Data Required for HDM-4.

| Parameter | Data Requirement |
|----------------------------|--|
| Material properties | Modulus of elasticity of concrete (E_c) Modulus of Rupture of concrete (MR28) Thermal coefficient of concrete (α_T) Drying shrinkage coefficient of concrete (γ) Poisson's ratio for concrete (μ) Modulus of elasticity of dowel bars (E_s) Modulus of elasticity of bases (E_{base}) Modulus of subgrade reaction (KSTAT) Thornthwaite Moisture Index Freezing Index Modulus of dowel support Modulus of elasticity of the dowel bar |
| Pavement structure | Slab thickness Base thickness Percentage of longitudinal steel reinforcement Base type Average joint spacing Dowel diameter Type of joint sealant |
| Traffic | Average annual daily traffic (AADT) Percentage of vehicle composition Types of axles Axle load Tire pressure Spacing between wheels |
| Drainage conditions | Drainage coefficient (C_d) Annual average precipitation (inches) |
| Other | Pavement age Efficiency of load transfer Efficiency of load transfer between slab and shoulder widened outside lanes initial roughness |

Table 2.13. HDM-4 Default Calibration Factors (Adapted from Kerali and Odoki 2000).

| Pavement Surface Type | Calibration Factor | Deterioration Model | Recommended Default Value |
|------------------------------|---|---|----------------------------------|
| JPCP | K_{jp_c} | Transverse cracking calibration factor | 1.0 |
| | K_{jp_n_f} | Faulting calibration factor in JP concrete pavements without dowels | 1.0 |
| | K_{jp_d_f} | Faulting calibration factor in JP concrete pavements with dowels | 1.0 |
| | K_{jp_s} | Joint spalling calibration factor | 1.0 |
| | K_{jp_r} | Roughness (IRI) progression calibration factor | 1.0 |
| JRCP | K_{jr_c} | Cracking deterioration calibration factor | 1.0 |
| | K_{jr_f} | Faulting calibration factor | 1.0 |
| | K_{jr_s} | Joint spalling calibration factor | 1.0 |
| | K_{jr_r} | Roughness progression calibration factor | 1.0 |
| CRCP | K_{cr_f} | Failures calibration factor | 1.0 |
| | K_{cr_r} | Roughness progression calibration factor | 1.0 |

In the following, the distresses modeled for JPCP, JRCP and will be presented and discussed.

2.3.2.1 Transverse Cracking

Transverse cracks are perpendicular to the central axis of the road. They occur in slabs subjected to high stress levels that are generally caused by the combined effect of thermal curling, moisture-induced curling and traffic loading (Huang 2004). Cracking can also be caused by defects originating from material fatigue. Transverse cracks can be classified into three severity levels according to the Strategic Highway Research Program (SHRP): low, medium and high. A low severity level of transverse cracking happens when cracks are less than 3 mm in width and have no visible spalling or faulting; or when cracks are well sealed with a non-determinable width. Medium severity level of transverse cracking occurs when there are cracks between 3 and 6 mm. It can also occur when there is spalling less than 75 mm or faulting less than 6 mm. On the other hand, a high severity level of transverse cracking occurs when the cracks have a width greater than 6 mm. It can also occur when there is spalling greater than 75 mm or faulting

greater than 6 mm (Kerali and Odoki 2000). Transverse cracking is modeled in HDM-4 for jointed plain and jointed reinforced concrete pavements. Transverse cracks in JPCP are recorded as a percentage while in JRCP they are recorded as the number of deteriorated cracks per mile.

2.3.2.2 Faulting

In concrete pavement, faulting occurs when a joint or a crack has a difference in elevation between both sides of the opening. It is caused either by the buildup of loose material under a trailing slab near a joint or crack or it can be caused by the depression of a leading slab. The buildup of this material underneath the slab is caused by pumping. Pumping, on the other hand, is caused by the presence of high levels of free moisture under a slab which carries heavy traffic loading. Insufficient load transfer can greatly contribute to faulting. Ultimately, faulting significantly increases road roughness (Huang 2004). In HDM-4, faulting is modeled for JPCP (with and without load transfer dowels) and for JRCP (Kerali and Odoki 2000). This distress is measured in inches.

2.3.2.3 Spalling

In HDM-4, spalling in the transverse joint is a distress that is also modeled for concrete pavements. Spalling occurs when the pavement cracks, breaks or chips off the slab edge within 2 ft (0.6m) of the opening. Spalled cracks do not usually penetrate the whole slab thickness, but they do extend until they intersect the joint at an angle. There are three levels of spalling according to SHRP (Kerali and Odoki 2000): low, medium and high. Low severity spalling is less than 75mm of distress width (which is measured from the center of the joint) with or without loss of material. A medium severity spall is also measured from the center of the joint. This level of spalling occurs between 75 and 150 mm of distress width with loss of material. High

severity spalling has the same characteristics as a medium level severity spall, but these spalls have measurements greater than 150 mm. In HDM-4, only medium and high level severity transverse spalling are modeled for JPCP and JRCP. It is recorded as the percent of spalled transverse joints.

2.3.2.4 Failures

A failure is a deterioration mode that is only modeled for continuously reinforced concrete pavement (CRCP). Failures include loosening and breaking of reinforcement steel and transverse crack spalling (Kerali and Odoki 2000). High tensile stresses created in the concrete and reinforcement steel, which are caused by traffic loading and changes in environmental factors, are the main causes of failures. Failures are measured in number per mile (or km).

2.3.2.5 Present Serviceability Rating

Present Serviceability Rating (PSR) is a subjective rating given by an individual of the ride quality of a specific roadway section. The ratings range from 0, which is the worst condition, to 5, which represents a pavement in extremely good condition. PSR is modeled for JRCP and CRCP in HDM-4. The ratings given are based on key distress types like transverse cracking, spalling and faulting for JRCP. As opposed to the PSR model used for JRCP, the PSR model for CRCP is based on pavement age since construction, cumulative ESALs and slab thickness.

2.3.2.6 Roughness

Roughness is usually the most important indicator of pavement condition according to the driving public. This is especially the case for higher speed limits (Huang 2004). Roughness can be described as a measure of the deviations of the surface from a true planar surface that can affect the riding quality of a driver. Roughness is modeled for all concrete pavement types:

JPCP, JRCP and CRCP. Nevertheless, in JPCP roughness is modeled as a function of faulting, spalling and transverse cracking while for JRCP and CRCP it is modeled as a function of PSR (Kerali and Odoki 2000).

A detailed description of the performance models used for HDM-4 is presented in Appendix A.

2.4 Mechanistic-Empirical Pavement Design Guide: Overview of Concrete

Pavement Performance Models

The Mechanistic-Empirical Pavement Design Guide (MEPDG) is software used in the design of flexible and rigid pavement structures. The user specifies a pavement structure for a trial pavement design and threshold values for evaluated structural and functional pavement performance indicators. The structural pavement condition is evaluated through pavement distresses. The functional pavement condition is evaluated through the ride quality of the pavement which is measured through IRI. Traffic, climate and pavement material characteristic inputs are also required since the software considers their effects on pavement condition behavior. MEPDG analyzes the suggested pavement design under the influence of all these factors to predict pavement performance. It predicts the performance by computing pavement responses to load (stresses and strains) which are used to compute damage (distresses and loss in ride quality) over the life of the pavement. The software determines whether the pavement design will meet the thresholds defined by the user. The MEPDG software is only used as a tool for determining the feasibility of the design; therefore, the user must go through a series of iterations to determine a design that will satisfy the thresholds. Given to this application of the software, MEPDG is a tool mostly aimed for project level management (Baus and Stires 2010).

2.4.1 MEPD Concrete Pavement Distress Performance Models

The performance models used in MEPDG are mechanistic-empirical models. The models are based on mechanistic engineering principles of the pavement's response to load (stresses and strains) and empirical relations to real pavement performance data. The models incorporate calibration factors that can be adjusted to represent pavements in different locations. Incorporating calibration factors is recommended since these can help account for the distress mechanisms that are too complex to be described by purely mechanistic models. The models in MEPDG can be divided into structural response models and transfer functions. The structural response models predict pavement condition by calculating incremental damage accumulation through the ISLAB2000 Finite Element Model (FEM) or neural network programs. The incremental damage is accumulated monthly or semi-monthly (depending to the frost condition) and is then converted to performance indicators through transfer functions. MEPD models evaluate performance indicators for flexible and rigid pavements. For rigid pavements, MEPD models JPCP and CRCP performance through various distresses. The distresses evaluated for JPCP are transverse slab cracking and mean joint faulting. For CRCP, punchouts are evaluated as a distress (NCHRP 2004a).

The input parameters needed to predict pavement distresses for JPCP and CRCP are presented in Table 2.14.

Table 2.14. Input parameters for Rigid Pavement Distress Performance Models (Adapted from NCHRP b,c,d).

| Input Parameter | Transverse Cracking (JPCP) | Transverse Joint Faulting (JPCP) | Punchouts (CRCP) |
|---|-----------------------------------|---|-------------------------|
| Design life | X (years) | X (month) | |
| Month of project opening | X | X | |
| PCC age at opening | X | X | |
| PCC strength for each month (psi) | X | X | |
| PCC modulus for each month (psi) | X | X | |
| PCC 28 day compressive strength | | | X |
| PCC elastic modulus | | | X |
| PCC 28 day tensile strength | | | X |
| PCC Modulus of Rupture | | | X |
| Joint spacing (ft) | X | X | |
| Dowel diameter (in) | X | X | |
| Steel bar diameter | | | X |
| Mean crack spacing | | | X |
| Shoulder joint stiffness | | | X |
| Loss of bond age | X | | |
| Lane-shoulder deflection load transfer efficiency (LTE) (%) | X | X | |
| LTE of base (alone) | | | X |
| Widened slab (yes/no) | X | X | |
| Poisson's ratio | X | X | X |
| PCC unit weight (pcf) | X | X | X |
| Coefficient of thermal expansion (°F) | X | X | X |
| Ultimate reversible shrinkage strain (10^{-6}) | X | X | X |
| Time to 50% ult. Shrinkage (days) | X | X | |
| Slab/base friction coefficient | | | X |
| Base thickness (in) | X | X | X |
| Base unit weight (pcf) | X | X | |
| base modulus (psi) | X | X | X |
| Base erodibility | | X | |
| Base/subbase erodibility index | | | X |
| Percent subgrade passing the number 200 sieve | | | X |
| Monthly effective subgrade k-value (psi/in) | X | X | X |
| Permanent curl/warp (°F) | X | X | |

Table 2.14. Input parameters for Rigid Pavement Distress Performance Models (Adapted from NCHRP b,c,d) (Continued).

| Input Parameter | Transverse Cracking (JPCP) | Transverse Joint Faulting (JPCP) | Punchouts (CRCP) |
|--|-----------------------------------|---|-------------------------|
| Mean annual precipitation | | | X |
| Raw annual axle load spectra for design lane (base year) | | | X |
| Edge-to-edge (outside) axle width (ft) | X | | |
| Lane width (ft) | X | X | |
| PCC zero-stress temperature | | X | |
| Mean wheel path (in) | X | X | |
| Traffic wander standard deviation (in) | X | X | |
| Annual truck growth factor | | | X |
| Monthly truck adjustment coefficient | | | X |
| Hourly temperature adjustment coefficient | | | X |
| Mean truck wheel path | | | X |
| Wheel path lateral standard deviation | | | X |
| Drying time (days from placement) | | | X |
| Slab width (ft) | X | X | |
| Slab thickness | | | X |
| PCC water/cement ratio | | | X |
| Depth to steel | | | X |
| Percent steel as fraction | | | X |
| Tire pressure (psi) | X | | |
| Axle spacing (in) | X | | |
| Dual wheel spacing (in) | X | | |
| Tire width (in) | X | | |
| Wheelbase-short, medium, and long (ft) | X | | |
| % trucks at each wheelbase (%) | X | | |

2.4.1.1 MEPD Jointed Plain Concrete Pavement Performance Models

2.4.1.1.1 Transverse Slab Cracking

MEPD models determine the amount of transverse slab cracking in a pavement section by considering the top-down (cracking initiates at the top and then propagates downward) and bottom-up cracking (cracking initiates at the bottom and works its way to the top). Both types of

cracking are considered since transverse cracking can initiate either at the top or bottom of the slab depending on loading, climate, material properties and conditions during construction (NCHRP 2003a). Bottom-up transverse cracking is caused by tensile bending stresses at the bottom of the slab (halfway between two transverse joints) which results from repeated traffic loading and high positive temperature gradients. Top-down transverse cracking is caused by bending stresses at the top of the slab induced by high negative temperature gradients and high axle loadings at opposite ends of the slab (Baus and Stires 2010). In MEPDG, cracking is calculated separately for both types of cracking and then added in the end to determine the total amount of transverse slab cracking. The equations used in this process are presented in Appendix A.

2.4.1.1.2 Mean Transverse Joint Faulting

Transverse joint faulting is one of the distresses that greatly affect the serviceability of jointed Portland cement pavements. As was previously stated, joint faulting is the difference in elevation between adjacent joints at a transverse joint. In MEPDG, transverse faulting is measured in inches. In this software, mean transverse joint faulting is calculated through incremental calculations. Given that the incremental design procedure requires thousands of monthly deflection calculations, the computations can take hours using finite element programs. As a result, neural network programs were developed to compute deflections faster (NCHRP 2003b). Faulting is calculated by summing the accumulated faulting throughout the pavement's life. The equations used for the calculation of faulting are presented in Appendix A.

2.4.1.2 MEPD Continuously Reinforced Concrete Pavement Performance Model for Punchouts

Given that the focus of the mechanistic-empirical CRCP structural design procedure is to control punchouts, the MEPDG software focuses on the punchout distress to evaluate the performance of CRCP. As was stated, the development of a punchout occurs with the formation of a longitudinal crack between two adjacent transverse cracks. The development of the longitudinal crack is associated to the accumulation of fatigue damage caused by the bending of the slab in the transverse direction. Therefore, the prediction of punchouts is considered in terms of the accumulated fatigue damage that forms longitudinal cracks in a process related to crack width, loss of load transfer and foundation support changes. In MEPDG, an incremental analysis is also applied to predict the number of punchouts in CRCP. Neural networks that were developed using a finite element structural model are used to compute critical top tensile stresses which help predict punchout development in a pavement. The equations used for the calculation of faulting are presented in Appendix A.

2.4.2 MEPD Concrete Pavement Roughness Performance Models

In MEPDG, pavement roughness is also evaluated for JPCP and CRCP as a measure of pavement performance. Pavement roughness is evaluated through the International Roughness Index (IRI). Pavement roughness can be described as the variation in surface elevation that affects the ride quality of a pavement and can therefore lead to user discomfort. IRI is calculated by the average rectified slope, which is a filtered ratio of a standard vehicle's accumulation suspension motion, divided by the vehicle's traveled distance during the evaluation. IRI is measured in meters per kilometer in MEPDG (NCHRP 2003d).

During the IRI model development for JPCP, structural, nonstructural, surface defects and maintenance factors were found to show some correlation with smoothness. Structural factors include faulting, corner breaks and transverse cracking. Nonstructural factors include joint spalling and longitudinal cracking. Surface defects include initial smoothness and map cracking. Maintenance includes patches of flexible and rigid materials. Pavement age was also found to be a factor that could represent other time dependent factors affecting the longitudinal profile (e.g. settlements, heaves, and swelling soils) that could not be represented in the model. As for CRC pavement, structural, surface defects and maintenance factors were found to show some correlation with pavement smoothness. Structural factors include punchouts, transverse cracking and pumping. Surface defects include initial IRI, scaling and map cracking. Maintenance includes patching. The equations used for the calculation of roughness for JPCP and CRCP are presented in Appendix A.

2.5 Summary

Pavement performance modeling is an important component of an effective pavement management system. Accurate predictions of pavement performance are essential for the development of pavement maintenance and rehabilitation strategies. Pavement performance can be represented through various types of models. Performance models can be broadly categorized as deterministic and probabilistic models. Deterministic models can be further divided into the following categories: primary response, structural, functional and damage models. Probabilistic models are further divided into survival curves and transition models. These models can be developed through mechanistic, empirical or mechanistic-empirical methods. The types of models and the modeling method used depend on the resources of an agency, its specific needs and the management level for which these models will be used for.

PMIS, MEPDG and HDM-4 are tools mainly used in pavement management in Texas, the United States and other countries around the world, respectively. Given that they target different management levels, the types of models used in each vary. PMIS is mainly aimed for the state and district network management levels. The models used in PMIS do not require an extensive amount of data to predict pavement condition. Given that not many factors are considered in the models, these pavement performance models can be easily calibrated. On the other hand, MEPDG is software that is of most use in the project management level. This software is mainly used as a pavement design tool. The data required for the prediction of pavement performance in MEPDG is very extensive. As a result, the models used in MEPDG consider enough detail to accurately predict the performance of one pavement section. These models can help determine a more specific pavement maintenance or rehabilitation strategy. Due to the large amount of input factors considered in the MEPD performance models, the models take various function forms (e.g. logarithmic or exponential forms). The large number of required input data also makes the calibration of the MEPD models more tedious. The HDM-4 software, which was also introduced, is applicable to all management levels: national, state and district network management levels and project level. The data required for the prediction of pavement performance is also very extensive. HDM-4 provides enough detail to accurately predict the performance of one pavement section. Nevertheless, its capacity also allows it to analyze more than one section at a time to provide the optimal maintenance or rehabilitation strategy for a whole network. As the MEPD models, the models in HDM-4 also take various forms (e.g. logarithmic, exponential and polynomial forms). The calibration of these models is also complicated by the large number of input data needed for the pavement performance prediction. Table 2.15 provides an overview of the models used in each management tool.

Table 2.15-Overview of PMIS, MEPDG and HDM-4 Pavement Management Tools.

| Descriptor | PMIS | MEPDG | HDM-4 |
|----------------------------------|--|--|--|
| JPCP distresses modeled | Failed joints and cracks, JCP failures, slabs with longitudinal cracks, shattered slabs, concrete patching, ride quality | Transverse slab cracking, transverse joint faulting, roughness (IRI) | Cracking, faulting, spalling, roughness |
| JRCP distresses modeled | Failed joints and cracks, JCP failures, slabs with longitudinal cracks, shattered slabs, concrete patching, ride quality | Not modeled | Cracking, faulting, spalling, serviceability loss (PSR), roughness (IRI) |
| CRCP distresses modeled | Spalled cracks, punchouts, ACP patches, PCC patches, ride quality | Punchouts, roughness (IRI) | Failures, serviceability loss (PSR), roughness (IRI) |
| Type of Performance Model | Deterministic (structural, functional) | Deterministic (uses output from response and damage models for structural and functional models) | Deterministic (structural, functional) |
| Modeling Method | empirical | Distress models are categorized as mechanistic-empirical models. Roughness models are categorized as empirical models that combine the effects of distress models. | HDM-4 classifies its pavement performance models as structural empirical, which are a form of mechanistic-empirical models. Roughness models are also classified as distress based. They also depend on the initial roughness. |

Table 2.1515. Overview of PMIS, MEPDG and HDM-4 Pavement Management Tools (continued).

| Overview | PMIS | MEPDG | HDM-4 |
|--|---|---|---|
| Region/ country of employment | The PMIS models were developed by the Center for Transportation Research in the University of Texas at Austin. The models were developed to be used in TxDOT's pavement management system. | The MEPD models were developed under a series of National Cooperative Highway Research Program (NCHRP) studies. MEPDG was developed for the adoption and distribution by the AASHTO. MEPDG is mainly used by highway agencies in the U.S. | HDM-4 was developed by the University of Birmingham in the United Kingdom through the International Study of Highway Development and Management Tools (ISOHDM). |
| Target management level | State and District Network management levels | Mainly focused in the project level | All management levels (national, state, district and project levels) |
| Input factors considered in performance model | Distresses are predicted based on pavement age. The models were designed to account for climate, traffic and subgrade properties, but these factors are not considered in the current models. | Climate; environment; temperature; traffic; traffic loads; pavement maintenance history; pavement geometry; slab, base and subgrade properties; drainage conditions; load transfer efficiency; pavement age; dowel and reinforcing steel properties | Climate; environment; temperature; traffic; traffic loads; pavement maintenance history; pavement geometry; slab, base and subgrade properties; drainage conditions; load transfer efficiency; pavement age; dowel and reinforcing steel properties |
| Output | Level of distress, percent ride quality lost | Distress measurements (percent and quantity), Present Serviceability Rating (PSR), International Roughness Index (IRI) | Distress measurements (percent and quantity), IRI |

Chapter 3: Overview of Hybrid Technique for the Calibration of CRC

Pavement Performance Network Level Models

3.1 Challenges when Calibrating CRCP Performance Network Level Models

Calibrating network level pavement performance models can pose a challenge depending on the amount and type of pavement data available and its quality. Due to the vast number of pavement sections in a network, it is challenging to collect and maintain performance data for all sections on a regular basis. Many agencies have to compromise the frequency of data collection, the pavement sampling size and extent of collected pavement performance data because of limited resources and funding. Changing policies and budgets affect the number of sections and the extent to which they are monitored. For example, the amount of collected information is reduced if it is desired to maintain records for the entire pavement network. On the other hand, the number of pavement sections monitored every year is limited if detailed information is needed for the network. Besides not providing adequate records of pavement performance, this inconsistency can also cause the absence of key information (e.g. pavement construction date and maintenance and rehabilitation history) for the calibration of network level performance models. Overall, missing information can cause uncertainties regarding distress development throughout time. This can pose a challenge in the calibration process and affect the reliability of the calibrated performance models.

Another challenge that may be experienced with network level databases is the data's vulnerability to data entry errors. These errors are prone to occur during the manual data entry process of large amounts of data. A large concentration of errors can cause uncertainties about the actual development of the given distress observed. Furthermore, pavement performance

databases without a large concentration of data errors or missing information can also pose a challenge depending on the data that is available. For example, the majority of pavement sections in TxDOT's PMIS database demonstrate no distress throughout their history. This is a good indication of the effectiveness of TxDOT's pavement management practices, but it does not give a clear understanding of the development of the distress in the later stages of the pavement's life.

3.2 Overcoming the Challenges through a Proposed Hybrid Technique

To overcome the challenges of calibrating pavement performance network level models, a hybrid technique was developed. This technique combines statistical analyses and expert judgment during the calibration process. Statistical measures provide a tool for modeling pavement behavior according to observed historical pavement performance data. The integration of expert opinion about CRC pavement deterioration complements the developed model by incorporating factors that cannot be accounted for with statistical measures. Incorporating expert judgment can also address deficiencies of the pavement performance data collected in a network level database. Data deficiencies can include data entry errors, missing data, and improper pavement performance monitoring.

Figure 3.1 generally outlines the proposed hybrid technique for the calibration of network level pavement performance models. The first phase consists of preliminary statistical analysis. In this phase, a sensitivity study of the parameters affecting pavement performance is conducted. The results from these analyses should then be analyzed by experts who will recommend data refinements and smart filters based on their observations. After the data is filtered and synthesized, non-linear regression analyses will be used to calibrate the performance models. Experts will be consulted once again to review the calibrated models' ability to adequately model

distress evolution. Based on expert judgment and statistical measures, recalibrations will be performed if needed. Experts will be consulted as needed until the final pavement performance models are selected. Through this iterative process, it is desired to obtain the most representative and reliable pavement performance models possible for the pavement network being studied.

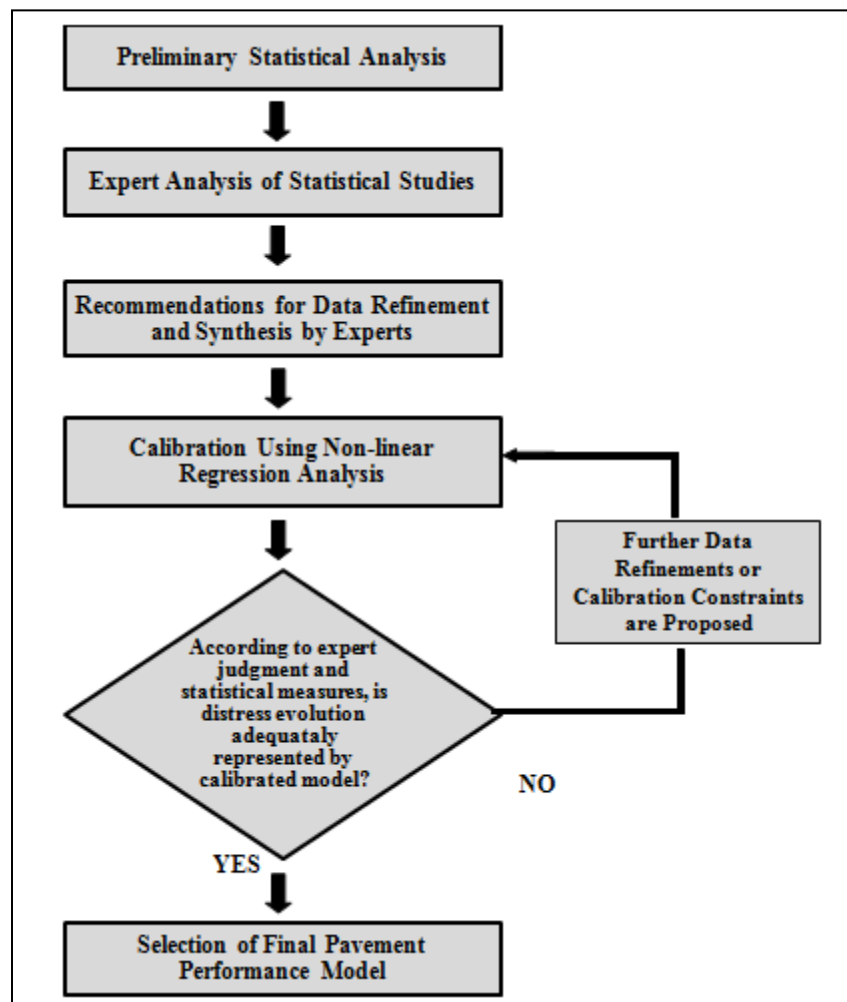


Figure 3. 1. Hybrid technique For The Calibration Of Network Level Pavement Performance Models.

3.3 Step by Step Methodology of the Hybrid technique.

The following steps present a more detailed step by step calibration process for network level pavement performance models using the hybrid technique.

1. Gather pavement distress information from historical records for all pavements in the network.
2. Perform an initial statistical analysis of the observed level of distress (L_i) for each distress to gain a better understanding of the data and condition of pavements.
3. Estimate the pavement age associated to L_i values used (if the year of construction of the pavement is not recorded or uncertain) using the following expert judgment criteria:
 - a. Pavement age can be assumed to increase according to the age increment between fiscal years of data collected.
 - b. A pavement can be assumed to have received major rehabilitation if it initially demonstrates deterioration through distresses ($L_i > 0$) and then demonstrates no distresses ($L_i = 0$). It can be assumed that pavement age is restored to zero when L_i decreases to zero.
 - c. It is also assumed that if a pavement section initially demonstrates no distresses ($L_i = 0$), then the year in which the evaluated distress is first observed ($L_i > 0$) should be given the age at which the given distress deterioration usually starts. This age is the distress starting age and should be determined for each distress before any data filtering or calibration is performed.
4. Create datasets of the performance data according to the “windows” method which consists of gathering performance data of pavement sections that have similar characteristics but different ages. The windows method can be used to account for factors like climate, environment, pavement design, traffic loads, pavement type, subgrade and construction practices by creating datasets for each variation of a given factor.

5. Prepare data for regression analysis by filtering outliers not representing the pavement distress evolution in the field.
6. Perform calibrations of the estimated pavement age with the filtered observed Li values using non-linear regression analysis to obtain the model coefficients that best fit the observed data. Carry out this analysis by an iterative nonlinear least squares fitting method which minimizes the sum of the squared residuals of the observed points and their corresponding fitted points through an iterative process. Validate the overall quality of the fit of the recalibrated models to the collected pavement performance data using the coefficient of determination, R^2 .
7. Review the results obtained from the calibrations and receive feedback from experienced District personnel to select the model that best represents each distress and ride quality. Perform recalibrations if needed based on feedback and statistical measures.

3.4 Validation of the Hybrid technique through the Calibration of CRCP

Performance Network Level Models

Currently, TxDOT's PMIS uses pavement performance models created in the early 1990's to predict pavement deterioration behavior in Texas. The performance models are used in PMIS's treatment needs analysis, budget allocation process and treatment strategy development. Given that the models are outdated and that pavement design and construction practices have changed, the current pavement performance models are not effective prediction tools. If the models are not improved to adequately forecast pavement deterioration, misleading predictions of pavement condition will occur. As a result, this can cause ineffective rehabilitation and reconstruction strategies that will lead to inadequate allocation of funds. Furthermore, this will increase the number of deteriorating pavements and road user needs will not be met. In order for PMIS to

remain a valuable pavement management tool, improvement of the current CRCP performance models is required.

The hybrid technique developed for the calibration of network level pavement performance models was used to improve the CRCP performance models of TxDOT's PMIS. Performance models were developed for CRCP distress types (spalled cracks, punchouts, ACP patches and PCC patches) and ride quality using PMIS historical pavement performance data from years 1993-2010. Chapters 4 through 6 will provide a more detailed presentation of the application of the hybrid technique to the calibration of TxDOT's PMIS pavement performance models.

3.5 Conclusion

Calibrating network level pavement performance models may present a challenge due to limitations of available performance data. Network level databases must maintain a vast number of records that are subject to data entry errors and missing records. Developing models with performance data that inadequately represents the deterioration of pavements can cause misleading performance predictions and consequently ineffective development of treatment strategies. To address these challenges, the hybrid technique is proposed in this research. The integration of statistical measures, data compilation and synthesis methods, and expert judgment can provide the tools for developing reliable pavement performance models. The integration of these methods can help incorporate factors not easily accounted for with the limited data of network level databases.

The hybrid technique provides a general calibration concept that can be applied and adapted to the needs and resources of a user agency. It is ideal to have a long and complete history of pavement performance data along with expert judgment for the performance model development. Nevertheless, flexibility of the method allows the agency to adapt to the feasible steps it can

perform. According to the available data and its quality, the agency can accordingly adapt the data compilation and synthesis methods of the technique as needed. The use of expert opinion and calibration constraints during the calibration process can compensate for limited data. Ultimately, the hybrid technique is a flexible method that provides network level pavement management systems the tools necessary for the development of the most reliable performance model possible.

Chapter 4- PMIS Data Collection and Statistical Analysis

4.1 Introduction

A statistical analysis was performed of all PMIS CRC pavement performance records in order to obtain a better understanding of the data and condition of CRC pavements in Texas. In order to conduct this analysis, PMIS data for 12,449 CRC pavement data collection sections was first extracted from 1993 to 2010. The data collected for each section includes general inventory core data, which is used to identify the section, and pavement performance data, which evaluates the condition of the pavement at the given year the data was collected. Inventory data describing the section includes: fiscal year when data was collected; responsible district; county; highway system; pavement type; signed highway roadbed identification; beginning reference marker; end reference marker; section length; speed limit; and average daily traffic (ADT). These data categories will be described further in this chapter. Although there are various forms through which PMIS evaluates pavement condition (e.g. level of distress (Li), pavement scores, number of distresses per data collection section, skid score measurements, IRI), only Li was analyzed since pavement performance models predict pavement condition through this performance indicator. As a result, Li data for each CRCP distress (spalled cracks, punchouts, ACP patches and PCC patches) and percent of ride quality lost (Li for ride quality) was extracted for each CRCP data collection section in the PMIS database. These performance indicators are described in Chapter 2 of this research.

In this chapter, a general overview of the data collected in PMIS will first be given to provide a better understanding of the PMIS database. The results of the statistical analysis will also be presented and discussed. The analysis includes the calculation of statistical parameters and the

development of descriptive statistical plots and graphs. Through the findings of the analysis, data preparation and filters will be recommended if needed.

4.2 Overview of the PMIS Database

The Pavement Management Information System stores, retrieves, analyzes and reports pavement inventory and condition data. PMIS stores data for all pavement data collection sections managed by TxDOT's districts. TxDOT is divided into 25 geographical districts which are responsible for overseeing the construction and maintenance of state highways within their jurisdiction (TxDOT 2012). The list of districts with their respective identification number and code are displayed in Table 4.1. The location of the districts can be observed in Figure 4.1.

PMIS collects and stores data for data collection sections which are usually 0.5 mile in length. A section can be as long as one mile or more (depending on the length of one reference marker to the next reference marker) or as short as 0.1 mile. The data collected in PMIS can be classified into four broad categories (TxDOT 2010): inventory, construction and rehabilitation, pavement evaluation data and pavement maintenance expenditure data.

Inventory core data includes location, traffic data and climate data. The location data describes the location of each section according to a beginning and ending reference marker. The traffic data describes traffic volume in the given section while climate data describes climate through different measurements (e.g. average county rainfall and average number of freeze-thaw cycles). Table 4. 2 lists the inventory data collected for this research.

Construction and Rehabilitation data includes information about the pavement structure and material properties. Information regarding maintenance and rehabilitation activities should also be included, but this type of data is commonly maintained in District office paper archives rather

than the PMIS database. Nevertheless, recommended treatment levels from the Needs Estimate Process in PMIS are recorded in the database.

Pavement evaluation data collected and stored in PMIS includes: surface distresses, ride quality, skid resistance and deflection. For rigid pavements, the surface distresses are evaluated through visual surveys. A rater counts the distress occurrences in the given evaluated section lane while traveling along the edge of the road at less than 15 miles per hour (TxDOT 2009). The number of observed distresses is stored in PMIS and also converted to an Li value in the database through the process described in Section 2.2.2 in Chapter 2. On the other hand, the ride quality is measured through TxDOT's Profiler/Rutbar. The Profiler measures the inertial profile of each wheelpath which is then converted to IRI by an on-board data storage computer. The IRI values measured for the wheelpaths are then converted into a single Serviceability Index (SI) value for PMIS (TxDOT 2010).

Although, PMIS stores a long history of pavement performance for the data collection sections, pavement condition data is not available for every fiscal year. Pavement evaluation surveys have not been conducted every year given to the vast amount of work required, limited resources and changing policies. For example, around the late 90's interstate highways were sampled every year, U.S. and state highways were sampled every other year, and Farm to Market and Ranch to Market roads (which have low traffic volumes) were sampled every four years (Dossey et al. 1998). As a result, pavement performance data cannot be found for every year of a pavement's life.

Table 4. 1. Texas Districts (TxDOT 2012).

| District Name | Identification Number | District Code |
|----------------------|------------------------------|----------------------|
| Paris | 1 | PAR |
| Fort Worth | 2 | FTW |
| Wichita Falls | 3 | WFS |
| Amarillo | 4 | AMA |
| Lubbock | 5 | LUB |
| Odessa | 6 | ODA |
| San Angelo | 7 | SJT |
| Abilene | 8 | ABL |
| Waco | 9 | WAC |
| Tyler | 10 | TYL |
| Lufkin | 11 | LFK |
| Houston | 12 | HOU |
| Yoakum | 13 | YKM |
| Austin | 14 | AUS |
| San Antonio | 15 | SAT |
| Corpus Christi | 16 | CRP |
| Bryan | 17 | BRY |
| Dallas | 18 | DAL |
| Atlanta | 19 | ATL |
| Beaumont | 20 | BMT |
| Pharr | 21 | PHR |
| Laredo | 22 | LAR |
| Brownwood | 23 | BWD |
| El Paso | 24 | ELP |
| Childress | 25 | CHD |

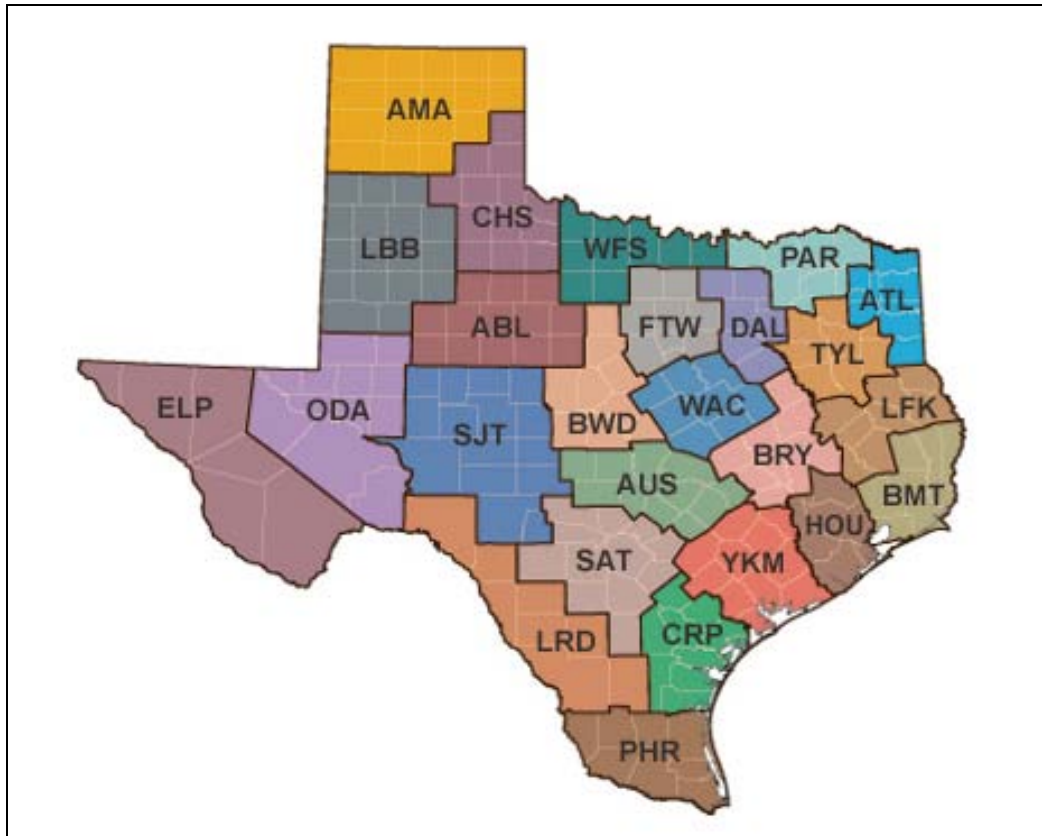


Figure 4. 1. Texas District Divisions (TxDOT 2012).

Table 4. 2. Inventory Data Collected for Calibration of PMIS Pavement Performance Models.

| Inventory Data | Description |
|--|---|
| Fiscal Year | Fiscal year in which the data collection begins. For visual distress surveys the data collection cycles are usually from September to December. The ride quality surveys usually take place from September to March. |
| Responsible District | The district responsible for rating and maintaining the data collection section. |
| County | Identifies one of the 254 geographic divisions within the Texas where the section is located. |
| Highway System | Broad category of highway the section is identified as (e.g. interstate highway (IH), U.S. Highway (US), Farm to Market (FM), Ranch to Market (RM)) |
| Pavement Type | This indicates the predominant travel lane pavement type. There are ten pavement types classified in PMIS: 01 - Continuously Reinforced Concrete (CRCP); 02 - Jointed Reinforced Concrete (JRCR); 03 - Jointed Plain Concrete (JPCP); 04 - Thick Asphaltic Concrete (Over 5.5"); 05 - Medium Thickness Asphaltic Concrete (2.5 - 5.5"); 06 - Thin Asphaltic Concrete (Under 2.5"); 07 - Composite (Asphalt Surfaced Concrete); 08 - Widened Composite Pavement; 09 - Overlaid And Widened Asphaltic Concrete Pavement; 10 - Surface Treatment Pavement (Or Seal Coat) |
| Signed Highway Roadbed Identification | This field includes the highway system, highway number, highway suffix and roadbed identification. The roadbed identification describes whether the lane evaluated for the pavement section is part of a single roadbed, multiple roadbeds or a frontage road. |
| Beginning Reference Marker | This is a number that identifies the beginning point location of the pavement section on a highway system. The number is assigned to a physical number on the highway or an imaginary marker at the highway's origin. |
| End Reference Marker | This is a number that identifies the ending point location of the pavement section on a highway system. The number is assigned to a physical number on the highway or an imaginary marker at the highway's origin. |
| Section Length | This field gives the length of the pavement in miles. |
| Speed Limit | This is the maximum legal speed limit in miles per hour posted for vehicles over the greater part of the section. |
| Average Annual Daily Traffic (AADT) | This is the average annual daily traffic of the section. |

4.3 Statistical Analysis

As was stated, PMIS CRCP distress data was extracted for 12,449 data collection pavement sections from 1993 to 2010. The statistical parameters calculated for the Li values of each distress and ride quality are presented in Table 4.3 (Mendenhall et al. 2009). Histograms, relative frequency histograms and box plots were also generated to study distress characteristics for spalled cracks, punchouts, ACP patches, and PCC patches. The histograms provide a graphical representation of the distribution of the data. The relative frequency histogram, which is a normalized histogram, shows the data set's distribution through the proportion of cases that fall into each category. This type of graph is especially useful for large data sets. On the other hand, the box plots display a visual representation of the statistics of the given data. Figure 4.2 provides a description of the box plots created. The whiskers extend to the furthest observation that is no more than 1.5 times the interquartile range (IQR). IQR is equal to the difference between the first and third quartile. The mild outliers are observations that are between 1.5IQR and 3 IQR from the edges of the box. The extreme outliers are the values that are greater than 3 IQR from the edges of the box (Mendenhall et al. 2009).

Table 4.3. Parameters Evaluated for Statistical Analysis.

| Statistical Parameter | Description/Calculation |
|-----------------------------|--|
| Mean | <p>The arithmetic average of the data.</p> $\frac{\sum_{i=1}^n x_i}{n}$ <p>Where x_i is a data point and n is the number of data points.</p> |
| Standard Deviation | <p>A statistical measure of the dispersion of the data.</p> $\sqrt{\frac{\sum_{i=1}^n (x_i - \bar{x})^2}{(n-1)}}$ <p>Where x_i is a data point, \bar{x} is the average of all data points x_i, and n is the number of data points.</p> |
| Median | The number in the middle of a range of data values that are arranged in ascending order. |
| Minimum | The smallest number in a range of data values. |
| Maximum | The largest number in a range of data values. |
| 1st Quartile | This is the value in the data set that is greater than one-fourth (25%) of the data and less than the remaining three-fourths (75%) of the data after the data has been arranged in ascending order. |
| 3rd Quartile | This is the value in the data set that is greater than three-fourths (75%) of the data and is less than the remaining one-fourth (25%) of the data after the data has been arranged in ascending order. |
| Frequency of Maximum | This is the number of times which the maximum value is present in the data set. |

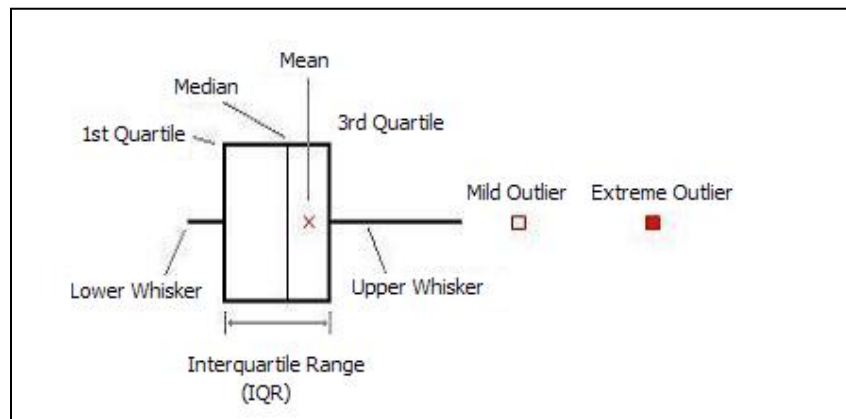


Figure 4. 2. Box Plot Structure.

4.3.1 Spalled Cracks

The Li spalled crack data has a large variation going from 0 to 1980 spalled cracks per mile. Seventy-one percent (71%) of the records report a Li value of 0. Figure 4.3 shows the histogram of the observed level of distress (Li) for spalled cracks. Figure 4.4 shows a relative frequency histogram for this distress.

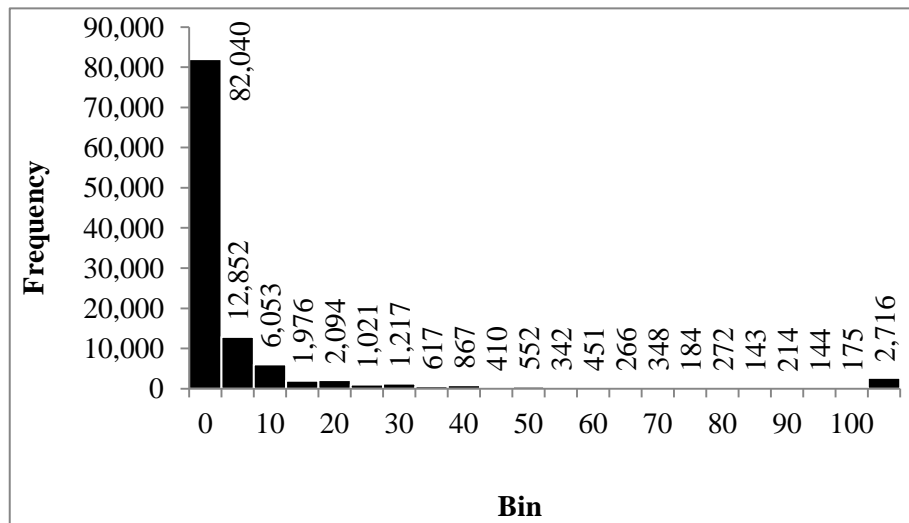


Figure 4. 3. Histogram of Observed Li for Spalled Cracks.

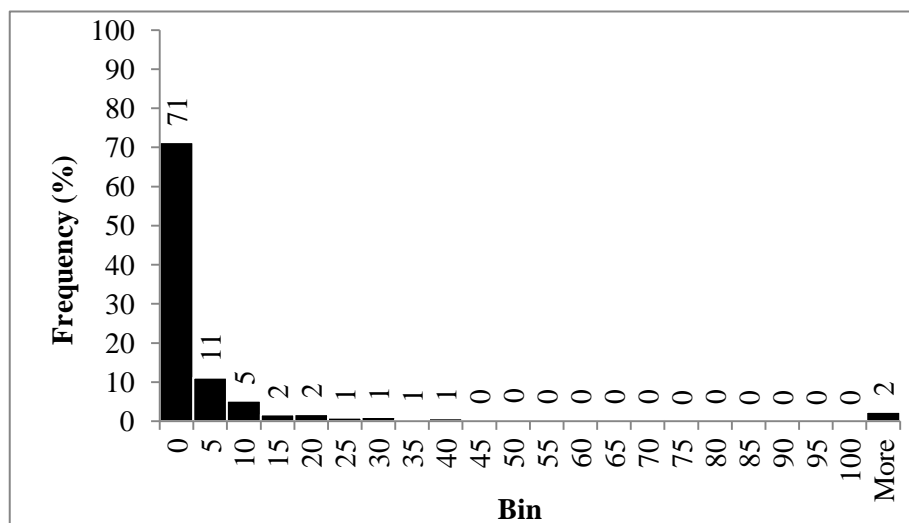


Figure 4. 4. Relative Frequency Histogram of Observed Li for Spalled Cracks.

Seventy-five percent (75%) of the records reported two spalled cracks per mile or less. Table 4.4 shows a summary of the mean, standard deviation, minimum, maximum, median, first quartile and third quartile of the Li for spalled cracks. Figure 4.5 shows the box plot of the Li values.

Table 4.4. Li Statistical Parameters for Spalled Cracks.

| Statistical Parameter | Li |
|-----------------------|-------|
| Mean | 9.73 |
| Standard Deviation | 45.73 |
| Median | 0 |
| Minimum | 0 |
| Maximum | 1980 |
| 1st Quartile | 0 |
| 3rd Quartile | 2 |
| Frequency of Maximum | 1 |

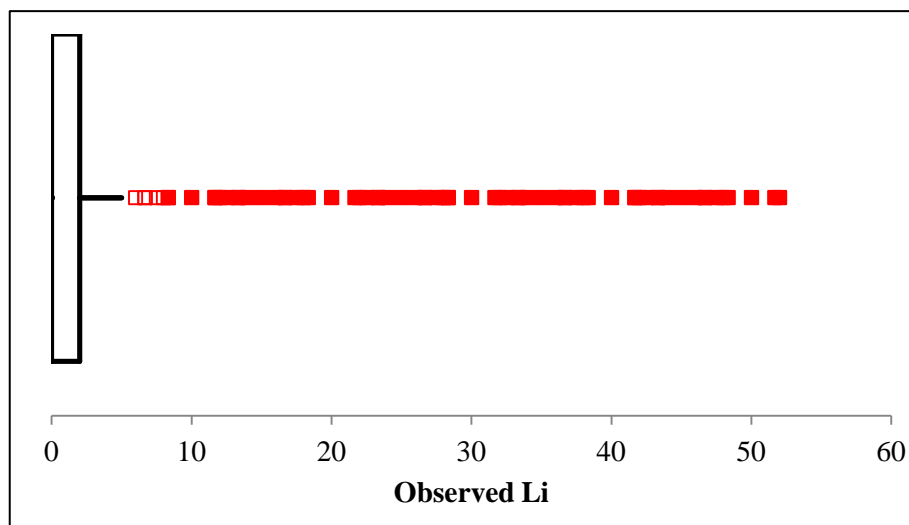


Figure 4.5. Box Plot of Observed Li for Spalled Cracks.

4.3.2 Punchouts

Eighty-nine percent (89%) of the PMIS records register zero punchouts. Figure 4.6 shows the histogram for Li for punchouts. Figure 4.7 shows a relative frequency histogram for this distress.

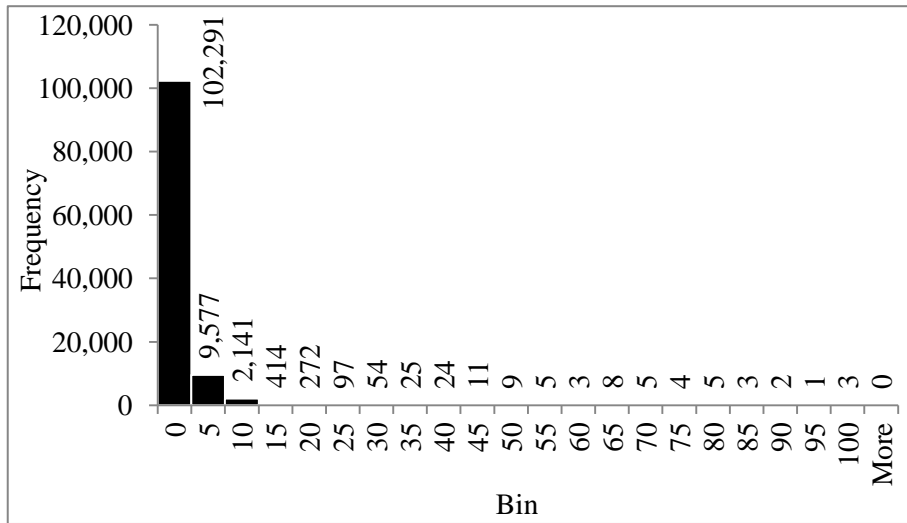


Figure 4. 6. Histogram of Li for Punchouts.

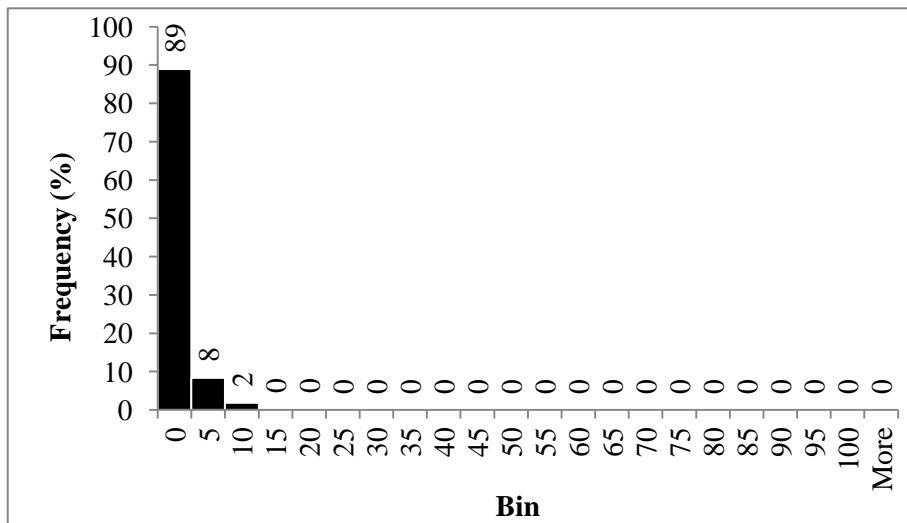


Figure 4.7. Relative Frequency Histogram of Li for Punchouts.

Table 4.5 displays the statistical parameters for the Li data of the punchout distress. Li ranges from 0 to 100 punchouts per mile with a mean of 0.54 and 2.57 as a standard deviation. Figure 4.8 shows the box plot for the punchouts Li data.

Table 4.5. Statistical Parameters for Li for Punchouts.

| Statistical Parameter | Li |
|-----------------------|------|
| Mean | 0.54 |
| Standard Deviation | 2.57 |
| Median | 0 |
| Minimum | 0 |
| Maximum | 100 |
| 1st Quartile | 0 |
| 3rd Quartile | 0 |
| Frequency of Maximum | 2 |

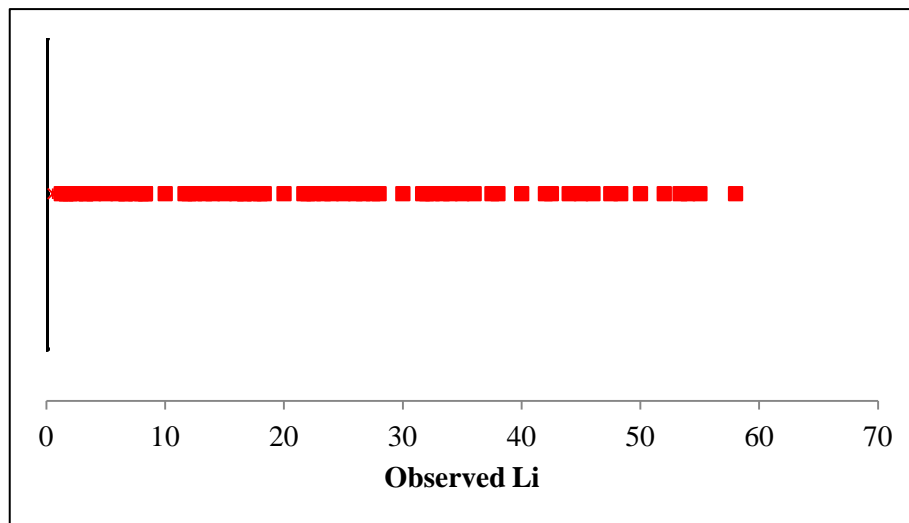


Figure 4.8. Box Plot of Li for Punchouts.

4.3.3 ACP Patches

The number of data collection section records with ACP patches is minimal. Ninety-eight percent (98%) of records show an Li value of 0 for ACP patches. Figure 4. 9 shows the histogram for the Li data for ACP patching. Figure 4.10 shows a relative frequency histogram for this distress.

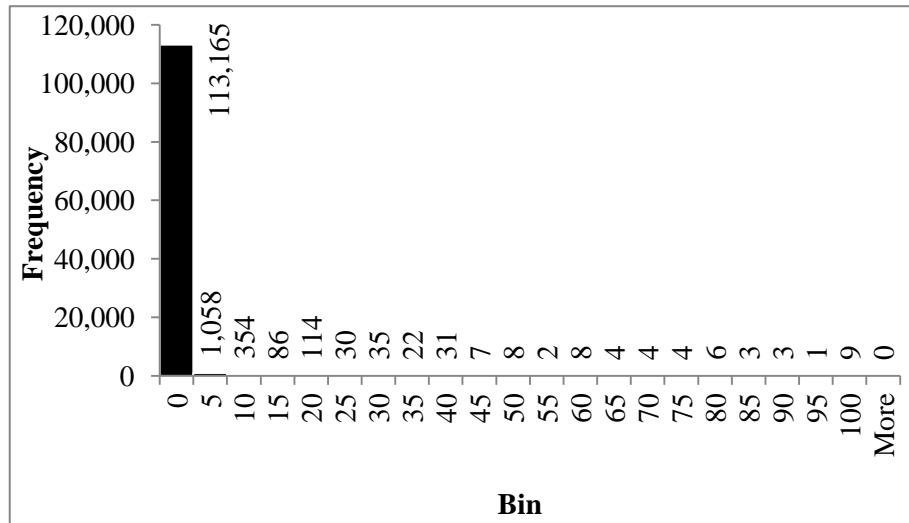


Figure 4.9. Histogram of Observed Li for ACP Patches.

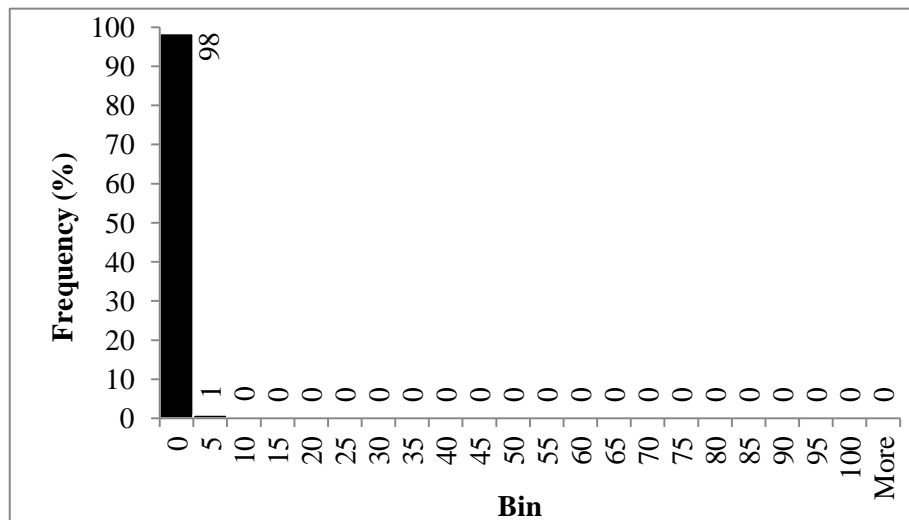


Figure 4.10. Relative Frequency Histogram of Observed Li for ACP Patches.

A summary of the statistical parameters for this distress is shown in Table 4.6. This distress does not show much variability given to the large concentration of zeros. Figure 4.11 shows the box plot of Li for ACP patches.

Table 4. 6. Li Statistical Parameters for ACP Patches.

| Statistical Parameter | Li |
|-----------------------|------|
| Mean | 0.14 |
| Standard Deviation | 2.08 |
| Median | 0 |
| Minimum | 0 |
| Maximum | 100 |
| 1st Quartile | 0 |
| 3rd Quartile | 0 |
| Frequency of Maximum | 8 |

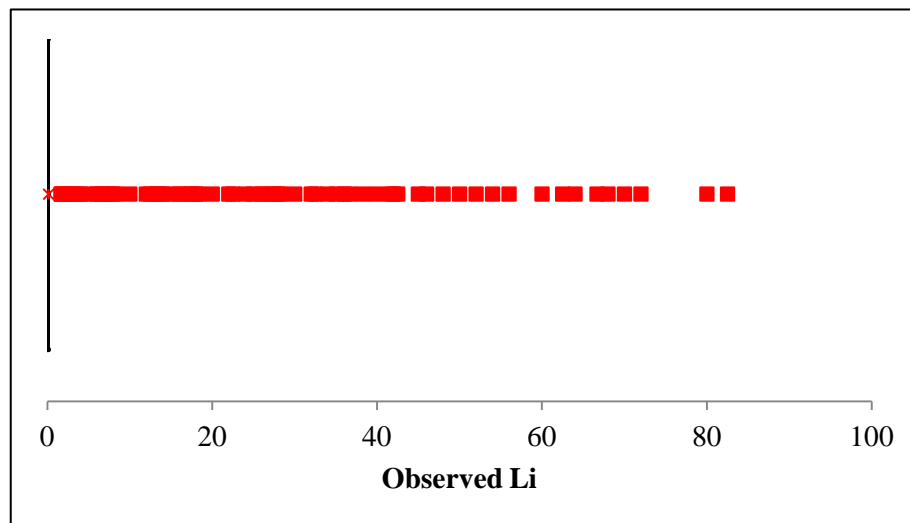


Figure 4.11. Box Plot of Observed Li for ACP Patches.

4.3.4 PCC Patches

Eighty-three percent (83%) of the PMIS records show no PCC patch. Figure 4.12 shows the histogram for the Li values for the PCC patches. Figure 4.13 shows a relative frequency histogram for this distress.

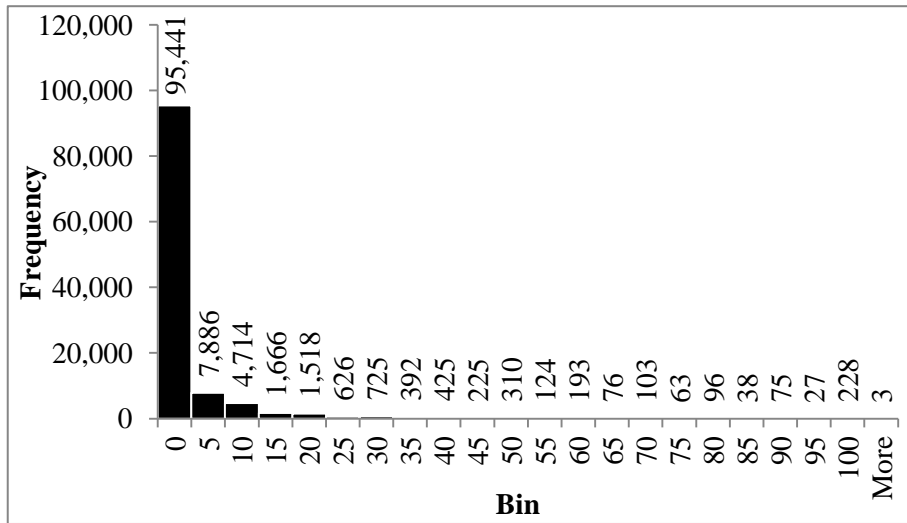


Figure 4. 12. Histogram of Li for PCC Patches.

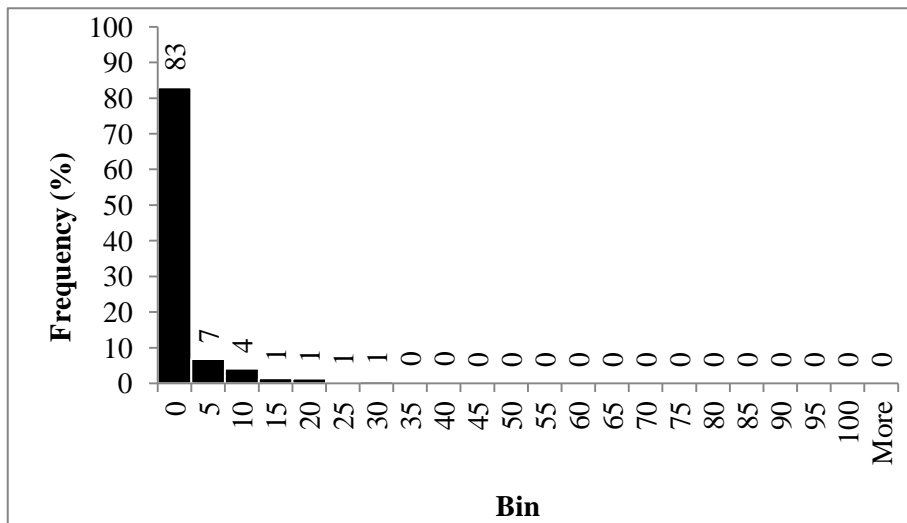


Figure 4.13. Relative Frequency Histogram of Li for PCC Patches.

Table 4.7 presents the statistical parameters for the Li data of PCC Patches. There is a greater variability in the number of PCC patches per mile which range from a minimum Li of 0 to a maximum of 205. Figure 4.14 shows the box plot for PCC patches.

Table 4.7. Li Statistical Parameters for PCC Patches.

| Statistical Parameter | Li |
|-----------------------|------|
| Mean | 2.41 |
| Standard Deviation | 9.25 |
| Median | 0 |
| Minimum | 0 |
| Maximum | 205 |
| 1st Quartile | 0 |
| 3rd Quartile | 0 |
| Frequency of Maximum | 1 |

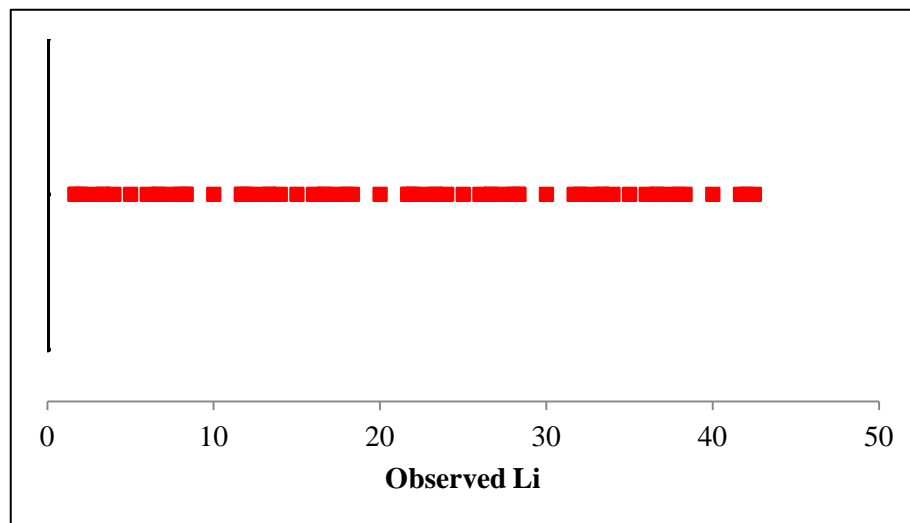


Figure 4. 14. Box Plot of Observed Li for PCC Patches.

4.3.5 Summary of CRCP Distresses by District

Table 4.8 displays the number of sections for a District that demonstrate a level of distress (Li) greater than zero, the total number of sections in the District and the percentage of sections with an Li greater than zero. This is displayed for all the districts fit for calibration. Districts displaying a hyphen are those districts where no calibrated performance model was obtained due to the lack of data. This table reinforces the findings of the statistical analysis previously presented. It can be concluded once again that there is a large concentration of Li values equal to

zero in the data. It can also be noted that spalled cracks and PCC patches are the most common distresses in CRC pavements in Texas given to their higher percentages of sections with Li values greater than zero.

Table 4. 8. Number of Sections with Level of Distress (Li) Greater than Zero.

| Districts | | Spalled Cracks | | | Punchouts | | | ACP Patches | | | PCC Patches | | |
|-----------|----------------|----------------|-------|------------|-----------|-------|------------|-------------|-------|------------|-------------|-------|------------|
| | | Li>0 | Total | Percentage | Li>0 | Total | Percentage | Li>0 | Total | Percentage | Li>0 | Total | Percentage |
| 1 | Paris | 51 | 160 | 32% | 76 | 160 | 48% | - | - | - | 67 | 163 | 41% |
| 2 | Fort Worth | 575 | 2165 | 27% | 315 | 2163 | 15% | 132 | 2155 | 6% | 576 | 2165 | 27% |
| 3 | Wichita Falls | 245 | 484 | 51% | 147 | 483 | 30% | - | - | - | 126 | 483 | 26% |
| 4 | Amarillo | 163 | 524 | 31% | 48 | 515 | 9% | - | - | - | 105 | 524 | 20% |
| 5 | Lubbock | 278 | 476 | 58% | 84 | 476 | 18% | 16 | 469 | 3% | 150 | 473 | 32% |
| 6 | Odessa | 1 | 10 | 10% | 0 | 9 | 0% | - | - | - | - | - | - |
| 7 | San Angelo | - | - | - | - | - | - | - | - | - | - | - | - |
| 8 | Abilene | - | - | - | - | - | - | - | - | - | 1 | 7 | |
| 9 | Waco | 39 | 126 | 31% | - | - | - | - | - | - | 31 | 110 | 28% |
| 10 | Tyler | 27 | 86 | 31% | 8 | 73 | 11% | - | - | - | 11 | 88 | 13% |
| 11 | Lufkin | - | - | - | - | - | - | - | - | - | - | - | - |
| 12 | Houston | 1305 | 3737 | 35% | 872 | 3737 | 23% | 23 | 3729 | 1% | 761 | 3737 | 20% |
| 13 | Yoakum | 54 | 163 | 33% | 23 | 156 | 15% | - | - | - | 28 | 157 | 18% |
| 14 | Austin | 9 | 287 | 3% | - | - | - | - | - | - | - | - | - |
| 15 | San Antonio | 11 | 74 | 15% | - | - | - | - | - | - | 2 | 74 | 3% |
| 16 | Corpus Christi | - | - | - | - | - | - | - | - | - | - | - | - |
| 17 | Bryan | 84 | 114 | 74% | 32 | 105 | 30% | 6 | 82 | 7% | 46 | 113 | 41% |
| 18 | Dallas | 565 | 1826 | 31% | - | - | - | - | - | - | 368 | 1824 | 20% |
| 19 | Atlanta | 34 | 84 | 40% | 10 | 84 | 12% | 3 | 61 | 5% | 12 | 85 | 14% |
| 20 | Beaumont | 94 | 587 | 16% | 112 | 585 | 19% | - | - | - | 103 | 587 | 18% |
| 21 | Pharr | 3 | 6 | 50% | - | - | - | - | - | - | - | - | - |
| 22 | Laredo | 1 | 23 | 4% | - | - | - | - | - | - | - | - | - |
| 23 | Brownwood | - | - | - | - | - | - | - | - | - | - | - | - |
| 24 | El Paso | 149 | 797 | 19% | 101 | 795 | 13% | - | - | - | 122 | 797 | 15% |
| 25 | Childress | 57 | 133 | 43% | 37 | 133 | 28% | - | - | - | 44 | 134 | 33% |
| Statewide | | 3745 | 11862 | 32% | 1865 | 9474 | 20% | 180 | 6496 | 3% | 2553 | 11521 | 22% |

4.3.6 Percent of Ride Quality Lost (Li)

A statistical analysis was also performed for the percent of ride quality lost (Li of the ride quality) statewide. Figure 4.15, Figure 4.16 and Figure 4.17 show the histogram, relative frequency histogram and box plot used to summarize the data, respectively. The concentration of zeros is minimal when compared to the CRCP distresses. Only 0.2% of the data has an Li value of zero. The statistical parameters are also displayed in Table 4.9.

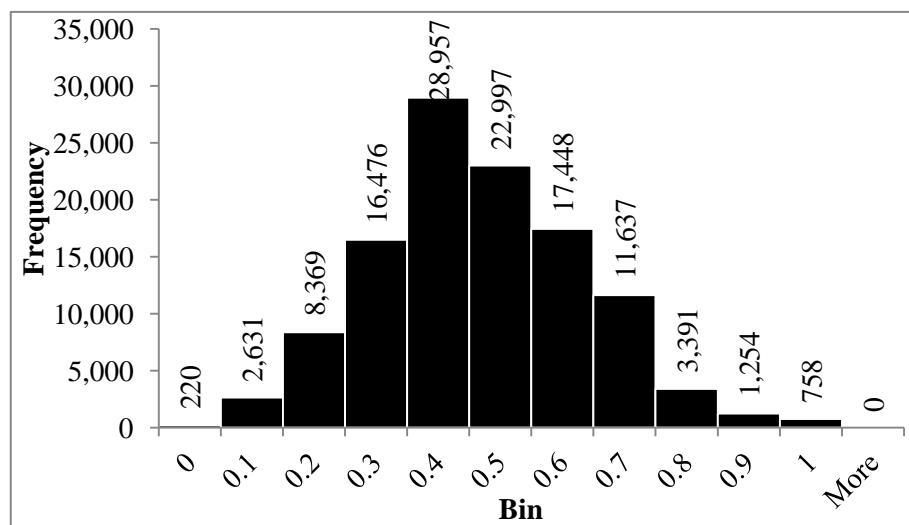


Figure 4. 15. Histogram of Li for CRCP Ride Quality.

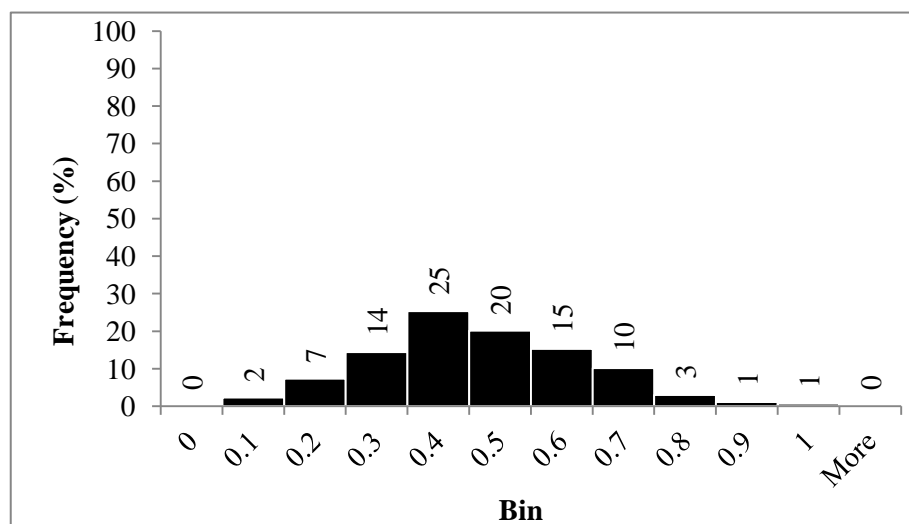


Figure 4. 16. Relative Frequency Histogram of Li for CRCP Ride Quality.

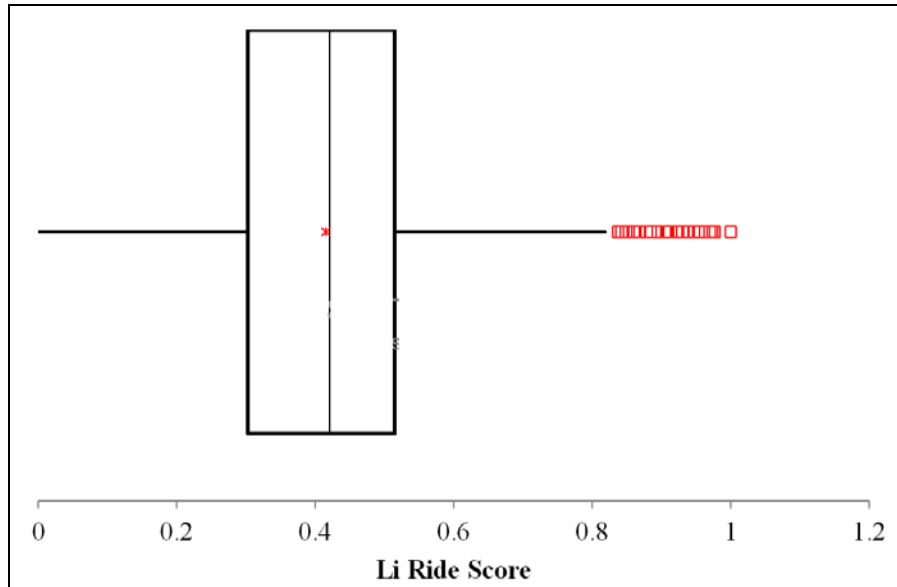


Figure 4. 17. Box Plot of Li for CRCP Ride Quality.

Table 4. 9. Li Statistical Parameters for CRCP Ride Quality.

| Statistical Parameter | Li |
|-----------------------|------|
| Mean | 0.42 |
| Standard Deviation | 0.17 |
| Median | 0.42 |
| Minimum | 0 |
| Maximum | 1 |
| 1st Quartile | 0.30 |
| 3rd Quartile | 0.52 |
| Frequency of Maximum | 319 |

4.4 Conclusions

PMIS CRC pavement performance data was gathered and statistically analyzed to obtain a better understanding of the available data and the condition of pavements in Texas. It was observed that there is a reasonable amount of information regarding the history of CRC pavements in PMIS. Nevertheless, the absence of key information for the calibration of the performance models can present a challenge. For example, the year of pavement construction is missing from the PMIS database. The database is also lacking a clear history of the maintenance and

rehabilitation activities performed by the Districts on the pavement sections. As was stated, the information regarding these activities is commonly maintained in District office paper archives rather than the PMIS database. If available, this type of information could help determine pavement age which is necessary for pavement performance prediction in PMIS models. Furthermore, the incomplete history of pavement condition data was also a problem. Pavement condition evaluation surveys are not frequently performed given to the amount of effort required and sampling policies. As a result, pavement condition data is not available for each year of the pavement's life. Missing records of the pavement's condition can cause uncertainties regarding the development of the distress throughout time.

Another challenge encountered with the data was the number of errors found. For example, the database contained data entry errors in which pavement condition evaluations were duplicated for a given section in one fiscal year. Also, for some sections there were unreasonable fluctuations in the amount of distress throughout a pavement's history. For example, 1,980 spalled cracks were observed for a record of a data collection section. The statistical analysis of spalled cracks for all CRC pavement sections in Texas showed that 75% of the data had an Li value of 2 or less; therefore, it can be concluded that 1,980 spalled cracks must be an error. This can be attributed to human mistakes occurring during data entry into the PMIS database. It was also observed that there were other fluctuations in the levels of distress observed which are not representative of pavement deterioration progression with time. It was observed that the amount of distress increased and decreased throughout a given pavement's condition history. For example, in the first, second, third and fourth fiscal years where data was recorded for one given section 4, 6, 2, and 7 spalled cracks were observed, respectively. This behavior is not representative of distress progression with time. The 2 spalled cracks observed in the third fiscal

year can be attributed to data entry errors or maintenance activities that alleviated but did not completely remove all pavement deterioration.

Furthermore, the results of the statistical analysis of the pavement performance data were presented and analyzed. It was observed that there is a large difference between the minimum and maximum of the level of distress observed for all CRCP distress types. Spalled cracks, punchouts, ACP patches and PCC patches varied from a minimum of 0 to a maximum of 1,980, 100, 100 and 250, respectively. It was also noted that the majority of pavement sections demonstrate no distress throughout their history ($Li=0$). There were 68%, 80%, 97%, and 78% of pavement sections statewide displaying no spalled cracks, punchouts, ACP patches and PCC patches, respectively. Although this is a good indication of the effectiveness of TxDOT's pavement management practices, it prevents obtaining a clear understanding of the development of the distress in the later stages of the pavement's life. On the other hand, the concentration of zeros for the percent of ride quality lost parameter is minimal when compared to the CRCP distresses. Only 0.2% of the data has an Li value of zero.

Overall, it can be inferred that the lack of the pavement age and a clear history of pavement performance will challenge the calibration process. The missing data can negatively affect the prediction capabilities and reliability of the calibrated models. The high percentage of Li values equal to zero may also interfere with the recalibration of reasonable models.

4.5 Recommendations

Through the findings and conclusions of the statistical analysis and the review of the available PMIS data, it was evident that there was a need to synthesize and filter the data for the calibration. Results from the analyses were reviewed by experts to determine the refinement and smart filters to be applied to the data. Given the lack of pavement age and clear history of

pavement performance in PMIS, it was first concluded that a methodology to determine pavement age would have to be developed. It was necessary to associate a pavement age with each performance record (Li value) in PMIS for the non-linear regression analysis of Equation 2.1. From the analysis, it was also concluded that different performance models could be proposed to account for the number of factors affecting pavement performance. As a result, calibrations would be performed of different pavement performance data sets created by the “windows” method. Finally, it was recommended to filter the data of outliers not representing the pavement distress evolution in the field. Through these steps it was desired to develop a set of models for each distress type from which the final pavement performance model recommended for PMIS could be selected.

Chapter 5- Data Compilation and Synthesis

5.1 Introduction

As was stated in Chapter 4, the need for data compilation and synthesis was recommended for the PMIS CRC pavement performance data. From the observations and results of this chapter, it was concluded that pavement age would have to be determined for the calibrations; categorization of performance data into datasets to account for different factors affecting performance needed to be performed; and data filters removing outliers and errors not representative of distress evolution in the field were required. As a response to these needs, a pavement age estimation procedure, data categorization based on the “windows” method, and data filters procedures were established. These procedures will be presented in the following sections. The application of the procedures in the PMIS historical CRC pavement performance data will be described.

5.2 Methodology for Pavement Age Estimation

The prediction of distress development in the current CRCP PMIS performance model is dependent on pavement age. This can be observed from Equation 2.1 in Chapter 2. As was stated, pavement age cannot be determined from the data provided in the PMIS database. Given that a pavement age needs to be associated with each observed L_i value for the calibration’s non-linear regression analysis, a method was developed to estimate the pavement age from the available PMIS data. This method is based on three major assumptions regarding distress development in a pavement:

- Assumption 1: Pavement age increases according to the increment between fiscal years in which performance data was collected for the given section.

- Figure 5.1 displays the pavement age estimation process for the Li records [R(1)] of each pavement section. The acronyms FY and $DSC_{distress}$ refer to the fiscal year the record was collected and the distress starting age, respectively. The process will continue from i equal to zero [R(1)] to the number of i-1 records.

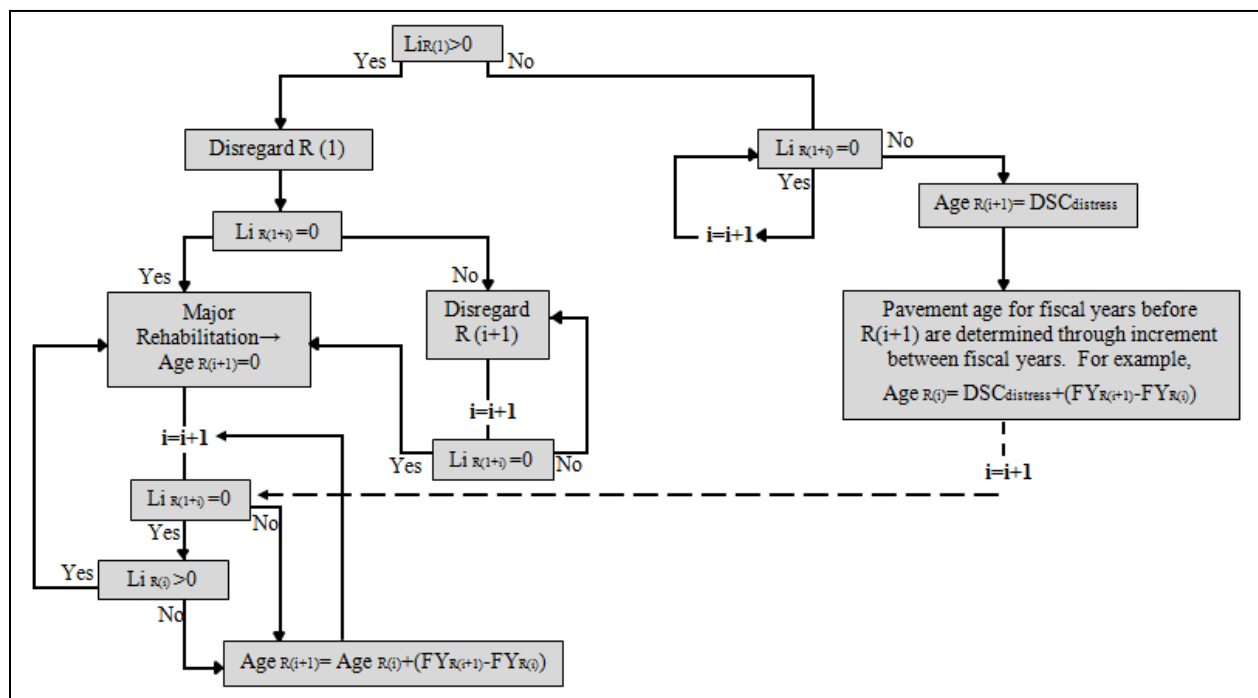


Figure 5. 1. Pavement Age Estimation Process for Li Records.

85

5.2.1 Assumption 1

The pavement's age increases according to the yearly increment between the year where data was collected and the year where age is to be estimated. For example, if data was collected for fiscal year 1994 and it was previously assumed that the pavement age corresponding to that fiscal year is 9 years, then the pavement age in 1996 is 11 years. The visual representation of this example is displayed in Figure 5.2.

| | Fiscal Year | Observed Li | Assumed Pavement Age | |
|-----------------------------------|-------------|-------------|----------------------|------------------------|
| | 1993 | 0 | 8 | |
| Age Increment: 1996-1994=2 yrs | 1994 | 16 | 9 | Age=9+ (Age Increment) |
| | 1996 | 52 | 11 | =9+2=11 |

Figure 5.2. Example of Pavement Age Estimation: Assumption 1.

5.2.2 Assumption 2

In a given section previously demonstrating surface distress, an age of zero will be given to the year where the distress decreases to an Li value of zero. For example, if a section had a distress of 10 spalled cracks per mile in 1994 and in 1996 the data showed no spalling (Li=0), then it is assumed that the pavement has received major rehabilitation. As a result, the age of the pavement is restored back to 0 at the year at which the distress is no longer present. The age for the following years is then increased by the increment between fiscal years when the data was collected. The visual representation of this example is displayed in Figure 5. 3.

| | Fiscal Year | Observed Li | Assumed Pavement Age |
|--|-------------|-------------|----------------------|
| | 1993 | 5 | |
| | 1994 | 10 | |
| | 1996 | 0 | 0 |
| | 1997 | 4 | 1 |
| | 1998 | 34 | 2 |

Age Increment: 1998-1997=1 yr

Age=1+ (Age Increment)
=1+1=2

Figure 5. 3. Example of Pavement Age Estimation: Assumption 2.

5.2.3 Assumption 3

It is assumed that if a pavement section initially demonstrates no distress ($L_i=0$), then the pavement age for the year in which the evaluated distress is first observed ($L_i>0$) should be assumed to be the distress starting age (pavement age at which the distress initiates) for the given distress type. Since the distress starting age varies according to the distress type being observed, the distress starting age should be determined for each distress before any data filtering or calibration is performed. The age for the previous and following fiscal years is then determined based on this distress starting age.

The distress starting age was estimated for each distress type based on historical L_i data and the current CRCP performance models. The pavement age was back calculated using Equation 2.1 and the historical performance data obtained for the sections. The age was plotted against L_i to determine an approximate distress starting age for each CRCP distress. From the plots, the distress starting age was estimated for each distress at: 9.5 years for spalled cracks, and 0 years for punchouts, ACP patches, and PCC patches. A zero distress starting age (or in this case the age at which ride quality starts to deteriorate) was also estimated for the ride quality. This

distress starting age estimation method was used to start the iterations when conducting the recalibration process.

An example of this assumption is displayed in the graph of Figure 5. 4. This graph shows the number of spalled cracks per mile (Observed Li) for each fiscal year that pavement performance data is available. It can be observed that there are no spalled cracks evident during the first fiscal years in which data was collected. In 1996, seven spalled cracks are then observed for the one mile section. As a result, a pavement age of 9.5 years (which was determined to be the distress starting age for spalled cracks) will be given for the pavement in the 1996 fiscal year. The pavement age for the fiscal years before and after the distress starting age are determined according to the year increments. For example, since it was determined that the pavement age in fiscal year 1996 is 9.5 years, then in fiscal year 1997 (which increases by one year from 1996) will be given a pavement age of 10.5 years (9.5 years + 1 year increment).

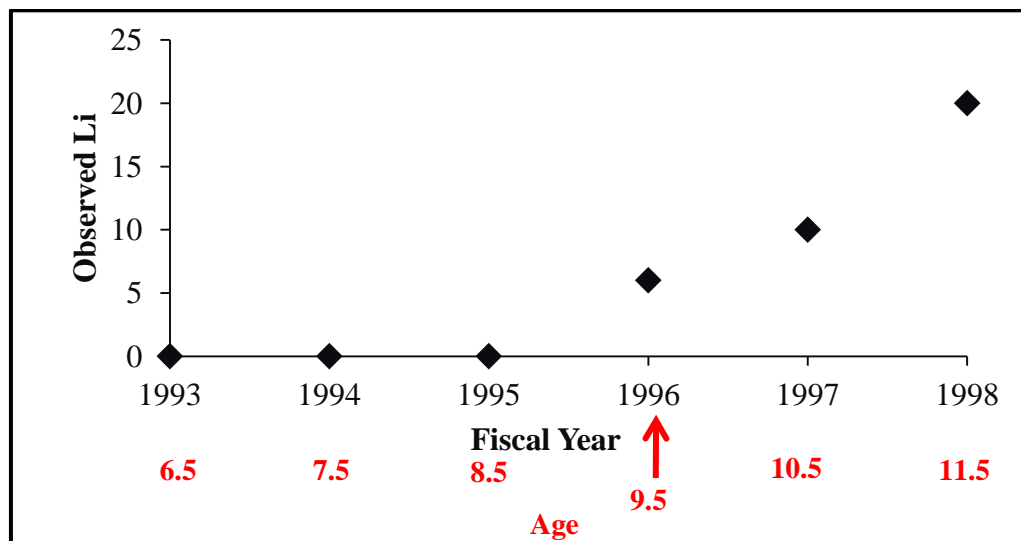


Figure 5. 4. Example of Pavement Age Estimation: Assumption 3.

An example of the pavement age estimation process using these three assumptions is shown in Figure 5.5. This information is also useful later for the regression analysis in order to determine

the maximum amount of distress growth, distress evolution rate and age of distress initiation related to α , β , ρ , respectively. The effects of these parameters on the shape of the sigmoidal model are also shown in Figure 5.5.

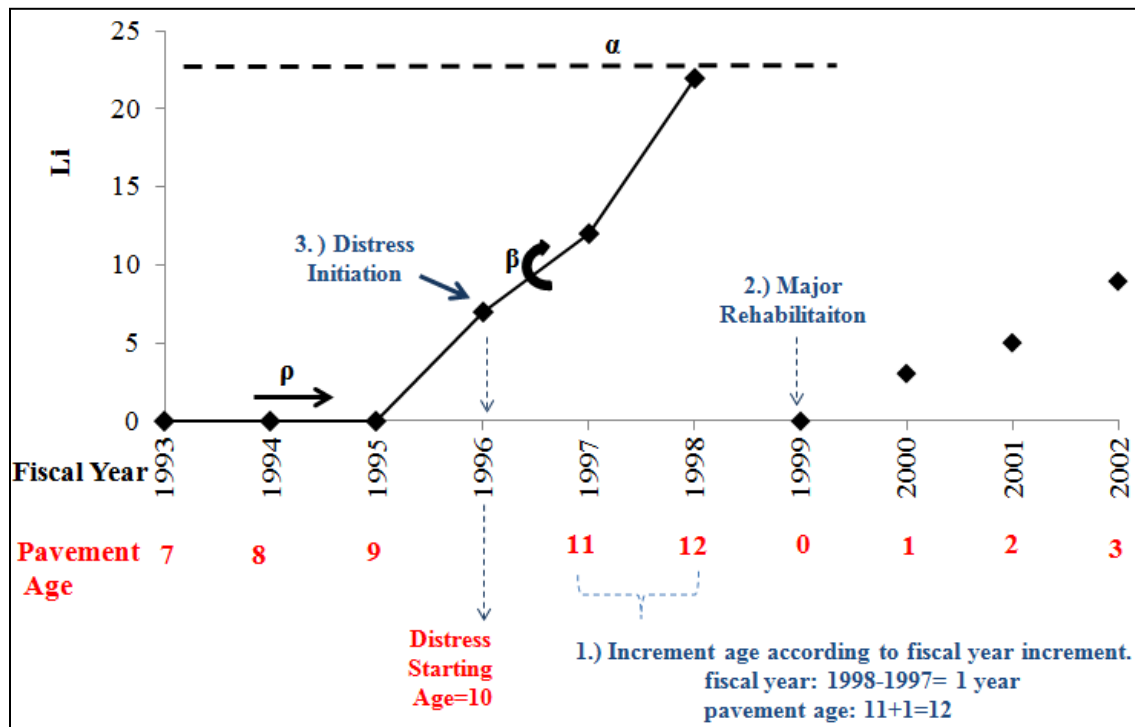


Figure 5.5. Example of Pavement Age Estimation Using Assumptions 1, 2 and 3.

5.3 “Windows” Method Datasets

The development of pavement distress is dependent on many factors like climate, environment, pavement design, traffic loads, pavement material, subgrade and construction practices. Given that Texas is a very large state, these factors widely vary between districts and are not easily accounted for. In order to account for all these factors in the calibrations, data sets of the collected performance data were created according to the “windows” method. Performance models were then calibrated for each “window” data set so the development of distress under various factors could be observed. Calibration of the performance models for each “window” data set may develop more representative and reliable models.

The “windows” method consists of creating datasets of pavement sections that have similar characteristics, but ages as different as possible. This method allows the evaluation of a large number of sections with similar characteristics which result in a wider calibration inference space (Bustos et al. 1998). The use of the “windows” technique is demonstrated in Figure 5. 6. For this example, pavement performance data is collected for pavement types A and B, which each represent certain pavement characteristics. The performance data is then grouped into two datasets named “type A” and “type B”, and a performance model is calibrated for each.

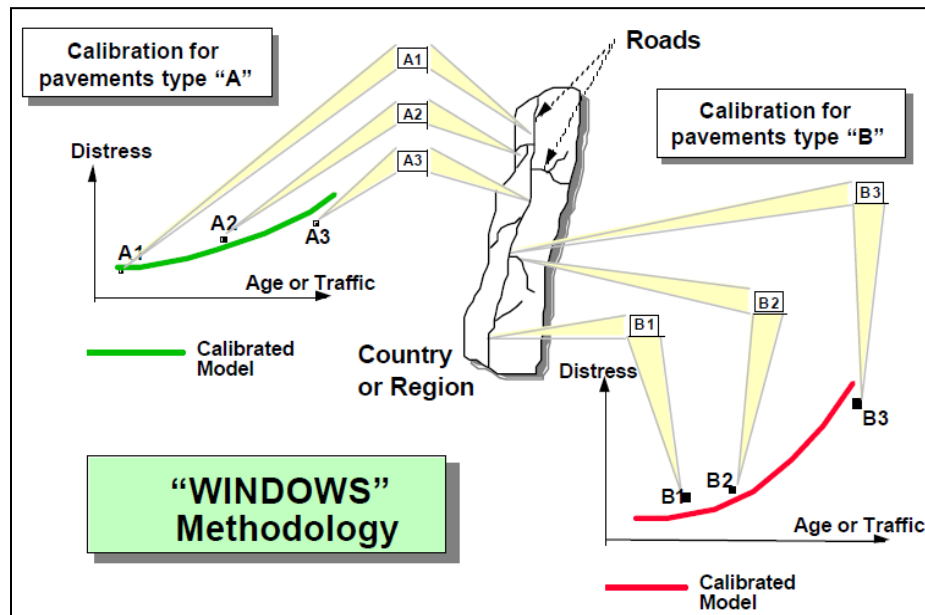


Figure 5. 6. Calibration of Pavement Performance Curves using the “Windows” Technique (Bustos et al. 1998).

In this study, the CRCP performance data collected was compiled into three data sets (or “windows”) with similar characteristics. The data sets created are the following:

- District Performance Data: Twenty-five data set categories were created which represent the performance of pavements in each of the 25 Texas districts. The separation of the

data into 25 districts can help account for the effects of the different construction practices, design practices and pavement material used by the districts.

- **Climate and Subgrade Zone Performance Data:** Four data set categories were created which represent the performance of pavements in the four climatic and subgrade zones in Texas. All counties in Texas are grouped into one of the four zones according to their climate and subgrade characteristics. Table 5.1 describes the characteristics for each zone. Pavement sections were grouped into the climate and subgrade zones according to their respective county. The areas of these zones in Texas are presented in Figure 5. 7.
- **Statewide Performance Data:** This data set includes performance data of all continuously reinforced concrete pavements in the state of Texas.

Table 5. 1. Climate and Subgrade Characteristics for Zones

| Zone | Climate and Subgrade Characteristics |
|-------------|--|
| Zone 1 | Wet-cold climate, and poor, very poor, or mixed subgrade |
| Zone 2 | Wet-warm climate, and poor, very poor, or mixed subgrade |
| Zone 3 | Dry-cold climate, and good, very good, or mixed subgrade |
| Zone 4 | Dry-warm climate, and good, very good, or mixed subgrade |

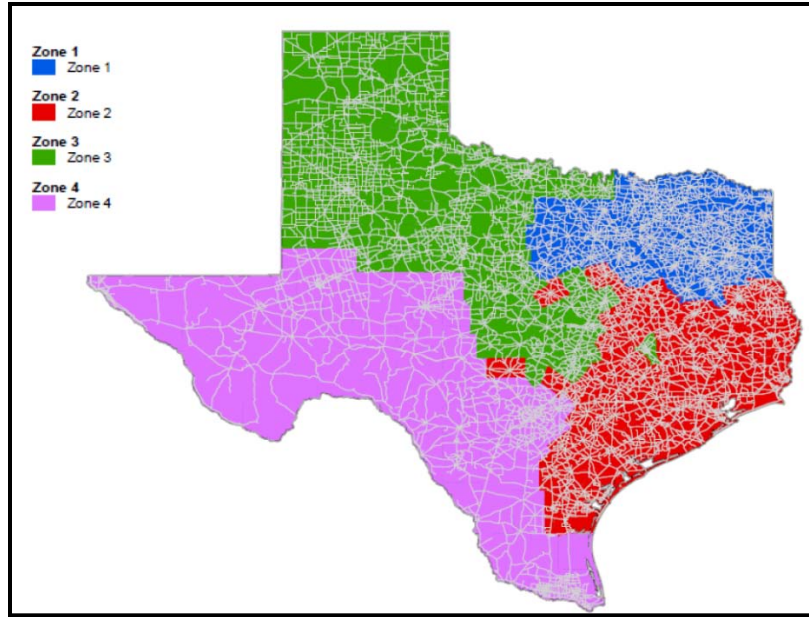


Figure 5.7. Climate and Subgrade Zones utilized for Calibration of CRCP Performance Curves (Gharaibeh et al. 2012).

5.4 Data Filters and Li Quartile and Li Median Subsets

As was stated in Chapter 4, there are a number of discrepancies found in the PMIS database which include duplicate records, data outliers and unexplained distress fluctuations. Overall, these discrepancies are not representative of distress evolution and therefore had to be removed through a series of filters determined through expert judgment and analysis. The first filter applied to the PMIS data removed duplicate data records. A second filter was then applied to address the fluctuations in distress development which were not representative of distress evolution with time. Li values for a given section where a decrease in distress is observed in consecutive fiscal years were removed. For example, if 4, 6, 2, and 7 spalled crack Li values are observed for the first, second, third and fourth consecutive fiscal years of pavement history, then the record for the third fiscal year (2 spalled cracks) was removed. A quartile filter, which will be explained later in the section, was also applied to remove extreme outliers not representative of distress evolution in the field.

As was observed during the statistical analysis, the Li data has a large concentration of zeros. The large number of zeros skewed preliminary calibrated performance curves and produced unreasonable models. This observation reinforced the need for a quartile filter (to reduce the large Li zero value concentration) and the preparation of the data to be calibrated. As a result, two Li data subsets of each “window” data set (district, climate and subgrade zones, and statewide data sets) were created during the data preparation process: Li Quartile and Li Median subsets. For each data set, separate calibrations were performed.

5.4.1 Li Quartile Subset

The first data subset was obtained by removing the first and fourth quartile of the Li values corresponding to each estimated age. This filter was performed by first grouping all Li values of a given distress according to the estimated age associated with it. For example, all Li values that correspond to an estimated pavement age of 13 years were grouped into the “thirteen year old pavement” age group. The Li values for each age group were then ordered from smallest to largest and the first and fourth quartiles were removed. The Li interquartile data (data between the first and third quartiles) for each age group were kept for the calibration. Figure 5. 8 displays the quartile filtering technique applied.

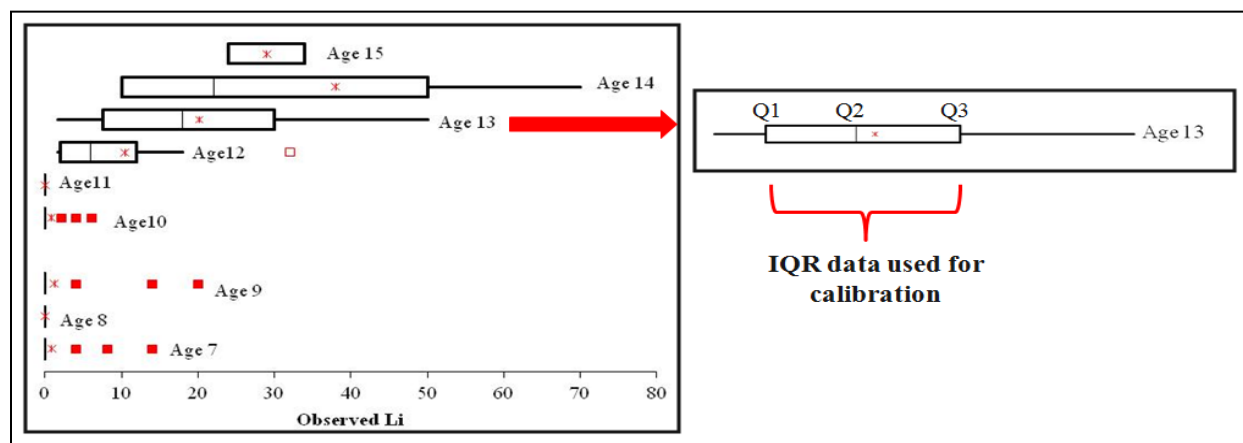


Figure 5. 8. Example of Li Quartile Filter Technique.

5.4.2 Li Median Subset

Given that the Li Quartile data subset was still greatly influenced by a large concentration of zeros, the need to further filter the data was observed. As a result, a second data subset, which consisted of Li Median values, was created. This data subset was created by first grouping all Li values according to the estimated age associated with it. The median of the Li values was then determined for each age group. This reduced the data subset to a single representative Li value for each estimated age of the given distress type. Figure 5.9 displays the Li Median technique applied.

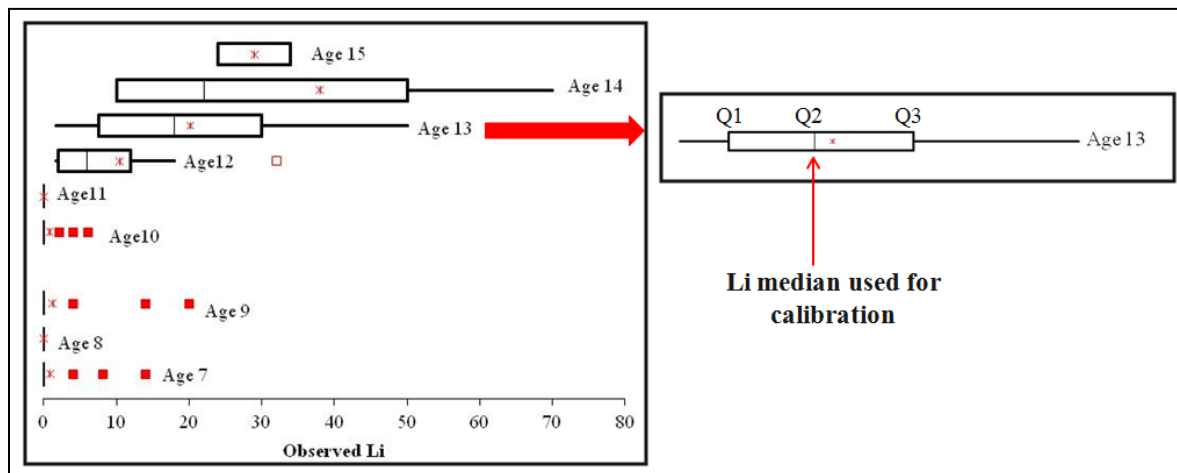


Figure 5.9. Example of Li Median Technique.

5.5 Conclusion

The pavement age estimation process, “windows” data set method and data filters presented in this chapter provide the necessary tools for the preparation of the performance data to be calibrated. Through these procedures, the utilizable pavement performance data representative of CRC pavement deterioration was obtained from the PMIS’s database and grouped for the calibrations. Figure 5.10 shows a diagram of the total number of sets of data created for the calibration for a given distress. This diagram is an example of the sets of data prepared for

spalled cracks; the same concept applies to the other distresses. A total of 60 data sets were created and calibrated for each of the four CRCP distress types (spalled cracks, punchouts, ACP patches and PCC patches).

Due to the need to filter and prepare a vast amount of pavement performance data, a macro code was developed in Excel's Microsoft Visual Basic to automate the data filtering and preparation process. An Excel file, which incorporated the macro, was created to group each data collection sections' performance data, filter the data according to the methods described, and create the data subsets. Part 1 of Appendix B provides a description of the Excel file developed and the process it followed for the compilation and synthesis of the data.

The data obtained from the hybrid technique's steps presented in this chapter can only be used to model the deterioration trend of the compiled and synthesized data. Consequently, expert opinion is still required to account for pavement deterioration trends that are not represented in the data prepared. Although the compiled and synthesized data represents an improvement from the original PMIS records, it does not fully describe CRC pavement deterioration in Texas. The calibration process and the applied expert judgment for the development of the final CRC pavement performance network level models will be presented in the next chapter.

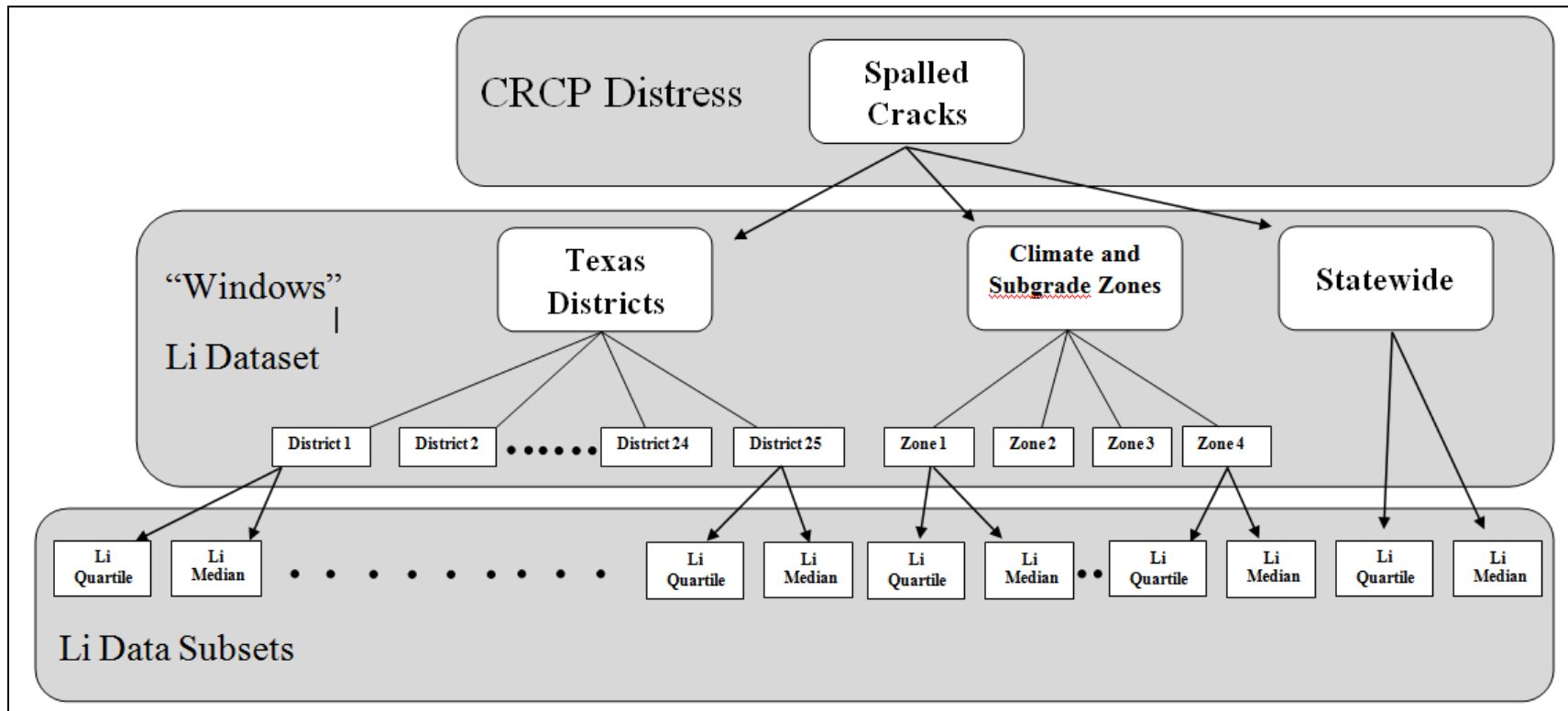


Figure 5. 10. Sets of Data Prepared for the Calibration: Spalled Crack Example.

Chapter 6: Calibration of CRC Pavement Performance Models

6.1 Introduction

Calibrations of the PMIS CRCP performance models were performed using the compiled and synthesized PMIS data. Due to the sigmoidal equation's favoring characteristics for modeling pavement distress progression, the current sigmoidal equation (Equation 2.1) used in the PMIS performance models was selected to be fitted for the calibration. A non-linear regression analysis was performed to calibrate the prepared PMIS CRCP distress data (Li data). The goal of the nonlinear regression was to adjust the model coefficients to find a model that best represents the observed pavement performance. This analysis was performed by an iterative nonlinear least squares fitting method. Calibrations were performed for each of the data subsets (Li Median and Li Quartile) of the "windows" data sets' categories (Texas districts, climate and subgrade, and statewide) presented in Chapter 5. Using expert judgment and statistical measures, recalibrations were performed until the most representative and reliable performance models could be obtained. In this chapter, the calibration process and the expert judgment criteria employed for the selection of the final models will be discussed. The final recommended CRC pavement performance models for PMIS will also be presented.

6.2 CRC Pavement Performance Models' Calibration Methodology

6.2.1 Selection of CRC Pavement Performance Model for Calibration

As was stated, the sigmoidal PMIS model was selected to be calibrated due to its flexibility for modeling pavement deterioration. The alpha (α), beta (β), and rho (ρ) coefficients of Equation 2.1 were calibrated for each pavement performance model. In the calibration, the chi (X), sigma (σ) and epsilon (ϵ) coefficients were not calibrated and were set to one. This was done due to the

findings of past research performed for TxDOT which concluded that considering ϵ , σ and X did not show significant improvements to the predictive capabilities of the models (Robinson et al. 1995). Furthermore, the ϵ , σ and X coefficients were also not considered in the calibration since they are not major players in the determination of the curve shape. The α , β and ρ are the main determinants of the shape and behavior of the sigmoidal curve. As a result, Equation 6.1 was calibrated and new α , β , and ρ coefficients were proposed.

$$L_i = \alpha e^{-\left(\frac{\rho}{Age}\right)^\beta} \quad \text{Equation 6.1}$$

where:

L_i = level of distress in a pavement section or percent of ride quality lost for the distress and ride quality performance models, respectively.

Alpha (α) = horizontal asymptote factor that represents the maximum range of distress growth.

Beta (β) = a slope factor that controls how steeply utility is lost in the middle of the model.

Rho (ρ) = prolongation factor that controls the time it takes before significant increases in distress occur.

Age=pavement age of section in years

6.2.2 Non-linear Regression Analysis

A non-linear regression analysis was performed to calibrate Equation 6.1 to the PMIS CRCP distress data. The goal of the analysis was to determine the coefficients that would best shape the sigmoidal curve to fit the observed L_i data from PMIS. The regression analysis was performed by an iterative nonlinear least squares fitting method. This method minimizes the

sum of the squares of the vertical distance between the observed points and their corresponding fitted points obtained from the calibrated equation through an iterative method. Equation 6.2 displays the equation used to calculate the sum of the squared residuals (SS). In this study, y_o represents the observed Li value corresponding to an estimated pavement age of a given section, n . The y_f variable represents the predicted Li value obtained from the calibrated model for the respective estimated age of the same section n . Figure 6.1 provides an overview of this method.

$$SS = \sum_{n=1}^n [y_o - y_f]^2 \quad \text{Equation 6.2}$$

By minimizing SS, the best fit model with minimal difference between observed and corresponding predicted values is achieved. In order to minimize the sum, an iterative process had to be followed. This process consists of making an initial estimate of the coefficients of the model to be calibrated. SS is then calculated based on these estimated coefficients. If SS is not minimized, a second iteration is performed by slightly changing the coefficient values. SS is then recalculated for the second iteration. This process continues until the minimum SS according to predetermined criteria is found. Several algorithms can be used for this iteration process (e.g. Gauss-Newton, Marquardt-Levenberg, Nelder-Mead, steepest descent method, and Generalized Reduced Gradient method) (Brown 2001).

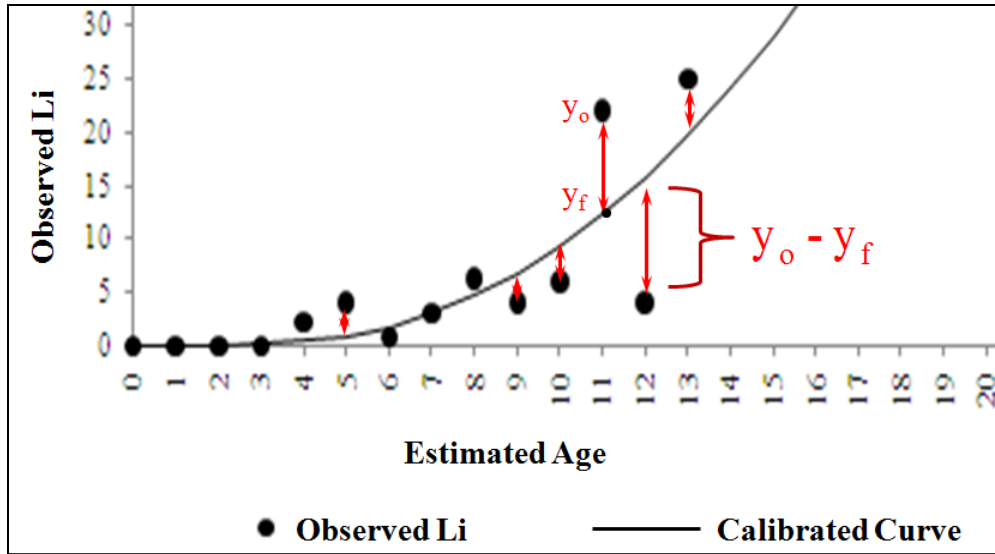


Figure 6. 1. Least Squares Method for Non-linear Regression Analysis.

6.2.3 Validation of Calibrated Models

The coefficient of determination, R^2 , was used to validate the overall quality of the fit of the recalibrated models to the observed pavement performance data. The coefficient of determination expresses the proportion of variance in a dataset that is accounted for by the recalibrated model. In other words, it describes how well the recalibrated model approximates to real observed data. The coefficient of determination is calculated using Equation 6.3 where y_o and y_f retain the meaning described in the previous section. The \bar{y}_o and \bar{y}_f represent the average of the observed Li values and calibrated Li values, respectively. This coefficient varies between 0 and 1. An R^2 equal to zero represents no relationship between the observed and predicted values while an R^2 equal to 1 indicates that the predicted values perfectly match the observed values (Brown 2001). Network level performance models usually have an R^2 value less than 0.9, while project level performance models have an R^2 value greater than 0.9 (Civil and Environmental Engineering 2012). In this study, R^2 is used as a statistical measure to judge the quality of the fit. It will be presented for all models calibrated.

$$R^2 = \left[\frac{\sum (y_o - \bar{y}_o)(y_f - \bar{y}_f)}{\sqrt{\sum (y_o - \bar{y}_o)^2 \sum (y_f - \bar{y}_f)^2}} \right]^2 \quad \text{Equation 6.3}$$

6.2.4 Calibrations with Constrained Alpha (α) Parameter

It was noted in preliminary calibrations that some alpha values of the performance models were calibrated to very large numbers. For example, for the Lubbock district the alpha value for the ACP patches performance model was calibrated to 15,045,539. This is unreasonable given that alpha is supposed to represent the maximum range of distress growth. It was therefore concluded that a second analysis should be performed for all data sets and subsets in which the alpha coefficient would be constrained. Alpha values were constrained within a 90% confidence interval. Equation 6.4 was used to calculate the maximum limit for the alpha value where \bar{x} and STDV are the mean and standard deviation, respectively, of the Li data to be calibrated. Calibrations were performed for all data sets with this constraint.

$$\alpha_{\text{Max}} = \bar{x} + 1.645 \text{ STDV} \quad \text{Equation 6. 4}$$

6.3 CRCP Distress Performance Model

Calibrations for each CRCP distress (spalled cracks, punchouts, ACP patches and PCC patches) were performed for each data subsets for all categories of the “windows” data sets. The Excel file and the macro mentioned in Chapter 5 were also tailored to perform the calibrations. A description of this macro and the process followed in the Excel file are presented in part 2 of Appendix B. In this section, only the coefficients of the calibrated performance models for the Li Median data subsets will be presented. The “ R^2 – Median” value, which measures the fit of the Li Median calibrated model to the Li Median data subset, and the “ R^2 – Quartile” value, which measures the fit of the Li Median calibrated model to the Li Quartile data subset, are also

presented for each set of calibrated models. A graph of the calibrated Li Median performance model will be presented in this section and in the Appendices. Furthermore, data sets displaying a hyphen are those data sets where a calibration was not feasible due to limited data or the large concentration of Li values equal to zero.

6.3.1 Districts

6.3.1.1 Unconstrained Calibrations

Table 6.1 shows a summary of the coefficients alpha (α), beta (β), and rho (ρ) obtained for the calibrated CRC pavement distress performance models for spalled cracks, punchouts, ACP patches, and PCC patches in each of the 25 Texas districts. In these calibrations, there were no constraints imposed on the coefficients. The calibrated distress performance model graphs for the Li Median subsets, and the coefficients and graphs of the calibrated performance models for the Li Quartile data subsets can be found in Appendix C.

Table 6. 1. Calibrated CRCP Distress Performance Models for Texas Districts (Li Median Subset).

| Districts | CRCP Distress | Calibrated Performance Model Coefficients | | | | |
|------------------|----------------|---|---------|----------------|------------------------|--------------------------|
| | | α | β | ρ | R ² -Median | R ² -Quartile |
| 01-Paris | Spalled Cracks | 3.00 | 53.57 | 9.34 | 0.95 | 0.26 |
| | Punchouts | 8.00 | 123.44 | 12.87 | 0.95 | 0.51 |
| | ACP Patches | - | - | - | - | - |
| | PCC Patches | 2,643.55 | 0.95 | 73.09 | 0.94 | 0.81 |
| 02-Fort Worth | Spalled Cracks | 13.18 | 4.78 | 11.15 | 0.54 | 0.07 |
| | Punchouts | 44.21 | 20.85 | 17.80 | 1.00 | 0.79 |
| | ACP Patches | 11,694.17 | 1.41 | 72.57 | 0.66 | 0.45 |
| | PCC Patches | 4.46 | 32.95 | 15.89 | 1.00 | 0.43 |
| 03-Wichita Falls | Spalled Cracks | 18.51 | 211.99 | 12.51 | 0.38 | 0.42 |
| | Punchouts | 1.72 | 170.92 | 14.15 | 0.91 | 0.40 |
| | ACP Patches | - | - | - | - | - |
| | PCC Patches | 4.09 | 24.07 | 12.61 | 0.99 | 0.40 |
| 04-Amarillo | Spalled Cracks | 0.86 | 275.00 | 9.07 | 0.18 | 0.14 |
| | Punchouts | 37.05 | 19.17 | 14.66 | 1.00 | 1.00 |
| | ACP Patches | - | - | - | - | - |
| | PCC Patches | 611.08 | 0.67 | 167.05 | 0.84 | 0.41 |
| 05-Lubbock | Spalled Cracks | 2.50 | 298.81 | 7.55 | 0.67 | 0.36 |
| | Punchouts | 59.72 | 14.79 | 16.29 | 1.00 | 0.67 |
| | ACP Patches | 15,045,539 | 0.17 | 247,096,415.20 | 0.35 | 0.14 |
| | PCC Patches | 396.00 | 0.65 | 151.19 | 0.80 | 0.46 |
| 06-Odessa | Spalled Cracks | 4.04 | 43.75 | 9.42 | 1.00 | 0.09 |
| | Punchouts | - | - | - | - | - |
| | ACP Patches | - | - | - | - | - |
| | PCC Patches | - | - | - | - | - |
| 07-San Angelo | Spalled Cracks | - | - | - | - | - |
| | Punchouts | - | - | - | - | - |
| | ACP Patches | - | - | - | - | - |
| | PCC Patches | - | - | - | - | - |
| 08-Abilene | Spalled Cracks | - | - | - | - | - |
| | Punchouts | - | - | - | - | - |
| | ACP Patches | - | - | - | - | - |
| | PCC Patches | 8.54 | 8.24 | 5.23 | 1.00 | 1.00 |

Table 6.1. Calibrated CRCP Distress Performance Models for Texas Districts (Li Median Subset) (continued).

| Districts | CRCP Distress | Calibrated Performance Model Coefficients | | | | |
|-------------------|----------------|---|---------|------------|------------------------|--------------------------|
| | | α | β | ρ | R ² -Median | R ² -Quartile |
| 09-Waco | Spalled Cracks | 2.22 | 250.00 | 9.07 | 0.17 | 0.06 |
| | Punchouts | - | - | - | - | - |
| | ACP Patches | - | - | - | - | - |
| | PCC Patches | 12.67 | 4.99 | 0.00 | 0.06 | 0.06 |
| 10-Tyler | Spalled Cracks | 2.89 | 142.08 | 8.61 | 0.91 | 0.34 |
| | Punchouts | 0.18 | 76.46 | 5.13 | 0.07 | 0.07 |
| | ACP Patches | - | - | - | - | - |
| | PCC Patches | 27.55 | 19.67 | 10.01 | 1.00 | 0.73 |
| 11-Lufkin | Spalled Cracks | - | - | - | - | - |
| | Punchouts | - | - | - | - | - |
| | ACP Patches | - | - | - | - | - |
| | PCC Patches | - | - | - | - | - |
| 12-Houston | Spalled Cracks | 11.96 | 11.41 | 9.77 | 0.82 | 0.41 |
| | Punchouts | 4.30 | 11.26 | 15.27 | 0.97 | 0.35 |
| | ACP Patches | 71.58 | 19.82 | 17.93 | 1.00 | 1.00 |
| | PCC Patches | 4,918.58 | 0.99 | 112.06 | 0.96 | 0.51 |
| 13-Yoakum | Spalled Cracks | 2,538.82 | 0.49 | 389.27 | 0.75 | 0.62 |
| | Punchouts | 59.72 | 14.79 | 16.29 | 1.00 | 0.42 |
| | ACP Patches | - | - | - | - | - |
| | PCC Patches | 171,632.50 | 0.25 | 220,138.48 | 0.31 | 0.03 |
| 14-Austin | Spalled Cracks | 4.00 | 237.94 | 9.49 | 0.84 | 0.79 |
| | Punchouts | - | - | - | - | - |
| | ACP Patches | - | - | - | - | - |
| | PCC Patches | - | - | - | - | - |
| 15-San Antonio | Spalled Cracks | 0.89 | 305.92 | 9.06 | 0.29 | 0.36 |
| | Punchouts | - | - | - | - | - |
| | ACP Patches | - | - | - | - | - |
| | PCC Patches | 0.50 | 148.38 | 7.09 | 0.10 | 0.12 |
| 16-Corpus Christi | Spalled Cracks | District 16 does not have CRC pavement. | | | | |
| | Punchouts | | | | | |
| | ACP Patches | | | | | |
| | PCC Patches | | | | | |
| 17-Bryan | Spalled Cracks | 4.20 | 294.63 | 9.06 | 0.48 | 0.40 |
| | Punchouts | 59.72 | 14.79 | 16.29 | 1.00 | 0.05 |
| | ACP Patches | 2.00 | 124.04 | 13.24 | 1.00 | 1.00 |
| | PCC Patches | 17.50 | 159.26 | 11.02 | 0.55 | 0.58 |

Table 6.1. Calibrated CRCP Distress Performance Models for Texas Districts (Li Median Subset) (continued).

| Districts | CRCP Distress | Calibrated Performance Model Coefficients | | | | |
|--------------|----------------|---|---------|------------|------------------------|--------------------------|
| | | α | β | ρ | R ² -Median | R ² -Quartile |
| 18-Dallas | Spalled Cracks | 157.13 | 1.19 | 37.90 | 0.55 | 0.43 |
| | Punchouts | - | - | - | - | - |
| | ACP Patches | - | - | - | - | - |
| | PCC Patches | 5.67 | 5.04 | 12.89 | 0.90 | 0.51 |
| 19-Atlanta | Spalled Cracks | 11.00 | 99.16 | 9.45 | 0.48 | 0.70 |
| | Punchouts | 10.08 | 1.43 | 10.16 | 0.96 | 0.34 |
| | ACP Patches | 24.60 | 7.34 | 8.20 | 1.00 | 0.47 |
| | PCC Patches | 2.00 | 35.79 | 5.94 | 1.00 | 0.71 |
| 20-Beaumont | Spalled Cracks | 140.67 | 1.14 | 16.02 | 0.43 | 0.24 |
| | Punchouts | 22.95 | 23.98 | 10.92 | 0.97 | 0.08 |
| | ACP Patches | - | - | - | - | - |
| | PCC Patches | 95,923.650 | 0.323 | 9766.617 | 0.640 | 0.430 |
| 21-Pharr | Spalled Cracks | 21.44 | 19.21 | 9.49 | 1.00 | 0.93 |
| | Punchouts | - | - | - | - | - |
| | ACP Patches | - | - | - | - | - |
| | PCC Patches | - | - | - | - | - |
| 22-Laredo | Spalled Cracks | 51.11 | 13.25 | 10.12 | 1.00 | 1.00 |
| | Punchouts | - | - | - | - | - |
| | ACP Patches | - | - | - | - | - |
| | PCC Patches | - | - | - | - | - |
| 23-Brownwood | Spalled Cracks | District 23 does not have CRC pavement. | | | | |
| | Punchouts | | | | | |
| | ACP Patches | | | | | |
| | PCC Patches | | | | | |
| 24-El Paso | Spalled Cracks | 2.20 | 79.28 | 9.22 | 0.96 | 0.27 |
| | Punchouts | 34,239.33 | 0.26 | 147,796.12 | 0.40 | 0.14 |
| | ACP Patches | - | - | - | - | - |
| | PCC Patches | 56.51 | 1.28 | 29.93 | 0.96 | 0.69 |
| 25-Childress | Spalled Cracks | 23.33 | 3.76 | 12.44 | 0.46 | 0.51 |
| | Punchouts | 7.44 | 30.34 | 17.15 | 1.00 | 1.00 |
| | ACP Patches | - | - | - | - | - |
| | PCC Patches | 1.00 | 105.62 | 12.29 | 1.00 | 0.33 |

1.2 Constrained Calibrations

In a second analysis, the maximum range of distress growth was limited by constraining the value of the alpha coefficient. As was stated, the alpha values were constrained within a 90%

confidence interval. Table 6.2 shows a summary of the calibrated coefficients for the CRCP distress performance models for each of the 25 Districts. The calibrated distress performance model graphs for the Li Median subsets, and the coefficients and graphs of the calibrated performance models for the Li Quartile data subsets can be found in Appendix C.

Table 6.2. Constrained Calibration of CRCP Distress Performance Models for Texas Districts (Li Median Subset).

| Districts | CRCP Distress | Calibrated Performance Model Coefficients | | | | |
|------------------|----------------|---|---------|--------|------------------------|--------------------------|
| | | α | β | ρ | R ² -Median | R ² -Quartile |
| 01-Paris | Spalled Cracks | 2.000 | 159.837 | 9.113 | 0.928 | 0.270 |
| | Punchouts | 3.000 | 250.000 | 12.245 | 0.935 | 0.499 |
| | ACP Patches | - | - | - | - | - |
| | PCC Patches | 23.000 | 18.689 | 12.576 | 0.838 | 0.711 |
| 02-Fort Worth | Spalled Cracks | 2.000 | 200.000 | 9.088 | 0.433 | 0.152 |
| | Punchouts | 1.000 | 147.770 | 16.153 | 1.000 | 0.791 |
| | ACP Patches | 1.000 | 250.000 | 14.194 | 0.598 | 0.651 |
| | PCC Patches | 1.000 | 250.000 | 15.132 | 0.889 | 0.466 |
| 03-Wichita Falls | Spalled Cracks | 5.000 | 55.802 | 9.251 | 0.263 | 0.297 |
| | Punchouts | 1.000 | 250.000 | 12.182 | 0.906 | 0.399 |
| | ACP Patches | - | - | - | - | - |
| | PCC Patches | 3.000 | 93.494 | 12.709 | 0.975 | 0.383 |
| 04-Amarillo | Spalled Cracks | 2.000 | 200.000 | 9.081 | 0.891 | 0.368 |
| | Punchouts | 1.000 | 250.000 | 13.179 | 1.000 | 1.000 |
| | ACP Patches | - | - | - | - | - |
| | PCC Patches | 3.000 | 59.533 | 10.360 | 0.764 | 0.262 |
| 05-Lubbock | Spalled Cracks | 2.000 | 300.000 | 7.570 | 0.670 | 0.361 |
| | Punchouts | 1.000 | 250.000 | 14.255 | 1.000 | 0.666 |
| | ACP Patches | 1.000 | 228.286 | 14.128 | 1.000 | 0.799 |
| | PCC Patches | 4.000 | 5.269 | 10.215 | 0.749 | 0.419 |
| 06-Odessa | Spalled Cracks | 2.000 | 206.782 | 9.100 | 0.886 | 0.136 |
| | Punchouts | - | - | - | - | - |
| | ACP Patches | - | - | - | - | - |
| | PCC Patches | - | - | - | - | - |
| 07-San Angelo | Spalled Cracks | - | - | - | - | - |
| | Punchouts | - | - | - | - | - |
| | ACP Patches | - | - | - | - | - |
| | PCC Patches | - | - | - | - | - |
| 08-Abilene | Spalled Cracks | - | - | - | - | - |
| | Punchouts | - | - | - | - | - |
| | ACP Patches | - | - | - | - | - |
| | PCC Patches | 2.000 | 400.000 | 4.219 | 1.000 | 1.000 |

Table 6.2. Constrained Calibration of CRCP Distress Performance Models for Texas Districts (Li Median Subset) (continued).

| Districts | CRCP Distress | Calibrated Performance Model Coefficients | | | | |
|-------------------|----------------|---|---------|--------|------------------------|--------------------------|
| | | α | β | ρ | R ² -Median | R ² -Quartile |
| 09-Waco | Spalled Cracks | 2.22 | 250.00 | 9.61 | 0.17 | 0.06 |
| | Punchouts | - | - | - | - | - |
| | ACP Patches | - | - | - | - | - |
| | PCC Patches | 12.67 | 4.99 | 0.00 | 0.06 | 0.06 |
| 10-Tyler | Spalled Cracks | 2.89 | 153.40 | 8.62 | 0.91 | 0.34 |
| | Punchouts | 0.18 | 71.30 | 5.13 | 0.07 | 0.07 |
| | ACP Patches | - | - | - | - | - |
| | PCC Patches | 4.00 | 300.00 | 9.10 | 1.00 | 0.73 |
| 11-Lufkin | Spalled Cracks | - | - | - | - | - |
| | Punchouts | - | - | - | - | - |
| | ACP Patches | - | - | - | - | - |
| | PCC Patches | - | - | - | - | - |
| 12-Houston | Spalled Cracks | 5.00 | 99.35 | 9.36 | 0.77 | 0.36 |
| | Punchouts | 1.00 | 215.00 | 14.13 | 0.90 | 0.27 |
| | ACP Patches | 1.00 | 200.00 | 16.14 | 1.00 | 1.00 |
| | PCC Patches | 2.00 | 177.99 | 12.17 | 0.64 | 0.40 |
| 13-Yoakum | Spalled Cracks | 14.00 | 9.54 | 9.25 | 0.67 | 0.58 |
| | Punchouts | 1.00 | 200.00 | 14.20 | 1.00 | 0.42 |
| | ACP Patches | - | - | - | - | - |
| | PCC Patches | 4.31 | 186.78 | 13.02 | 0.55 | 0.11 |
| 14-Austin | Spalled Cracks | 3.00 | 246.83 | 9.47 | 0.84 | 0.79 |
| | Punchouts | - | - | - | - | - |
| | ACP Patches | - | - | - | - | - |
| | PCC Patches | - | - | - | - | - |
| 15-San Antonio | Spalled Cracks | 0.89 | 300.00 | 9.06 | 0.29 | 0.36 |
| | Punchouts | - | - | - | - | - |
| | ACP Patches | - | - | - | - | - |
| | PCC Patches | 0.50 | 118.81 | 7.13 | 0.10 | 0.12 |
| 16-Corpus Christi | Spalled Cracks | District 16 does not have CRC pavement. | | | | |
| | Punchouts | | | | | |
| | ACP Patches | | | | | |
| | PCC Patches | | | | | |
| 17-Bryan | Spalled Cracks | 4.20 | 294.63 | 9.06 | 0.48 | 0.40 |
| | Punchouts | 2.00 | 200.00 | 14.23 | 1.00 | 0.05 |
| | ACP Patches | 1.00 | 250.00 | 13.12 | 1.00 | 1.00 |
| | PCC Patches | 10.00 | 28.16 | 10.01 | 0.47 | 0.51 |

Table 6.2. Constrained Calibration of CRCP Distress Performance Models for Texas Districts (Li Median Subset) (continued).

| Districts | CRCP Distress | Calibrated Performance Model Coefficients | | | | |
|--------------|----------------|---|---------|--------|------------------------|--------------------------|
| | | α | β | ρ | R ² -Median | R ² -Quartile |
| 18-Dallas | Spalled Cracks | 4.00 | 34.15 | 9.32 | 0.41 | 0.34 |
| | Punchouts | - | - | - | - | - |
| | ACP Patches | - | - | - | - | - |
| | PCC Patches | 3.00 | 20.08 | 11.62 | 0.87 | 0.44 |
| 19-Atlanta | Spalled Cracks | 10.00 | 0.72 | 5.96 | 0.15 | 0.12 |
| | Punchouts | 2.00 | 5.74 | 4.93 | 0.90 | 0.34 |
| | ACP Patches | 1.00 | 162.68 | 6.11 | 1.00 | 0.47 |
| | PCC Patches | 2.00 | 46.77 | 5.59 | 1.00 | 0.71 |
| 20-Beaumont | Spalled Cracks | 28.00 | 7.19 | 7.09 | 0.38 | 0.16 |
| | Punchouts | 2.00 | 132.11 | 13.13 | 0.97 | 0.24 |
| | ACP Patches | - | - | - | - | - |
| | PCC Patches | 10.000 | 8.085 | 7.381 | 0.496 | 0.364 |
| 21-Pharr | Spalled Cracks | 8.00 | 127.22 | 8.67 | 1.00 | 0.93 |
| | Punchouts | - | - | - | - | - |
| | ACP Patches | - | - | - | - | - |
| | PCC Patches | - | - | - | - | - |
| 22-Laredo | Spalled Cracks | 3.00 | 374.00 | 8.63 | 1.00 | 1.00 |
| | Punchouts | - | - | - | - | - |
| | ACP Patches | - | - | - | - | - |
| | PCC Patches | - | - | - | - | - |
| 23-Brownwood | Spalled Cracks | District 23 does not have CRC pavement. | | | | |
| | Punchouts | | | | | |
| | ACP Patches | | | | | |
| | PCC Patches | | | | | |
| 24-El Paso | Spalled Cracks | 1.00 | 215.00 | 9.08 | 0.96 | 0.29 |
| | Punchouts | 1.00 | 145.40 | 13.19 | 1.00 | 0.10 |
| | ACP Patches | - | - | - | - | - |
| | PCC Patches | 3.00 | 11.81 | 9.69 | 0.76 | 0.49 |
| 25-Childress | Spalled Cracks | 3.00 | 236.18 | 9.07 | 0.35 | 0.35 |
| | Punchouts | 1.00 | 250.00 | 16.15 | 1.00 | 1.00 |
| | ACP Patches | - | - | - | - | - |
| | PCC Patches | 1.00 | 275.00 | 12.15 | 1.00 | 0.33 |

6.3.2 Climate and Subgrade Zones

6.3.2.1 Unconstrained Calibrations

Calibrations were also performed based on climate and subgrade zones to obtain models that are representative of the effects of temperature, moisture and subgrade quality on CRC pavements. Table 6.3 presents the results obtained for the unconstrained calibration of the CRCP performance models for each of the four climate and subgrade zones. The calibrated distress performance model graphs for the Li Median subsets, and the coefficients and graphs of the calibrated performance models for the Li Quartile data subsets can be found in Appendix D.

Table 6.3. Calibrated CRCP Distress Performance Models for Climate and Subgrade Zones (Li Median Subset).

| Zone | CRCP Distress | Calibrated Performance Model Coefficients | | | | |
|--------|----------------|---|---------|---------|------------------------|--------------------------|
| | | α | β | ρ | R ² -Median | R ² -Quartile |
| Zone 1 | Spalled Cracks | 15.729 | 2.323 | 13.602 | 0.766 | 0.181 |
| | Punchouts | 44.211 | 20.854 | 17.801 | 1.000 | 0.787 |
| | ACP Patches | 9.8 | 45.3479 | 16.74 | 0.97253 | 0.2763 |
| | PCC Patches | 5.268 | 13.707 | 14.232 | 0.891 | 0.460 |
| Zone 2 | Spalled Cracks | 99.866 | 0.929 | 44.017 | 0.734 | 0.451 |
| | Punchouts | 3.246 | 17.9479 | 14.72 | 0.95652 | 0.4215 |
| | ACP Patches | 71.58 | 19.818 | 17.93 | 1 | 1 |
| | PCC Patches | 585.746 | 1.207 | 58.058 | 0.943 | 0.468 |
| Zone 3 | Spalled Cracks | 4.166 | 94.121 | 9.182 | 0.860 | 0.597 |
| | Punchouts | 7.436 | 30.341 | 17.15 | 1 | 0.992 |
| | ACP Patches | 1.8E-13 | 0.65692 | 1.21 | - | 0.0011 |
| | PCC Patches | 7.338 | 4.957 | 13.884 | 0.870 | 0.567 |
| Zone 4 | Spalled Cracks | 2.200 | 79.276 | 9.223 | 0.964 | 0.275 |
| | Punchouts | 393333 | 0.224 | 1696612 | 0.406 | 0.142 |
| | ACP Patches | - | - | - | - | - |
| | PCC Patches | 56.507 | 1.278 | 29.925 | 0.961 | 0.663 |

6.3.2.2 Constrained Calibrations

Table 6.4 presents the results obtained for the alpha constrained calibration of the CRCP performance models for each of the four climate and subgrade zones. The calibrated distress performance model graphs for the Li Median subsets, and the coefficients and graphs of the calibrated performance models for the Li Quartile data subsets can be found in Appendix D.

Table 6.4. Constrained Calibration of CRCP Distress Performance Models for Climate and Subgrade Zones (Li Median Subset).

| Zone | CRCP Distress | Calibrated Performance Model Coefficients | | | | |
|--------|----------------|---|---------|----------|------------------------|--------------------------|
| | | α | β | ρ | R ² -Median | R ² -Quartile |
| Zone 1 | Spalled Cracks | 3.000 | 230.000 | 9.088 | 0.664 | 0.258 |
| | Punchouts | 1.000 | 225.000 | 16.161 | 1.000 | 0.787 |
| | ACP Patches | 1.000 | 250.000 | 14.214 | 0.397 | 0.375 |
| | PCC Patches | 3.000 | 31.930 | 13.648 | 0.844 | 0.466 |
| Zone 2 | Spalled Cracks | 5.000 | 8.994 | 9.463 | 0.778 | 0.429 |
| | Punchouts | 1.000 | 162.997 | 14.150 | 0.926 | 0.338 |
| | ACP Patches | 1.000 | 250.000 | 16.132 | 1.000 | 1.000 |
| | PCC Patches | 2.000 | 163.899 | 12.187 | 0.712 | 0.395 |
| Zone 3 | Spalled Cracks | 2.000 | 200.000 | 9.084 | 0.860 | 0.599 |
| | Punchouts | 1.000 | 250.000 | 16.145 | 1.000 | 0.992 |
| | ACP Patches | 0.001 | 0.001 | 53687092 | - | 0.000 |
| | PCC Patches | 2.000 | 12.913 | 10.640 | 0.683 | 0.466 |
| Zone 4 | Spalled Cracks | 1.000 | 200.000 | 9.090 | 0.963 | 0.299 |
| | Punchouts | 1.000 | 145.397 | 13.192 | 1.000 | 0.099 |
| | ACP Patches | - | - | - | - | - |
| | PCC Patches | 3.000 | 11.805 | 9.691 | 0.760 | 0.484 |

6.3.3 Statewide

6.3.3.1 Unconstrained Calibrations

Table 6.5 displays the results for the calibrated statewide CRC pavement distress performance models. Figure 6.2, Figure 6.3, Figure 6.4 and Figure 6.5 show the calibrated Li Median distress

statewide performance models for spalled cracks, punchouts, ACP patches, and PCC patches, respectively.

Table 6.5. Calibrated Statewide CRCP Distress Performance Models (Li Median Subset).

| Dataset | CRCP Distress | Calibrated Performance Model Coefficients | | | | |
|-----------|----------------|---|---------|--------|------------------------|--------------------------|
| | | α | β | ρ | R ² -Median | R ² -Quartile |
| Statewide | Spalled Cracks | 134.932 | 0.833 | 63.405 | 0.40 | 0.353 |
| | Punchouts | 27.133 | 23.001 | 17.654 | 1.00 | 0.546 |
| | ACP Patches | 16.609 | 39.999 | 16.848 | 1.00 | 0.742 |
| | PCC Patches | 5.365 | 10.526 | 13.375 | 0.93 | 0.529 |

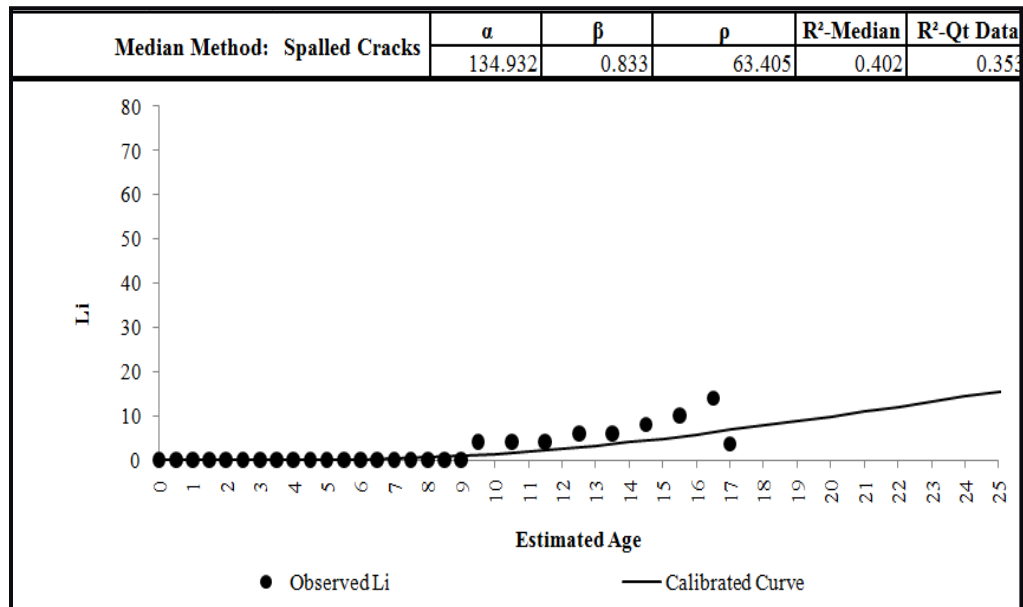


Figure 6.2. Calibrated CRCP Spalled Cracks Performance Model, Statewide, Li Median Subset (Unconstrained).

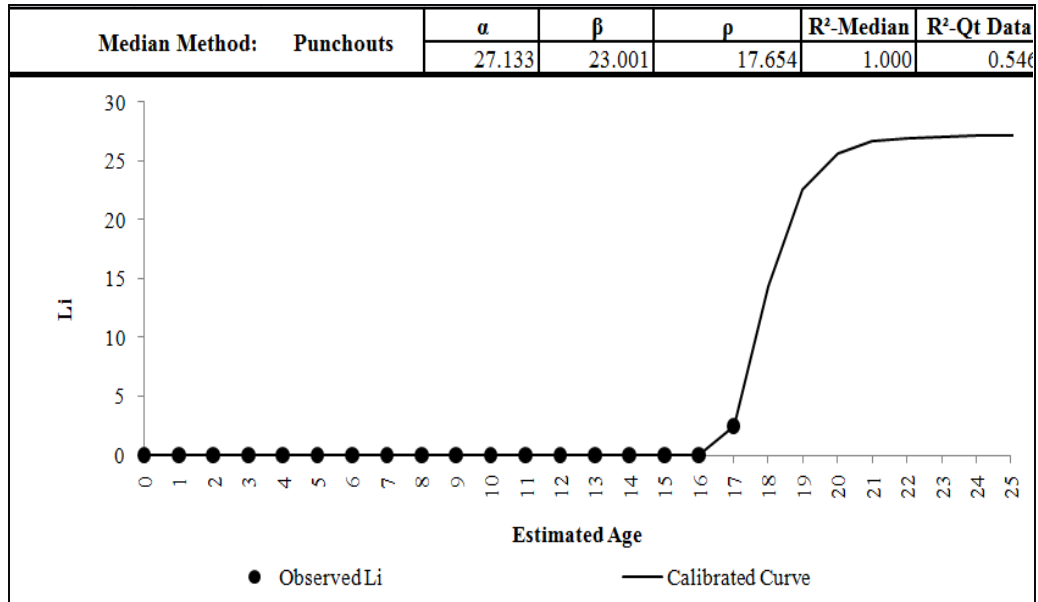


Figure 6.3. Calibrated CRCP Punchouts Performance Model, Statewide, Li Median Subset (Unconstrained).

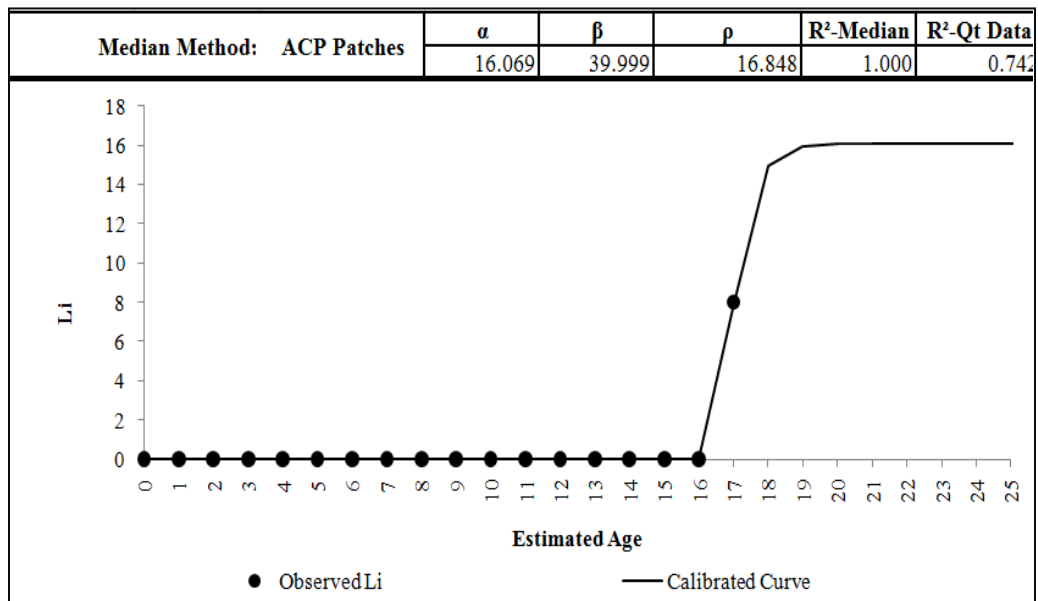


Figure 6.4. Calibrated CRCP ACP Patches Performance Model, Statewide, Li Median Subset (Unconstrained).

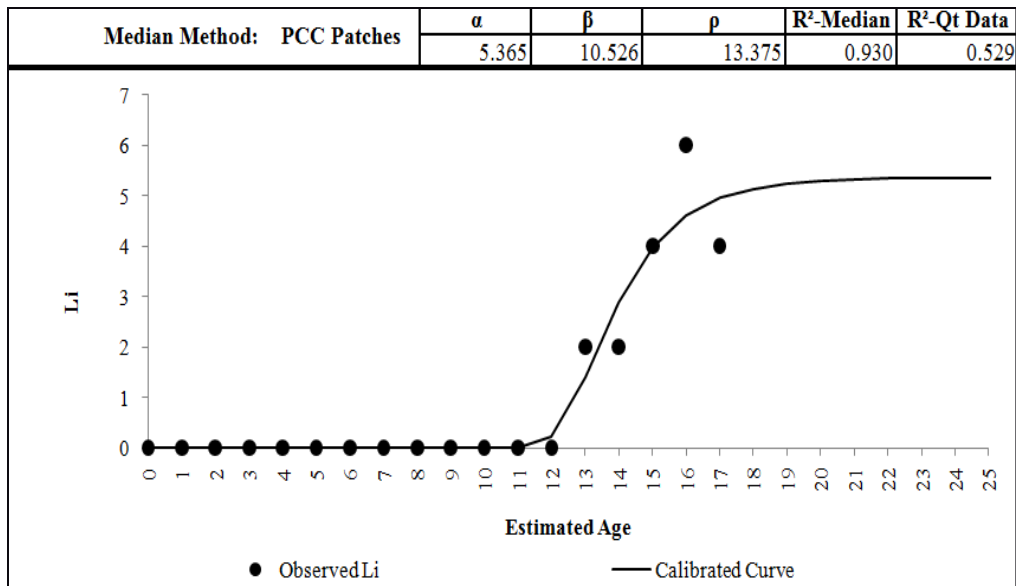


Figure 6.5. Calibrated CRCP PCC Patches Performance Model, Statewide, Li Median Subset (Unconstrained).

6.3.3.2 Constrained Calibrations

Table 6.6 displays the results for the alpha constrained calibrated statewide CRC pavement distress performance models. The coefficients and the “ R^2 -Median” and “ R^2 -Quartile” values for the Li Median calibrated models are presented. Figure 6.6, Figure 6.7, Figure 6.8 and Figure 6.9 show the Li Median calibrated distress statewide performance models for spalled cracks, punchouts, ACP patches, and PCC patches, respectively.

Table 6.6. Constrained Calibration of Statewide CRCP Distress Performance Models (Li Median Subset).

| Dataset | CRCP Distress | Calibrated Performance Model Coefficients | | | | |
|-----------|----------------|---|---------|--------|---------------|-----------------|
| | | α | β | ρ | R^2 -Median | R^2 -Quartile |
| Statewide | Spalled Cracks | 3.00 | 16.86 | 9.142 | 0.56 | 0.328 |
| | Punchouts | 1.00 | 250.00 | 16.287 | 1.00 | 0.587 |
| | ACP Patches | 1.00 | 200.00 | 16.150 | 1.00 | 0.742 |
| | PCC Patches | 2.00 | 77.987 | 12.262 | 0.809 | 0.425 |

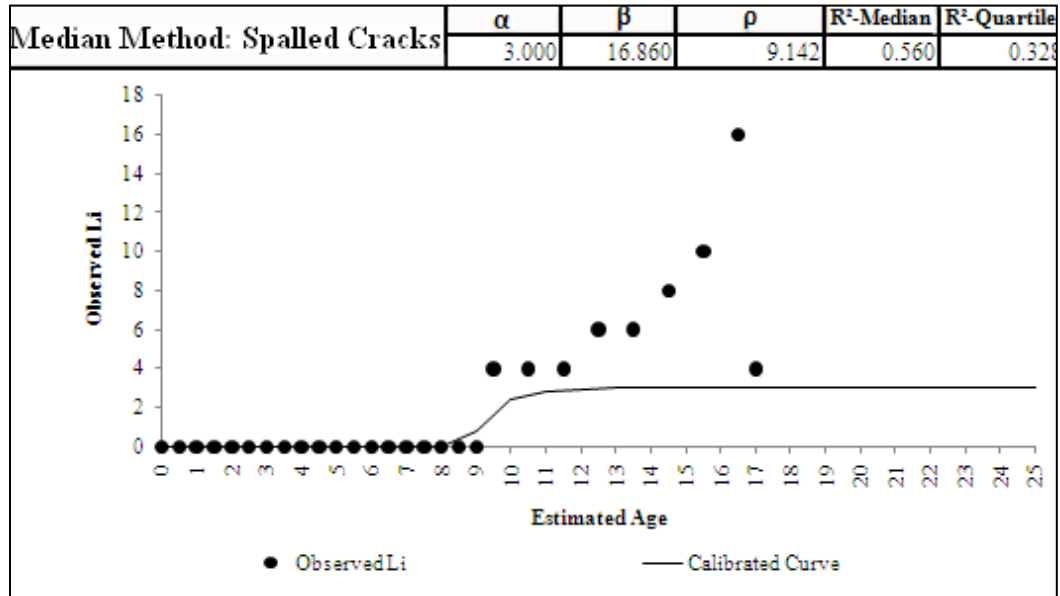


Figure 6.6. Calibrated CRCP Spalled Cracks Performance Model, Statewide, Li Median Subset (Constrained).

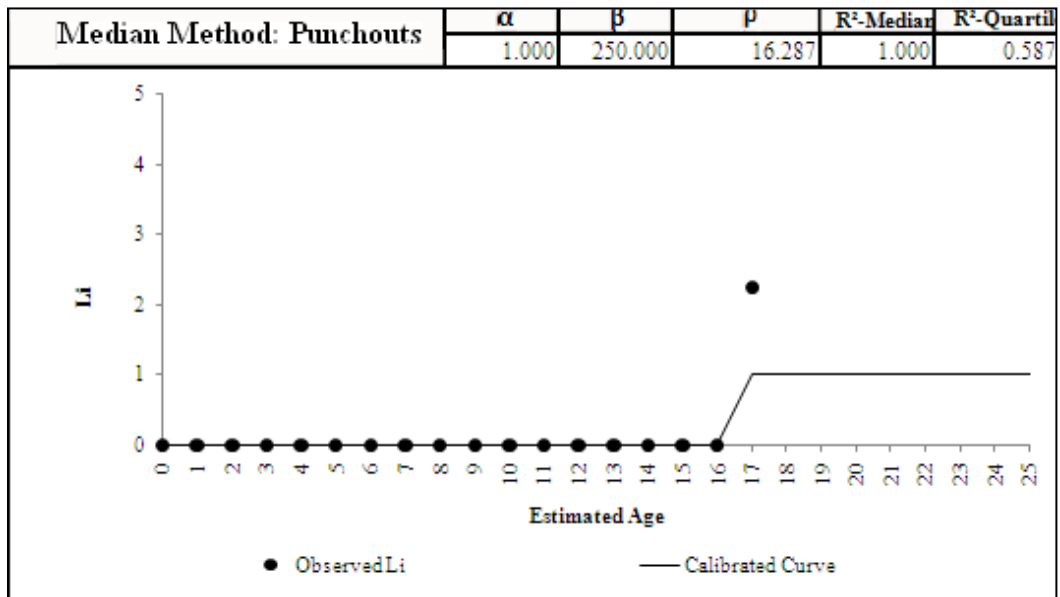


Figure 6.7. Calibrated CRCP Punchouts Performance Model, Statewide, Li Median Subset (Constrained).

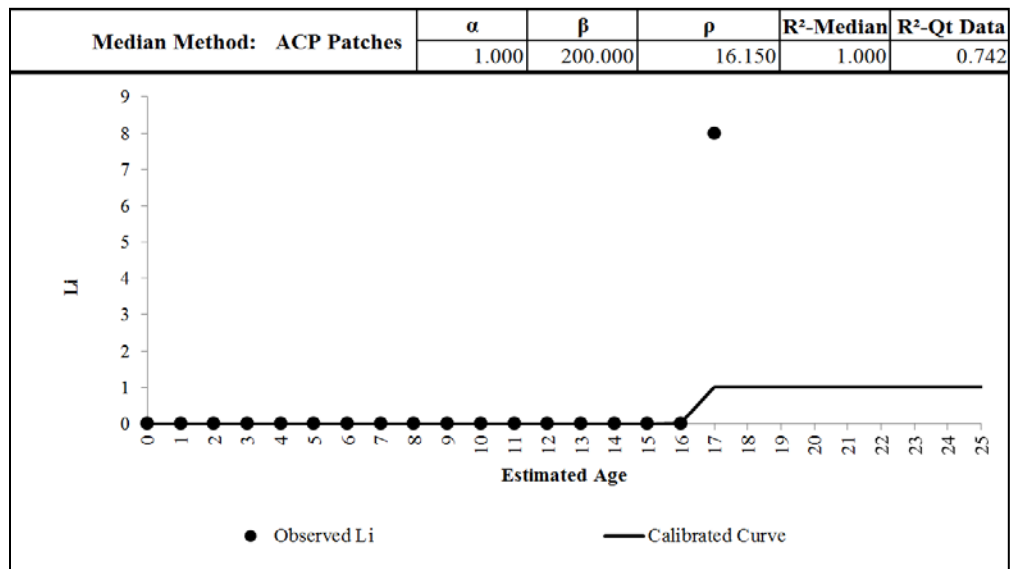


Figure 6.8. Calibrated CRCP ACP Patches Performance Model, Statewide, Li Median Subset (Constrained).

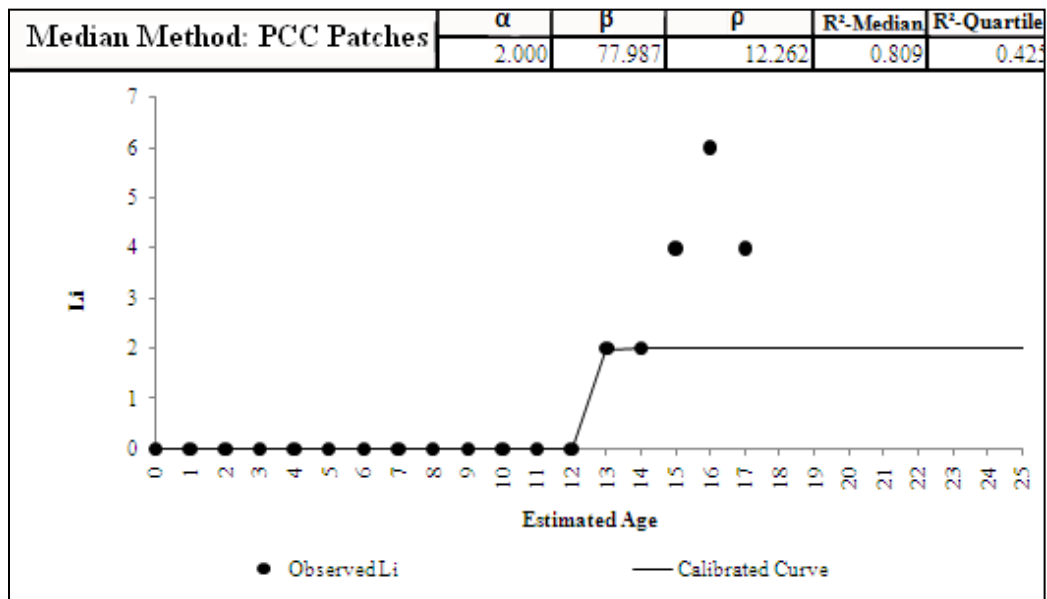


Figure 6.9. Calibrated CRCP PCC Patches Performance Model, Statewide, Li Median Subset (Constrained).

6.3.4 Recommended CRC Pavement Performance Models

The calibrated performance models were reviewed for the different “window” data sets in each distress type. The recalibrated performance models were compared between the three “window” data sets (district, climate and subgrade zones, and statewide) to select the set of CRC pavement performance models that best represent pavement deterioration in Texas. The following trends were noticed for the recalibrated models of all CRCP distresses:

- For the district data set, performance models could not be recalibrated for all districts. It was noted that in some districts the pavements were in very good condition. As a result, the concentration of Li values equal to zero was very high and there were only a few data points where Li had values greater than zero. For example, in the Fort Worth district there were 27%, 15%, 6%, and 27% of sections with Li values greater than zero for spalled cracks, punchouts, ACP patches and PCC patches, respectively. The high concentration of zeros was especially noted for punchouts and ACP patches. Punchouts are not common since they are given maintenance priority. This distress is granted priority given that it is a serious structural distress that can critically degrade pavement ride quality and pose safety hazards to the driving public. On the other hand, ACP patches are not common since they are a temporary method to cover surface or structural defects. The large concentration of zeros prevented the recalibration of some models given that there were no distresses to model.
- The trend observed for the district data set was also observed for the climate and subgrade zone dataset. There was a large concentration of Li values equal to zero for punchouts and ACP patches. Performance models could not be properly recalibrated

given that there were no distresses to model. This was especially observed for Zone 4 ACP patches performance model which could not be recalibrated.

- The recalibrated ACP patches and punchouts performance models for the statewide data were also affected by the large concentration of Li values equal to zero. Nevertheless, all distresses were recalibrated for the statewide data.
- Overall, the Li Median data set for all distress types was concluded to give the most reasonable recalibrated performance models when compared to the Li Quartile dataset models. The Li Quartile data set performance models were not chosen since they were greatly influence by the large concentration of Li values equal to zero.

Given that not all the Texas districts and the climate and subgrade data sets could be recalibrated, it was concluded that the Li Median recalibrated statewide models would be recommended as the new CRC pavement performance models for PMIS. The recalibrated constrained and unconstrained statewide models were then presented to TxDOT personnel for further revision and recalibration recommendations. The performance models were revised and re-calibrated based on feedback from TxDOT personnel and statistical analysis of PMIS data. The recalibrated CRCP distress performance models are based on the following reasoning:

- In the recalibration, the beta (β) parameter was constrained to 50. This constraint was set based on feedback from expert judgment.
- For the spalled cracks performance model, it was concluded that the most representative distress model is the unconstrained model. According to expert feedback, this model represents the slow appearance of this distress.

- The alpha (α) of the punchouts performance model was constrained to 2. Given that punchouts are a serious structural distress and that they need to be addressed quickly, it was recommended to limit the maximum number of acceptable punchouts per mile to 2.
- The alpha (α) of the ACP patches performance model was constrained to 1 since according to the statistical analysis performed, this distress is not very common in CRC pavements. Ninety-eight percent of the data analyzed showed no ACP patching distress (ACP Patch Li was equal to zero). This constraint was also found reasonable according to expert feedback. The rho (ρ) parameter was also constrained to greater than 13 to control the age at which ACP patches start to occur (distress starting age). Given that patches are used to address punchout problems, it is reasonable for punchouts (which have a distress starting age of around 13) to start earlier than ACP Patches.
- According to expert feedback, the alpha (α) of the PCC patches performance model was suggested to be constrained at 4. It was concluded that this is a reasonable maximum acceptable number of PCC patches per mile.

Table 6.7 shows the coefficients and “R²– Median” and “R²– Quartile” values corresponding to the final recommended recalibrated statewide CRCP distress performance models. The coefficients of the current PMIS models are also presented along with the “R²– Median” and “R²– Quartile” values of these models compared to the Li Median and Quartile data subsets, respectively. It can be generally observed that the R²-Quartile and R²– Median values are higher for the recommended models than for the current PMIS models.

Table 6.7. Recommended Statewide CRCP Performance Curve Coefficients.

| CRCP Distress | | Calibrated Statewide Performance Model Coefficients | | | | |
|----------------|------------|---|---------|---------|------------------------|--------------------------|
| | | α | β | ρ | R ² -Median | R ² -Quartile |
| Spalled Cracks | Calibrated | 134.932 | 0.833 | 63.405 | 0.402 | 0.348 |
| | PMIS | 1.690 | 22.090 | 10.270 | 0.315 | 0.248 |
| Punchouts | Calibrated | 1.574 | 15.831 | 15.000 | 0.526 | 0.433 |
| | PMIS | 101.517 | 0.438 | 538.126 | 0.095 | 0.259 |
| ACP Patches | Calibrated | 1.000 | 50.000 | 15.812 | 0.729 | 0.385 |
| | PMIS | 96.476 | 0.375 | 824.139 | 0.222 | 0.015 |
| PCC Patches | Calibrated | 4.000 | 16.910 | 12.936 | 0.913 | 0.522 |
| | PMIS | 146.000 | 1.234 | 40.320 | 0.874 | 0.560 |

Figure 6.10 to Figure 6.13 show the final statewide recalibrated CRCP distress performance models recommended, the current PMIS performance curves and the Li Median data subset for each distress evaluated (presented as Li Observed). The calibrated models coincide with the expert recommendations previously discussed regarding distress initiation (determined by the rho coefficient), distress evolution rate (determined by beta coefficient) and maximum allowable amount of distress growth (determined by alpha coefficient).

According to the calibrated spalled cracks performance model displayed in Figure 6.10, spalled cracks start to appear in pavements around a pavement age of 8 years and slowly progress with time. The maximum number of spalled cracks per mile is about 135, but it is unlikely this amount will be reached given that this happens at a pavement age in which the pavement has exceeded its design life and has more than likely been reconstructed or rehabilitated. This differs from the current PMIS curve which describes spalled cracks as appearing around a pavement age of 10 years and quickly increasing within a year to the maximum allowable amount of 1.69 spalled cracks per mile.

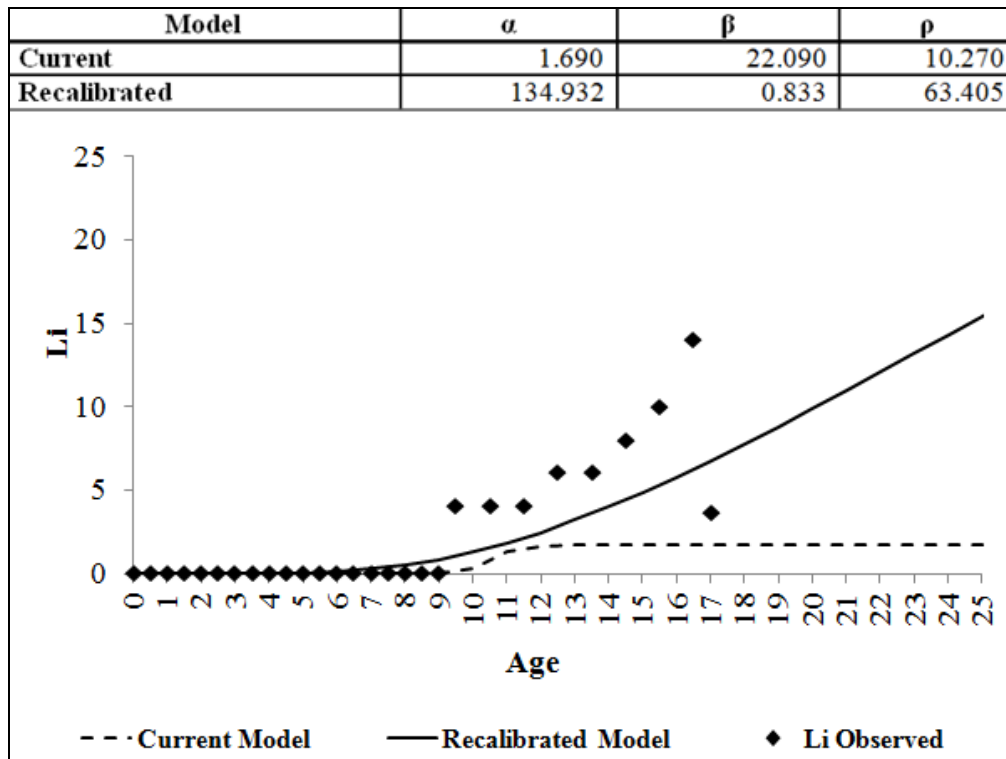


Figure 6. 10. Recommended Statewide CRCP Spalled Cracks Performance Curve, Median Method.

From Figure 6.11, it can be noted that the recalibrated performance model for punchouts differs from the current PMIS model in that the age in which the distress initiates is larger; the evolution of the number of punchouts per mile is faster; and that the maximum allowable number of punchouts per mile is considerably less (1.6) than those allowed by the current PMIS model (101.5).

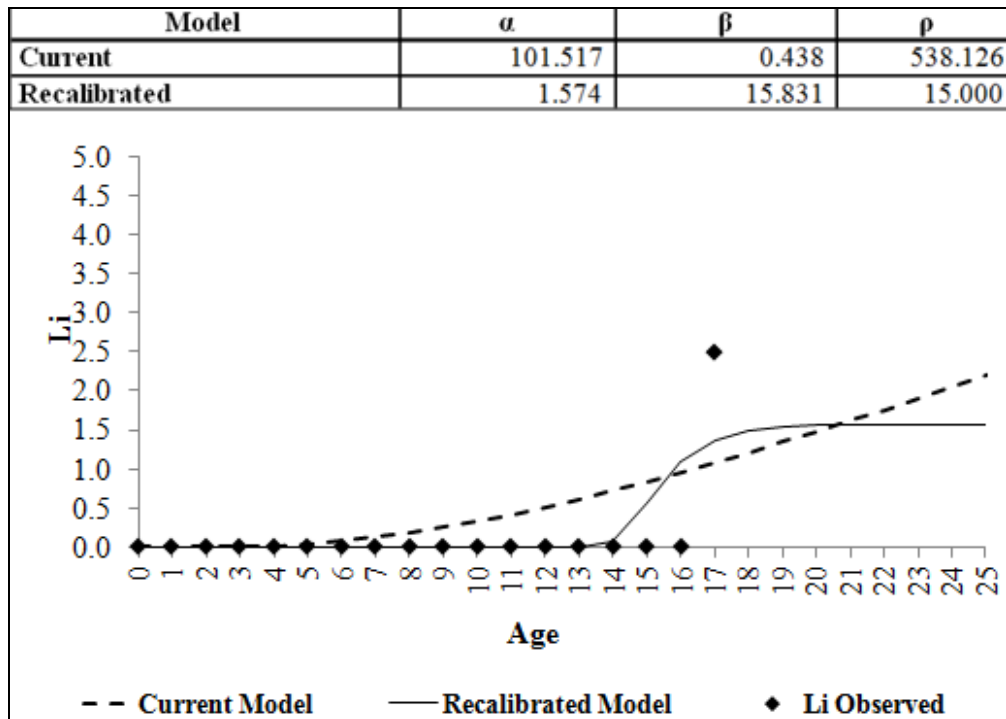


Figure 6.11. Recommended Statewide CRCP Punchouts Performance Curve, Median Method.

On the other hand, the calibrated ACP patches performance model displayed in Figure 6.12 differs from the current PMIS performance model in that the age in which the distress initiates is larger; the number of ACP patches rapidly increase to its maximum allowable number within two years from its distress starting age; and the maximum allowable number of ACP patches per mile is considerably reduced from about 96.5 to 1.

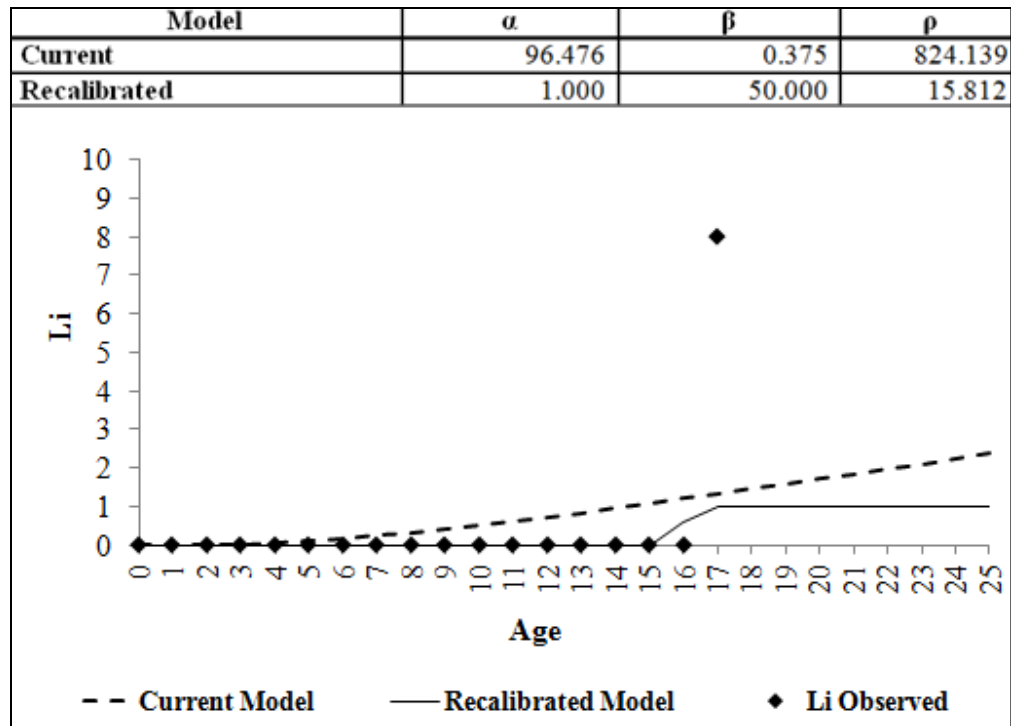


Figure 6. 12.Recommended Statewide CRCP ACP Patches Performance Curve, Median Method.

In Figure 6.13, it can be noted that the calibrated PCC patches performance model displayed differs from the current PMIS performance model in that the age in which the distress initiates is larger; the number of PCC patches rapidly increases to its maximum allowable distress; and the maximum allowable number of PCC patches per mile is considerably reduced from about 146 to 4.

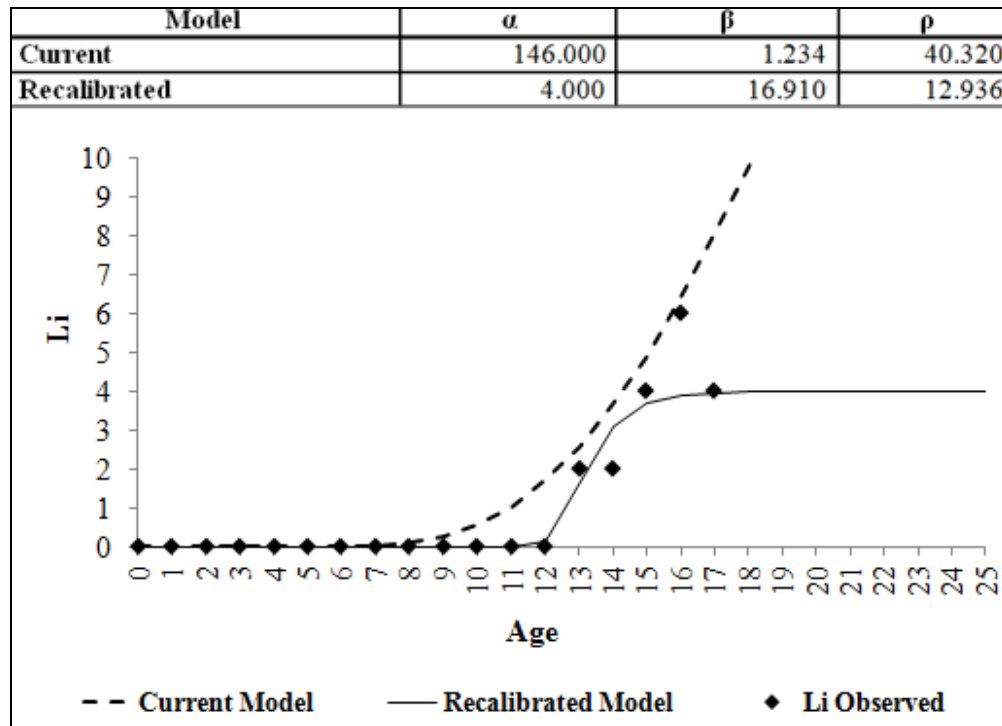


Figure 6. 13. Recommended Statewide CRCP PCC Patches Performance Curve, Median Method.

6.4 CRCP Ride Quality Performance Models

Calibrations for the ride quality pavement performance models were also performed for each data subset of all “windows” data sets. The calibrations were performed using the macro Excel file developed. In this section, only the coefficients of the calibrated performance models for Li Median data subsets will be presented. The “ R^2 – Median” and “ R^2 – Quartile” values, which retain the same meaning as described in section 6.3, are also presented for each set of calibrated models. Graphs with the calibrated Li Median performance model will be presented in this section and in the Appendices. Furthermore, data sets displaying a hyphen are those data sets where a calibration was not feasible due to limited data. The results obtained for the Texas district, climate and subgrade zones, and statewide “windows” datasets are presented in the following.

6.4.1 Ride Quality Performance Model Calibration Process

The calibration of the CRCP ride quality performance model was also performed with the hybrid technique and Equation 6.1. As was stated, the ride quality performance model measures ride quality performance in terms of percent ride quality lost, Li. The following steps outline the process followed to calibrate the ride quality models:

1. Gather historical ride quality data from PMIS records for all continuously reinforced concrete pavements.
2. The ride quality of a pavement is stored as Ride Score in the PMIS database while the performance models interpret ride quality as the percent of ride quality lost. As a result, the Ride Score for each data collection section has to be converted to the percent of ride quality lost, Li, for the calibrations. This is done with the conversion process described in Section 2.2.2.2 of Chapter 2.
3. After Ride Score is converted to Li, Steps 2 through 7 of the hybrid technique described in Chapter 3 were followed for the calibration of the CRCP ride quality performance models.

As stated, the calibration process was also carried out using the macro developed in the Excel file. An Excel file for each category of the “windows” datasets was also created for ride quality data.

6.4.2 Districts

Table 6.8 shows a summary of the coefficients alpha (α), beta (β), and rho (ρ) obtained for the calibrated CRC pavement ride quality performance models for each of the 25 Texas districts. The results obtained for the unconstrained and alpha constrained calibrations are displayed in

this table. The calibrated ride quality performance model graphs for the Li Median subsets, and the coefficients and graphs of the calibrated performance models for the Li Quartile data subsets can be found in Appendix E.

Table 6.8. Calibrated CRCP Ride Quality Performance Models for Texas Districts (Li Median Subset).

| Districts | Method | α | β | ρ | R ² -Median | R ² -Quartile |
|------------------|---------------|----------|---------|---------|------------------------|--------------------------|
| 01-Paris | Unconstrained | 50.010 | 1.254 | 22.362 | 0.520 | 0.345 |
| | Constrained | 7.000 | 7.454 | 9.671 | 0.461 | 0.275 |
| 02-Fort Worth | Unconstrained | 8.015 | 5.204 | 5.409 | 0.859 | 0.615 |
| | Constrained | 8.000 | 5.230 | 5.407 | 0.859 | 0.615 |
| 03-Wichita Falls | Unconstrained | 9.507 | 4.703 | 8.433 | 0.951 | 0.714 |
| | Constrained | 6.000 | 22.005 | 7.892 | 0.902 | 0.651 |
| 04-Amarillo | Unconstrained | 8.923 | 5.627 | 6.499 | 0.699 | 0.585 |
| | Constrained | 8.921 | 5.626 | 6.498 | 0.699 | 0.585 |
| 05-Lubbock | Unconstrained | 11.208 | 26.092 | 12.632 | 0.998 | 0.608 |
| | Constrained | 4.000 | 250.000 | 12.103 | 0.959 | 0.584 |
| 06-Odessa | Unconstrained | 0.857 | 57.489 | 3.110 | 0.400 | 0.077 |
| | Constrained | 0.857 | 57.489 | 3.110 | 0.400 | 0.077 |
| 07-San Angelo | Unconstrained | - | - | - | - | - |
| | Constrained | - | - | - | - | - |
| 08-Abilene | Unconstrained | - | - | - | - | - |
| | Constrained | - | - | - | - | - |
| 09-Waco | Unconstrained | 23.603 | 9.727 | 7.154 | 0.882 | 0.778 |
| | Constrained | 18.000 | 18.899 | 6.983 | 0.867 | 0.762 |
| 10-Tyler | Unconstrained | - | - | - | - | - |
| | Constrained | - | - | - | - | - |
| 11-Lufkin | Unconstrained | - | - | - | - | - |
| | Constrained | - | - | - | - | - |
| 12-Houston | Unconstrained | 1288.140 | 0.406 | 634.180 | 0.865 | 0.396 |
| | Constrained | 9.000 | 4.867 | 6.612 | 0.697 | 0.403 |
| 13-Yoakum | Unconstrained | 80.300 | 0.249 | 152.901 | 0.459 | 0.366 |
| | Constrained | 18.000 | 0.730 | 3.544 | 0.446 | 0.367 |

Table 6.8. Calibrated CRCP Ride Quality Performance Models for Texas Districts (Li Median Subset) (Continued).

| Districts | Method | α | B | ρ | R ² -Median | R ² -Quartile |
|-------------------|---------------|---|---------|--------|------------------------|--------------------------|
| 14-Austin | Unconstrained | 6.039 | 4.601 | 6.786 | 0.686 | 0.347 |
| | Constrained | 4.000 | 9.240 | 6.240 | 0.660 | 0.335 |
| 15-San Antonio | Unconstrained | 17.678 | 34.778 | 2.122 | 0.629 | 0.555 |
| | Constrained | 17.678 | 34.778 | 2.122 | 0.629 | 0.555 |
| 16-Corpus Christi | Unconstrained | District 16 does not have CRC pavement. | | | | |
| | Constrained | | | | | |
| 17-Bryan | Unconstrained | 2.922 | 41.001 | 13.673 | 1.000 | 0.202 |
| | Constrained | 2.000 | 250.000 | 13.203 | 0.966 | 0.195 |
| 18-Dallas | Unconstrained | 204.861 | 0.585 | 82.505 | 0.958 | 0.612 |
| | Constrained | 8.000 | 5.385 | 6.660 | 0.730 | 0.499 |
| 19-Atlanta | Unconstrained | 16.803 | 39.638 | 3.145 | 0.560 | 0.541 |
| | Constrained | 16.786 | 53.166 | 3.121 | 0.560 | 0.541 |
| 20-Beaumont | Unconstrained | 12.630 | 3.820 | 2.887 | 0.356 | 0.518 |
| | Constrained | 12.630 | 3.820 | 2.887 | 0.356 | 0.518 |
| 21-Pharr | Unconstrained | - | - | - | - | - |
| | Constrained | - | - | - | - | - |
| 22-Laredo | Unconstrained | 41.378 | 0.193 | 69.951 | 0.739 | 0.354 |
| | Constrained | 12.000 | 0.503 | 1.020 | 0.724 | 0.347 |
| 23-Brownwood | Unconstrained | District 23 does not have CRC pavement. | | | | |
| | Constrained | | | | | |
| 24-El Paso | Unconstrained | 15.009 | 2.936 | 8.615 | 0.875 | 0.623 |
| | Constrained | 7.000 | 8.248 | 6.806 | 0.768 | 0.564 |
| 25-Childress | Unconstrained | - | - | - | - | - |
| | Constrained | - | - | - | - | - |
| Statewide | Unconstrained | 32.343 | 1.164 | 17.629 | 0.974 | 0.440 |
| | Constrained | 7.000 | 5.859 | 7.647 | 0.867 | 0.406 |

6.4.3 Climate and Subgrade Zones

Table 6.9 shows a summary of the coefficients alpha (α), beta (β), and rho (ρ) obtained for the calibrated CRC pavement ride quality performance models for each of the climate and subgrade zones. The results obtained for the unconstrained and alpha constrained calibrations are

displayed in this table. The calibrated ride quality performance model graphs for the Li Median subsets, and the coefficients and graphs of the calibrated performance models for the Li Quartile data subsets can be found in Appendix F.

Table 6.9. Calibrated CRCP Ride Quality Performance Models for Climate and Subgrade Zones (Li Median Subset).

| Zone | Method | α | β | ρ | R ² -Median | R ² -Quartile |
|--------|---------------|----------|---------|---------|------------------------|--------------------------|
| Zone 1 | Unconstrained | 15.161 | 1.223 | 8.610 | 0.949 | 0.619 |
| | Constrained | 8.000 | 3.443 | 5.585 | 0.910 | 0.593 |
| Zone 2 | Unconstrained | 237.176 | 0.449 | 161.720 | 0.840 | 0.435 |
| | Constrained | 9.000 | 3.793 | 5.665 | 0.660 | 0.422 |
| Zone 3 | Unconstrained | 11.804 | 4.605 | 11.816 | 0.912 | 0.479 |
| | Constrained | 4.000 | 300.000 | 10.091 | 0.829 | 0.456 |
| Zone 4 | Unconstrained | 17.160 | 2.298 | 8.995 | 0.882 | 0.607 |
| | Constrained | 7.000 | 6.869 | 6.368 | 0.749 | 0.532 |

6.4.4 Statewide

Table 6.10 shows a summary of the coefficients alpha (α), beta (β), and rho (ρ) obtained for the unconstrained and alpha constrained calibrated statewide CRCP ride quality performance models. The respective R² values for each are also displayed. Figure 6.14 and Figure 6.15 show the best fit calibrated ride quality statewide performance models for the constrained and unconstrained calibrations.

Table 6.10. Calibrated Statewide CRCP Ride Quality Performance Models (Li Median Subset).

| Method | α | B | ρ | R ² -Median | R ² -Quartile |
|---------------|----------|-------|--------|------------------------|--------------------------|
| Unconstrained | 0.309 | 0.605 | 3.410 | 0.863 | 0.763 |
| Constrained | 0.304 | 0.616 | 3.297 | 0.863 | 0.763 |

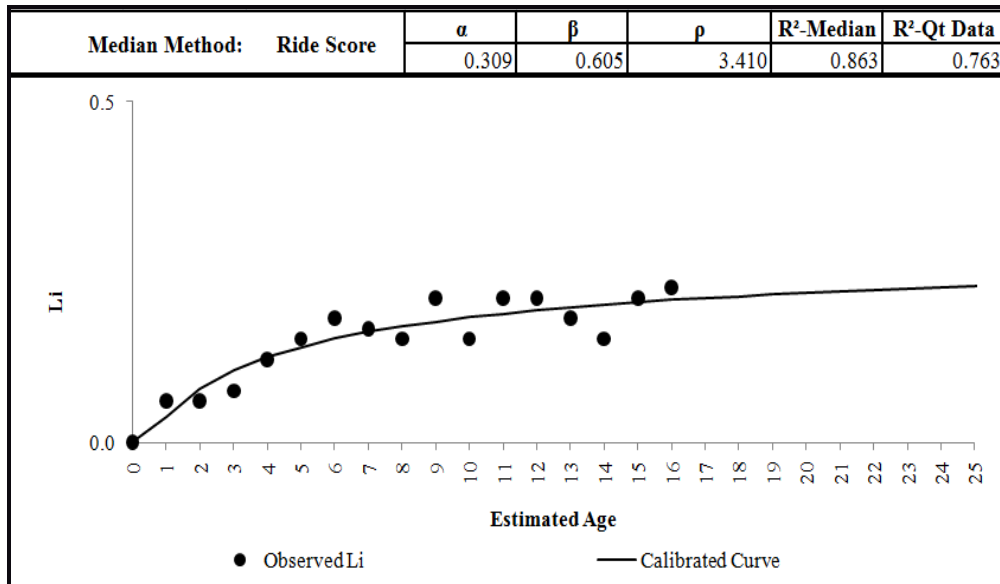


Figure 6.14. Calibrated CRCP Ride Quality Performance Model, Statewide, Li Median Subset (Unconstrained).

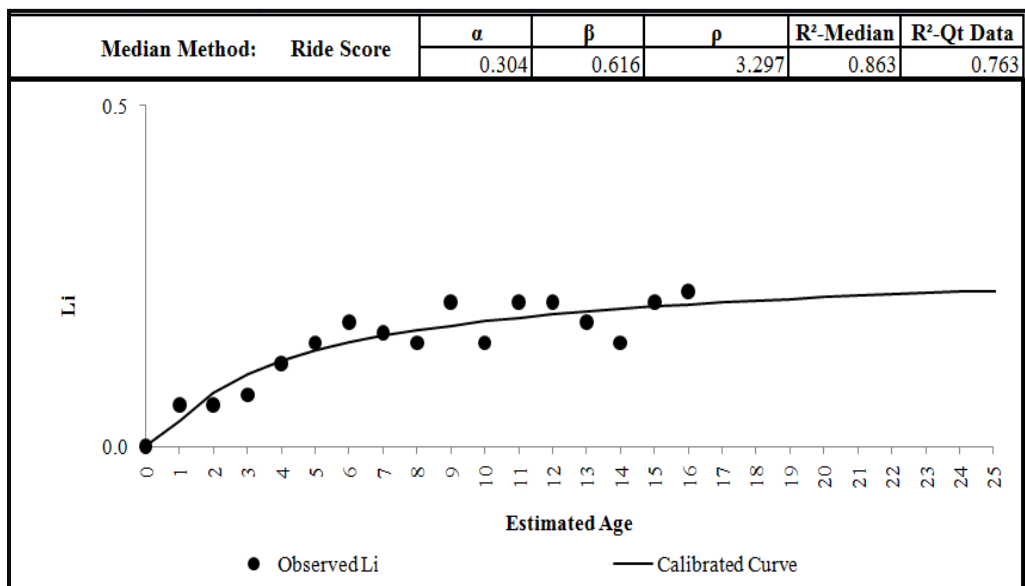


Figure 6.15. Calibrated CRCP Ride Quality Performance Model, Statewide, Li Median Subset (Constrained).

6.4.5 Recommended CRCP Ride Quality Pavement Performance Curves

Since it was desired to use the same type of datasets for the recommended ride quality calibrated models, the statewide ride quality performance models calibrated with the Li Median data subset

(constrained and unconstrained) were presented to TxDOT personnel for feedback. Given that the unconstrained and constrained calibrated models did not show a significant difference between each other, the unconstrained statewide ride quality performance model was proposed as the final model to represent the performance of CRC pavement ride quality. Table 6.11 shows the calibrated coefficients and “R²– Median” and “R²– Quartile” values corresponding to the final recommended statewide CRCP ride quality performance model. The coefficients of the current PMIS model are also presented along with its corresponding “R²– Median” and “R²– Quartile” values. The R²-Quartile and R²– Median values are higher for the recommended models than for the current PMIS models.

Table 6. 11.Recommended Statewide CRCP Ride Quality Performance Curve Coefficients.

| Ride Quality Model | Calibrated Statewide Performance Model Coefficients | | | | |
|---------------------------|--|---------------------------|--------------------------|-----------------------------|-------------------------------|
| | α | β | ρ | R²-Median | R²-Quartile |
| Calibrated | 0.309 | 0.605 | 4.410 | 0.863 | 0.763 |
| PMIS | 1.000 | 1.000 | 25.000 | 0.477 | 0.424 |

Figure 6.16 shows the final recommended ride quality performance model, the current PMIS performance curve and the Li Median data subset calibrated. It can be noted in this figure that the calibrated performance model displayed differs from the current PMIS model in that the ride quality starts to deteriorate soon after the pavement is built, there is a slower ride quality deterioration rate, and the maximum percentage of ride quality allowed to be lost is 31% (or 0.399) rather than the 100% (or 1.000).

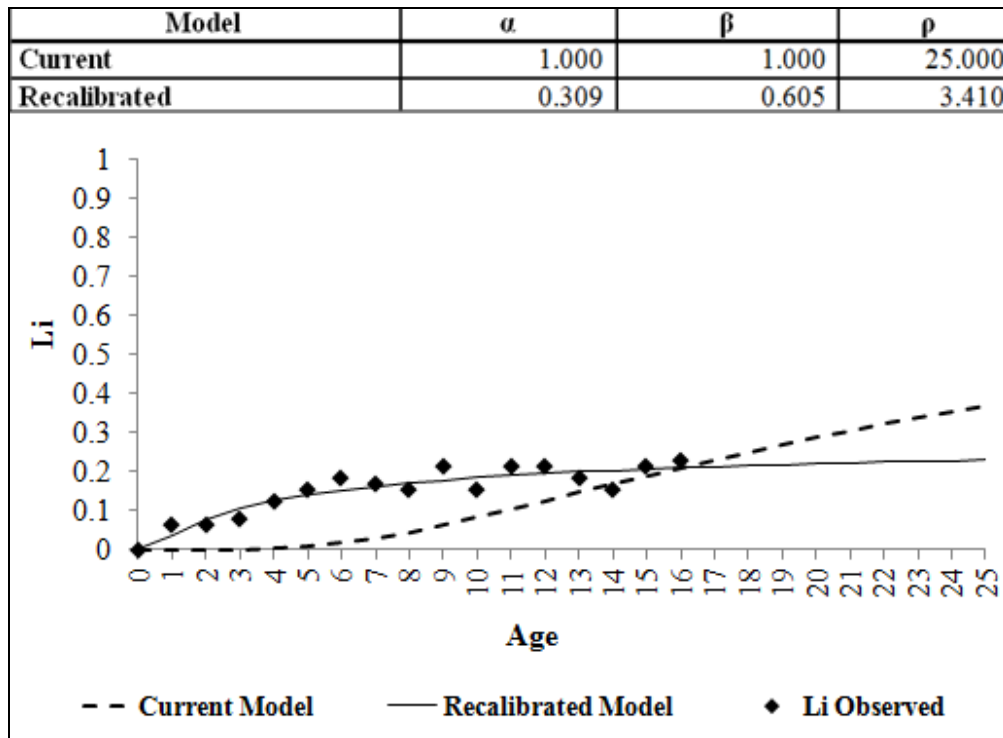


Figure 6. 16. Calibrated CRCP Ride Quality Performance Model, Statewide, Li Median Subset (Constrained).

6.6 Summary, Conclusions and Recommendations

TxDOT's PMIS CRCP network level pavement performance models were calibrated using the hybrid technique. Preliminary calibrations of the synthesized pavement performance data were performed using an iterative nonlinear least squares fitting method. Calibrations were performed for each "windows" dataset's Li Median and Li Quartile data subsets. In an iterative process the performance models were reviewed by TxDOT personnel and recalibrated according to the expert's feedback. This was repeated until the final performance models were selected. Ultimately, pavement performance models that best fit the data according to statistical measures and expert's opinion about Texas' CRC pavement deterioration trends were finally recommended for PMIS. Performance models for the four distress types (spalled cracks,

punchouts, ACP patches, and PCC patches) and ride quality monitored in TxDOT were developed and proposed in this chapter.

The large concentration of Li values equal to zero (no observed distress) in the data sets presented a challenge during the calibration. This large concentration was especially observed for Punchouts and ACP patches. The trend can be attributed to TxDOT's maintenance and rehabilitation strategies: punchouts are considered a serious structural distress that is given priority and ACP patches are a temporary method to cover surface distresses. The large zero concentration prevented the calibration of various Texas district and climate and subgrade zone models since there were no distresses to model. Statewide performance models were also affected by the large concentration of Li zero values; nevertheless, the statewide models were not greatly influenced since the larger dataset includes more records with visible distress ($Li > 0$). All statewide distress and ride performance models were calibrated. The concentration of Li values equal to zero also had a great influence in the calibrations of the Li Quartile data subsets. Overall, the Li Median data set was concluded to give the most reasonable calibrated performance models when compared to the models of the Li Quartile dataset. Based on these conclusions, the statewide Li Median models were proposed for further refinement based on expert feedback.

The performance models were then revised and re-calibrated based on comments from TxDOT personnel and statistical analysis of PMIS data. A number of constraints were recommended to be applied on the model coefficients during calibration. It was first observed that the alpha coefficient, which represents the maximum range of distress growth, had unreasonably high values. Therefore, one of the first recommendations was to constrain alpha within a 90% confidence interval. It was observed that the calibrated coefficients of the unconstrained and

alpha constrained models greatly differed in the distress performance models. The opposite was observed for the ride quality performance models since both methods produced very similar curves. This can be attributed to the fact that there was not a great Li zero value concentration in ride quality as there is for the distresses. Furthermore, the beta coefficient was constrained to 50 in all performance models due to limitations of the PMIS software mainframe. Further constraints on the coefficients were also set according to experts' knowledge of distress development trends in CRCP and statistical measures. According to expert opinion, spalled cracking is a distress that slowly develops in CRCP. In addition, punchouts need to be addressed quickly and should therefore have a maximum limit of 2 punchouts per mile. From the statistical analysis, ACP patches were the least observed distress in CRCP. It was therefore recommended by experts to limit alpha to one ACP patch per mile. A constraint on the distress starting age of ACP patches was also imposed according to the appearance of punchouts. According to expert feedback, four PCC patches per mile is the recommended maximum allowable number of patches. No constraints were set on the coefficients of the ride quality model. Table 6.12 presents the recommended distress and ride quality models that provide the most representative curves according to this feedback and historical performance data. The R^2 values for each recalibrated model are also shown. Furthermore, this table also presents the coefficients and R^2 values for the current PMIS performance models. It can be generally observed that the R^2 -Quartile value is higher for the recommended models than for the current PMIS models.

Table 6.12. Final Recommended Statewide CRCP Distress and Ride Quality Performance Model Coefficients.

| CRCP Performance Model | | Calibrated Statewide Performance Model Coefficients | | | | |
|------------------------|------------|---|---------|---------|------------------------|--------------------------|
| | | α | β | ρ | R ² -Median | R ² -Quartile |
| Spalled Cracks | Calibrated | 134.932 | 0.833 | 63.405 | 0.402 | 0.348 |
| | PMIS | 1.690 | 22.090 | 10.270 | 0.315 | 0.248 |
| Punchouts | Calibrated | 1.574 | 15.831 | 15.000 | 0.526 | 0.433 |
| | PMIS | 101.517 | 0.438 | 538.126 | 0.095 | 0.259 |
| ACP Patches | Calibrated | 1.000 | 50.000 | 15.812 | 0.729 | 0.385 |
| | PMIS | 96.476 | 0.375 | 824.139 | 0.222 | 0.015 |
| PCC Patches | Calibrated | 4.000 | 16.910 | 12.936 | 0.913 | 0.522 |
| | PMIS | 146.000 | 1.234 | 40.320 | 0.874 | 0.560 |
| Ride Quality | Calibrated | 0.309 | 0.605 | 4.410 | 0.863 | 0.763 |
| | PMIS | 1.000 | 1.000 | 25.000 | 0.477 | 0.424 |

The observations made during the calibration process of the PMIS performance models emphasized the importance of the integration of expert opinion in network level performance model development. The quality of the data is a challenge that can be generally encountered in network level databases. The integration of expert opinion can compensate for database deficiencies and provide a tool for the development of more representative pavement performance models. In this study, it is recommended to use the Li Median data subsets, and set constraints according to expert judgment and limitations of the PMS software used by the agency. Nevertheless, these are general recommendations that may change according to the type of modes being developed and the quality of the pavement records in an agency's database.

Chapter 7. Adapting the Hybrid Technique for the Calibration of HDM-4 and MEPD Concrete Pavement Performance Models

7.1 Introduction

The hybrid technique provides a very effective tool for modeling pavement performance at the network level. The flexibility of this technique, provided by the integration of various methods, was a key factor in its successful implementation in the calibration of TxDOT's PMIS CRCP performance models. The technique proved to be a very effective tool during the development of the models since it provided the necessary methods to address the challenges encountered in the PMIS database (e.g. missing data and data entry errors). Due to the adaptive nature of this technique, it is recommended for the calibration of performance models used by other pavement management agencies. Agencies calibrating HDM-4 and MEPD models can benefit from the methods proposed by the hybrid technique. Although these models are based on mechanistic empirical principles, which require more effort to calibrate, they can still benefit from the technique during the model development. In this chapter, the implementation of the hybrid technique for the calibration of HDM-4 and MEPD models will be discussed.

7.2 Calibration of HDM-4 and MEPD Rigid Pavement Performance Models Overview

7.2.1 Challenges Encountered in the Calibration of HDM-4 and MEPD Models

Generally, the HDM-4 and MEPD pavement performance models predict one type of distress through structural response and transfer functions. Structural response functions predict pavement condition according to stresses, strains and deflections in the pavement caused by traffic loads. These functions are used for the theoretical computation of damage. On the other

hand, the transfer functions are used to relate the theoretical damage with the observed distress measured in the field (NCHRP 2004). These transfer functions account for influential factors on pavement deterioration that cannot be accounted for by theoretical models. Depending on the distress being modeled, it may be possible to adapt both functions to represent pavement deterioration in the field through calibration parameters. Nevertheless, calibrating both functions can present a challenge since they are dependent on one another for the prediction of deterioration. This challenge is encountered in MEPD models which have calibration parameters for the structural and transfer functions.

Given that HDM-4 and MEPD pavement performance models use mechanistic-empirical principles to predict pavement deterioration, the structural functions require a vast amount of information to accurately predict pavement response to traffic load. If the required data is not available for the structural functions, then the pavement damage cannot be properly predicted. Misleading pavement damage predictions may negatively impact the calibration of transfer functions. As a result, the reliability of the calibrated pavement performance models can be jeopardized.

Calibrating HDM-4 and MEPD models may also be a challenging task if the distresses evaluated in a pavement management agency are different than those evaluated in HDM-4 and MEPDG. Also, the type of measurement used to evaluate pavement deterioration may differ between the agency and these management tools. For example, an agency may evaluate and record transverse cracks according to the width of the crack or number of cracks while HDM-4 and MEPDG evaluate this distress as the percentage of slabs with transverse cracks.

7.2.2 Recommendations for Adapting Hybrid Technique for the Calibration of HDM-4 and MEPD Performance Models

Due to the mechanistic-empirical nature of the HDM-4 and MEPD models, a few modifications of the hybrid technique are required so the method can be successfully implemented. These modifications help address the challenges that may be encountered during the calibration of HDM-4 and MEPD models. The following is recommended to adapt the hybrid technique:

- Given that a vast amount of information is needed to predict pavement distress in MEPDG and HDM-4, it is recommended to select pavement sections with the most detailed and complete records possible. It is also desired to select pavement sections with available performance data for the entire pavement design life.
- A more extensive database regarding pavement structure and material characteristics, traffic composition (percentage of vehicle class types), traffic flow (AADT), axle types and loads, climate characteristics and environment characteristics is required. Using test sections to acquire this type of data may be needed if data is not available.
- When pavement deterioration is measured by an agency with different measurement units than those used in the HDM-4 and MEPD models, it is recommended to develop transfer functions to convert the units. The transfer function may be either a mathematical relationship or a table. It is recommended to conduct parallel surveys with local measurements and measurements used in HDM-4 or MEPDG (whichever is being calibrated). Fifteen to twenty sections with a total length of at least 20 km are recommended to be surveyed (Bennett and Paterson 2000). The local measurements and the HDM4 (or MEPDG) measurements should then be correlated with some type of transfer function.

- It is recommended to perform a sensitivity analysis of the calibration parameters of each pavement performance model to acquire a better understanding of their influence in modeling pavement deterioration. Understanding the effect of each calibration parameter can assist in defining constraints during the calibration process.
- The present serviceability rating (PSR) and roughness models used in HDM-4 for JRCPC and JPCPC, respectively, are dependent on distress predictions; therefore, it is recommended to calibrate the distress performance models first. The JRCPC and CRCP roughness models are dependent on PSR predictions; therefore it is recommended to calibrate the PSR model before the roughness model.
- The MEPD roughness models for JPCPC and CRCP are dependent on pavement distress predictions; therefore, the distress models need to be calibrated before the roughness models.
- MEPDG requires the calibration of some structural functions used for the prediction of transverse slab cracking and mean transverse joint faulting for JPCPC, and punchouts for CRCP. Therefore, structural and transfer functions need to be calibrated for each distress. It is recommended to calibrate the transfer function while setting the coefficients of the structural function to one. The structural function should then be calibrated while fixing the coefficients of the transfer function to the calibrated values previously obtained.
- The observed pavement performance data used for the calibrations of MEPD transfer functions would have to be further synthesized to describe pavement condition as an increment (e.g. distress increment between two consecutive years of a pavement's life) rather than an absolute value (e.g. observed distress at a certain pavement age).

7.3 Case Study: Recommendations for the Calibration of HDM-4 and MEPD Transverse Cracking Performance Models using the Hybrid Technique

7.3.1 JPCP Transverse Cracking Models

To illustrate the application of the hybrid technique for the calibration of the HDM-4 and MEPD performance models, the calibration process of the transverse cracking model for JPCP is presented as an example. This performance model was chosen for the comparison because it is a distress modeled in all pavement management tools and has related units of measurement. The HDM-4 and MEPD transverse cracking model define this distress as cracks perpendicular to the central axis of the road. These models use traffic to predict the percentage of slabs that are cracked. Nevertheless, HDM-4 uses the number of ESAL repetitions during a temperature gradient, while MEPDG does not employ ESALs and uses the applied number of load applications for a given axle type and load level. PMIS also considers cracks perpendicular to the central axis of the road as transverse cracks, but it only rates cracks demonstrating spalling. In the transverse cracking performance model, PMIS evaluates spalled joints, transverse cracks and the asphalt patches of spalled joints and transverse cracks. The PMIS model uses pavement age to predict the percentage of transverse cracks and failed joints. A more detailed definition of these models can be found in Chapter 2 and Appendix A.

In order to obtain a better understanding of how the transverse cracking performance curves model pavement deterioration, it is necessary to comprehend the effects of each calibration parameter in the shape of the model. The HDM-4 transverse cracking model uses one calibration parameter to integrate pavement deterioration behavior observed in the field. The MEPD and PMIS models use 4 and 3 calibration parameters, respectively.

7.3.1.1 PMIS Failed Joints and Transverse Cracks Performance Model for JPCP

As was stated, the PMIS performance models are sigmoidal models (Equation 2.1) that use α , β and ρ to determine the shape of the model and ϵ , σ and X parameters as curve modifiers. As is observed in Figure 7.1, the α coefficient determines the maximum range of distress growth. In Figure 7. 2, it can be observed that β determines the slope in the middle of the model that controls the rate of distress progression with pavement age. On the other hand, the ρ coefficient is the prolongation factor that determines how long it takes until the pavement shows significant distress. This can be observed in Figure 7. 3. The ϵ , σ and X curve modifiers can increase or decrease the pavement life if they are greater or less than one, respectively.

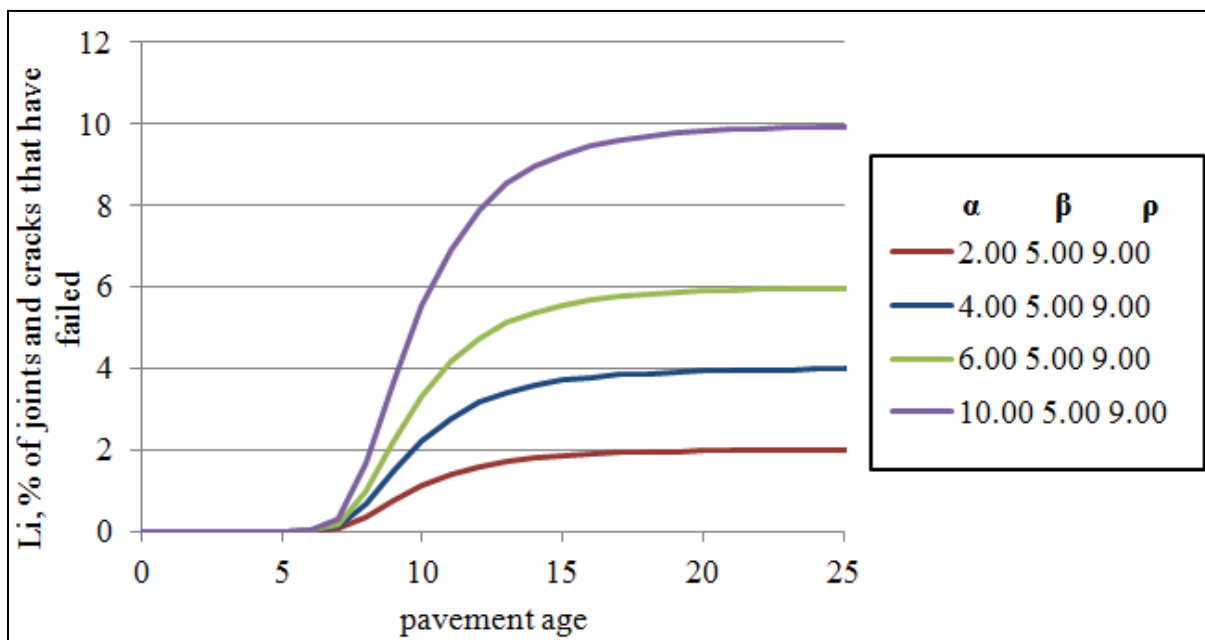


Figure 7.1. PMIS Failed Joints and Transverse Cracks Model with Varying Coefficient alpha (α).

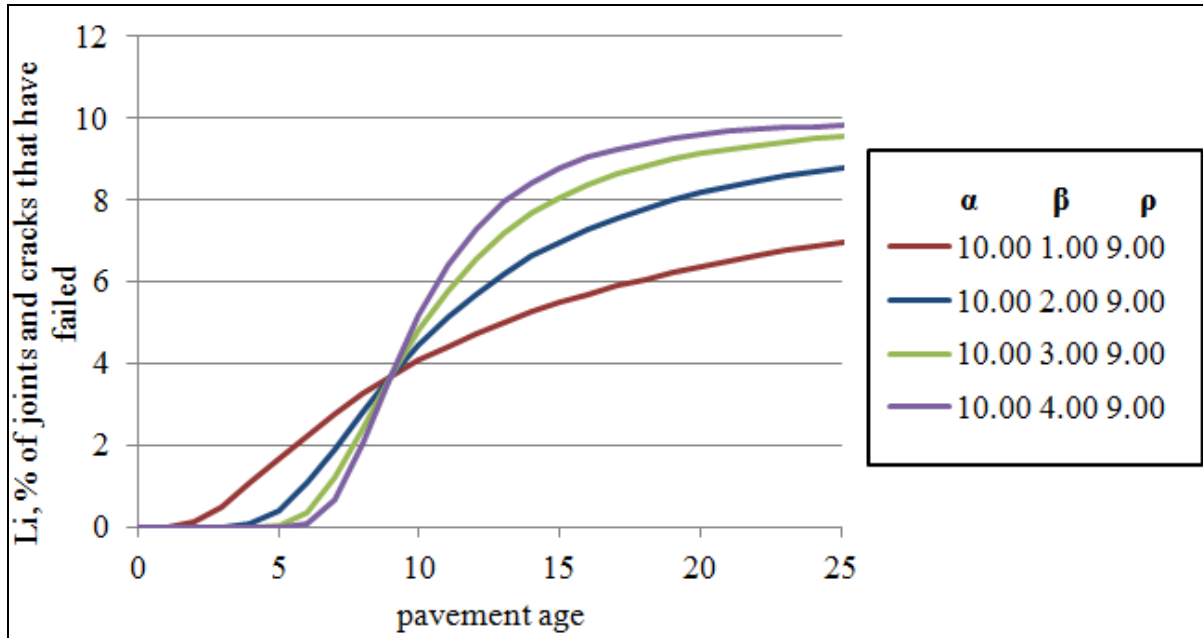


Figure 7. 2. PMIS Failed Joints and Transverse Cracks Model with Varying Coefficient beta (β).

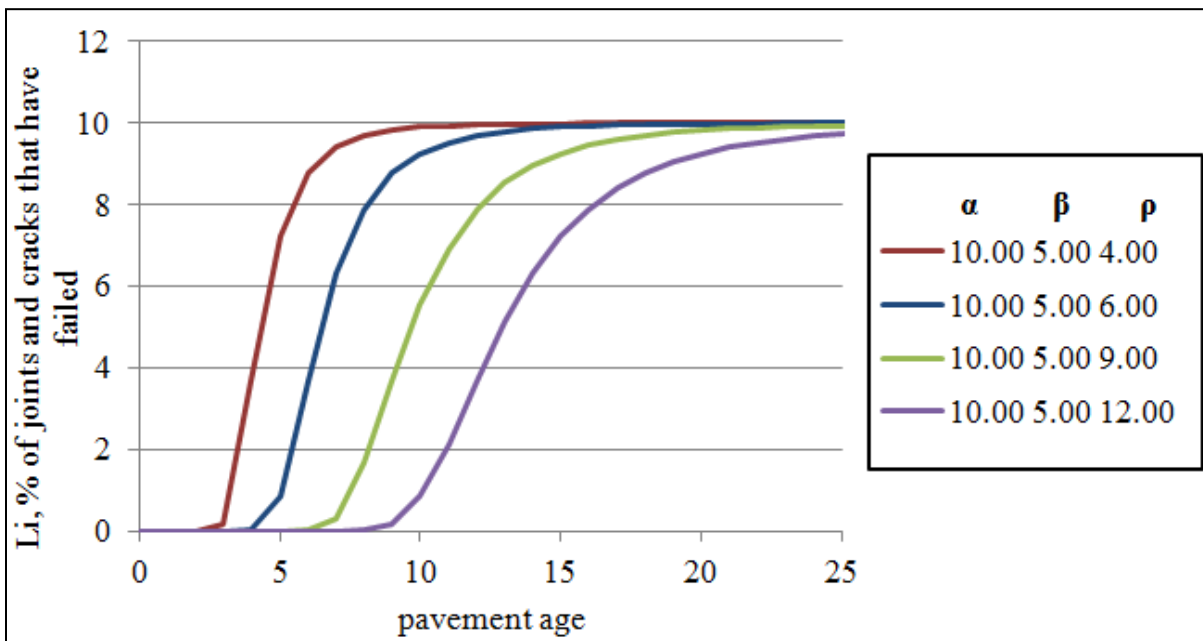


Figure 7. 3. PMIS Failed Joints and Transverse Cracks Model with Varying Coefficient rho (ρ).

7.3.1.2 HDM-4 Transverse Cracking Performance Model for JPCP

HDM-4 uses Equation 7.1 to describe the percentage of slabs demonstrating transverse cracking in respect to the amount of the accumulated damage factor, FD. The damage factor is determined through structural response functions that do not have calibration coefficients (Kerali and Odoki 2000). Given that HDM-4 considers various factors to calculate the damage factor, it is recommended to calculate FD using the HDM-4 software.

Equation 7.1 has only one calibration parameter. As can be observed in Figure 7.4, the K_{jpc} parameter determines the maximum range of distress growth. Having one calibration parameter does not give much flexibility to adapt the logarithmic curve to represent transverse cracking observed in the field. According to this equation, the pavement starts to develop transverse cracks shortly after it is constructed. If this is not observed in the pavements under the agency's jurisdiction, then this can lead to unreliable deterioration predictions. This may therefore result in early unnecessary applications of treatments and misuse of available budget.

$$PCRACK = K_{jpc} \times \frac{100}{1 + 1.41 \times FD^{-1.66}}$$

Equation 7. 1

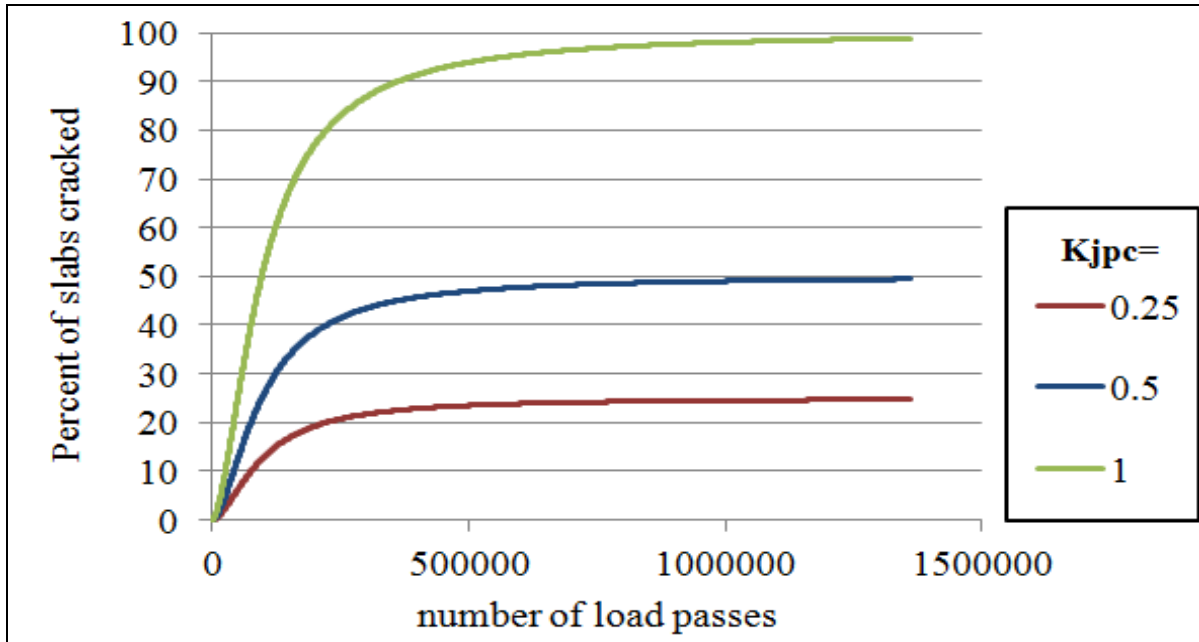


Figure 7. 4 HDM-4 Transverse Cracking Model with Varying Coefficient K_{jpc} .

7.3.1.3 MEPD Transverse Cracking Performance Model for JPCP

MEPDG uses Equation 7.2 to predict the percentage of slabs demonstrating top-down or bottom-up transverse cracking. Equation 7.3 integrates Equation 7.2 and is used to predict the total percentage of slabs with top-down (TD) and bottom-up (BU) transverse cracking. These transfer functions, which take a sigmoidal form, have two calibration coefficients C_4 and C_5 . Both of these equations depend on the total accumulated fatigue damage (FD) which is calculated through Equation 7.4. Equation 7.5, which is used to calculate the allowable number of load applications for Equation 7.4, has calibration coefficients C_1 and C_2 (NCHRP 2003a).

$$\text{Crack} = \frac{100}{1 + C_4 \times \text{FD}^{C_5}}$$

Equation 7. 2

TotalCrack = 100

$$* \left[\frac{1}{1 + C4 \times BU^{C5}} + \frac{1}{1 + C4 \times TD^{C5}} - \left(\frac{1}{1 + C4 \times BU^{C5}} \right) \times \left(\frac{1}{1 + C4 \times TD^{C5}} \right) \right]$$

Equation 7. 3

$$FD = \sum \frac{n_{i,j,k,l,m,n}}{N_{i,j,k,l,m,n}}$$

Equation 7. 4

Where:

FD=total accumulated fatigue damage (top-down or bottom-up)

$n_{i,j,k,l,m,n}$ =applied number of load applications at condition i,j,k,l,m,n

$N_{i,j,k,l,m,n}$ =allowable number of load applications at condition i,j,k,l,m,n.

i=age

j= month

k= axle type

l=load level

m=temperature difference

n=traffic path

$$\log(N_{i,j,k,l,m,n}) = C_1 \times \left(\frac{MR_i}{\sigma_{i,j,k,l,m,n}} \right)^{C_2} + 0.4371$$

Equation 7. 5

Where:

$N_{i,j,k,l,m,n}$ = allowable number of load applications at condition i,j,k,l,m,n

MR_i = PCC modulus of rupture at age i, psi

$\sigma_{i,j,k,l,m,n}$ = applied stress at condition i,j,k,l,m,n

C_1 = calibration constant= 2.0

C_2 = calibration constant= 1.22

From Figure 7.5, it can be observed that the C4 calibration parameter is the prolongation factor that determines how long it takes until the pavement shows significant distress. The calibration parameter C5 determines the slope in the middle of the model that controls the rate of distress evolution with number of loads applied. This can be observed from Figure 7.6. As can be observed from Figure 7.7 and Figure 7.8, the C1 and C2 calibration parameters are shape modifiers and can be used to prolong the pavement's life. As these factors increase, the pavement life is extended. The opposite occurs as the factors decrease. The max range of distress growth is controlled by the transfer function and is defined to be 100 percent of slabs with transverse cracks.

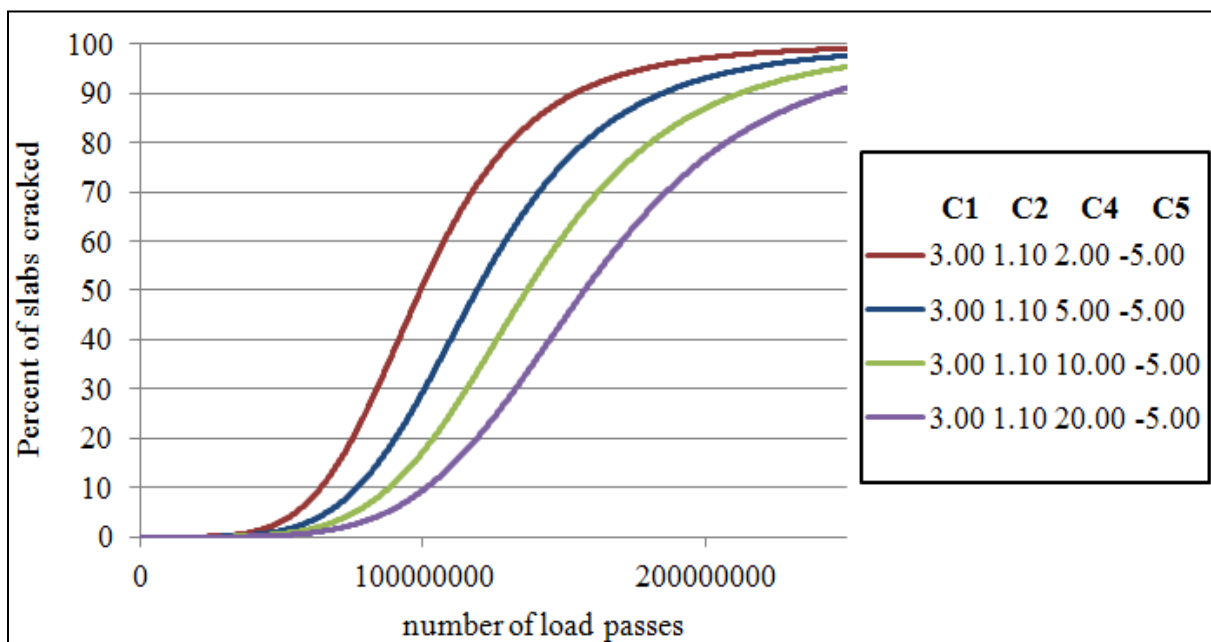


Figure 7. 5. MEPD Transverse Cracking Model with Varying Coefficient C4.

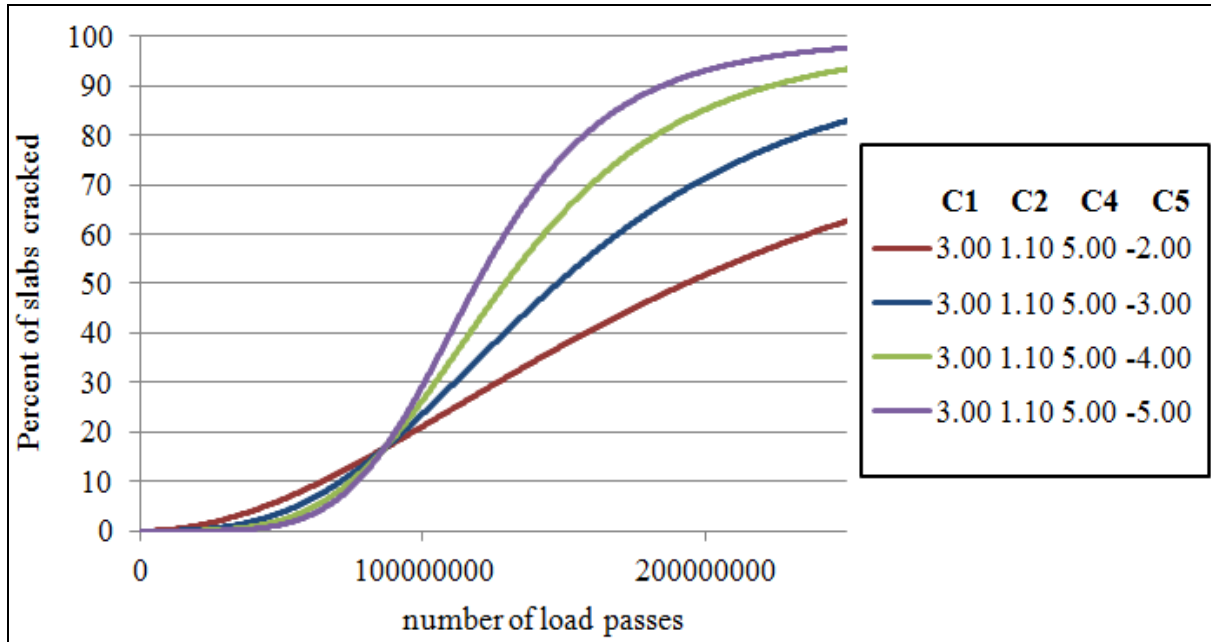


Figure 7. 6. MEPD Transverse Cracking Model with Varying Coefficient C5.

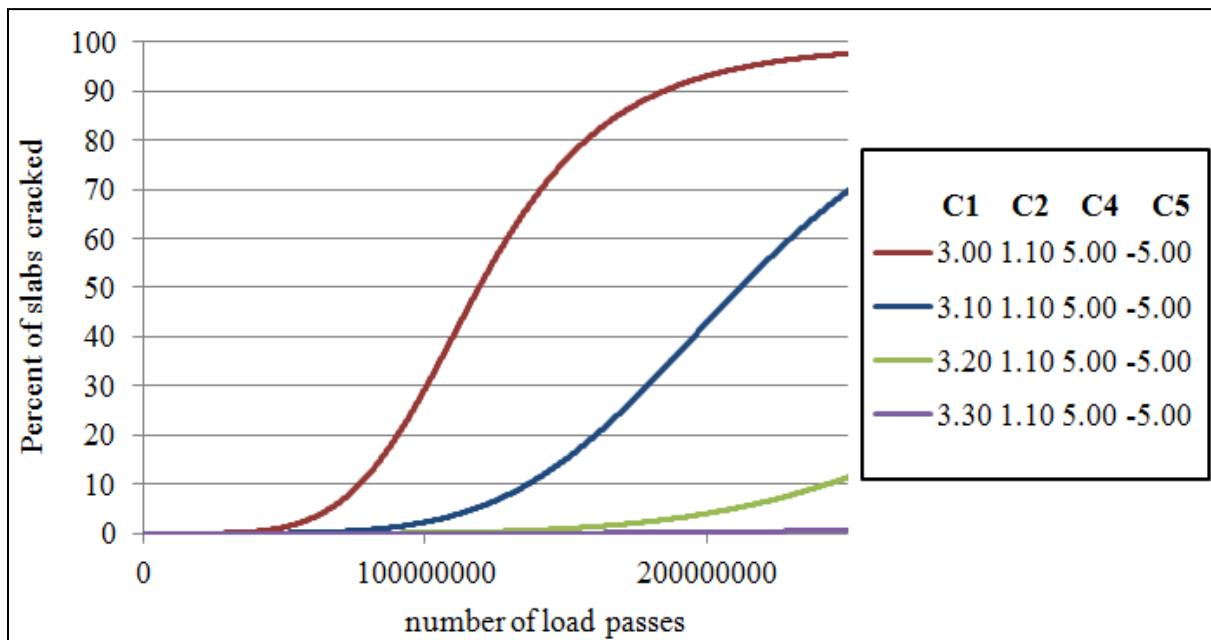


Figure 7. 7. MEPD Transverse Cracking Model with Varying Coefficient C1.

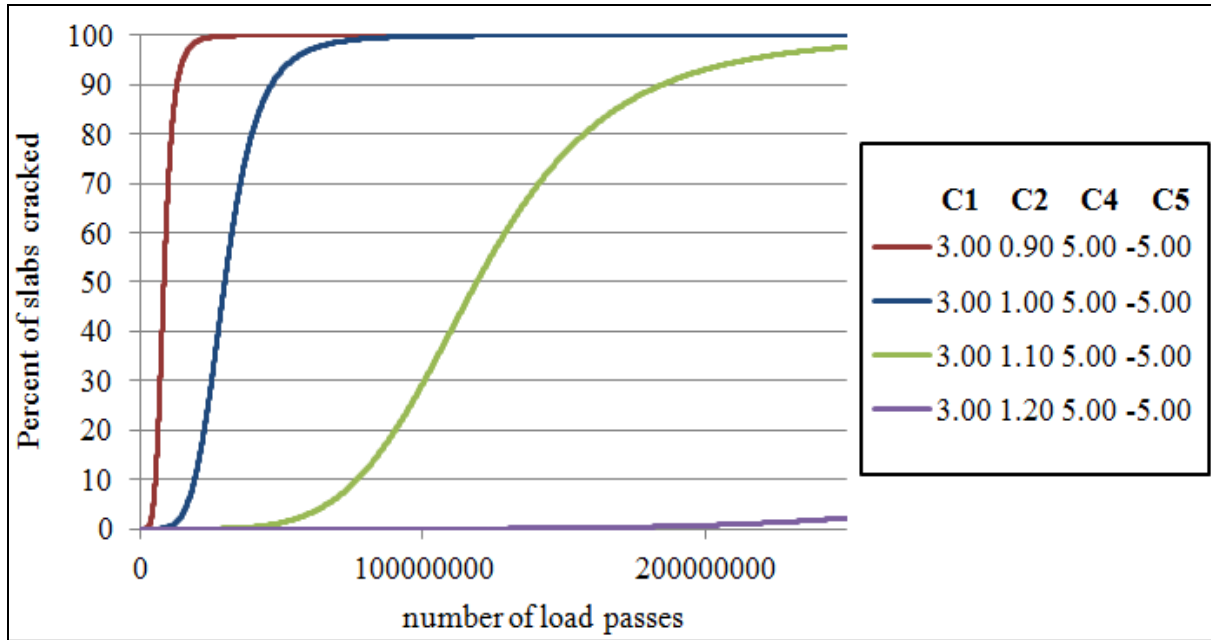


Figure 7.8.MEPD Transverse Cracking Model with Varying Coefficient C2.

7.3.2 Adapting Hybrid Technique to HDM-4 Model

Given that HDM-4 only requires to calibrate the transfer function, there are not many modifications needed to adapt the hybrid technique. To calibrate the HDM-4 transverse cracking model using the hybrid technique, the following steps should be performed:

1. Collect information needed to predict percentage of slabs with transverse cracking according to the required input factors needed for HDM-4. Table 2.12 in Chapter 2 gives a general overview of the input factors needed. Default values may be used for factors where data is not available.
2. Perform step 1 of the hybrid technique.
3. Determine whether the current model adequately represents the progression of transverse cracking by comparing the observed percentage of slabs with transverse cracking (from step 2) with the predicted percentage of slabs with transverse cracking according to the current HDM-4 models. To obtain the predicted distress according to the current model,

execute HDM-4 software using the available design inputs. According to how well the current models' predictions fit the observed data, determine whether the models should or should not be calibrated. If models need to be calibrated, proceed with the next steps.

4. Perform steps 2 through 5 of the hybrid technique. If pavement age is available in the database, omit step 3.
5. To determine the accumulated damage associated with transverse cracking needed for the calibration of Equation 7.1, HDM-4 software may be used. A non-linear regression analysis using the least squares method may then be performed with the damage computations obtained, the observed transverse cracking in the field, and Equation 7.1. Through this analysis, the calibration parameter K_{jpc} can be determined.
6. Perform step 7 of the hybrid technique. The effect of the calibration parameter on the model can be considered when setting constraints in the calibration.

7.3.3 Adapting Hybrid Technique to MEPD Model

Since MEPDG consists of a transfer and structural response function which have calibration coefficients, the two functions must be calibrated. The transfer function includes both top-down and bottom-up cracking; therefore, having pavement performance field data identifying both types of cracking would be ideal for the development of a more reliable model. It can be recommended to have coring samples of the pavement to confirm the cracking initiation location and therefore conclude what type of transverse cracking is observed (NCHRP 2003e).

To calibrate the MEPD transverse cracking model using the hybrid technique, the following steps should be performed:

1. Collect information needed to predict percentage of slabs with transverse cracking according to the required input factors needed for MEPDG. These are listed in Table 2.14 in Chapter 2. Default values may be used for factors where data is not available.
2. Perform step 1 of the hybrid technique.
3. Determine whether the current models adequately represents the progression of transverse cracking by comparing the observed percentage of slabs with transverse cracking with the predicted percentage of slabs with transverse cracking according to the current MEPD models. To obtain the predicted distress according to the current model, execute MEPDG design software using the available design inputs. According to how well the current models' predictions fit the observed data, determine whether the models should or should not be calibrated. If models need to be calibrated, proceed with the next steps.
4. Perform steps 2 through 5 of the hybrid technique. If pavement age is available in the database, omit step 3.
5. Perform the calibration of the transfer function: To determine the accumulated damage associated with top down and bottom up transverse cracking needed for the calibration of Equation 7.3, MEPDG software may be used. During this process, set coefficients C1 and C2 equal to 1. A non-linear regression analysis using the least squares method may then be performed with the damage computations obtained, the observed transverse cracking in the field, and Equation 7.3. Through this analysis, the calibration parameters C4 and C5 can be determined.
6. Perform the calibration of the structural response function: Calibrating the coefficients C1 and C2 of the structural response function (Equation 7.5) may present a challenge

given that fatigue damage for top-down and bottom-up cracking are needed in the calibration and this information is not usually recorded in network level databases. If this data is not available, then the MEPDG default coefficients can be used ($C1=2$ and $C2=1.22$). If fatigue damage associated with top-down and bottom-up cracking are available, then the following steps may be followed. This recommended process simplifies the calibration process by calibrating the coefficients according to yearly fatigue damage increments instead of considering the accumulated damage.

- a) Calculate the “observed” accumulated fatigue damage for top-down cracking using Equation 7.2, the calibrated $C4$ and $C5$ parameters obtained using the previous step, and the observed percentage of slab with top-down transverse cracking for each pavement age, i .
- b) Calculate the fatigue damage increment between each year by subtracting the ‘observed’ accumulated fatigue damage for a given age, i , from the “observed” accumulated fatigue damage from previous year, $i-1$. This gives the observed fatigue damage increment $FDo_{i-(i-1)}$.
- c) Using the MEPDG software, obtain the PCC modulus of rupture, MR_i , at age i .
- d) Calculate the applied number of load applications, n_i , for each pavement age i according to recommendations from Chapter 2 Part 4 of the Guide for Mechanistic-Empirical Design (NCHRP 2004b).
- e) Calculate the applied stress, σ_i , at pavement age i according to recommendations from Appendix QQ of the Guide for Mechanistic-Empirical Design (NCHRP 2003e).
- f) Repeat steps a through e for bottom-down cracking.

- g) Using Equation 7.6, which was obtained from incorporating Equation 7.4 and Equation 7.5, and the corresponding values obtained from the previous steps, calibrate the parameters C1 and C2 using non-linear regression analysis.

$$FDo_{i-(i-1)} = \frac{n_i}{10 \left(C1 \left(\frac{MR_i}{\sigma_i} \right)^{C2} + 0.4371 \right)}$$

Equation 7. 6

7. Perform step 7 of the hybrid technique. Recalibrate the structural response and transfer function according to expert feedback. The effect of each calibration parameter on the model can be considered when setting constraints in the calibration.

This recommended process is a general basic process that can be improved if test sections are used to collect more detailed data.

7.4 Conclusion

Overall, it can be concluded that the hybrid technique can be applied for the calibration of the HDM-4 and MEPD performance models. Modifications regarding the amount of data collected; transfer functions between different distress measurement units; calibration sequence of distress, roughness and serviceability models; further data synthesis for the representation of distress progression in increments (for the MEPD model); and the calibration of the MEPD model's transfer and structural response functions are recommended. It can be concluded that adapting the hybrid technique to the MEPD model requires more modifications than those required for the HDM-4 model. Nevertheless, the HDM-4 transverse cracking model, which takes a logarithmic form, does not have as much flexibility to model pavement deterioration in the field as MEPD's and PMIS' sigmoidal models. The HDM-4 model has only one calibration

coefficient that does not give such flexibility. The sigmoidal form used in PMIS and MEPDG is ideal to incorporate factors like the maximum amount of distress growth, rate of distress evolution and the pavement age at which the distress starts to develop. Incorporating these factors when developing the performance models is critical especially when the pavement management database is susceptible to deficiencies and the calibrations heavily rely on expert opinion. Therefore, from these conclusions, the MEPD and PMIS models are further recommended to be used in the calibration of network level performance models.

Chapter 8: Summary, Conclusions and Recommendations

8.1 Summary

Performance models are used to predict future pavement condition by projecting distress development and ride quality loss throughout the pavement's life. Through these predictions, pavement managers are able to forecast future treatment and budget needs. Justifications of maintenance expenditures and standards are also achieved through the use of pavement performance models. Given the role they play in pavement management, it is important to have reliable models so they can remain a valuable tool in the pavement management system. Pavement performance models exist in various forms to cater to the different needs and resources of pavement management agencies. The complexity and capabilities of each model also vary depending on the management level at which they will be applied. Developing network level models may present a challenge due to the limitations of performance data kept in network level databases. The vast amount of pavement records in a network level database is vulnerable to data entry errors and missing information. Overall, these limitations can cause uncertainties regarding distress development throughout time, negatively influence performance model development, and ultimately result in models that are not truly representative of pavement deterioration.

To address these challenges a hybrid technique was developed for the calibration of network level CRC pavement performance models. It was desired to develop a general tool for pavement performance model development that could be easily adapted by network level pavement management systems. This technique combines expert knowledge and statistical tools which can be applied for the calibration of other performance models. Expert opinion can compensate for deficiencies encountered in calibrated models developed through observed performance data and

statistical techniques. Expert opinion can also complement statistically calibrated models by incorporating factors that cannot be accounted for through these calibrations. For example, the maximum allowed amount of a given distress according to the managing agency's policies and practice can be controlled through constraints. Furthermore, construction practices, climate, environment, pavement design, traffic loads, pavement type, and pavement materials can also be accounted for in model development through recommended data categorization techniques. The hybrid technique can be generally summarized as follows: first, pavement performance data is collected; second, statistical analysis of the data is performed to gain a better understanding of the available data and pavement deterioration; third, pavement age is estimated for all performance records; fourth, data sets are created according to the "windows" method; fifth, filters are applied as recommended by experts and data subsets are created; sixth, calibrations are performed through a non-linear regression analysis; and finally, data is reviewed by CRCP experts and recommended recalibrations are performed until the final pavement performance model is selected.

In this study, network level CRC pavement performance models were calibrated for TxDOT's PMIS using the hybrid technique. Improved PMIS models are needed to address the current models' reliability deficiencies in pavement performance prediction. Performance models are used in TxDOT for determining treatment needs, formulating treatment strategies, and allocating maintenance and rehabilitation budgets. Therefore, it is imperative to improve the outdated performance models so they can remain a valuable tool in PMIS. Using the hybrid technique performance models were developed for CRCP distress types (spalled cracks, punchouts, ACP patches and PCC patches) and ride quality using PMIS historical pavement performance data. The final recommended models are presented in Table 6.11.

Given the successful implementation of the hybrid technique for the calibration of PMIS' CRCP performance models, recommendations for the application of this technique for the calibration of HDM-4 and MEPD models were also presented.

8.2 Conclusions

Based on the observations made during the development of the PMIS CRCP performance models, the following conclusions were made:

1. Data entry errors (e.g. duplicate records, extreme outliers) and missing key information (e.g. pavement construction date, maintenance and rehabilitation history) are generally observed in network level PMS databases. These deficiencies prevent the calibration analysis from capturing actual CRC pavement deterioration behavior. In order to address these deficiencies, compilation and filters of the data are usually needed. Expert opinion can complement deficient pavement performance records by providing the necessary interpretations to understand pavement deterioration.
2. In general, CRC pavements are not allowed to deteriorate without being repaired by TxDOT in the short term. Punchouts and ACP patches are not common distresses in CRC pavements in Texas due to TxDOT's pavement preservation strategies. This can be concluded by the large concentration of Li values equal to zero (which means no visible distress) in the PMIS CRCP database. There were 68%, 80%, 97%, and 78% of pavement sections statewide displaying no spalled cracks, punchouts, ACP patches and PCC patches, respectively. The lack of data at a later deterioration stage made it challenging to develop performance curves to forecast future distresses; therefore, expert judgment was heavily relied on.

3. The data obtained from the data synthesis and compilation can only be used to model the deterioration trend of the records in the PMIS database. Although the compiled and synthesized data represents an improvement from the original PMIS records, the quality of the data prevents from obtaining a clear understanding of CRCP deterioration in Texas. Solely relying on the PMIS data would not give the most reliable models. Therefore, the need for expert opinion to compensate for the deficiencies of the available performance data during model development was emphasized.
4. In preliminary calibrations, the large concentration of Li values equal to zero in the data sets prevented the calibration of some Texas district and climate and subgrade zone datasets. The large Li zero value concentration represents a distress free pavement network; therefore, there are no distresses to model. On the other hand, all statewide datasets were calibrated. Furthermore, the concentration of Li values equal to zero significantly influenced the calibrations of the Li Quartile data subsets. Overall, the Li Median data subset was concluded to give the most reasonable calibrated performance models when compared to the models of the Li Quartile data subset. It was finally concluded that models calibrated with the statewide Li Median data for CRCP distresses and ride quality would be candidates for further refinement.
5. According to expert opinion and statistical analysis, CRC pavements in Texas demonstrate the following trends in distress development: spalled cracks slowly develop in CRCP; punchouts have treatment priority and should therefore be limited to a maximum of 2 punchouts per mile; ACP patches are not common in CRCP and should therefore be limited to a maximum value of one ACP patch per mile; ACP patches are used to address punchouts and should therefore have a distress starting age greater than

that of punchouts; and the maximum acceptable number of PCC patches per mile is 4. Recalibrations were therefore based on these recommendations.

6. When comparing the recalibrated distress models with the current models, it is observed that the maximum allowable amount of distress is reduced, the age at which the distress initiates is increased, and the rate of distress evolution is increased for punchouts, ACP patches and PCC patches. The opposite is observed with the spalled cracks distress.

When comparing the calibrated ride quality performance model with the current PMIS model, it was observed that the calibrated model differs in that the ride quality starts to deteriorate soon after the pavement is built, there is a slower ride quality deterioration rate, and the maximum percentage of ride quality allowed to be lost is significantly reduced (from 1.000 to 0.309).

7. The newly calibrated CRCP distress performance models using the hybrid technique represent an improvement when compared to field observations and expert judgment's opinion. As a result of the application of the hybrid technique, TxDOT has more reliable CRC pavement performance models for pavement management applications. The improvement of the calibrated PMIS curves was statistically quantified through the higher coefficient of determination value (R^2) of the recommended models when compared to the current PMIS models.
8. The hybrid technique provides a very effective tool for modeling pavement performance at the network level. The flexibility of this technique, provided by the integration of various methods, provides the necessary tools to address the challenges encountered in network level databases. These tools were a key factor in the successful implementation of the technique during the calibration of TxDOT's PMIS CRCP performance models.

Due to its adaptive nature, it is recommended for the calibration of performance models used by other pavement management agencies. .

9. Understanding the model shaping characteristics of the calibration parameters and expected field observations is imperative during the calibration process specially when there is insufficient data. Sigmoidal models are ideal for these circumstances given that its calibration parameters α , β , and ρ allow to model the maximum amount of distress permitted by the agency, the rate of pavement deterioration, and the age at which the given distress starts, respectively. Constraining the calibration parameters allows to capture expert judgment and to model pavement deterioration more accurately.

8.3 Recommendations

Based on the PMIS calibration results and the observations made during the application of the hybrid technique, the following recommendations are proposed:

1. Further refinements can be applied to the calibration's constraints to better represent any specific pavement network considered. Surveys catered to obtain a better understanding of CRCP distress development from experts can be developed. It is ideal to target CRCP experts that are familiar with the pavements whose performance is being modeled.
2. It is recommended that the performance models be recalibrated based on treatment levels because pavement deterioration varies after treatment application depending on the treatment applied. Defining different performance models for the treatment levels can provide more reliable pavement performance predictions as well as better comparisons of the effectiveness of different treatment alternatives. This can ultimately result in a better condition of the road networks and cost savings.

3. It is recommended to further validate the developed PMIS CRCP performance models by comparing their distress predictions with more complete pavement performance records. Pavement records used for the comparison should include pavement construction date, maintenance and rehabilitation history, and a complete performance history with no missing records.
4. In future research, an economic and impact analysis can be performed to determine the effect of the recalibrated performance models in budget allocation. The cost savings and improvement in pavement condition, if any, should be quantified by comparing the effectiveness of treatment strategies developed through the use of the recalibrated PMIS models with the effectiveness of strategies developed with the current PMIS models.
5. The calibration methodology presented in this research can be applied for the calibration of network level performance models for different pavement families or individual pavement sections. This methodology can also be easily implemented in other network level pavement management agencies where the amount of pavement data is not readily available.
6. The hybrid technique can be applied for the calibration of the HDM-4 and MEPD performance models. Nevertheless, modifications regarding data collection and synthesis, and calibration of multiple functions for a given distress performance model are recommended. Understanding the models used and the model shaping characteristics of the calibration parameters is imperative during the calibration process especially if databases are deficient and expert opinion is heavily relied on. The multiple calibration parameters of the MEPD and PMIS JPCP transverse

cracking sigmoidal models increase the flexibility to model pavement deterioration and allow the incorporation of expert opinion in the calibration process. Therefore, these models are especially recommended for network level pavement performance models calibrated with incomplete databases.

References

- Baus, R.L., and Stires, N.R. (2010). “Mechanistic-Empirical Pavement Design Guide Implementation.” *Department of Civil and Environmental Engineering University of South Carolina*, South Carolina, Report No. FHWA-SC-10-01.
- Bennett, C.R., Paterson, W.D.O. (2000). *A Guide to Calibration and Adaption*, Highway Development and Management Series, Vol. 5, International Study of Highway Development and Management, World Road Association, Paris.
- Brown, A. M. (2001). “A step-by-step guide to non-linear regression analysis of experimental data using a Microsoft Excel spreadsheet.” *Computer Methods and Programs in Biomedicine*, 65, 191-200.
- Bustos, M., Solminihac, H.E., Darter, M.I., Caroca, A., and Covarrubias, J.P. (1998). “Calibration of Performance Models for Jointed Plain Concrete Pavements Using Long-Term Pavement Performance Database.” *Transportation Research Record* 1629, 1947, 110-120.
- Choi, J., Chen, R.H.L. (2005). “Design of Continuously Reinforced Concrete Pavement Using Glass Fiber Reinforced Polymer Rebar.” *West Virginia Univ. and Federal Highway Administration*, Morgantown, WV, Report No. FHWA-HRT-05-081.
- Civil and Environmental Engineering Department of Michigan Technological University.
“Performance Models.” Department of Civil and Environmental Engineering,
<<http://www.cee.mtu.edu/~balkire/CE5403/Lec16.pdf>> (April 30, 2012).

Dossey, T., Turen, T., McCullough B.F. (1998). "The Rigid Pavement Database: Overview and Data Collection Plan." *Center for Transportation Research*, Austin, Texas, Report No. TX-98/2952-1.

Federal Highway Administration. (2010). "Local Calibration of the MEPDG Using Pavement Management Systems Final Report Volume 1." *Federal Highway Administration Office of Asset Management*, Washington, DC, Report No. HIF-11-026.

Gharaibeh, N., Saliminejad, S., Wimsatt, A., Freeman, T., Chang-Albitres, C., Weissman, A., Weissman, J., Gurganus, C. (2012). "Evaluation and Development of Pavement Scores, Performance Models and Needs Estimates for the TxDOT Pavement Management Information System Final Report." *Texas Transportation Institute*; College Station, Texas, Report No. FWHA/TX-12/0-6386-3.

Huang, Y. H. (2004). *Pavement analysis and design*, 2nd Ed., Pearson Prentice Hall.

Kerali, H.R. and Odoki, J.B. (2000). *Analytical framework and model descriptions*, Highway Development and Management Series, Vol. 4, International Study of Highway Development and Management, World Road Association, Paris.

Kerali, H.R., Robinson, R., and Paterson, W.D. O. (1988). "Role of the new HDM-4 in highway management." *Proc., 4th Int. Conf. on Managing Pavements*, 2, 801–814.

Liebertz, J.P. (2010). "Colombia Pike The History of an Early Turnpike." *Arlington County Historic Preservation Office*.

Lytton, R. L. (1987). “Concepts of pavement performance prediction and modeling.” *Proc., 2nd North American Pavement Management Conf.*, Vol. 2, Canada, 2.4–2.19.

Mendenhall, W., Beaver, R.J., and Beaver, B.M. (2009). *Introduction to probability and statistics*, 13th ed., Duxbury Press, Pacific Grove, California.

Muench, S. T., Mahoney, J. P., and Pierce, L. M. (2003). *WSDOT pavement guide interactive* (CD-ROM), Washington State Dept. of Transportation, Olympia, Washington.

National Cooperative Highway Research Program (NCHRP). (2003a). “Guide for Mechanistic-Empirical Design of New and Rehabilitated Pavement Structures. Final Report for Project 1-37A. Appendix KK: Transverse Cracking of JPCP.” *NCHRP, Transportation Research Board, National Research Council*, Washington, D.C.

National Cooperative Highway Research Program (NCHRP). (2003b). “Guide for Mechanistic-Empirical Design of New and Rehabilitated Pavement Structures. Final Report for Project 1-37A. Appendix JJ: Transverse Joint Faulting Model.” *NCHRP, Transportation Research Board, National Research Council*, Washington, D.C.

National Cooperative Highway Research Program (NCHRP). (2003c). “Guide for Mechanistic-Empirical Design of New and Rehabilitated Pavement Structures. Final Report for Project 1-37A. Appendix LL: Punchouts in Continuously Reinforced Concrete Pavements.” *NCHRP, Transportation Research Board, National Research Council*, Washington, D.C.

National Cooperative Highway Research Program (NCHRP). (2003d). “Guide for Mechanistic-Empirical Design of New and Rehabilitated Pavement Structures. Final Report for Project 1-

37A. Appendix PP: Smoothness Prediction for Rigid Pavements.” *NCHRP, Transportation Research Board, National Research Council*, Washington, D.C.

National Cooperative Highway Research Program (NCHRP). (2003e). “Guide for Mechanistic-Empirical Design of New and Rehabilitated Pavement Structures. Final Report for Project 1-37A. Appendix QQ: Structural Response Models for Rigid Pavements.” *NCHRP, Transportation Research Board, National Research Council*, Washington, D.C.

National Cooperative Highway Research Program (NCHRP). (2004a). “Guide for Mechanistic-Empirical Design of New and Rehabilitated Pavement Structures. Final Report for Project 1-37A. Part 1, Chapter 1.” *NCHRP, Transportation Research Board, National Research Council*, Washington, D.C.

National Cooperative Highway Research Program (NCHRP). (2004b). “Guide for Mechanistic-Empirical Design of New and Rehabilitated Pavement Structures. Final Report for Project 1-37A. Part 2, Chapter 4.” *NCHRP, Transportation Research Board, National Research Council*, Washington, D.C.

Rao, R.V. (2011). “Advanced Modeling and Optimization of Manufacturing Processes” *Springer-Verlag London*, New York, New York.

Rauhut, J.B., and Gendel, D.S. (1987). “Proposed Development of Pavement Performance Prediction Models from SHRP/LTPP Data.” *2nd North American Pavement Management Conference*.

Robinson, C.A., Anderson, V., Dossey, T., and Hudson, W.R. (1995). “Improved Distress Prediction Models for Rigid Pavements in Texas.” *Center for Transportation Research and Texas Department of Transportation*, Austin, Texas, Report No. TX+1908-4.

Saba, R.G. (2007). “Performance Prediction Models for Flexible Pavements.” *Nordic Road and Transport Research No. 1*, Norway.

Sadek, A.W., Freeman, T.E., and Demetsky, M.J. (1996). “Deterioration Prediction Modeling of Virginia’s Interstate Highway System.” *Transportation Research Record*, 1524, 118-129.

Shiraz, D.T., Wu, C.L., Plei, M. (2001). “Performance of Continuously Reinforced Concrete Pavements in the LTPP Program” *7th International Conference on Concrete Pavements*, Orlando, Florida.

Texas Department of Transportation (TxDOT). (2012). “Local Information.” *Texas Department of Transportation*, <http://www.txdot.gov/local_information/> (March 30, 2012).

Texas Department of Transportation Construction Division, Materials and Pavements Section (TxDOT). (2010). “PMIS Technical Manual.” *Texas Department of Transportation*, Austin, Texas.

Texas Department of Transportation. (2009). “Pavement Management Information System Rater’s Manual Fiscal Year 2010.” *Texas Department of Transportation*, Austin, Texas.

Appendix A: HDM-4 and MEPD Pavement Performance Models for Rigid Pavement

HDM-4 Pavement Performance Models for Rigid pavement

A.1. Transverse Cracking

A.1.1 Jointed Plain Concrete Pavement

For jointed plain concrete pavement, transverse cracking is a function of cumulative fatigue damage in slabs. Equation A.1 is a deterministic model used to determine the percent of the slab that is cracked.

$$\text{PCRACK} = K_{\text{jpc}} \times \frac{100}{1 + 1.41 \times \text{FD}^{-1.66}} \quad \text{Equation A.1}$$

K_{jpc} is the calibration factor, which is by default set to 1. FD is the cumulative fatigue damage which is a dimensionless factor obtained from Equation A.2. It is calculated by summing the damage index over each slab thermal condition or temperature gradient and axle load distribution (Kerali and Odoki 2000).

$$\text{FD} = \sum_{\text{tg}=1}^G \frac{n_{\text{tg}}}{N_{\text{tg}}} \quad \text{Equation A.2}$$

The variable n_{tg} , which is expressed in ESALS per lane, is the number of 18 kip equivalent single axle load passes during temperature gradient tg. N_{tg} is the maximum number of 18 kip equivalent standard axle load repetitions during temperature gradient tg before flexural failure occurs. It is also expressed in ESALS per lane. The variables n_{tg} and N_{tg} are calculated by Equation A.3 and Equation A.4, respectively (Kerali and Odoki 2000).

$$n_{\text{tg}} = \frac{\text{NE4}}{\text{LCR}_{\text{tg}}} \times \text{FREQ}_{\text{tg}} \quad \text{Equation A.3}$$

$$\log_{10} N_{\text{tg}} = 2.13 \times \text{SR}_{\text{tg}}^{-1.2} \quad \text{Equation A.4}$$

where:

NE4= cumulative number of ESALs since construction of pavement, in millions 18-kip axles per lane

FREQ_{tg}= frequency of each temperature gradient tg. This value can be obtained from field data or a default data set based on climate zones provided in HDM-4 Manual Volume 4.

LCR_{tg}=lateral coverage ratio of traffic, for temperature gradient tg. This is a measure of the likelihood that the wheel loading will pass through the critical edge location. Equation A.5 is used to calculate this value.

SR_{tg}= ratio between combined stress in slab and the Modulus of Rupture of concrete for temperature gradient tg. This is calculated with Equation A.6.

$$LCR_{tg} = 418.9 - 1148.6 \times SR_{tg} + 1259.9 \times SR_{tg}^2 - 491.55 \times SR_{tg}^3 \quad \text{Equation A.5}$$

$$SR_{tg} = \frac{SIGMA_{tg}}{MR} \quad \text{Equation A.6}$$

The variable MR is the modulus of rupture of concrete which is expressed in psi. The variable SIGMA_{tg} is the combined stress (in psi) in the slab edge due to loading and curling for the temperature gradient tg. It is calculated through Equation A.7.

$$SIGMA_{tg} = f_{SB} \times (\sigma_{load(tg)} + R_{tg} \times \sigma_{curl(tg)}) \quad \text{Equation A.7}$$

where:

f_{SB}=adjustment factor for stabilized bases. This is calculated through Equation A.8.

σ_{load(tg)}=stress in slab edge due to traffic loading (psi). This stress is produced by traffic loads. It is calculated through Equation A.11.

R_{tg}=regression coefficient. This coefficient is calculated with Equation A.17.

σ_{curl(tg)}=stress in slab edge due to curling (psi). This stress is calculated through Equation A.21.

$$f_{SB} = \frac{2 \times (SLABTHK - NAXIS)}{EFFETHK} \quad \text{Equation A.8}$$

where:

SLABTHK=slab thickness (inches)

NAXIS=location of the neutral axis. This is calculated with Equation A.9.

EFFTHK=effective slab thickness (inches). This is calculated by using Equation A.10.

$$NAXIS = \frac{0.5 \times SLABTHK^2 + \frac{E_{base}}{E_c} \times BASETHK \times (SLABTHK + 0.5 \times BASETHK)}{SLABTHK^2 + \frac{E_{base}}{E_c} \times BASETHK}$$

Equation A.9

$$EFFETHK = \left[SLABTHK^2 + BASETHK^2 \times \frac{E_{base} \times BASETHK}{E_c \times SLABTHK} \right]^{0.5}$$

Equation A.10

where:

E_{base} =modulus of elasticity of stabilized base (psi)

E_c =modulus of elasticity of concrete (psi)

BASETHK=thickness of the stabilized base (inches)

In order to calculate the stress in slab edge due to traffic loading, σ_{load} , Equation A.11 was used.

$$\sigma_{load} = f_{ES} \times f_{WL} \times \sigma_e$$

Equation A.11

Where:

f_{ES} =adjustment factor for edge support (for example, shoulder support). This is calculated with Equation A.12.

f_{WL} = adjustment factor for widened outside lanes. This is calculated with Equation A.13.

σ_e =edge stress obtained from Westergaard's equations. This is calculated using Equation A.15.

$$f_{ES} = \frac{100}{100 + L_{TESH}}$$

Equation A.12

where:

LTE_{SH}=efficiency load transfer between slab and edge support (%). A default value of 20 can be used if concrete shoulders are placed during initial construction. If they are placed after initial construction, then a value of 10 should be used.

$$f_{WL} = 0.454147 + \frac{0.013211 \times \ell}{DW} + 0.386201 \times \left(\frac{a}{DW}\right) - 0.24565 \times \left(\frac{a}{DW}\right)^2 + 0.053891 \times \left(\frac{a}{DW}\right)^3$$

Equation A.13

where:

ℓ =radius of relative stiffness of the slab-foundation system (inches). This is calculated using Equation A.14.

DW= average wheels location, given by the average distance of the exterior wheel to slab edge (inches).

a= load application radius for single-wheel single axle (inches).

$$\ell = \left[\frac{E_c \times \text{SLABTHK}^3}{12 \times (1 - \mu^2) \times \text{KSTAT}} \right]^{0.25}$$

Equation A.14

where:

E_c = modulus of elasticity of concrete (psi)

μ = Poisson's ratio

KSTAT= modulus of subgrade reaction (pci)

The edge stress in the slab is calculated using Westergard's equation for a circular load (Equation A.15).

$$\sigma_e = \frac{3 \times (1 + \mu) \times P}{\pi(3 + \mu) \times \text{SLABTHK}^2} \left[\ln \left(\frac{E_c \times \text{SLABTHK}^3}{100 \times \text{KSTAT} \times a_{eq}^4} \right) + 1.84 - \frac{4\mu}{3} + \frac{1 - \mu}{2} + 1.18 \right. \\ \left. \times (1 + 2\mu) \frac{a_{eq}}{\ell} \right]$$

Equation A.15

Where:

P=total load applied by each wheel of a single-axle dual wheel (lb). A default value of 9,000 lb can be used.

a_{eq}=equivalent load application radius for a dual-wheel single axle (inches). This is calculated using Equation A.16.

$$\frac{a_{eq}}{a} = \left[0.909 + 0.339485 \times \left(\frac{SP}{a} \right) + 0.103946 \times \left(\frac{a}{\ell} \right) - 0.017881 \times \left(\frac{SP}{a} \right)^2 - 0.045229 \right. \\ \times \left(\frac{SP}{a} \right)^2 + 0.000436 \times \left(\frac{SP}{a} \right)^3 - 0.301805 \times \left(\frac{SP}{a} \right) \times \left(\frac{a}{\ell} \right)^3 + 0.034664 \times \left(\frac{SP}{a} \right)^2 \\ \left. + 0.001 \times \left(\frac{SP}{a} \right)^3 \times \left(\frac{a}{\ell} \right) \right]$$

Equation A.16

Limits: $0 \leq \frac{SP}{a} \leq 20$

$0 \leq \frac{a}{\ell} \leq 0.5$

where:

a= load application radius for a single-wheel single axle (inches). This is calculated by the square root of (P/π)*p.

p=tire pressure

SP=spacing between central wheels of dual wheel single axle (inches)

$$\begin{aligned}
R = & 86.97 \times Y^3 - (1.051 \times 10^{-9} \times E_c \times dT \times KSTAT + 1.7487 \times dT) \times Y^2 \\
& - (1.068 - 0.387317 \times dT - 1.84 \times 10^{-11} \times E_c \times dT^2 \times KSTAT + 8.16396 \\
& \times dT^2) \times Y \\
& + (1.062 - 1.5757 \times 10^{-2} \times dT - 8.76 \times 10^{-5} \times KSTAT \\
& + (1.17 - 0.181 \times dT) \times 10^{-11} \times E_c \times dT \times KSTAT)
\end{aligned}$$

Equation A.17

The variables Y and dT can be calculated with Equation A.18 and Equation A.19, respectively.

$$Y = \frac{12 \times \text{JTSPACE}}{100 \times \ell} \quad \text{Equation A.18}$$

$$dT = \alpha_T \times \Delta T_s \times 10^5 \quad \text{Equation A.19}$$

where:

JTSPACE=average transverse joint spacing (ft)

α_T =thermal coefficient of concrete (per °F)

ΔT_s = adjusted difference in temperature at the top and bottom of the slab (°F). This can be calculated with Equation A.20.

$$\Delta T_s = \Delta T - \left[a_0 + \frac{a_1 \times (\text{SLABTHK} - 2)}{\text{SLABTHK}^3} \right] \quad \text{Equation A.20}$$

The model coefficients a0 and a1 are based on climate zones and can be determined from Table A.1.

Table 6. A.13. Model Coefficient for Temperature Correction (adapted from Volume 4 of HDM-4 Manual).

| Climate Type | a0 | a1 |
|----------------------|------|--------|
| Dry with freezing | 6.29 | 436.36 |
| Dry without freezing | 7.68 | 436.36 |
| Wet with freezing | 5.03 | 327.27 |
| Wet without freezing | 6.66 | 218.18 |

The stress in the slab edge due to curling can be calculated through Equation A.21.

$$\sigma_{\text{curl}} = \frac{\text{COEF} \times E_c \times \alpha_T \times \Delta T_s}{2} \quad \text{Equation A.21}$$

Where:

E_c = modulus of elasticity of concrete (psi)

α_T = thermal coefficient of concrete (per °F)

ΔT_s = adjusted difference in temperature at the top and bottom of the slab (°F).

COEF = curling stress coefficient. This variable is calculated with the help of Equation A.22.

$$\text{COEF} = 1 - \left[\frac{2 \times \cos \lambda \times \cosh \lambda}{\sin 2\lambda + 2 \times \sinh \lambda \times \cosh \lambda} \right] \times \left[\tan \lambda \times \cosh \lambda + \left(\frac{\sinh \lambda}{\cosh \lambda} \right) \right] \quad \text{Equation A.22}$$

The variable λ , which is an intermediate parameter expressed in sexagesimal degrees, can be calculated through Equation A.23. JTSPACE is the average transverse joint spacing and ℓ is radius of relative stiffness of the slab-foundation system.

$$\lambda = \frac{12 \times \text{JTSPACE}}{\ell \times \sqrt{8}} \quad \text{Equation A.23}$$

Given that there are a large number of equations used to calculate transverse cracking in jointed plain concrete pavement, a diagram showing the relationships between the equations was developed. Figure A.1 shows the dependency between equations in the calculation of transverse cracking.

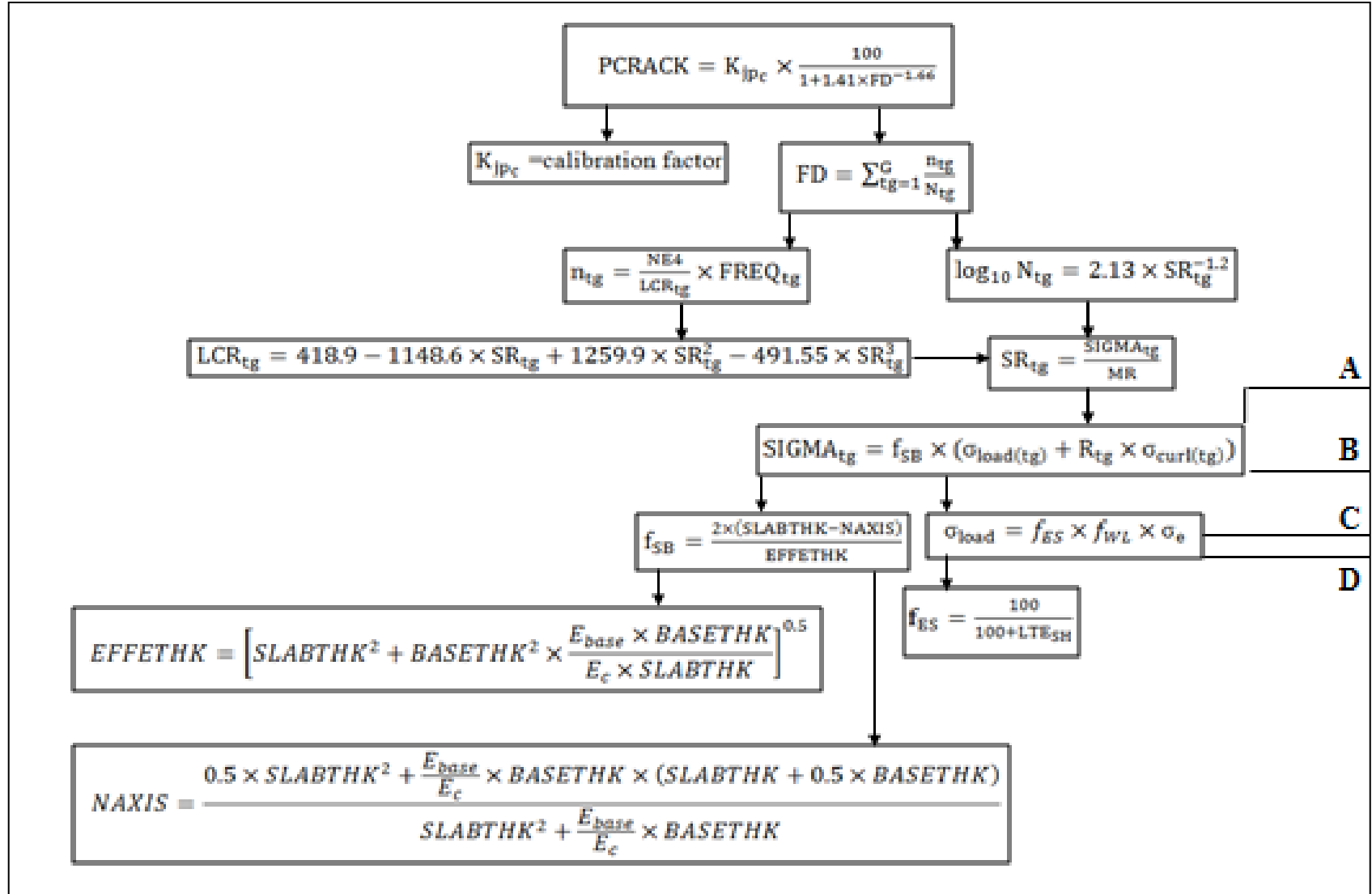


Figure 6. A.17. Relationship Diagram of Equations used for Calculating Transverse Cracking in Jointed Plain Concrete Pavement (Part A).

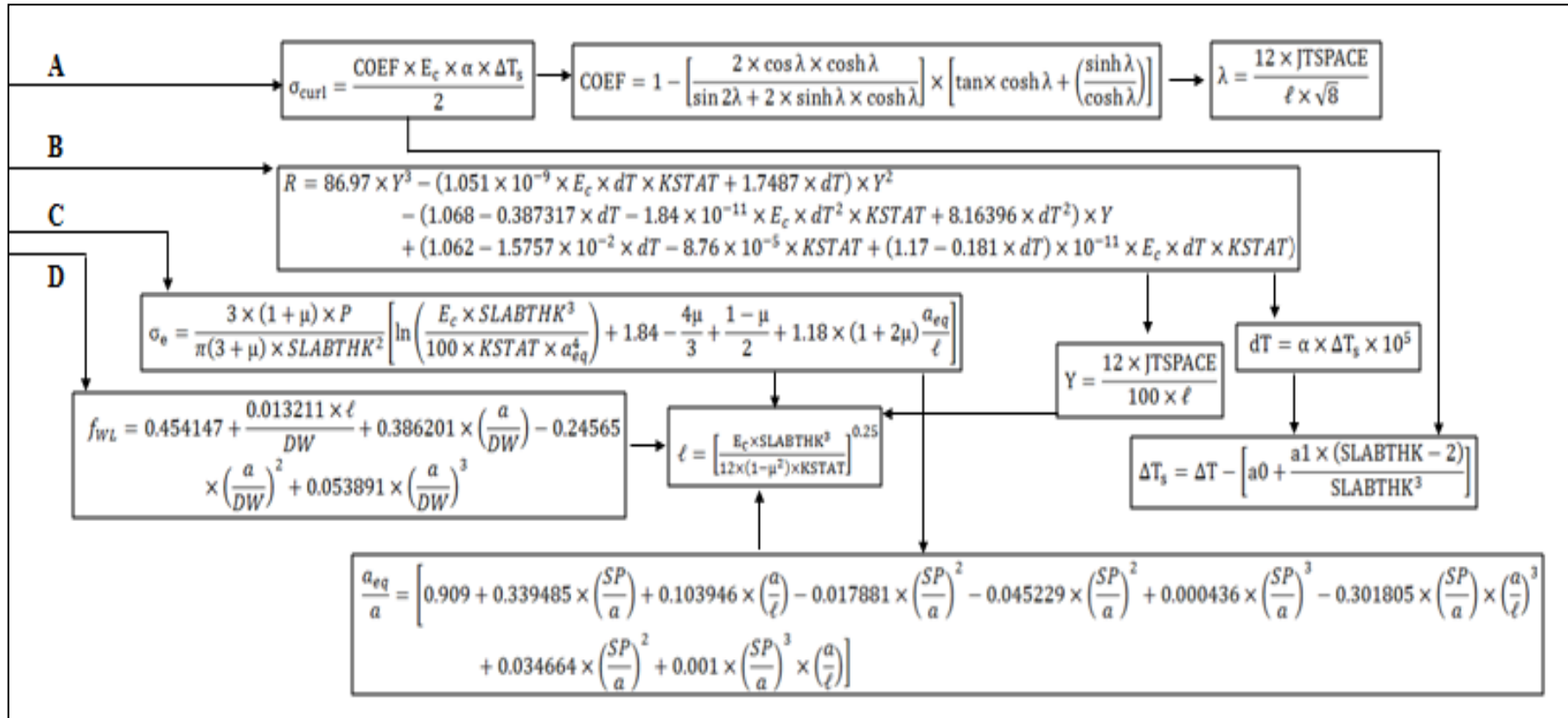


Figure 6. A.18. Relationship Diagram of Equations used for Calculating Transverse Cracking in Jointed Plain Concrete Pavement (Part B).

A.1.2 Jointed Reinforced Concrete Pavement

The number of deteriorated cracks per mile for JRCP is calculated using Equation A.24.

$$\begin{aligned} \text{DCRACK} = & K_{jr_c} \times \text{AGE}^{2.5} \\ & \times \left[6.88 \times 10^{-5} \times \frac{\text{FI}}{\text{SLABTHK}} + \text{NE4} \times (0.116 - 0.073 \times \text{BASE}) \right. \\ & \times (1 - \exp(-0.032 \times \text{MI})) \\ & \left. \times \exp[7.5518 - 66.5 \times \text{PSTEEL} - (1 - 5 \times \text{PSTEEL}) \times E_c \times 10^{-6}] \right] \end{aligned}$$

Equation A.24

Where:

AGE=number of years since pavement construction

FI=freezing index (°F-days)

SLABTHK=slab thickness (inches)

NE4=cumulative ESALs since pavement construction

BASE= base type:

0 if not stabilized

1 if stabilized

MI=Thornthwaite moisture index

PSTEEL=percentage of longitudinal steel reinforcement

E_c =Modulus of elasticity of concrete (psi)

K_{jr_c} =calibration factor (default=1)

A.2 Faulting

A.2.1 Jointed Plain Concrete Pavement without Load Transfer Dowels

The average transverse joint faulting for JPCP, which is measured in inches, is modeled with Equation A.25.

$$\begin{aligned}
\text{FAULT} = & K_{jpn_f} \times NE4^{0.25} \\
& \times \left[0.2347 - 0.1516 \times C_d - 0.00025 \times \left(\frac{SLABTHK^2}{JTSPACE^{0.25}} \right) \right. \\
& - (0.0115 \times \text{BASE} + 7.78 \times 10^{-8} \times FI^{1.5} \text{PRECIP}^{0.25}) \\
& \left. - (0.002478 \times \text{DAYS90}^{0.5} - 0.0415 \times \text{WIDENED}) \right]
\end{aligned}$$

Equation A.25

Where:

NE4=cumulative ESALs since pavement construction

C_d =drainage coefficient

SLABTHK=slab thickness (inches)

JTSPACE=average transverse joint spacing (ft)

BASE= base type:

0 if not stabilized

1 if stabilized

FI=freezing index (°F-days)

PRECIP=annual average precipitation (inches)

DAYS90=number of days with mean temperature greater than 90°F

WIDENED= widened lane:

0 if not widened

1 if widened

K_{jpn_f} = calibration factor (default=1.0)

A.2.2 Jointed Plain Concrete Pavement with Load Transfer Dowels

Transverse joint faulting in JPCP with load transfer dowels is predicted using Equation A.26.

$$\begin{aligned}
\text{FAULT} = & K_{jpd_f} \times NE4^{0.25} \\
& \times [0.0628 \times (1 - C_d) + 3.673 \times 10^{-9} \times \text{BSTRESS}^2 \\
& + (4.116 \times 10^{-6} \times \text{JTSPACE}^2 + 7.466 \times 10^{-10} \times FI^2 \times \text{PRECIP}^{0.5}) \\
& - (0.009503 \times \text{BASE} - 0.01917 \times \text{WIDENED} + 0.0009217 \times \text{AGE})]
\end{aligned}$$

Equation A.26

Where:

NE4=cumulative ESALS since pavement construction

C_d=drainage coefficient

BSTRESS=maximum concrete bearing stress in the dowel-concrete system (psi). This variable is calculated using Equation A.27.

JTSPACE=average transverse joint spacing (ft)

FI=freezing index (°F-days)

PRECIP=annual average precipitation (inches)

BASE= base type:

0 if not stabilized

1 if stabilized

WIDENED= widened lane:

0 if not widened

1 if widened

AGE=number of years since pavement construction

Kjpd_f=calibration factor (default=1.0)

$$BSTRESS = \frac{DFAC \times P \times LT \times K_d \times (2 + BETA \times OPENING)}{4 \times E_s \times INERT \times BETA^3}$$

Equation A.27

where:

DEFAC=distribution factor which is calculated by $\frac{24}{(\ell+12)}$. The variable ℓ is the radius of relative stiffness which is calculated using Equation A.14.

P=total load applied by each wheel of a single-axle dual wheel (lb). The default value used is 9,000.

LT=percentage of load transfer between joints. The default value used is 45.

K_d=modulus of dowel support, in pci (default=1.5x10⁶ psi/in)

BETA=relative stiffness of the dowel-concrete system. This value is calculated using

Equation A.28.

OPENING=average transverse joint opening (inches). This value is calculated using Equation A.29.

E_s =modulus of elasticity of dowel bar (psi)

INERT=moment of inertia of the transverse section of the dowel bar (in⁴). Inert is calculated using Equation A.30.

$$BETA = \left[\frac{K_d \times DOWEL}{4 \times E_s \times INERT} \right]^{0.25}$$

Equation A.28

where:

K_d =modulus of dowel support, in pci (default=1.5x10⁶ psi/in)

DOWEL=dowel diameter (inches)

E_s =modulus of elasticity of dowel bar (psi)

INERT=moment of inertia of the transverse section of the dowel bar (in⁴)

$$OPENING = 12 \times CON \times JTSPACE \times \left[\left(\frac{\alpha_T \times TRANGE}{2} \right) + \gamma \right]$$

Equation A.29

where:

CON=adjustment factor due to base/slab frictional restraint:

0.80 if not stabilized base

0.65 if stabilized base

JTSPACE=average transverse joint spacing (ft)

α_T =thermal coefficient of concrete (per °F)

TRANGE=temperature range (the mean monthly temperature range obtained from data on the difference between the maximum and the minimum temperature for each month) (°F)

γ =drying shrinkage coefficient of concrete

$$INERT = 0.25 \times \pi \times \left(\frac{DOWEL}{2} \right)^4$$

Equation A.30

where:

DOWEL=dowel diameter (inches)

A.2.3 Jointed Reinforced Concrete Pavement

Equation A.31 shows the model used for jointed reinforced concrete pavement model for faulting (Kerali and Odoki 2000).

$$\begin{aligned} \text{FAULT} = & K_{jr_f} \times \text{NE4}^{0.25} \\ & \times [0.0628 \times (1 - C_d) + 3.673 \times 10^{-9} \times \text{BSTRESS}^2 \\ & + (4.116 \times 10^{-6} \times \text{JTSPACE}^2 + 7.446 \times 10^{-10} \times \text{FI}^2 \times \text{PRECIP}^{0.5}) \\ & - (0.009503 \times \text{BASE} - 0.01917 \times \text{WIDENED} + 0.0009217 \times \text{AGE})] \end{aligned}$$

Equation A.31

where:

NE4=cumulative ESALS since pavement construction

C_d=drainage coefficient, modified AASHTO

BSTRESS=maximum concrete bearing stress, in the dowel-concrete system (psi)

JTSPACE=average transverse joint spacing (ft)

FI=freezing index (°F-days)

PRECIP=annual average precipitation (inches)

BASE= base type:

0 if not stabilized

1 if stabilized

WIDENED= widened lane:

0 if not widened

0.5 if concrete shoulders are placed after initial construction

1 if widened or shoulders provided during initial construction

AGE=number of years since pavement construction

K_{jr_f}=calibration factor (default=1.0)

A.3 Spalling

A.3.1 Jointed Plain Concrete Pavement

The percentage of spalled transverse cracks in JPCP is modeled through Equation A.32 (Kerali and Odoki 2000).

$$\begin{aligned} \text{SPALL} = & K_{jp_s} \times \text{AGE}^2 \times \text{JTSPACE} \times 10^{-6} \\ & \times [549.9 - 895.7 \times (\text{LIQSEAL} + \text{PREFSEAL}) + 1.11 \times \text{DAYS90}^3 \times 10^{-3} + 375 \\ & \times \text{DWLCOR} + (29.01 - 27.6 \times \text{LIQSEAL}) \times \text{FI} \\ & - (28.59 \times \text{PREFSEAL} + 27.09 \times \text{SILSEAL})] \end{aligned}$$

Equation A.32

where:

SPALL=percentage of spalled transverse joints

AGE=age since pavement construction (years)

JTSPACE=average transverse joint spacing (ft)

LIQSEAL=presence of liquid sealant in joint

0 if not present

1 if present

PREFSEAL=presence of pre-formed sealant in joint

0 if not present

1 if present

DAYS90=number of days with temperature greater than 90°F

DWLCOR=dowel corrosion protection:

0 if no dowels exist, or are protected from corrosion

1 if dowels are not protected from corrosion

FI=freezing index (°F-days)

SIPSEAL=presence of silicone sealant in joint:

0 if not present

1 if present

K_{jp_s} =calibration factor (default=1.0)

A.3.2 Jointed Reinforced Concrete Pavement

As for JRCP, the transverse joint spalling is predicted using Equation A.33.

$$\text{SPALL} = K_{jr_s} \times \text{AGE}^3 \times \text{JTSPACE} \times 10^{-5} \\ \times [1.94 \times \text{DWLCOR} + 8.819 \times \text{BASE} \times (1 - \text{PREFSEAL}) + 7.01 \times \text{FI} \times 10^{-3}]$$

Equation A.33

where:

AGE=age since pavement construction (years)

JTSPACE=average transverse joint spacing (ft)

DWLCOR=dowel corrosion protection:

0 if no dowels exist, or are protected from corrosion

1 if dowels are not protected from corrosion

PREFSEAL=presence of pre-formed sealant in joint

0 if not present

1 if present

BASE= base type:

0 if not stabilized

1 if stabilized

FI=freezing index (°F-days)

K_{jr_s} =calibration factor (default=1.0)

A.4 Failures for CRCP

Equation A.34 is used to predict the number of failures per mile in the more trafficked lane of a CRC pavement.

$$\log_e \text{FAIL} = K_{cr_f} \\ \times [6.8004 - 0.0334 \times \text{SLABTHK}^2 - 6.5858 \times \text{PSTEEL} + 1.2875 \times \log_e \text{NE4} \\ - 1.1408 \times \text{AB} - 0.9367 \times \text{SB} - 0.8908 \times \text{GB} - 0.1258 \times \text{CHAIRS}]$$

Equation A.34

where:

SLABTHK=slab thickness (in)

PSTEEL=percentage of longitudinal reinforcement steel (%)

NE4=cumulative equivalent standard axle load (ESALs) since pavement construction (millions per lane)

AB 1 if base type is asphaltic

0 in other cases

SB 1 if base type is cement stabilized

0 in other cases

GB 1 if base type is granular

0 in other cases

CHAIRS

1 if chairs are used for installation of the reinforcement

0 if tubes are used

Kcrf=calibration factor (default=1.0)

A.5 Present Serviceability Rating

A.5.1 Jointed Reinforced Concrete Pavement

Equation A.35 shows the model used to predict PSR for JRCP in HDM-4.

$$PSR = 4.165 - 0.06694 \times TFAULT^{0.5} - 0.00003228 \times DCRACK^2 - 0.1447 \times SPALL^{0.25}$$

Equation A.35

where:

TFAULT=total transverse joint faulting per mile (in/mile). This is calculated using Equation 42.

DCRACK=number of deteriorated transverse cracks per mile. This is calculated using Equation A.24.

SPALL=percentage of spalled joints. This is calculated using Equation A.33.

$$TFAULT = \frac{FAULT \times 5280}{JTSPACE}$$

Equation A.36

where:

FAULT=average transverse joint faulting (in). This is calculated using Equation A.31.

JTSPACE= average transverse joint spacing (ft).

A.5.2 Continuously Reinforced Concrete Pavement

Equation A.37 is used to model serviceability loss for continuously reinforced concrete pavements.

$$\begin{aligned} \log_{10}(PSR_0 - PSR_t) \\ = [0.79 - 1.3121 \\ \times \log_{10} SLABTHK + 0.1849 \times \log_{10} AGE + 0.2634 \times \log_{10} NE4] \end{aligned}$$

Equation A.37

where:

PSR₀=initial PSR at the time of pavement construction (default=4.5)

PSR_t=predicted PSR value at time t

SLABTHK=slab thickness (in)

AGE=age since pavement construction (years)

NE4=cumulative equivalent standard axle load

A.6 Roughness

A.6.1 Jointed Plain Concrete Pavement

Roughness on JPCP pavement is calculated using Equation A.38.

$$RI_t = K_{jp_r} \times (RI_0 + 2.6098 \times TFAULT + 1.8407 \times SPALL + 2.2802 \times 10^{-6} \times TCRACKS^3)$$

Equation A.38

where:

RI_t =roughness at time t (in/mile)

RI_0 =initial roughness at the time of pavement construction (in/mile) (default=98.9)

TFAULT=total transverse joint faulting per mile (in/mile). This is calculated using Equation A.36.

SPALL=percentage of spalled joints. This is calculated using Equation A.32.

TCRACKS=Total number of cracked slabs per mile. This is calculated using Equation A.39.

K_{jp_r} =calibration factor (default=1.0)

$$TCRACKS = \frac{PCRACK \times 5280}{JTSPACE \times 100} \quad \text{Equation A.39}$$

where:

PCRACK=percent of slabs cracked. This is calculated using Equation A.1.

JTSPACE=average transverse joint spacing (ft).

A.6.2 Jointed Reinforced Concrete Pavement

Roughness on JRCp pavement is calculated using Equation A.40.

$$RI_t = K_{jr_r} \times \left[-\log_e \left(\frac{0.2 \times PSR_t}{0.0043} \right) \right] \quad \text{Equation A.40}$$

where:

RI_t =roughness at time t (in/mile)

PSR_t =serviceability rating at time t

K_{jr_r} =calibration factor (default=1.0)

A.6.3 Continuously Reinforced Concrete Pavement

Roughness on CRC pavement is calculated using Equation A.41.

$$RI_t = K_{cr_r} \times \left[-\log_e \left(\frac{0.2 \times PSR_t}{0.0043} \right) \right] \quad \text{Equation A.41}$$

where:

RI_t =roughness at time t (in/mile)

PSR_t =serviceability rating at time t

Kcr_r=calibration factor (default=1.0)

MEPD Pavement Performance Models for Rigid pavement

A.7 Jointed Plain Concrete Pavement

A.7.1 Transverse Slab Cracking

Since damage accumulates differently for both types of cracking, the damage for each needs to be computed separately. Equation A.42 is used to calculate the transverse cracking for each type of transverse cracking. The accumulated fatigue damage (FD) is calculated through structural response models on a monthly basis considering daytime and nighttime hourly thermal gradients. Other factors considered in the calculation of the fatigue damage include: age, month, axle type, load level, temperature difference and traffic path (NCHRP 2003a).

$$CRK = \frac{1}{1 + FD^{-1.68}}$$

Equation A.42

where:

CRK=predicted amount of bottom-up or top-down cracking (fraction)

FD=accumulated fatigue damage calculated through Equation A.43

$$FD = \sum \frac{n_{i,j,k,l,m,n}}{N_{i,j,k,l,m,n}}$$

Equation A.43

Where:

FD=total accumulated fatigue damage (top-down or bottom-up)

$n_{i,j,k,l,m,n}$ =applied number of load applications at condition i,j,k,l,m,n

$N_{i,j,k,l,m,n}$ =allowable number of load applications at condition i,j,k,l,m,n. This factor is the number of load cycles at which the fatigue failure is expected. Fatigue failure is assumed to occur at 50 percent slab cracking. The allowable number of load repetitions

is a function of the applied stress and PCC strength. It is calculated through Equation A.44.

i=age (accounts for change in PCC modulus of rupture, layer bond condition, and deterioration of shoulder LTE)

j= month (accounts for change in base and effective dynamic modulus of subgrade reaction)

k= axle type (single, tandem, and tridem for bottom-up cracking; short, medium and long wheelbase for top-down cracking)

l=load level (incremental load for each axle type)

m=temperature difference

n=traffic path

$$\log(N_{i,j,k,l,m,n}) = C_1 \times \left(\frac{MR_i}{\sigma_{i,j,k,l,m,n}} \right)^{C_2} + 0.4371$$

Equation A.44

Where:

$N_{i,j,k,l,m,n}$ = allowable number of load applications at condition i,j,k,l,m,n

MR_i = PCC modulus of rupture at age i, psi

$\sigma_{i,j,k,l,m,n}$ = applied stress at condition i,j,k,l,m,n

C_1 = calibration constant= 2.0

C_2 = calibration constant= 1.22

After calculating the damage for top-down and bottom-up transverse cracking, Equation A.45 is used to calculate the total transverse cracking. Since top-down and bottom-up cracking cannot occur at the same time, Equation A.45 eliminates this possibility through the inclusion of the third term of the equation (NCHRP 2003a).

$$TCRACK = [CRK_{Bottom-up} + CRK_{top-down} - (CRK_{Bottom-up} \times CRK_{top-down})] \times 100\%$$

Equation A.45

where:

TCRACK=total transverse cracking (percent)

CRK_{Bottom-up}=predicted amount of bottom-up cracking (fraction). This is obtained through Equation A.42.

CRK_{top-down}=predicted amount of top-down cracking (fraction). This is obtained through Equation A.42.

A.7.2 Mean Transverse Joint Faulting

Faulting is calculated by summing the accumulated faulting from all previous months. Equation A.46 is used to determine the mean joint faulting at the end of the month, m.

$$\text{Fault}_m = \sum_{i=1}^m \Delta\text{Fault}_i$$

Equation A.46

Where:

ΔFault_i =incremental change in mean transverse joint faulting during month i, inches.

The increment in faulting in a given month is calculated through Equation A.47.

m=month

$$\Delta\text{Fault}_i = C_{34} \times (\text{FMAX}_{i-1} - \text{FAULT}_{i-1})^2 \times \text{DE}_i$$

Equation A.47

Where:

$$C_{34} = C_3 + C_4 \times \text{FR}^{0.25}$$

C_3 and C_4 are calibration coefficients

FR=Base Freezing Index

$C_3=0.001725$

$C_4=0.0008$

$FMAX_{i-1}$ =maximum mean transverse joint faulting for the previous month, inches. This is calculated with Equation A.48.

$FAULT_{i-1}$ =mean joint faulting at the end of the previous month, inches. This is calculated with Equation A.46.

DE_i = Differential energy density of subgrade deformation accumulated for month i. This is calculated with Equation A.50. This parameter is calculated based on coefficient of subgrade reaction (k_{month}) and the loaded slab ($\delta_{L,i,A}$) and unloaded slab ($\delta_{U,i,A}$) deflections caused by axle loading. The differential energy density of subgrade deformation is directly and indirectly dependent on the following factors: mean transverse joint spacing, temperature, pavement material properties, load transfer efficiency of shoulder and joint, axle type, traffic, load (axle weight), pavement weight, subgrade properties, joint stiffness, humidity, aggregate joint shear capacity, joint opening, joint spacing, and slab shrinkage strain.

$$FMAX_i = FMAX_{i-1} + C_7 \times DE_i \times [\log(1 + C_5 \times 5^{EROD})]^{C_6}$$

Equation A.48

Where:

$FMAX_i$ = maximum mean transverse joint faulting for month i, inches.

$FMAX_{i-1}$ =maximum mean transverse joint faulting for the previous month, inches. This is also calculated using Equation A.48. If i is equal to month 1, then FMAX is $FMAX_0$ which is the initial maximum faulting. $FMAX_0$ is calculated with Equation A.49. $FMAX_0$ is directly and indirectly dependent on the following factors: pavement material

properties, subgrade, temperature, mean transverse joint spacing, and shrinkage strain determined according to humidity.

DEi= Differential energy density of subgrade deformation accumulated for month i. This is calculated with Equation A.50.

EROD=erodibility of the base layer. This is a factor based on the erodibility of the base layer.

$C_5=250$

$C_6=0.4$

$C_7=1.2$

$$FMAX_0 = C_{12} \times \delta_{\text{eff,max}} \times \left[\log \frac{P_{200} \times \text{WetDays}}{P_s} \log(1 + C_5 \times 5^{\text{EROD}}) \right]^{C_6}$$

Equation A.49

where:

$FMAX_0$ =initial maximum faulting. This value is the maximum faulting that can occur according to the maximum deflection experienced from any of the monthly deflections computed within the previous year.

P_{200} =percent subgrade material passing 0.075 mm (#200) sieve

EROD=erodibility of the base layer. This is a factor based on the erodibility of the base layer

WetDays= number of wet days per year

$\delta_{\text{eff,max}}$ =maximum corner deflection due to curling

$$C_{12} = C_1 + C_2 \times FR^{0.25}$$

C_1, C_2, C_5 and C_6 are calibration coefficients

FR=Base Freezing Index

$$C_1=1.29$$

$$C_2=1.1$$

$$C_5=250$$

$$C_6=0.4$$

$$DE_i = \sum_{A=1}^3 \sum_{i=1}^{N_A} n_{i,A} \left(k_i \frac{\delta_{L,i,A}^2}{2} - k_i \frac{\delta_{U,i,A}^2}{2} \right)$$

Equation A.50

where:

$\delta_{L,i,A}$ = corner deflection of the loaded slab caused by axle loading

$\delta_{U,i,A}$ = corner deflection of the unloaded slab caused by axle loading

$n_{i,A}$ = number of axle load applications for current increment and load group i.

N_A = number of load categories for the axle type A

A.8 Continuously Reinforced Concrete Pavement

A.8.1 Punchouts

Equation A.51 is used to predict punchout development in CRCP (NCHRP 2003c).

$$PO_i = \sum_{i=1}^{Life} \frac{a}{1 + b \times D_i^c}$$

Equation A.51

where:

PO_i =total predicted number of punchouts per mile at the end of i^{th} monthly increment

D_i =accumulated fatigue damage (due to slab bending in the transverse direction) at the end of the i^{th} monthly increment. This damage is calculated with Equation A.52.

a,b,c=calibration constants for the nationally calibrated model (105.26, 4.0, -0.38, respectively)

$$D_i = \sum_{h=1}^{h=24} D_{hi} \times m_days_i$$

Equation A.52

where:

D_i =Accumulated fatigue damage during monthly increment i

D_{hi} =damage accumulated at critical point during progressive monthly increment i and cyclic hourly increment h due to all applied loads. As was stated, neural networks are used to calculate the incremental bending stress which is used to calculate the fatigue damage. D_{hi} is directly and indirectly dependent on the following factors: pavement material properties, traffic, applied axle load applications, slab bending stress, load transfer efficiency, temperature gradient, ambient temperature and humidity, subgrade properties, loss in shear capacity, transverse crack stiffness, mean crack width and slab structure.

m_days_i =number of days in monthly increment i

A.9 Roughness for JPCP and CRCP

A.9.1 Jointed Plain Concrete Pavement

MEPDG developed Equation A.53 to describe the pavement roughness in JPCP in terms of IRI (NCHRP 2003d).

$$IRI = IRI_I + 0.013 \times TC + 0.007 \times SPALL + 0.005 \times PATCH + 0.0015 \times TFAUL + 0.4 \times SF$$

Equation A.53

where:

IRI_I =initial smoothness measured as IRI, m/km

TC=percentage of slabs with transverse cracking (all severities)

SPALL=percentage of joints with spalling (all severities)

PATCH= percent of pavement surface area with flexible and rigid patching (all severities)

TFAULT=total joint faulting accumulated per km, mm

SF=site factor. This is calculated through Equation A.54.

Age= pavement age in years

FI=freezing index, °C days

P200=percent subgrade material passing the 0.075-mm sieve

$$SF = \frac{\text{Age} \times (1 + FI) \times (1 + P200)}{1000000}$$

Equation A.54

A.9.2 Continuously Reinforced Concrete Pavement

MEPDG developed Equation A.55 to describe the pavement roughness in CRCP in terms of IRI.

$$IRI = IRI_I + 0.003 \times TC + 0.008 \times PUNCH + 0.45 \times SF + 0.2 \times PATCH$$

Equation A.55

where:

IRI_I=initial IRI, m/km

TC= number of medium and high transverse cracks/km

PUNCH=number of medium and high severity punchouts/km

PATCH=percentage pavement surface with patching (medium to high severity, flexible and rigid)

SF=site factor

AGE=pavement age in years

FI=freezing index, °C days

P200=percent subgrade material passing the 0.075 mm sieve

**Appendix B: Microsoft Visual Basic Excel File for the Calibration of CRCP
Performance Models**

PART 1: DATA COMPILATION AND SYNTHESIS

The data preparation and filtering process using the developed Excel file is the following:

1. The pavement data for each of the “windows” datasets was first extracted from the PMIS database in Microsoft Outlook. A Standard Query Language (SQL) code in Microsoft Outlook was developed to extract the pavement inventory and distress data described in Chapter 4. Duplicates in the data to be calibrated were removed manually.
2. After the data was extracted, it was inserted in a sheet of the Excel file developed that was designated for the data.
3. The macro in the Excel file was run. Steps a through f were repeated by the macro for each of the four CRCP distresses. After the completion of step f for each distress, an Excel file for that particular distress was automatically saved with the final data to be used for the calibration. As a result, four Excel files for each category of the “windows” data sets (e.g. “zone 1” for the climate and subgrade “windows” dataset) were created.
 - a. The macro first grouped together the historical performance data of each data collection section. The sections which had less than two fiscal years of pavement history were removed from the data to be calibrated since their pavement age could not be estimated according to the pavement age estimation process.
 - b. Li values where a decrease in distress was observed in consecutive fiscal years were removed from the data to be calibrated.
 - c. Through the use of Excel functions the macro applied the age assumptions to the pavement performance data to estimate the pavement age for each Li value in record. Li values for which the pavement age could not be assumed were removed from the data to be calibrated.
 - d. Steps a through c terminated the phase of the first filtering process and provided the Li data to be used for the creation of the Li data subsets. Li values were first grouped by the macro according to their corresponding estimated pavement age.
 - e. The quartile filter was then applied to the Li data of each estimated pavement age group to create the quartile data subsets. The macro ordered the Li data of each age group in ascending order, calculated the Li value of quartiles 1 and 3, and removed all the Li data that was less than quartile 1 and greater than quartile 3 Li

values. This process was repeated for each estimated age group existing for the given distress type. The interquartile data remaining for all pavement age groups was then grouped and the Li Quartile data subset created. This data was then stored by the macro in one of the sheets of the Excel file.

- f. In another sheet of the Excel file, the data remaining from step d was used for the calculation of the median of each estimated pavement age existing for the given distress type. As was stated, this reduced the data to a subset that contained a single representative Li value for each existing estimated age.

Using steps 1 through 3, the data was filtered and data subsets were prepared for each category of the “windows” data sets.

PART 2: DATA CALIBRATION PROCESS

B.1 General Overview of Calibration Process

The Microsoft Visual Basic macro in the Excel file described in Chapter 5 was also tailored for the calibration process. As was stated in Chapter 5, an Excel file was created for each “windows” dataset category for each distress type. For example, one Excel file was created for Spalled Cracks for Texas’ District 1. In this Excel file, the data was filtered and prepared to create the Li Median and Li Quartile subsets. A sheet in the Excel file was designated for the Li Median subset data and another sheet was designated for the Li Quartile subset data. Each of these sheets was prepared for the calibration process that would be carried out through Excel. For illustrative purposes, Table B.1 is presented to describe the calibration process in the sheets. As can be noted, the estimated pavement age and respective observed Li for the data subset are placed in columns A and B, respectively. The calibrated Li value is calculated in column C through Equation 6.1 presented in Chapter 6, where *Age* is the corresponding estimated age for the given row and α , β , and ρ are the coefficients to be calibrated. In column D, the squared residual of the observed (y_o) and fitted (y_f) Li values, which are in columns B and C, respectively, is calculated for each row using the equation displayed. Through an iterative process the α , β , and ρ coefficients are changed with the goal of minimizing the sum of the squared residuals of column D. The iteration process is continued until the coefficients of the best fit model, according to the smallest possible SS, are determined. The coefficient of determination, R^2 , is then calculated to evaluate the fit of the calibrated model using the observed Li values (column B) and their corresponding calibrated Li values (column C).

Table B.1.Example of Calculated Values for Calibration Process.

| | A | B | C | D |
|---|---------------|-------------|--|---------------------------------------|
| 1 | Estimated Age | Observed Li | Calibrated Li $L_i = \alpha e^{-\left(\frac{\rho}{Age}\right)^\beta}$ | Squared Residual $= [y_o - y_f]^2$ |
| 2 | 1 | 4 | 5 | 1 |
| 3 | 2 | 7 | 7 | 0 |
| 4 | 3 | 10 | 12 | 4 |
| 5 | 4 | 14 | 16 | 4 |

B.2 Microsoft Excel SOLVER for Regression Analysis

In this study, the SOLVER function in Microsoft Excel was used to perform the iteration process of the non-linear regression analysis. This function is ideally suited for fitting non-linear functions to a given set of data. SOLVER carries out the iterations for minimizing SS by an iteration protocol that is based on the generalized reduced gradient (GRG) method (Microsoft Support 2011). GRG is a precise and accurate method for solving non-linear programming problems. It is one of a class of techniques called reduced-gradient or gradient projection methods which are based on extending methods for linear constraints to non-linear constraints (Rao 2011).

To use SOLVER, the user must first estimate the coefficients of the initial iteration. In this study, the α , β , and ρ coefficients were estimated to equal to one to start the iteration process. SOLVER then iterates until the convergence criteria of SS set by the user is met (Brown 2001). Criteria for convergence can include maximum iteration time, number of iterations, precision, tolerance and convergence. These parameters control the precision level of the iteration process and its duration. Table B.2 describes the convergence criteria (Brown 2011) and the values used for each for the calibrations. Default Excel values for these parameters were used in this study.

Table B.2. Convergence Criteria for SOLVER function in Microsoft Excel.

| Parameter | Definition | Value |
|--------------|---|--------------------|
| Maximum time | Maximum time limits the time taken by the solution process. | 100 seconds |
| Iterations | This parameter limits the time taken by the solution process by limiting the number of calculations. | 100 |
| Precision | Precision controls the precision of solutions by using the number that you entered to determine whether the value of a constraint meets a target or satisfies a lower or upper bound. | 1×10^{-6} |
| Tolerance | The percentage by which a target cell (SS in this study) of a solution satisfying the integer constraints can differ from the true optimal value and still be considered acceptable. | 5 percent |
| Convergence | This value tells excel when to stop the iterative process. Solver stops when the relative change in the target cell is less than the convergence number entered for the last five iterations. | 0.001 |

B.3 Procedure for the Calibration of Network Level Pavement Performance Models using Microsoft Excel Macro

The macro in the Excel file was extended to automate this calibration process. Figure B.1 displays a screenshot of the result summary sheet of the Excel file in which the results of the calibration for the Li Median and the Li Quartile data subsets are presented. In the result summary sheet, the distress evaluated and the distress starting age predetermined from data analysis are entered by the user in the left corner. An age cap (maximum limit for pavement age) can also be entered. An age cap can be set to determine the maximum pavement age to which the model must be calibrated. For example, if the age cap is 17 years, then all observed Li data corresponding to an estimated age of 17 years or less will be calibrated. Li data with estimated ages greater than 17 years will be omitted. Through an age cap, the pavement life of interest to

the agency can be modeled. In the table labeled “Constraints for Calibration of Performance Curves”, constraints for the coefficients to be calibrated can be set by the user. This allows to set constraints for the maximum and/or minimum values. It also allows to fix a coefficient for the calibration. If no constrain is desired, then “na” is entered for cells.

After these parameters are entered, the PMIS Li data is ready to be grouped by the macro according to the respective pavement sections. This is done by pressing the “Group Sections” button in the upper left section of the result summary sheet. The data is then filtered and compiled into data subsets by the macro by pressing the “Filter Data” button. Finally, the Li Quartile and the Li Median data subsets are calibrated by pressing the “Calibrate” button. The macro will run SOLVER with the constraints defined by the user. After the best fit model is obtained according to the optimum minimum SS, the coefficient of determination is calculated. The calibrated coefficients and R^2 for the Li Quartile and Li Median data subsets will be displayed next to “Quartile Filter: Spalled Cracks” and “Median Method: Spalled Cracks” cells, respectively, in the result summary screen. The “ R^2 – Qt Data” presented for “Quartile Filter: Spalled Cracks” measures how well the Li Quartile calibrated model fits the Li Quartile data subset. The “ R^2 – Median” value presented for “Median Method: Spalled Cracks” measures how well the Li Median calibrated model fits the Li Median data subset. The “ R^2 – Qt Data” value presented for “Median Method: Spalled Cracks” measures how well the Li Median calibrated model fits the Li Quartile data subset. In the “Quartile Filter: Spalled Cracks” section, a bubble graph with the Li Quartile data and calibrated performance model for this subset is displayed in the lower left corner. A bubble graph is a type of chart that gives a visual representation of the density of a point defined by the x and y axes. The density is represented by a bubble that increases in size according to the frequency of the given point in the dataset. The larger the frequency of a given point in the data set, the bigger the bubble will become. In this study, the bubbles represent the observed Li data. In the “Median Method: Spalled Cracks” section, a graph with the Li Median data and calibrated performance model for this subset is displayed in the lower right corner. If it is desired to recalibrate the performance curve with new constraints, this can be done by changing the constraints and pressing the “Calibrate” button once again. This can be repeated until the desired results are obtained.

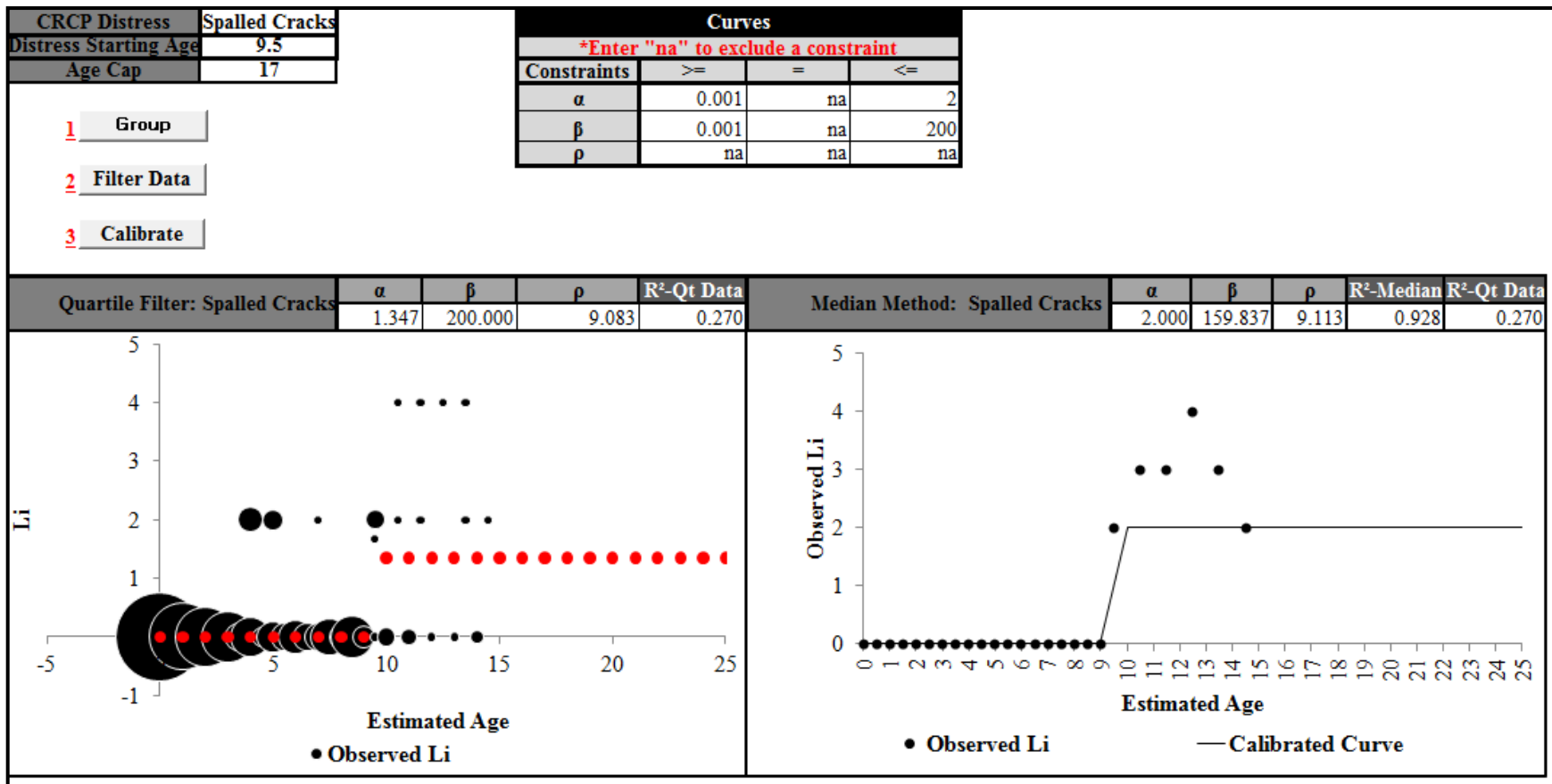


Figure B.1. Main Screen of CRC Pavement Performance Model Calibration Excel File.

Appendix C: Calibrated CRCP Distress Performance Models for Texas Districts

Paris District 01-Spalled Cracks

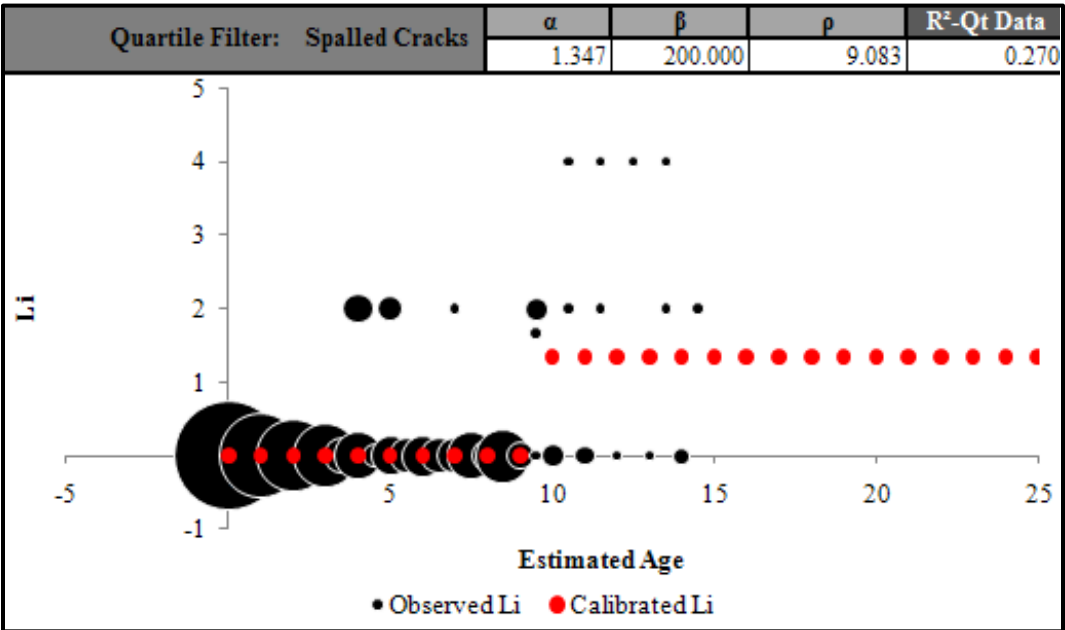


Figure C 1.1. Calibrated Performance Model for Paris District, Li Quartile Method (Unconstrained).

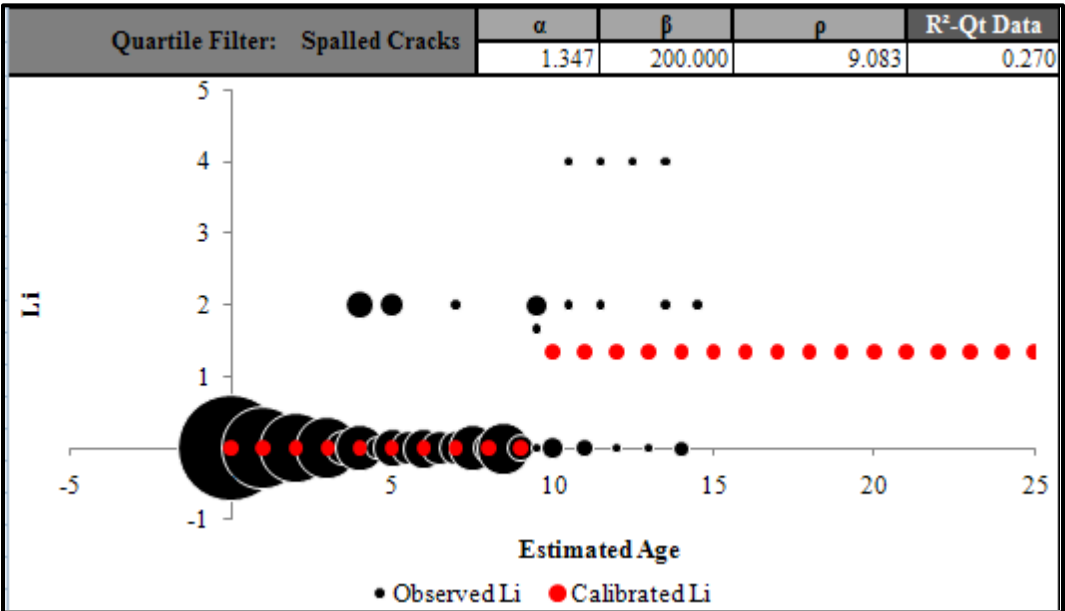


Figure C 1.2. Calibrated Performance Model for Paris District, Li Quartile Method (Constrained).

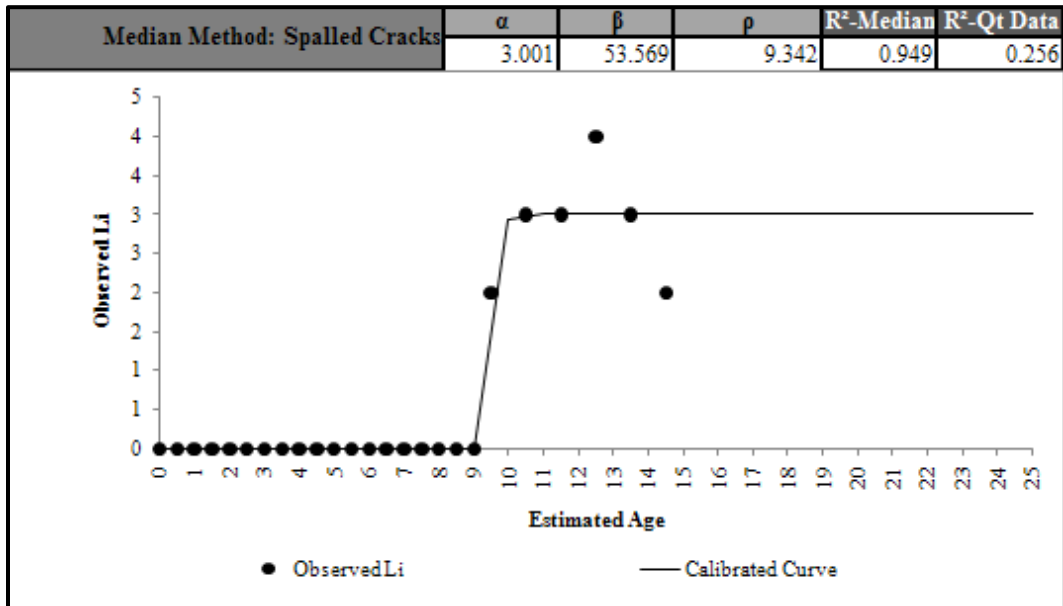


Figure C 1.3. Calibrated Performance Model for Paris District, Li Median Method (Unconstrained).

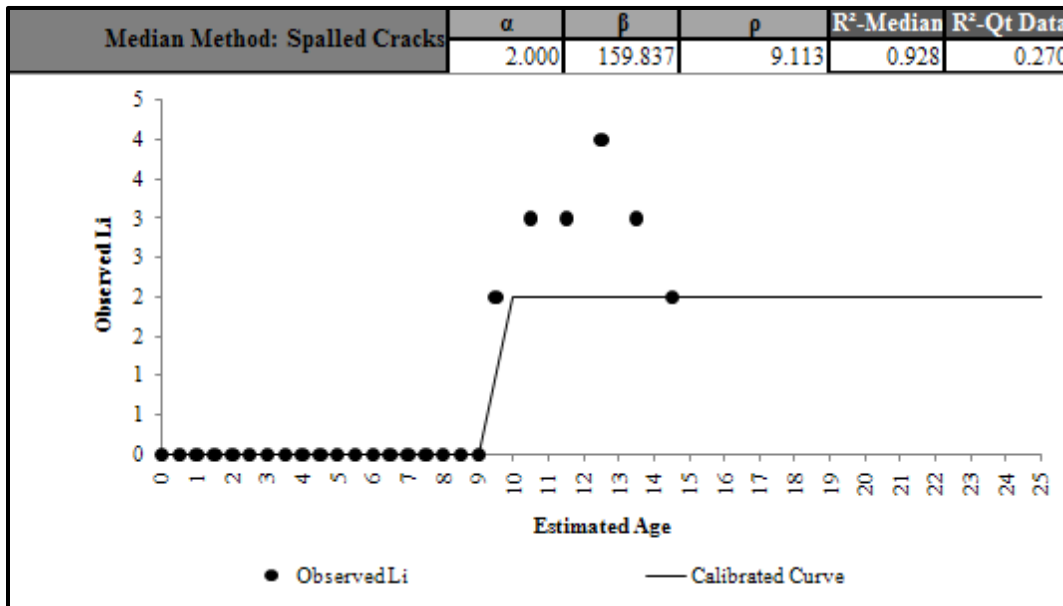


Figure C 1.4. Calibrated Performance Model for Paris District, Li Median Method (Constrained).

Paris District 01-Punchouts

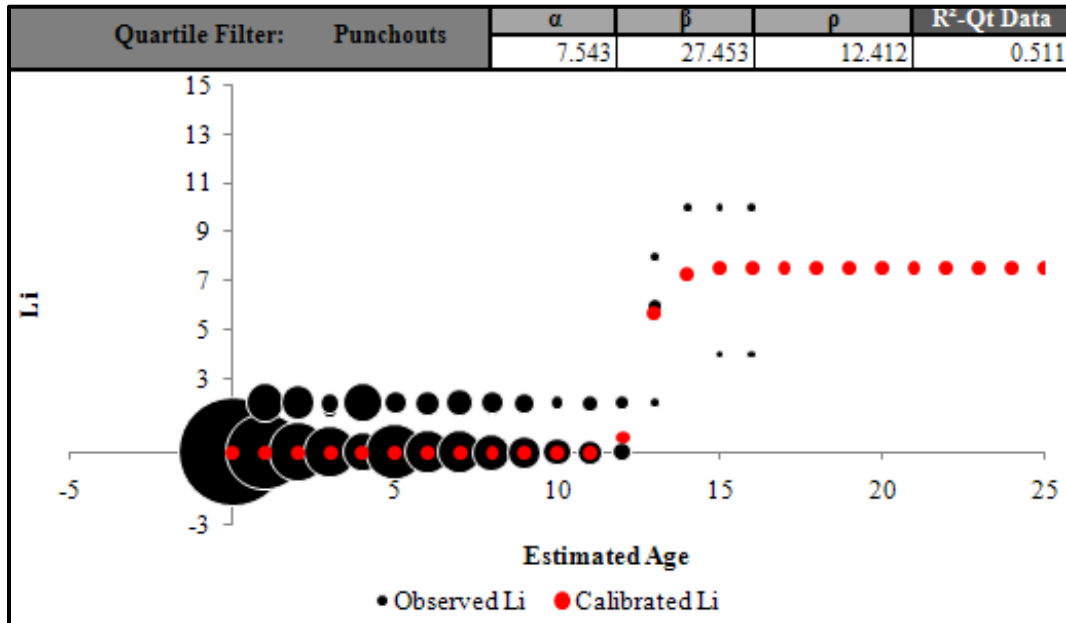


Figure C 1.5. Calibrated Performance Model for Paris District, Li Quartile Method (Unconstrained).

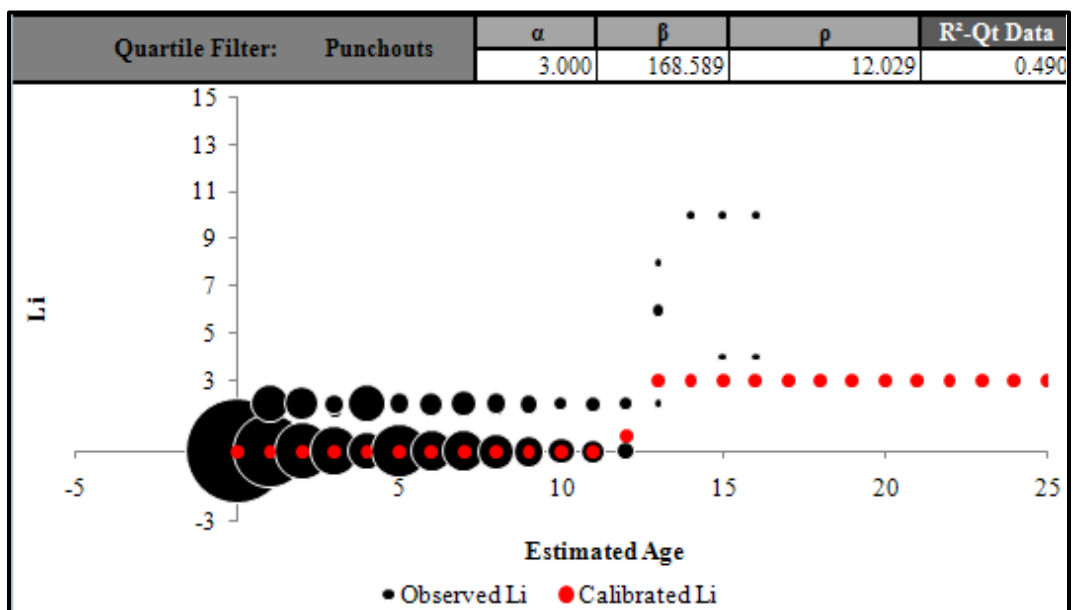


Figure C 1.6. Calibrated Performance Model for Paris District, Li Quartile Method (Constrained).

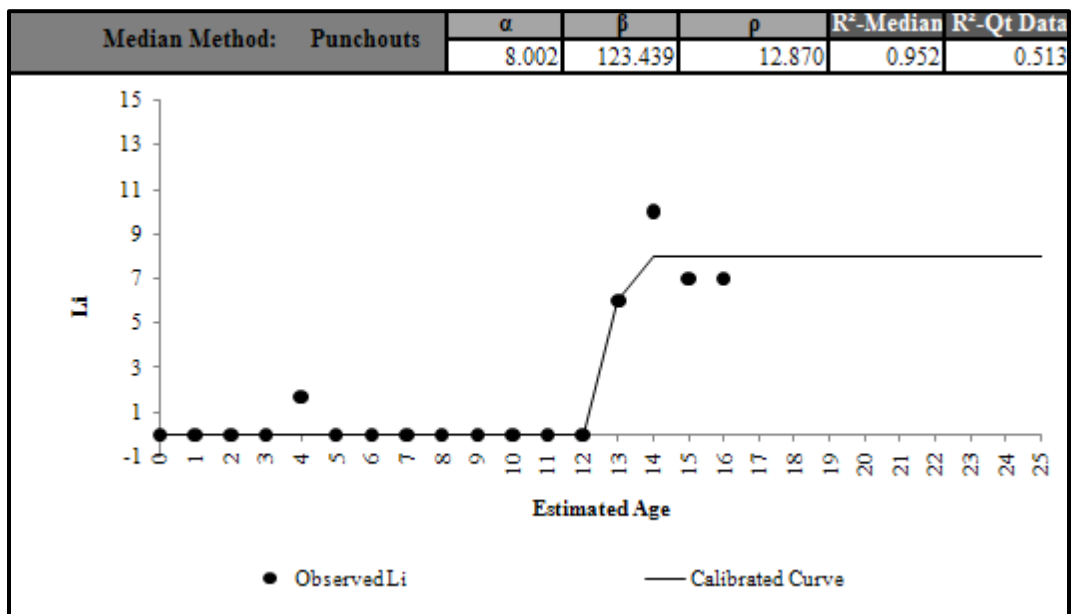


Figure C 1.7. Calibrated Performance Model for Paris District, Li Median Method (Unconstrained).

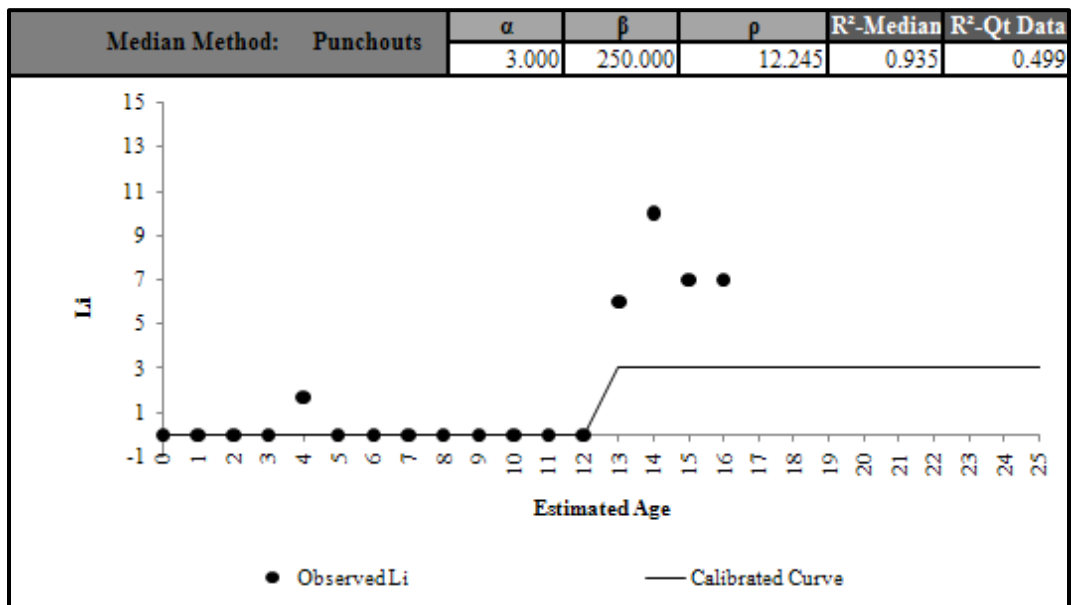


Figure C 1.8. Calibrated Performance Model for Paris District, Li Median Method (Constrained).

Paris District 01-PCC Patches

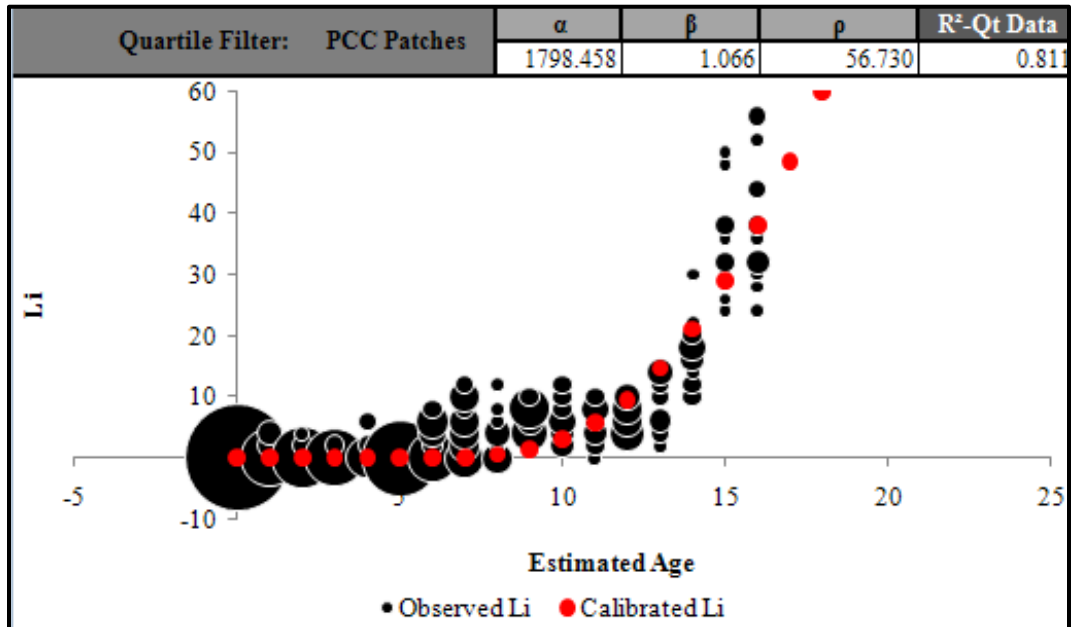


Figure C 1.9. Calibrated Performance Model for Paris District, Li Quartile Method (Unconstrained).

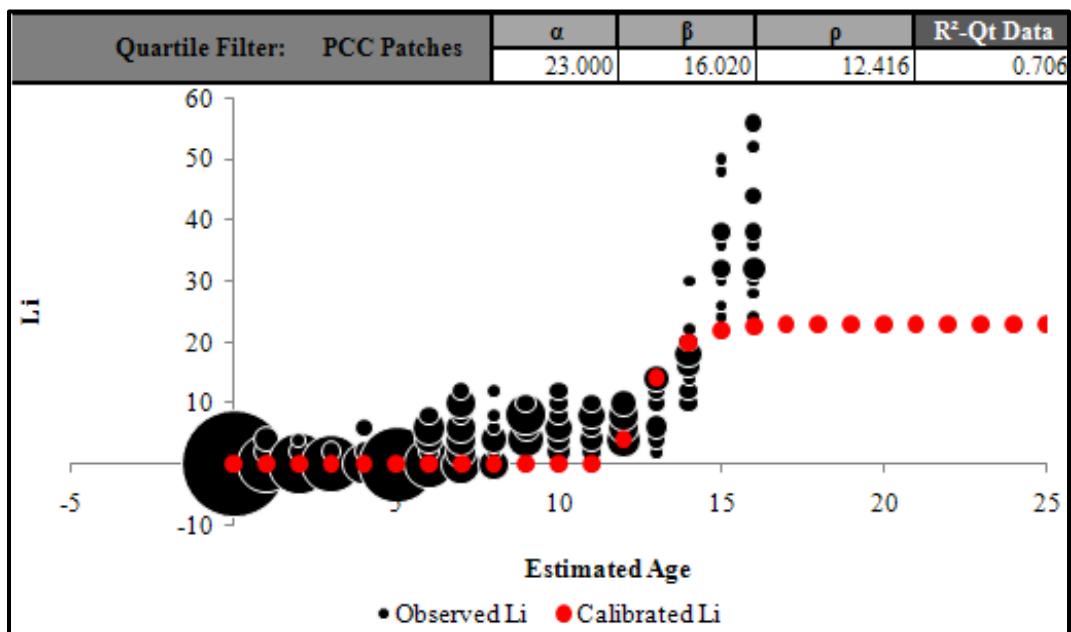


Figure C 1.10. Calibrated Performance Model for Paris District, Li Quartile Method (Constrained).

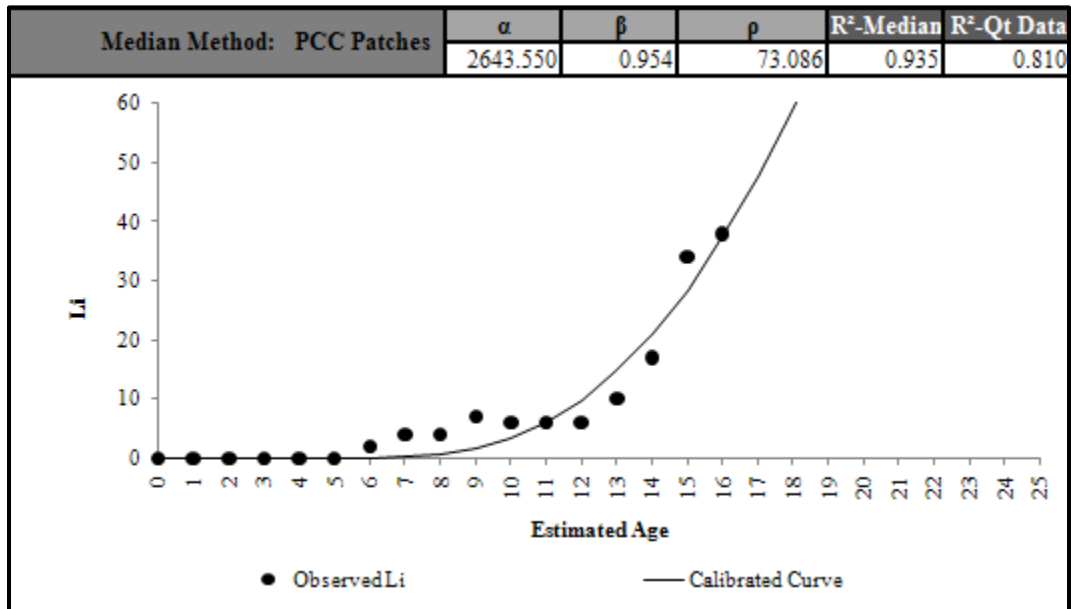


Figure C 1.11. Calibrated Performance Model for Paris District, Li Median Method (Unconstrained).

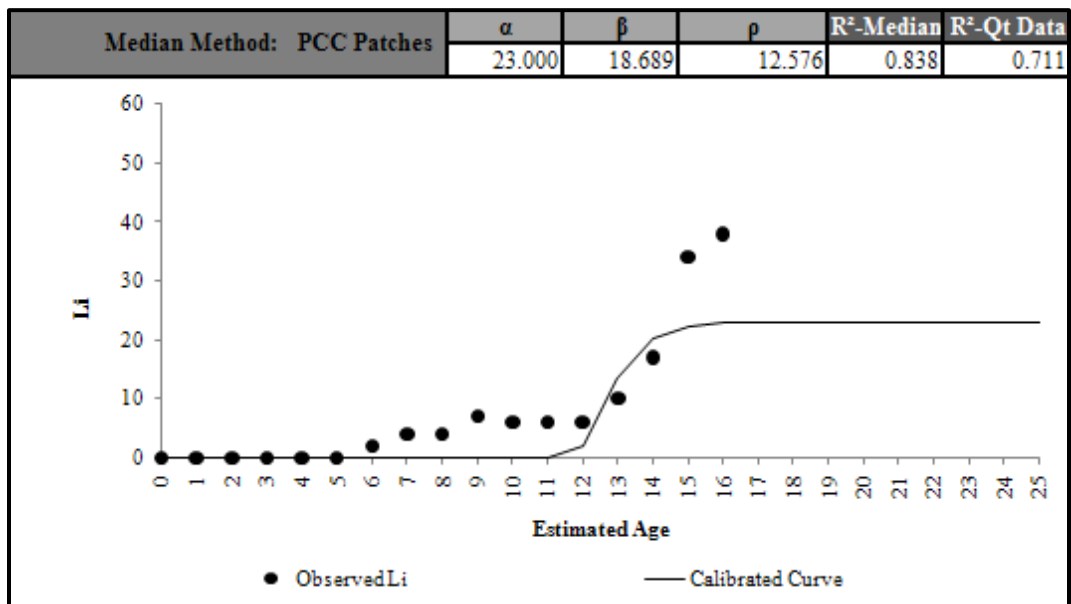


Figure C 1.12. Calibrated Performance Model for Paris District, Li Median Method (Constrained).

Fort Worth District 02-Spalled Cracks

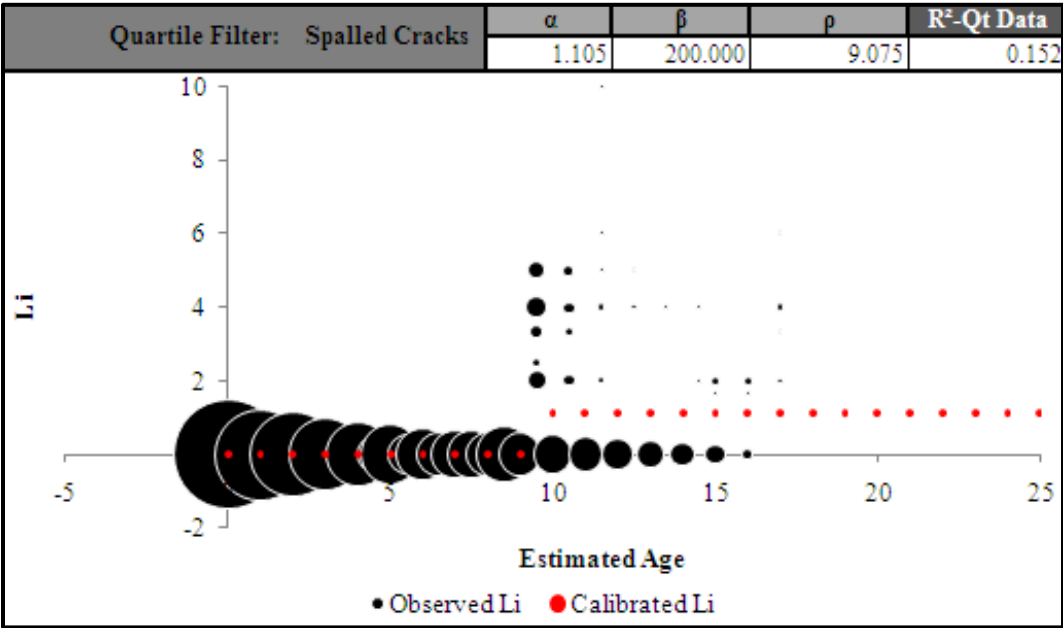


Figure C 2.1. Calibrated Performance Model for Fort Worth District, Li Quartile Method (Unconstrained).

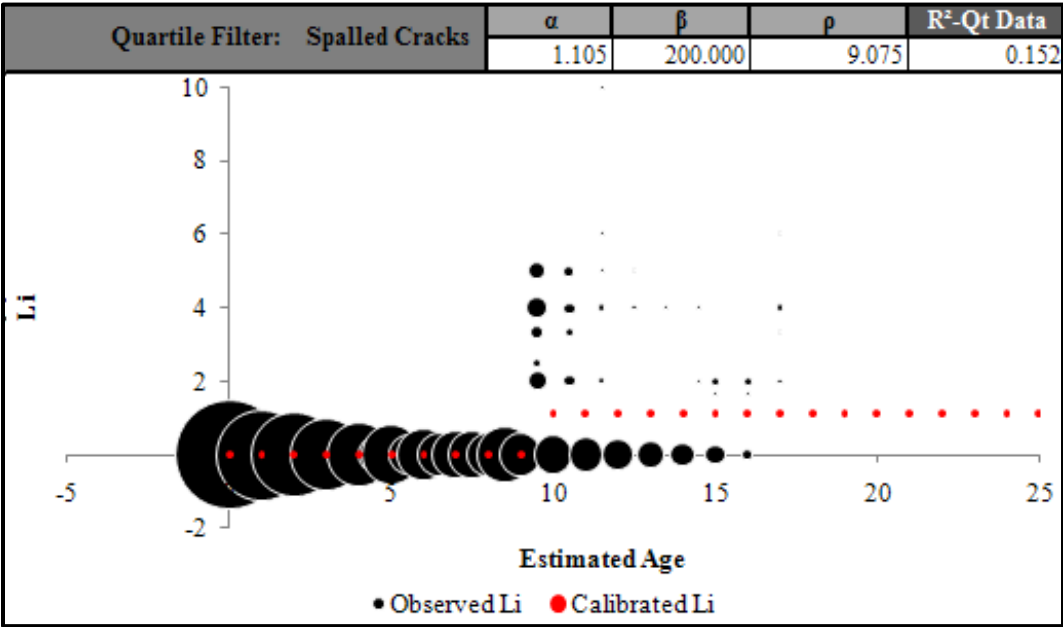


Figure C 2.2. Calibrated Performance Model for Fort Worth District, Li Quartile Method (Constrained).

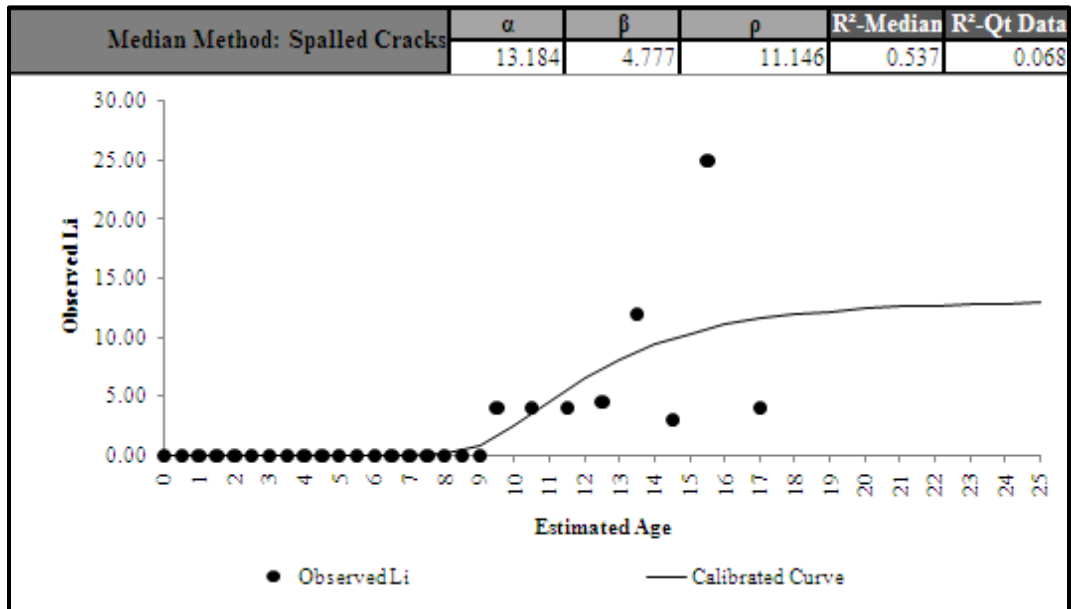


Figure C 2.3. Calibrated Performance Model for Fort Worth District, Li Median Method (Unconstrained).

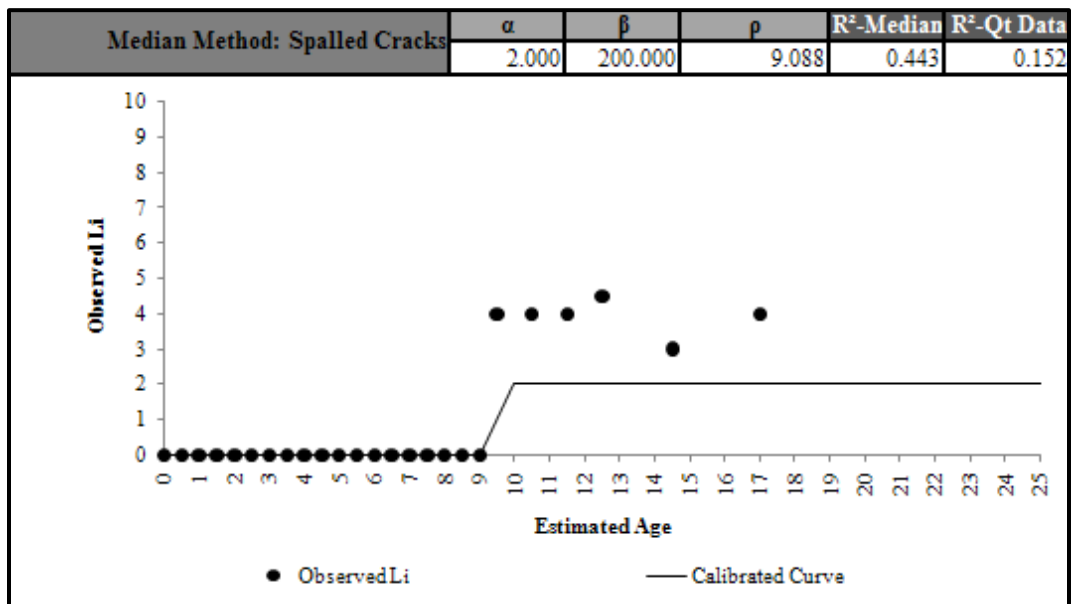


Figure C 2.4. Calibrated Performance Model for Fort Worth District, Li Median Method (Constrained).

Fort Worth District 02-Punchouts

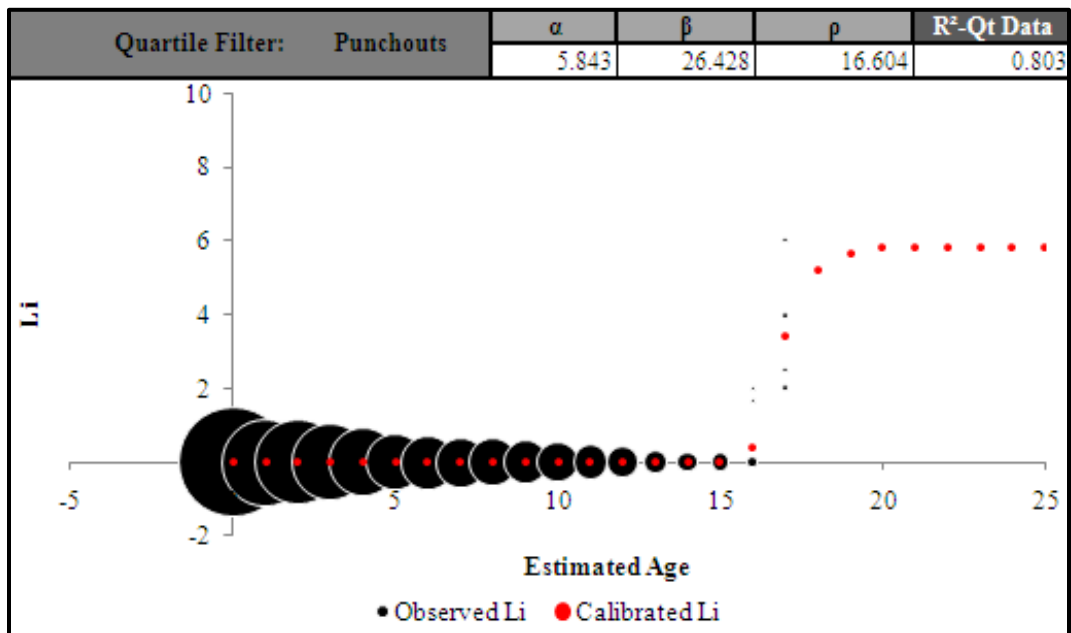


Figure C 2.5. Calibrated Performance Model for Fort Worth District, Li Quartile Method (Unconstrained).

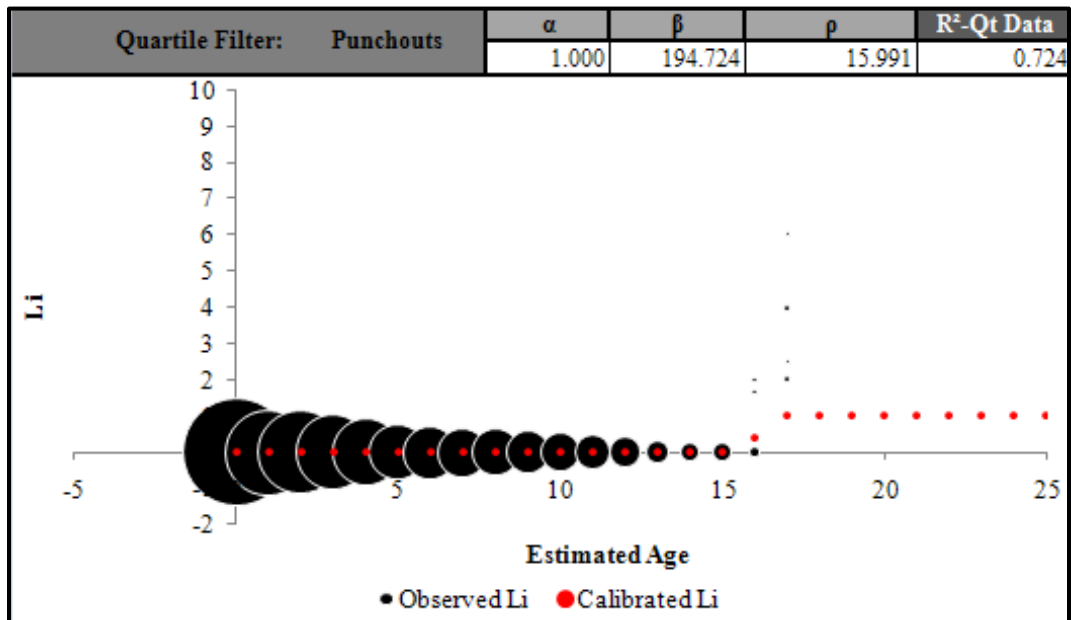


Figure C 2.6. Calibrated Performance Model for Fort Worth District, Li Quartile Method (Constrained).

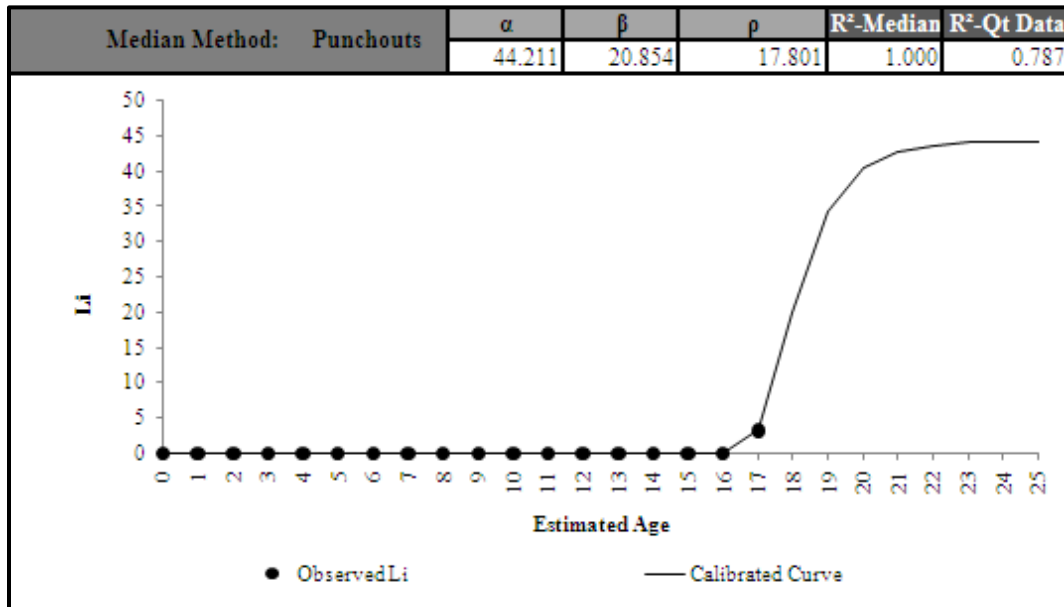


Figure C 2.7. Calibrated Performance Model for Fort Worth District, Li Median Method (Unconstrained).

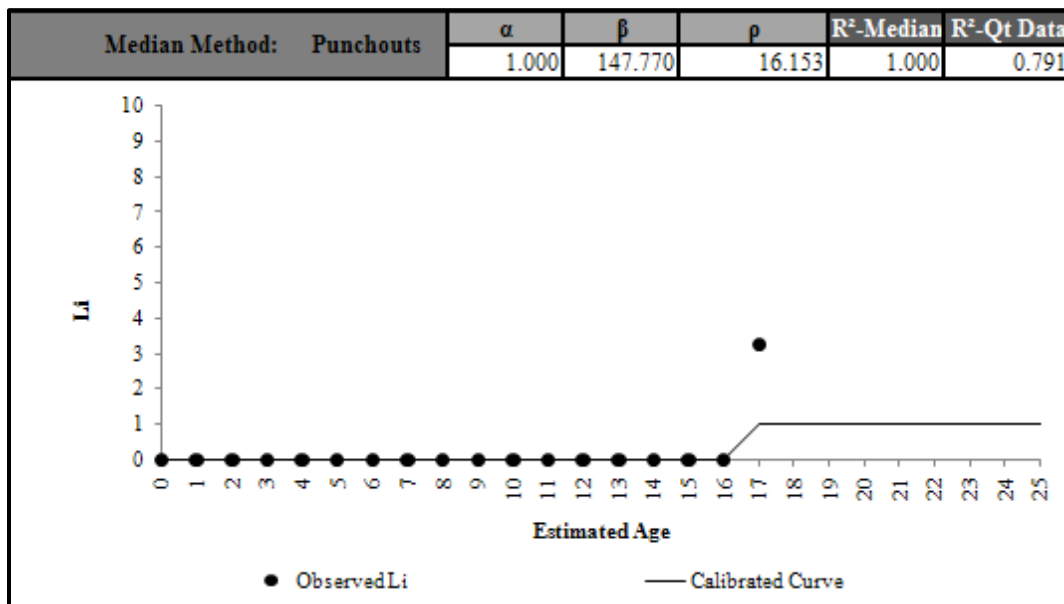


Figure C 2.8. Calibrated Performance Model for Fort Worth District, Li Median Method (Constrained).

Fort Worth District 02-ACP Patches

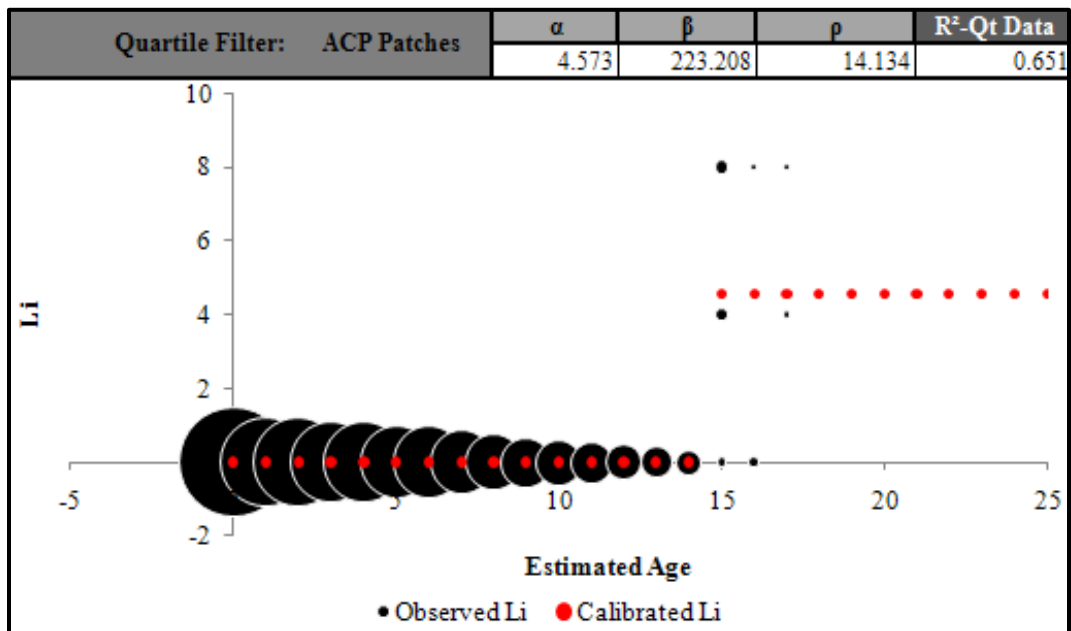


Figure C 2.9. Calibrated Performance Model for Fort Worth District, Li Quartile Method (Unconstrained).

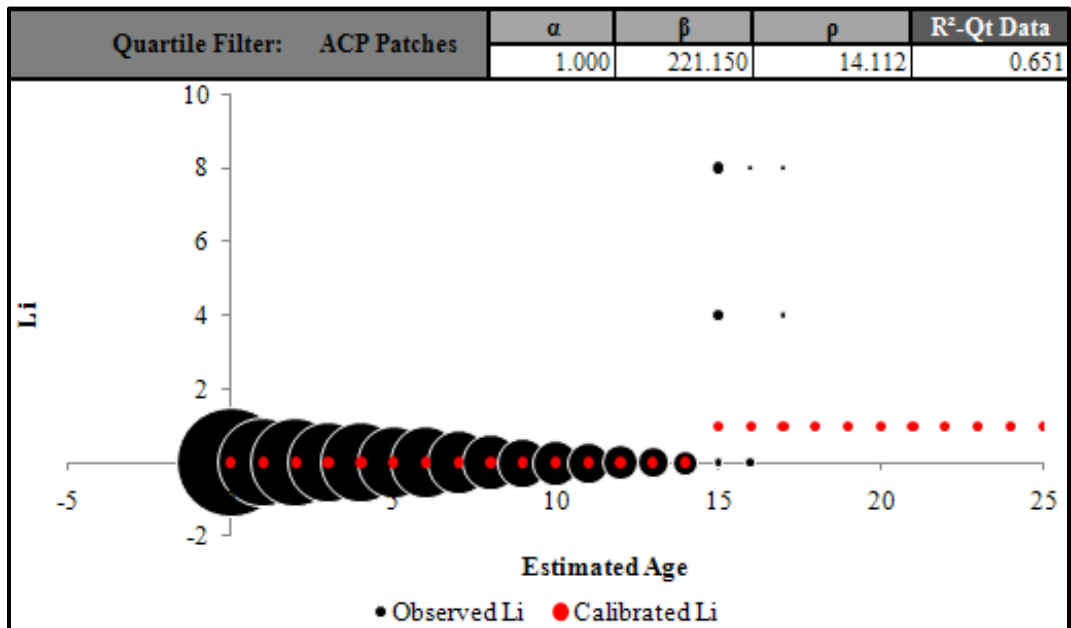


Figure C 2.10. Calibrated Performance Model for Fort Worth District, Li Quartile Method (Constrained).

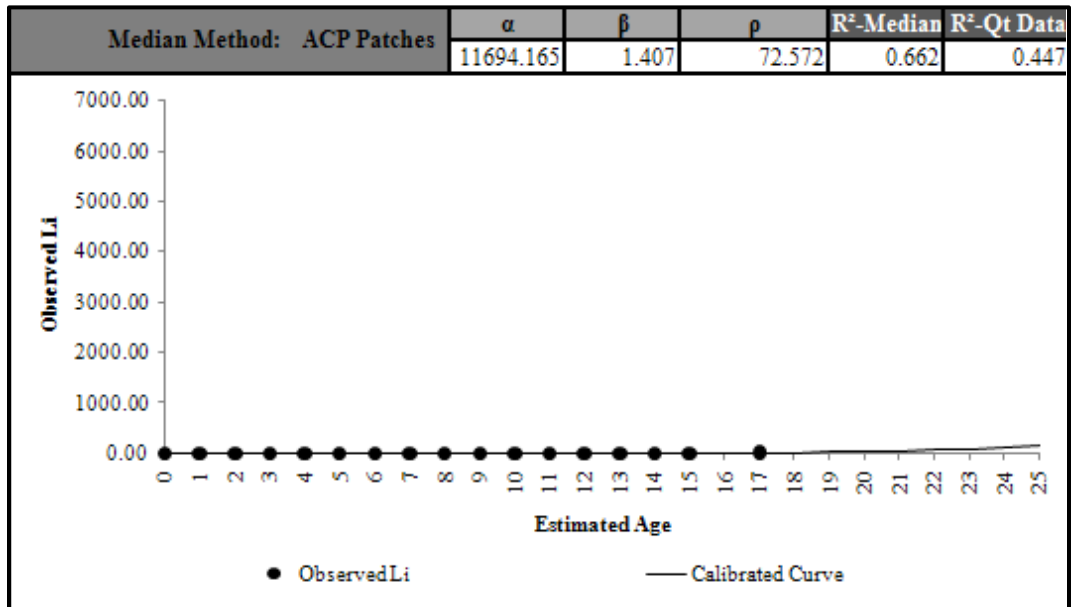


Figure C 2.11. Calibrated Performance Model for Fort Worth District, Li Median Method (Unconstrained).

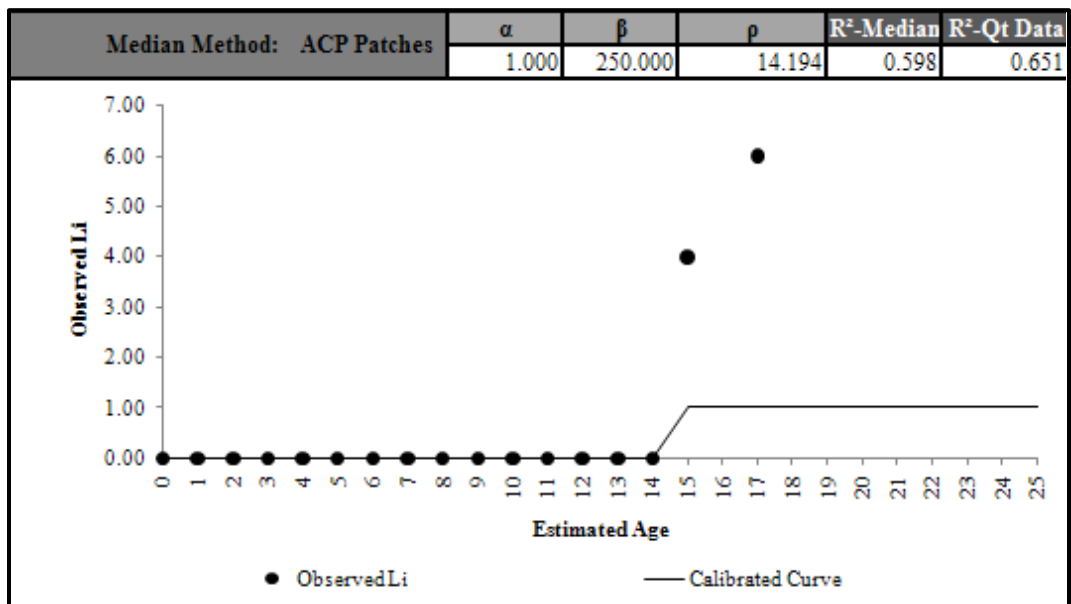


Figure C 2.12. Calibrated Performance Model for Fort Worth District, Li Median Method (Constrained).

Fort Worth District 02-PCC Patches

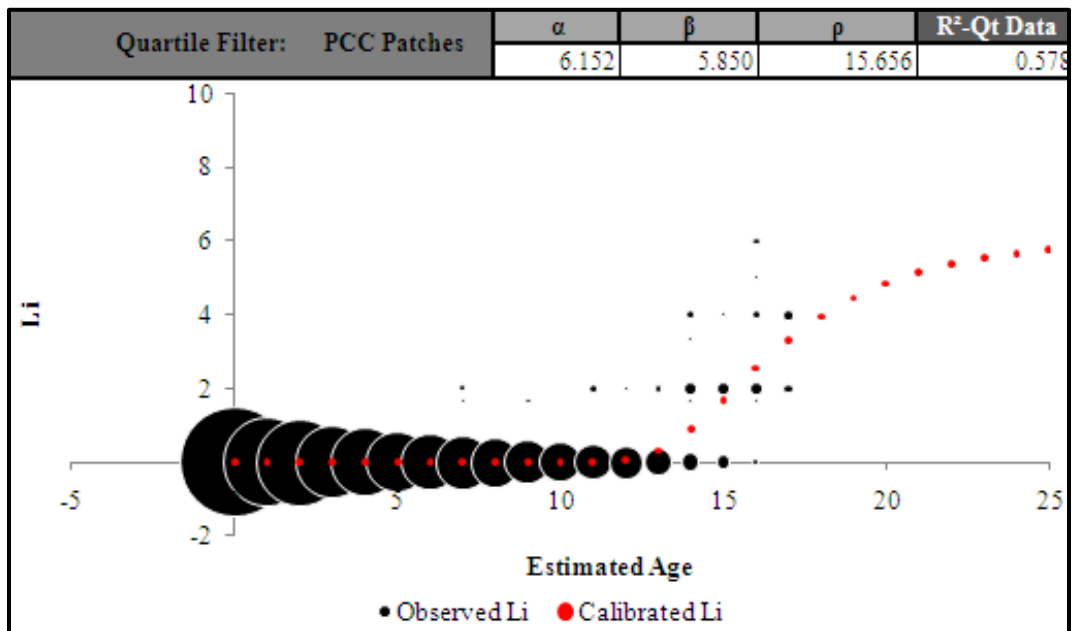


Figure C 2.13. Calibrated Performance Model for Fort Worth District, Li Quartile Method (Unconstrained).

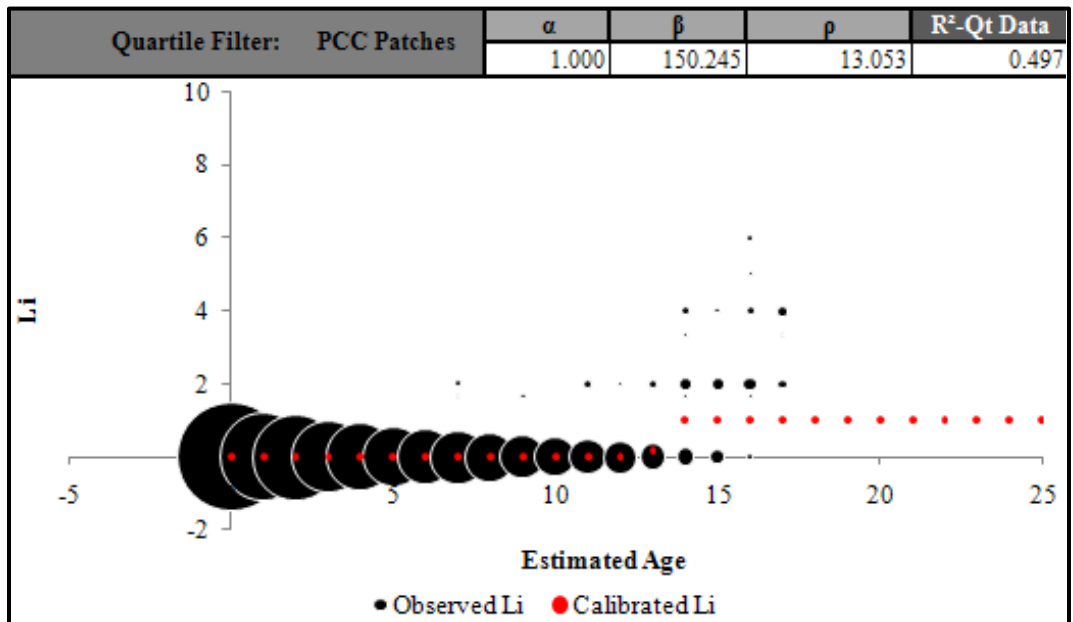


Figure C 2.14. Calibrated Performance Model for Fort Worth District, Li Quartile Method (Constrained).

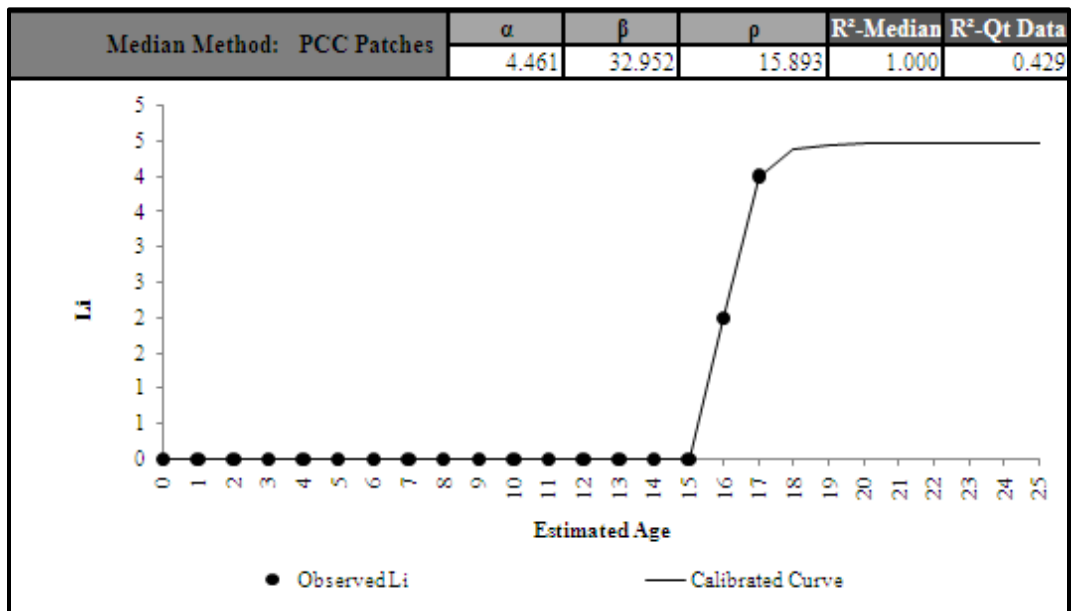


Figure C 2.15. Calibrated Performance Model for Fort Worth District, Li Median Method (Unconstrained).

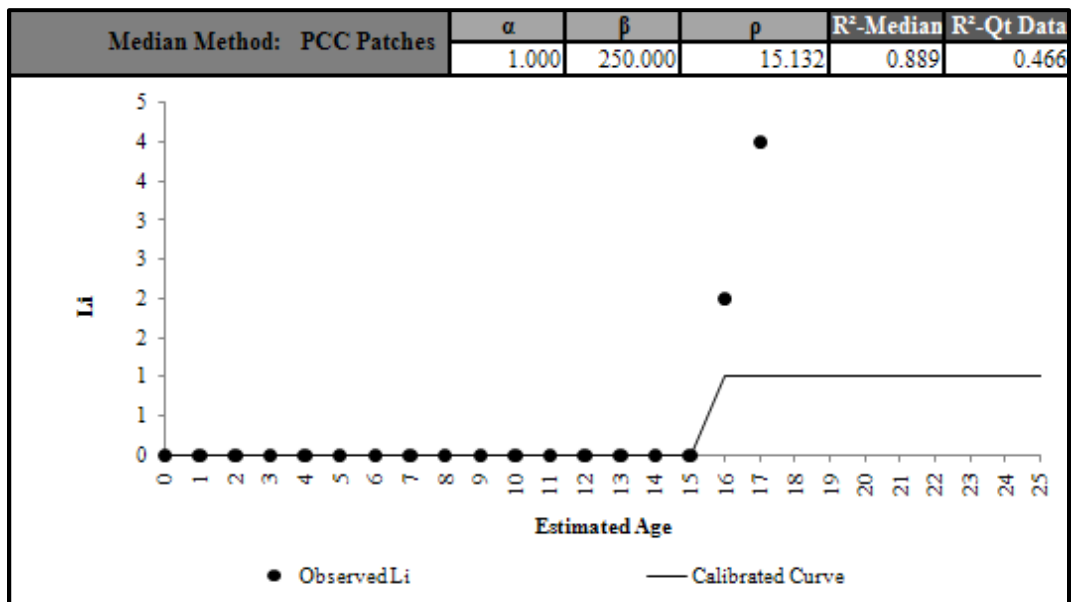


Figure C 2.16. Calibrated Performance Model for Fort Worth District, Li Median Method (Constrained).

Wichita Falls District 03-Spalled Cracks

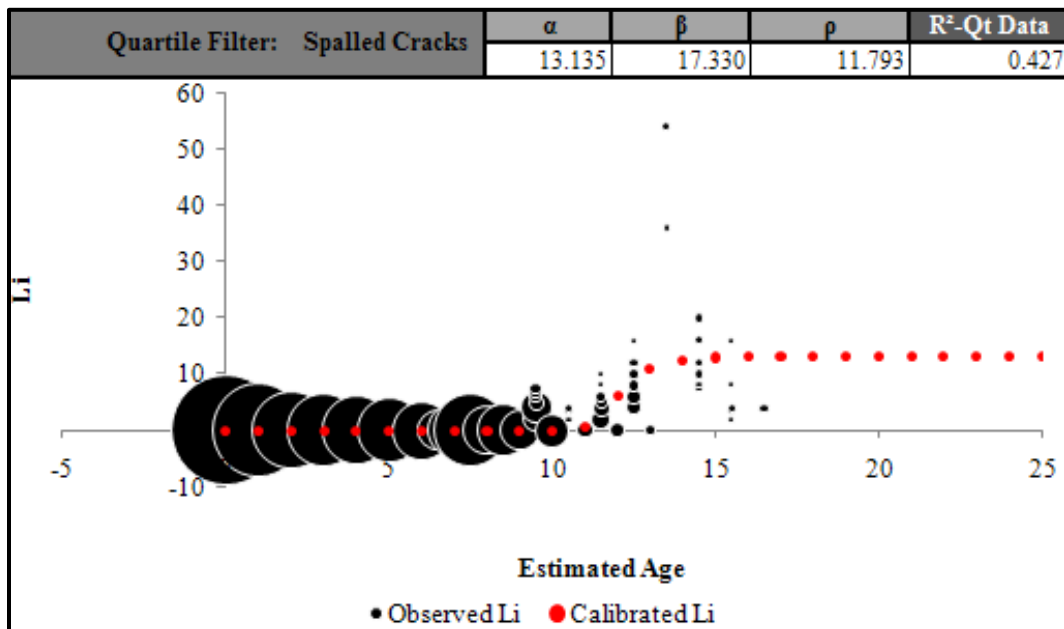


Figure C 3.1. Calibrated Performance Model for Wichita Falls District, Li Quartile Method (Unconstrained).

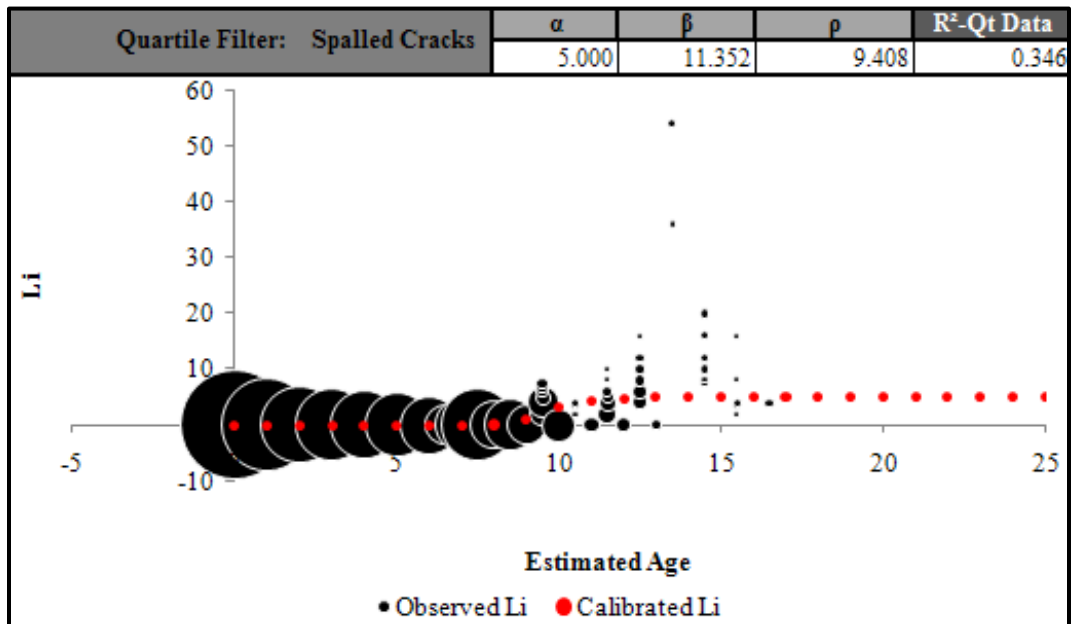


Figure C 3.2. Calibrated Performance Model for Wichita Falls District, Li Quartile Method (Constrained).

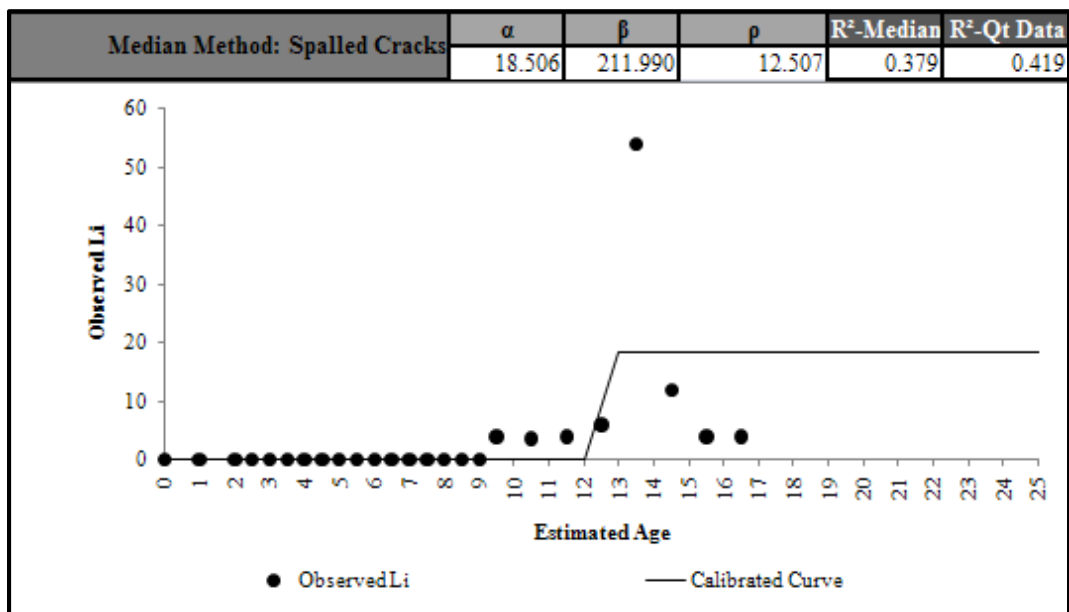


Figure C 3.3. Calibrated Performance Model for Wichita Falls District, Li Median Method (Unconstrained).

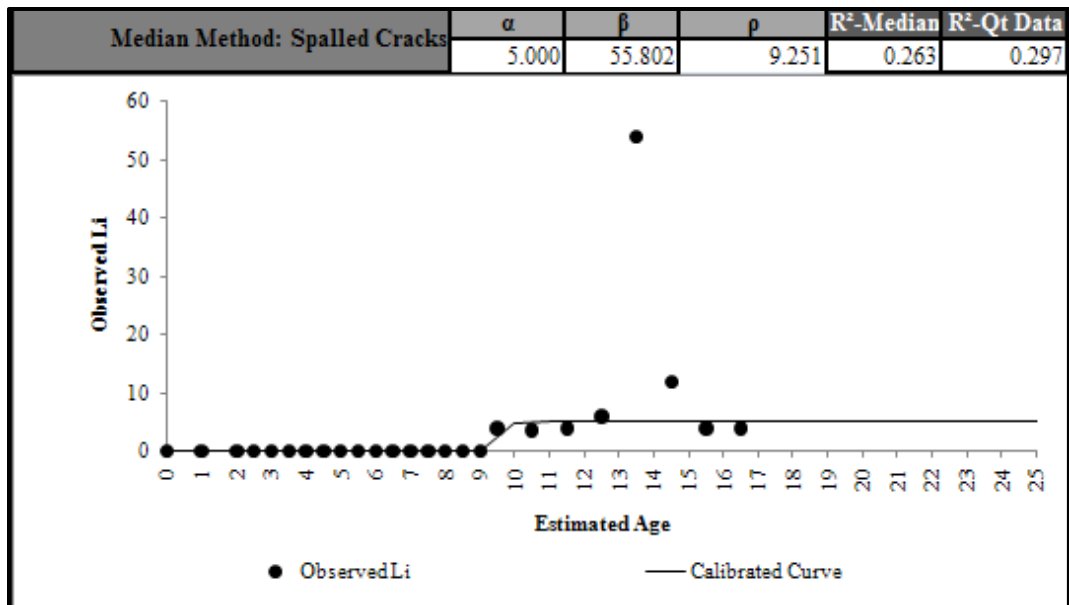


Figure C 3.4. Calibrated Performance Model for Wichita Falls District, Li Median Method (Constrained).

Wichita Falls District 03-Punchouts

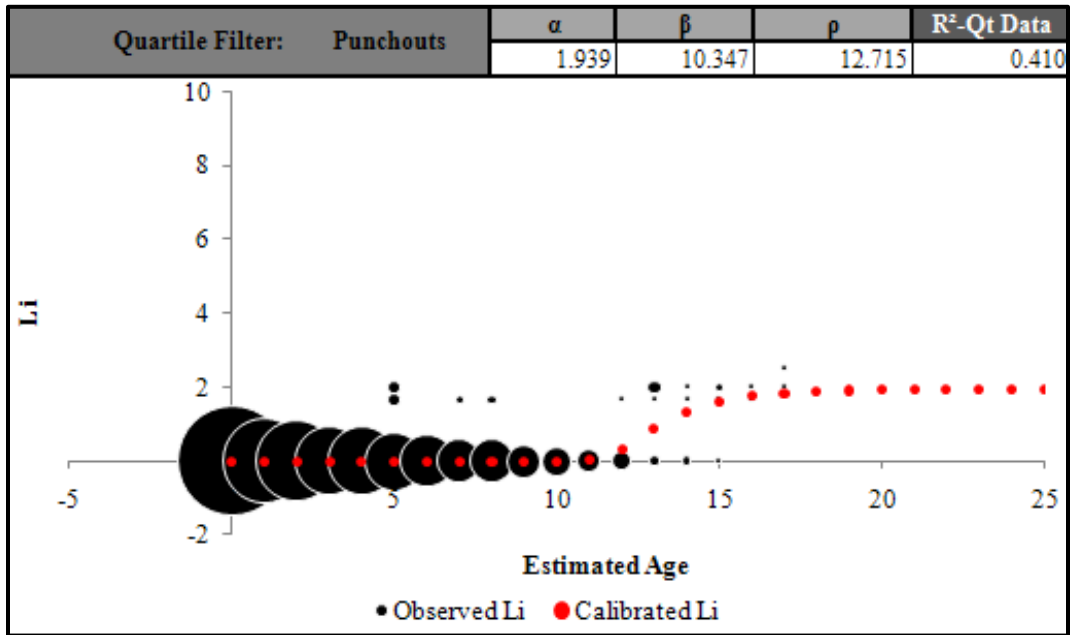


Figure C 3.5. Calibrated Performance Model for Wichita Falls District, Li Quartile Method (Unconstrained).

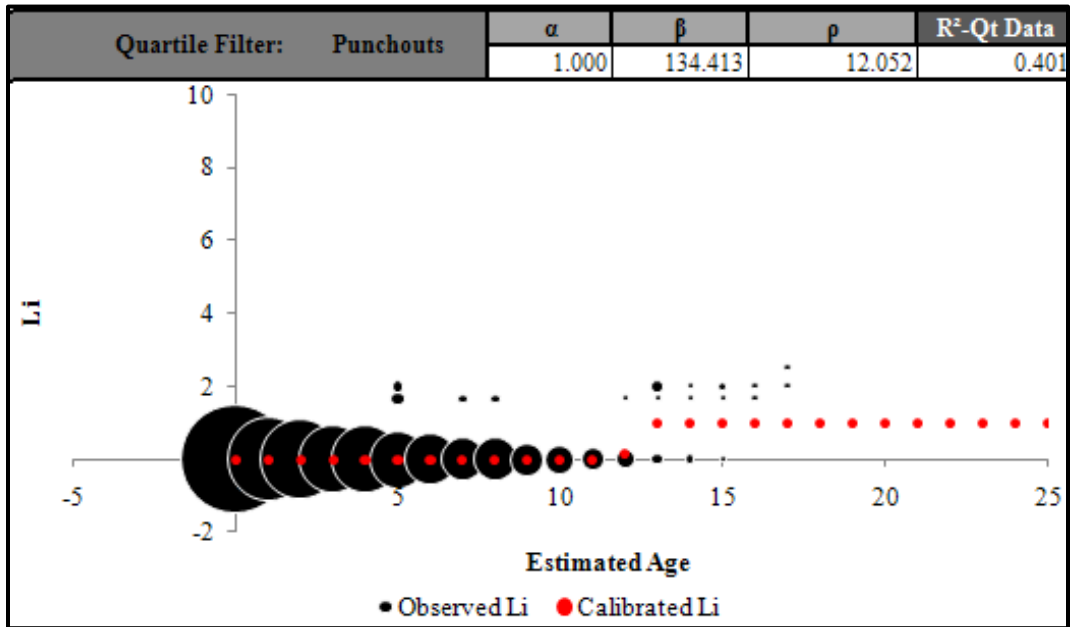


Figure C 3.6. Calibrated Performance Model for Wichita Falls District, Li Quartile Method (Constrained).

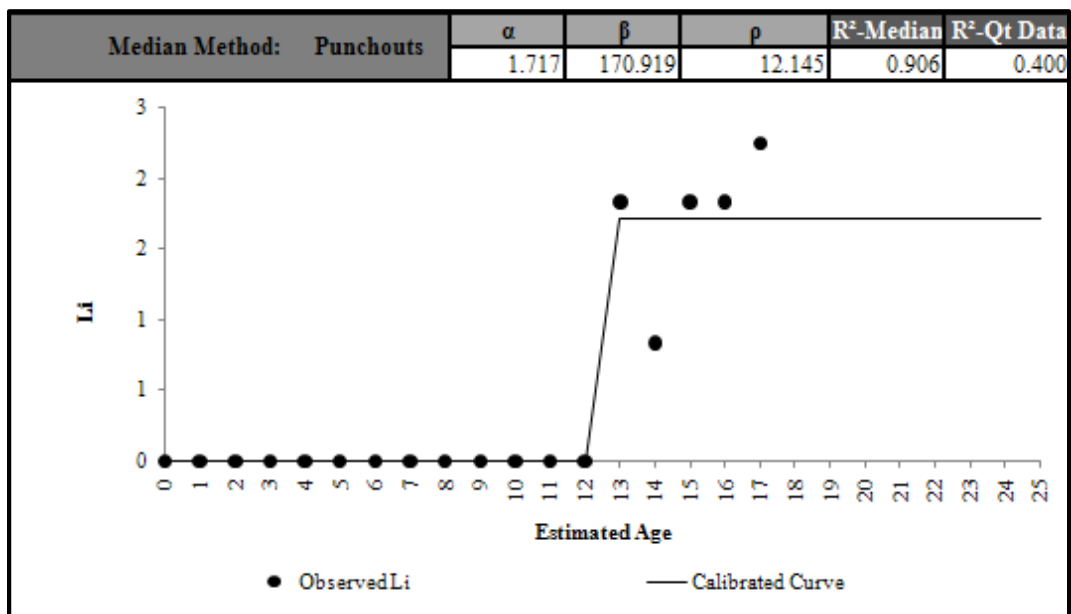


Figure C 3.7. Calibrated Performance Model for Wichita Falls District, Li Median Method (Unconstrained).

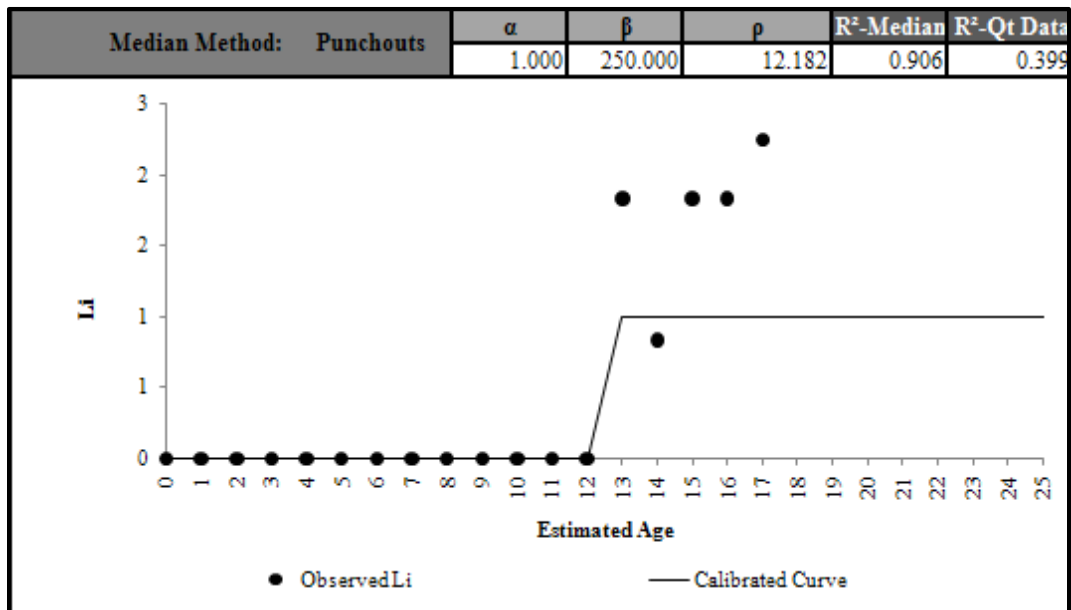


Figure C 3.8. Calibrated Performance Model for Wichita Falls District, Li Median Method (Constrained).

Wichita Falls District 03-PCC Patches

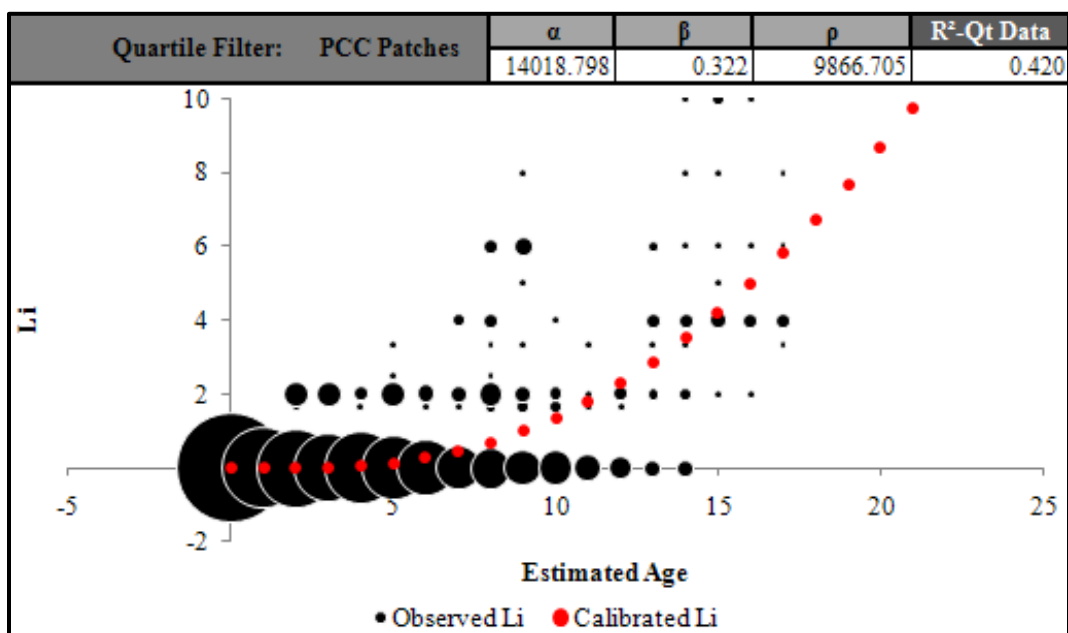


Figure C 3.9. Calibrated Performance Model for Wichita Falls District, Li Quartile Method (Unconstrained).

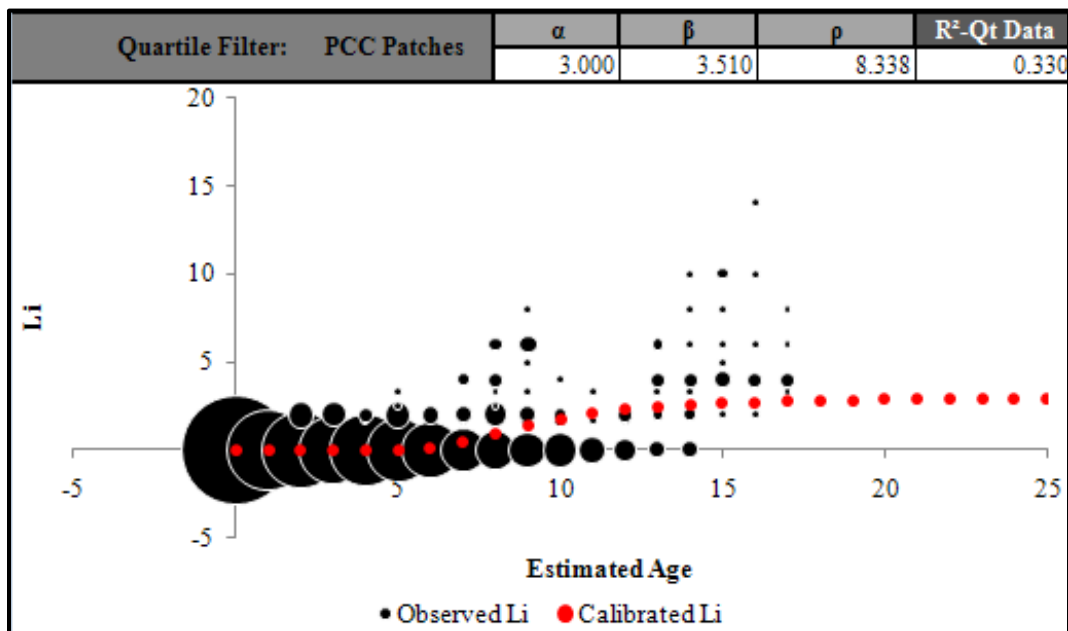


Figure C 3.10. Calibrated Performance Model for Wichita Falls District, Li Quartile Method (Constrained).

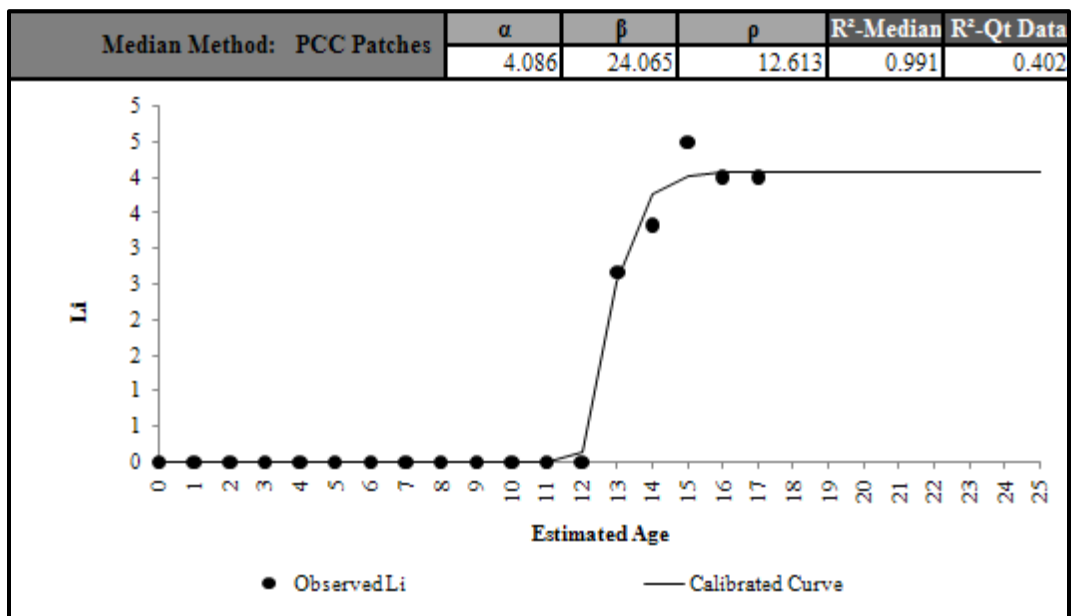


Figure C 3.11. Calibrated Performance Model for Wichita Falls District, Li Median Method (Unconstrained).

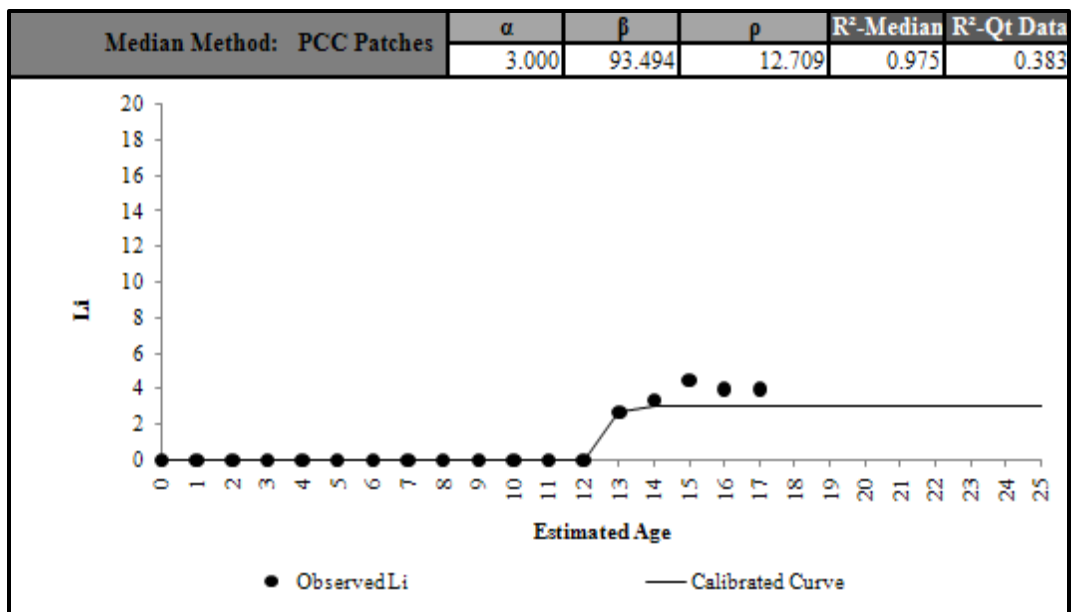


Figure C 3.12. Calibrated Performance Model for Wichita Falls District, Li Median Method (Constrained).

Amarillo District 04-Spalled Cracks

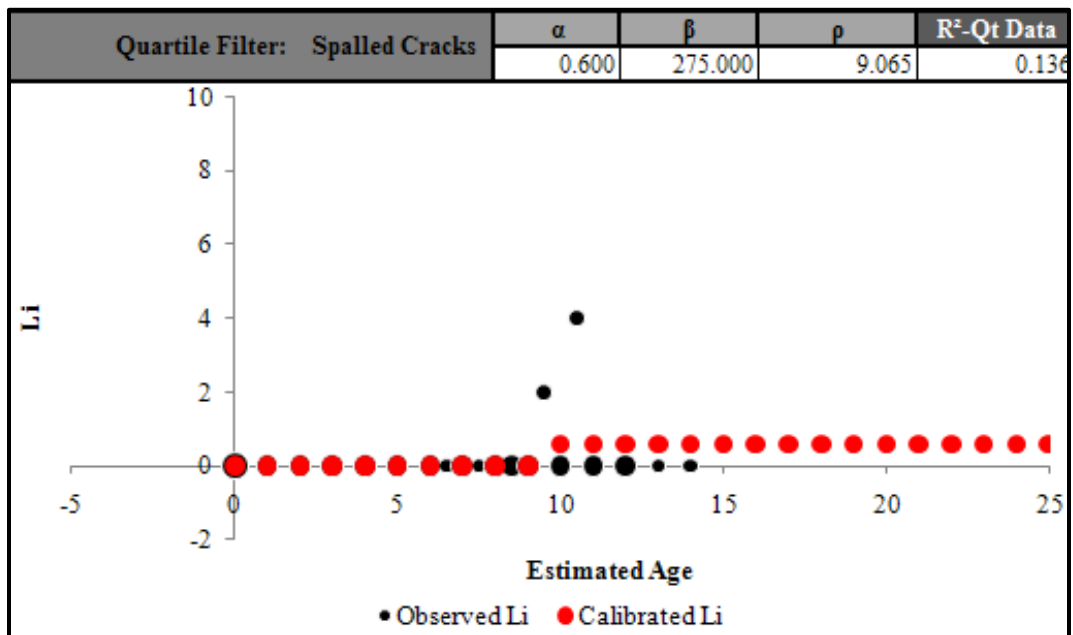


Figure C 4.1. Calibrated Performance Model for Amarillo District, Li Quartile Method (Unconstrained).

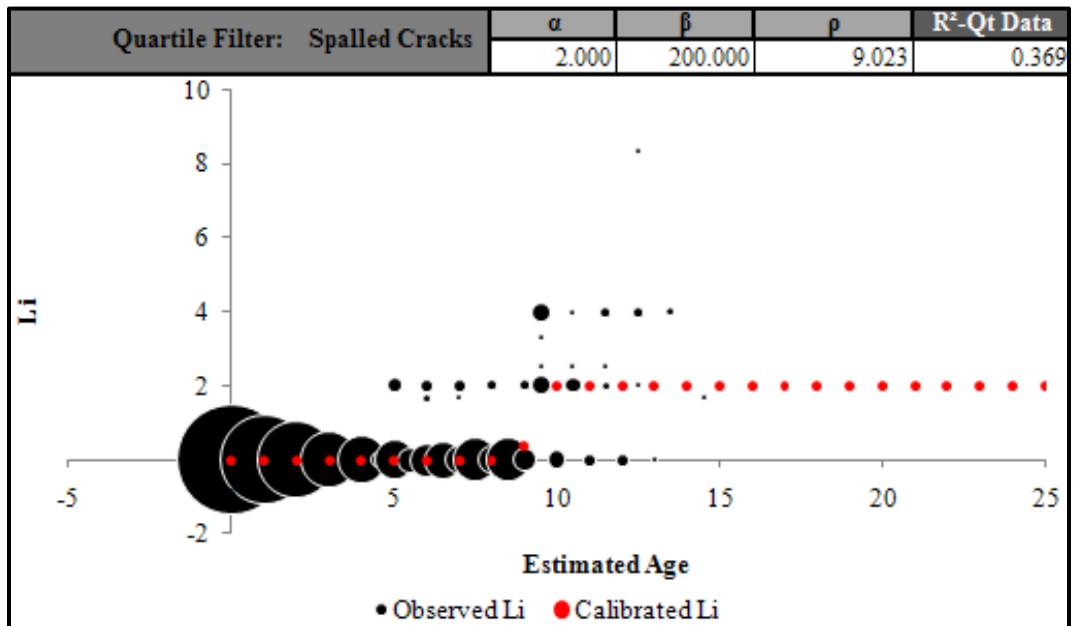


Figure C 4.2. Calibrated Performance Model for Amarillo District, Li Quartile Method (Constrained).

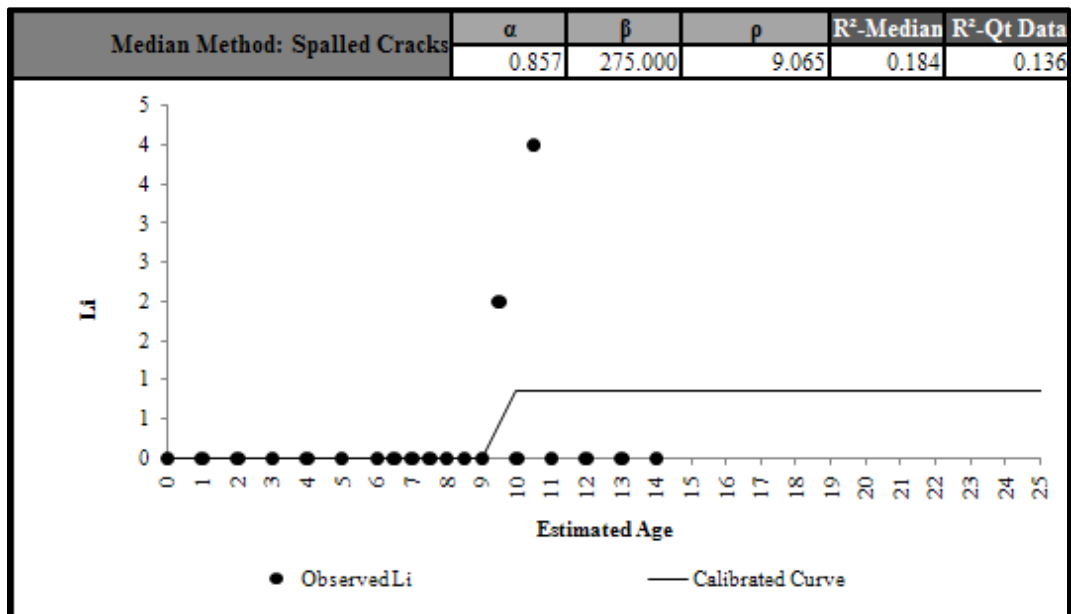


Figure C 4.3. Calibrated Performance Model for Amarillo District, Li Median Method (Unconstrained).

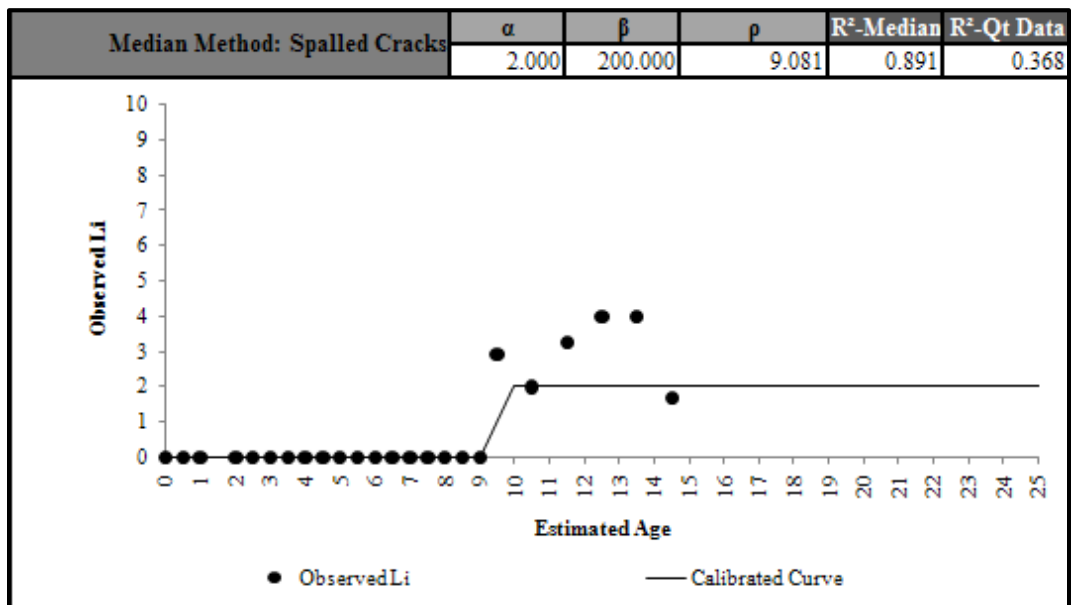


Figure C 4.4. Calibrated Performance Model for Amarillo District, Li Median Method (Constrained).

Amarillo District 04-Punchouts

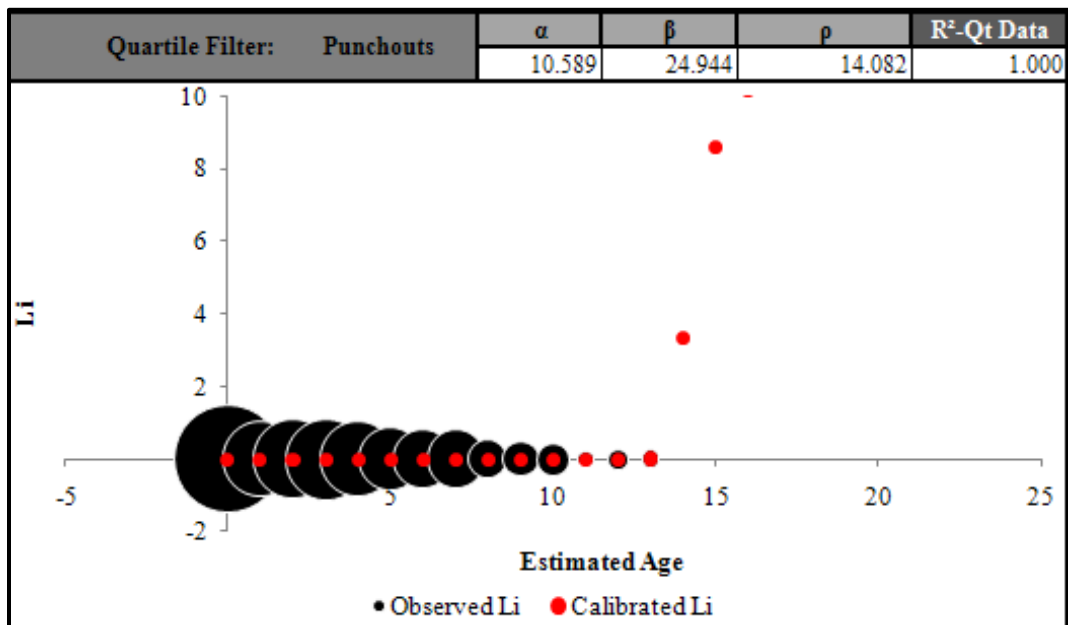


Figure C 4.5. Calibrated Performance Model for Amarillo District, Li Quartile Method (Unconstrained).

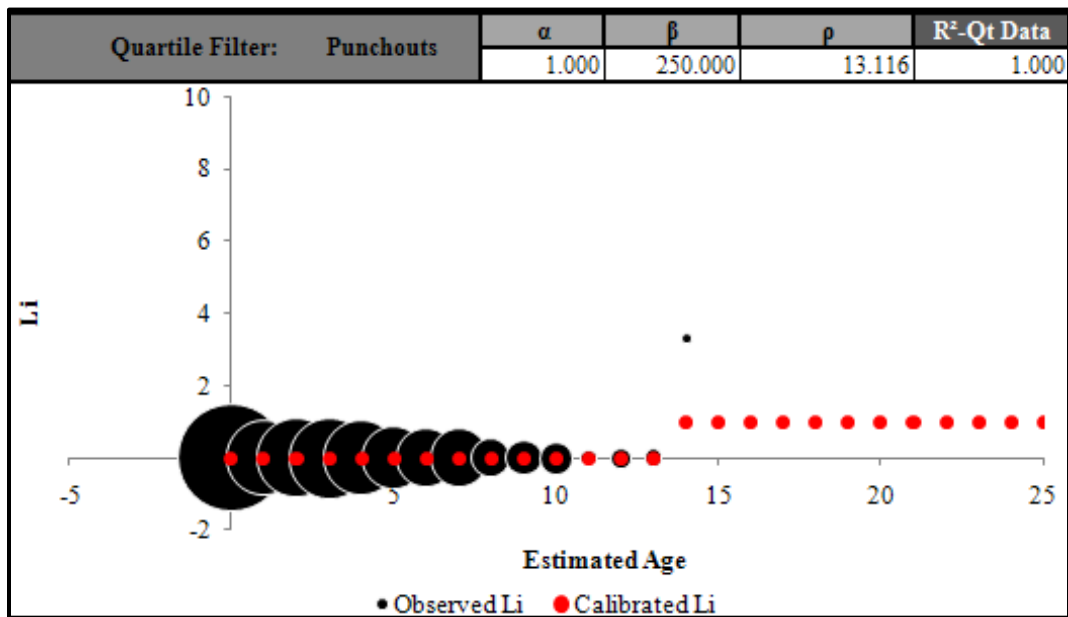


Figure C 4.6. Calibrated Performance Model for Amarillo District, Li Quartile Method (Constrained).

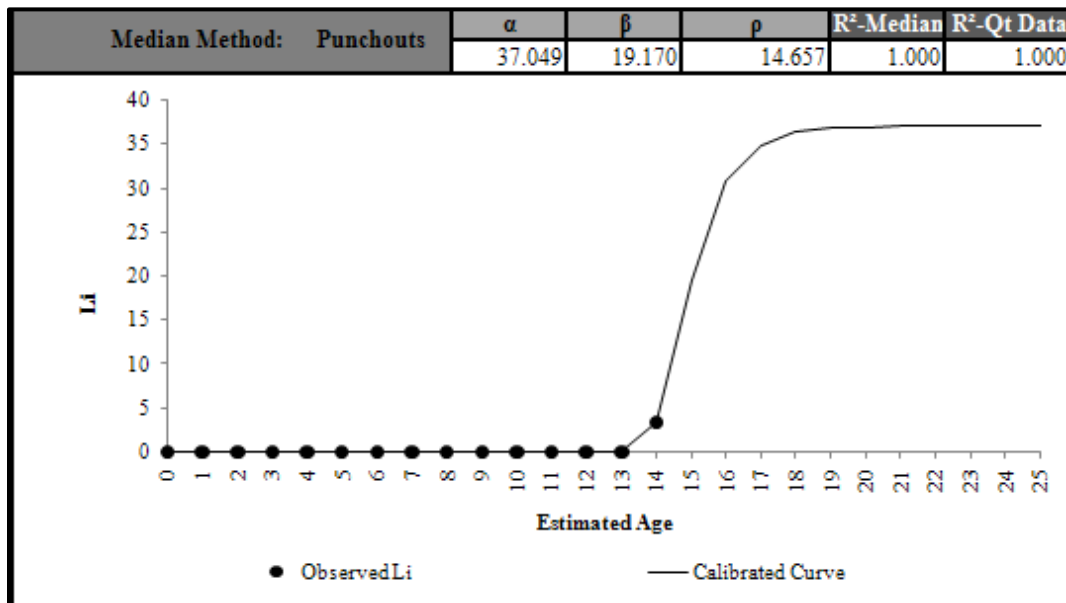


Figure C 4.7. Calibrated Performance Model for Amarillo District, Li Median Method (Unconstrained).

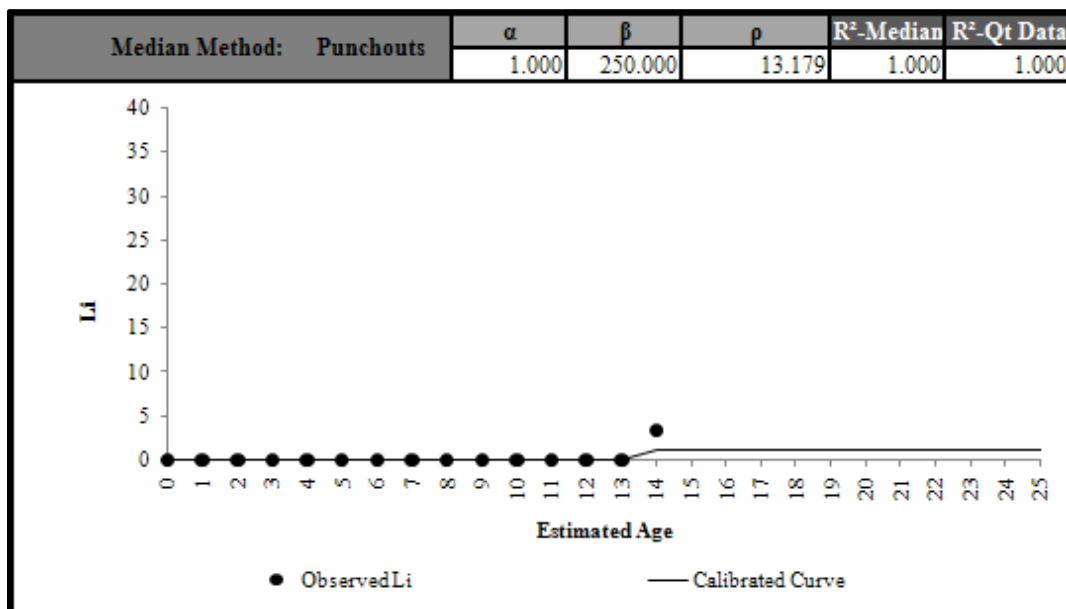


Figure C 4.8. Calibrated Performance Model for Amarillo District, Li Median Method (Constrained).

Amarillo District 04-PCC Patches

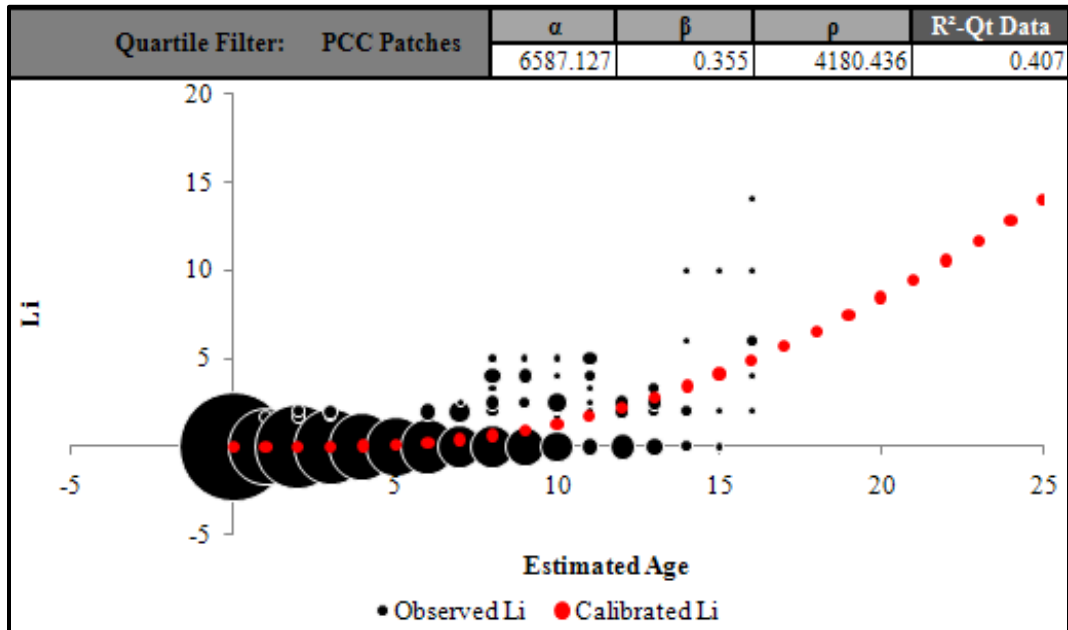


Figure C 4.9. Calibrated Performance Model for Amarillo District, Li Quartile Method (Unconstrained).

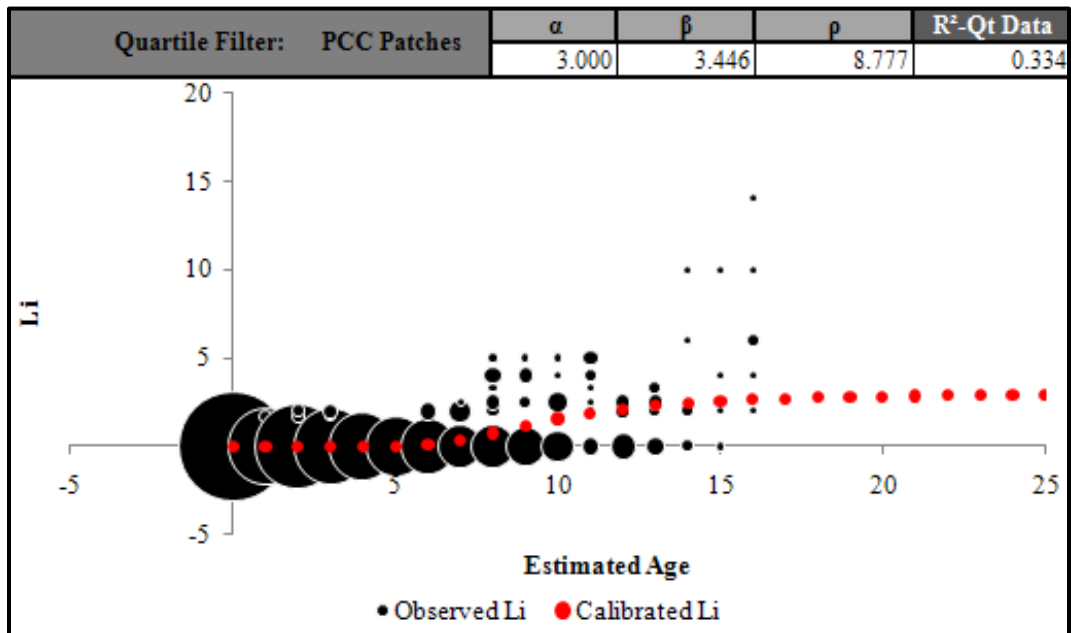


Figure C 4.10. Calibrated Performance Model for Amarillo District, Li Quartile Method (Constrained).

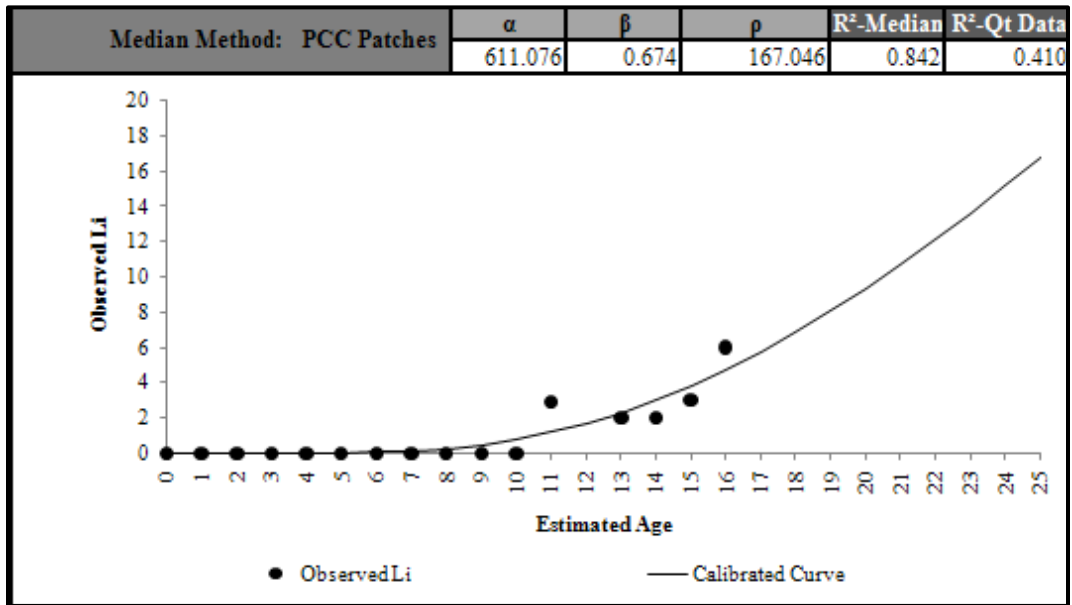


Figure C 4.11. Calibrated Performance Model for Amarillo District, Li Median Method (Unconstrained).

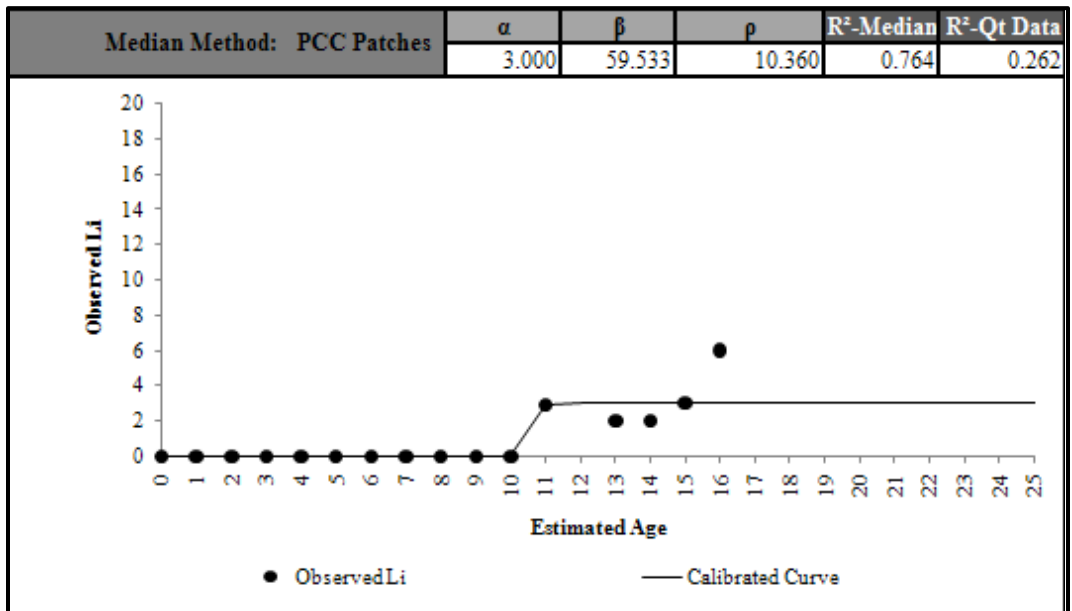


Figure C 4.12. Calibrated Performance Model for Amarillo District, Li Median Method (Constrained).

Lubbock District 05-Spalled Cracks

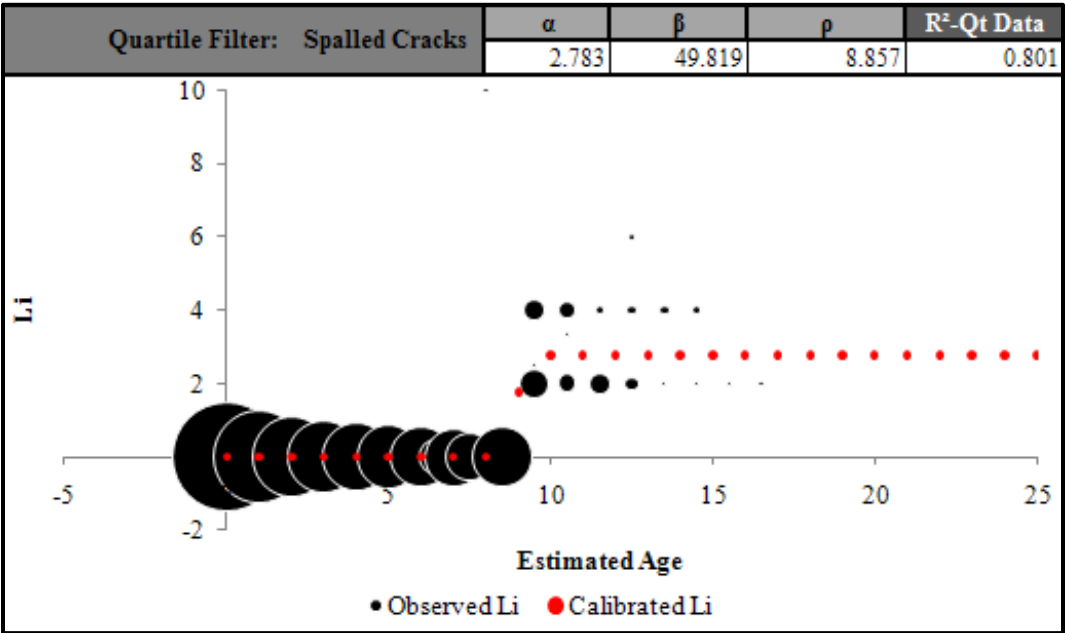


Figure C 5.1. Calibrated Performance Model for Lubbock District, Li Quartile Method (Unconstrained).

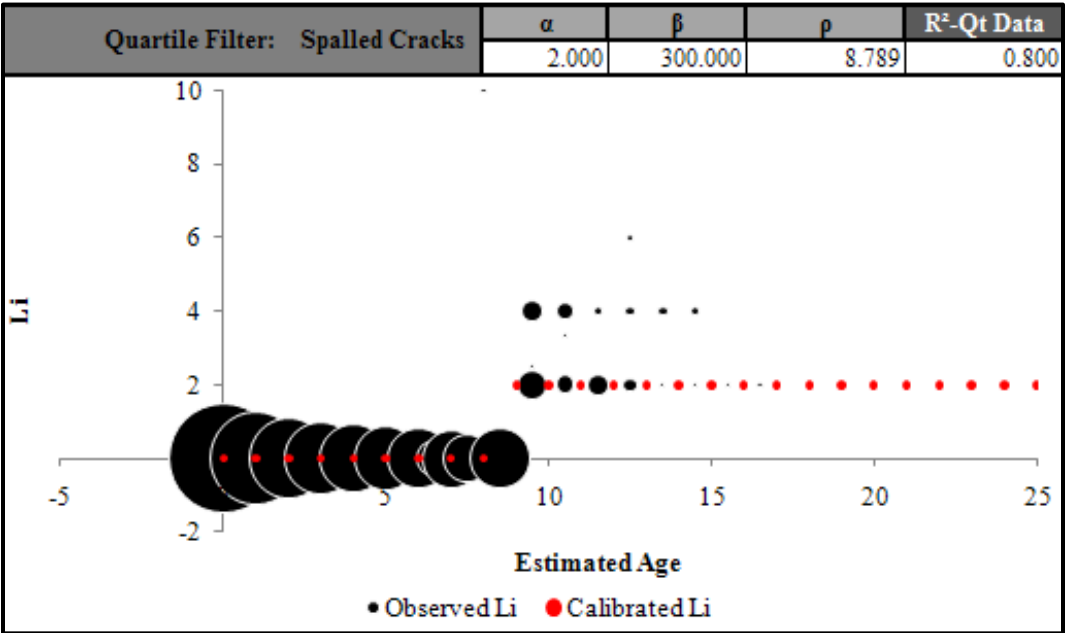


Figure C 5.2. Calibrated Performance Model for Lubbock District, Li Quartile Method (Constrained).

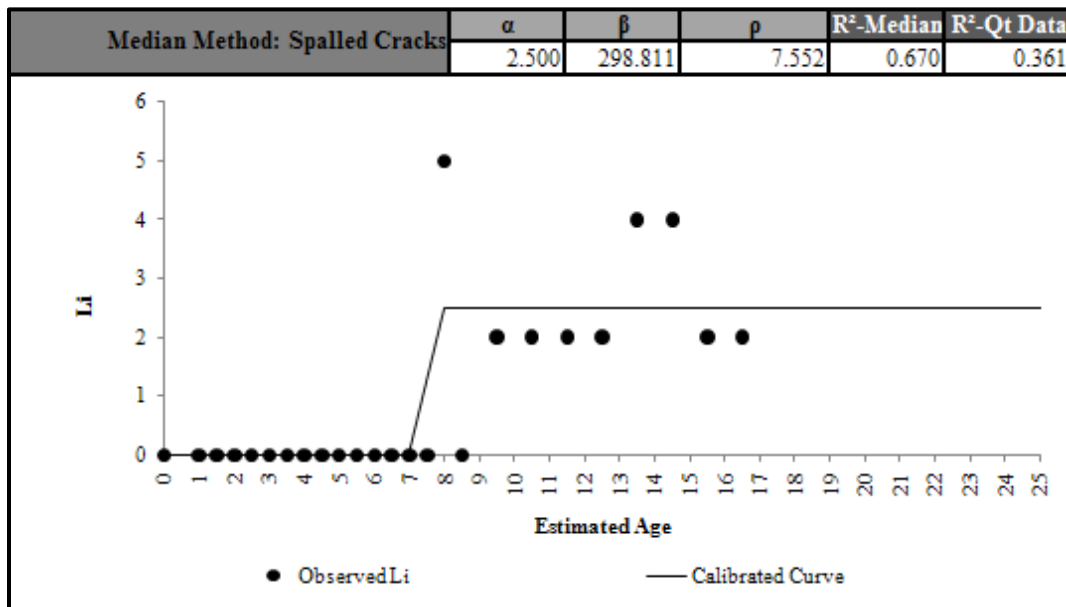


Figure C 5.3. Calibrated Performance Model for Lubbock District, Li Median Method (Unconstrained).

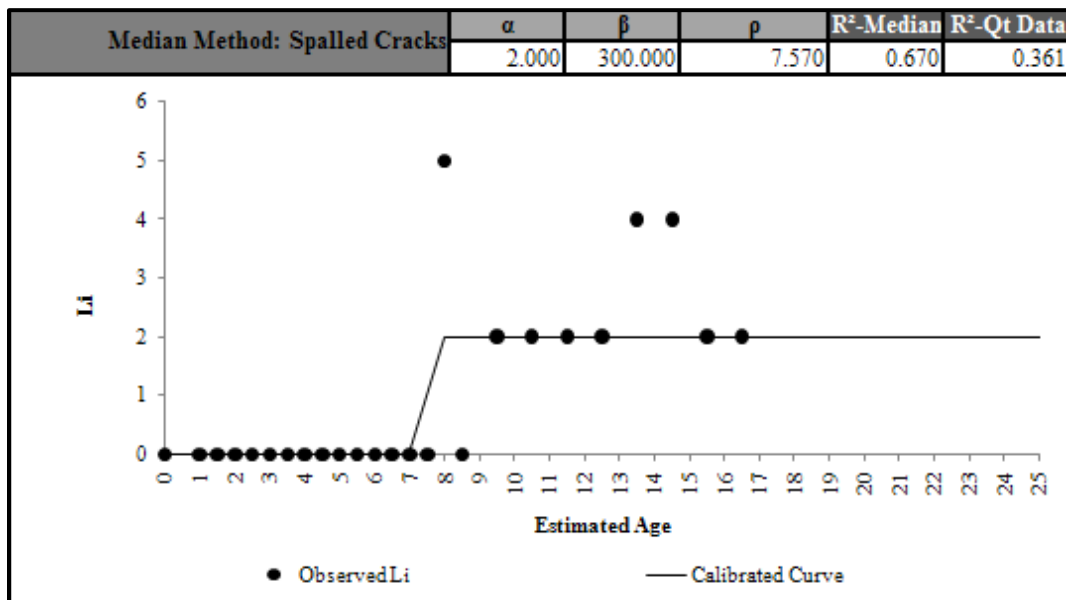


Figure C 5.4. Calibrated Performance Model for Lubbock District, Li Median Method (Constrained).

Lubbock District 05-Punchouts

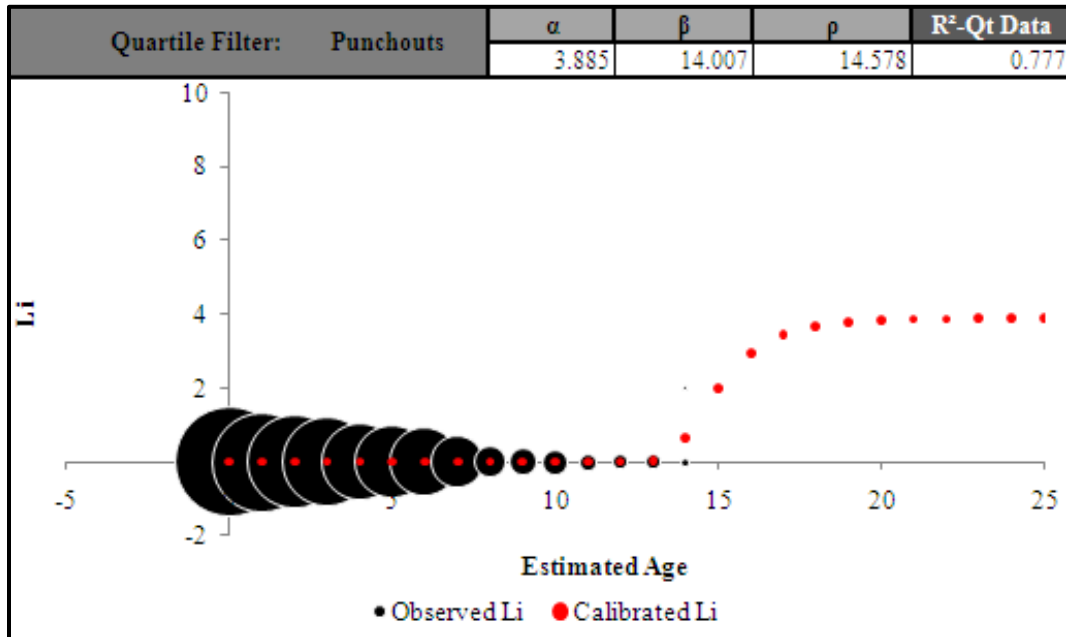


Figure C 5.5. Calibrated Performance Model for Lubbock District, Li Quartile Method (Unconstrained).

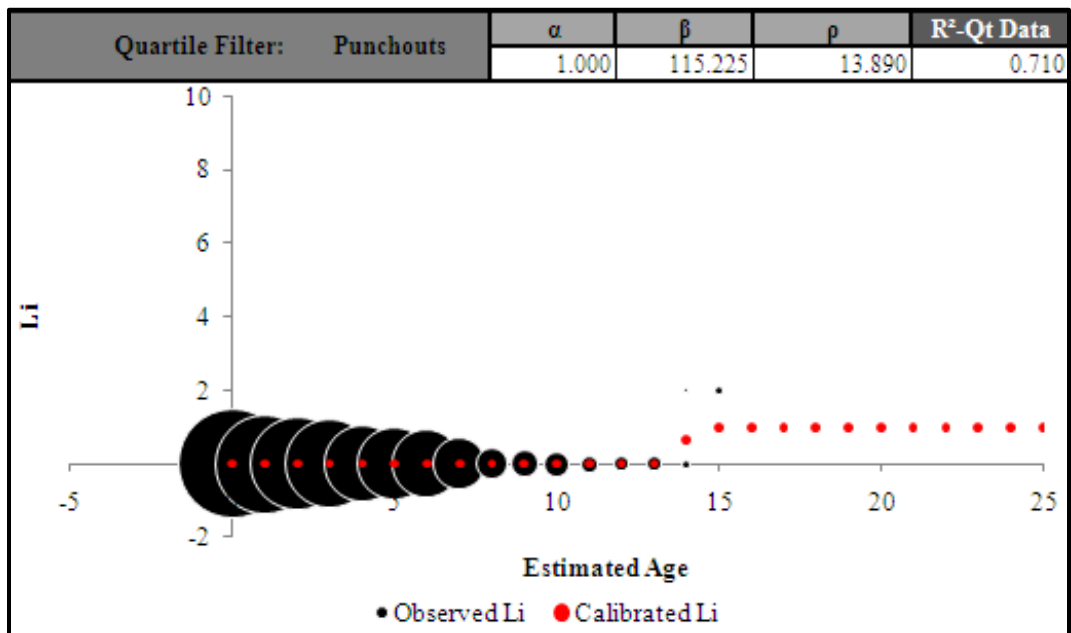


Figure C 5.6. Calibrated Performance Model for Lubbock District, Li Quartile Method (Constrained).

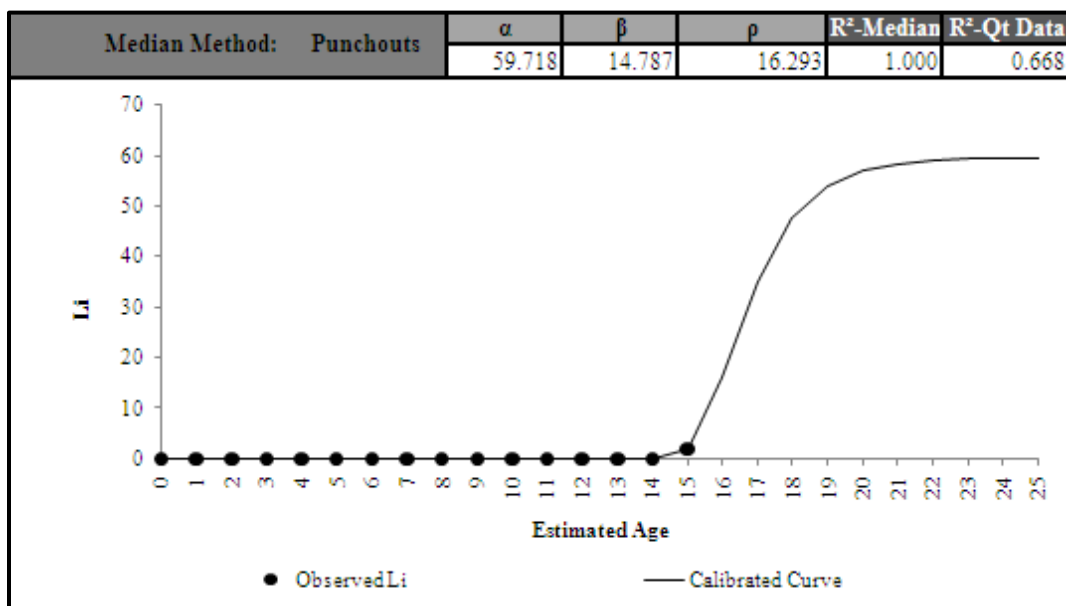


Figure C 5.7. Calibrated Performance Model for Lubbock District, Li Median Method (Unconstrained).

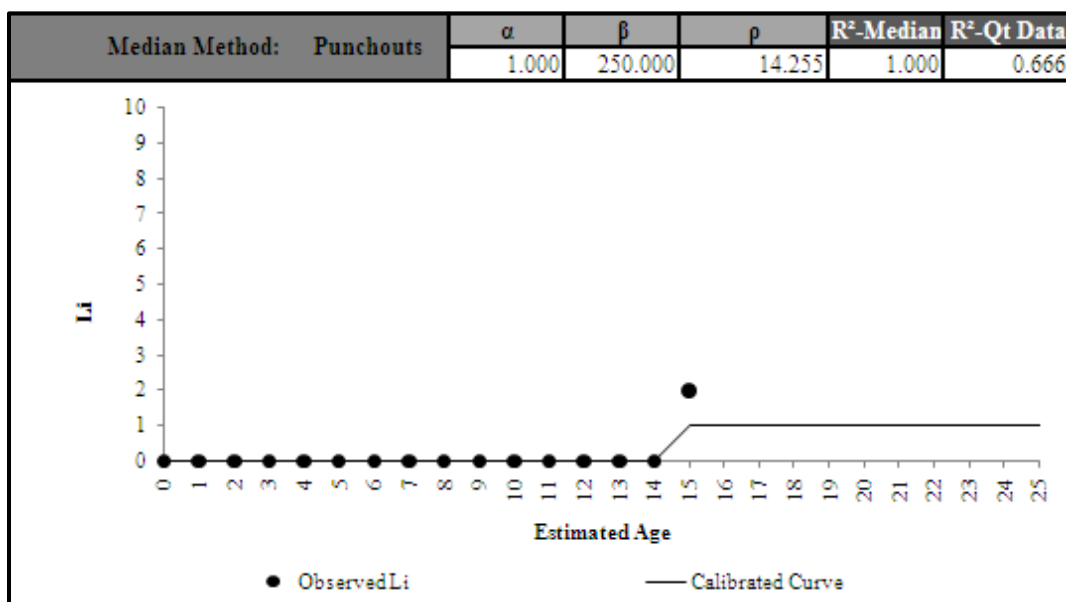


Figure C 5.8. Calibrated Performance Model for Lubbock District, Li Median Method (Constrained).

Lubbock District 05-ACP Patches

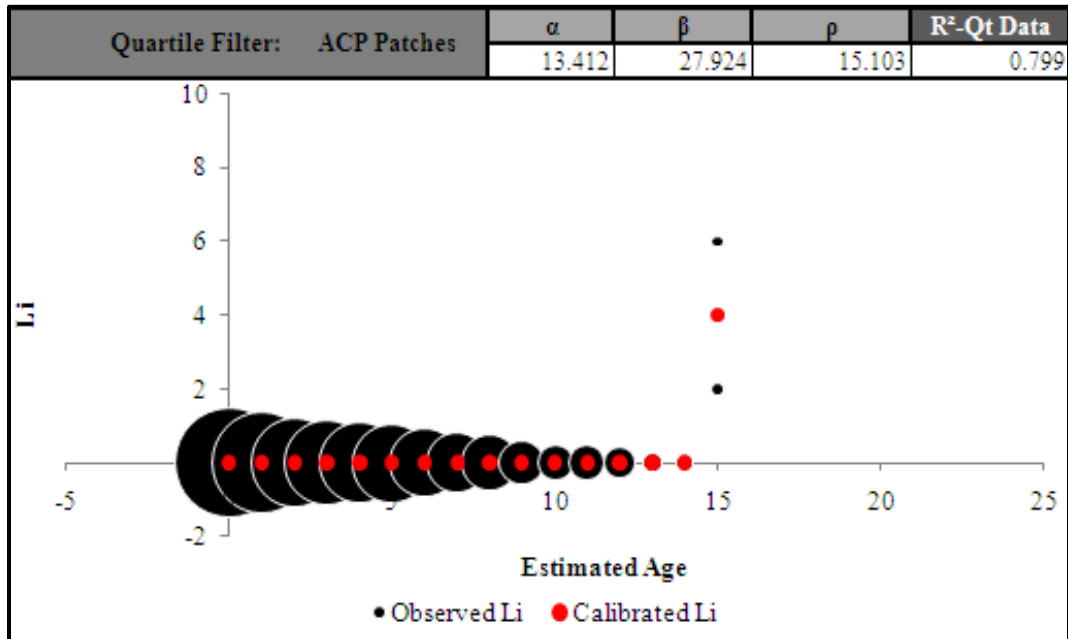


Figure C 5.9. Calibrated Performance Model for Lubbock District, Li Quartile Method (Unconstrained).

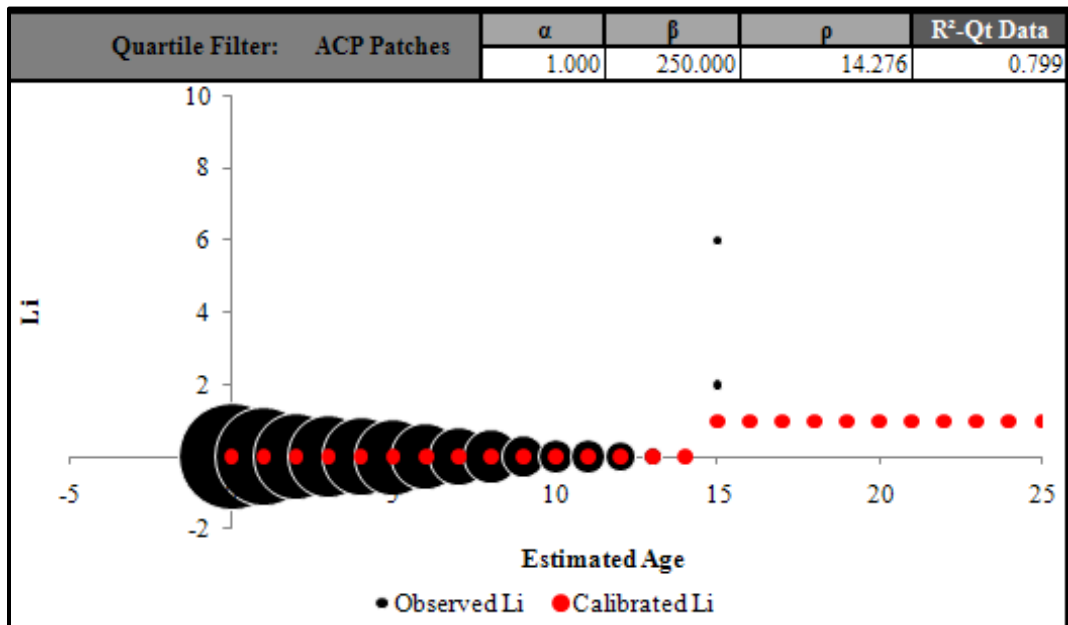


Figure C 5.10. Calibrated Performance Model for Lubbock District, Li Quartile Method (Constrained).

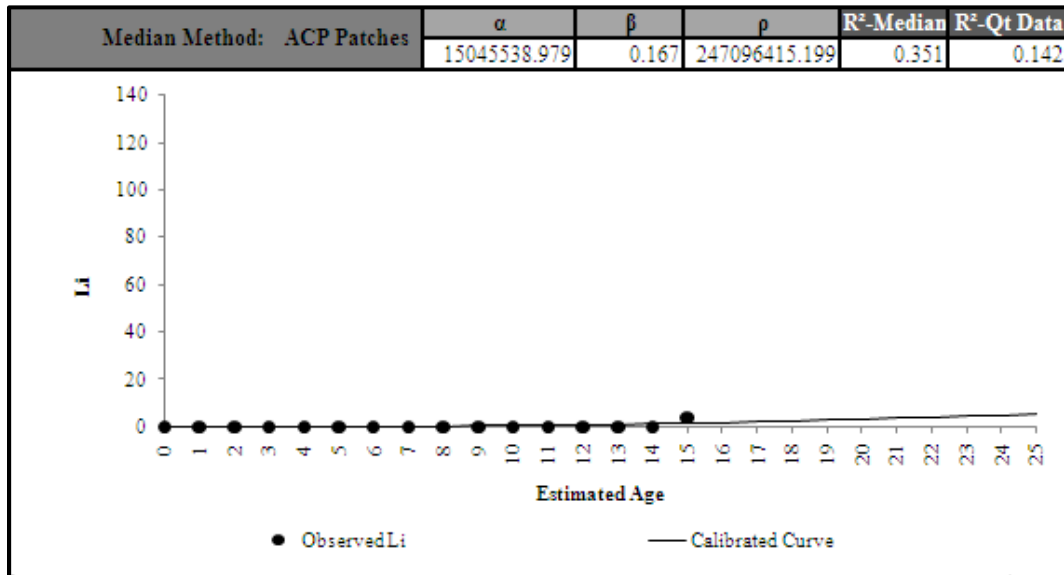


Figure C 5.11. Calibrated Performance Model for Lubbock District, Li Median Method (Unconstrained).

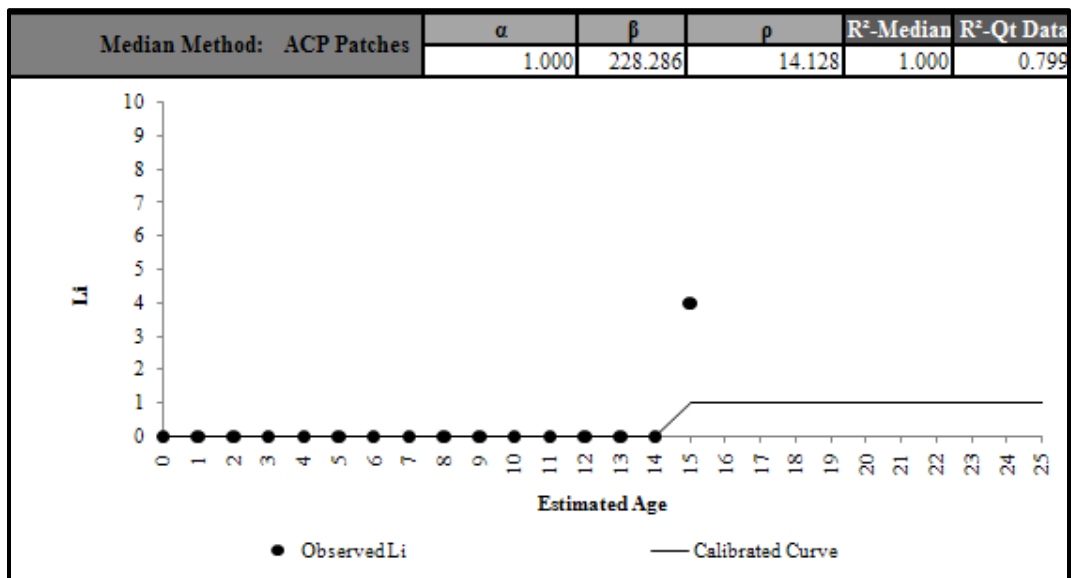


Figure C 5.12. Calibrated Performance Model for Lubbock District, Li Median Method (Constrained).

Lubbock District 05-PCC Patches

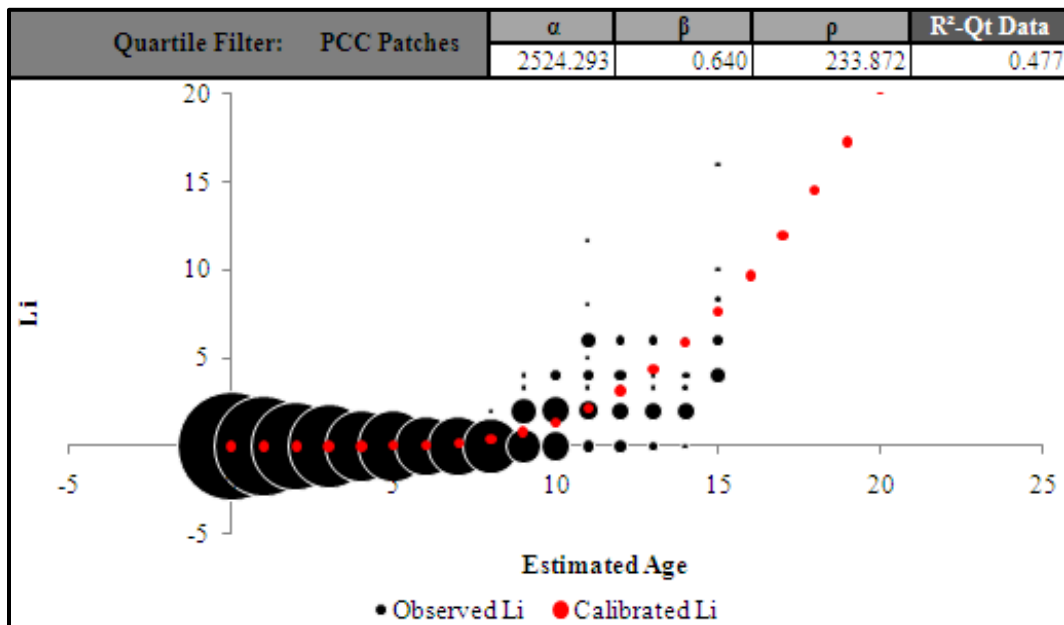


Figure C 5.13. Calibrated Performance Model for Lubbock District, Li Quartile Method (Unconstrained).

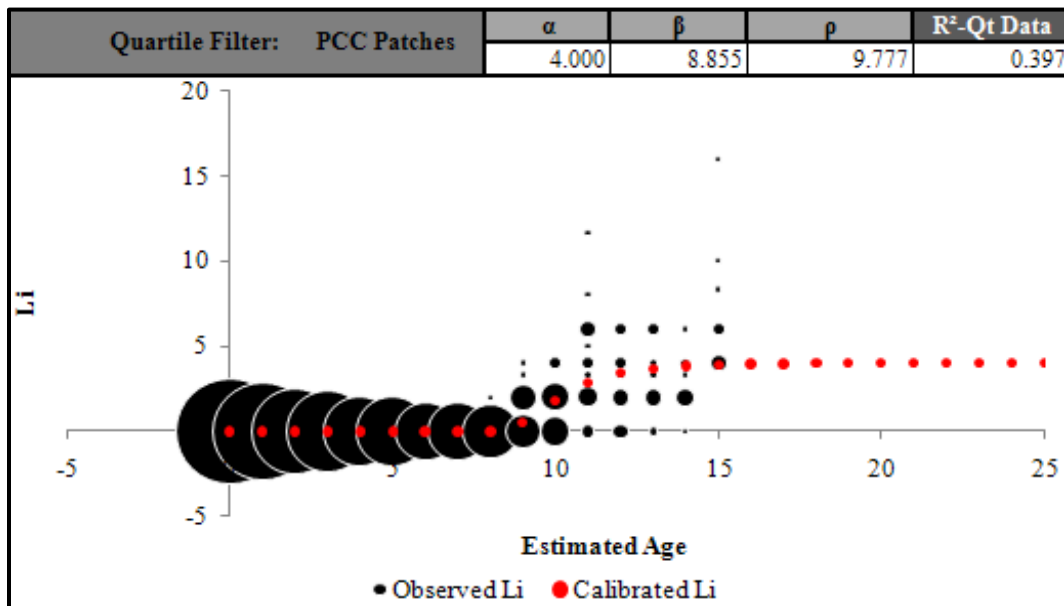


Figure C 5.14. Calibrated Performance Model for Lubbock District, Li Quartile Method (Constrained).

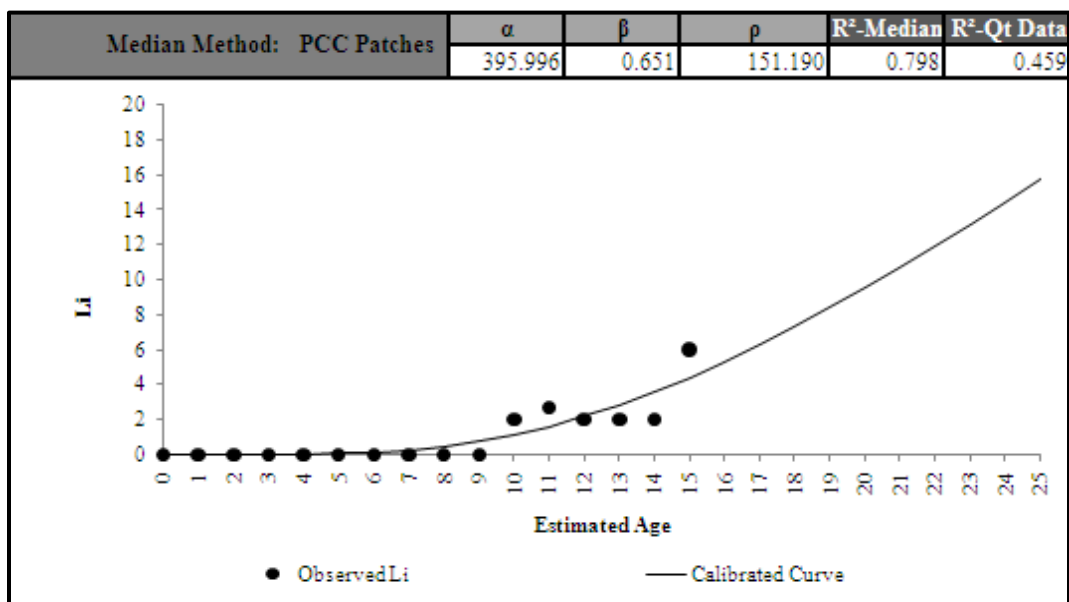


Figure C 5.15. Calibrated Performance Model for Lubbock District, Li Median Method (Unconstrained).

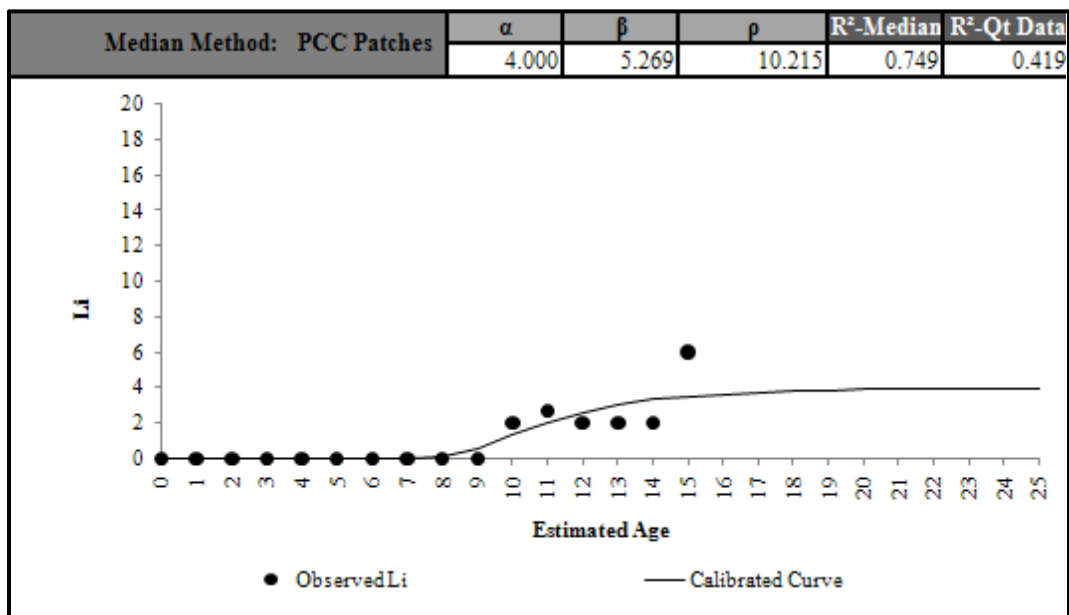


Figure C 5.16. Calibrated Performance Model for Lubbock District, Li Median Method (Constrained).

Odessa District 06-Spalled Cracks

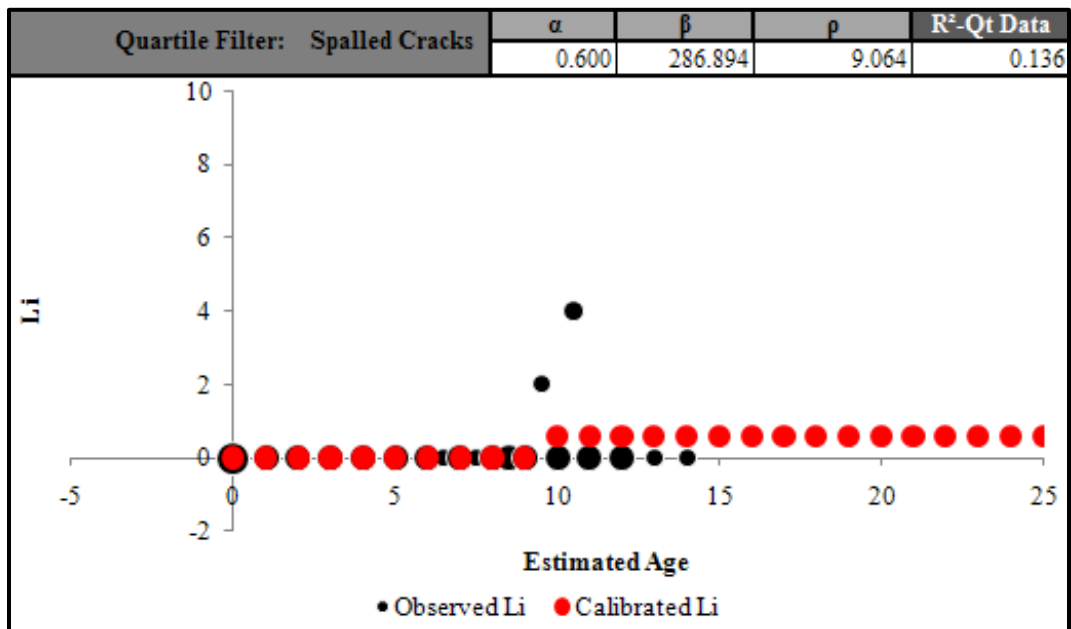


Figure C 6.1. Calibrated Performance Model for Odessa District, Li Quartile Method (Unconstrained).

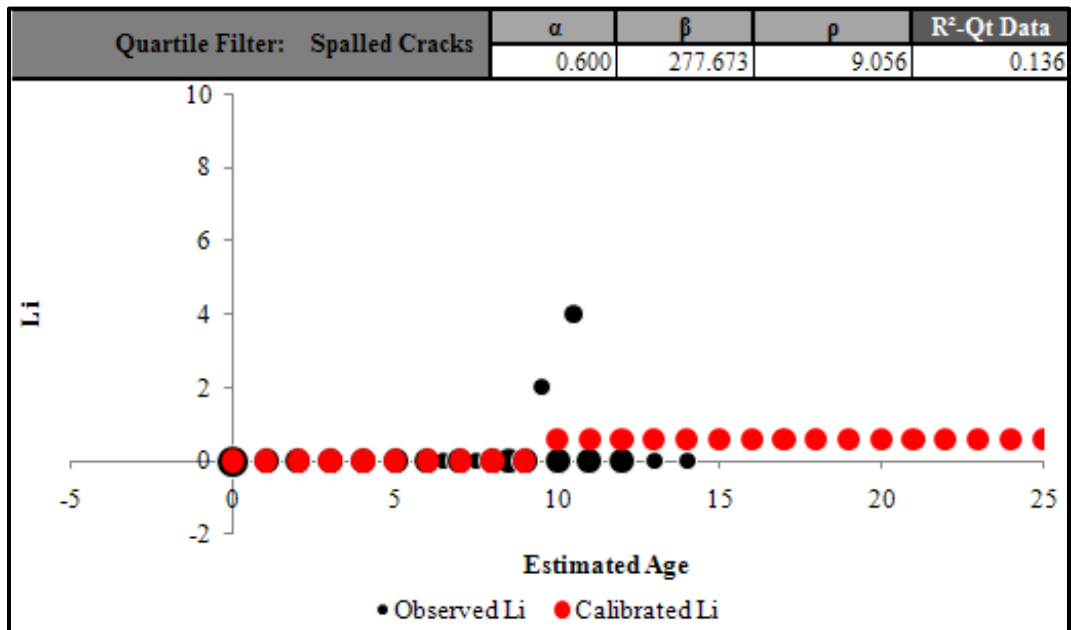


Figure C 6.2. Calibrated Performance Model for Odessa District, Li Quartile Method (Constrained).

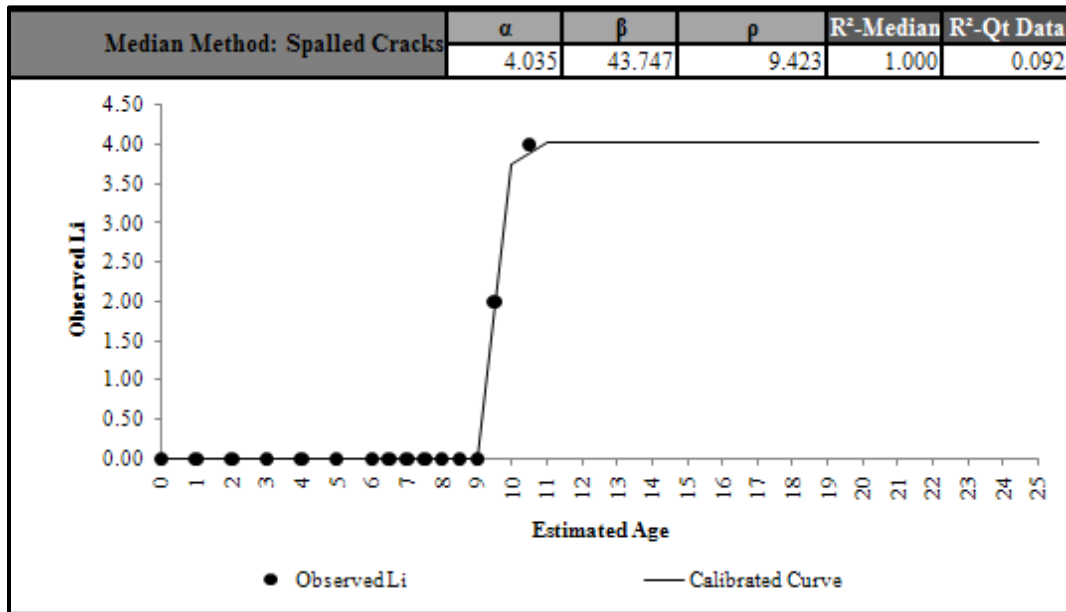


Figure C 6.3. Calibrated Performance Model for Odessa District, Li Median Method (Unconstrained).

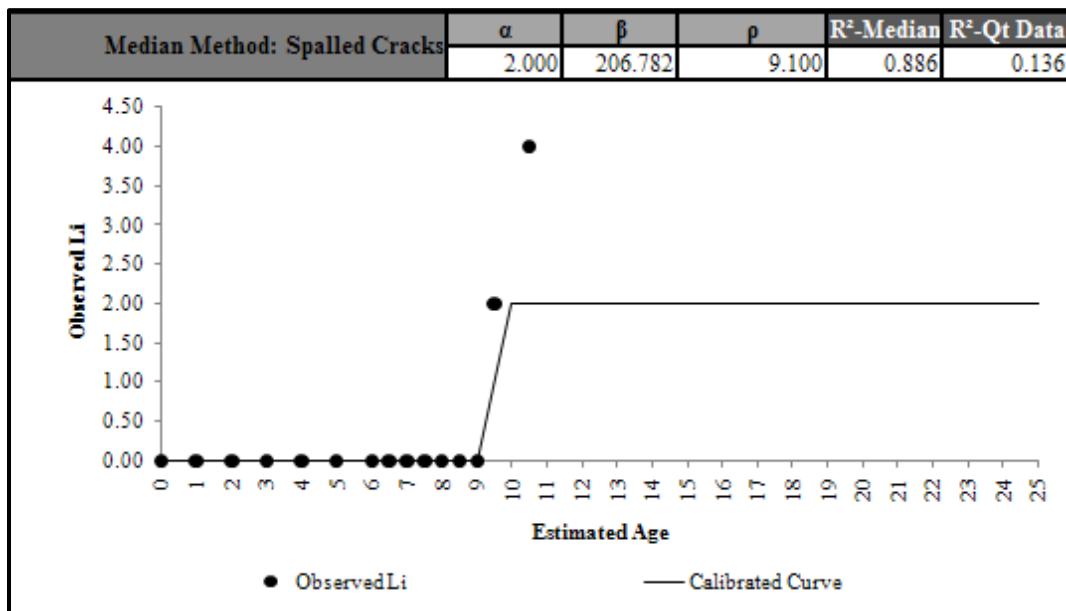


Figure C 6.4. Calibrated Performance Model for Odessa District, Li Median Method (Constrained).

Abilene District 08-PCC Patches

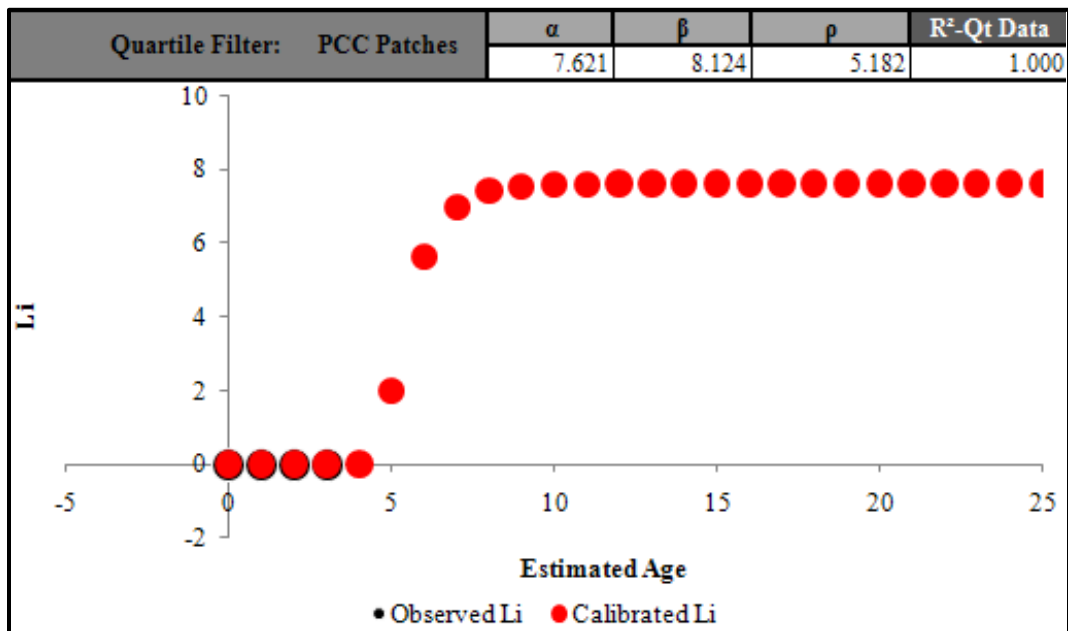


Figure C 8.1. Calibrated Performance Model for Abilene District, Li Quartile Method (Unconstrained).

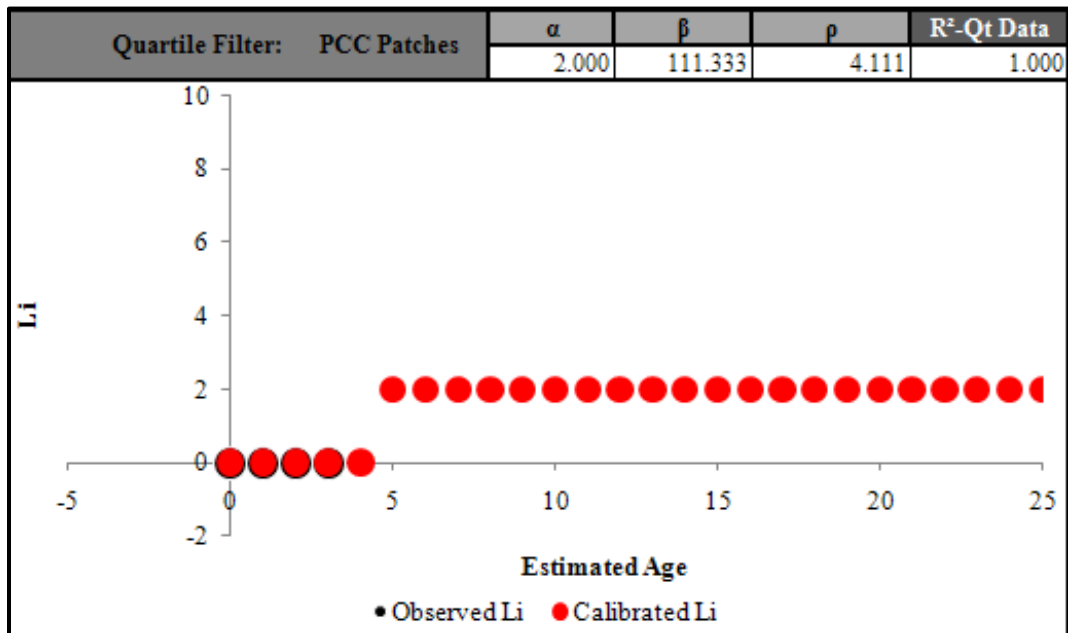


Figure C 8.2. Calibrated Performance Model for Abilene District, Li Quartile Method (Constrained).

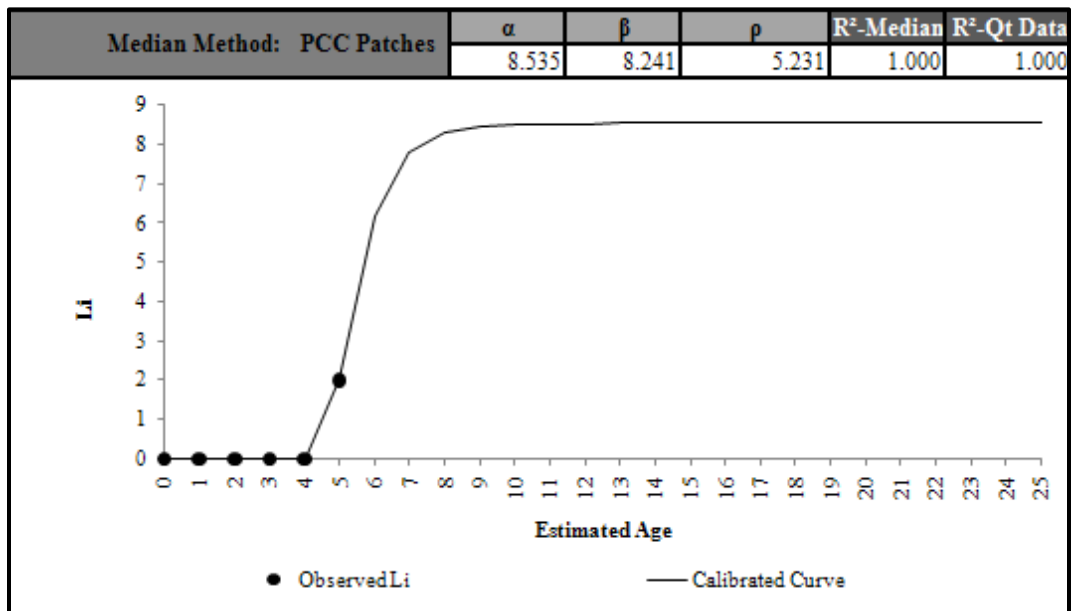


Figure C 8.3. Calibrated Performance Model for Abilene District, Li Median Method (Unconstrained).

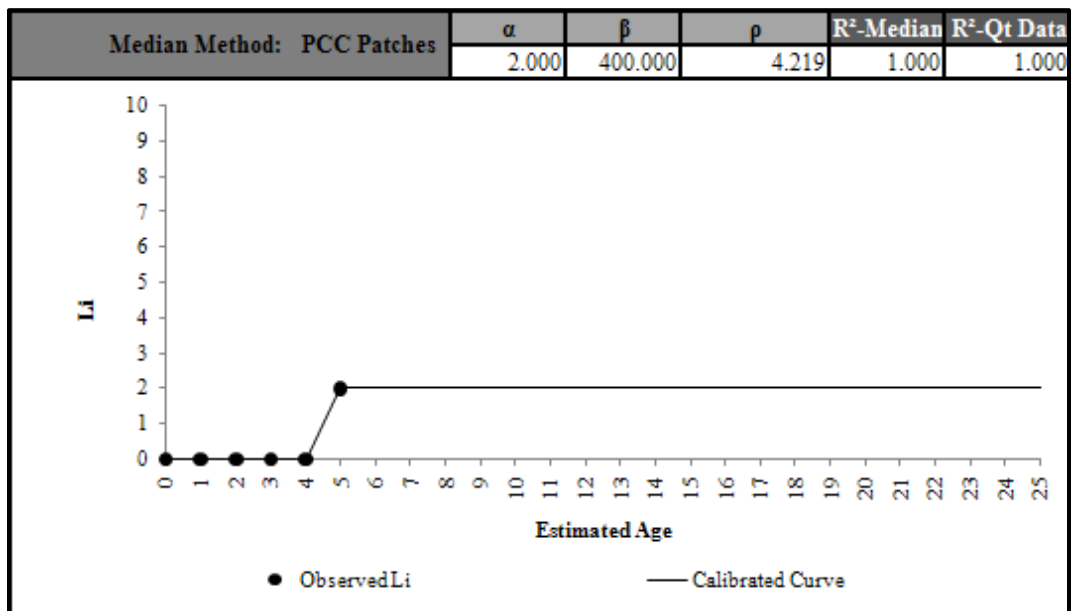


Figure C 8.4. Calibrated Performance Model for Abilene District, Li Median Method (Constrained).

Waco District 09-Spalled Cracks

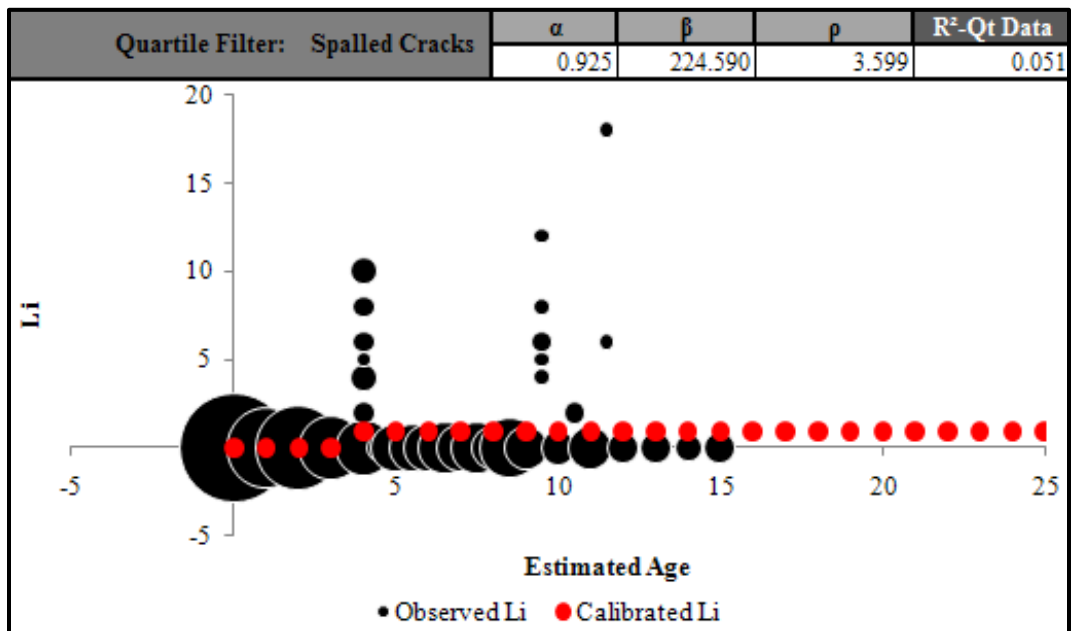


Figure C 9.1. Calibrated Performance Model for Waco District, Li Quartile Method (Unconstrained).

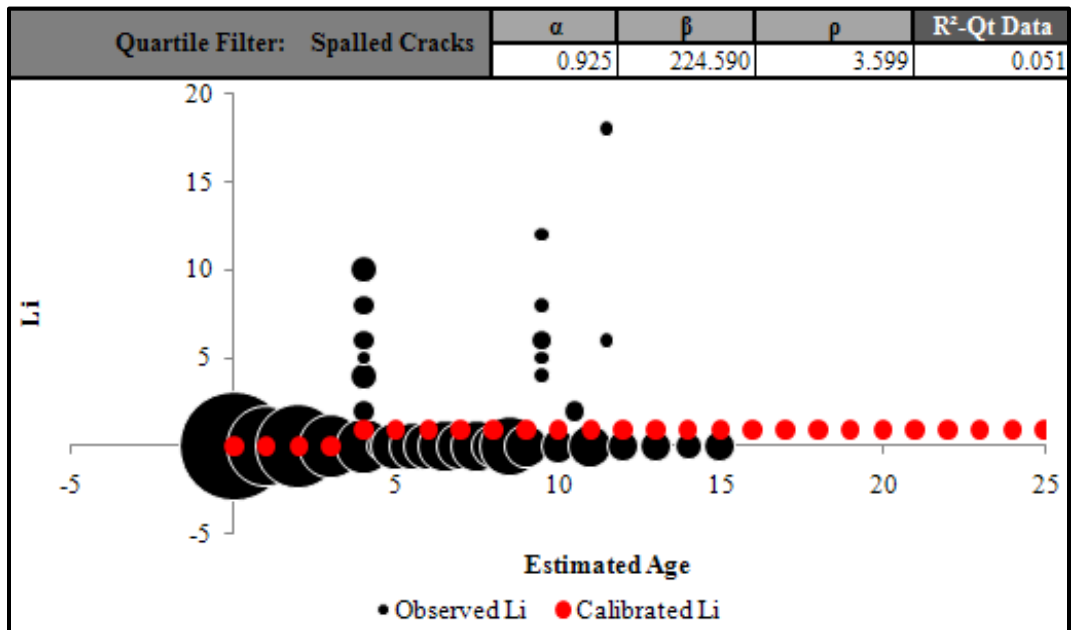


Figure C 9.2. Calibrated Performance Model for Waco District, Li Quartile Method (Constrained).

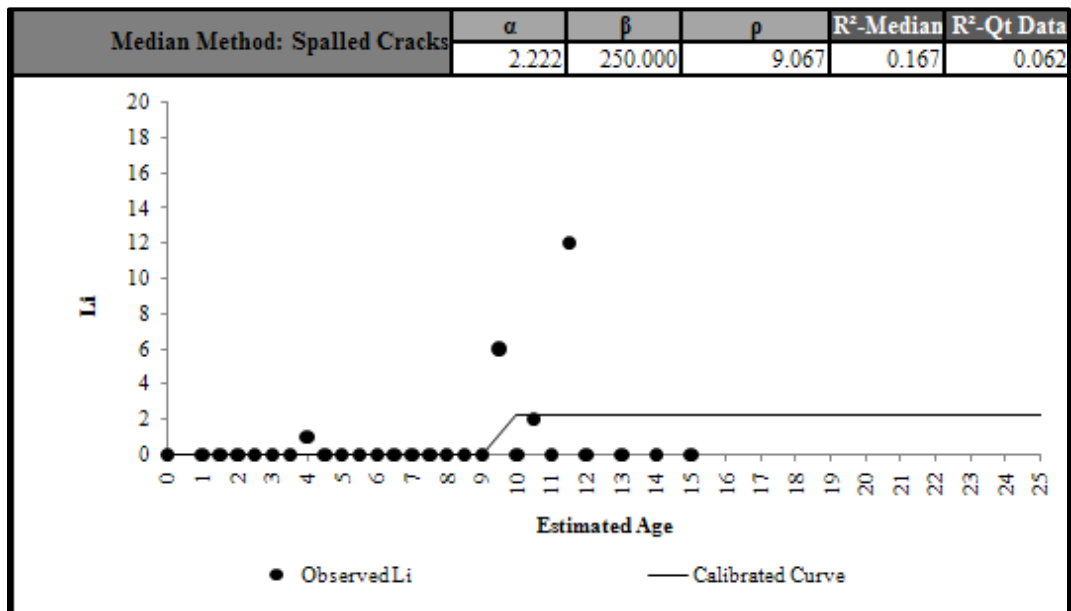


Figure C 9.3. Calibrated Performance Model for Waco District, Li Median Method (Unconstrained).

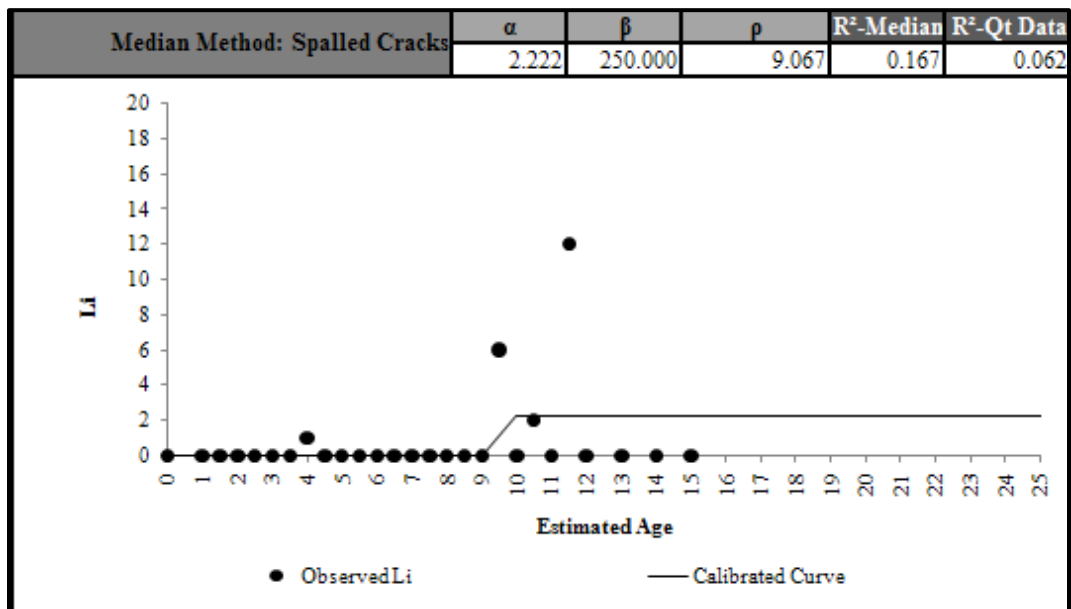


Figure C 9.4. Calibrated Performance Model for Waco District, Li Median Method (Constrained).

Waco District 09-PCC Patches

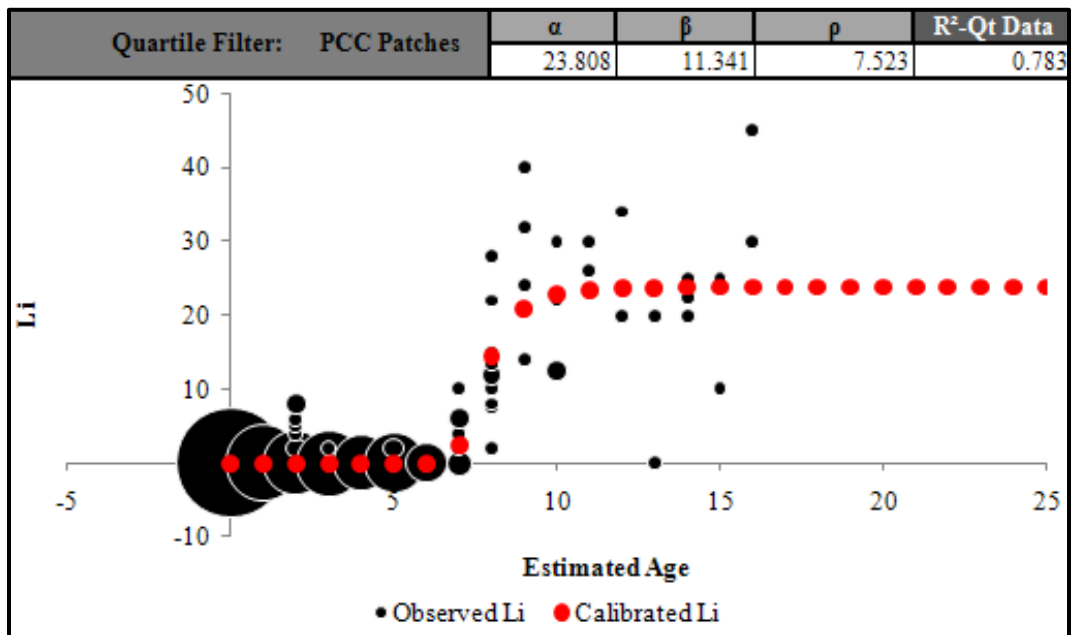


Figure C 9.5. Calibrated Performance Model for Waco District, Li Quartile Method (Unconstrained).

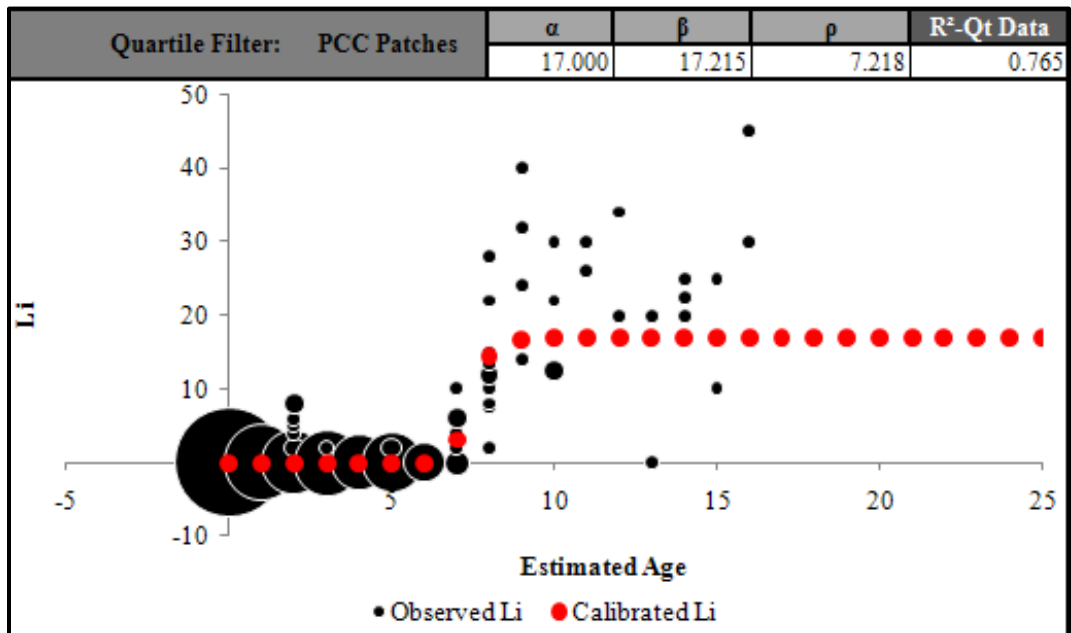


Figure C 9.6. Calibrated Performance Model for Waco District, Li Quartile Method (Constrained).

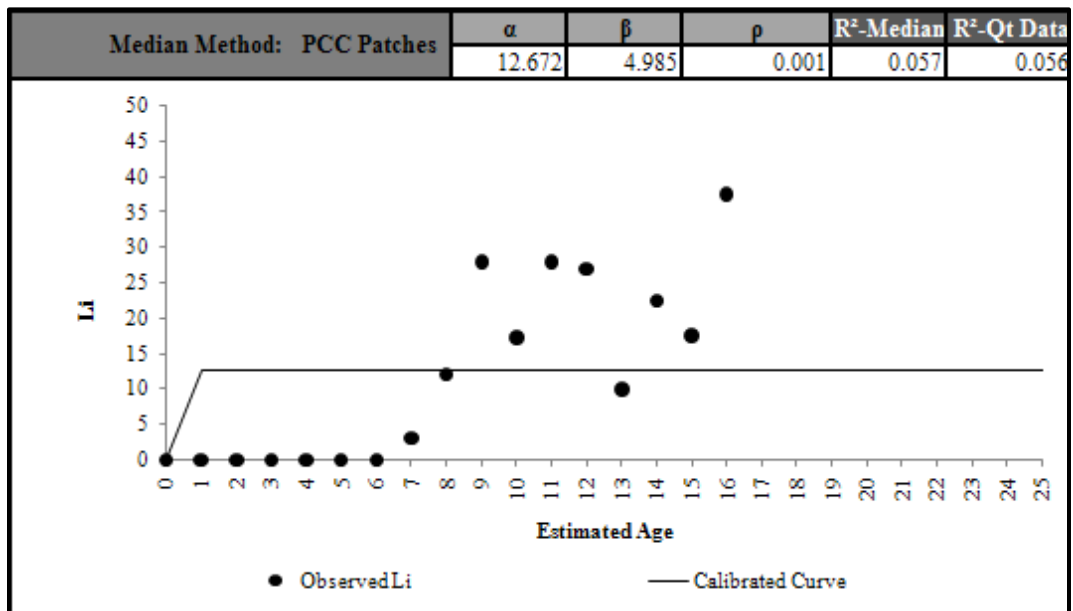


Figure C 9.7. Calibrated Performance Model for Waco District, Li Median Method (Unconstrained).

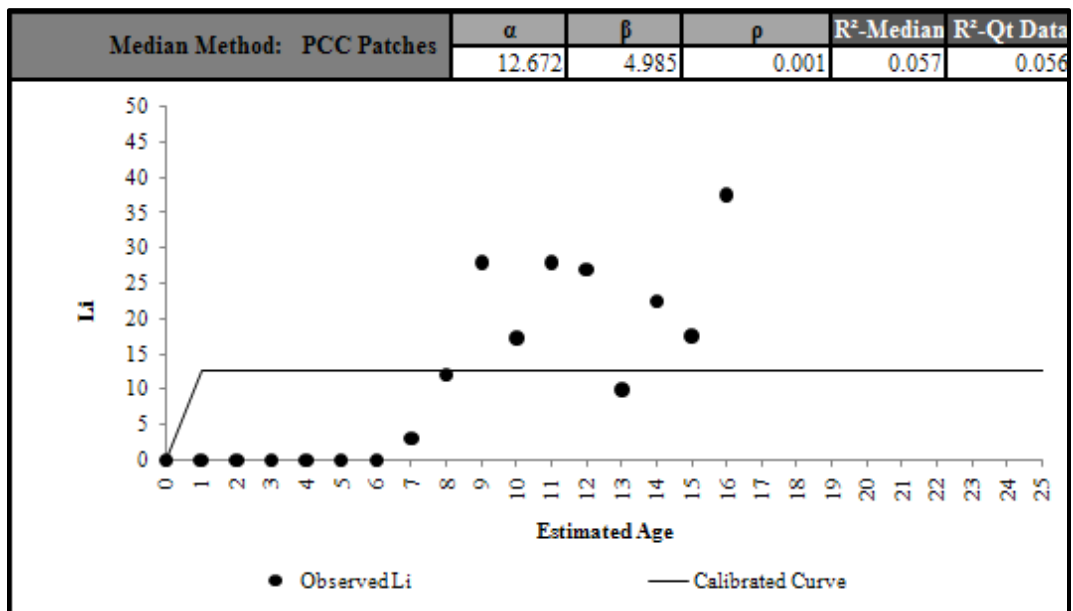


Figure C 9.8. Calibrated Performance Model for Waco District, Li Median Method (Constrained).

Tyler District 10-Spalled Cracks

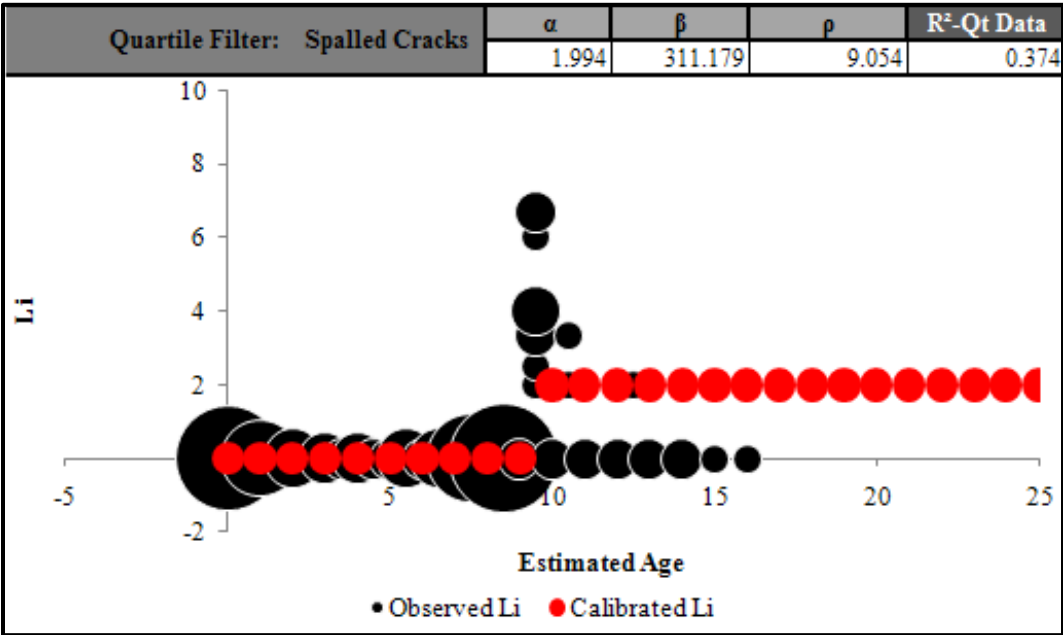


Figure C 10.1. Calibrated Performance Model for Tyler District, Li Quartile Method (Unconstrained).

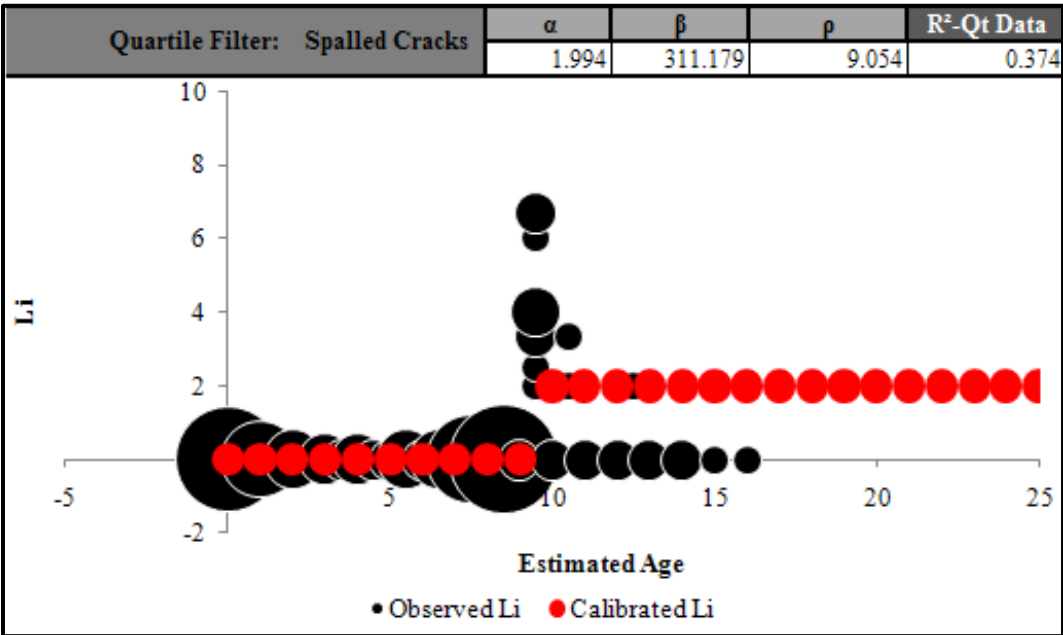


Figure C 10.2. Calibrated Performance Model for Tyler District, Li Quartile Method (Constrained).

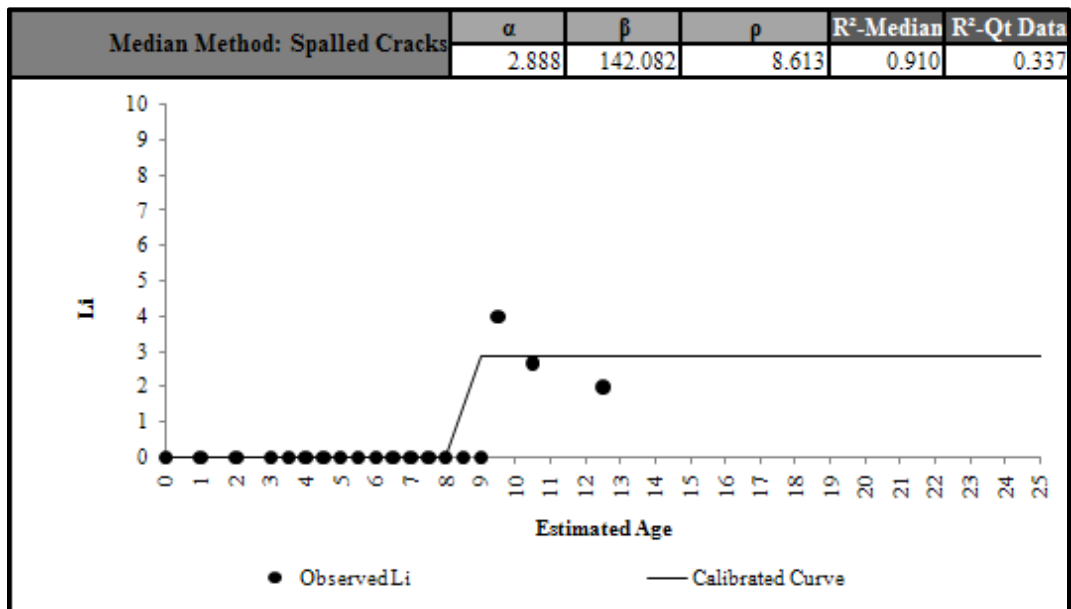


Figure C 10.3. Calibrated Performance Model for Tyler District, Li Median Method (Unconstrained).

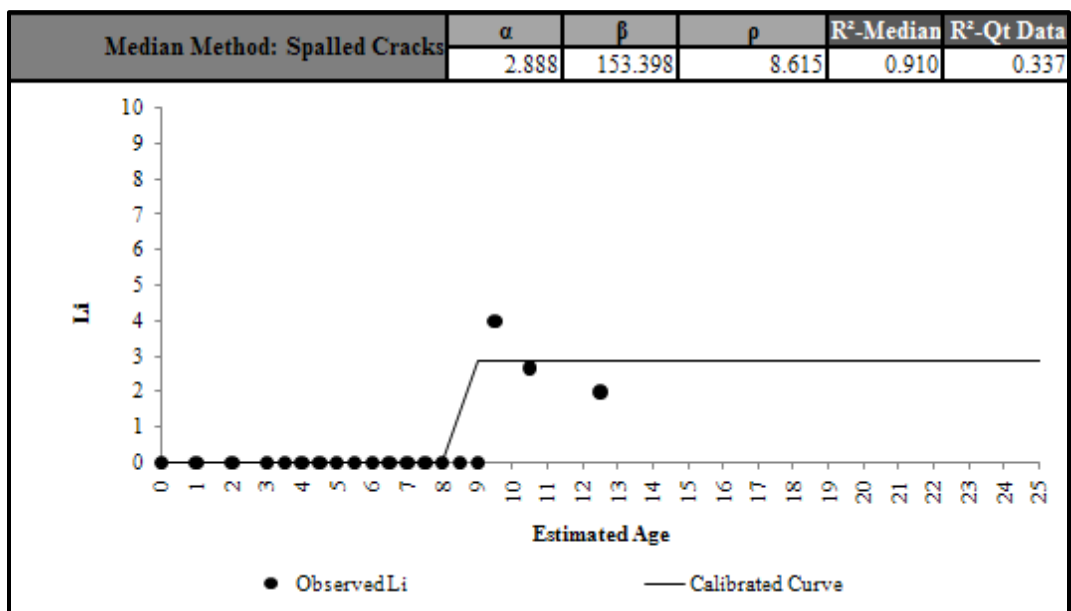


Figure C 10.4. Calibrated Performance Model for Tyler District, Li Median Method (Constrained).

Tyler District 10-Punchouts

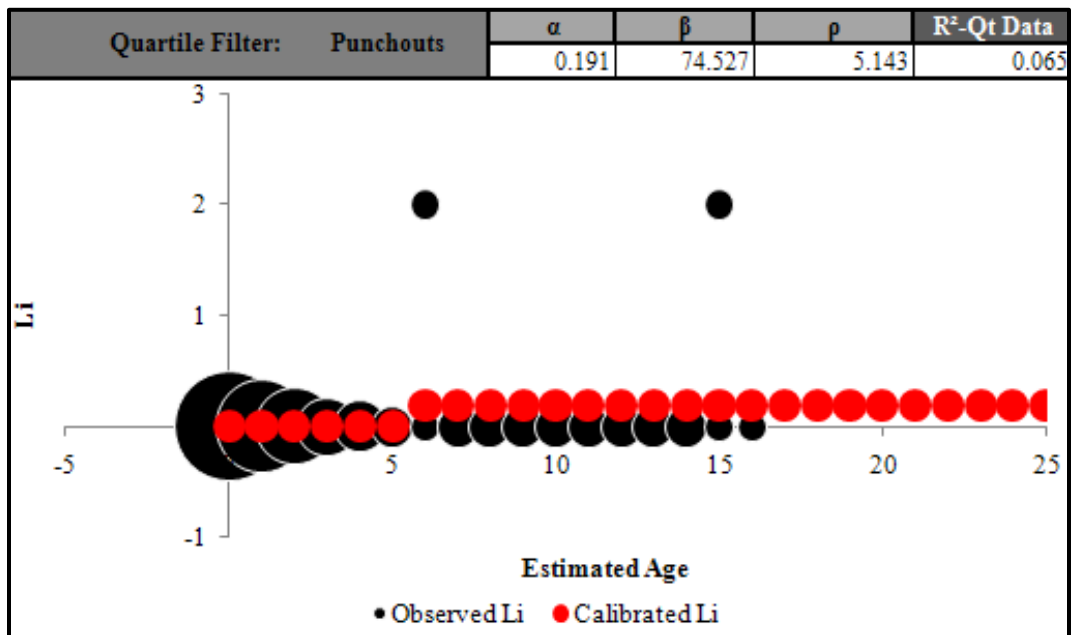


Figure C 10.5. Calibrated Performance Model for Tyler District, Li Quartile Method (Unconstrained).

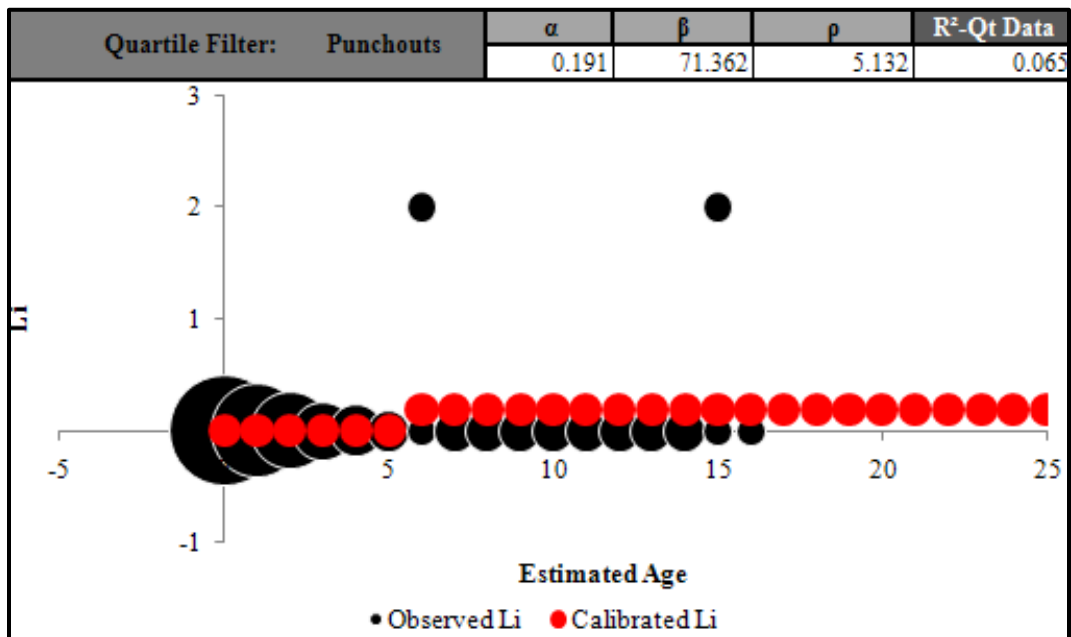


Figure C 10.6. Calibrated Performance Model for Tyler District, Li Quartile Method (Constrained).

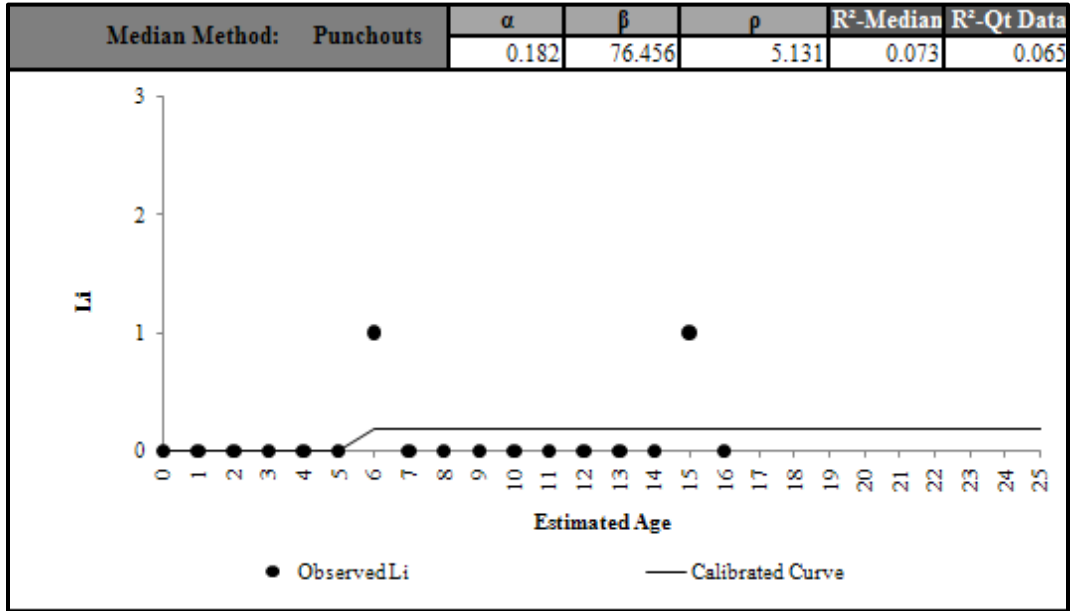


Figure C 10.7. Calibrated Performance Model for Tyler District, Li Median Method (Unconstrained).

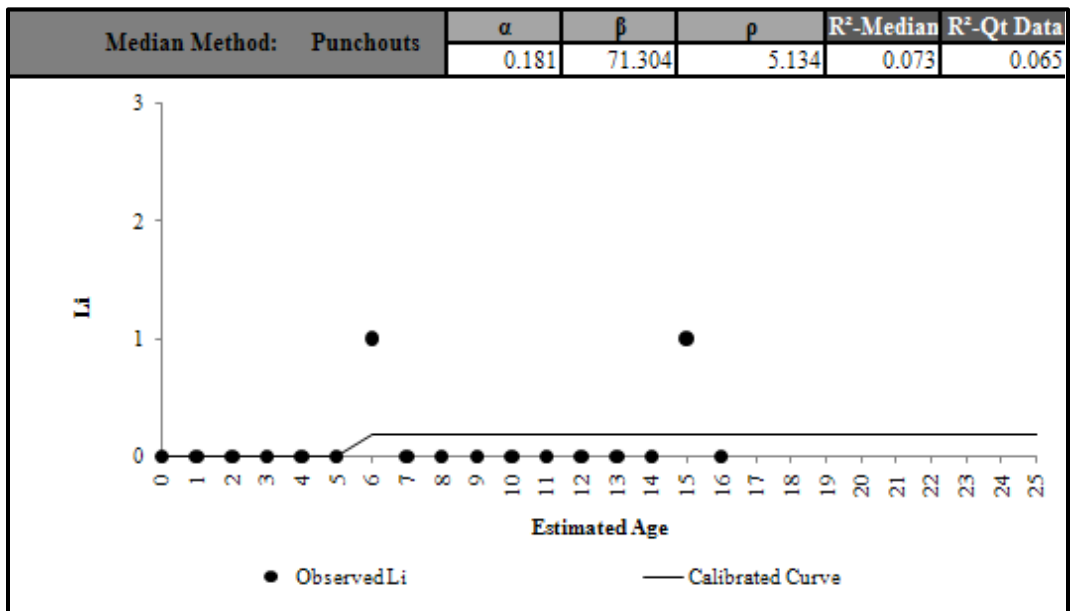


Figure C 10.8. Calibrated Performance Model for Tyler District, Li Median Method (Constrained).

Tyler District 10-PCC Patches

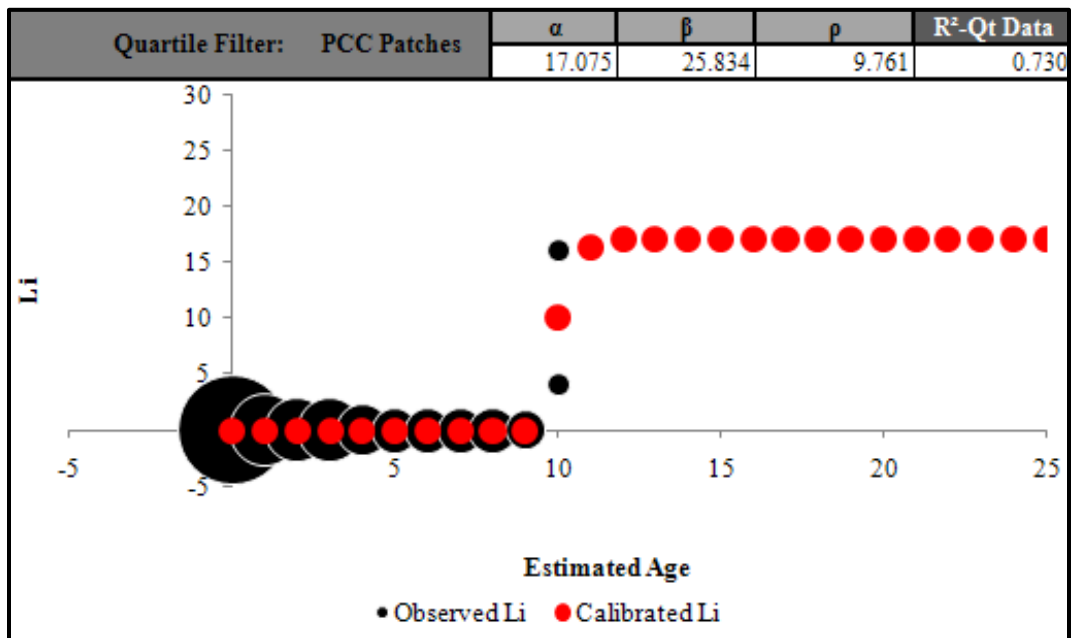


Figure C 10.9. Calibrated Performance Model for Tyler District, Li Quartile Method (Unconstrained).

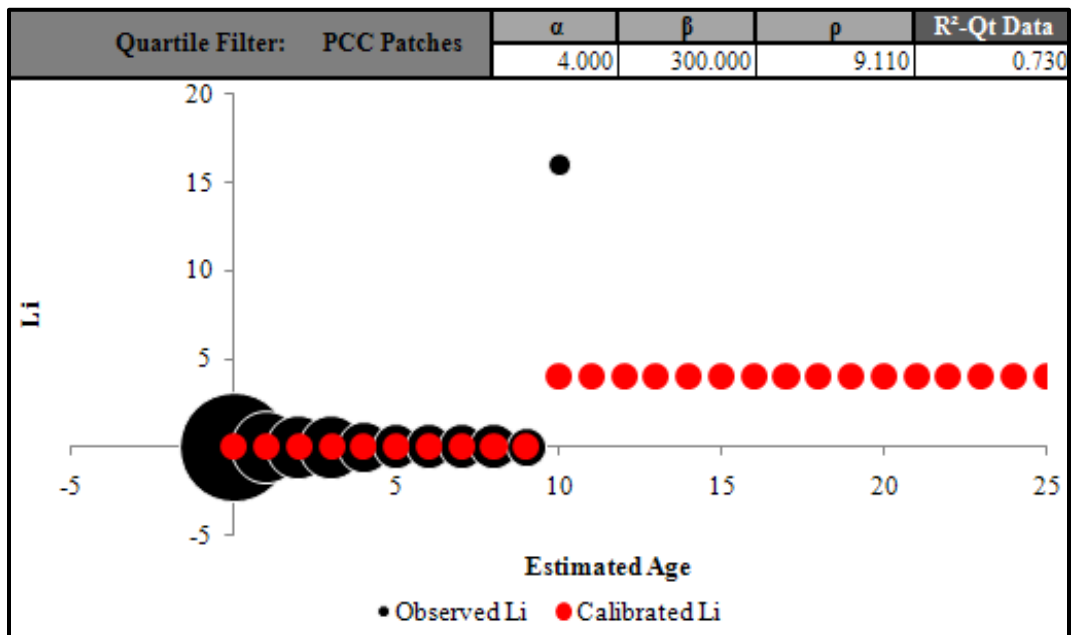


Figure C 10.10. Calibrated Performance Model for Tyler District, Li Quartile Method (Constrained).

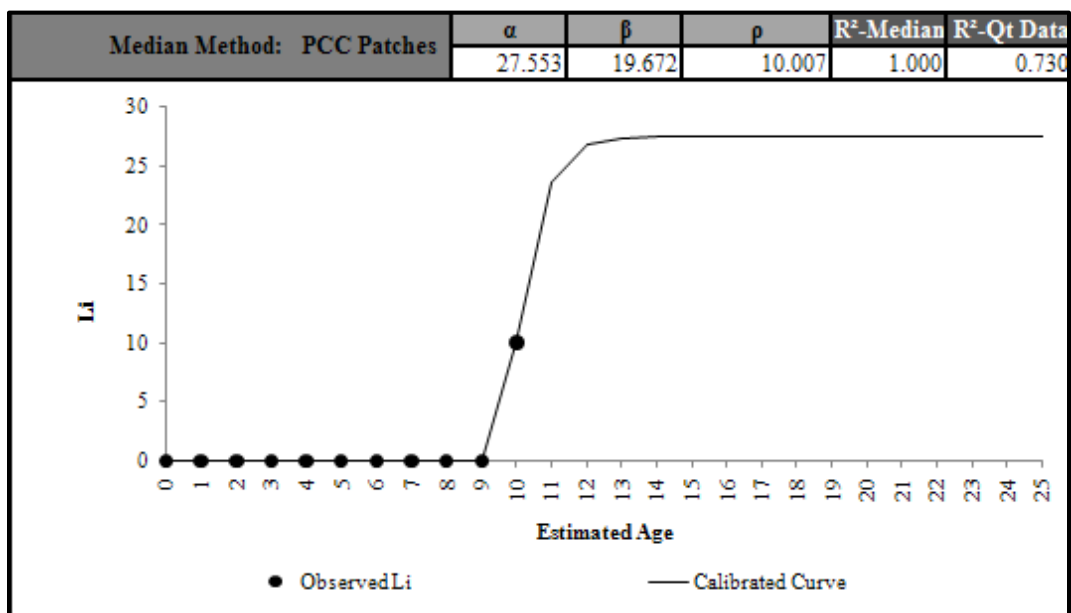


Figure C 10.11. Calibrated Performance Model for Tyler District, Li Median Method (Unconstrained).

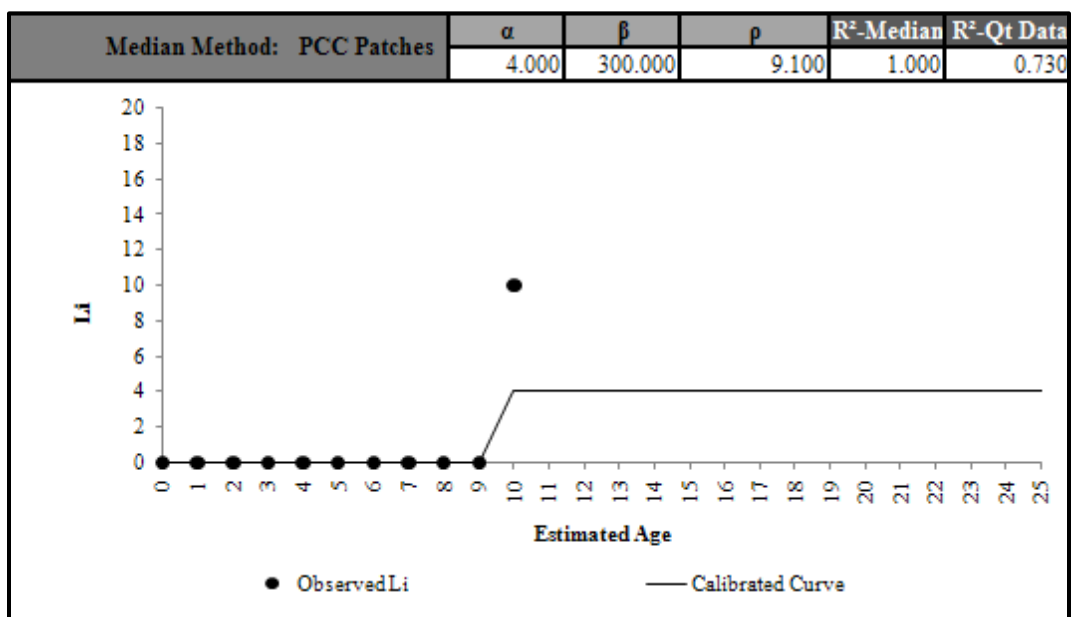


Figure C 10.12. Calibrated Performance Model for Tyler District, Li Median Method (Constrained).

Houston District 12-Spalled Cracks

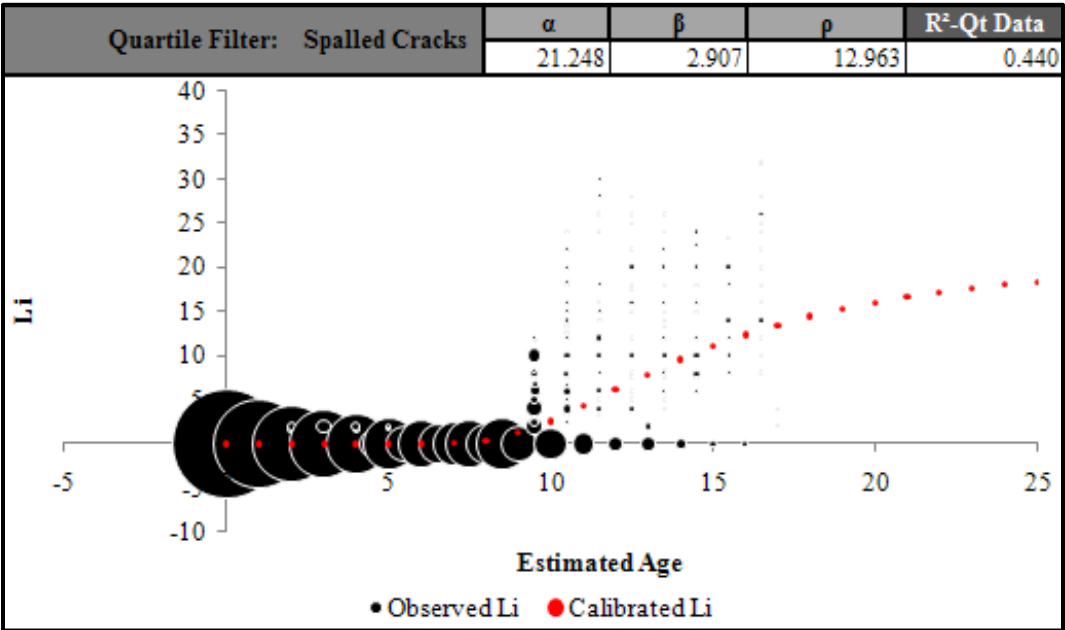


Figure C 12.1. Calibrated Performance Model for Houston District, Li Quartile Method (Unconstrained).

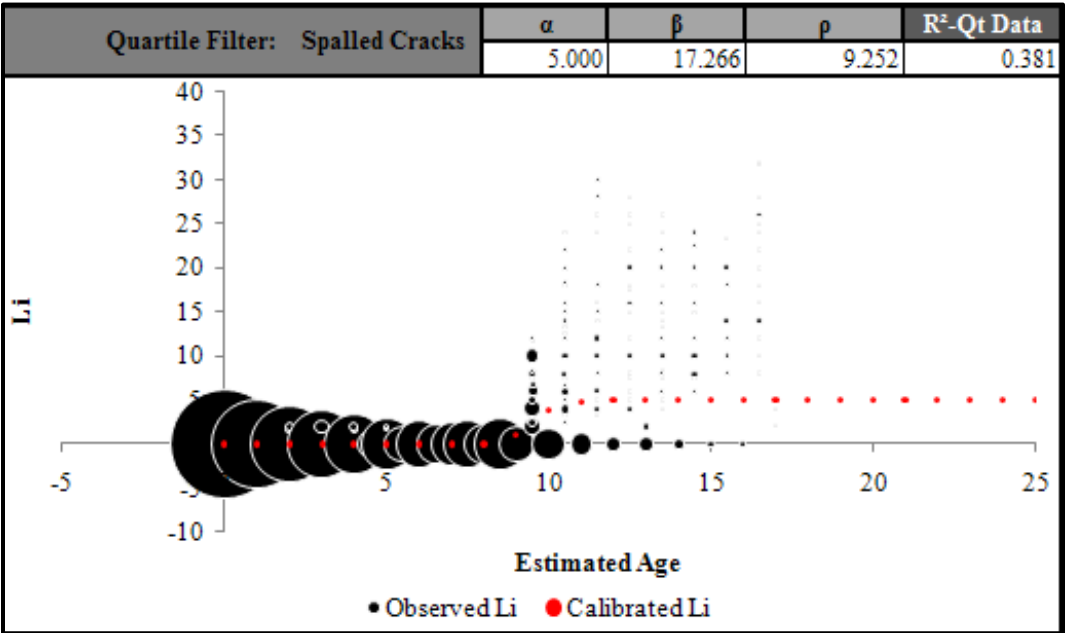


Figure C 12.2. Calibrated Performance Model for Houston District, Li Quartile Method (Constrained).

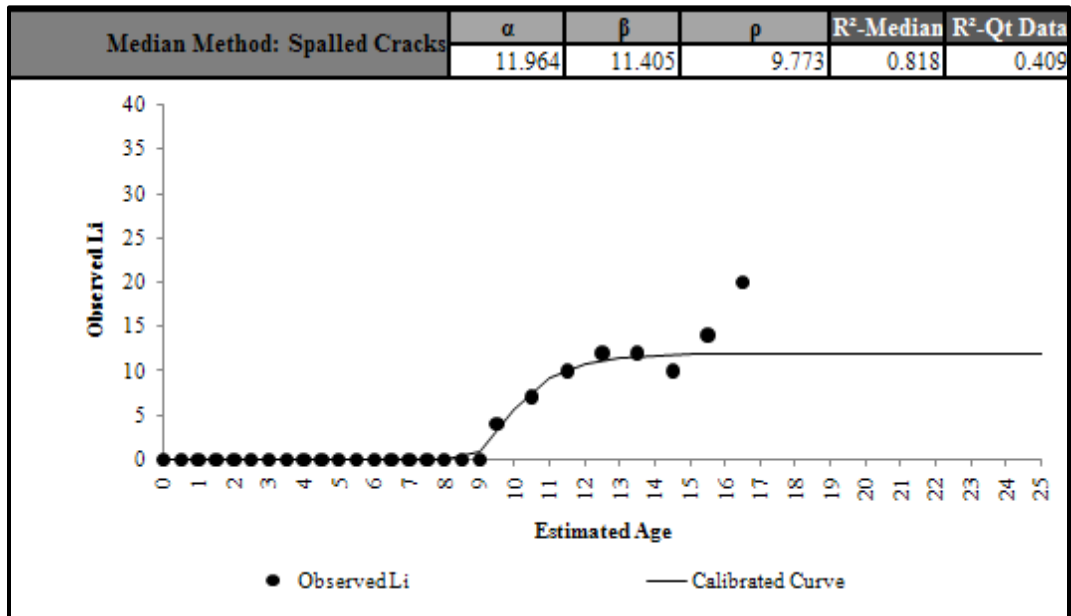


Figure C 12.3. Calibrated Performance Model for Houston District, Li Median Method (Unconstrained).

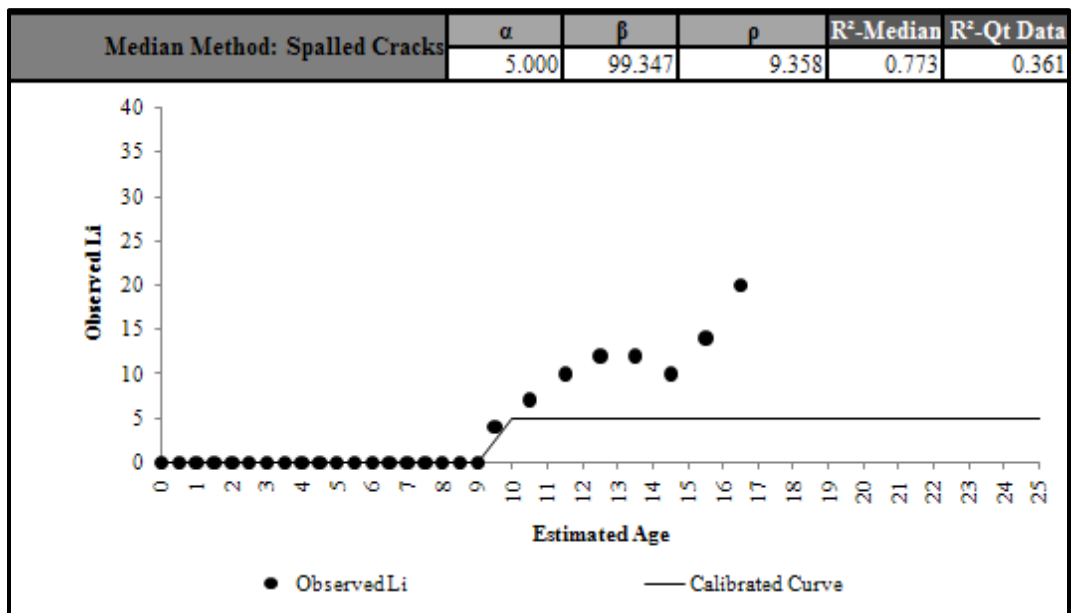


Figure C 12.4. Calibrated Performance Model for Houston District, Li Median Method (Constrained).

Houston District 12-Punchouts

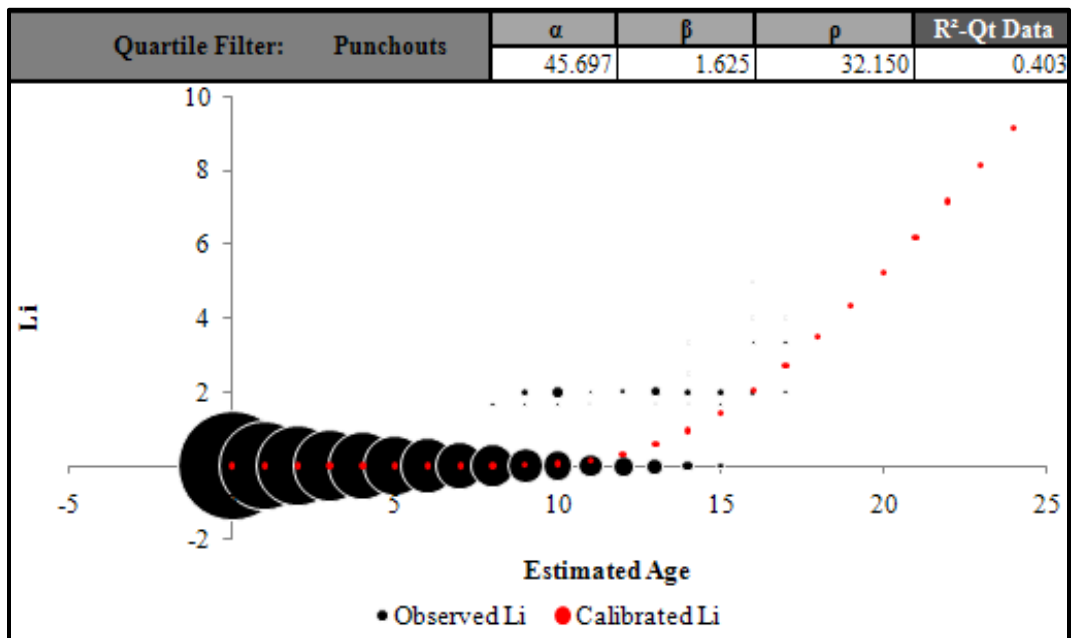


Figure C 12.5. Calibrated Performance Model for Houston District, Li Quartile Method (Unconstrained).

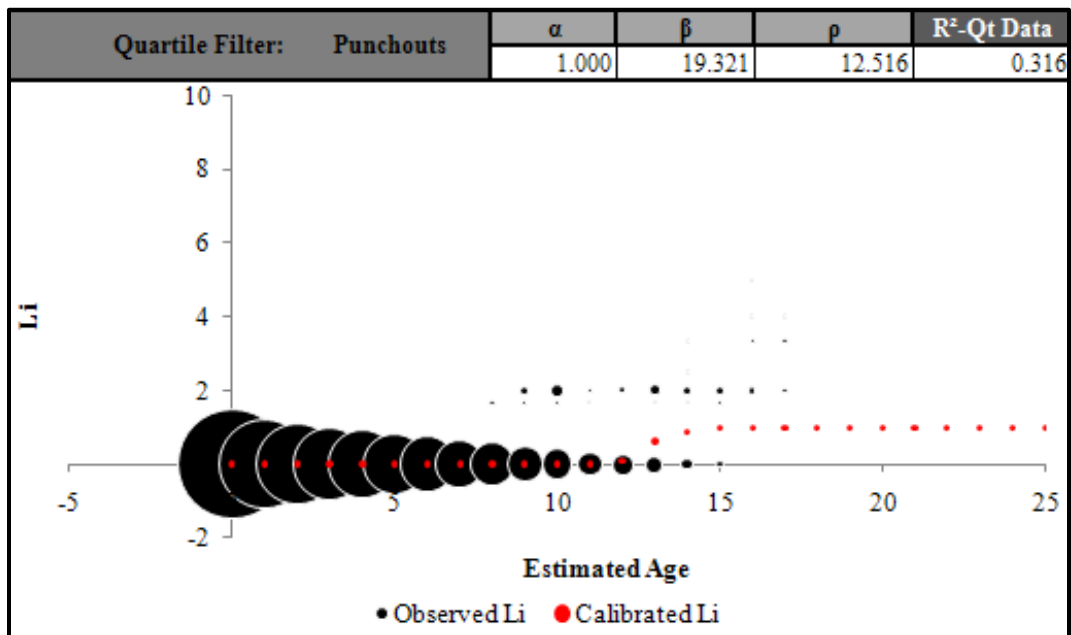


Figure C 12.6. Calibrated Performance Model for Houston District, Li Quartile Method (Constrained).

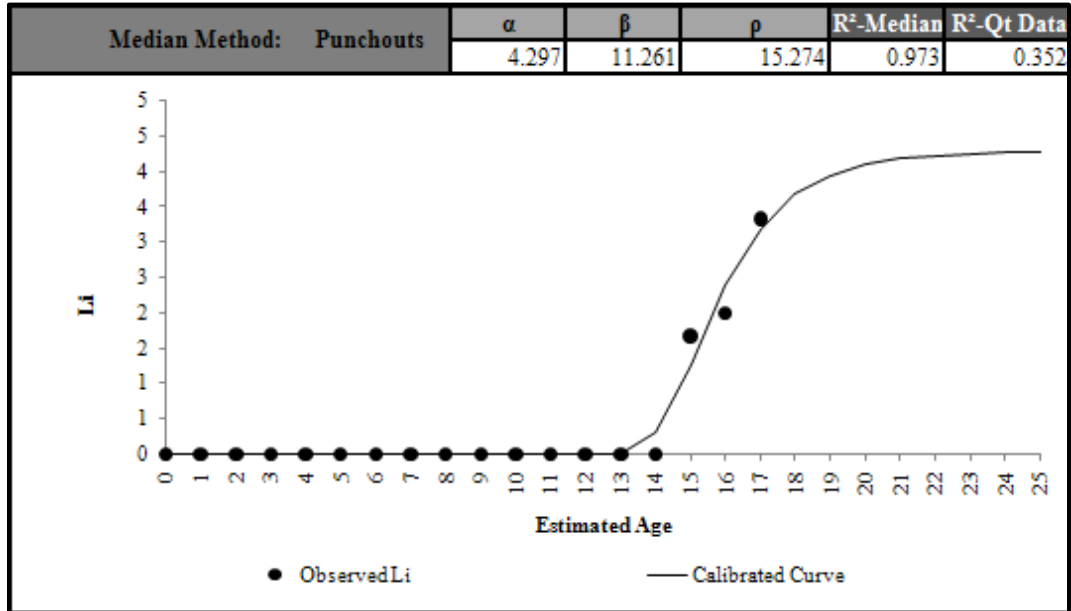


Figure C 12.7. Calibrated Performance Model for Houston District, Li Median Method (Unconstrained).

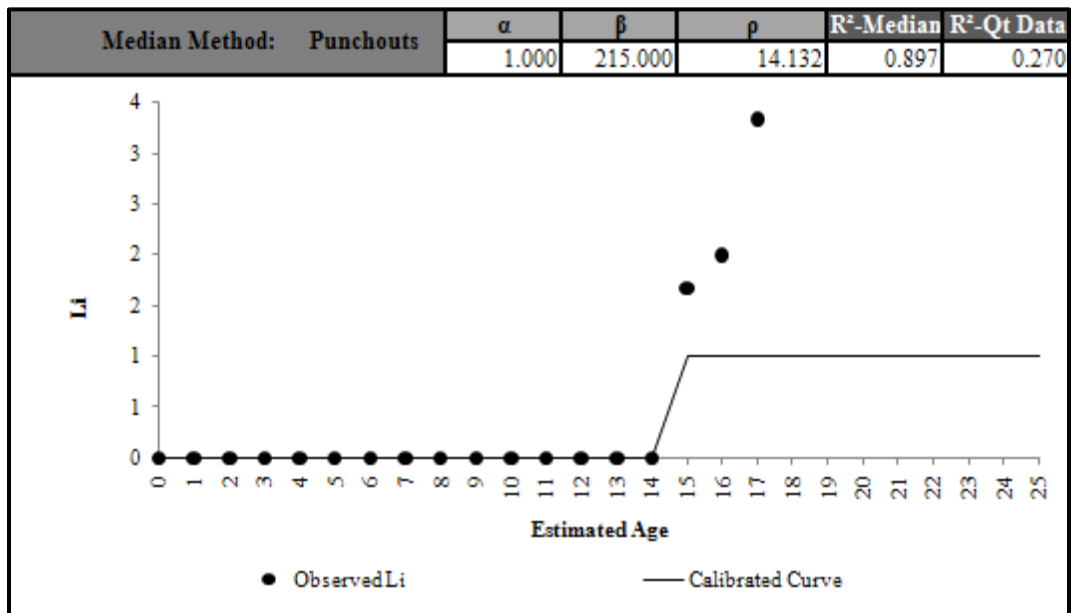


Figure C 12.8. Calibrated Performance Model for Houston District, Li Median Method (Constrained).

Houston District 12-ACP Patches

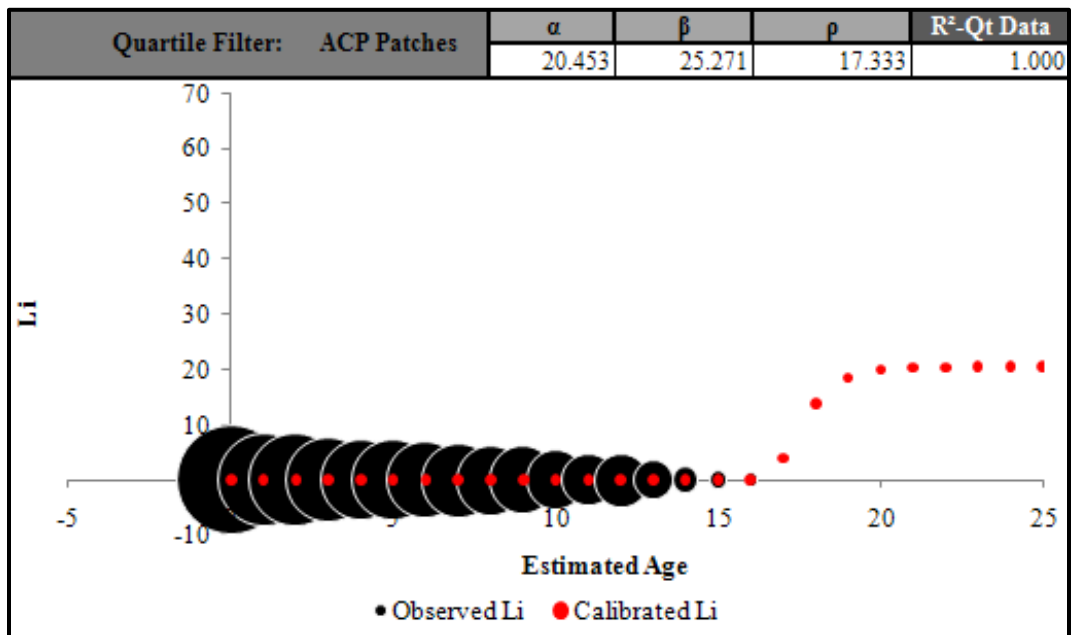


Figure C 12.9. Calibrated Performance Model for Houston District, Li Quartile Method (Unconstrained).

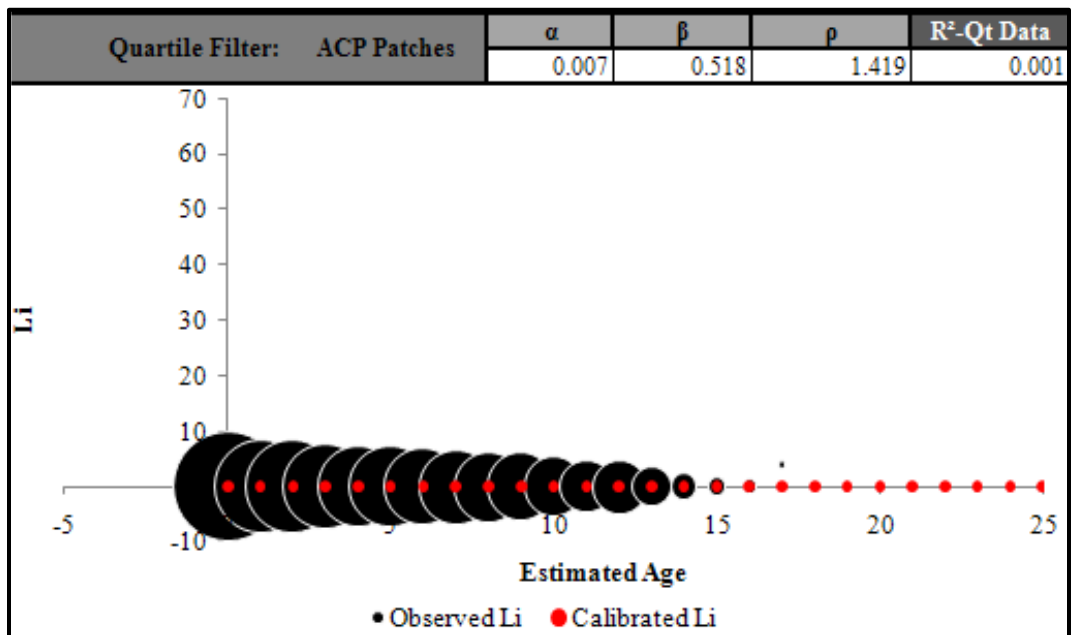


Figure C 12.10. Calibrated Performance Model for Houston District, Li Quartile Method (Constrained).

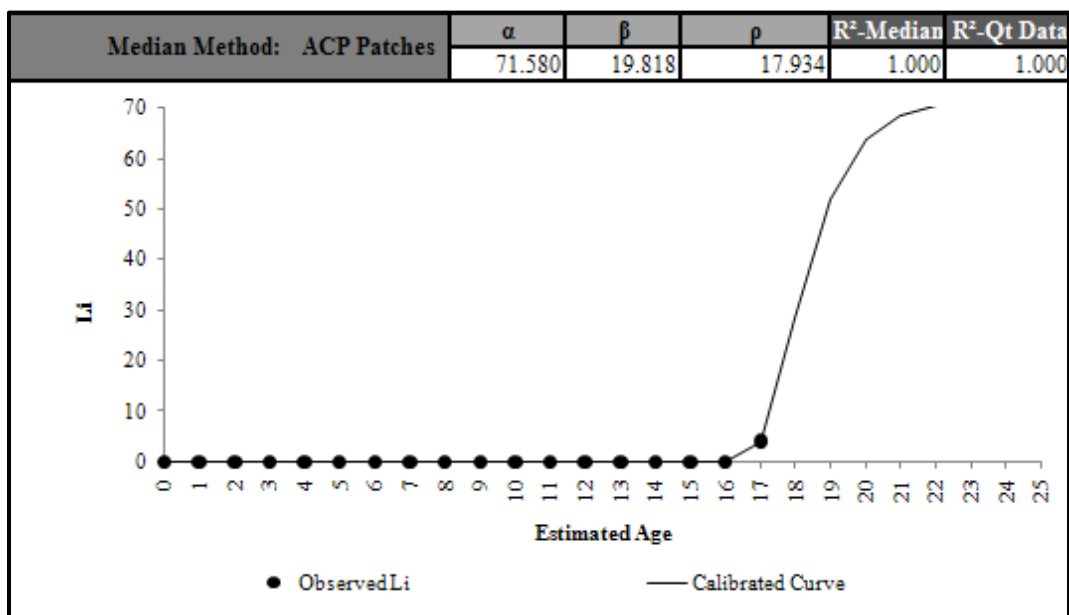


Figure C 12.11. Calibrated Performance Model for Houston District, Li Median Method (Unconstrained).

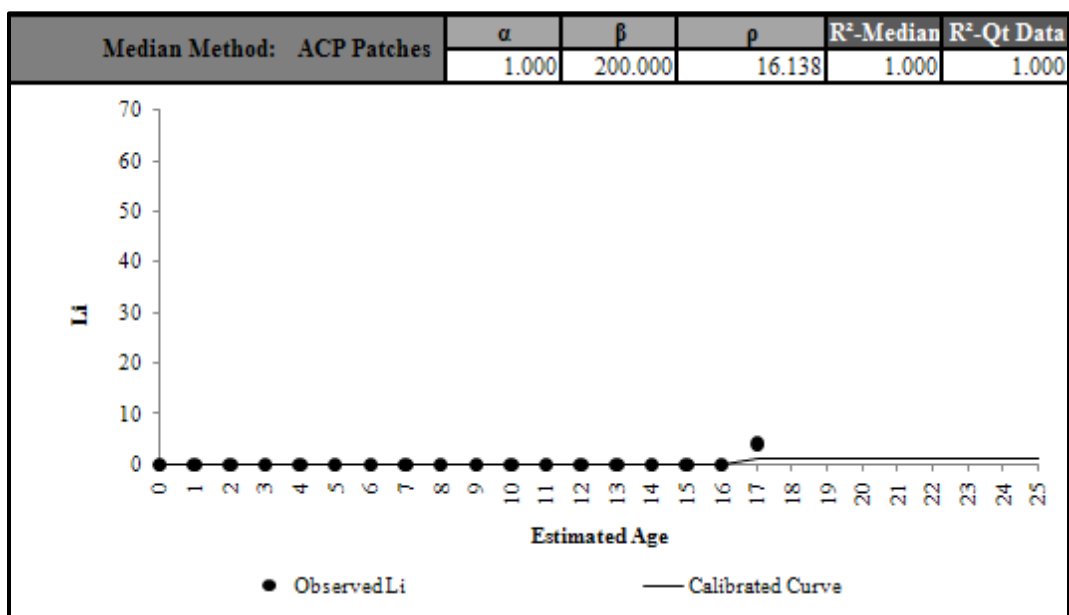


Figure C 12.12. Calibrated Performance Model for Houston District, Li Median Method (Constrained).

Houston District 12-PCC Patches

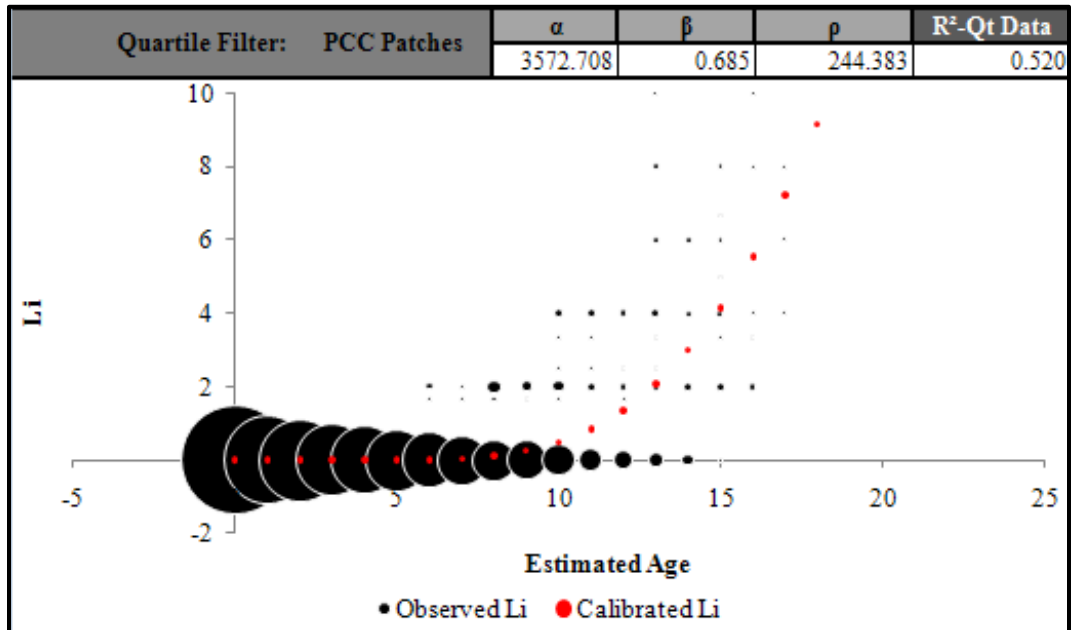


Figure C 12.13. Calibrated Performance Model for Houston District, Li Quartile Method (Unconstrained).

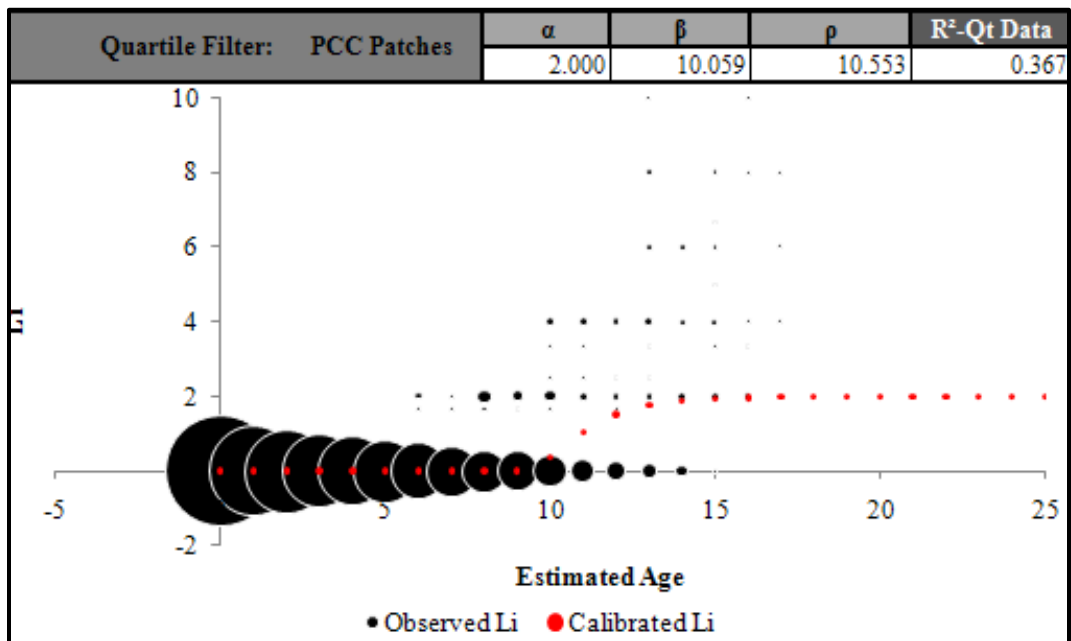


Figure C 12.14. Calibrated Performance Model for Houston District, Li Quartile Method (Constrained).

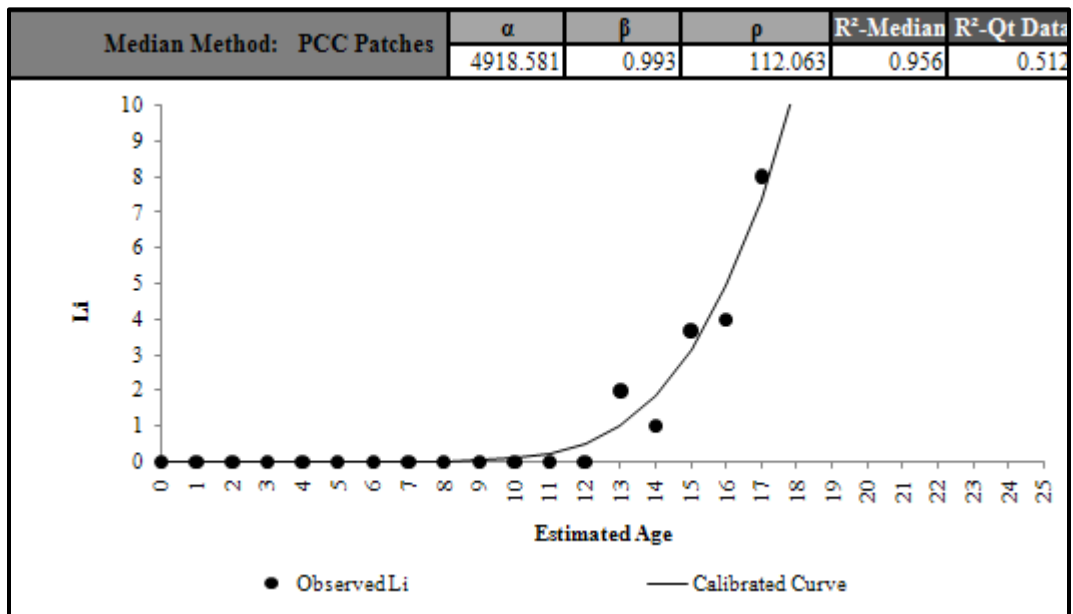


Figure C 12.15. Calibrated Performance Model for Houston District, Li Median Method (Unconstrained).

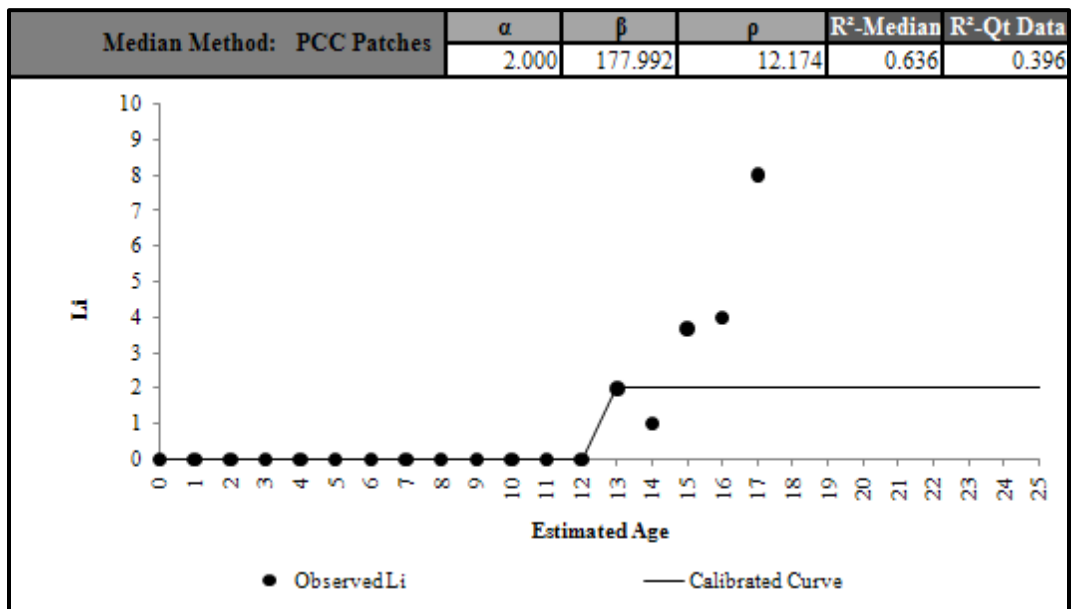


Figure C 12.16. Calibrated Performance Model for Houston District, Li Median Method (Constrained).

Yoakum District 13-Spalled Cracks

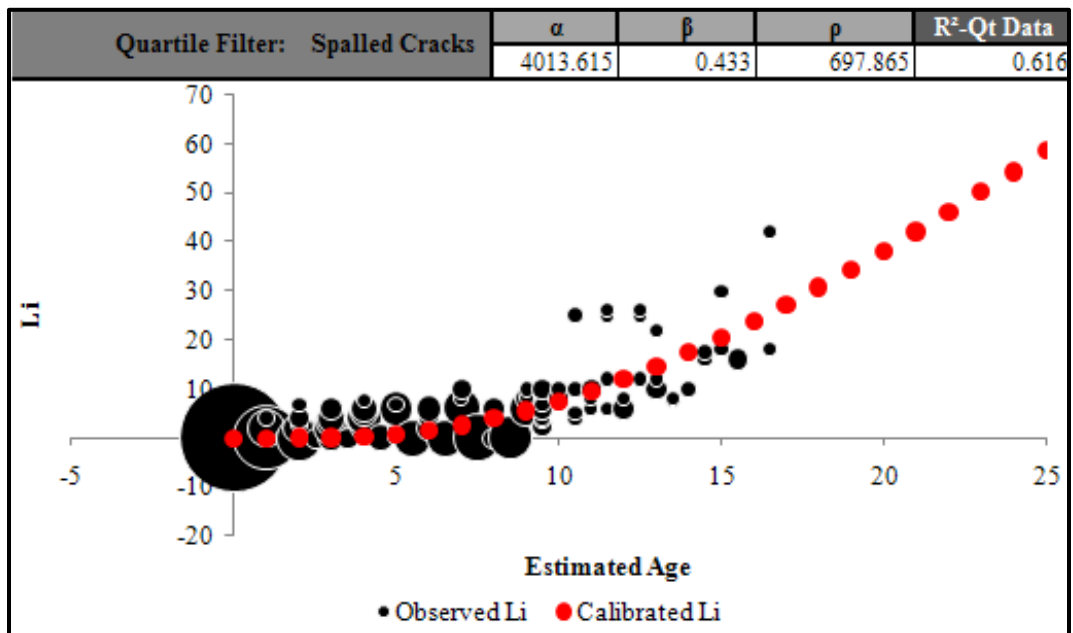


Figure C 13.1. Calibrated Performance Model for Yoakum District, Li Quartile Method (Unconstrained).

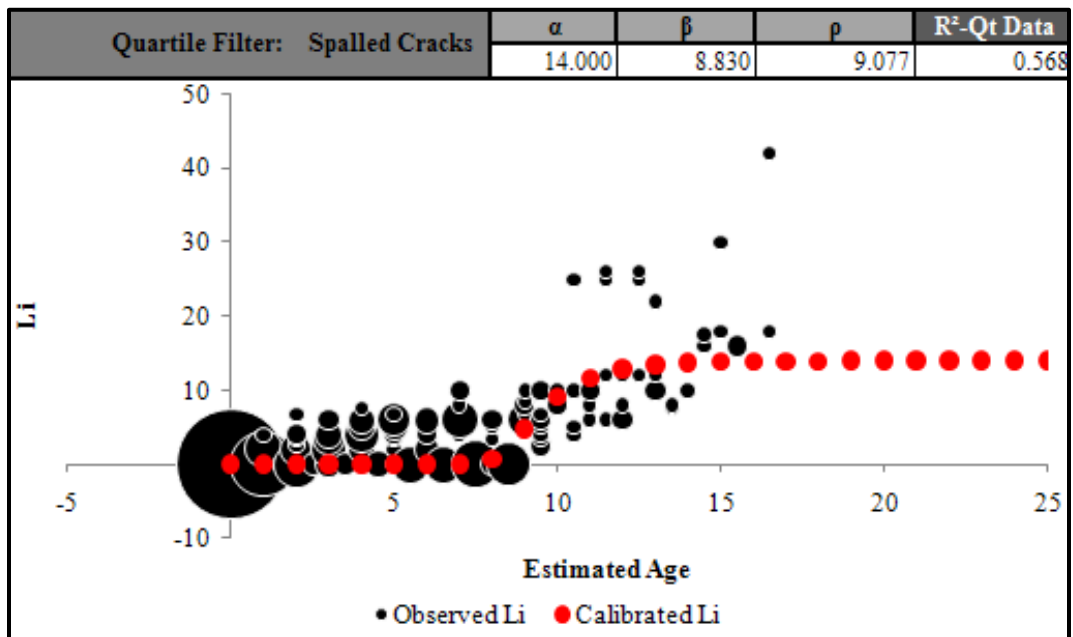


Figure C 13.2. Calibrated Performance Model for Yoakum District, Li Quartile Method (Constrained).

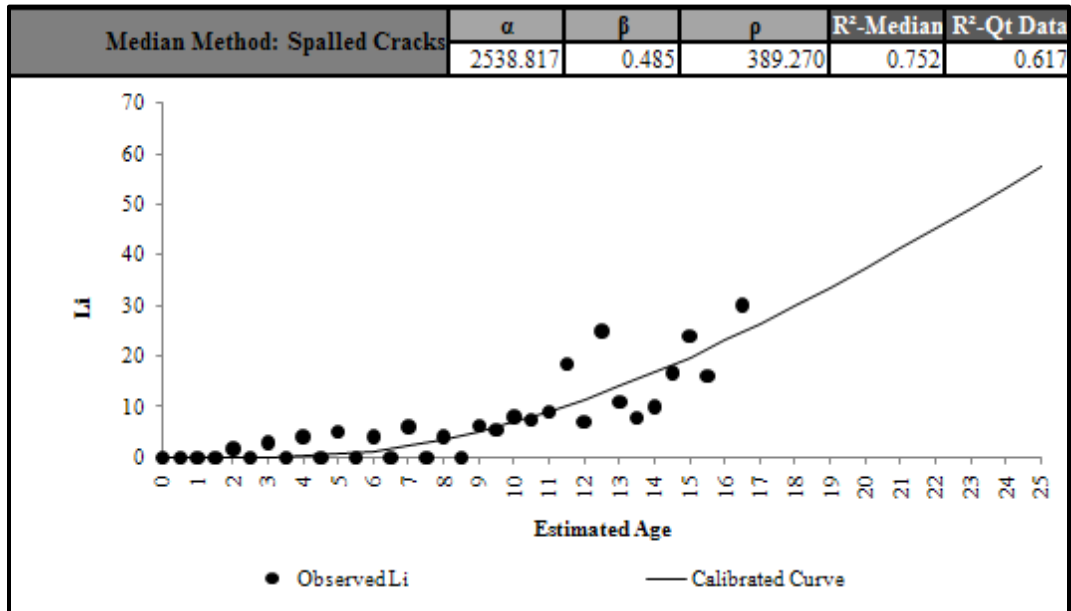


Figure C 13.3. Calibrated Performance Model for Yoakum District, Li Median Method (Unconstrained).

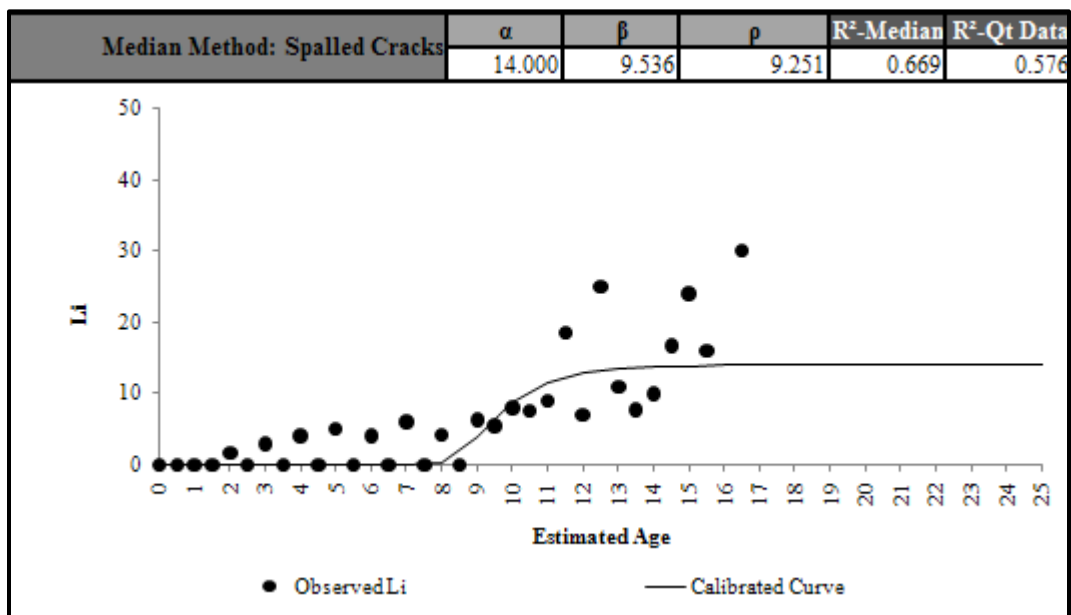


Figure C 13.4. Calibrated Performance Model for Yoakum District, Li Median Method (Constrained).

Yoakum District 13-Punchouts

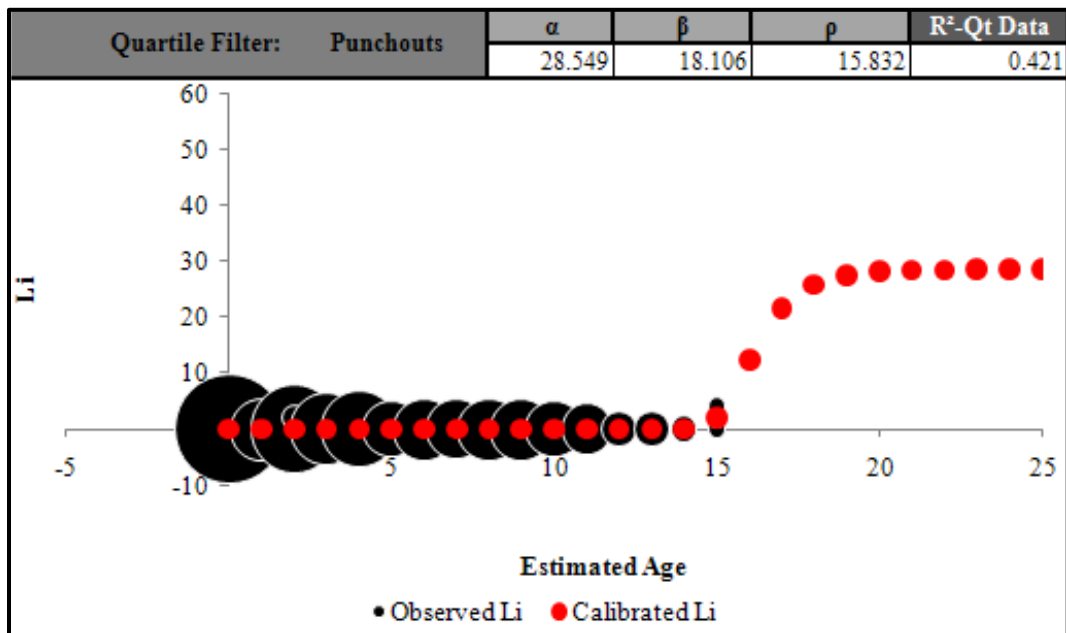


Figure C 13.5. Calibrated Performance Model for Yoakum District, Li Quartile Method (Unconstrained).

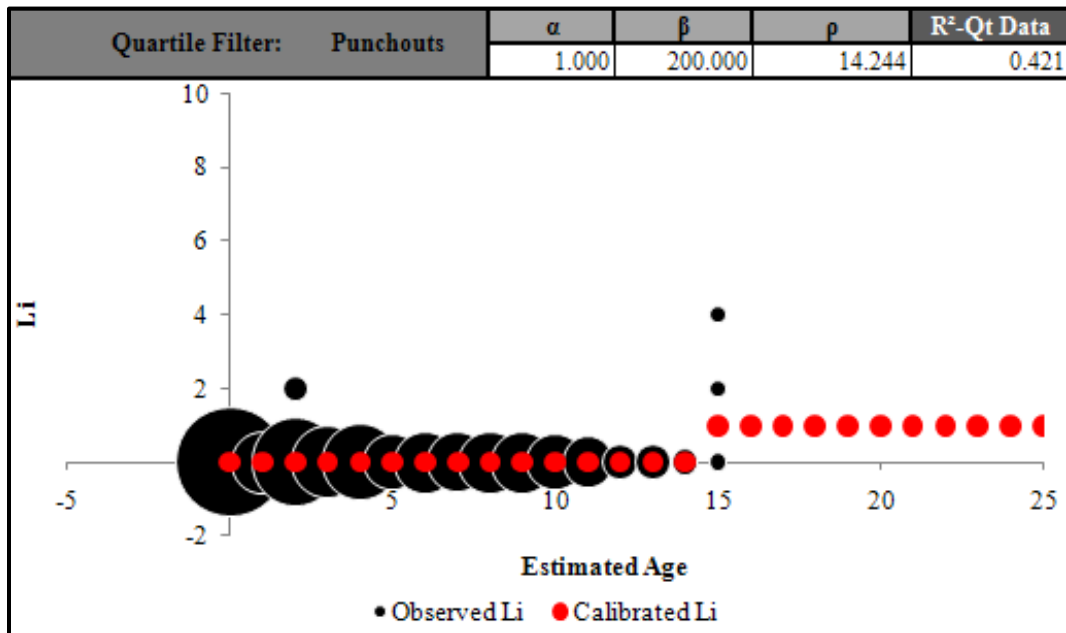


Figure C 13.6. Calibrated Performance Model for Yoakum District, Li Quartile Method (Constrained).

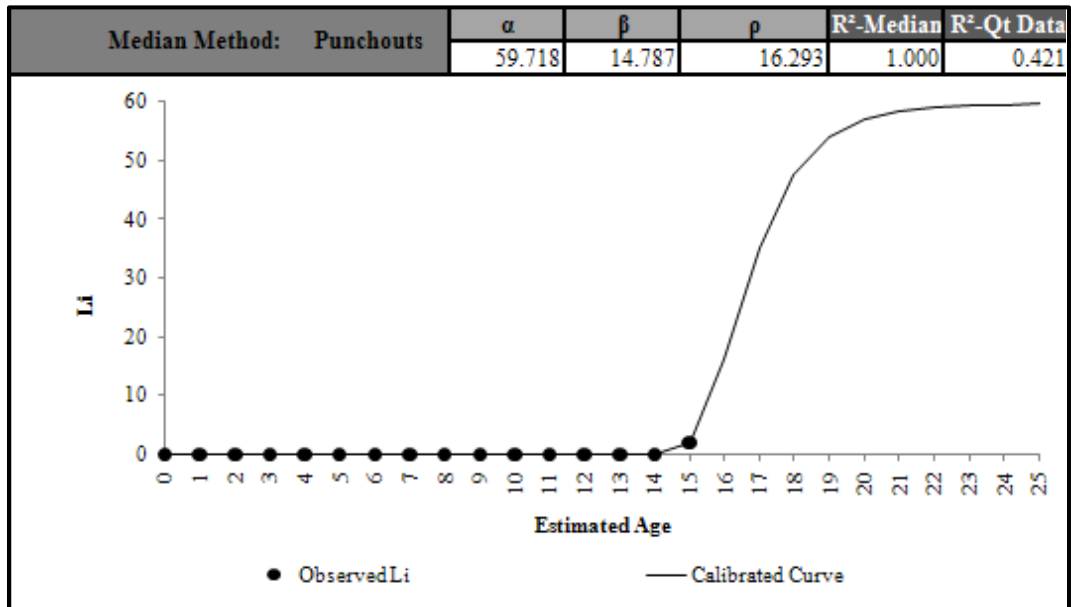


Figure C 13.7. Calibrated Performance Model for Yoakum District, Li Median Method (Unconstrained).

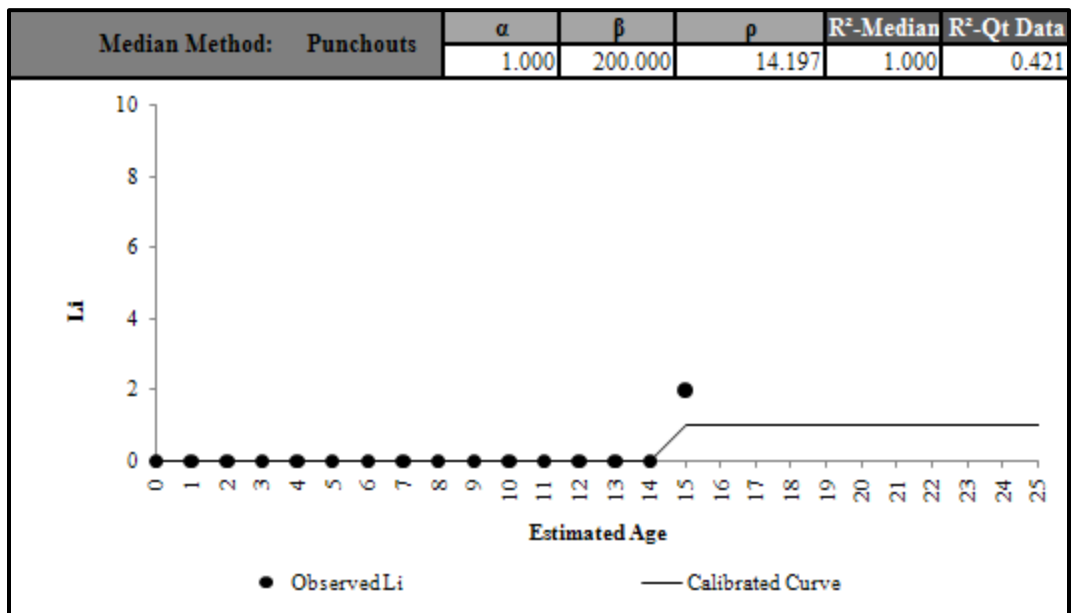


Figure C 13.8. Calibrated Performance Model for Yoakum District, Li Median Method (Constrained).

Yoakum District 13-PCC Patches

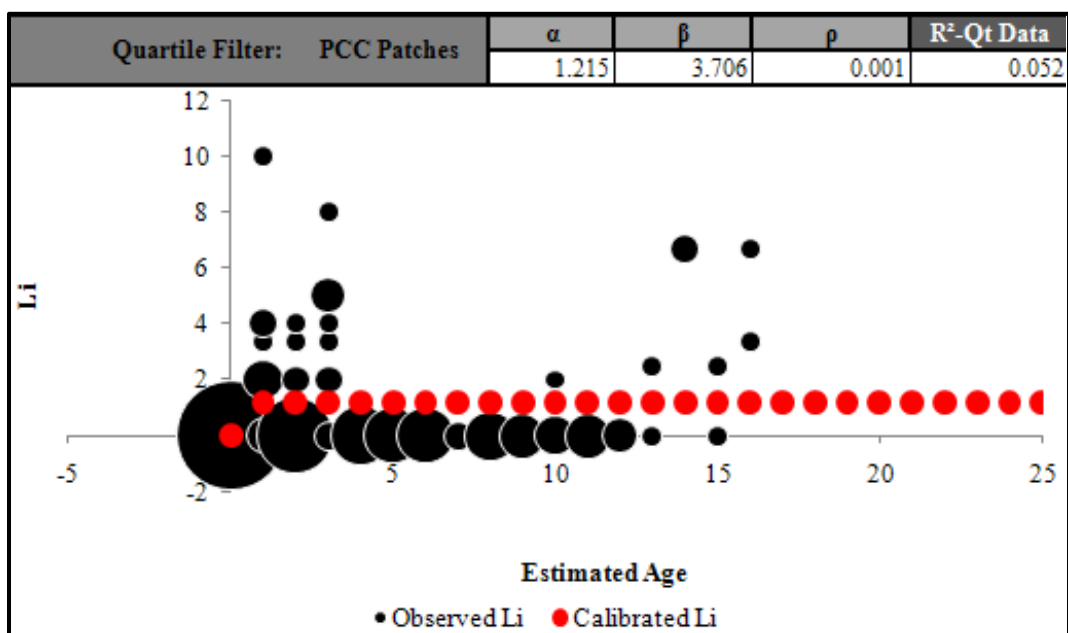


Figure C 13.9. Calibrated Performance Model for Yoakum District, Li Quartile Method (Unconstrained).

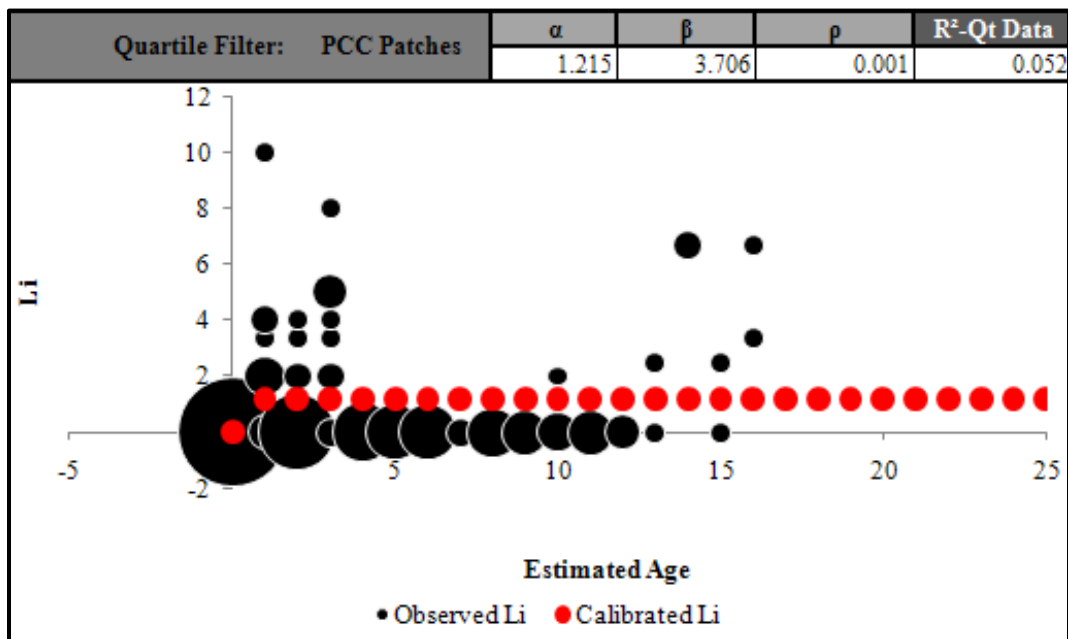


Figure C 13.10. Calibrated Performance Model for Yoakum District, Li Quartile Method (Constrained).

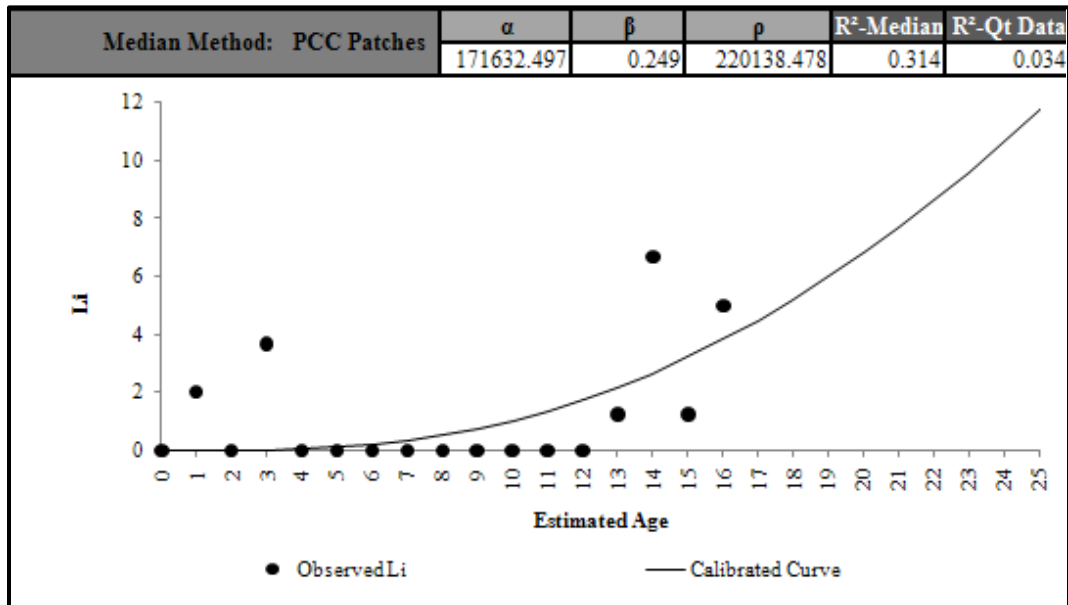


Figure C 13.11. Calibrated Performance Model for Yoakum District, Li Median Method (Unconstrained).

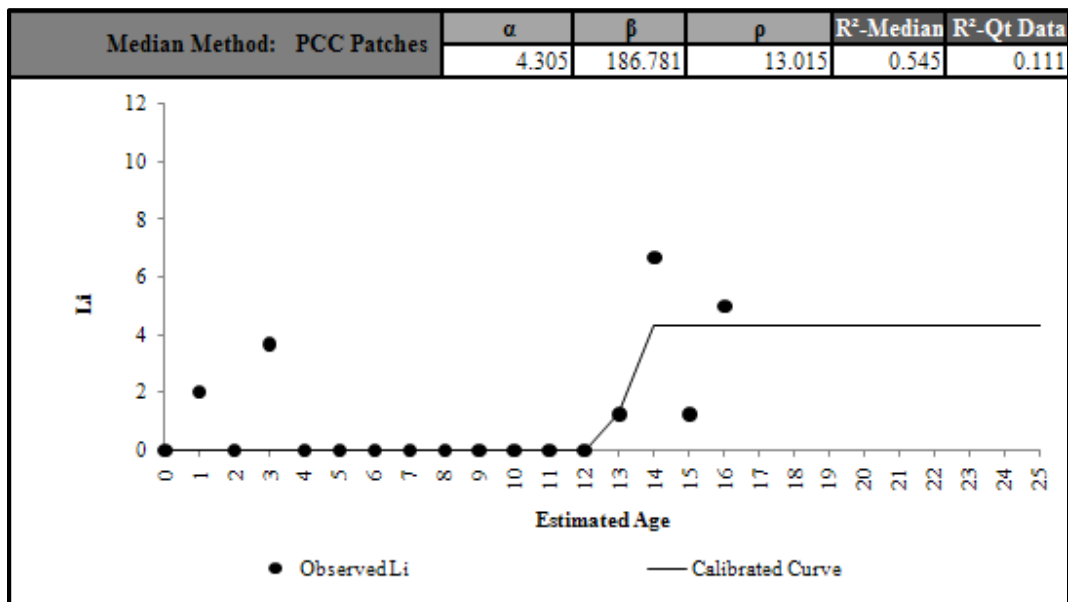


Figure C 13.12. Calibrated Performance Model for Yoakum District, Li Median Method (Constrained).

Austin District 14-Spalled Cracks

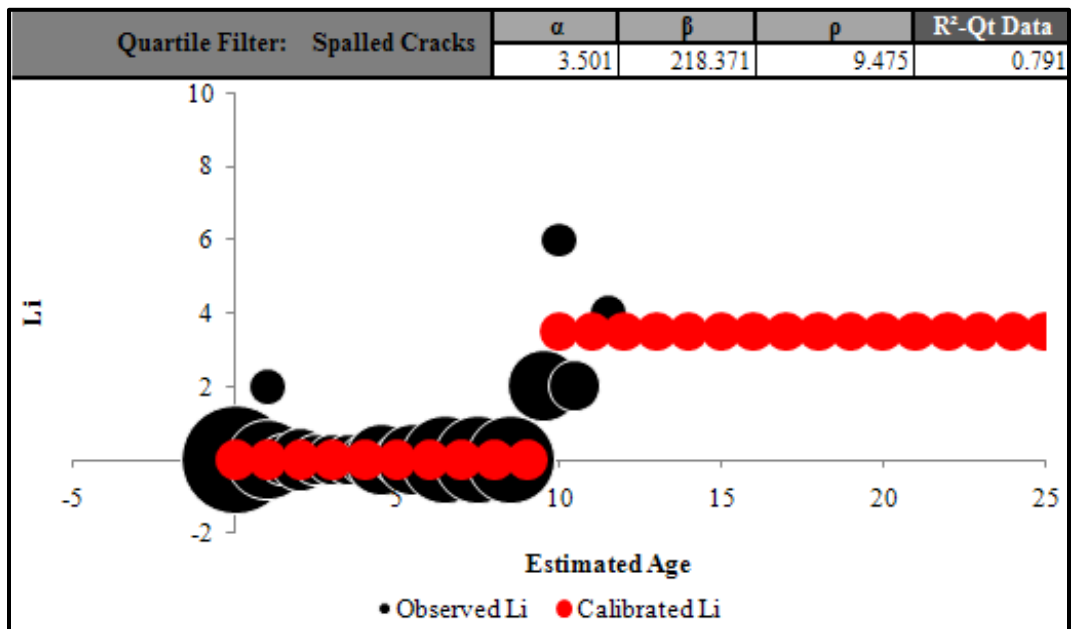


Figure C 14.1. Calibrated Performance Model for Austin District, Li Quartile Method (Unconstrained).

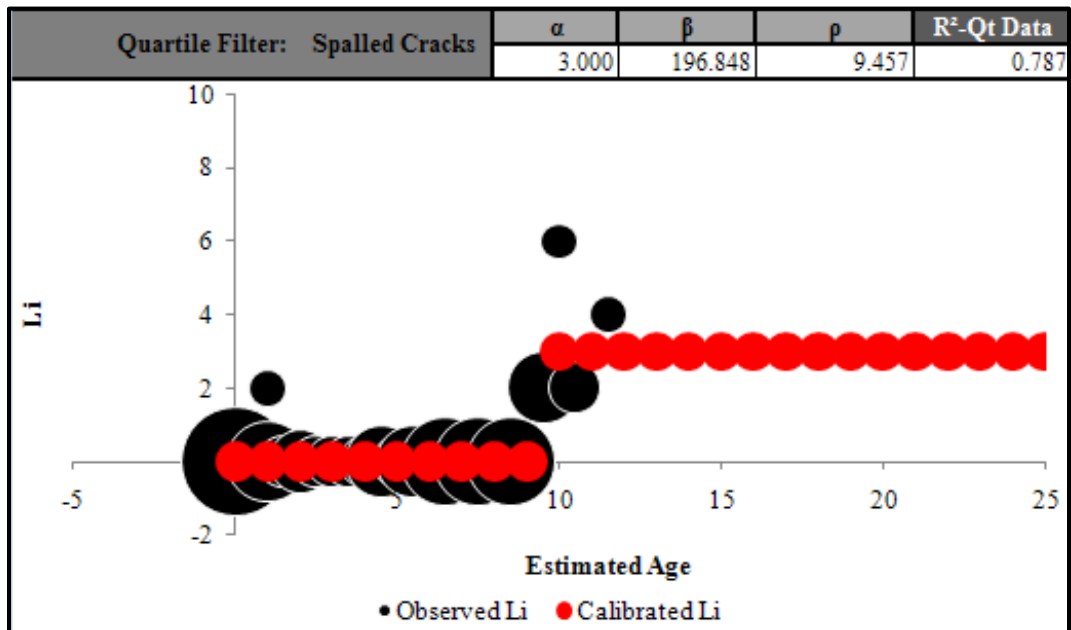


Figure C 14.2. Calibrated Performance Model for Austin District, Li Quartile Method (Constrained).

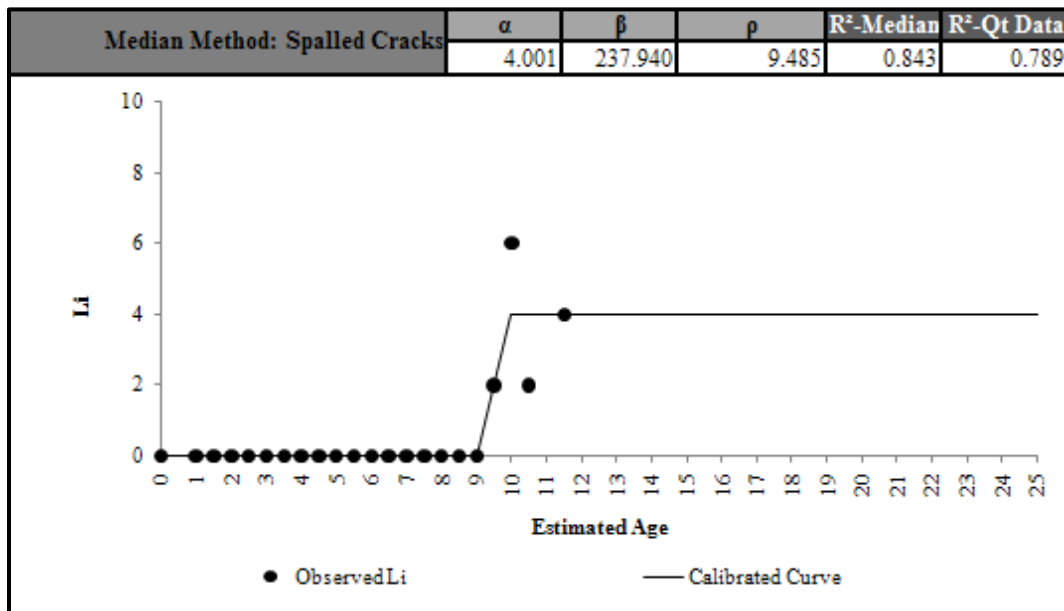


Figure C 14.3. Calibrated Performance Model for Austin District, Li Median Method (Unconstrained).

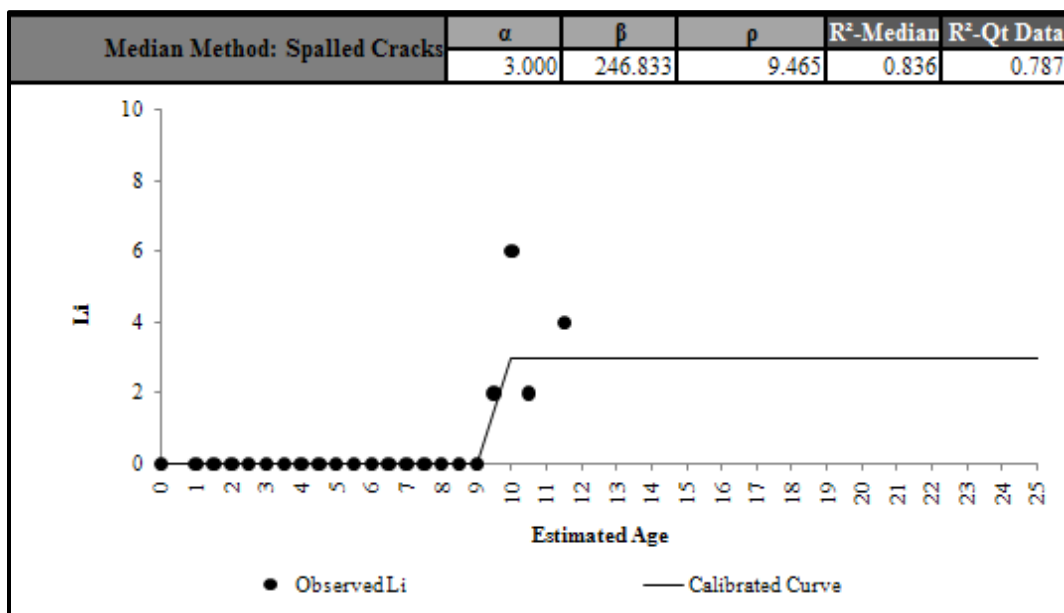


Figure C 14.4. Calibrated Performance Model for Austin District, Li Median Method (Constrained).

San Antonio District 15-Spalled Cracks

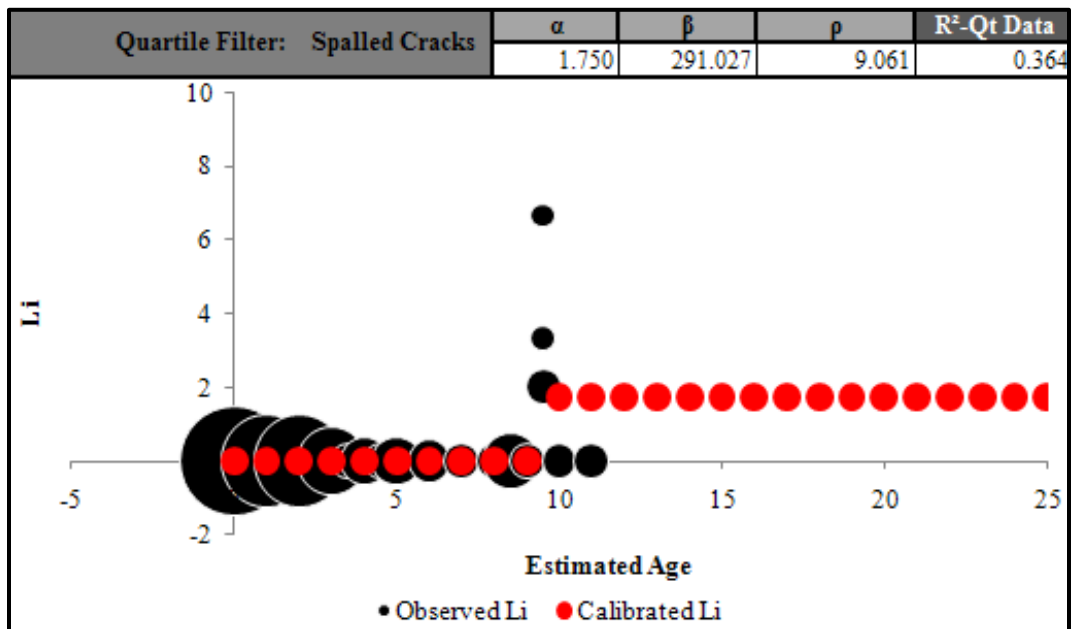


Figure C 15.1. Calibrated Performance Model for San Antonio District, Li Quartile Method (Unconstrained).

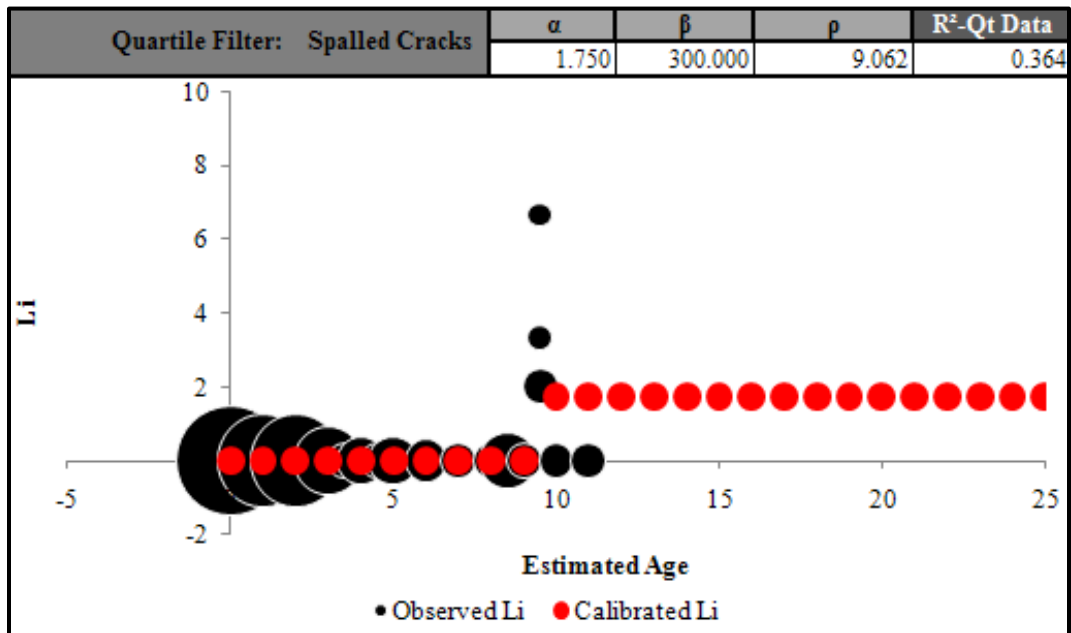


Figure C 15.2. Calibrated Performance Model for San Antonio District, Li Quartile Method (Constrained).

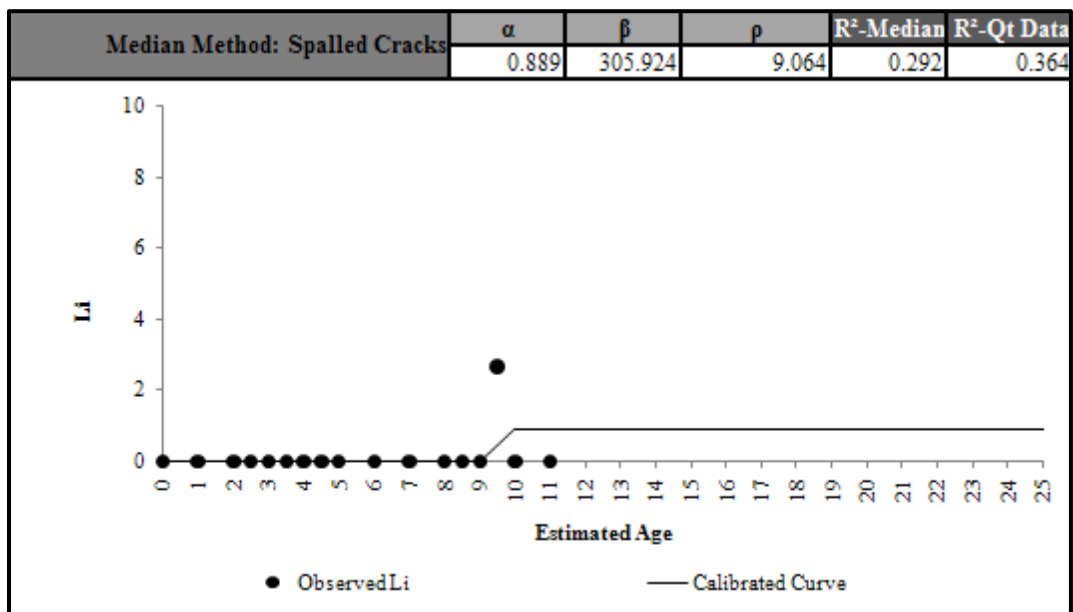


Figure C 15.3. Calibrated Performance Model for San Antonio District, Li Median Method (Unconstrained).

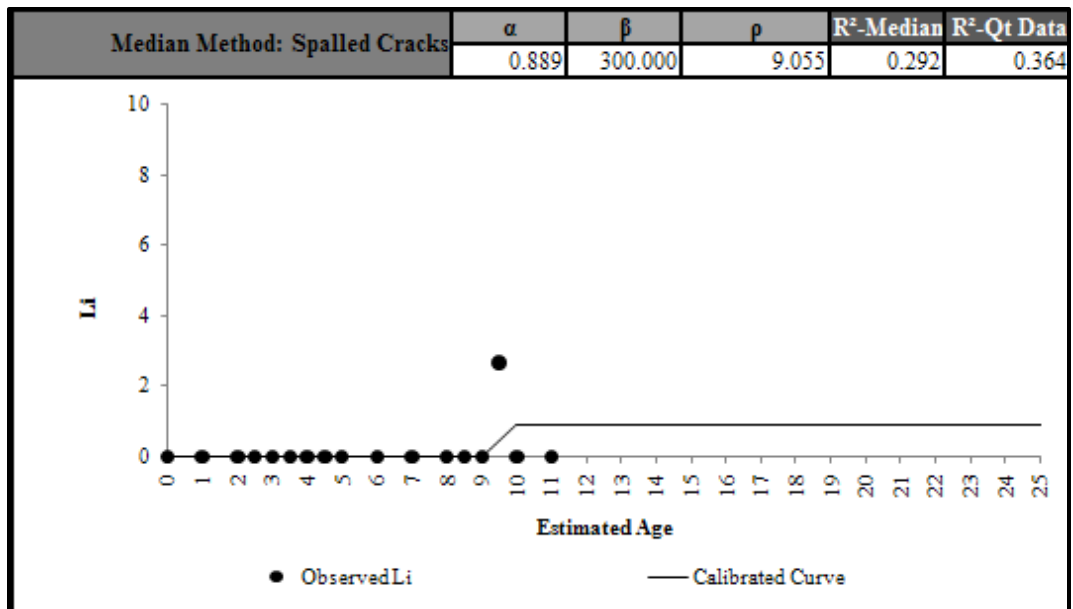


Figure C 15.4. Calibrated Performance Model for San Antonio District, Li Median Method (Constrained).

San Antonio District 15-PCC Patches

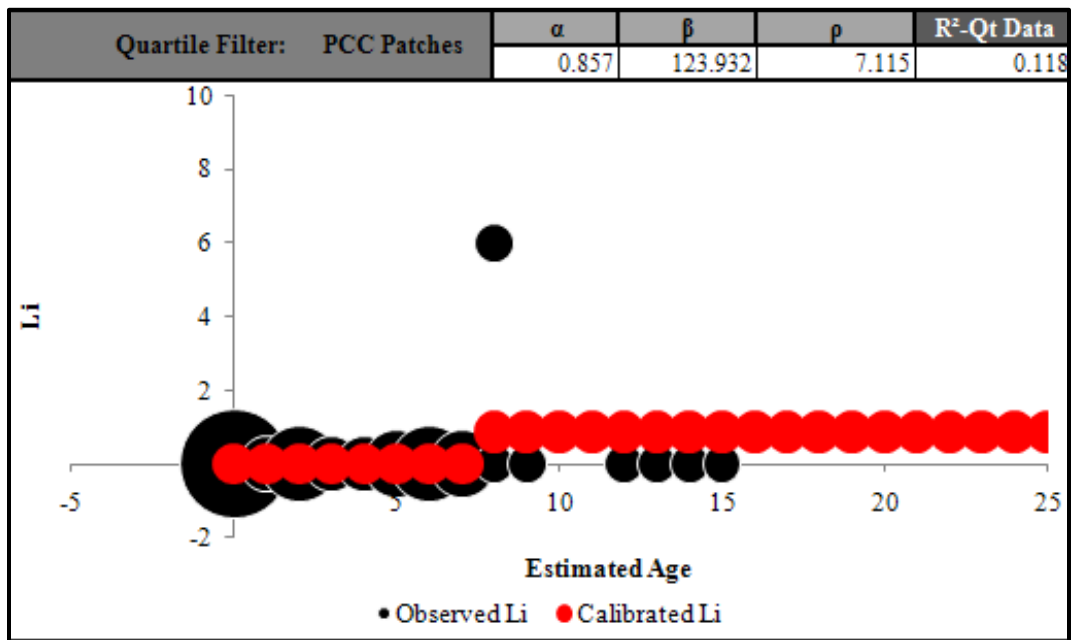


Figure C 15.5. Calibrated Performance Model for San Antonio District, Li Quartile Method (Unconstrained).

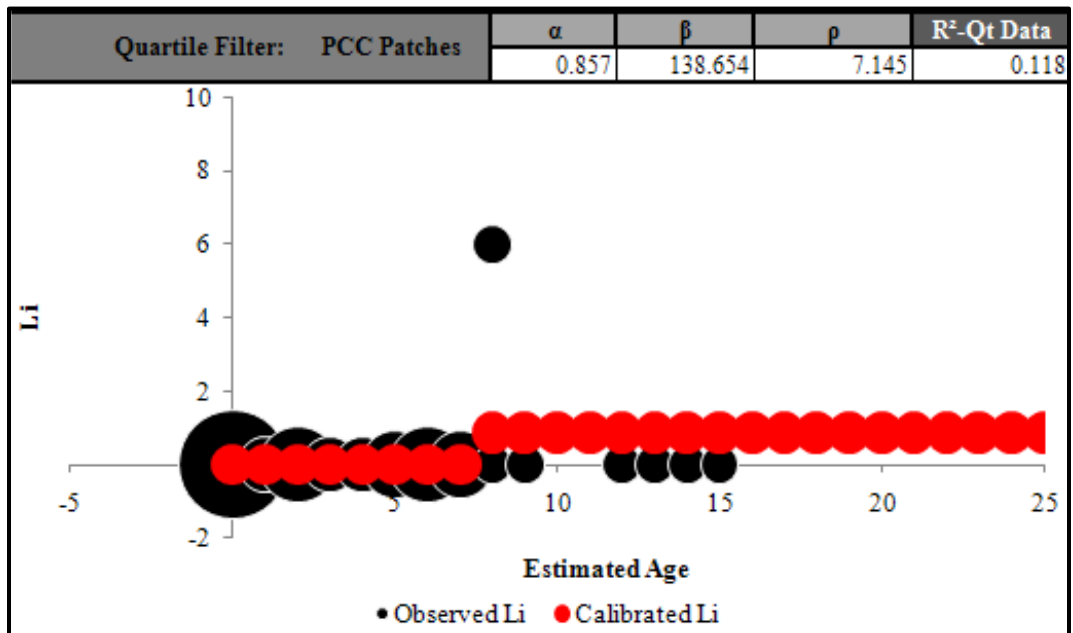


Figure C 15.6. Calibrated Performance Model for San Antonio District, Li Quartile Method (Constrained).

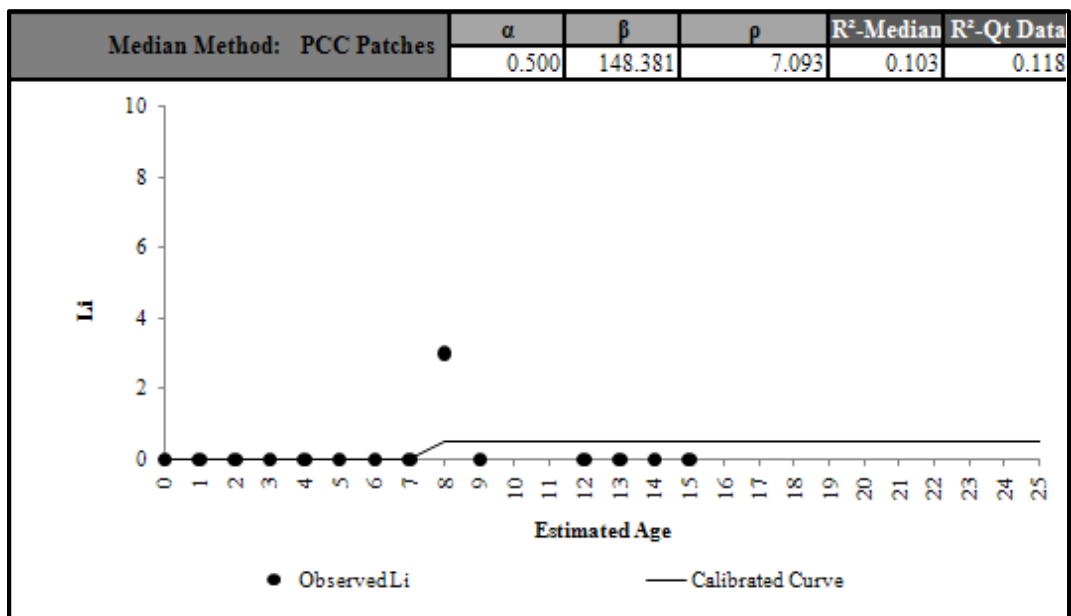


Figure C 15.7. Calibrated Performance Model for San Antonio District, Li Median Method (Unconstrained).

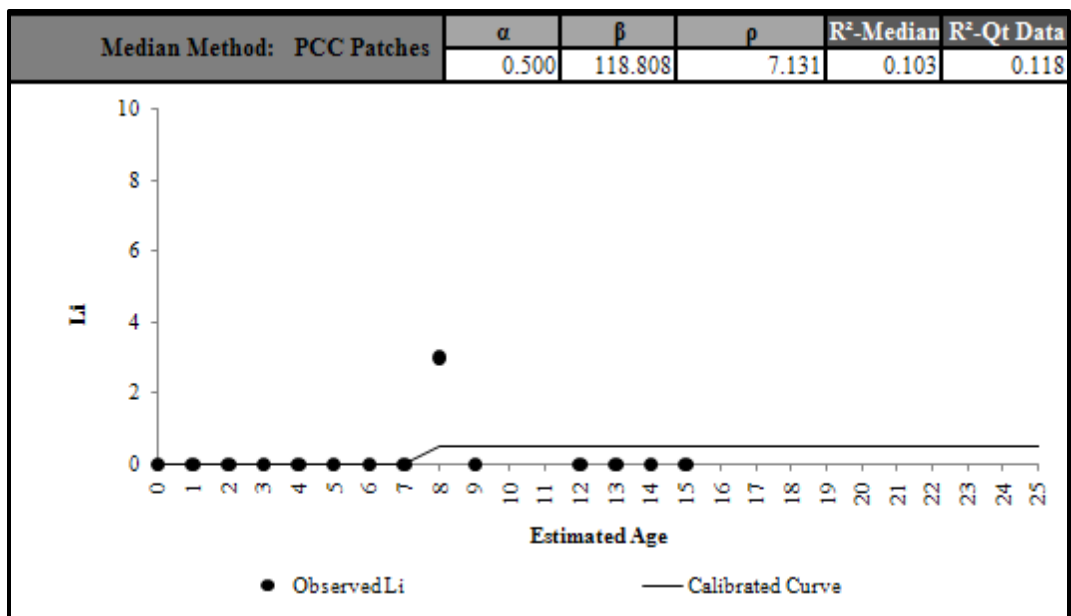


Figure C 15.8. Calibrated Performance Model for San Antonio District, Li Median Method (Constrained).

Bryan District 17-Spalled Cracks

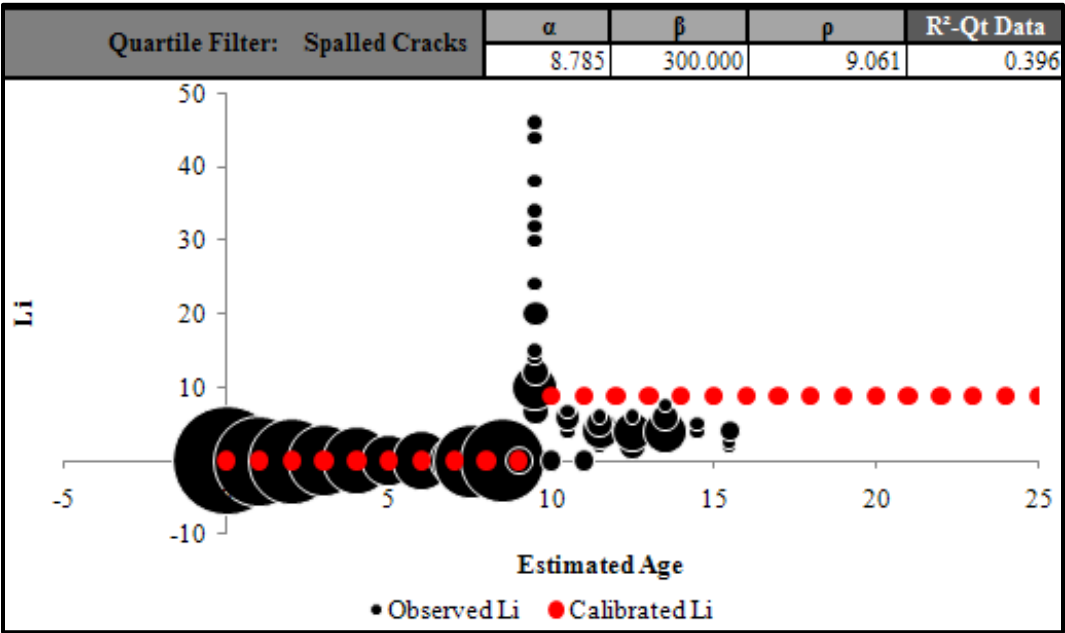


Figure C 17.1. Calibrated Performance Model for Bryan District, Li Quartile Method (Unconstrained).

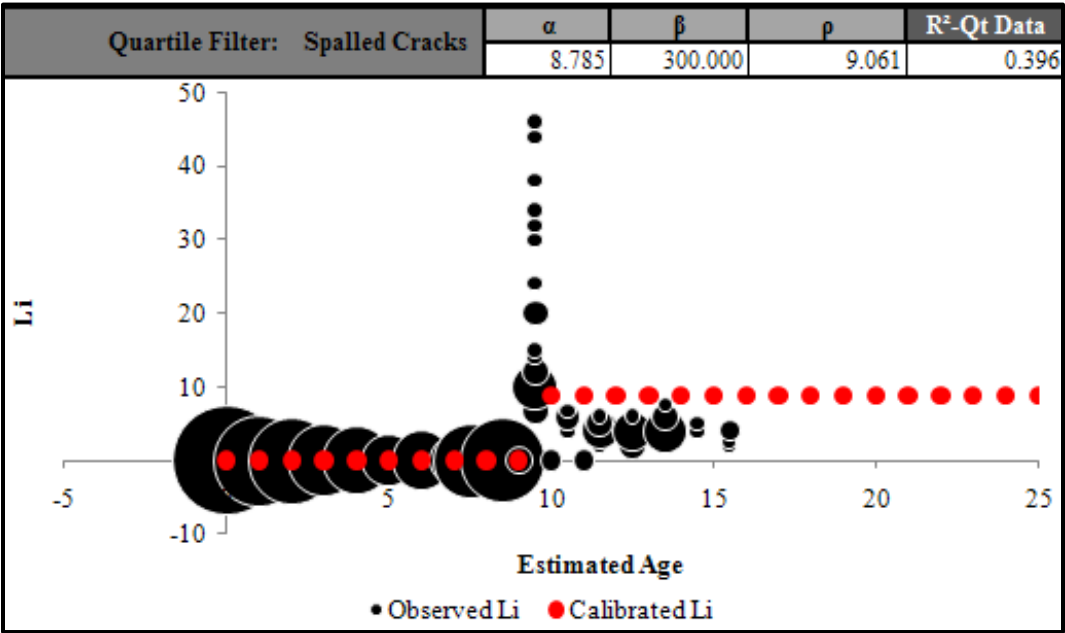


Figure C 17.2. Calibrated Performance Model for Bryan District, Li Quartile Method (Constrained).

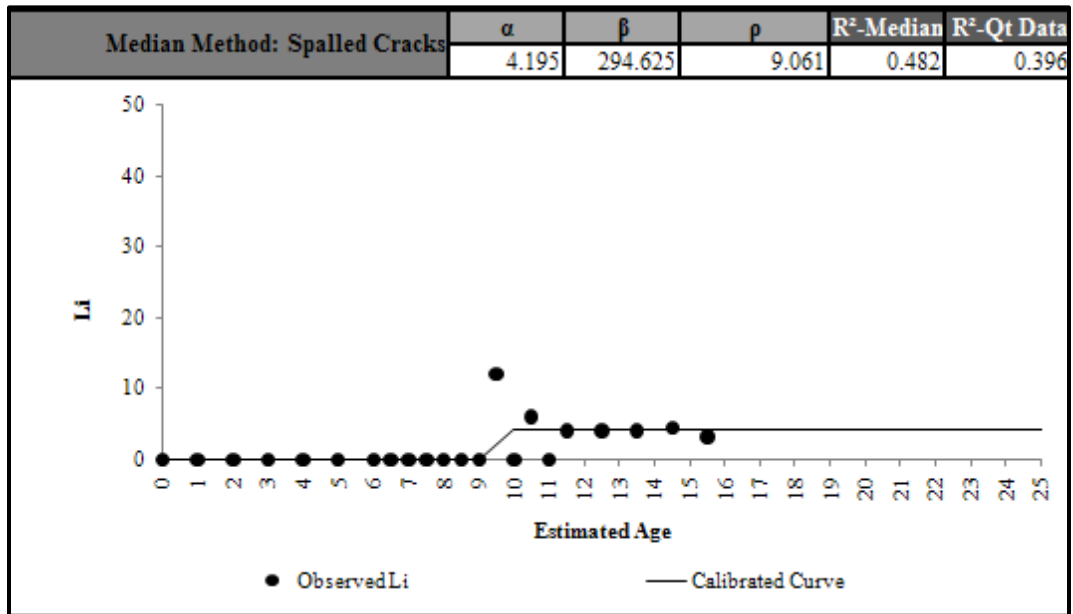


Figure C 17.3. Calibrated Performance Model for Bryan District, Li Median Method (Unconstrained).

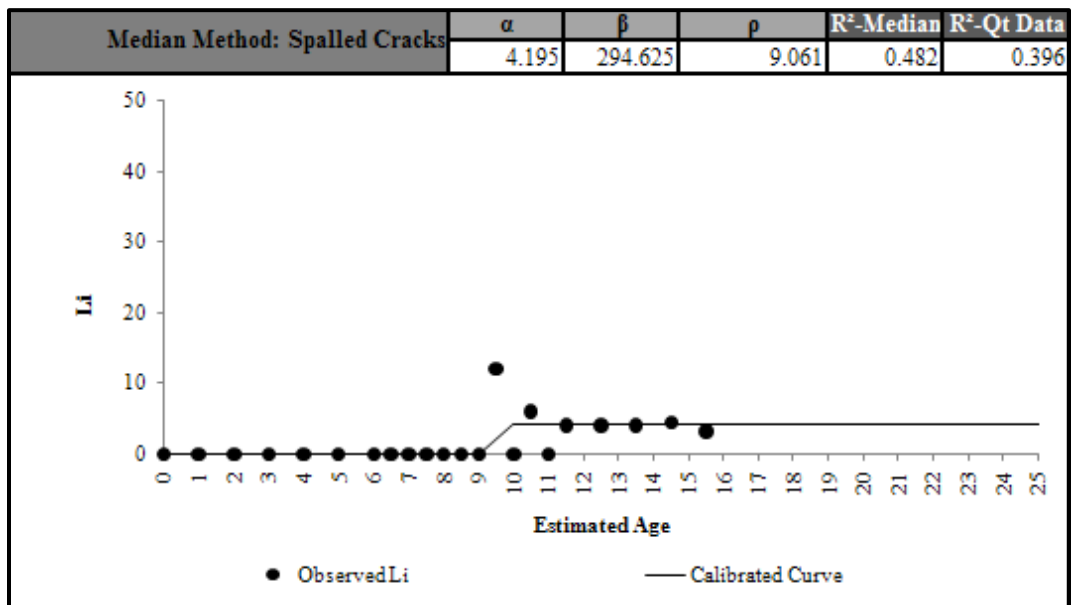


Figure C 17.4. Calibrated Performance Model for Bryan District, Li Median Method (Constrained).

Bryan District 17-Punchouts

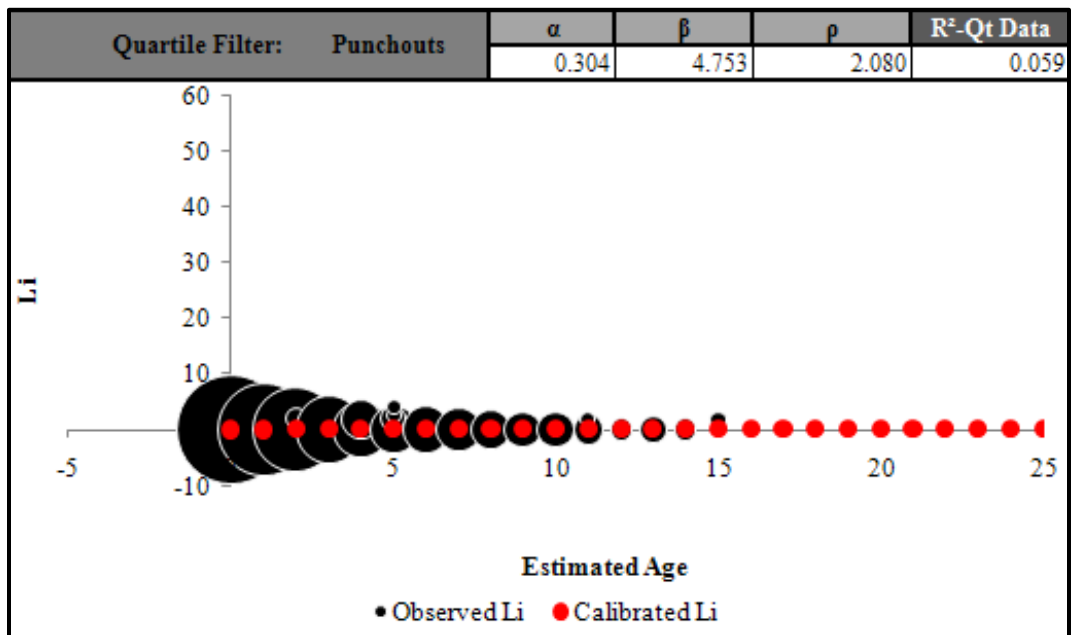


Figure C 17.5. Calibrated Performance Model for Bryan District, Li Quartile Method (Unconstrained).

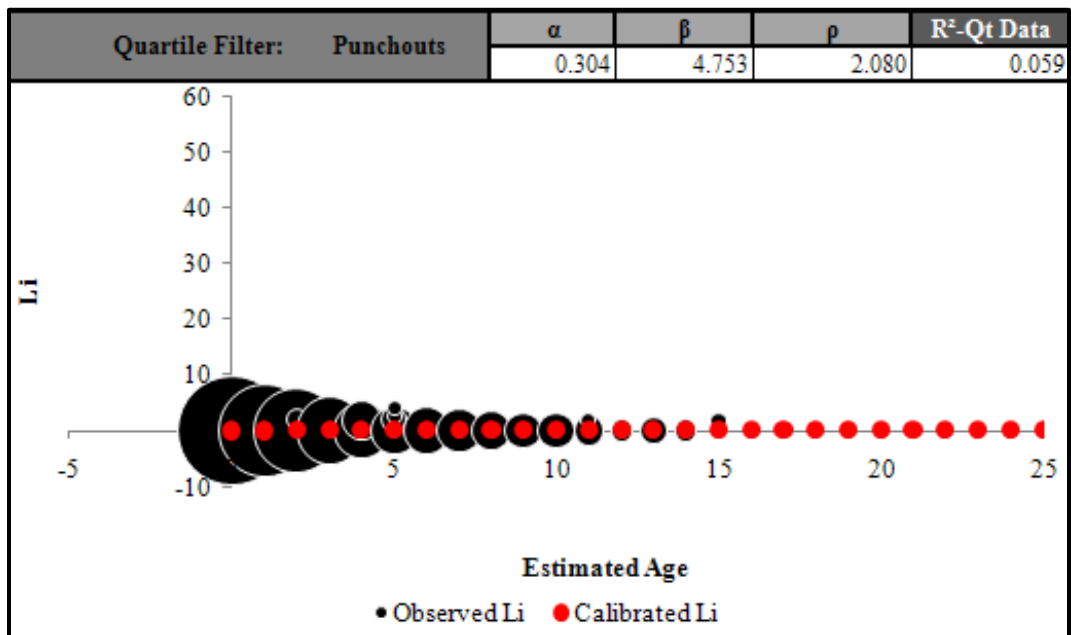


Figure C 17.6. Calibrated Performance Model for Bryan District, Li Quartile Method (Constrained).

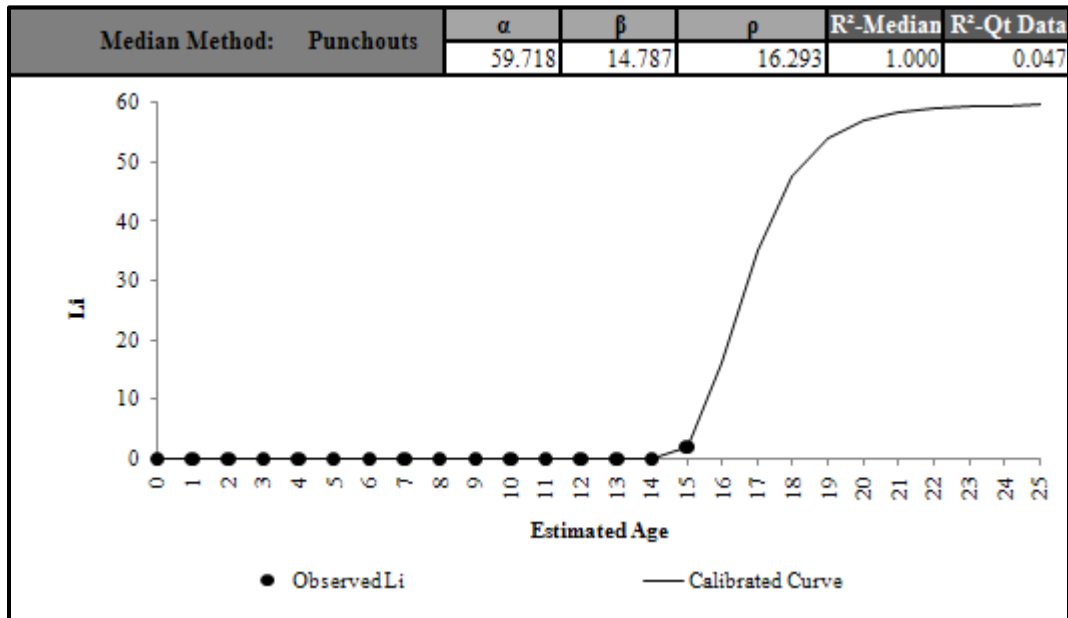


Figure C 17.7. Calibrated Performance Model for Bryan District, Li Median Method (Unconstrained).

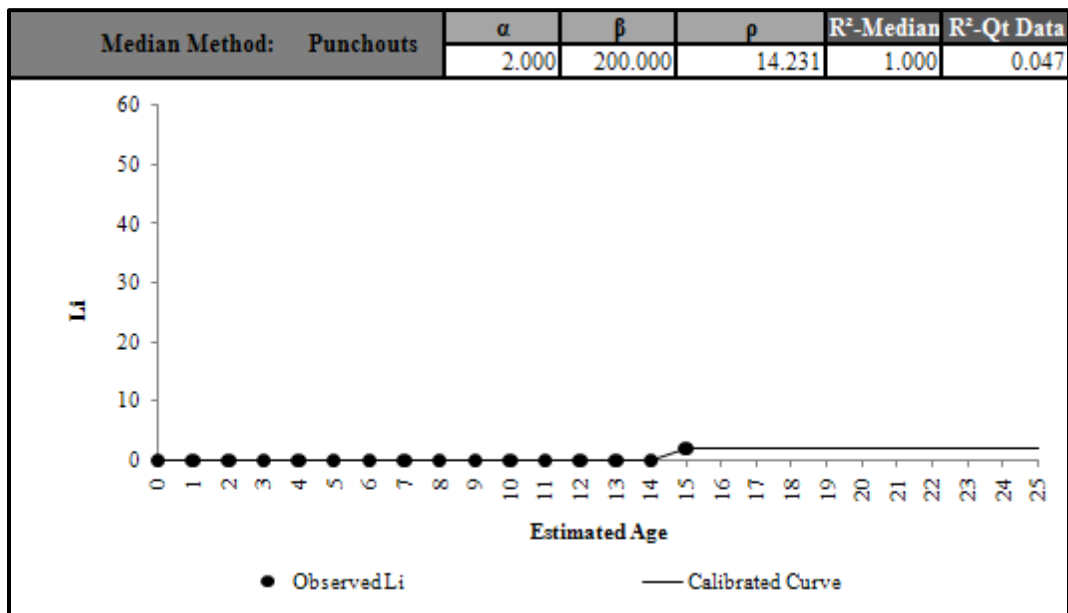


Figure C 17.8. Calibrated Performance Model for Bryan District, Li Median Method (Constrained).

Bryan District 17-ACP Patches

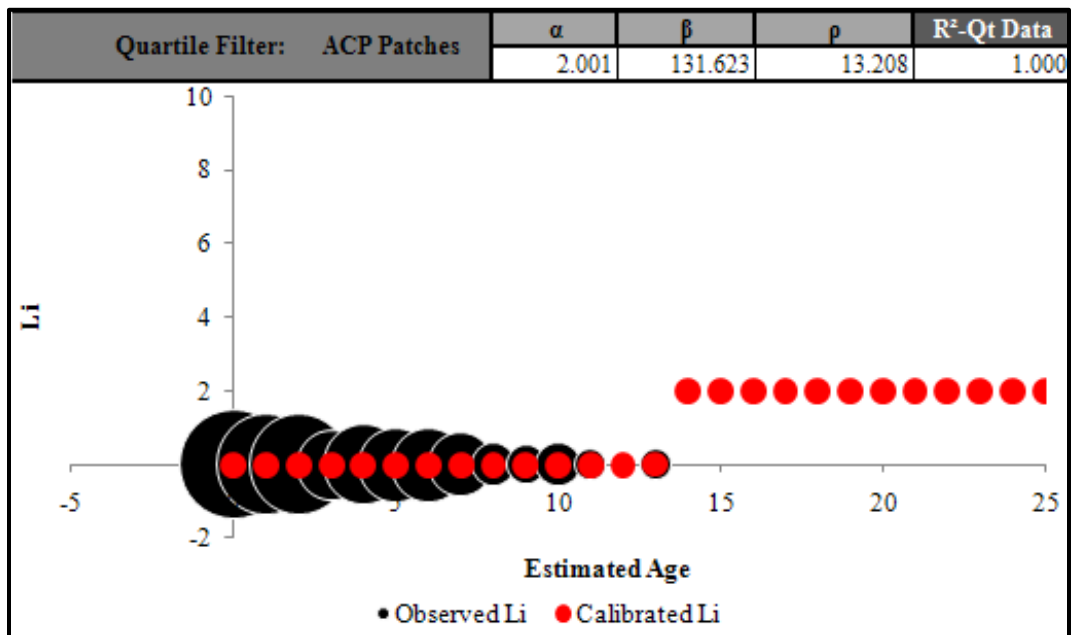


Figure C 17.9. Calibrated Performance Model for Bryan District, Li Quartile Method (Unconstrained).

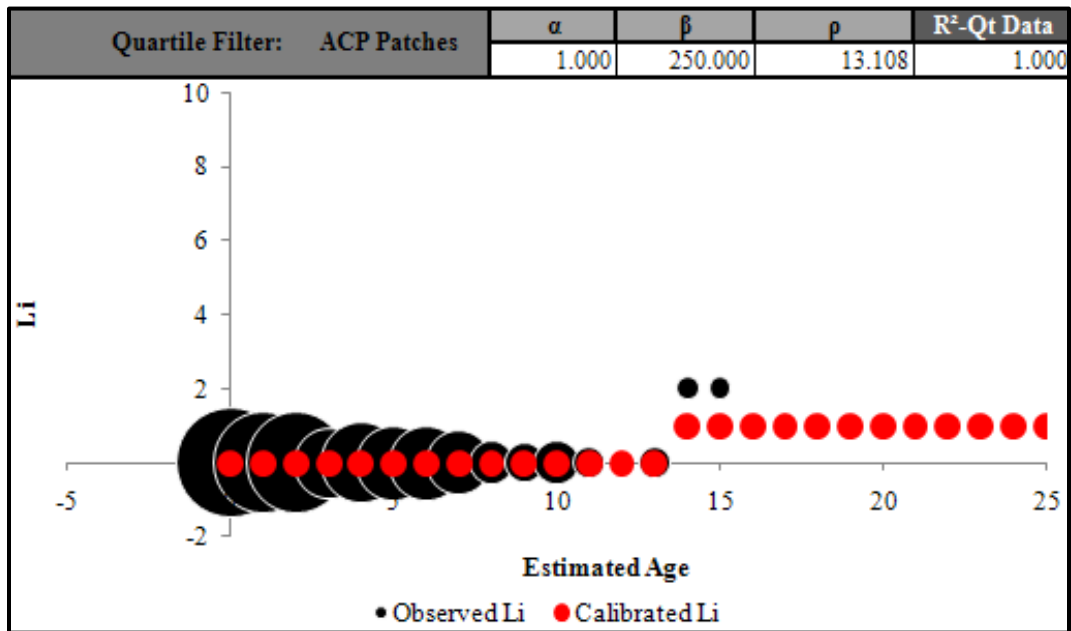


Figure C 17.10. Calibrated Performance Model for Bryan District, Li Quartile Method (Constrained).

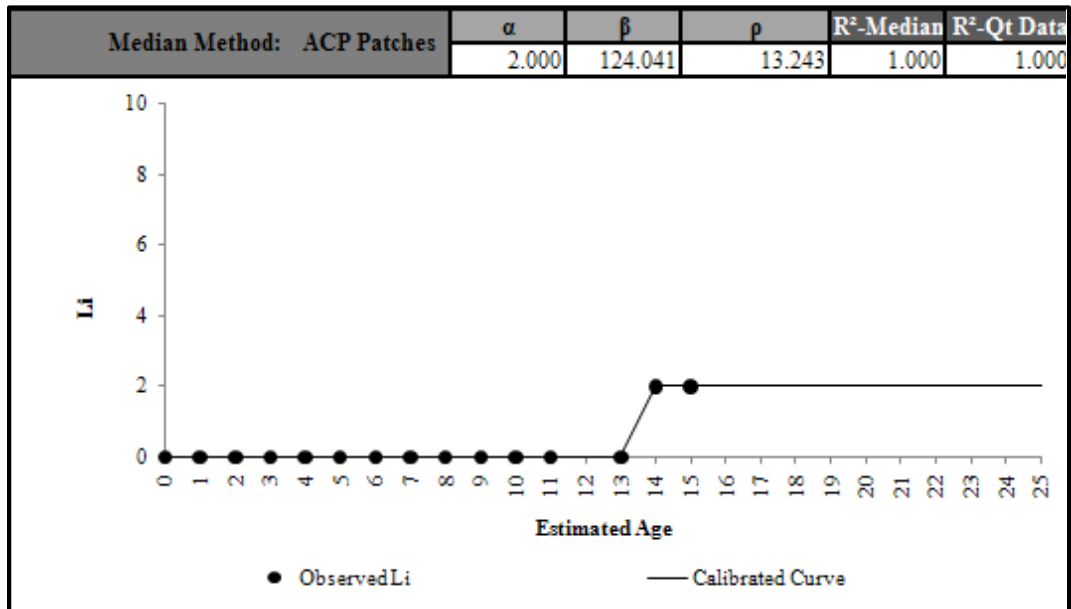


Figure C 17.11. Calibrated Performance Model for Bryan District, Li Median Method (Unconstrained).

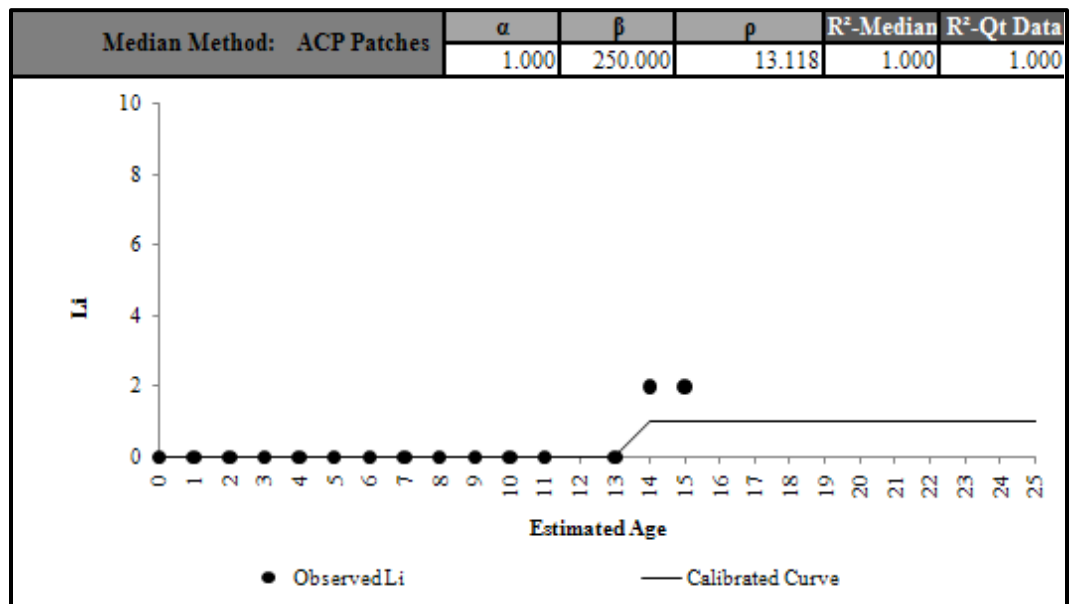


Figure C 17.12. Calibrated Performance Model for Bryan District, Li Median Method (Constrained).

Bryan District 17-PCC Patches

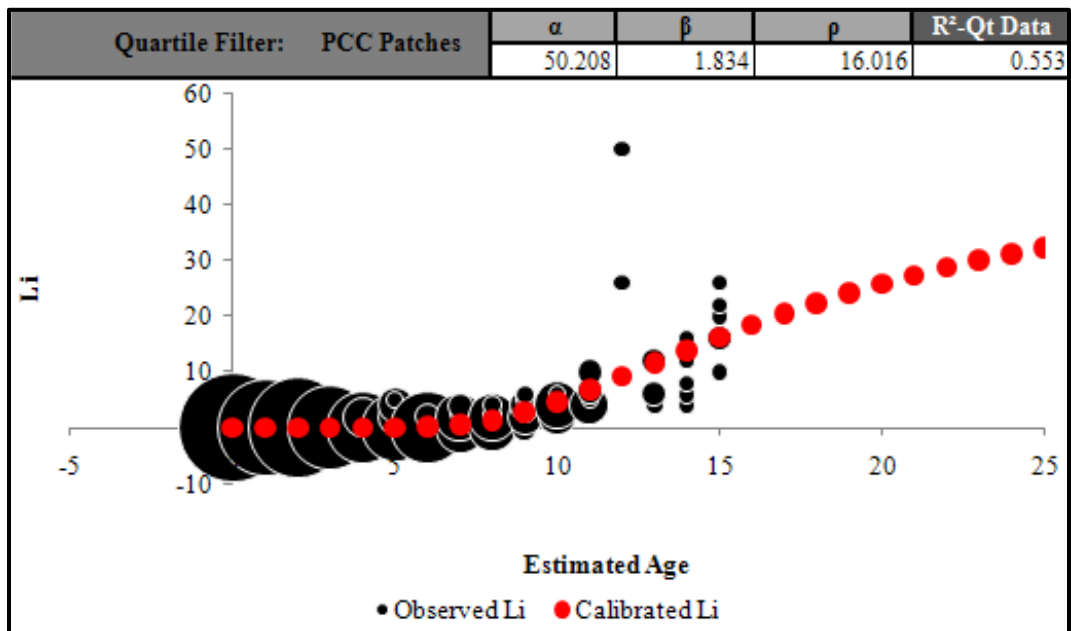


Figure C 17.13. Calibrated Performance Model for Bryan District, Li Quartile Method (Unconstrained).

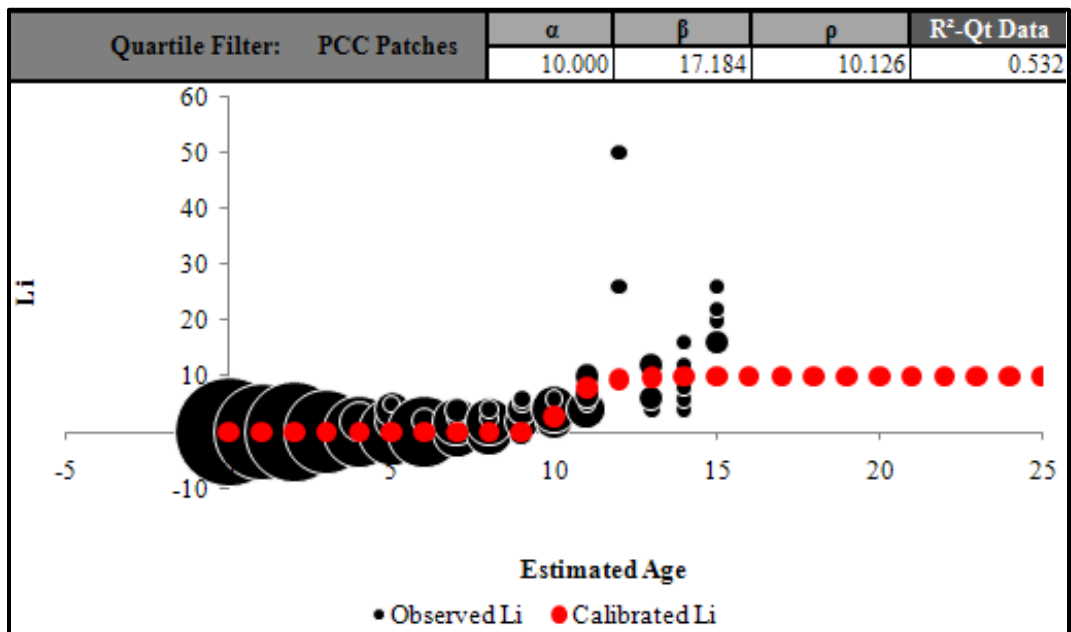


Figure C 17.14. Calibrated Performance Model for Bryan District, Li Quartile Method (Constrained).

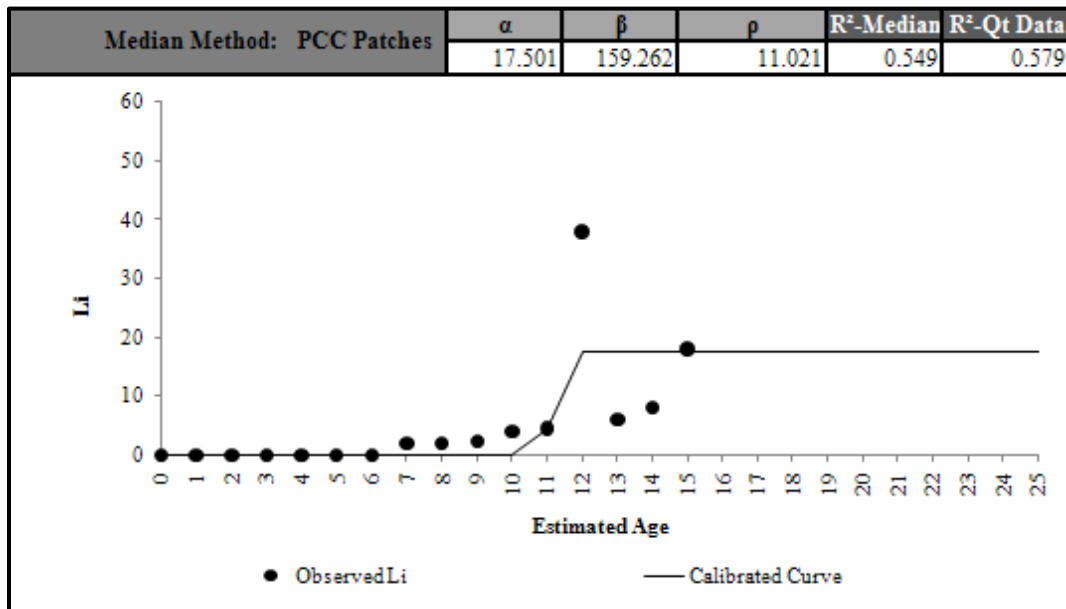


Figure C 17.15. Calibrated Performance Model for Bryan District, Li Median Method (Unconstrained).

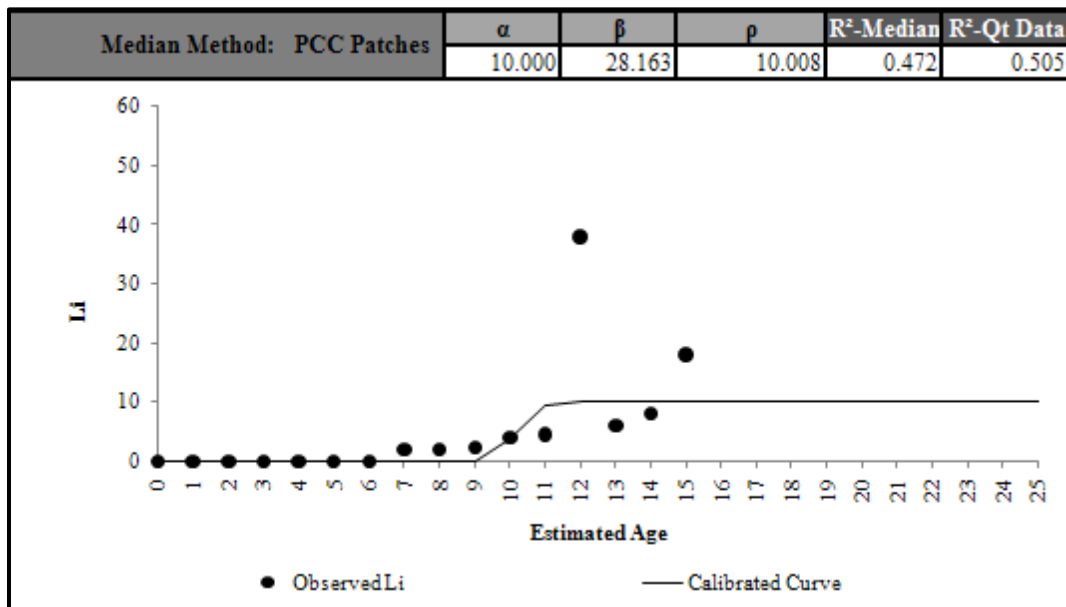


Figure C 17.16. Calibrated Performance Model for Bryan District, Li Median Method (Constrained).

Dallas District 18-Spalled Cracks

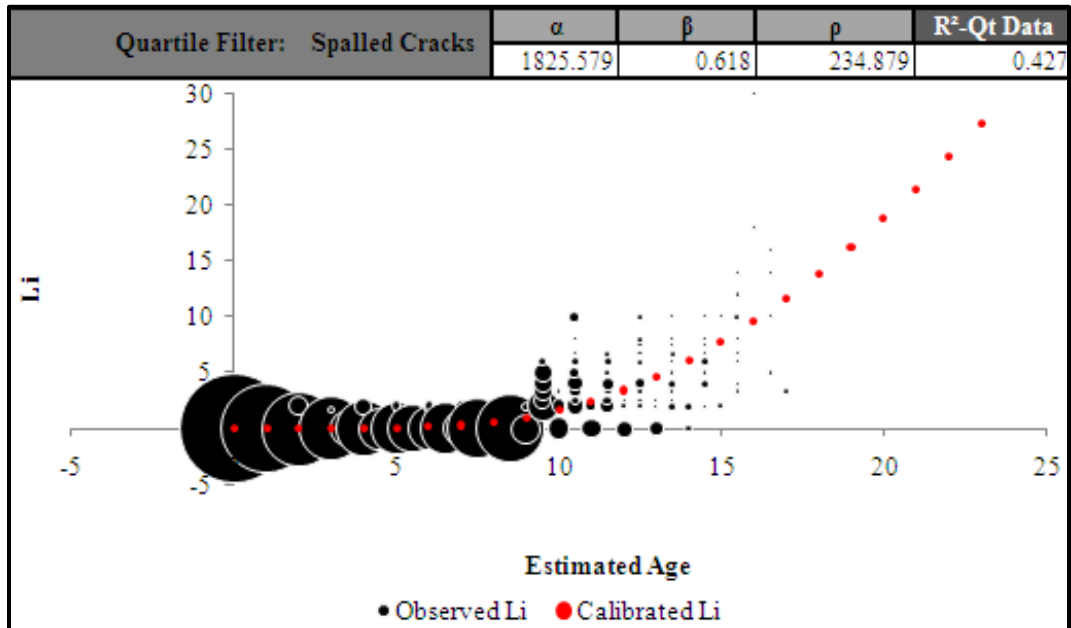


Figure C 18.1. Calibrated Performance Model for Dallas District, Li Quartile Method (Unconstrained).

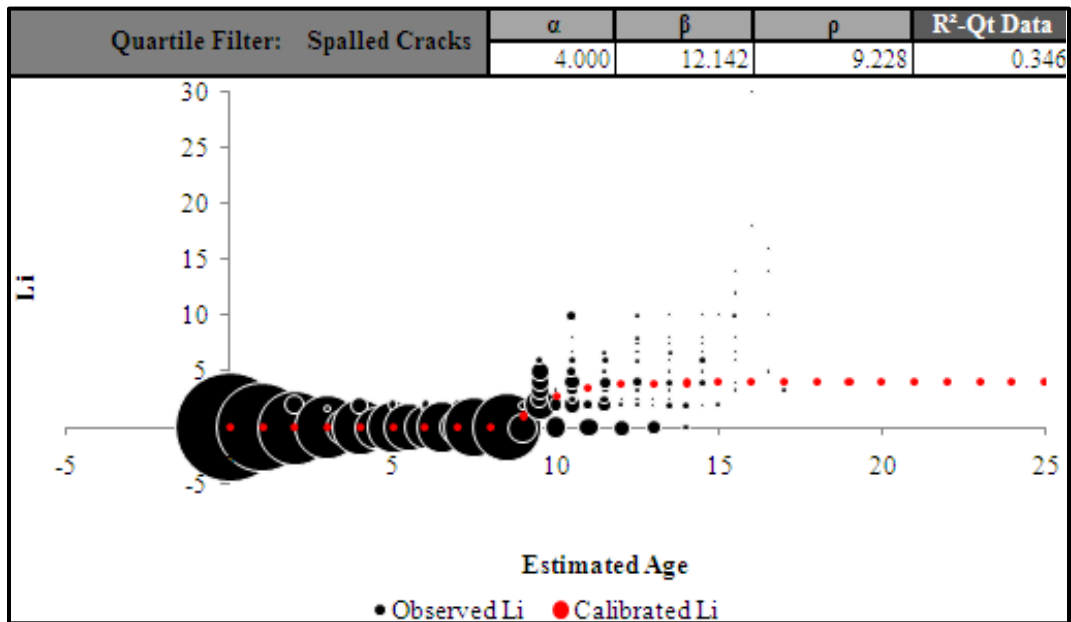


Figure C 18.2. Calibrated Performance Model for Dallas District, Li Quartile Method (Constrained).

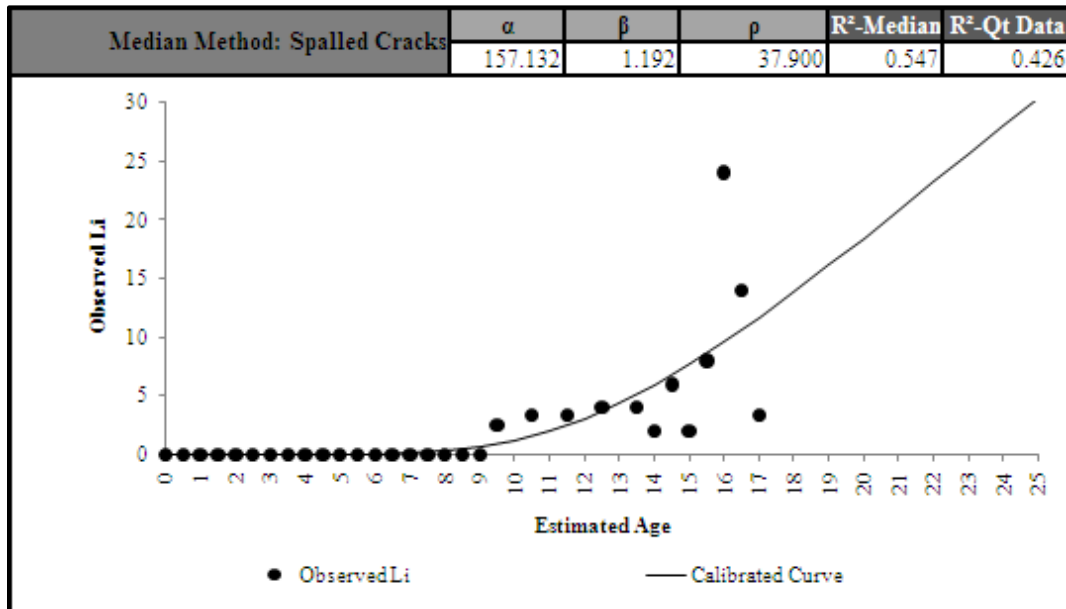


Figure C 18.3. Calibrated Performance Model for Dallas District, Li Median Method (Unconstrained).

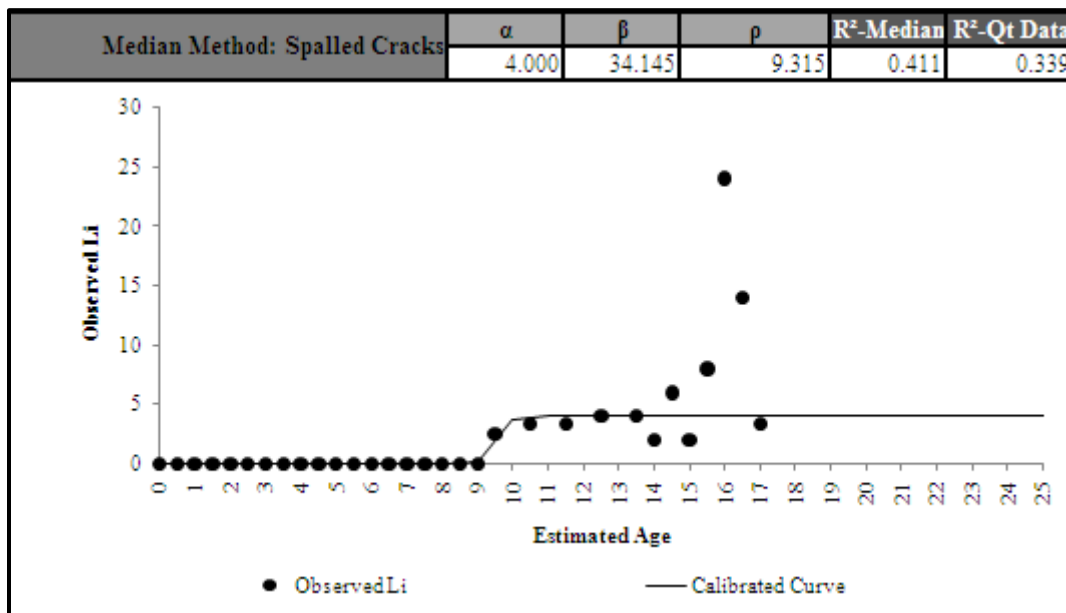


Figure C 18.4. Calibrated Performance Model for Dallas District, Li Median Method (Constrained).

Dallas District 18- PCC Patches

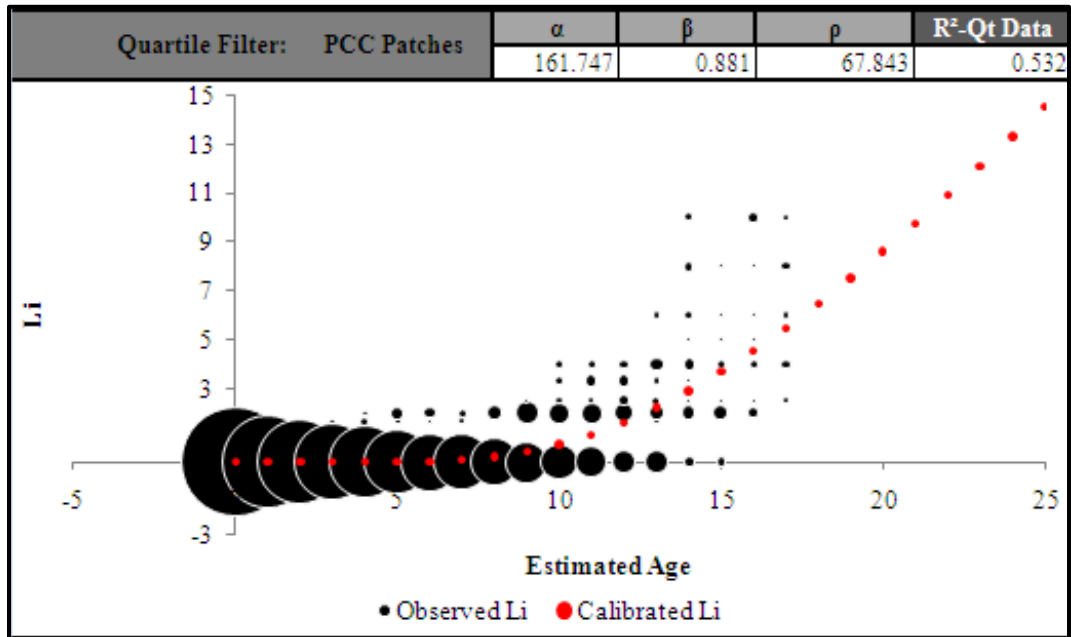


Figure C 18.5. Calibrated Performance Model for Dallas District, Li Quartile Method (Unconstrained).

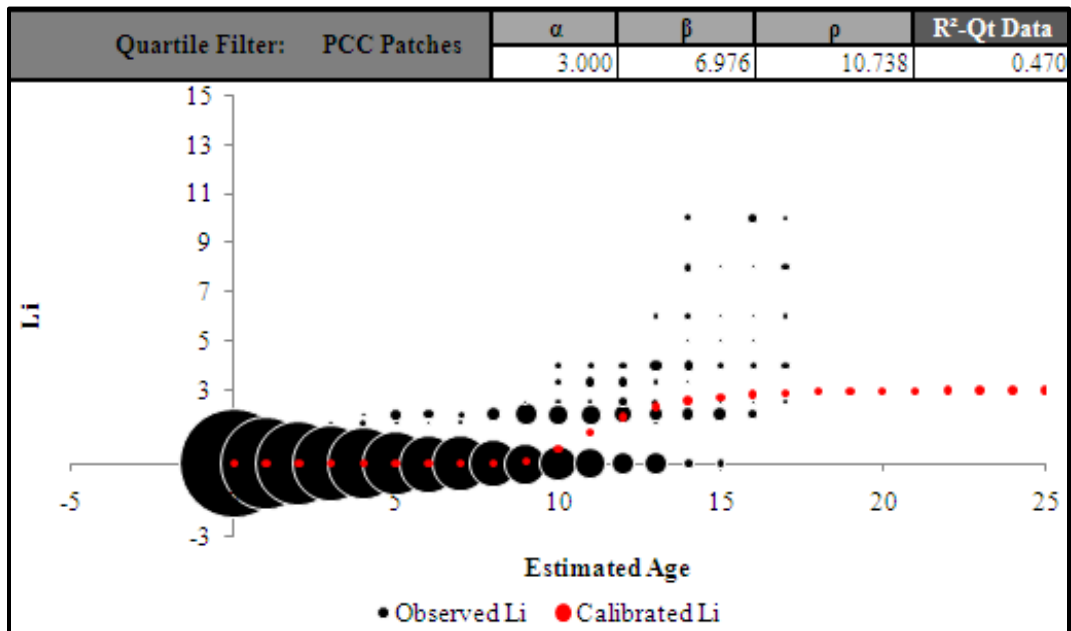


Figure C 18.6. Calibrated Performance Model for Dallas District, Li Quartile Method (Constrained).

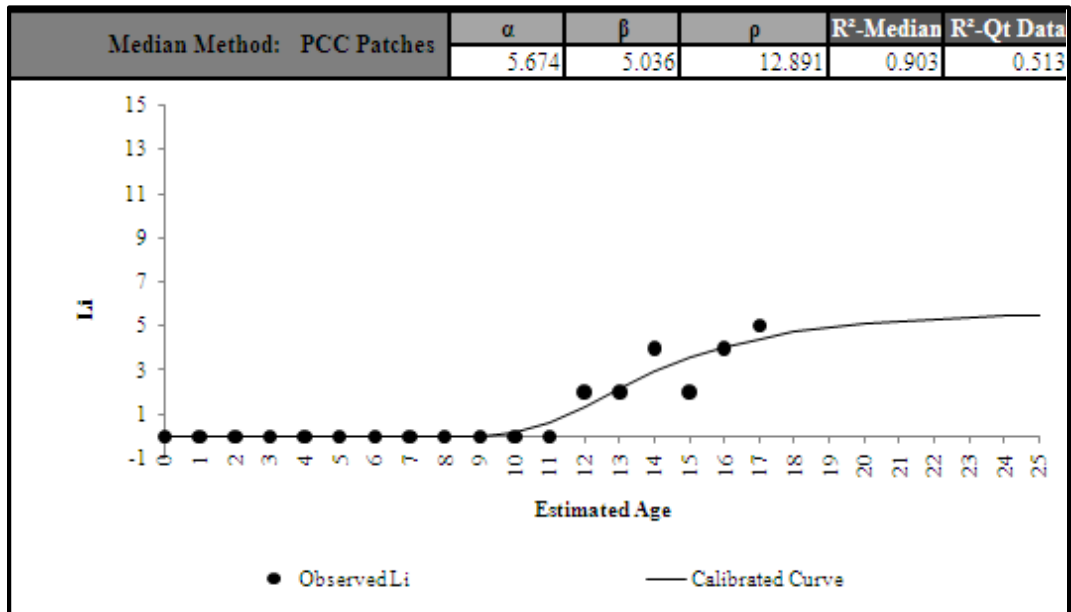


Figure C 18.7. Calibrated Performance Model for Dallas District, Li Median Method (Unconstrained).

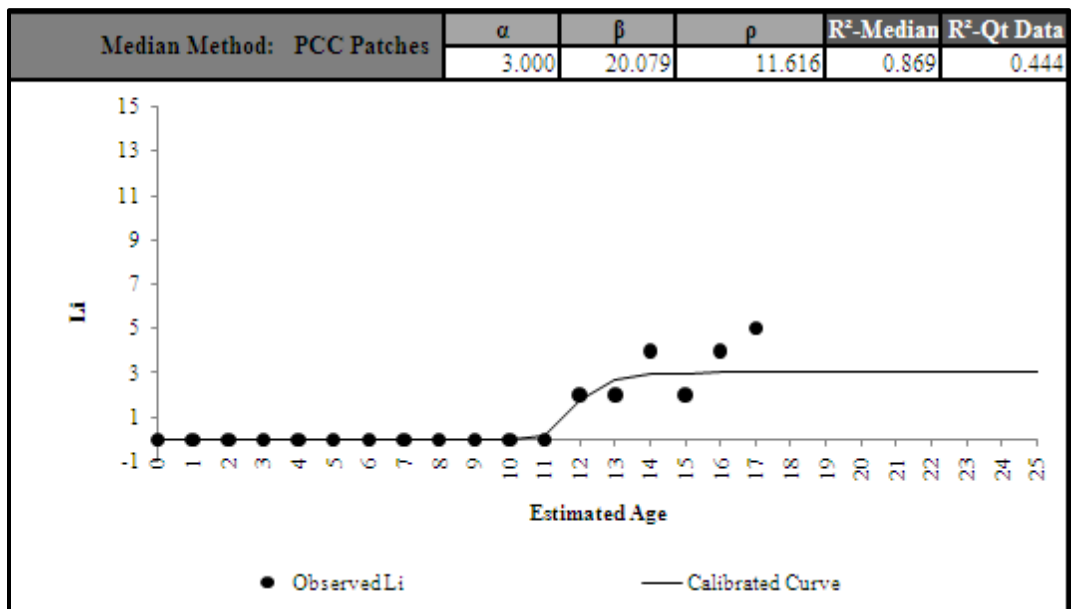


Figure C 18.8. Calibrated Performance Model for Dallas District, Li Median Method (Constrained).

Atlanta District 19-Spalled Cracks

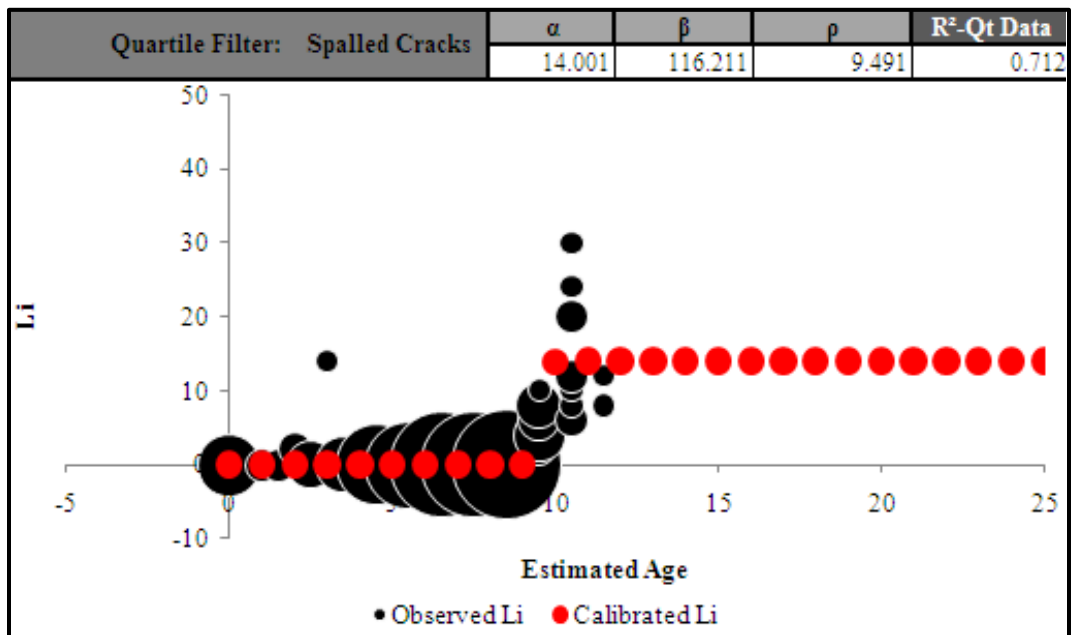


Figure C 19.1. Calibrated Performance Model for Atlanta District, Li Quartile Method (Unconstrained).

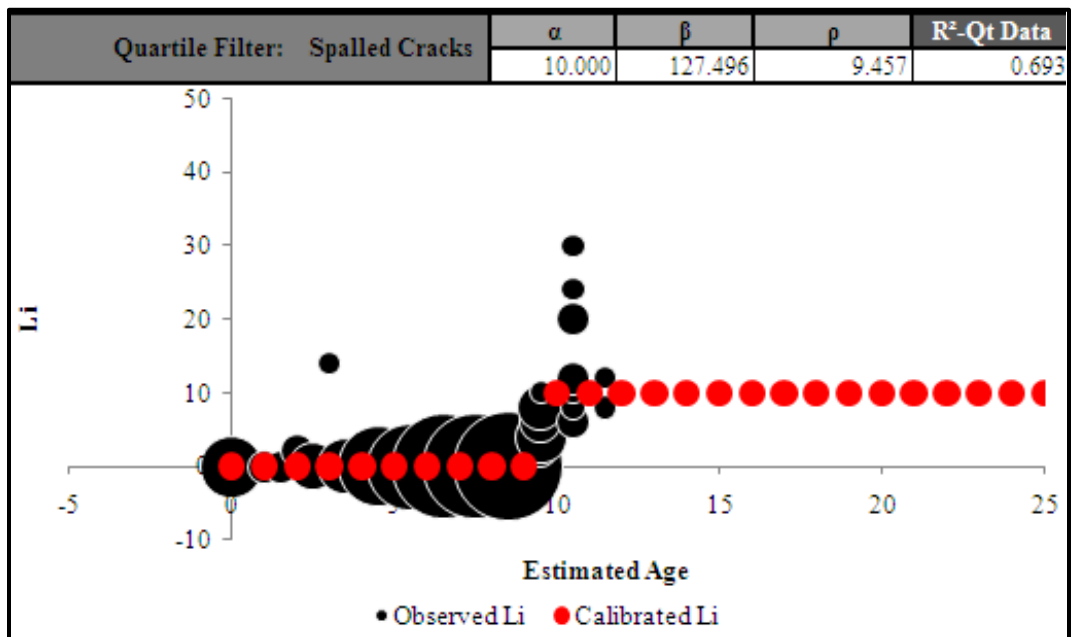


Figure C 19.2. Calibrated Performance Model for Atlanta District, Li Quartile Method (Constrained).

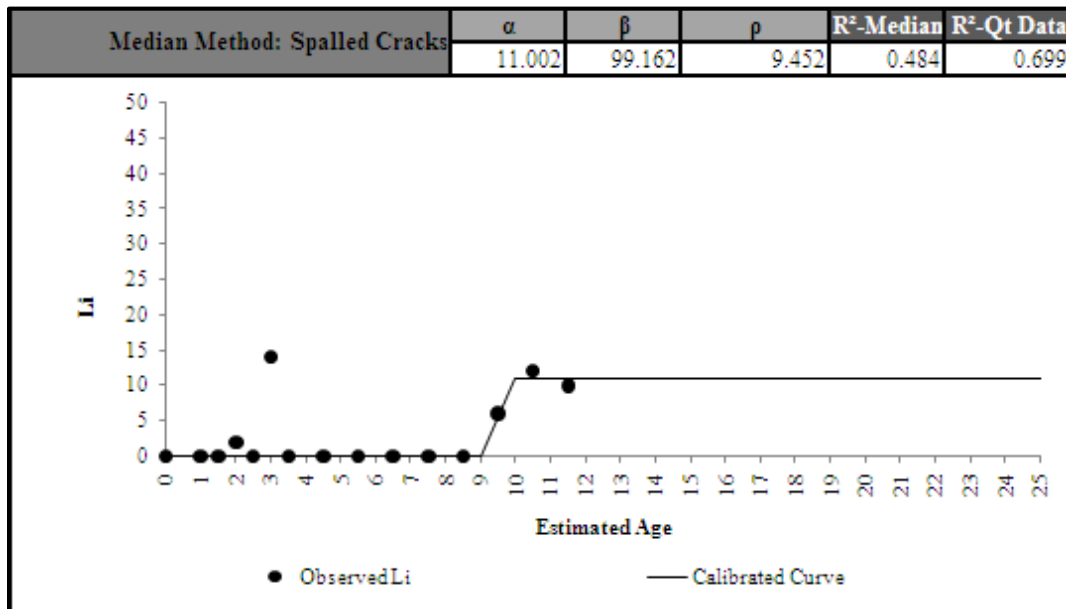


Figure C 19.3. Calibrated Performance Model for Atlanta District, Li Median Method (Unconstrained).

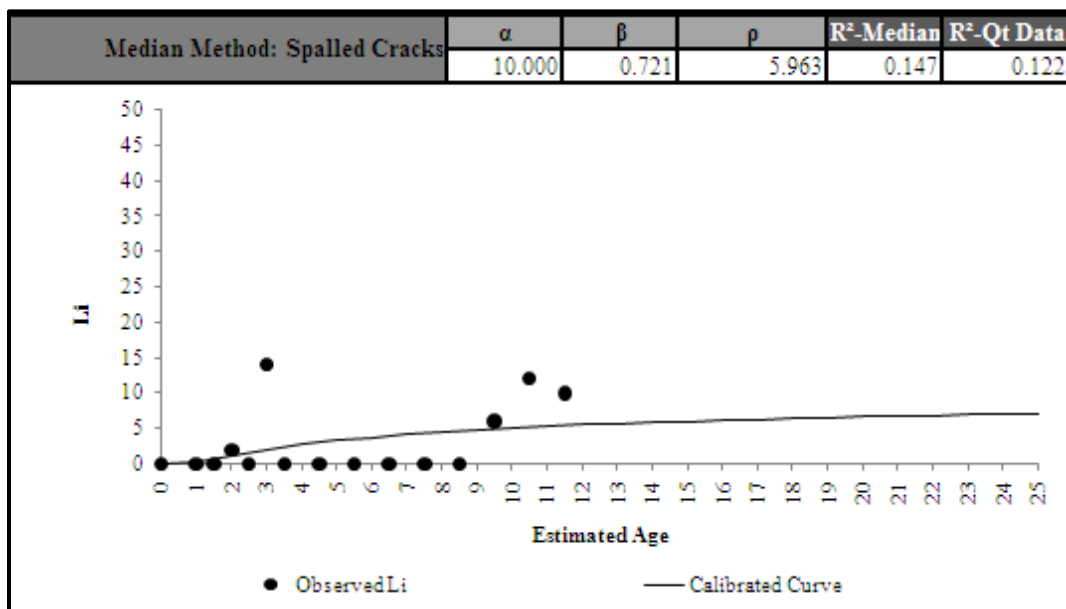


Figure C 19.4. Calibrated Performance Model for Atlanta District, Li Median Method (Constrained).

Atlanta District 19-Punchouts

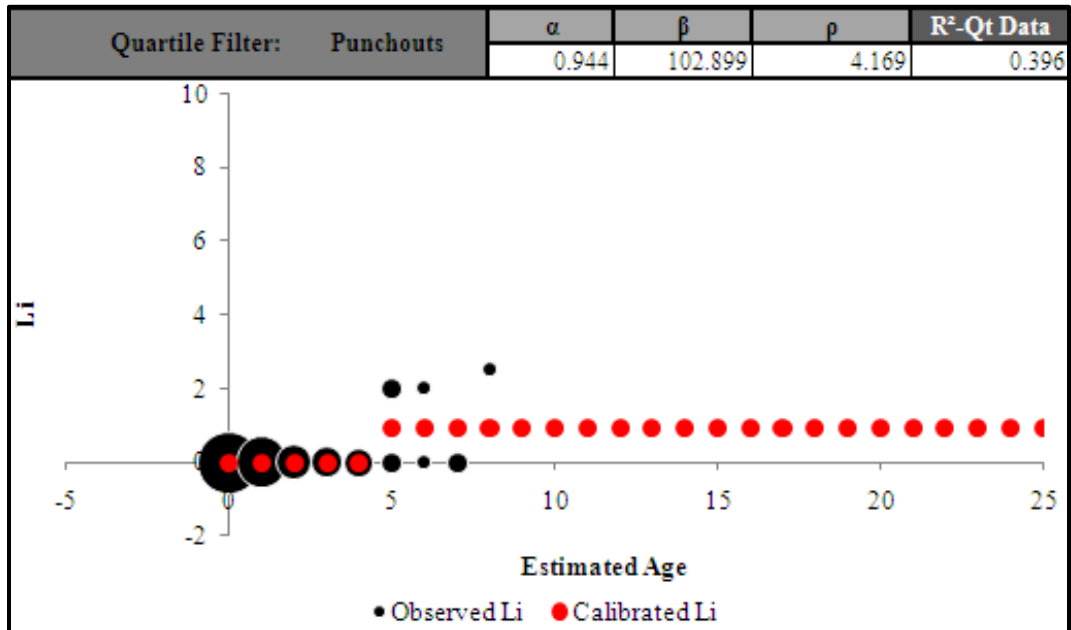


Figure C 19.5. Calibrated Performance Model for Atlanta District, Li Quartile Method (Unconstrained).

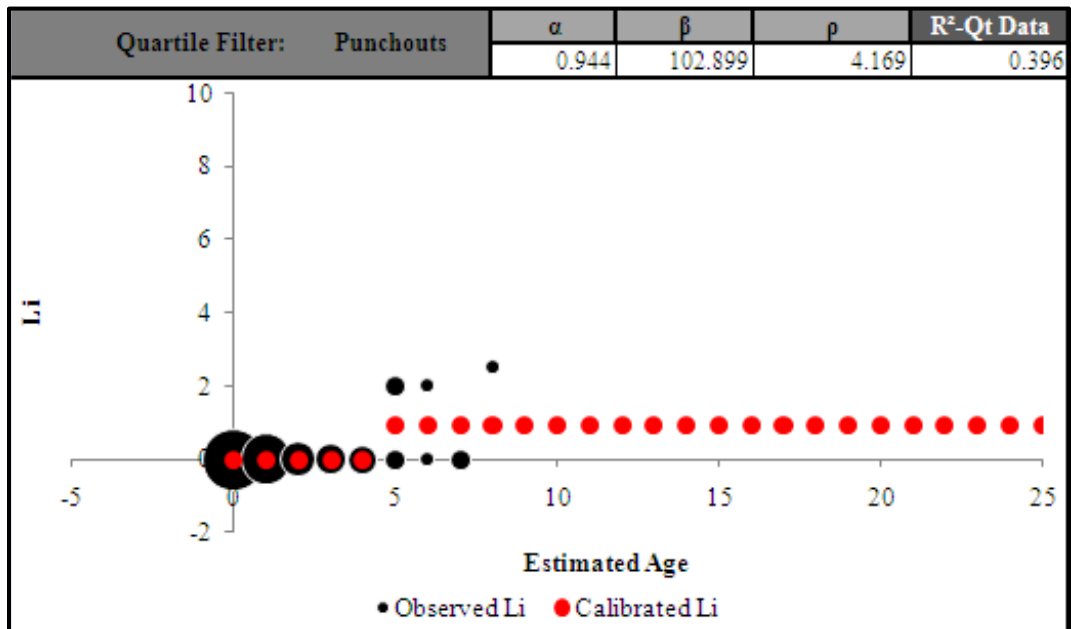


Figure C 19.6. Calibrated Performance Model for Atlanta District, Li Quartile Method (Constrained).

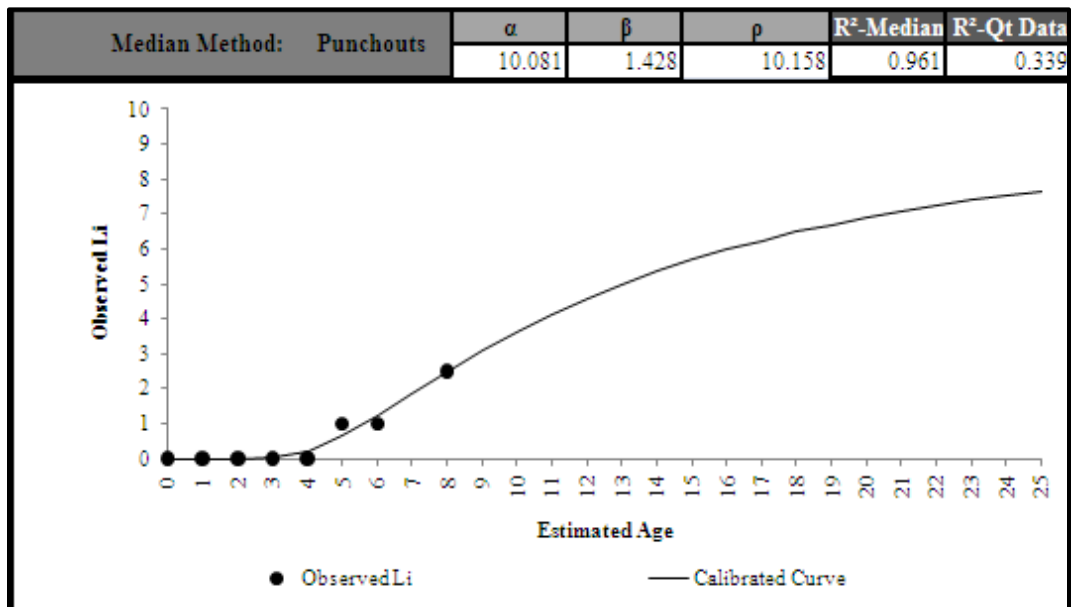


Figure C 19.7. Calibrated Performance Model for Atlanta District, Li Median Method (Unconstrained).

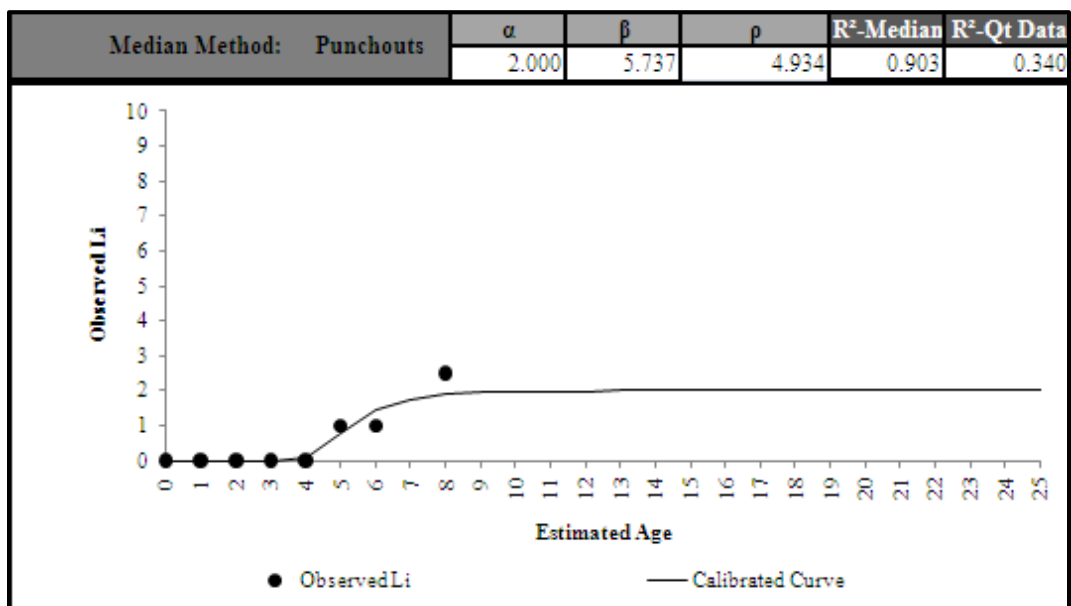


Figure C 19.8. Calibrated Performance Model for Atlanta District, Li Median Method (Constrained).

Atlanta District 19-ACP Patches

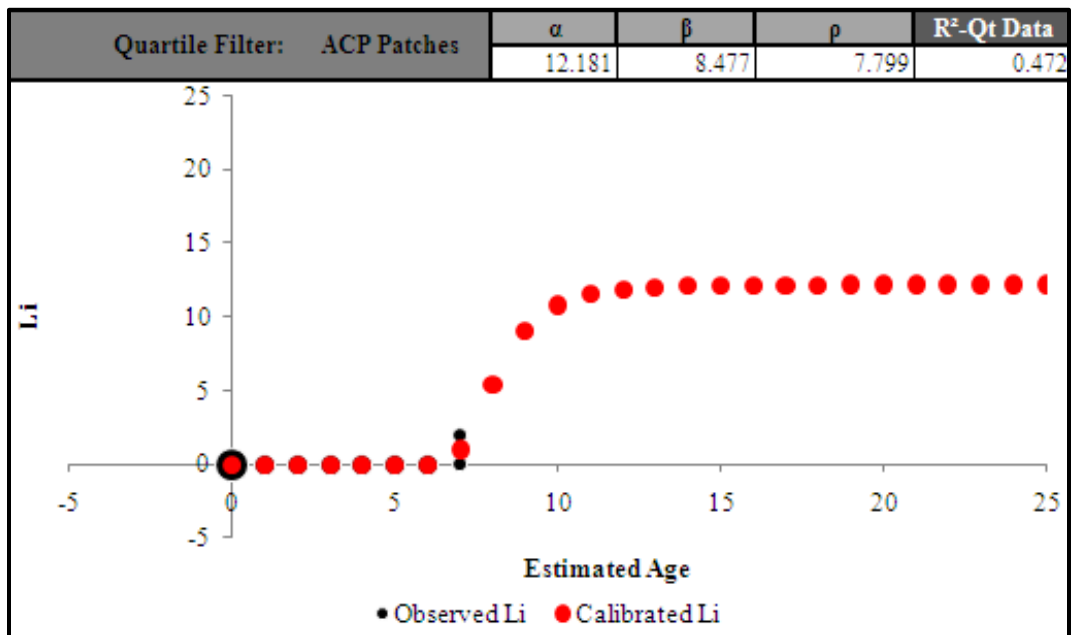


Figure C 19.9. Calibrated Performance Model for Atlanta District, Li Quartile Method (Unconstrained).

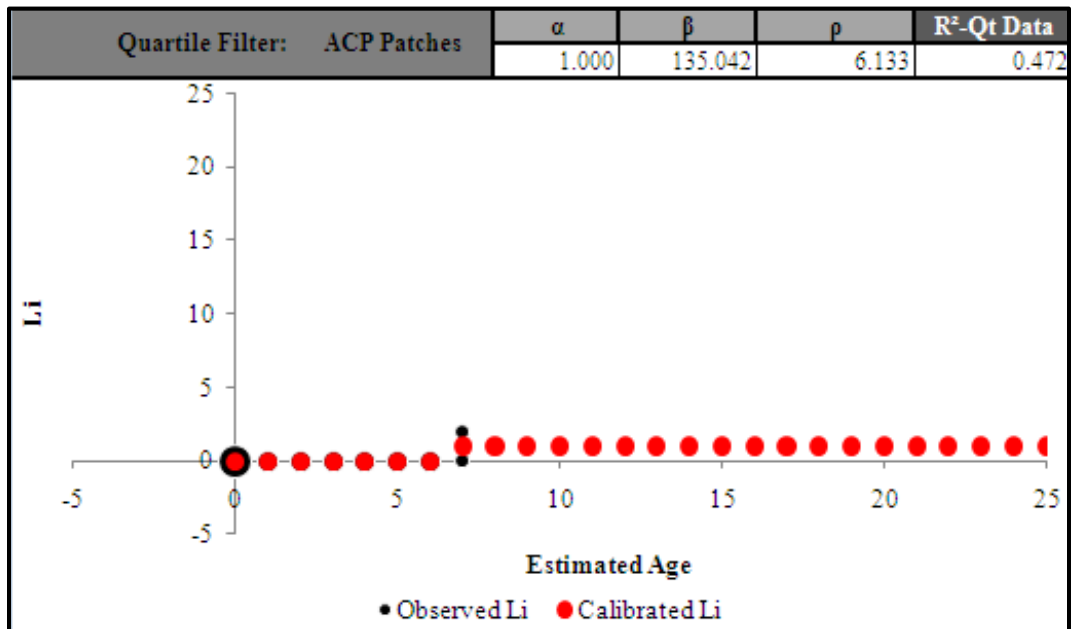


Figure C 19.10. Calibrated Performance Model for Atlanta District, Li Quartile Method (Constrained).

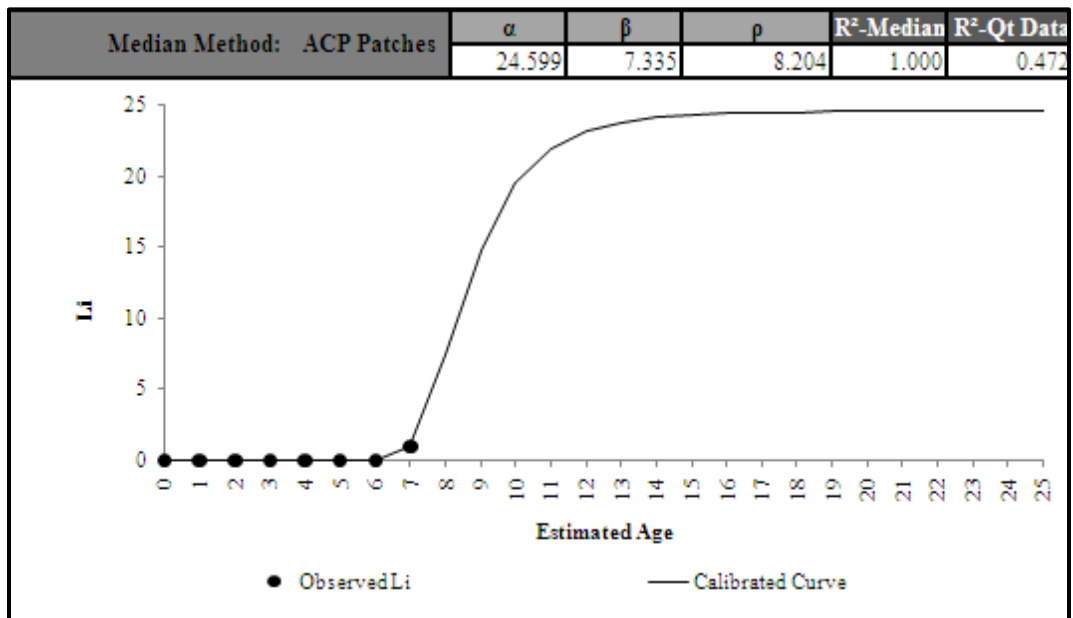


Figure C 19.11. Calibrated Performance Model for Atlanta District, Li Median Method (Unconstrained).

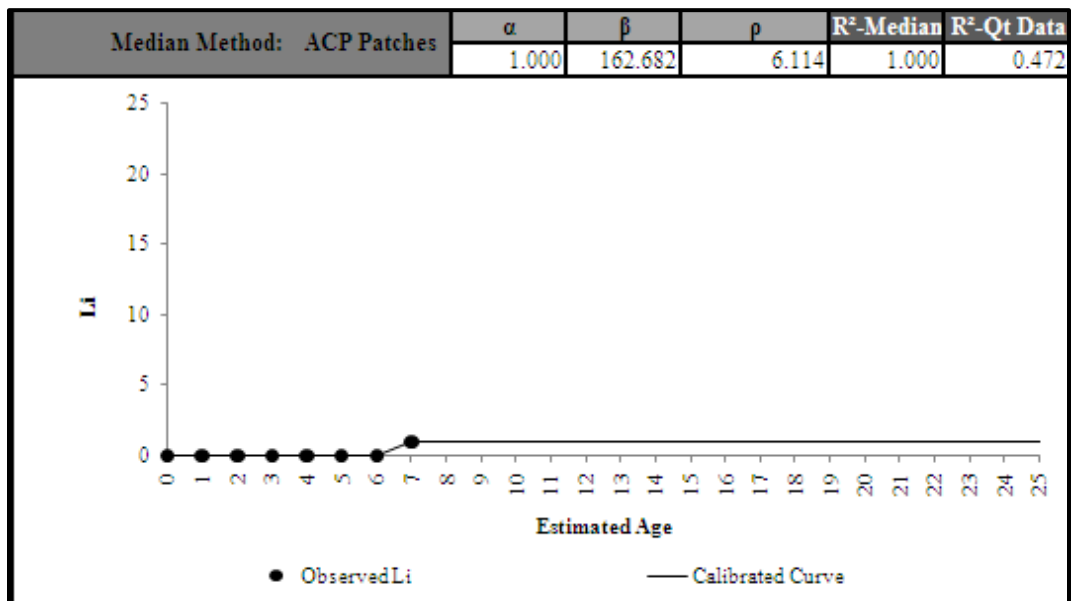


Figure C 19.12. Calibrated Performance Model for Atlanta District, Li Median Method (Constrained).

Atlanta District 19-PCC Patches

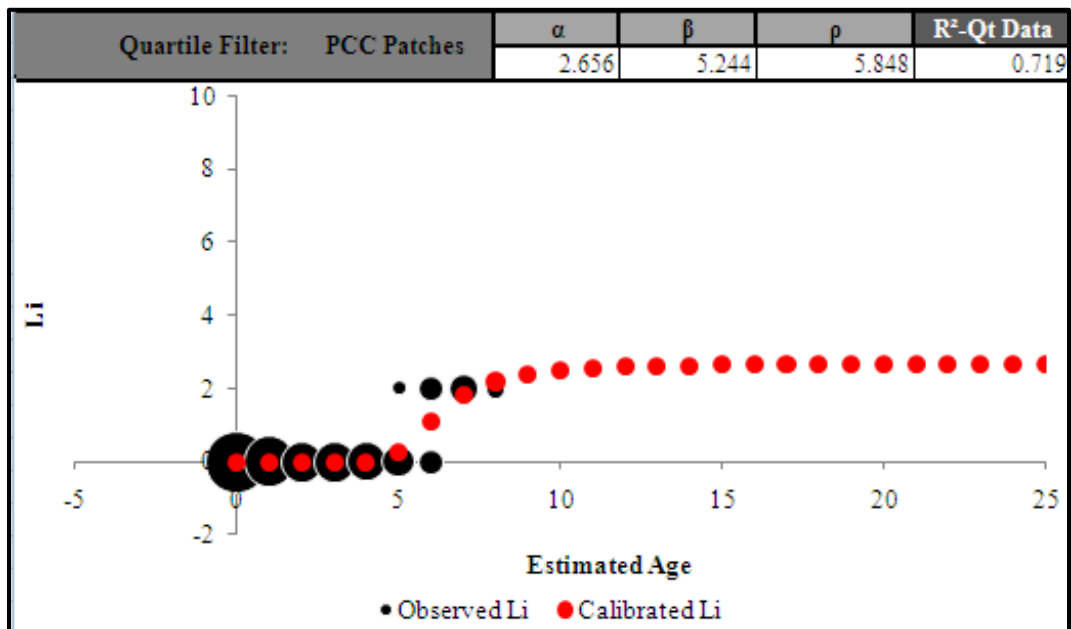


Figure C 19.13. Calibrated Performance Model for Atlanta District, Li Quartile Method (Unconstrained).

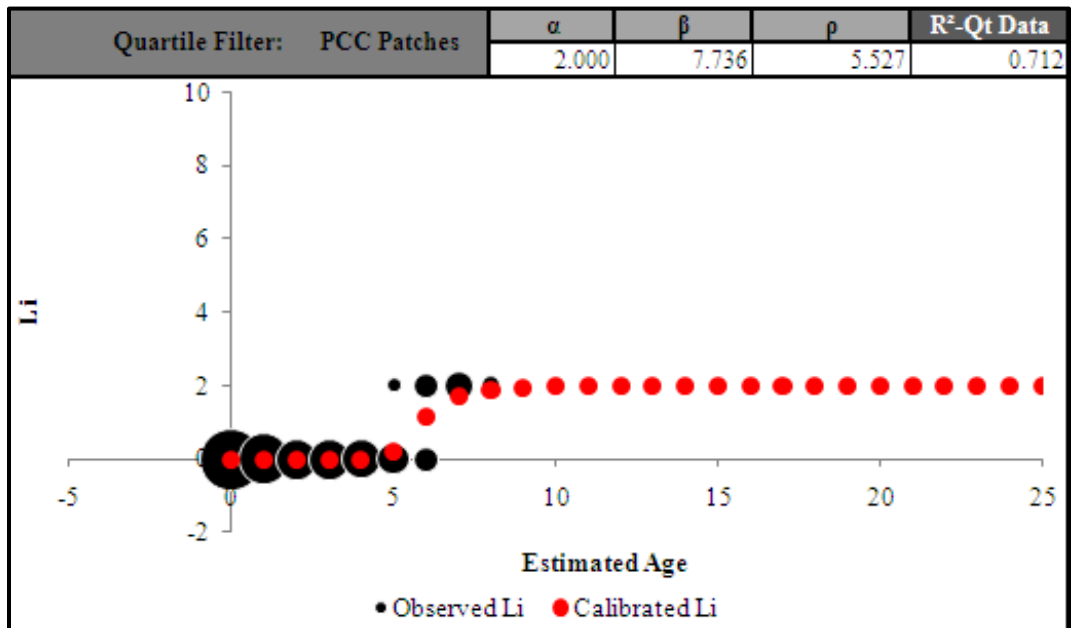


Figure C 19.14. Calibrated Performance Model for Atlanta District, Li Quartile Method (Constrained).

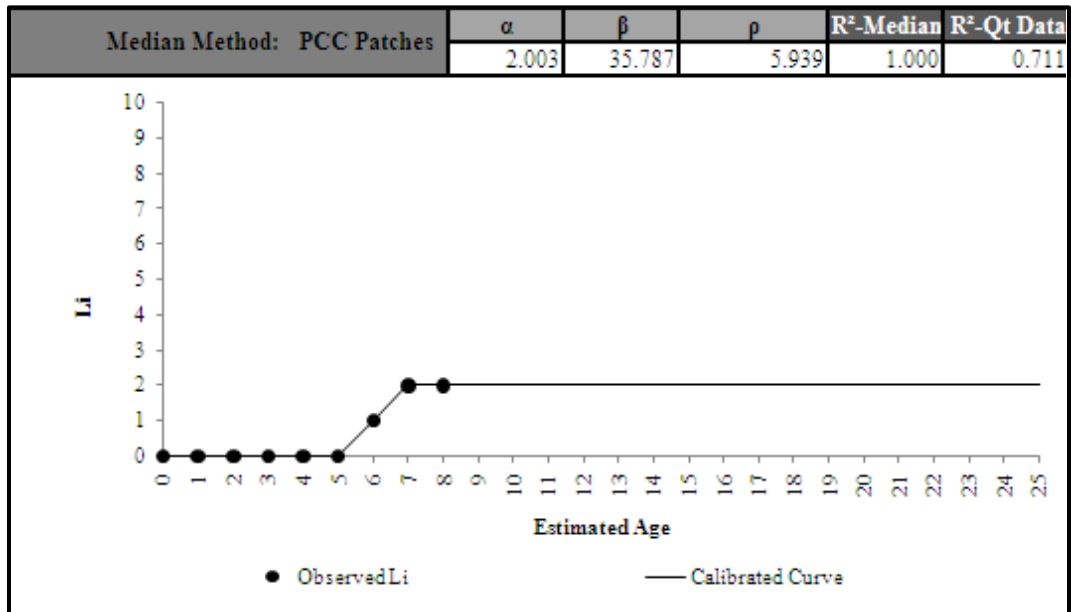


Figure C 19.15. Calibrated Performance Model for Atlanta District, Li Median Method (Unconstrained).

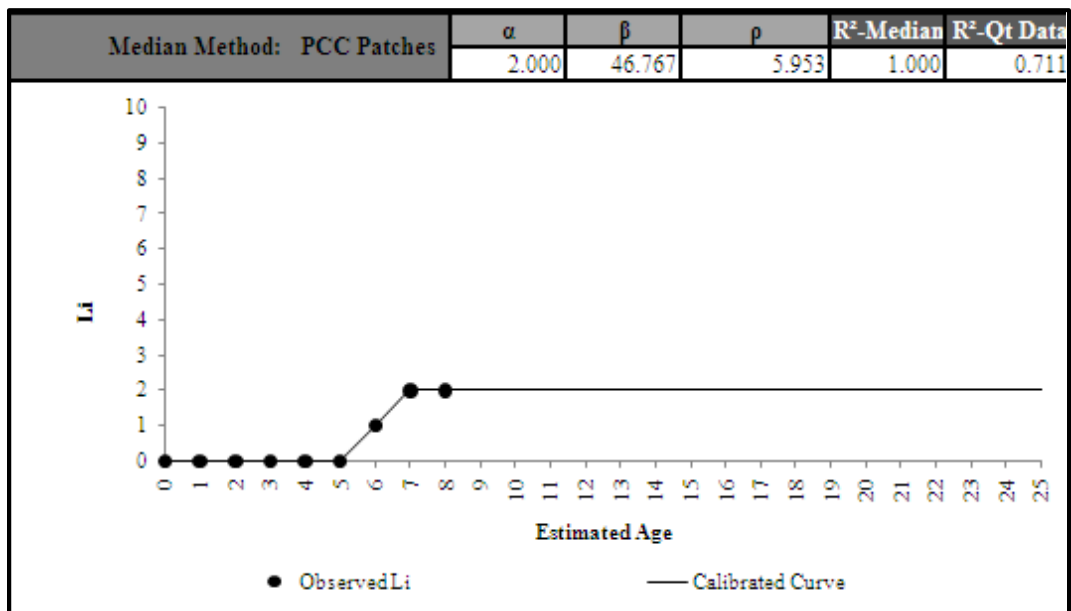


Figure C 19.16. Calibrated Performance Model for Atlanta District, Li Median Method (Constrained).

Beaumont District 20-Spalled Cracks

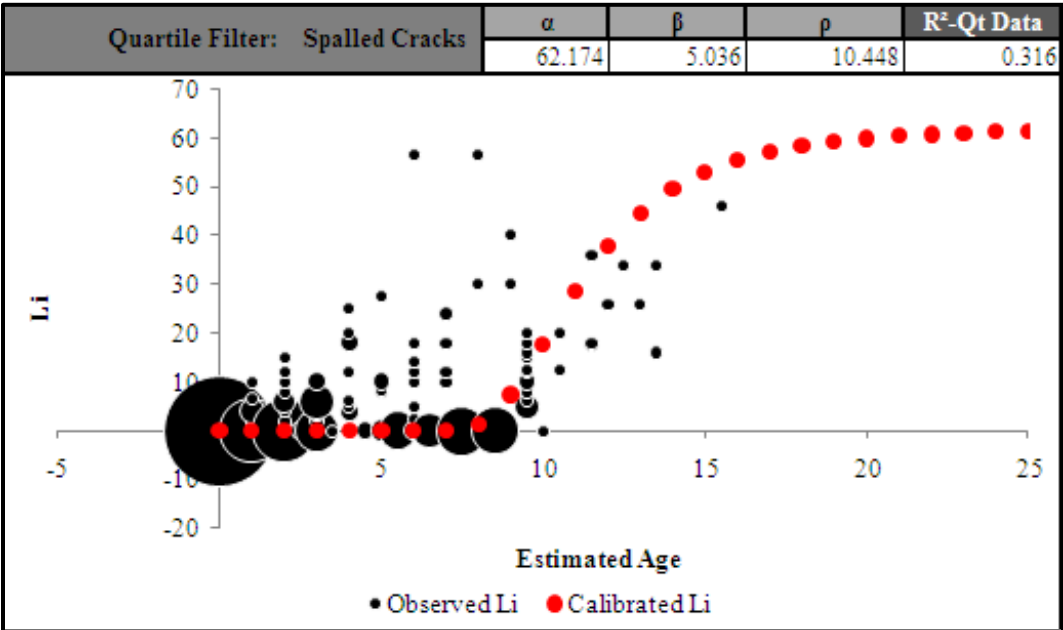


Figure C 20.1. Calibrated Performance Model for Beaumont District, Li Quartile Method (Unconstrained).

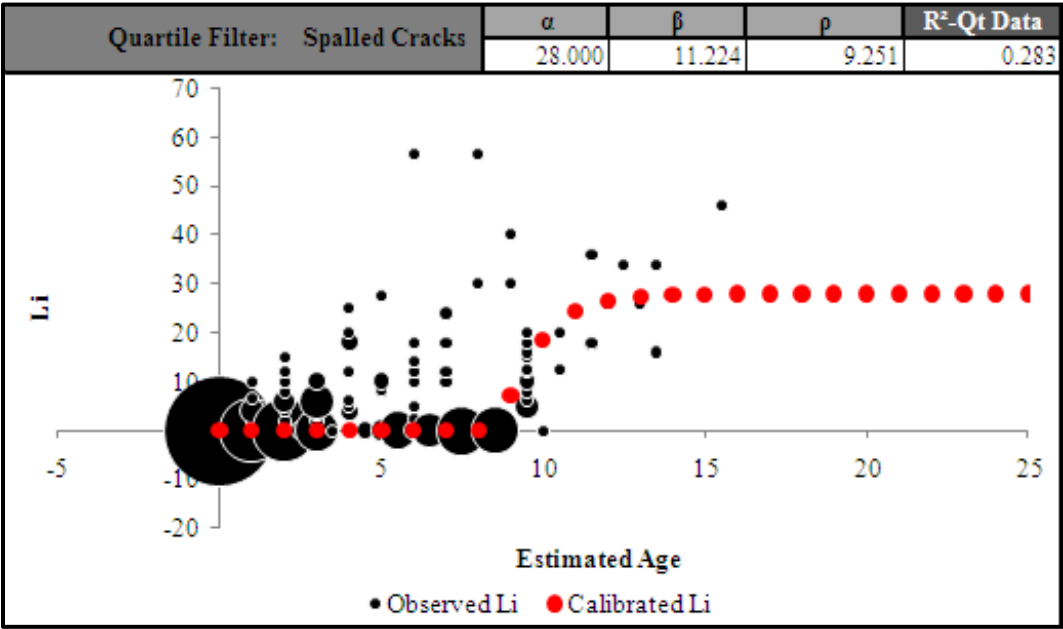


Figure C 20.2. Calibrated Performance Model for Beaumont District, Li Quartile Method (Constrained).

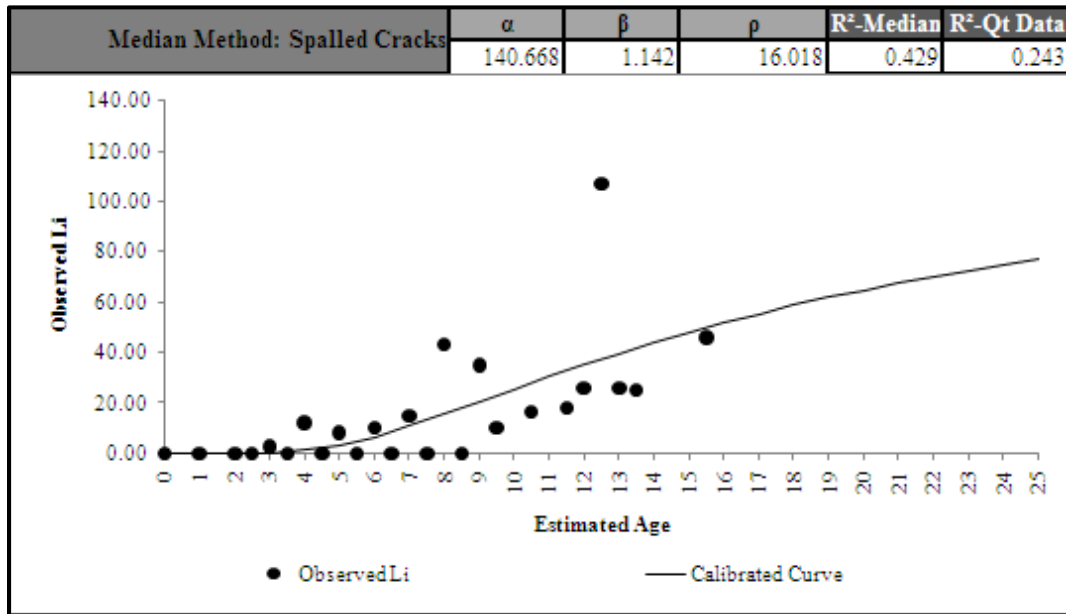


Figure C 20.3. Calibrated Performance Model for Beaumont District, Li Median Method (Unconstrained).

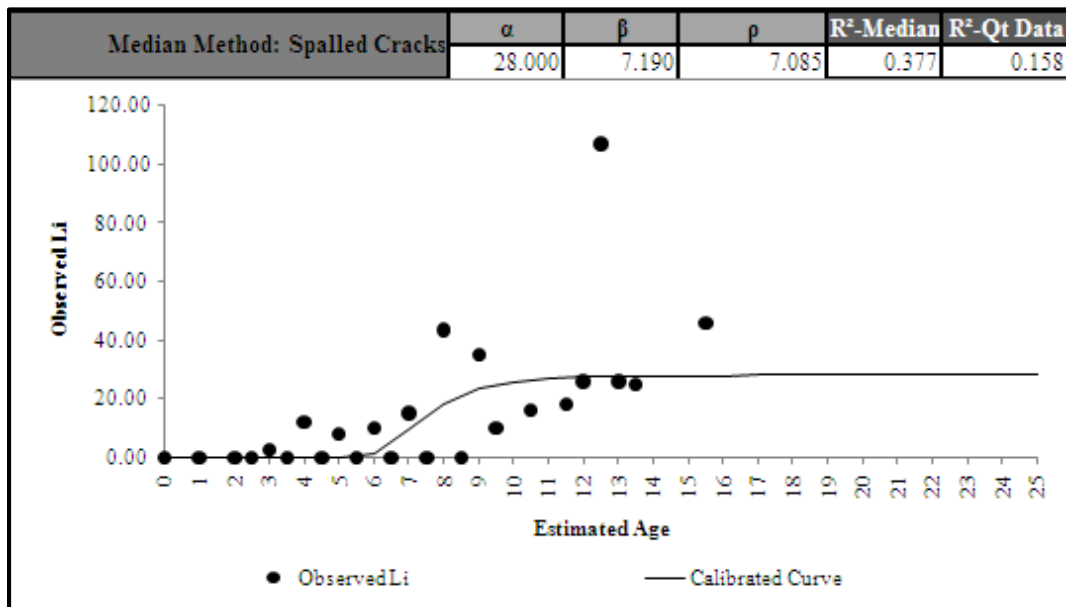


Figure C 20.4. Calibrated Performance Model for Beaumont District, Li Median Method (Constrained).

Beaumont District 20-Punchouts

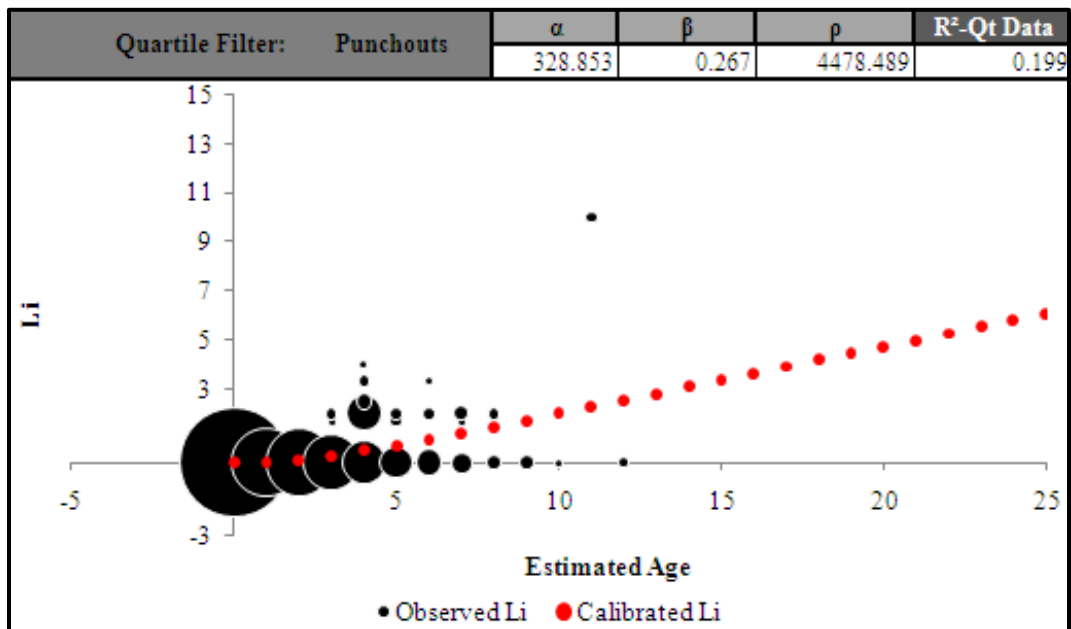


Figure C 20.5. Calibrated Performance Model for Beaumont District, Li Quartile Method (Unconstrained).

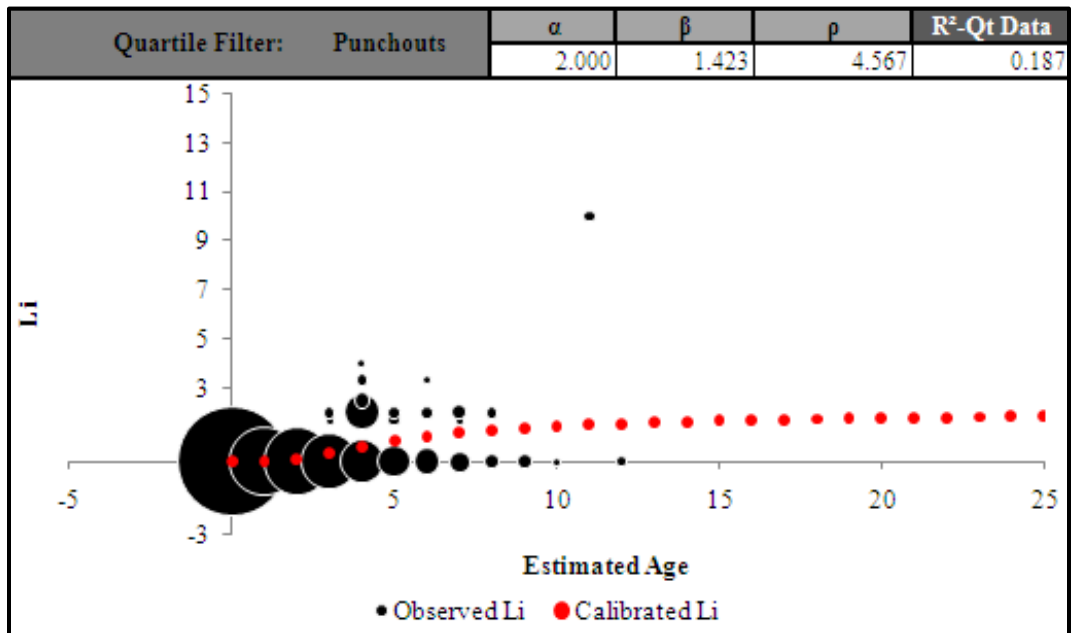


Figure C 20.6. Calibrated Performance Model for Beaumont District, Li Quartile Method (Constrained).

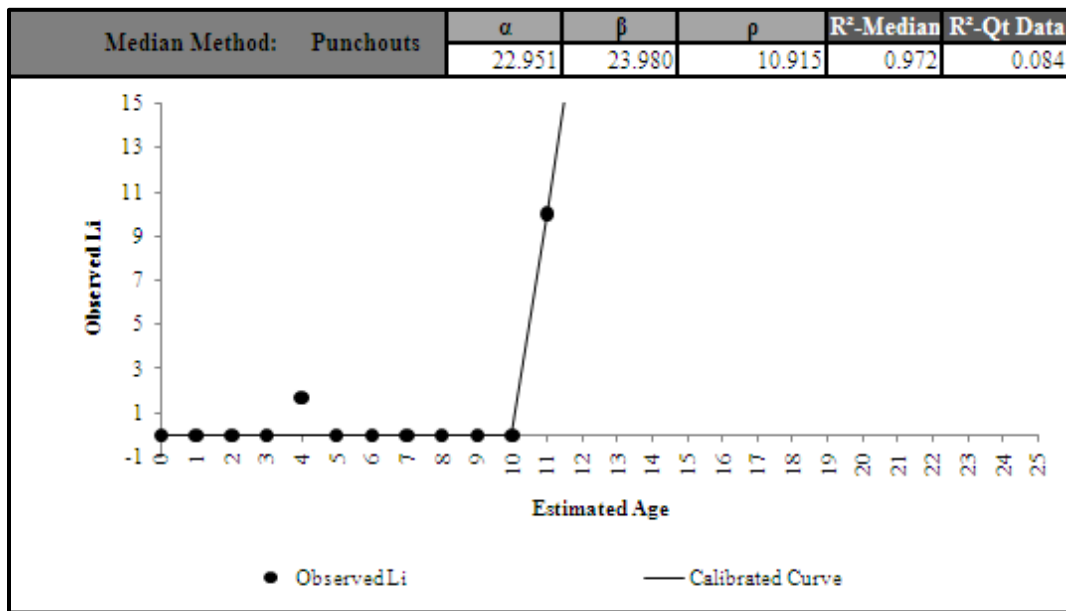


Figure C 20.7. Calibrated Performance Model for Beaumont District, Li Median Method (Unconstrained).

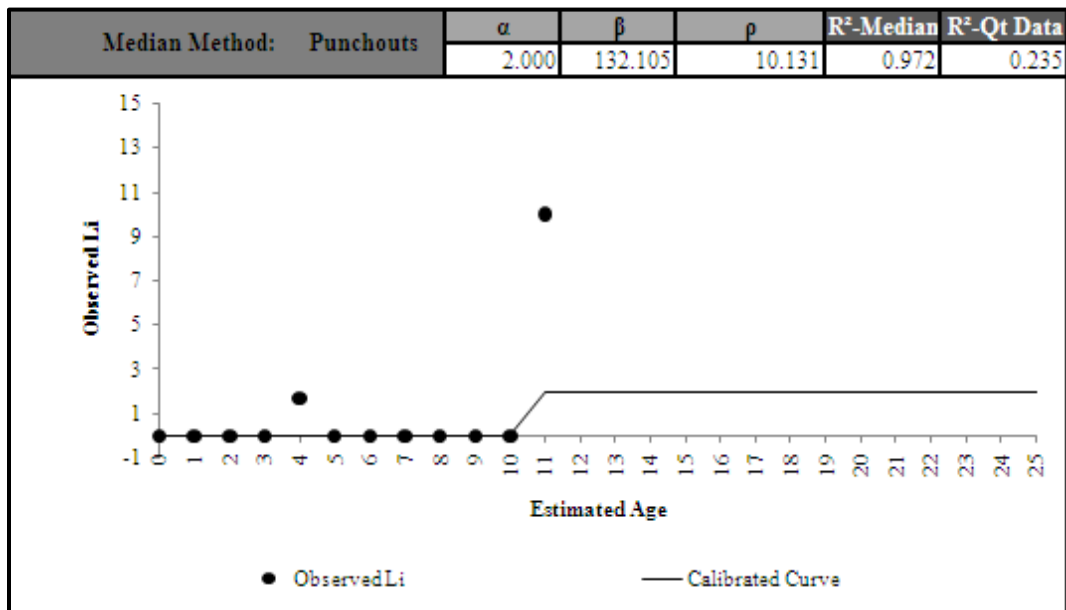


Figure C 20.8. Calibrated Performance Model for Beaumont District, Li Median Method (Constrained).

Beaumont District 20-PCC Patches

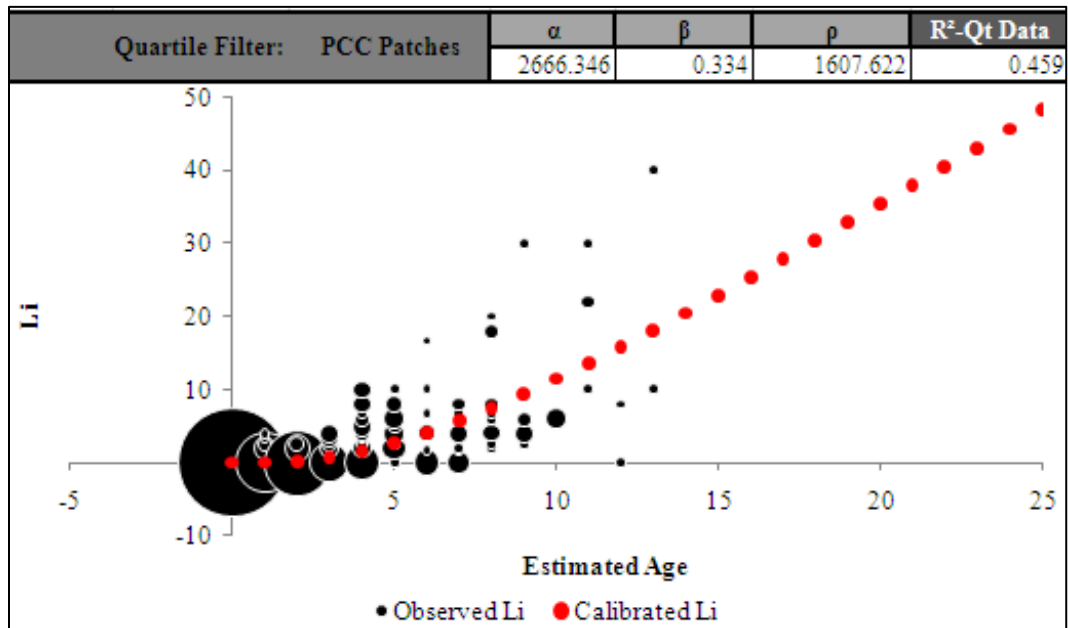


Figure C 20.9. Calibrated Performance Model for Beaumont District, Li Quartile Method (Unconstrained).

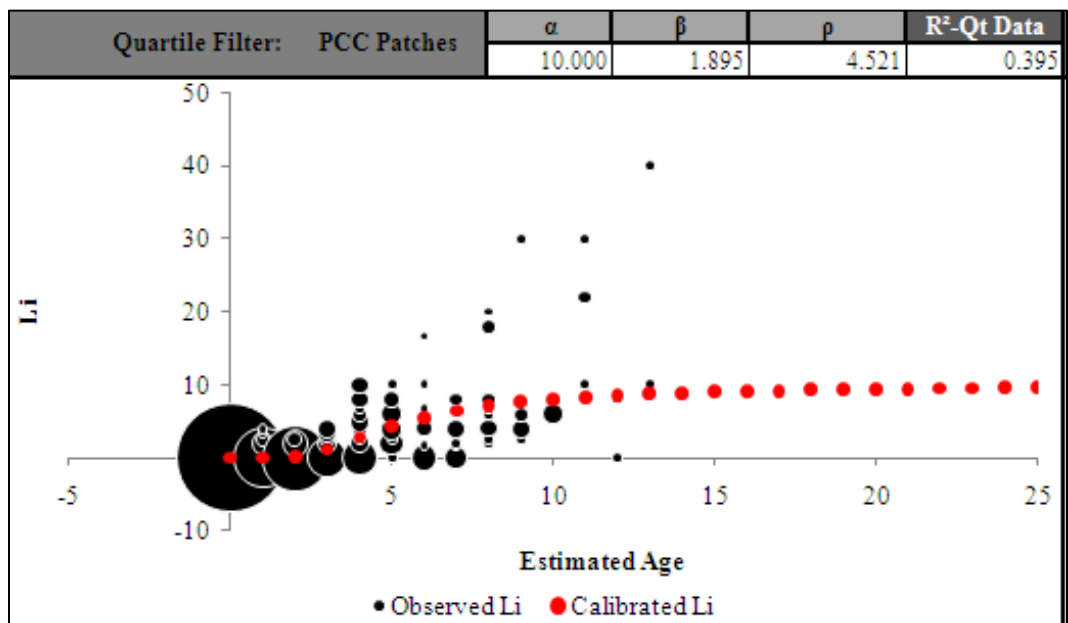


Figure C 20.10. Calibrated Performance Model for Beaumont District, Li Quartile Method (Constrained).

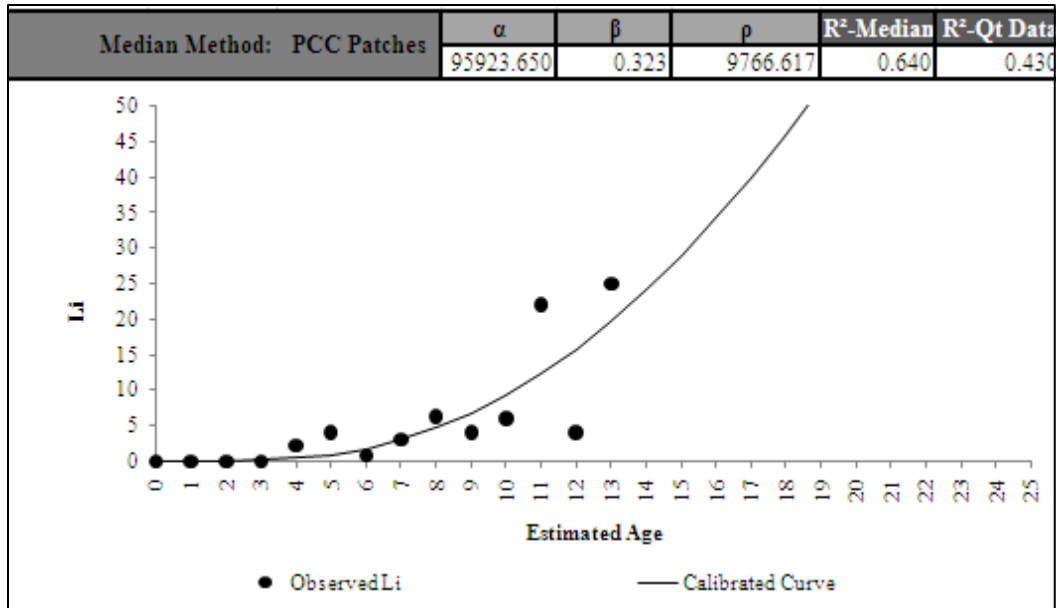


Figure C 20.11. Calibrated Performance Model for Beaumont District, Li Median Method (Unconstrained).

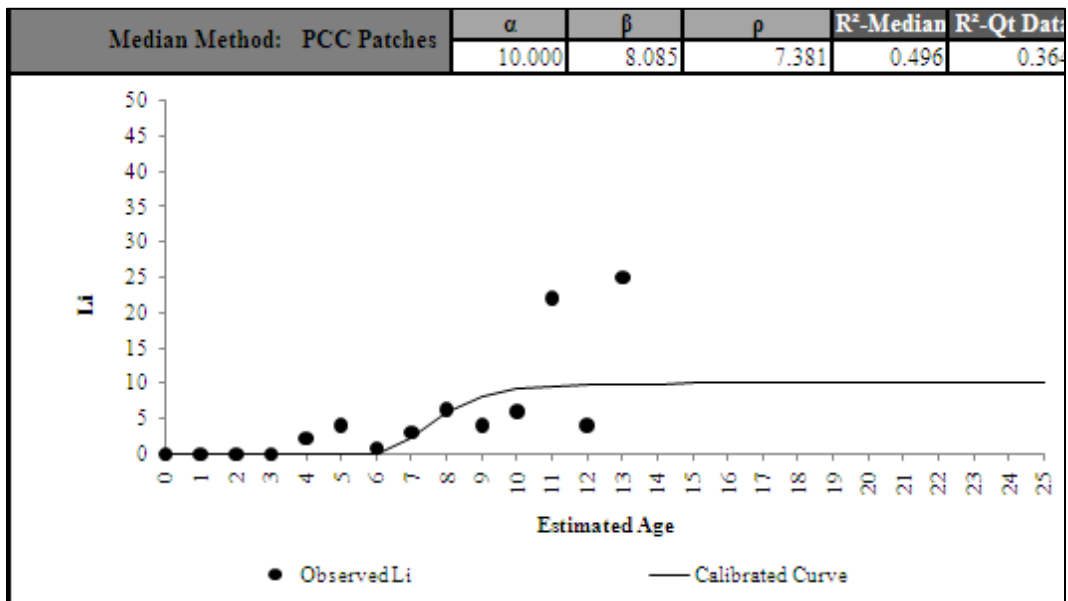


Figure C 20.12. Calibrated Performance Model for Beaumont District, Li Median Method (Constrained).

Pharr District 21-Spalled Cracks

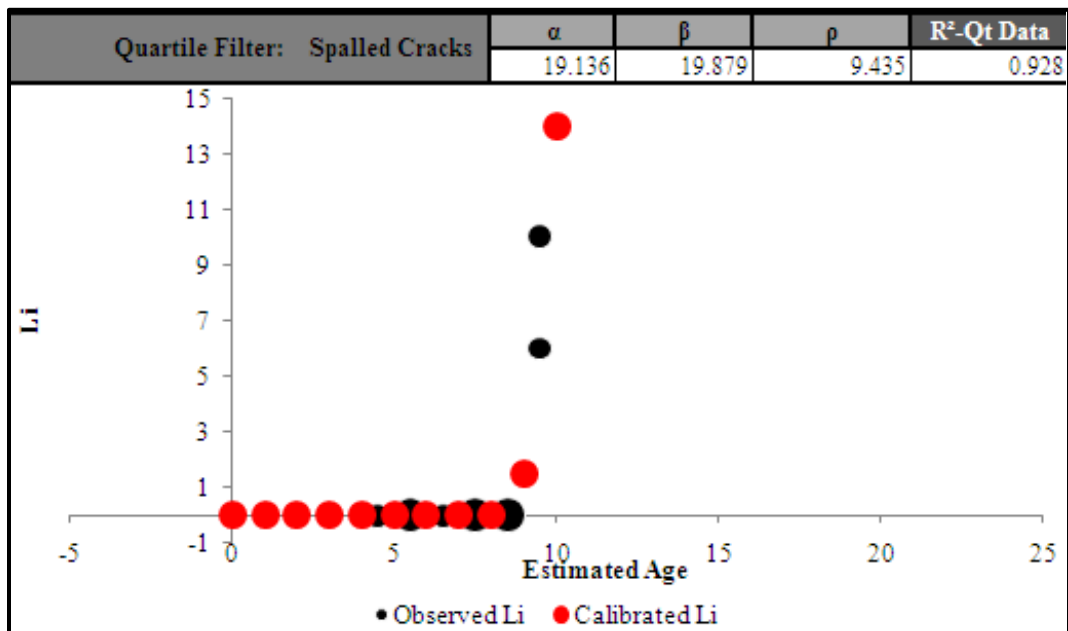


Figure C 22.1. Calibrated Performance Model for Pharr District, Li Quartile Method (Constrained).

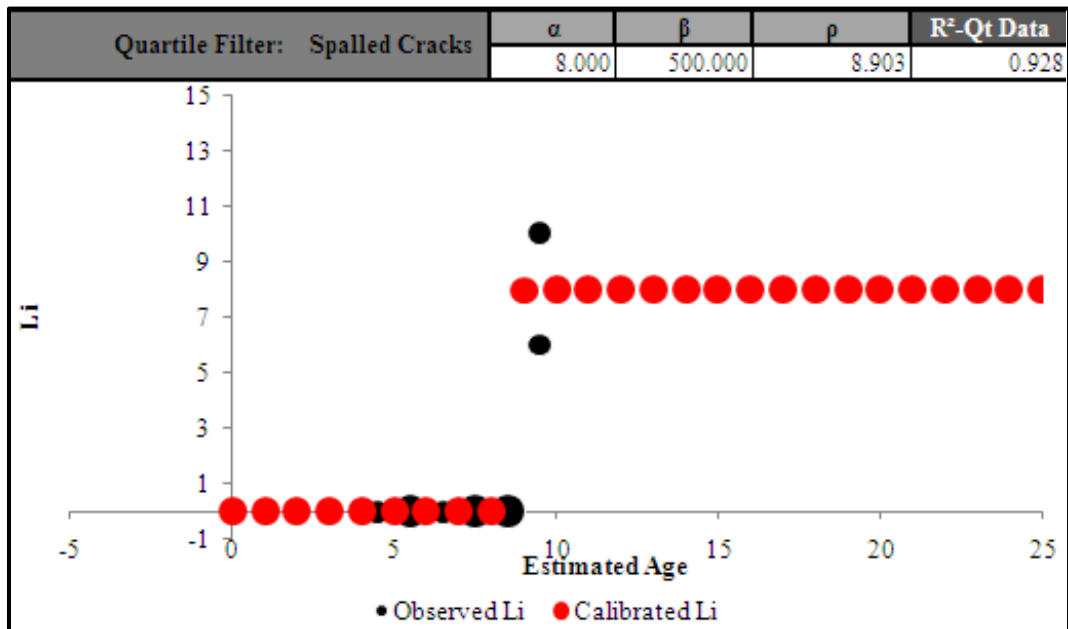


Figure C 21.2. Calibrated Performance Model for Pharr District, Li Quartile Method (Constrained).

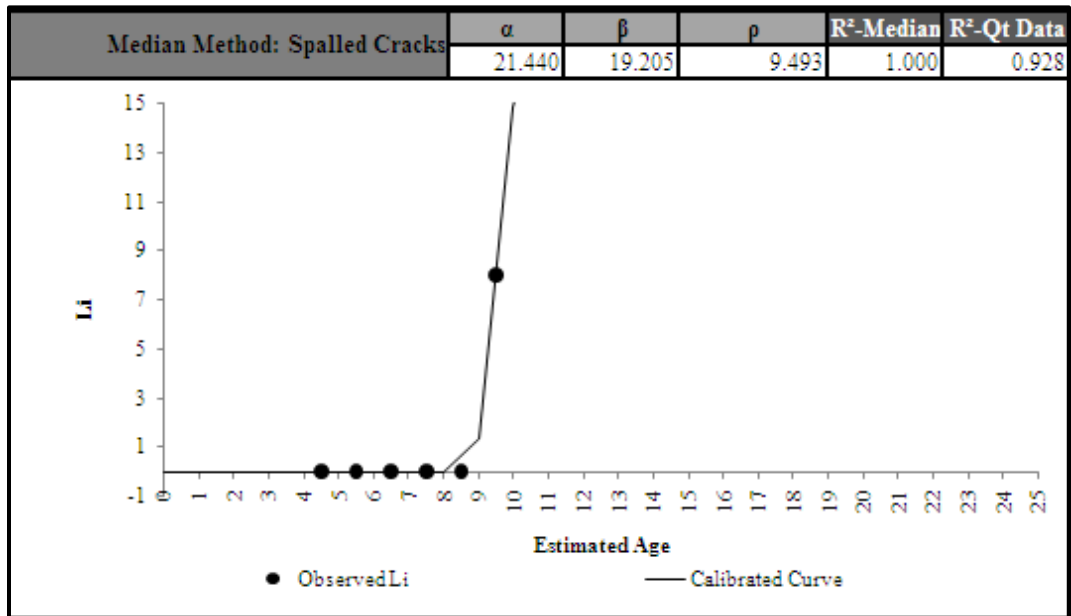


Figure C 21.3. Calibrated Performance Model for Pharr District, Li Median Method (Constrained).

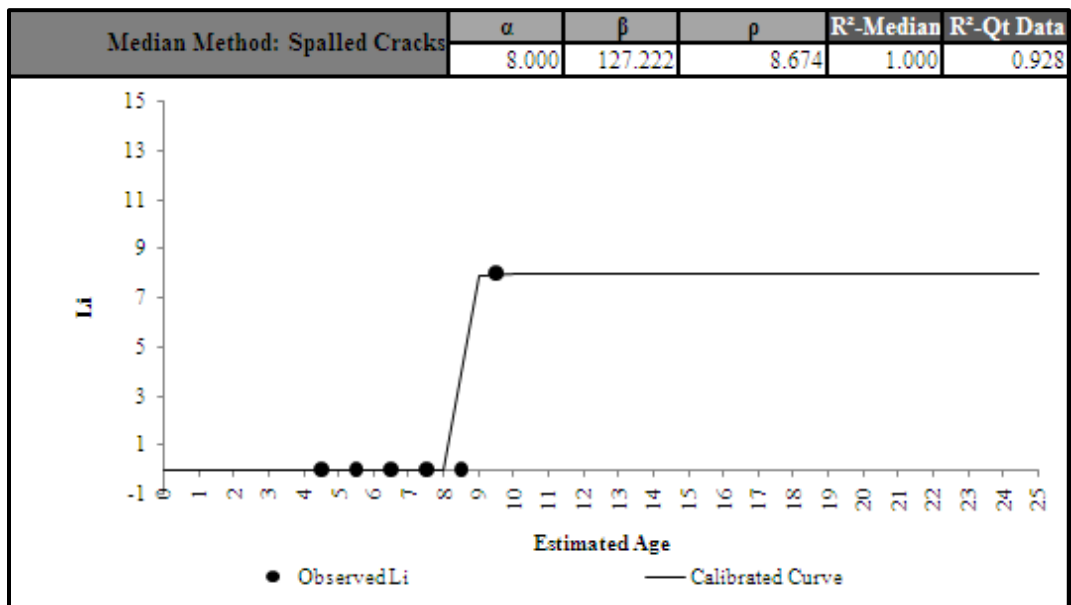


Figure C 21.4. Calibrated Performance Model for Pharr District, Li Median Method (Constrained).

Laredo District 22-Spalled Cracks

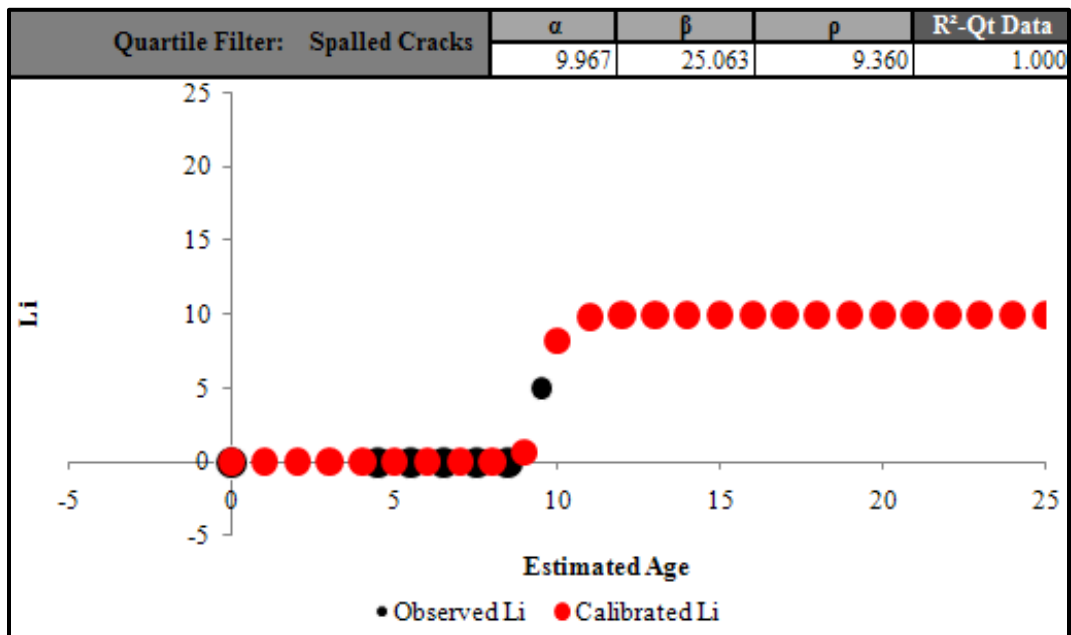


Figure C 22.1. Calibrated Performance Model for Laredo District, Li Quartile Method (Constrained).

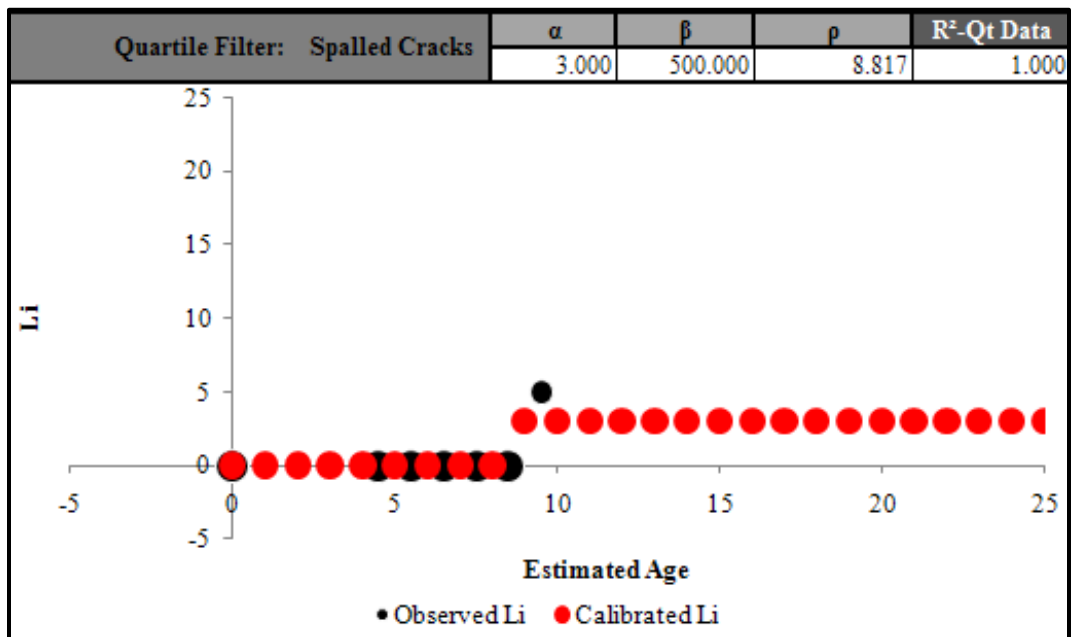


Figure C 22.2. Calibrated Performance Model for Laredo District, Li Quartile Method (Constrained).

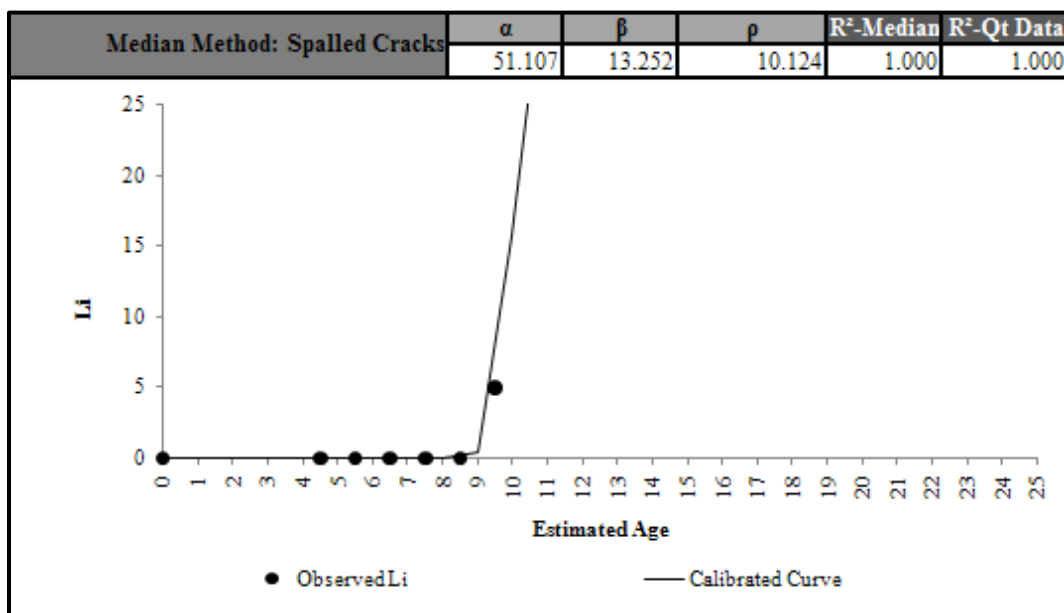


Figure C 22.3. Calibrated Performance Model for Laredo District, Li Median Method (Constrained).

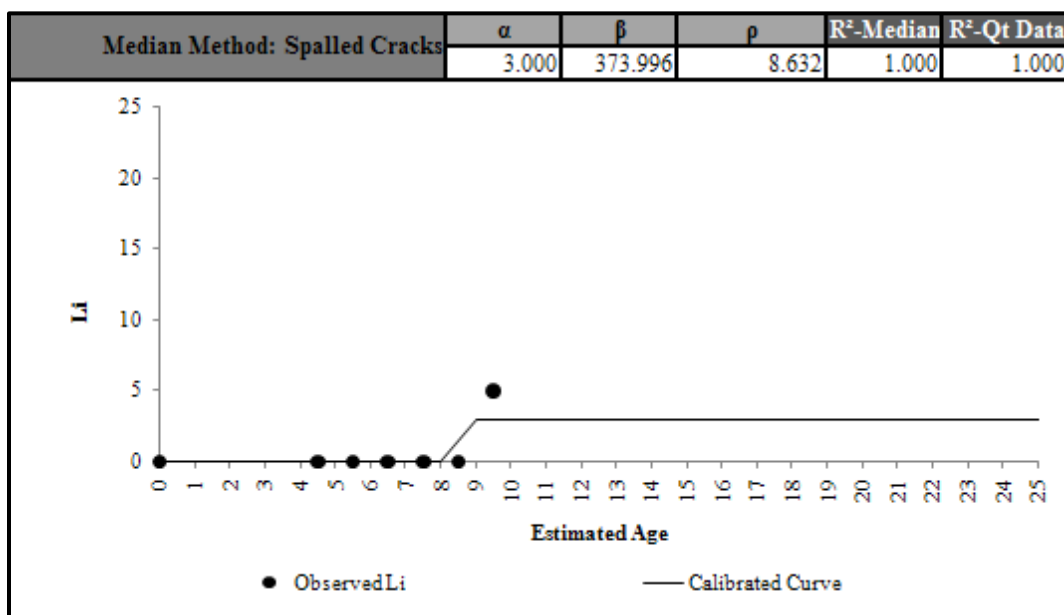


Figure C 22.4. Calibrated Performance Model for Laredo District, Li Median Method (Constrained).

El Paso District 24-Spalled Cracks

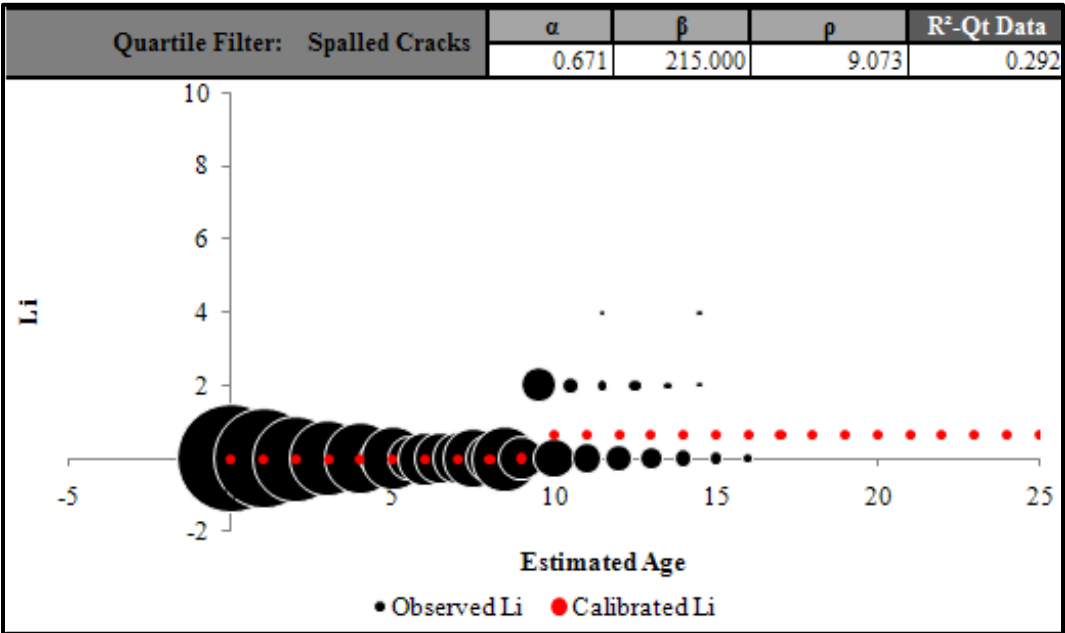


Figure C 24.1. Calibrated Performance Model for El Paso District, Li Quartile Method (Constrained).

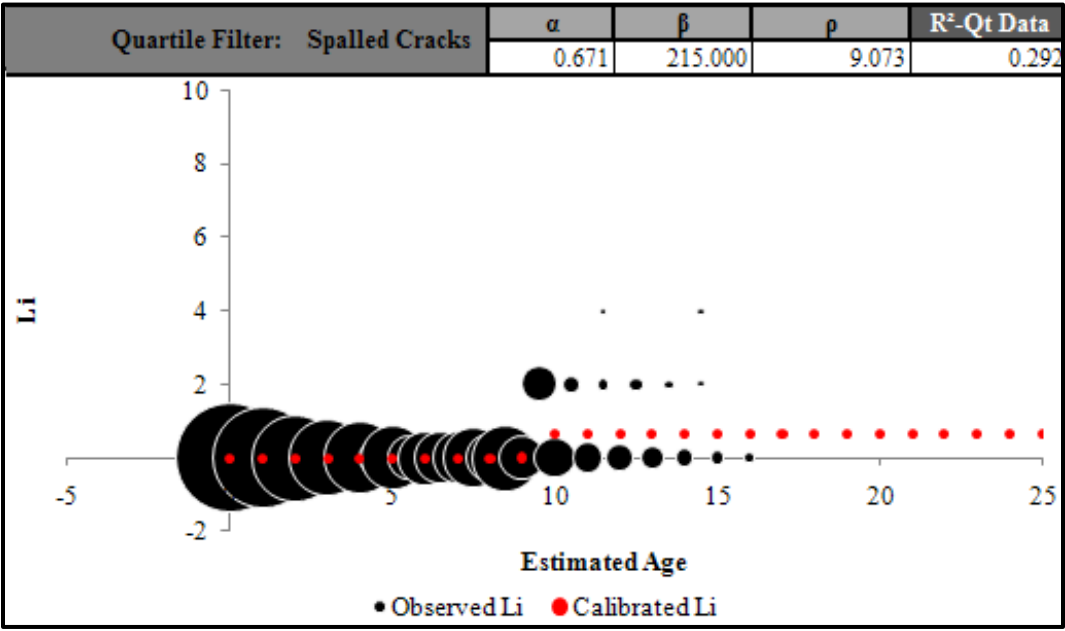


Figure C 24.2. Calibrated Performance Model for El Paso District, Li Quartile Method (Constrained).

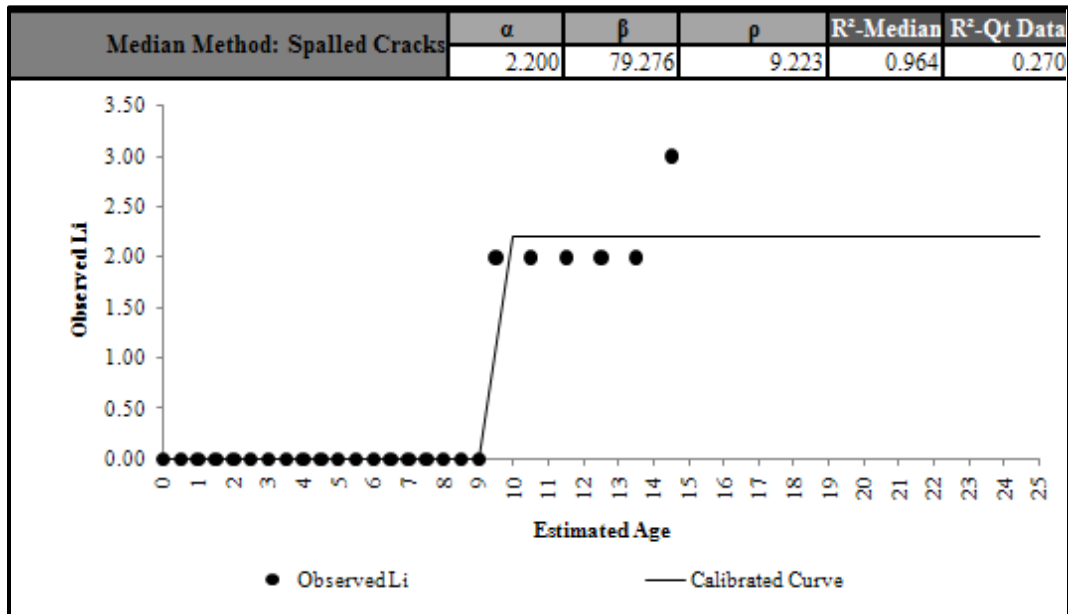


Figure C 24.3. Calibrated Performance Model for El Paso District, Li Median Method (Unconstrained).

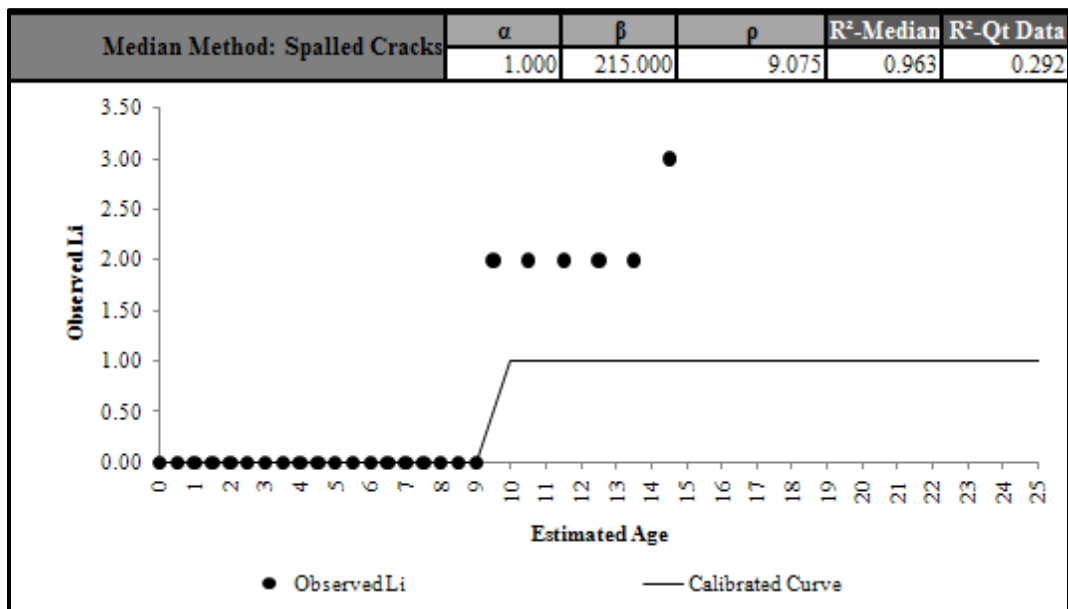


Figure C 24.4. Calibrated Performance Model for El Paso District, Li Median Method (Constrained).

El Paso District 24-Punchouts

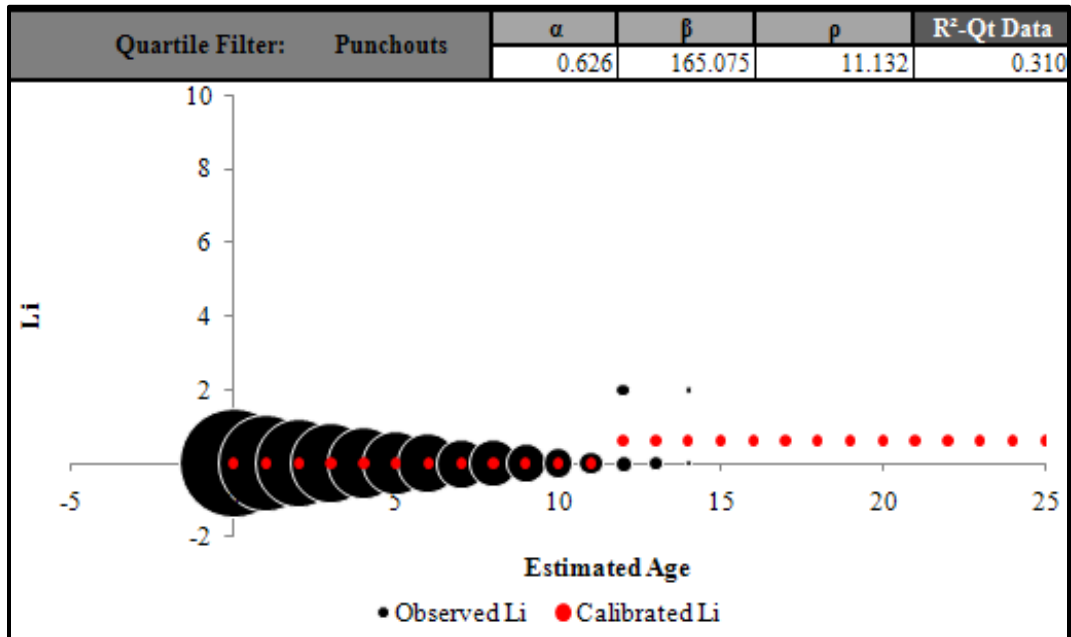


Figure C 24.5. Calibrated Performance Model for El Paso District, Li Quartile Method (Unconstrained).

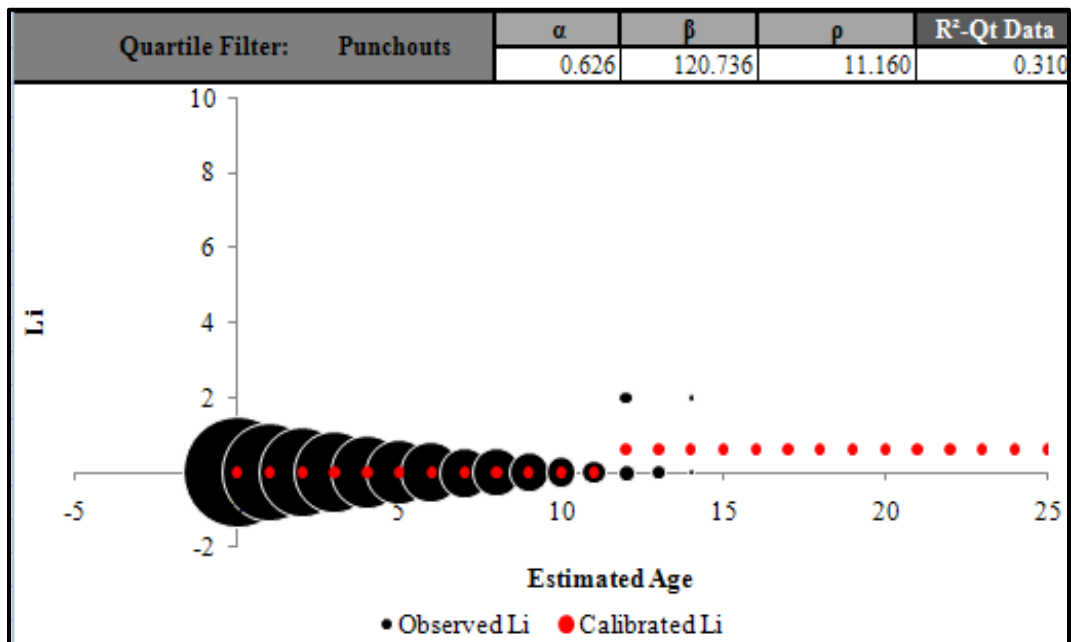


Figure C 24.6. Calibrated Performance Model for El Paso District, Li Quartile Method (Constrained).

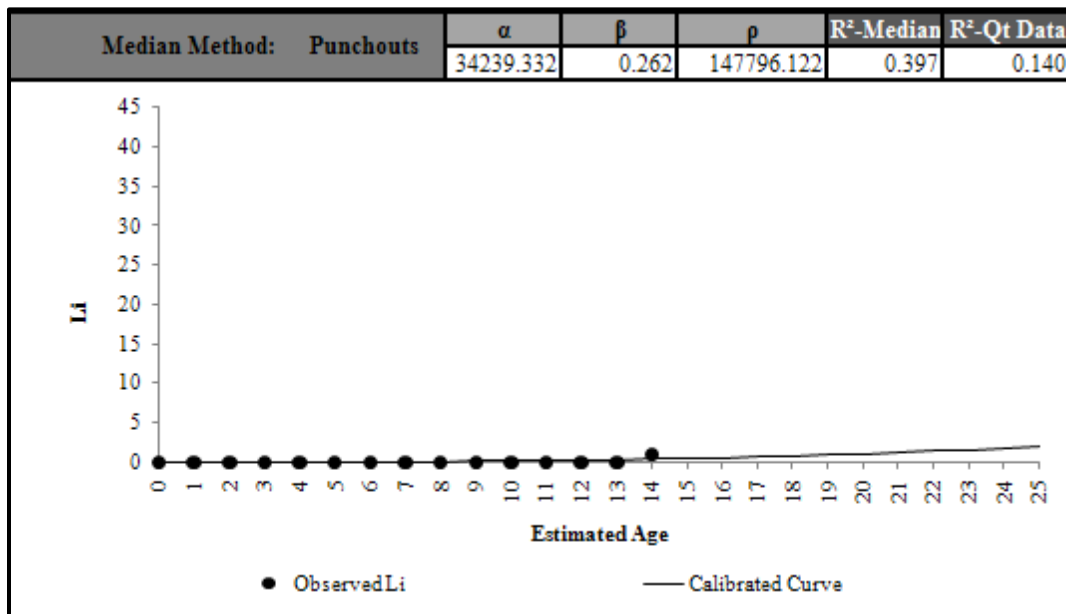


Figure C 24.7. Calibrated Performance Model for El Paso District, Li Median Method (Unconstrained).

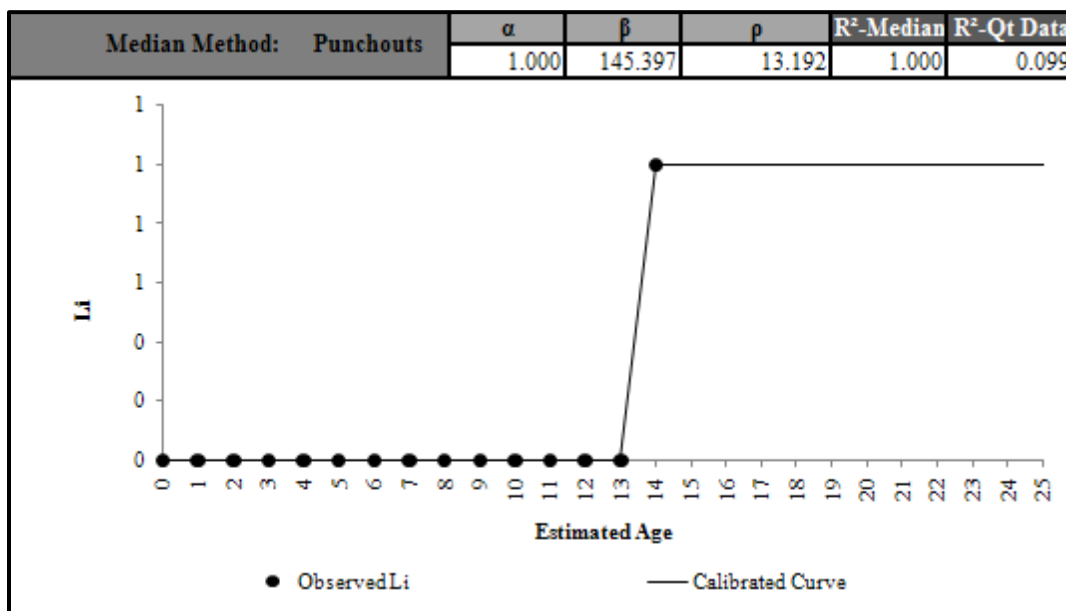


Figure C 24.8. Calibrated Performance Model for El Paso District, Li Median Method (Constrained).

El Paso District 24-PCC Patches

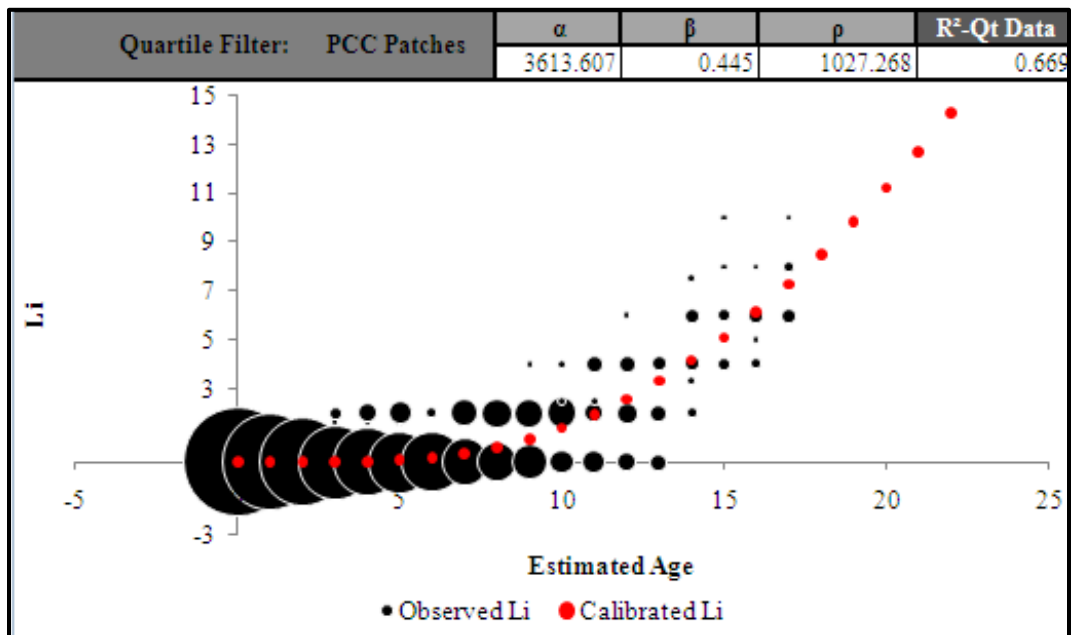


Figure C 24.9. Calibrated Performance Model for El Paso District, Li Quartile Method (Unconstrained).

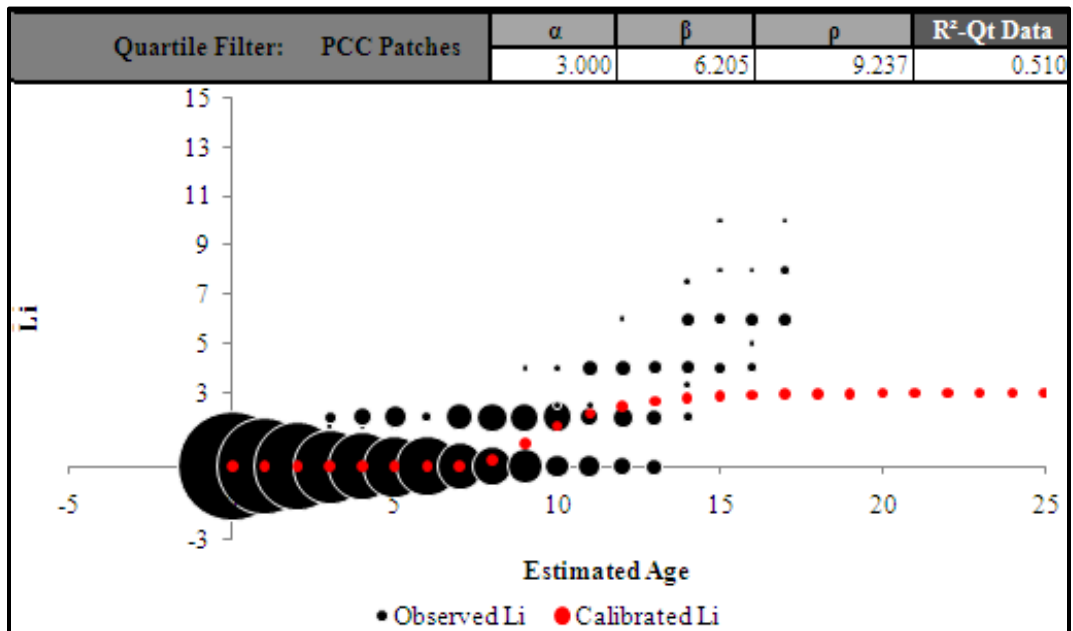


Figure C 24.10. Calibrated Performance Model for El Paso District, Li Quartile Method (Constrained).

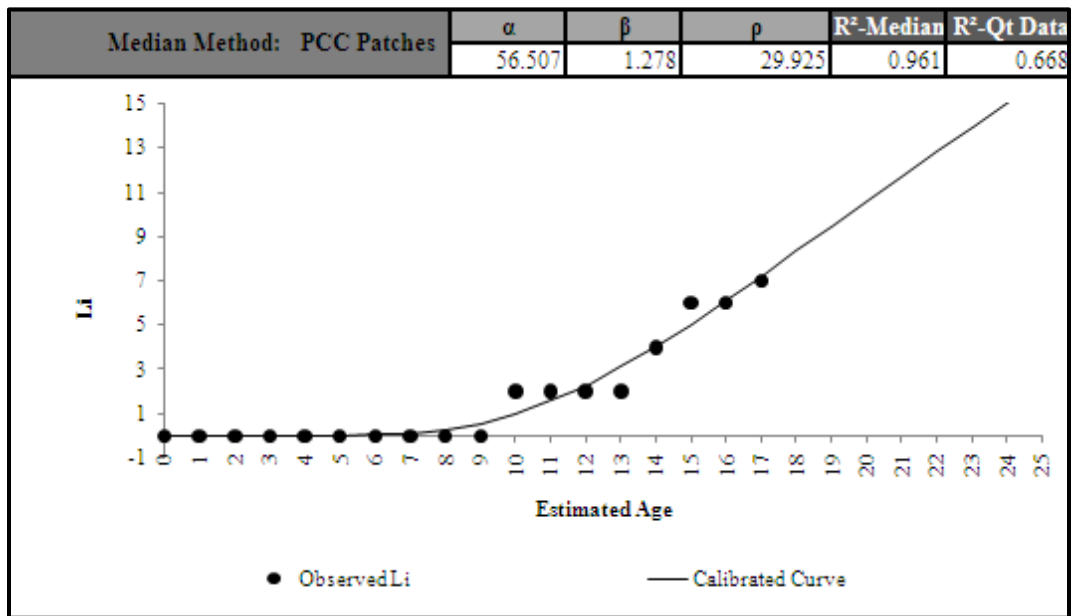


Figure C 24.11. Calibrated Performance Model for El Paso District, Li Median Method (Unconstrained).

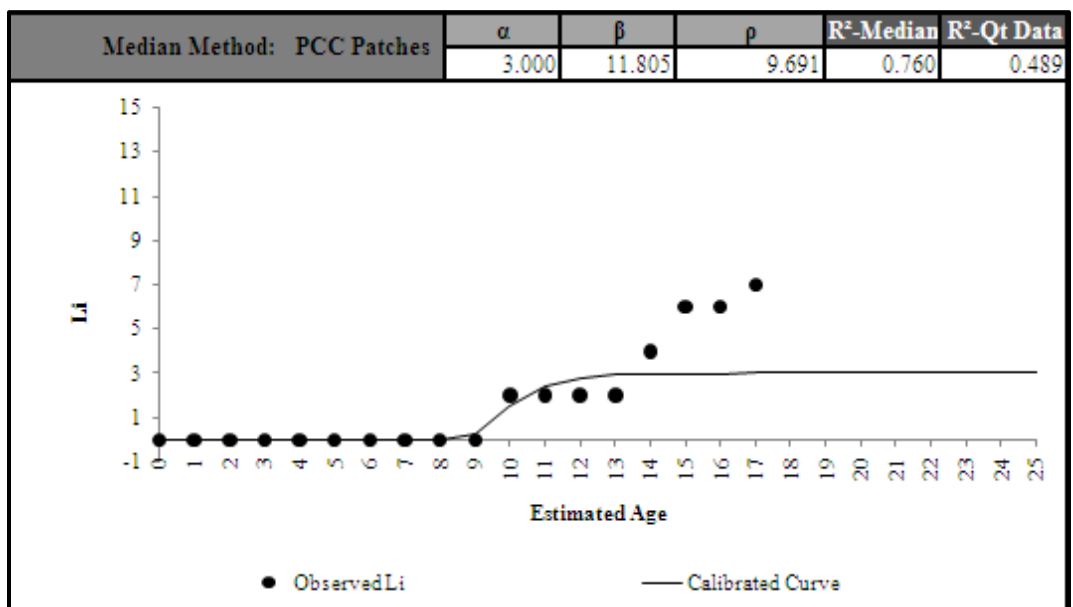


Figure C 24.12. Calibrated Performance Model for El Paso District, Li Median Method (Constrained).

Childress District 25-Spalled Cracks

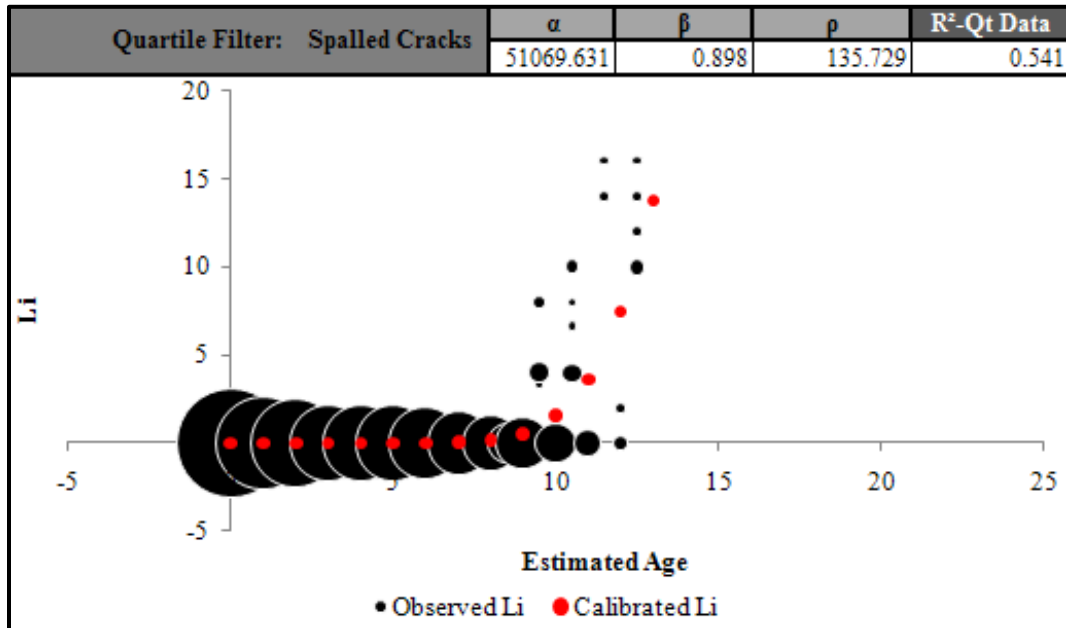


Figure C 25.1. Calibrated Performance Model for Childress District, Li Quartile Method (Unconstrained).

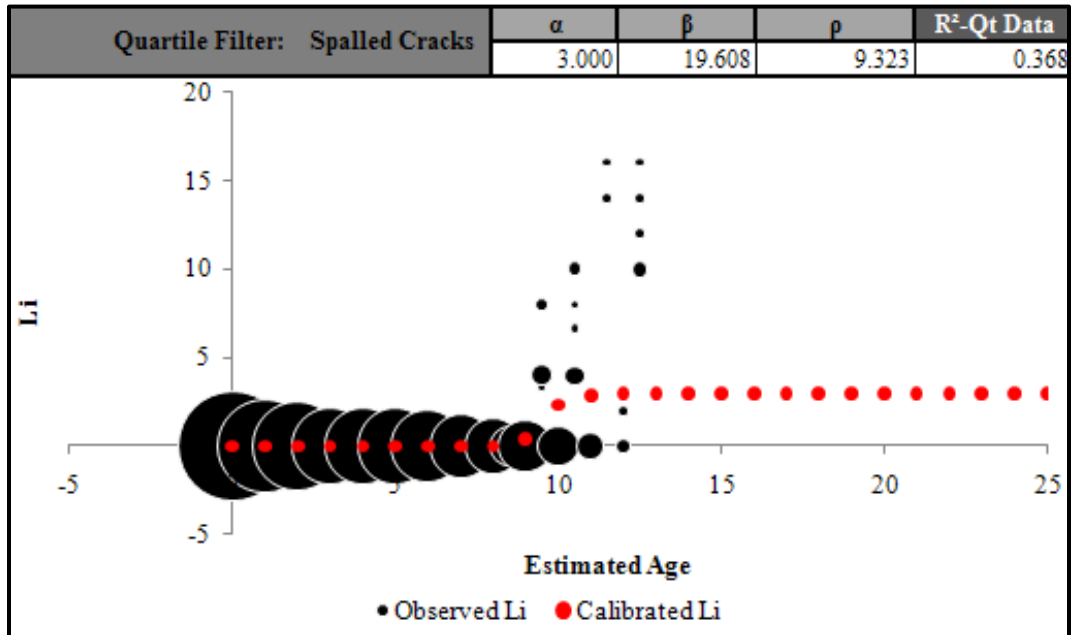


Figure C 25.2. Calibrated Performance Model for Childress District, Li Quartile Method (Constrained).

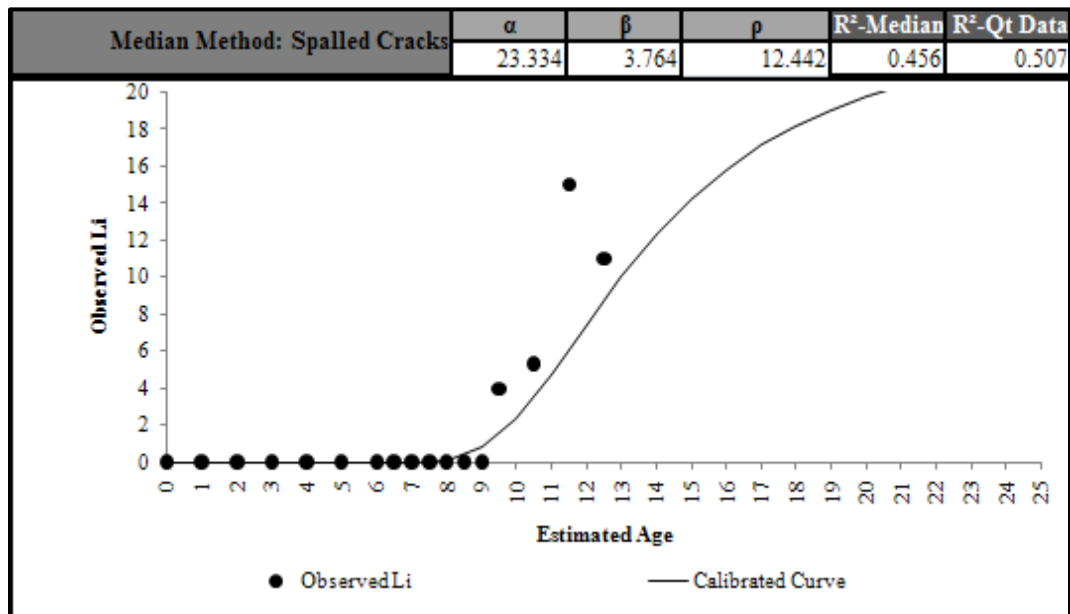


Figure C 25.3. Calibrated Performance Model for Childress District, Li Median Method (Unconstrained).

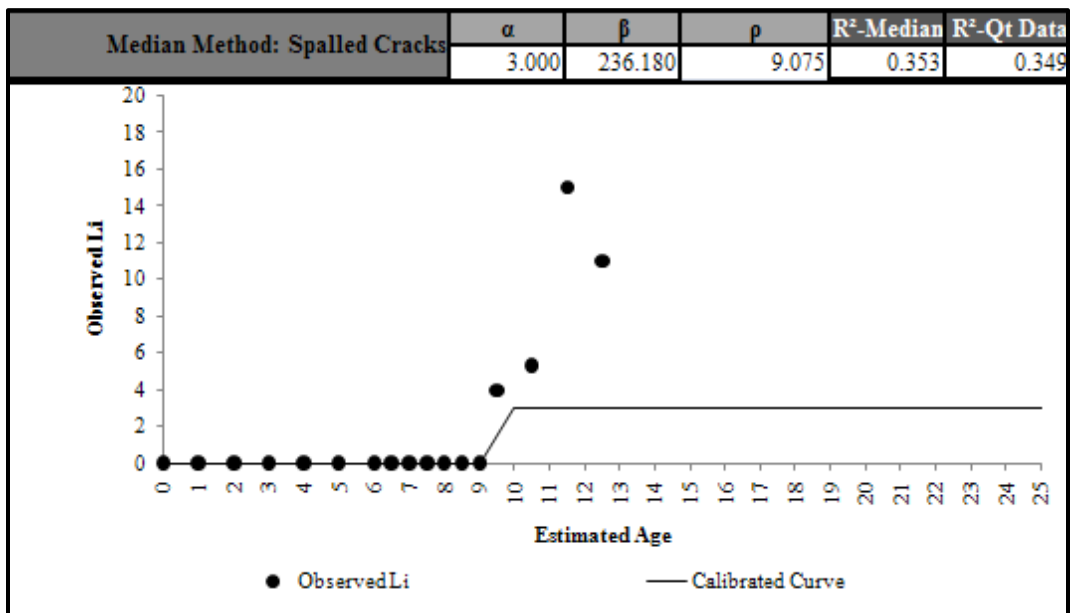


Figure C 25.4. Calibrated Performance Model for Childress District, Li Median Method (Constrained).

Childress District 25-Punchouts

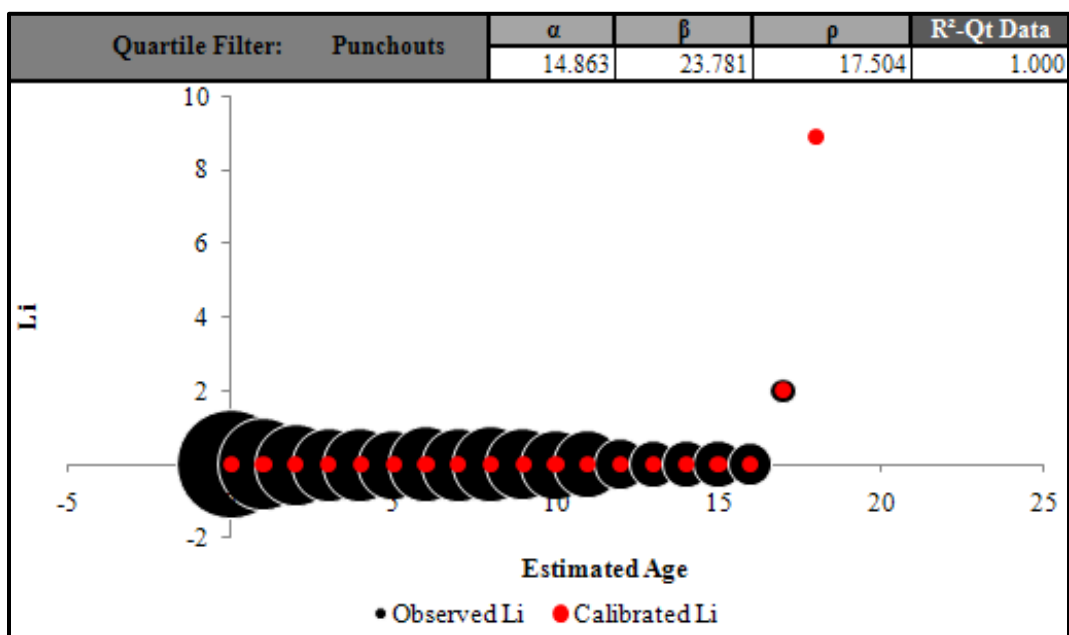


Figure C 25.5. Calibrated Performance Model for Childress District, Li Quartile Method (Unconstrained).

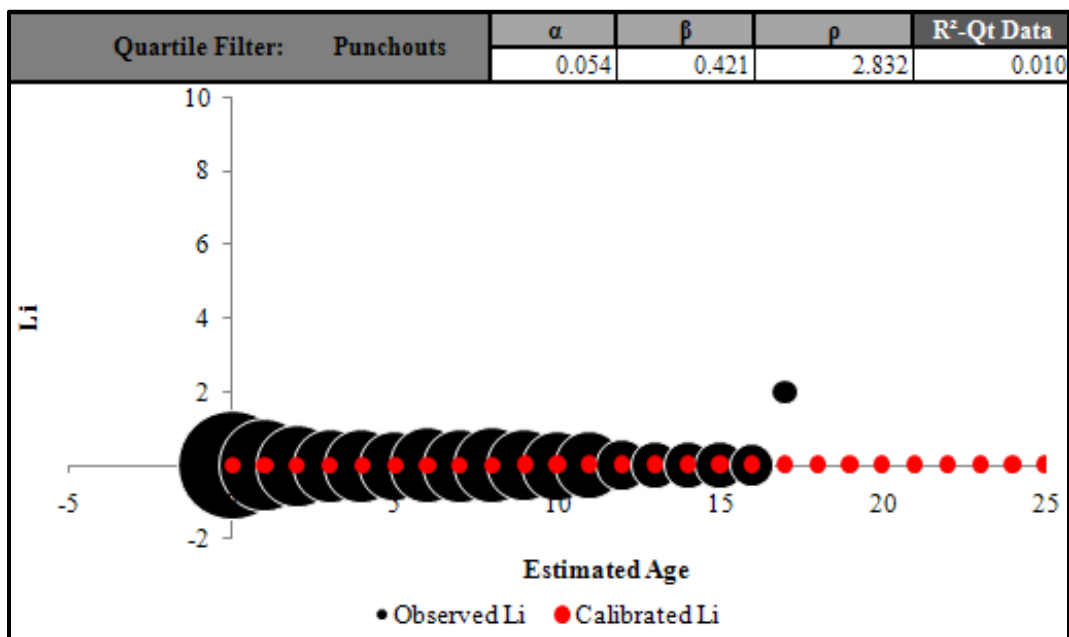


Figure C 25.6. Calibrated Performance Model for Childress District, Li Quartile Method (Constrained).

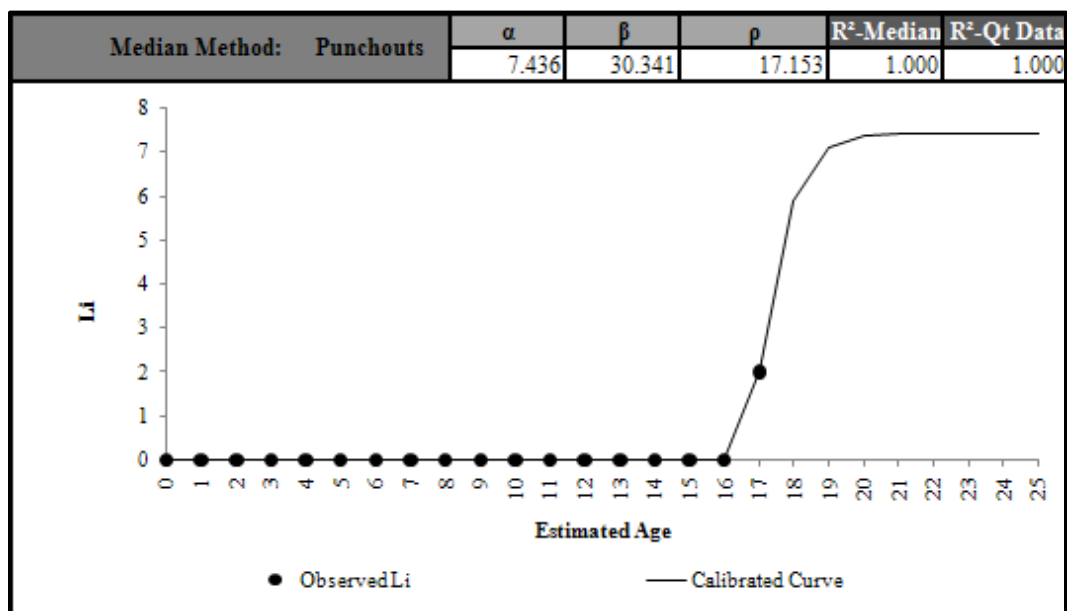


Figure C 25.7. Calibrated Performance Model for Childress District, Li Median Method (Unconstrained).

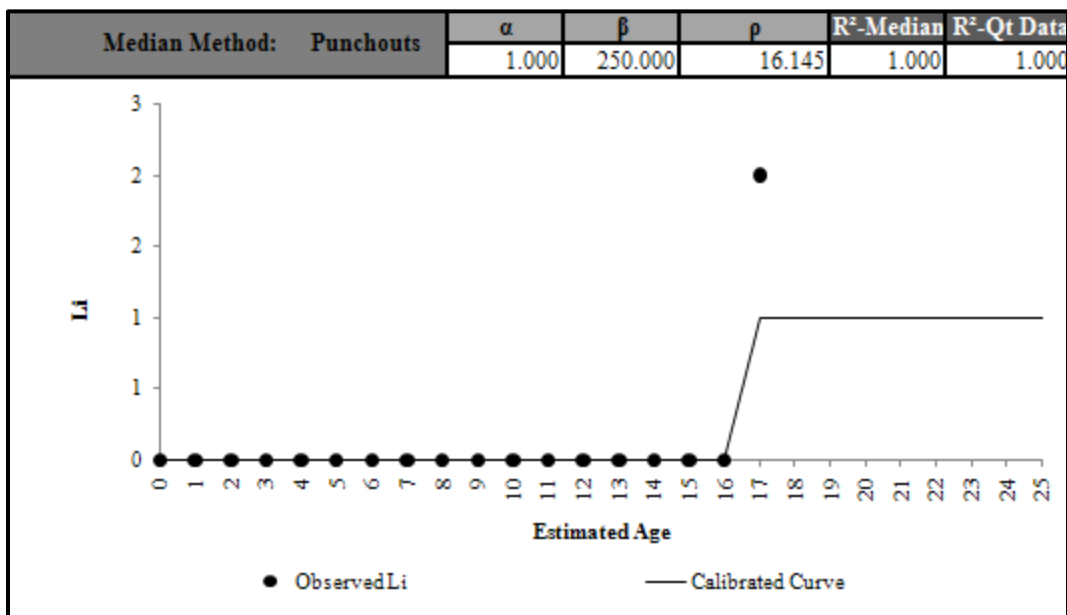


Figure C 25.8. Calibrated Performance Model for Childress District, Li Median Method (Constrained).

Childress District 25-PCC Patches

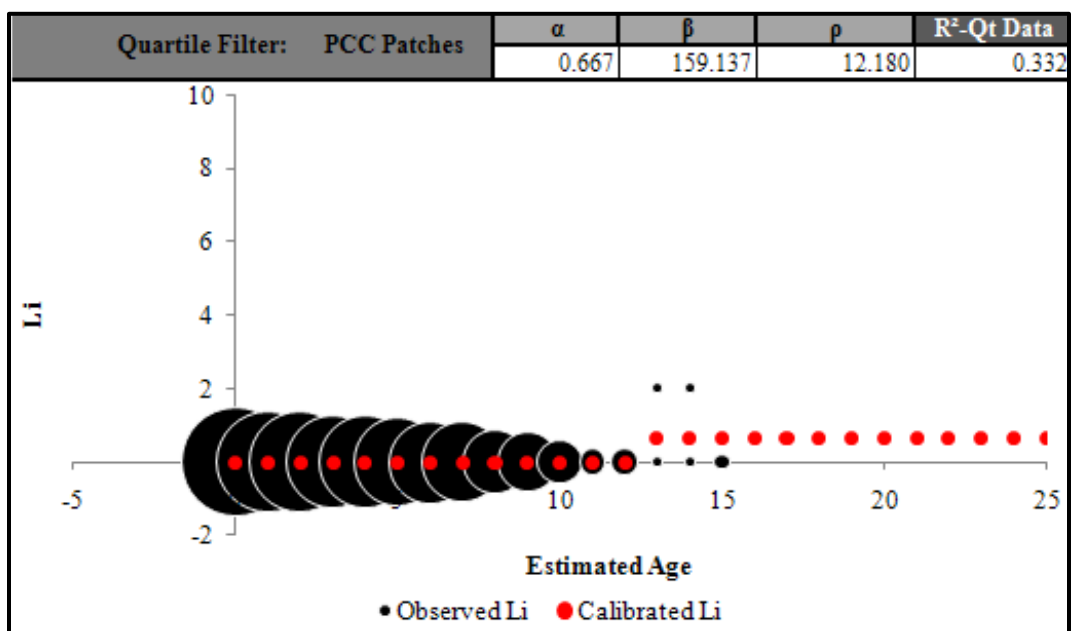


Figure C 25.9. Calibrated Performance Model for Childress District, Li Quartile Method (Unconstrained).

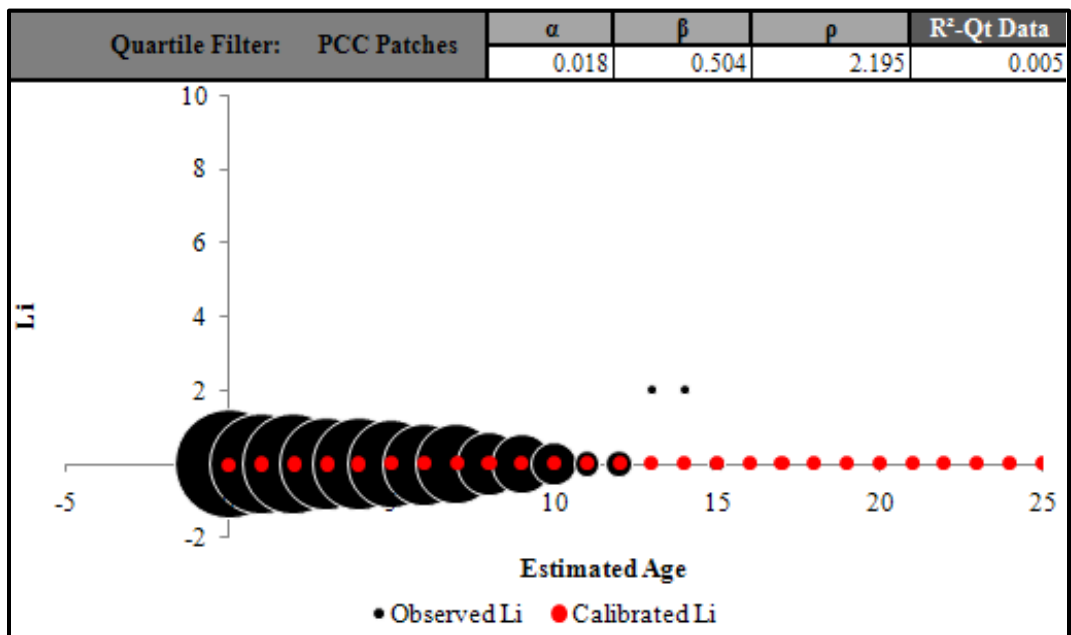


Figure C 25.10. Calibrated Performance Model for Childress District, Li Quartile Method (Constrained).

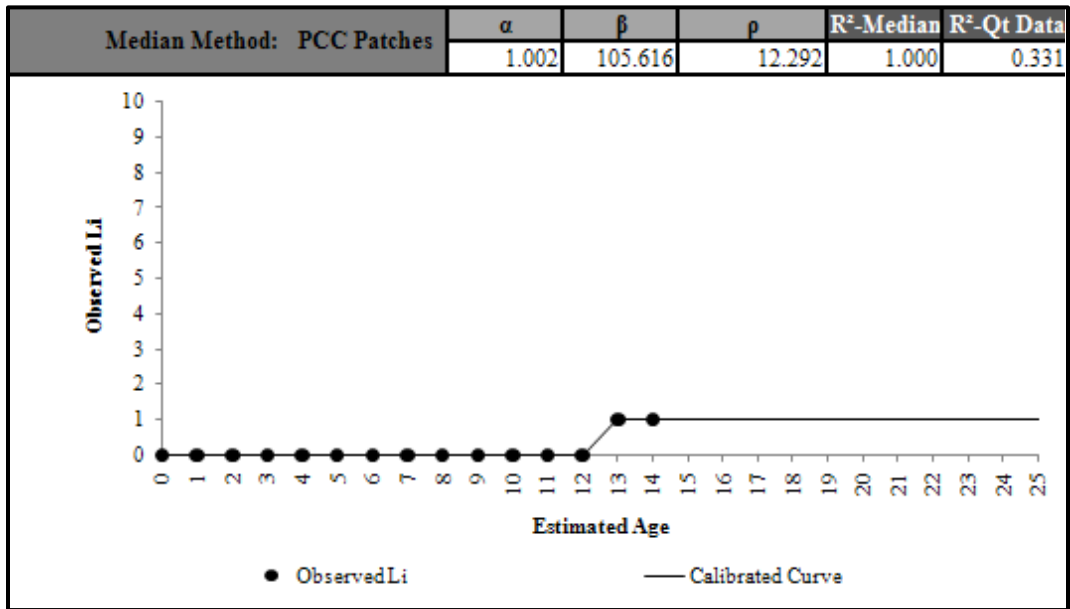


Figure C 25.11. Calibrated Performance Model for Childress District, Li Median Method (Unconstrained).

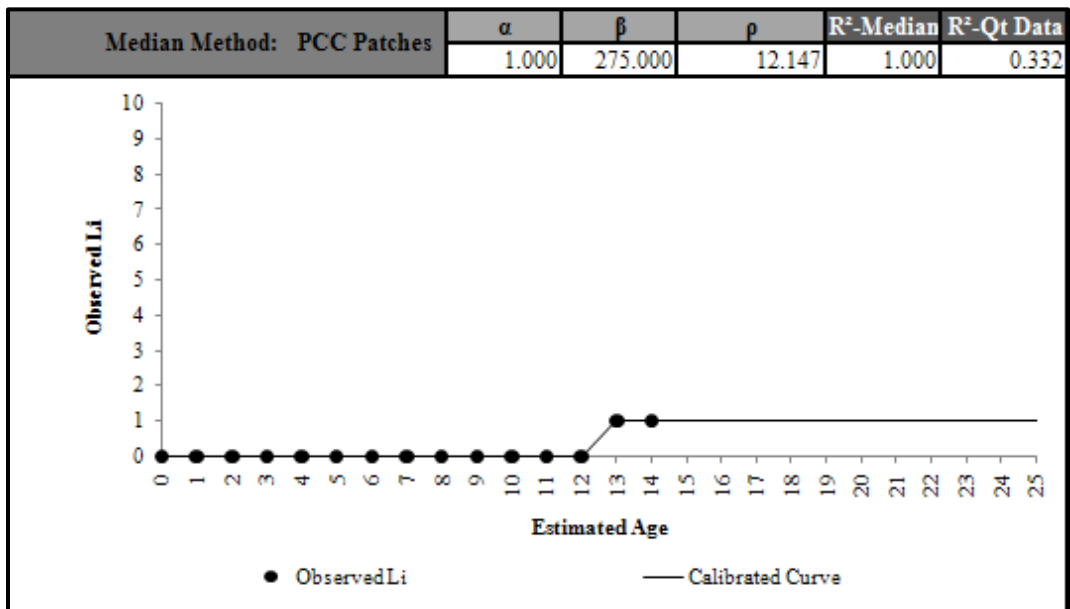


Figure C 25.12. Calibrated Performance Model for Childress District, Li Median Method (Constrained).

Statewide-Spalled Cracks

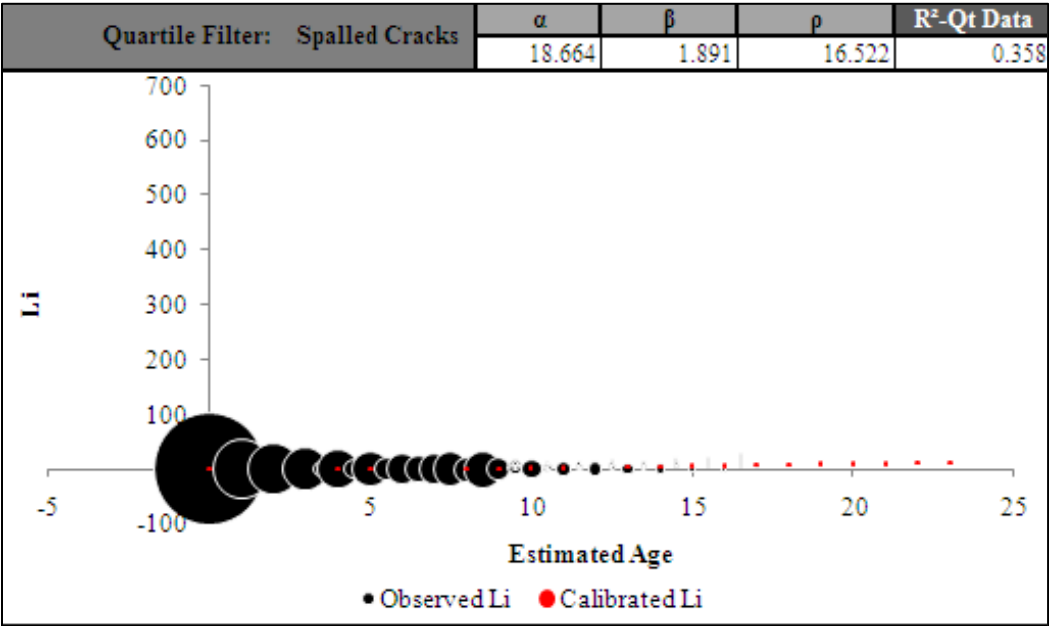


Figure C 26.1. Calibrated Performance Model, Statewide, Li Quartile Method (Unconstrained).

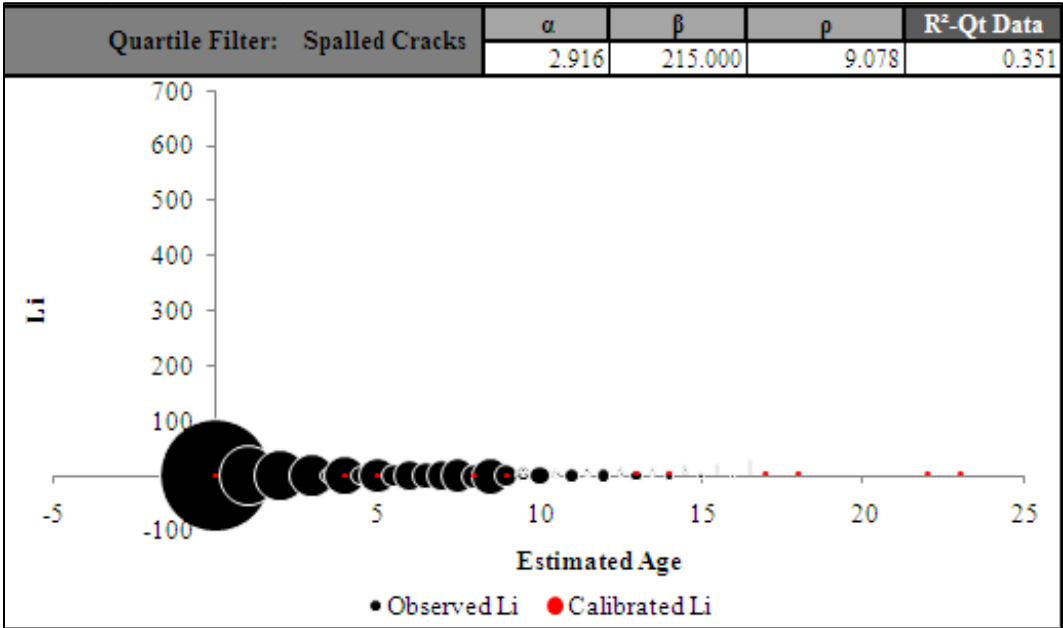


Figure C 26.2. Calibrated Performance Model, Statewide, Li Quartile Method (Constrained).

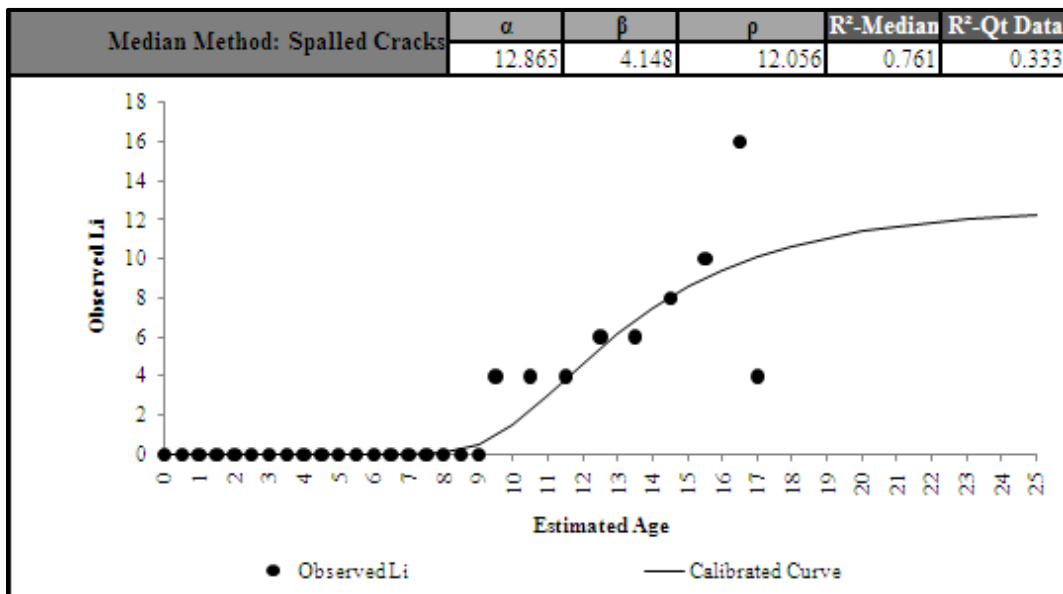


Figure C 26.3. Calibrated Performance Model, Statewide, Li Median Method (Unconstrained).

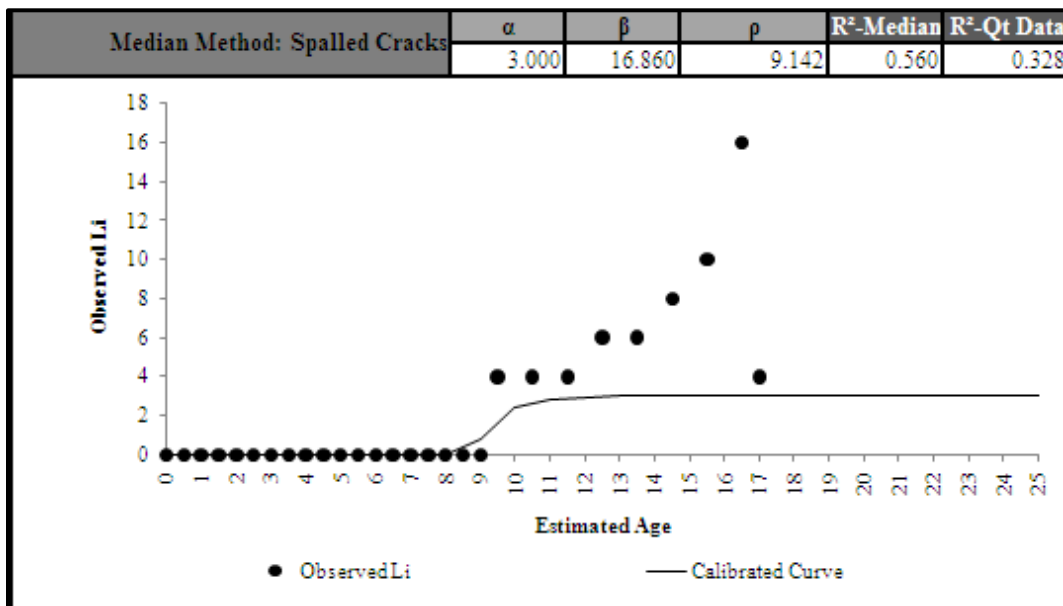


Figure C 26.4. Calibrated Performance Model, Statewide, Li Median Method (Constrained).

Statewide-Punchouts

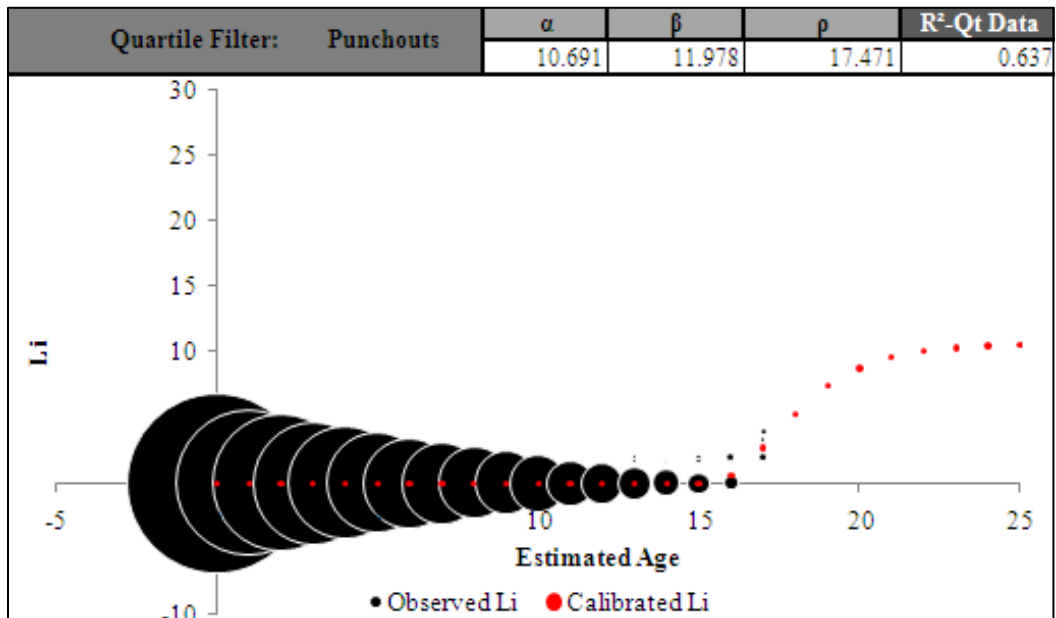


Figure C 26.5. Calibrated Performance Model, Statewide, Li Quartile Method (Unconstrained).

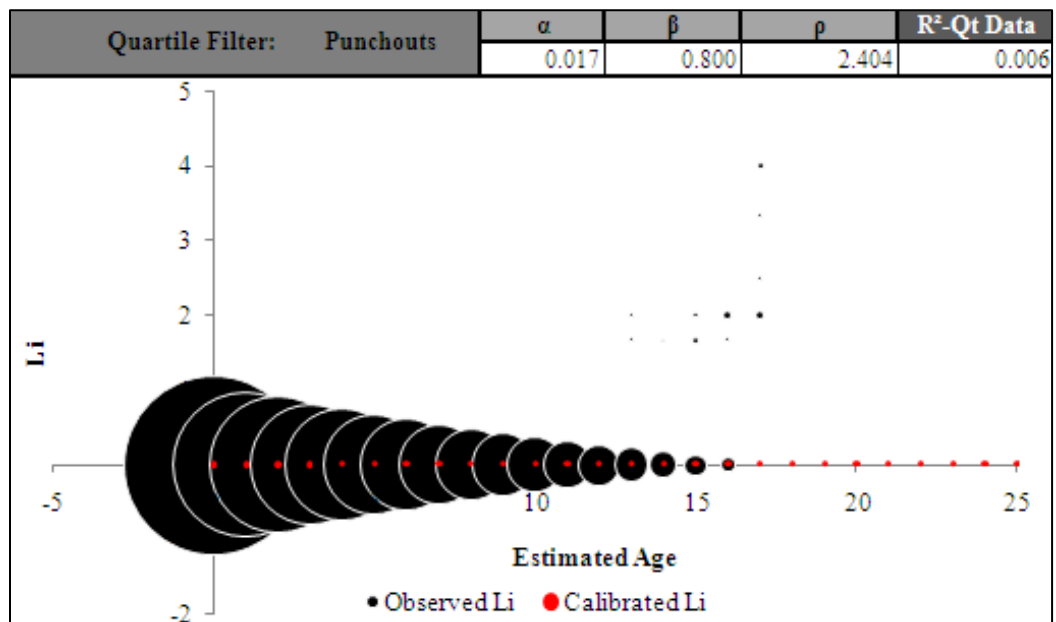


Figure C 26.6. Calibrated Performance Model, Statewide, Li Quartile Method (Constrained).

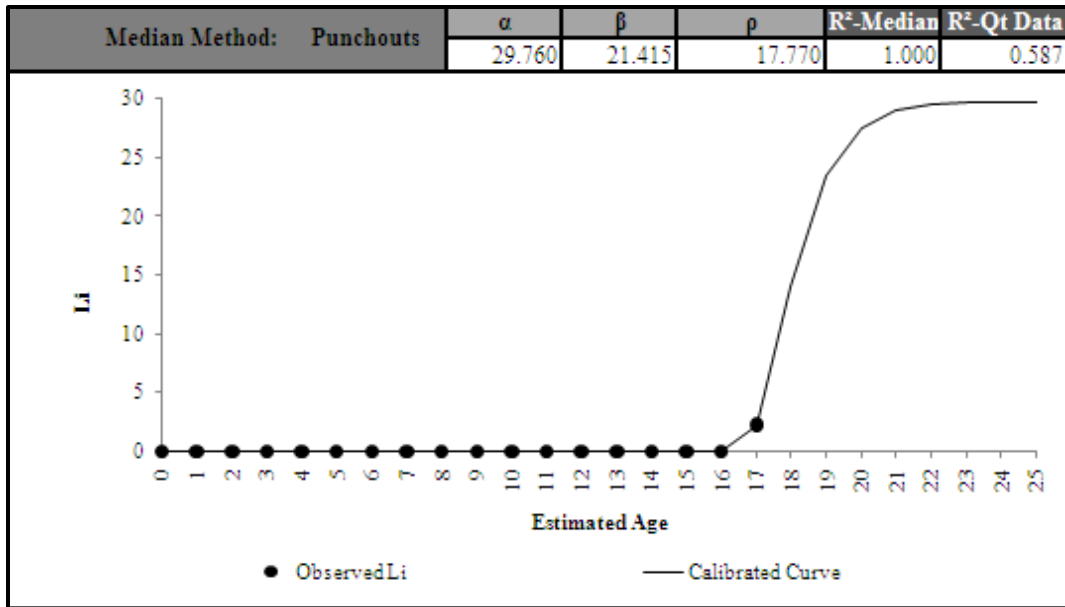


Figure C 26.7. Calibrated Performance Model, Statewide, Li Median Method (Unconstrained).

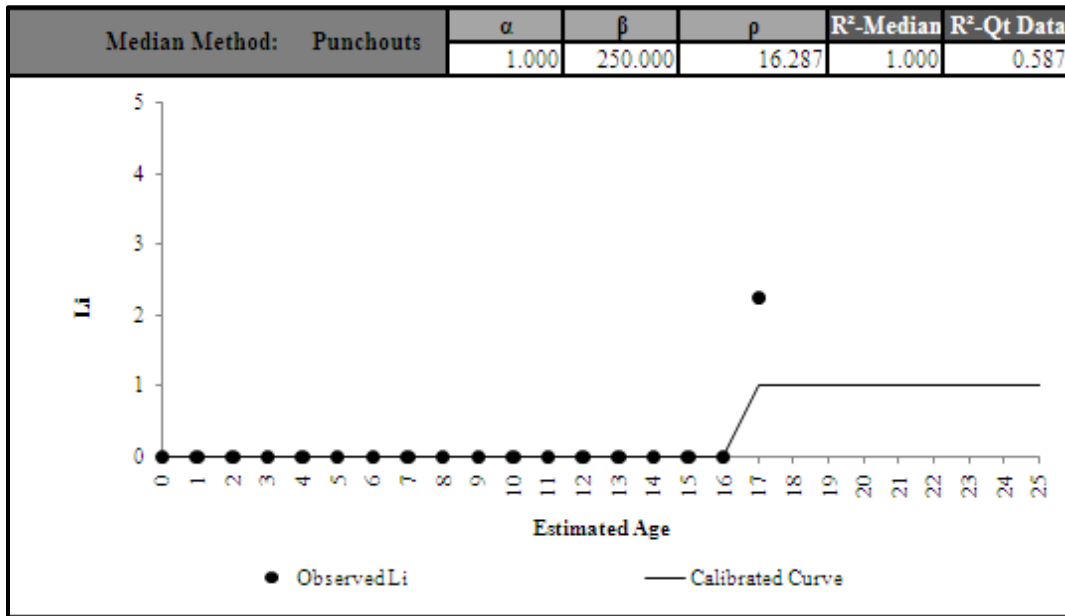


Figure C 26.8. Calibrated Performance Model, Statewide, Li Median Method (Constrained).

Statewide-ACP Patches

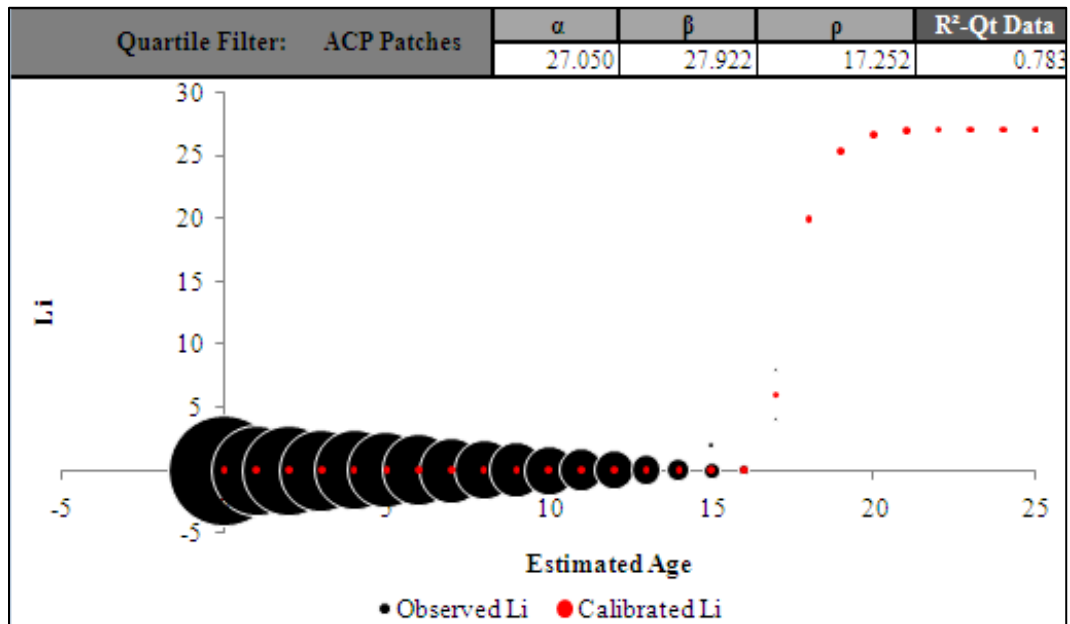


Figure C 26.9. Calibrated Performance Model, Statewide, Li Quartile Method (Unconstrained).

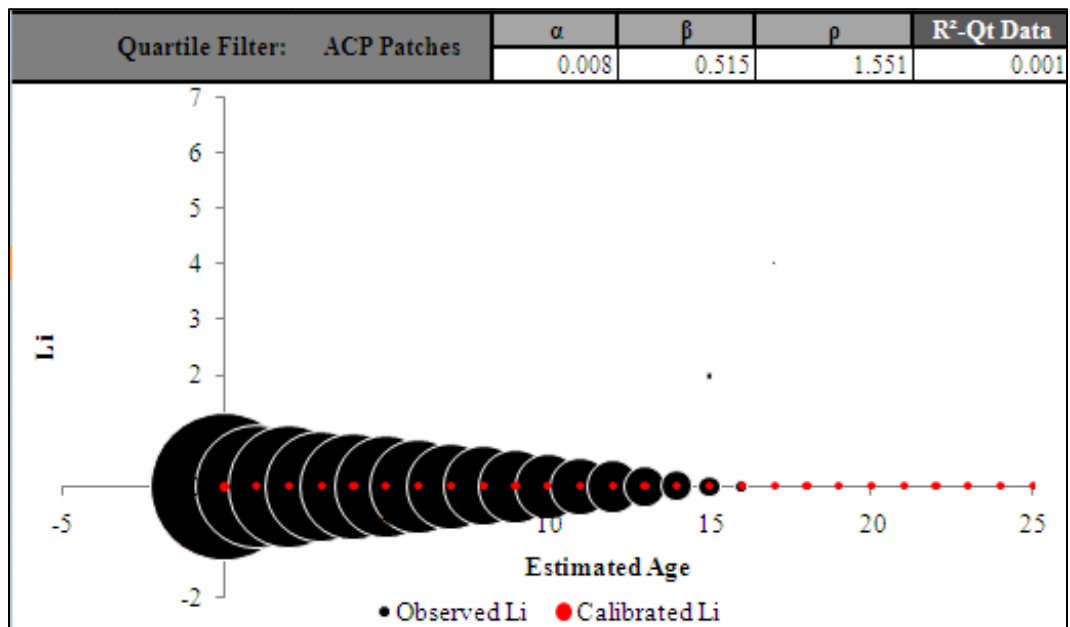


Figure C 26.10. Calibrated Performance Model, Statewide, Li Quartile Method (Constrained).

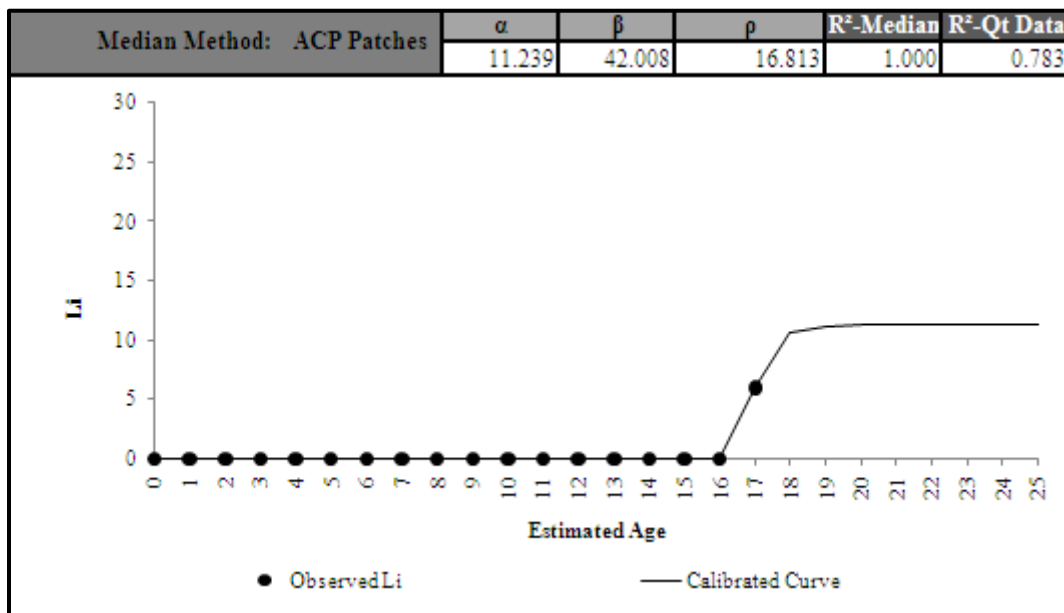


Figure C 26.11. Calibrated Performance Model, Statewide, Li Median Method (Unconstrained).

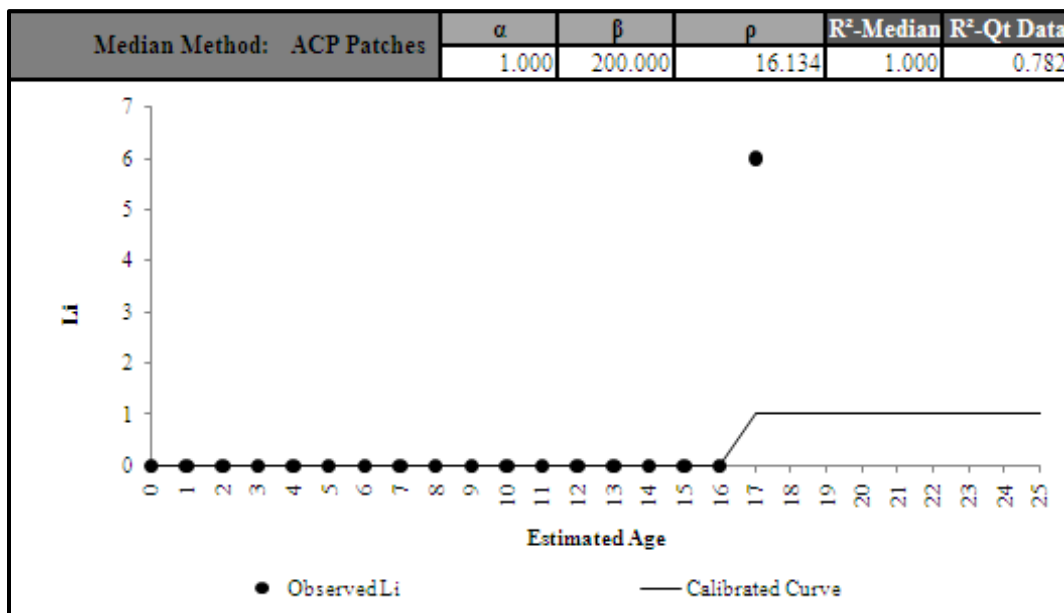


Figure C 26.12. Calibrated Performance Model, Statewide, Li Median Method (Constrained).

Statewide-PCC Patches

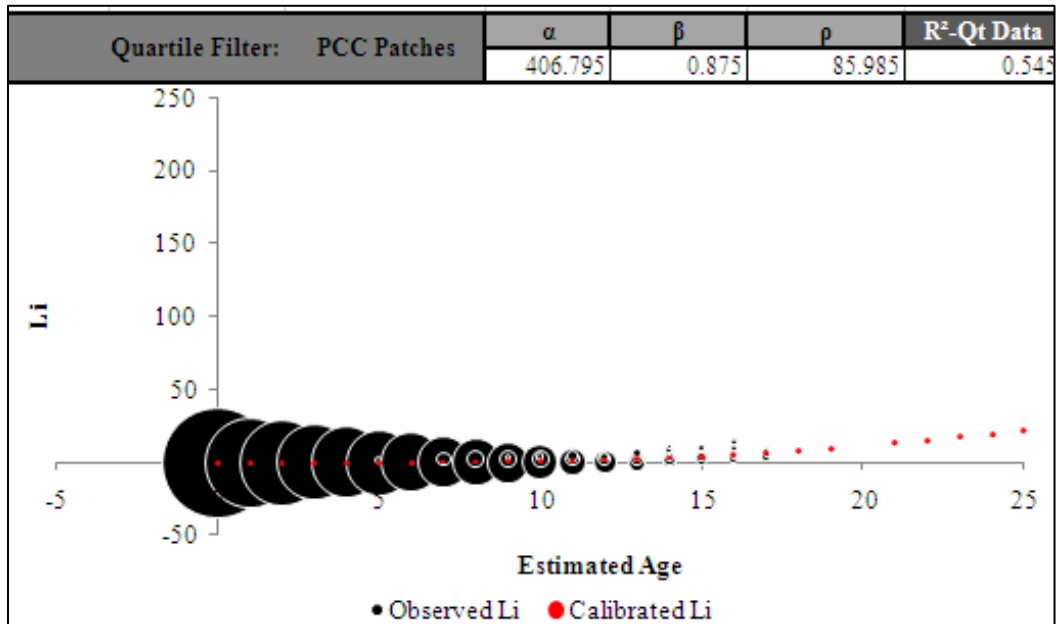


Figure C 26.13. Calibrated Performance Model, Statewide, Li Quartile Method (Unconstrained).

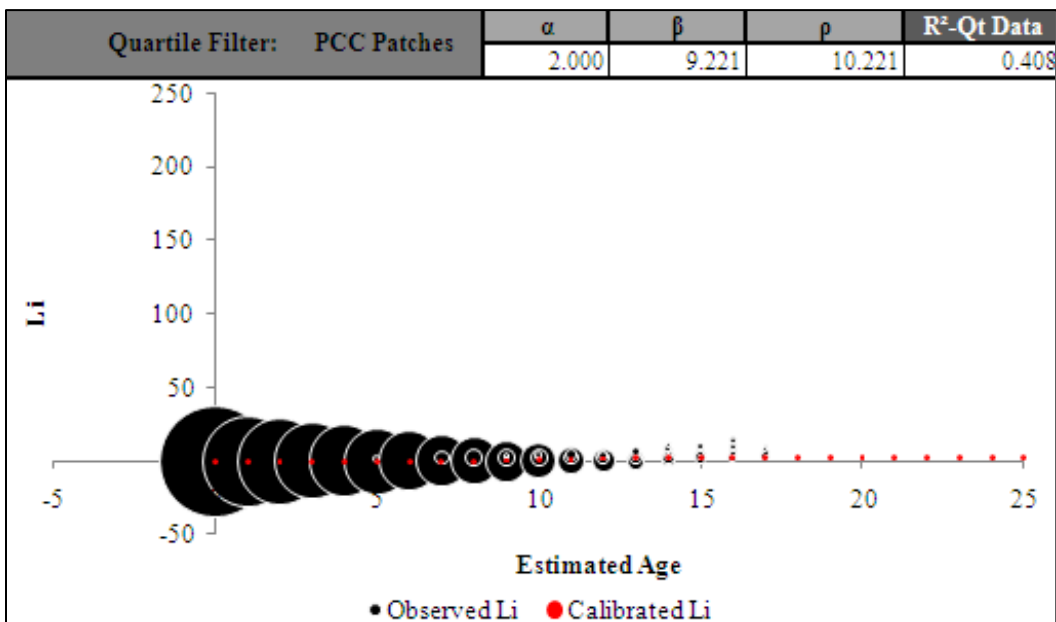


Figure C 26.14. Calibrated Performance Model, Statewide, Li Quartile Method (Constrained).

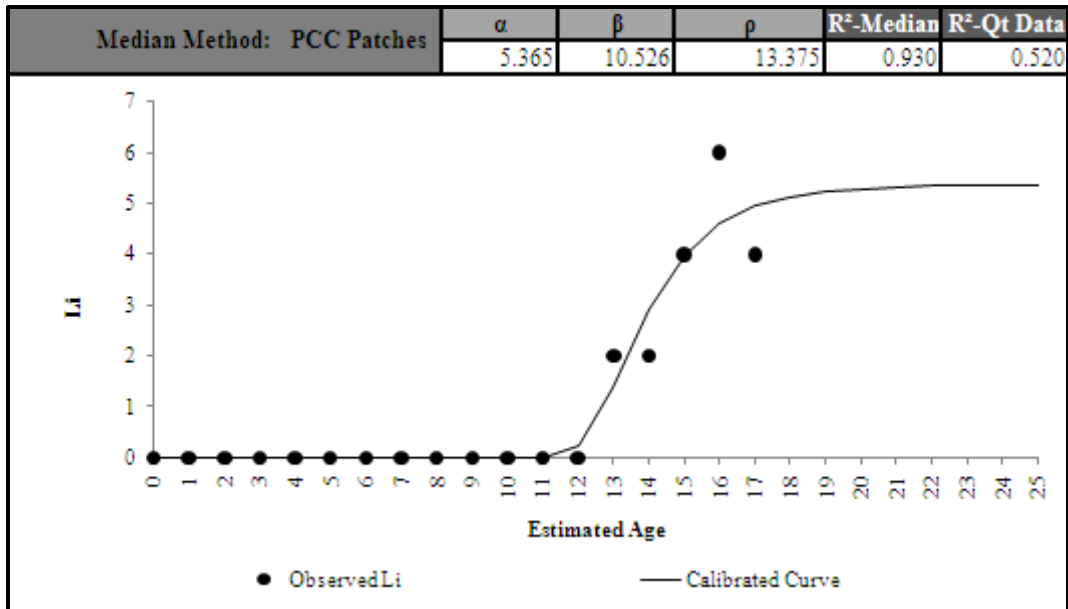


Figure C 26.15. Calibrated Performance Model, Statewide, Li Median Method (Unconstrained).

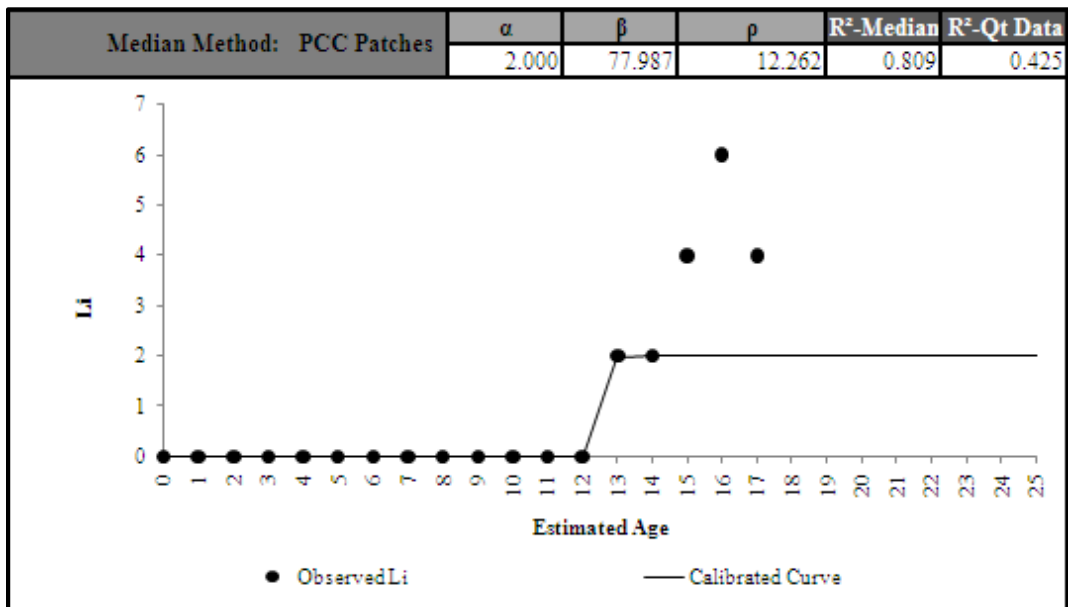


Figure C 26.16. Calibrated Performance Model, Statewide, Li Median Method (Constrained).

Appendix D: Calibrated CRCP Distress Performance Models for Climate and Subgrade Zones

Zone 1-Spalled Cracks

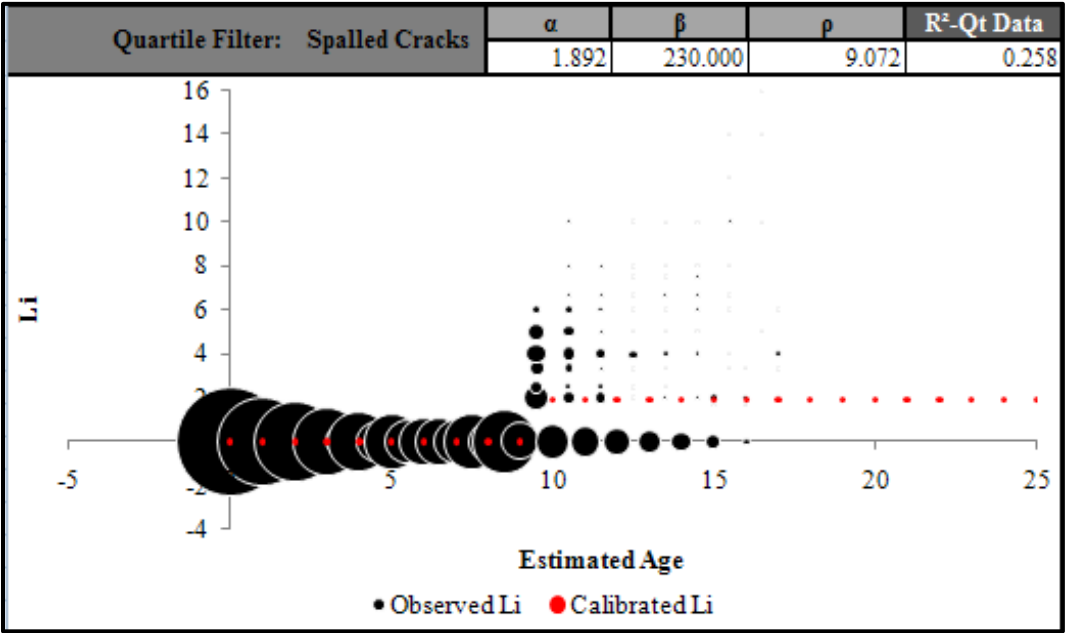


Figure D 1.1. Calibrated Performance Model for Paris District, Li Quartile Method (Unconstrained).

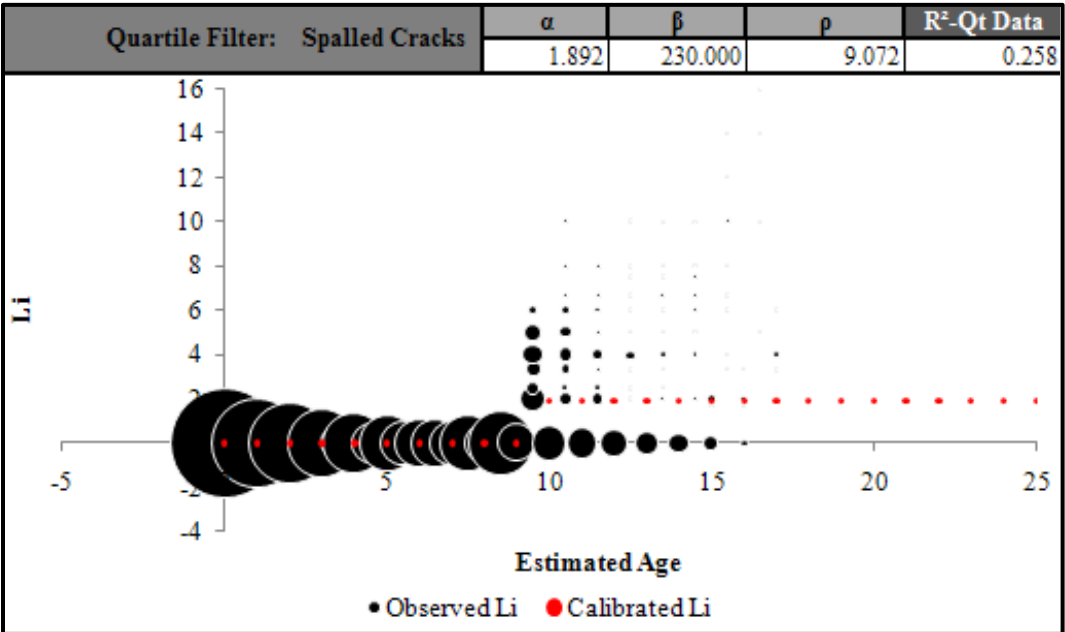


Figure D 1.2. Calibrated Performance Model for Paris District, Li Quartile Method (Constrained).

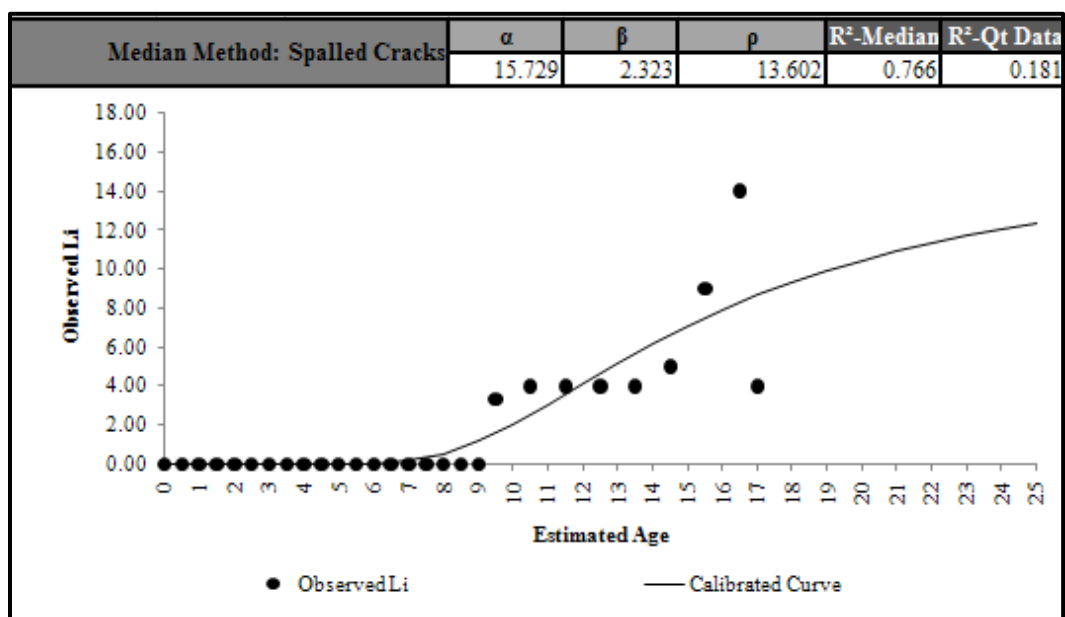


Figure D 1.3. Calibrated Performance Model for Paris District, Li Median Method (Unconstrained).

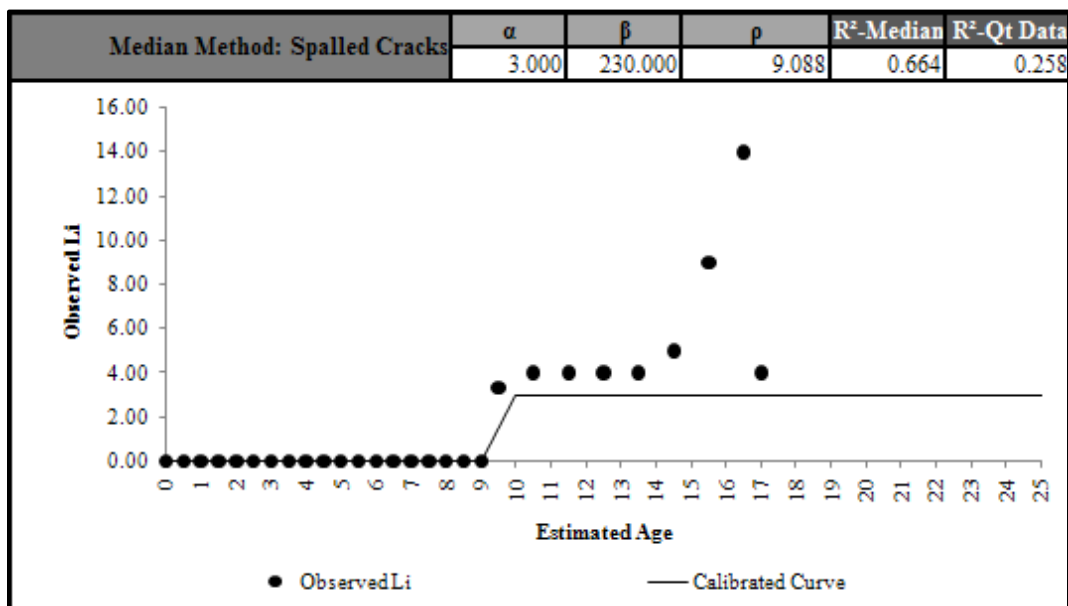


Figure D 1.4. Calibrated Performance Model for Paris District, Li Median Method (Constrained).

Zone 1-Punchouts

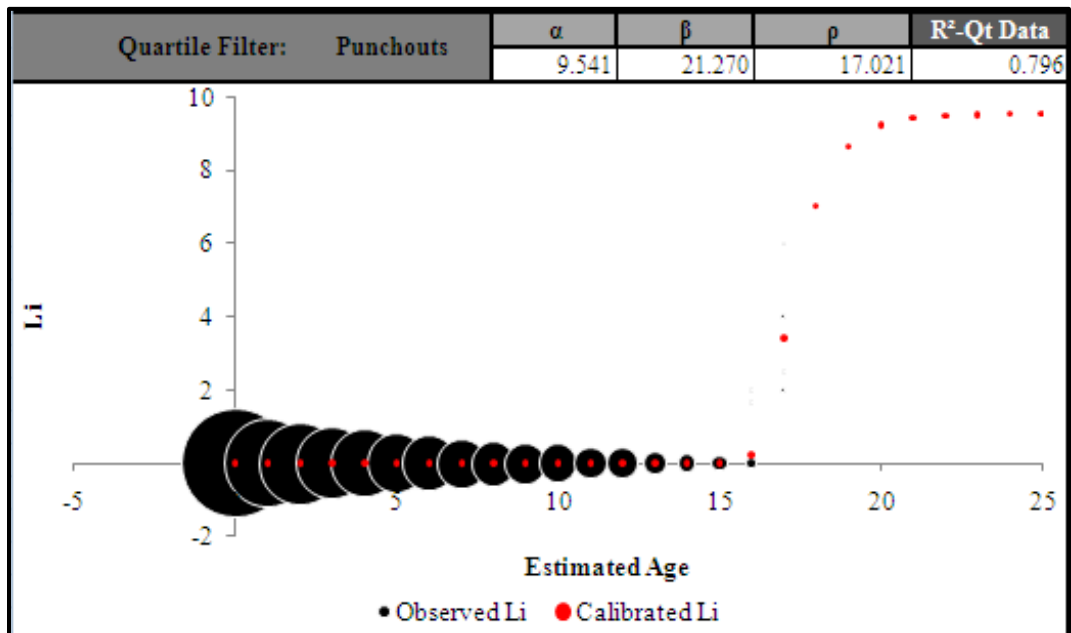


Figure D 2.1. Calibrated Performance Model for Fort Worth District, Li Quartile Method (Unconstrained).

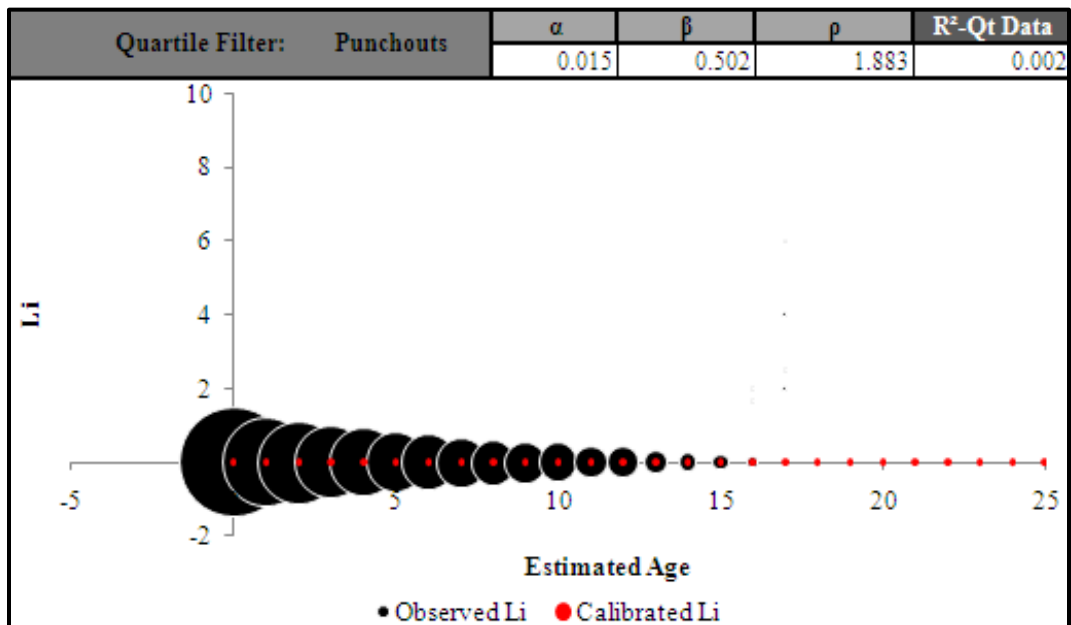


Figure D 2.2. Calibrated Performance Model for Fort Worth District, Li Quartile Method (Constrained).

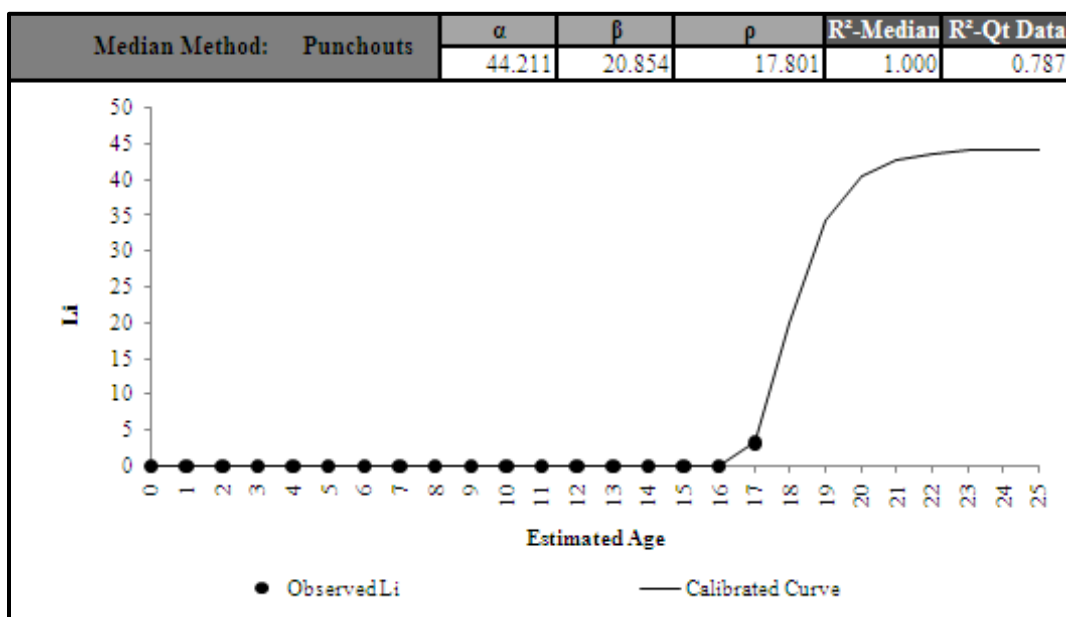


Figure D 2.3. Calibrated Performance Model for Fort Worth District, Li Median Method (Unconstrained).

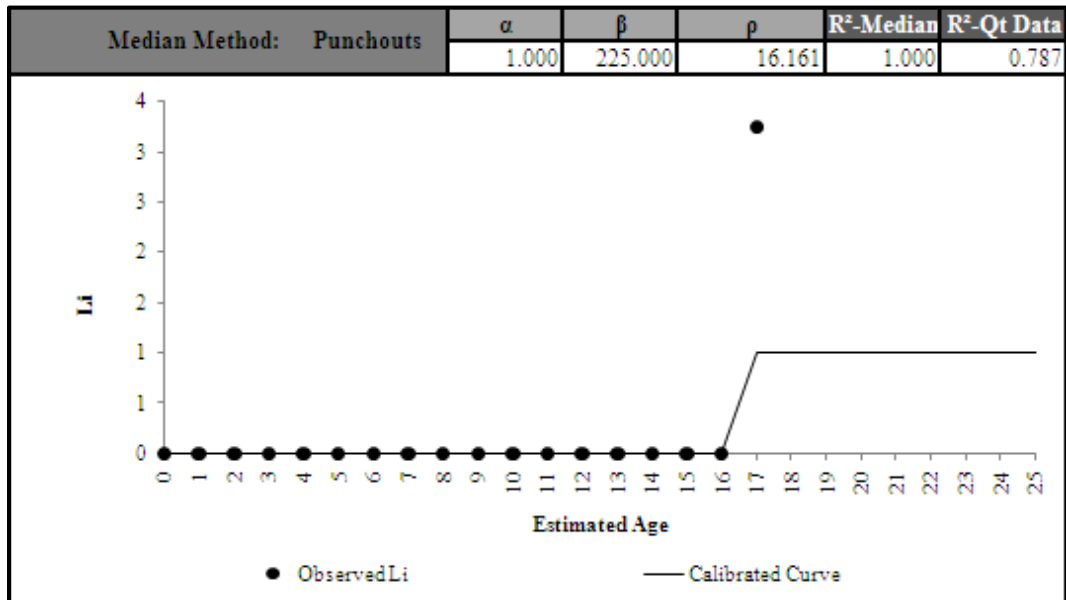


Figure D 2.4. Calibrated Performance Model for Fort Worth District, Li Median Method (Constrained).

Zone 1-ACP Patches

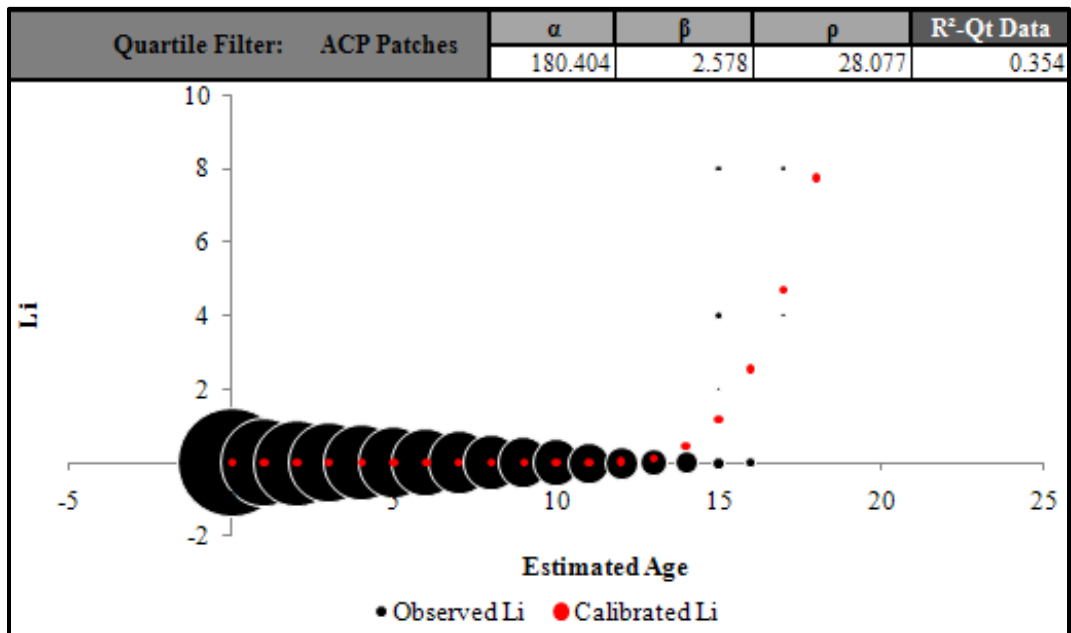


Figure D 3.1. Calibrated Performance Model for Wichita Falls District, Li Quartile Method (Unconstrained).

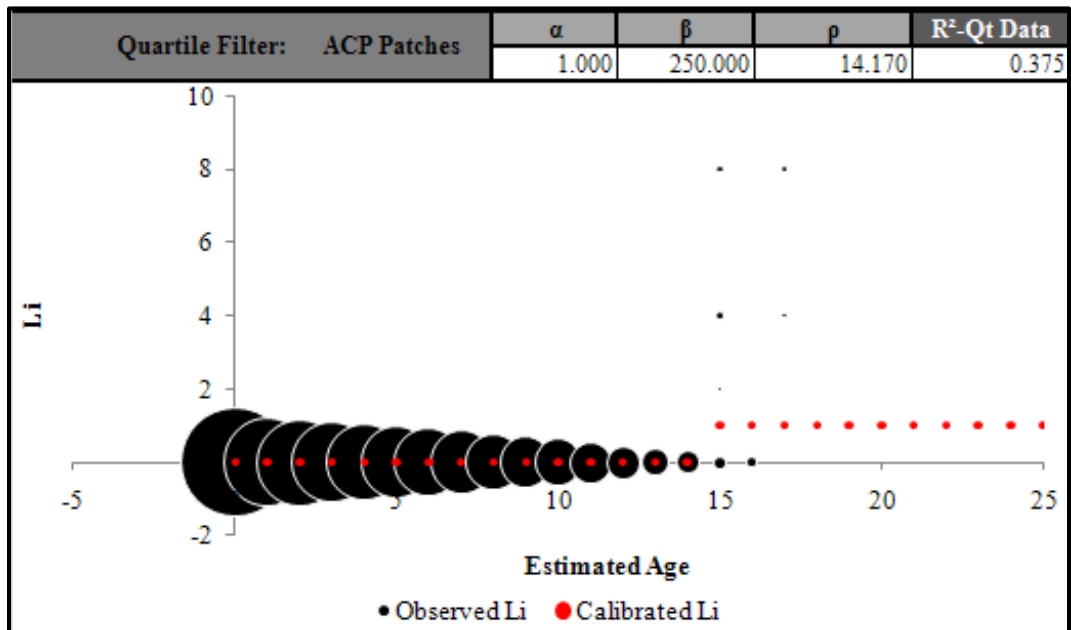


Figure D 3.2. Calibrated Performance Model for Wichita Falls District, Li Quartile Method (Constrained).

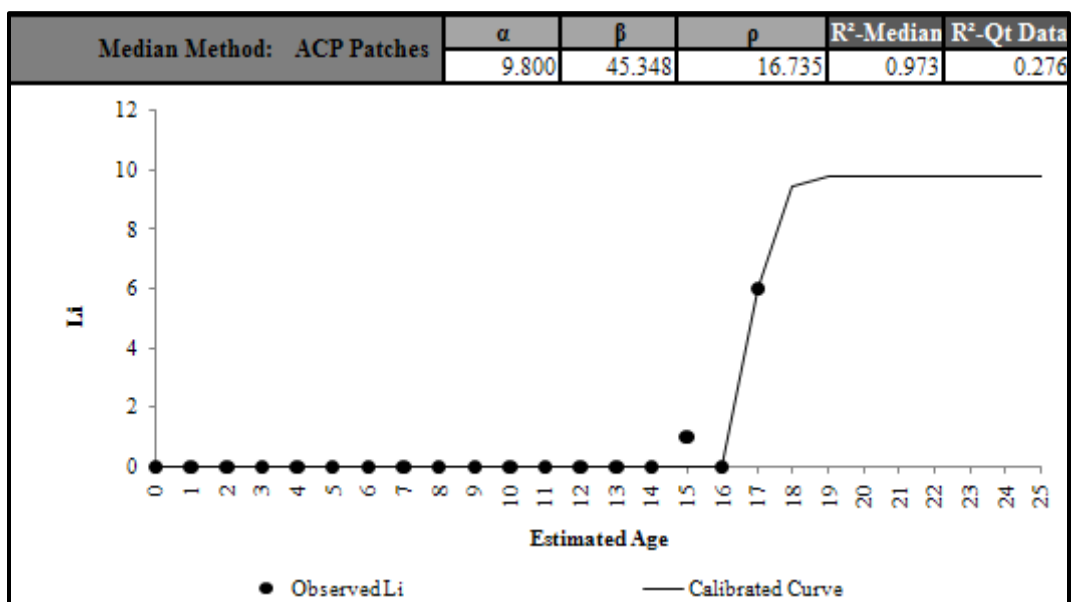


Figure D 3.3. Calibrated Performance Model for Wichita Falls District, Li Median Method (Unconstrained).

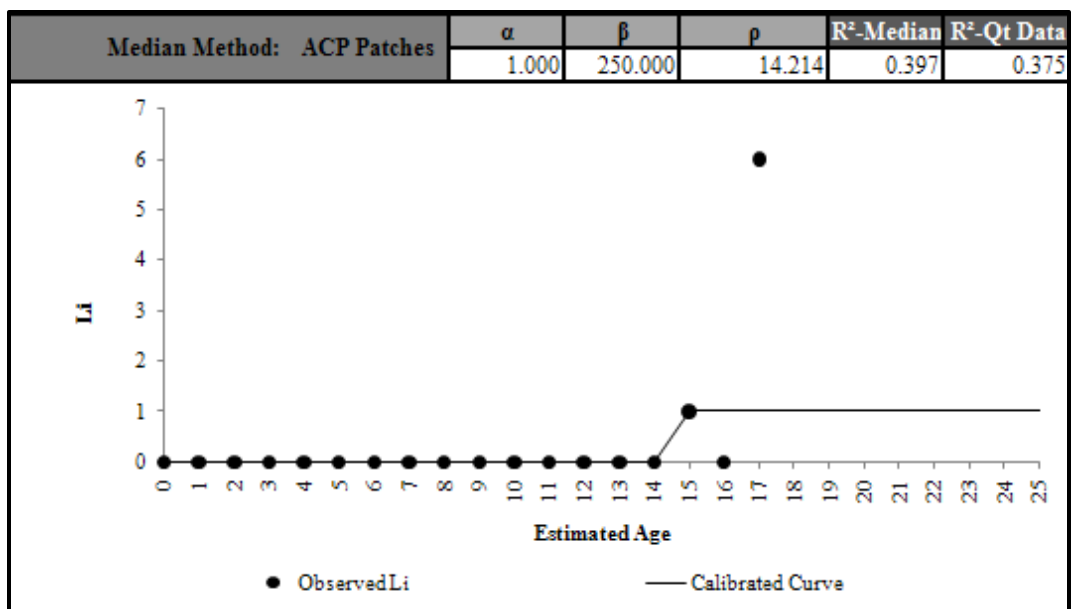


Figure D 3.4. Calibrated Performance Model for Wichita Falls District, Li Median Method (Constrained).

Zone 1-PCC Patches

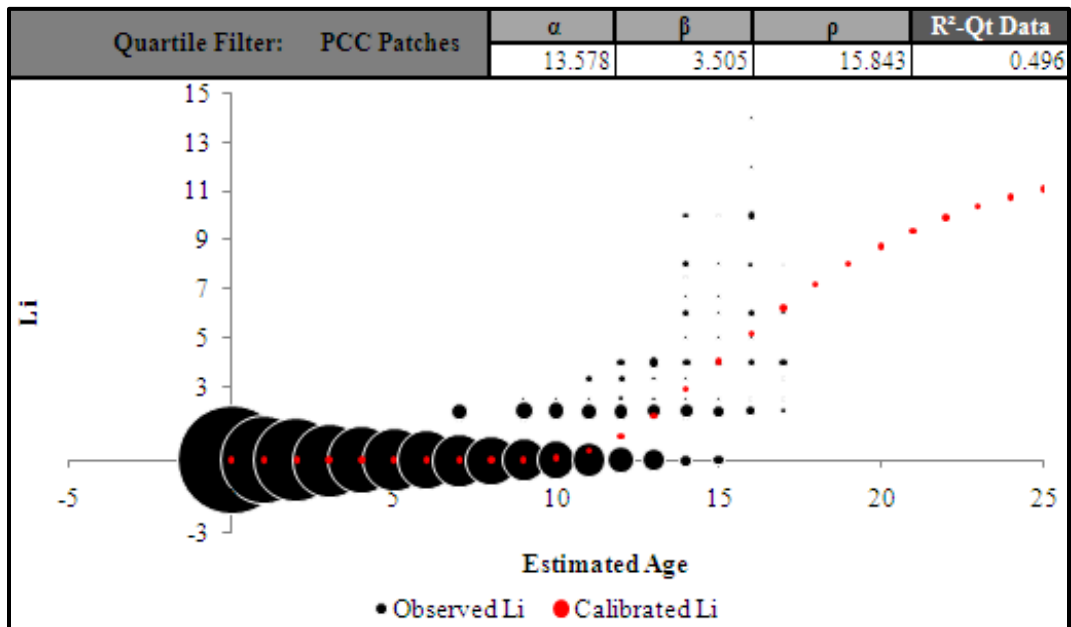


Figure D 4.1. Calibrated Performance Model for Amarillo District, Li Quartile Method (Unconstrained).

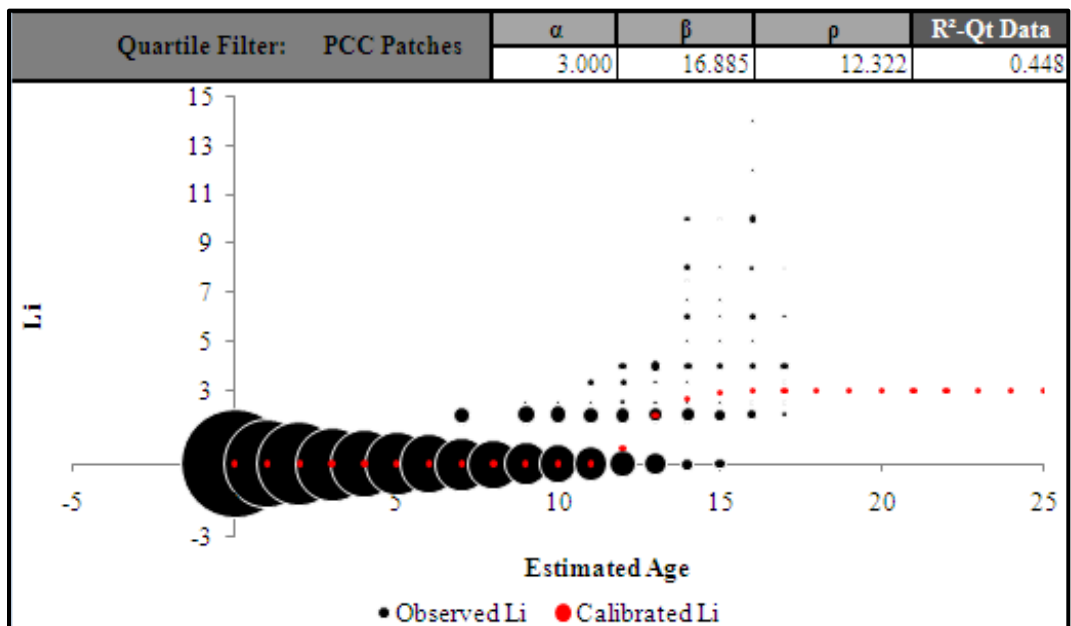


Figure D 4.2. Calibrated Performance Model for Amarillo District, Li Quartile Method (Constrained).

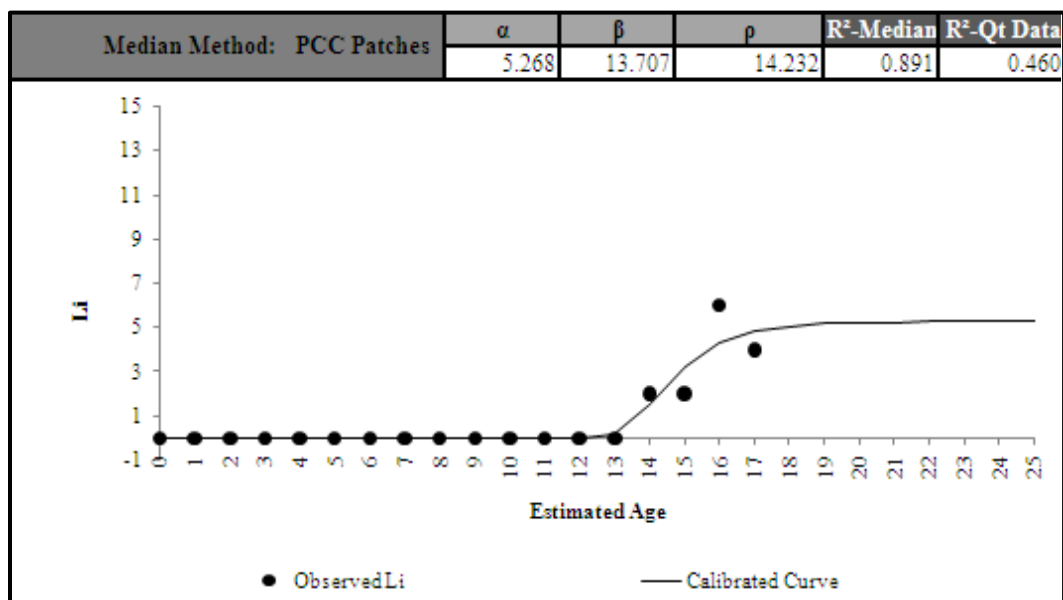


Figure D 4.3. Calibrated Performance Model for Amarillo District, Li Median Method (Unconstrained).

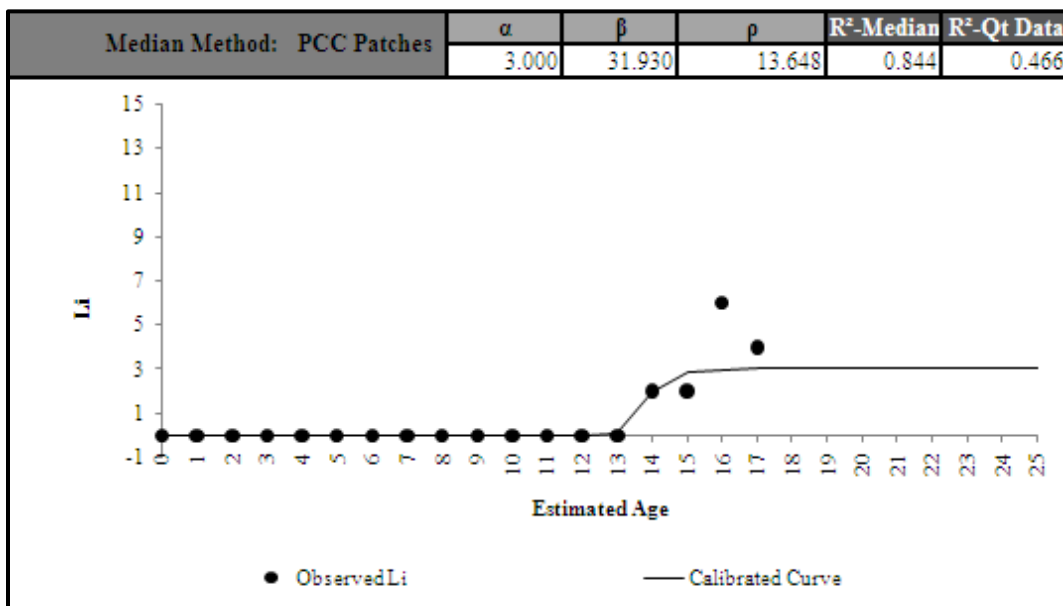


Figure D 4.4. Calibrated Performance Model for Amarillo District, Li Median Method (Constrained).

Zone 2-Spalled Cracks

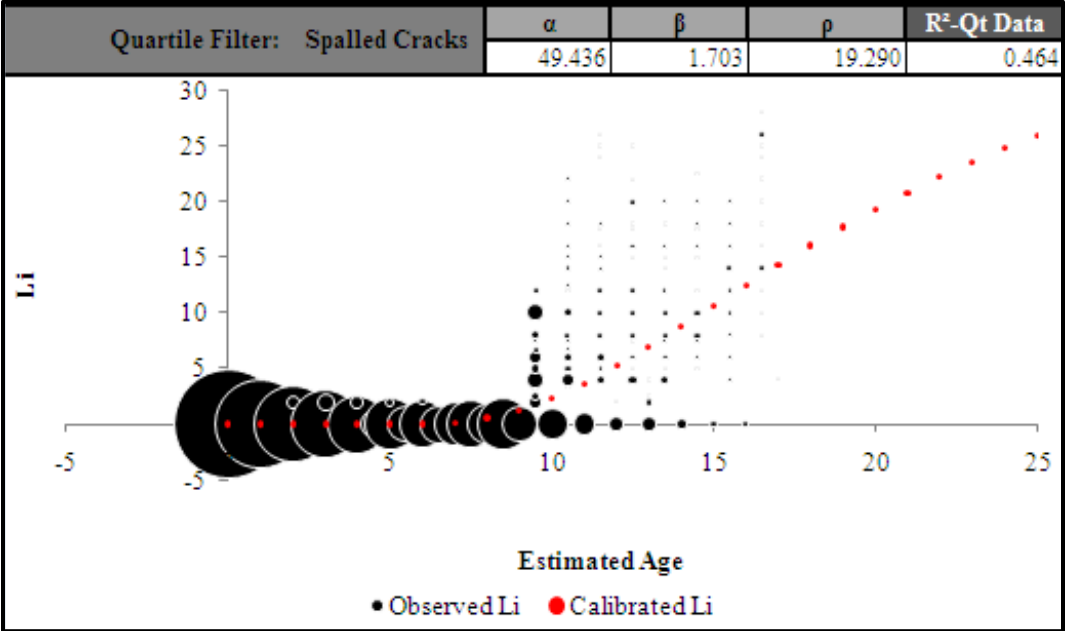


Figure D 5.1. Calibrated Performance Model for Paris District, Li Quartile Method (Unconstrained).

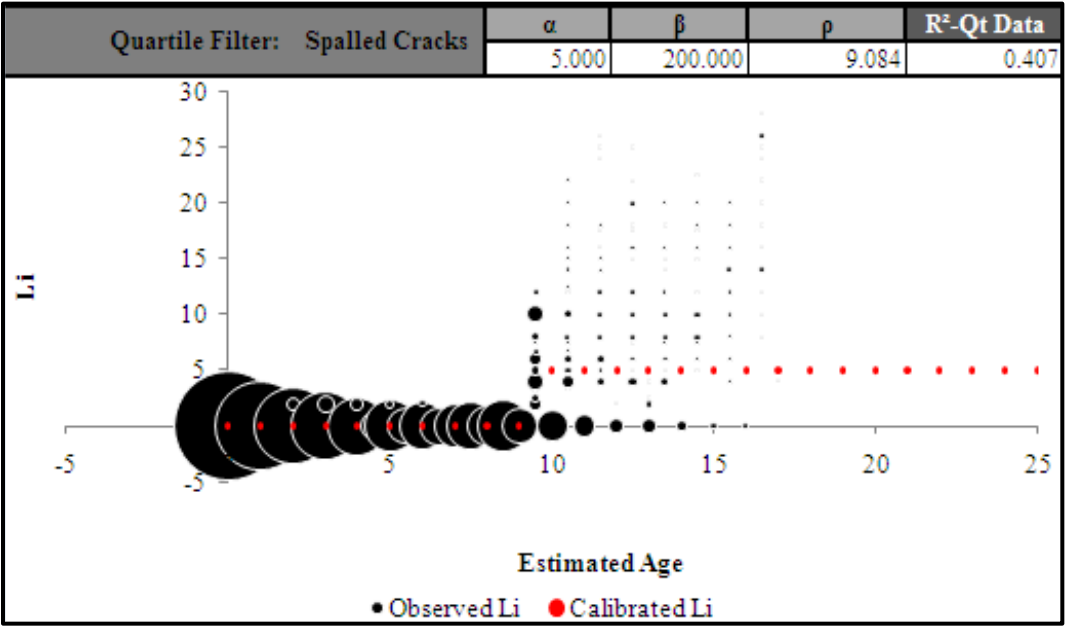


Figure D 5.2. Calibrated Performance Model for Paris District, Li Quartile Method (Constrained).

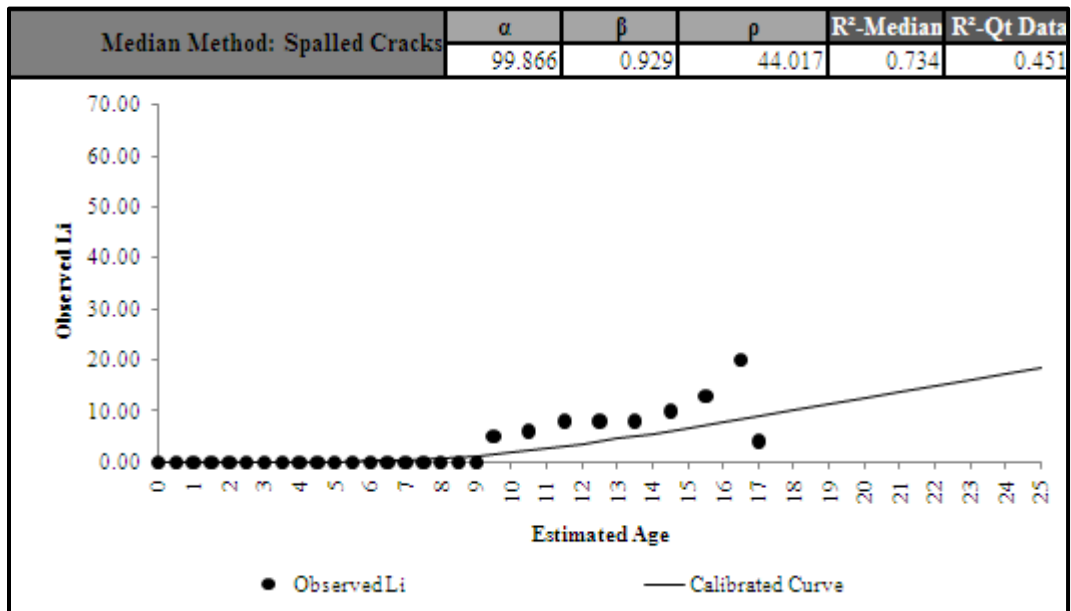


Figure D 5.3. Calibrated Performance Model for Paris District, Li Median Method (Unconstrained).

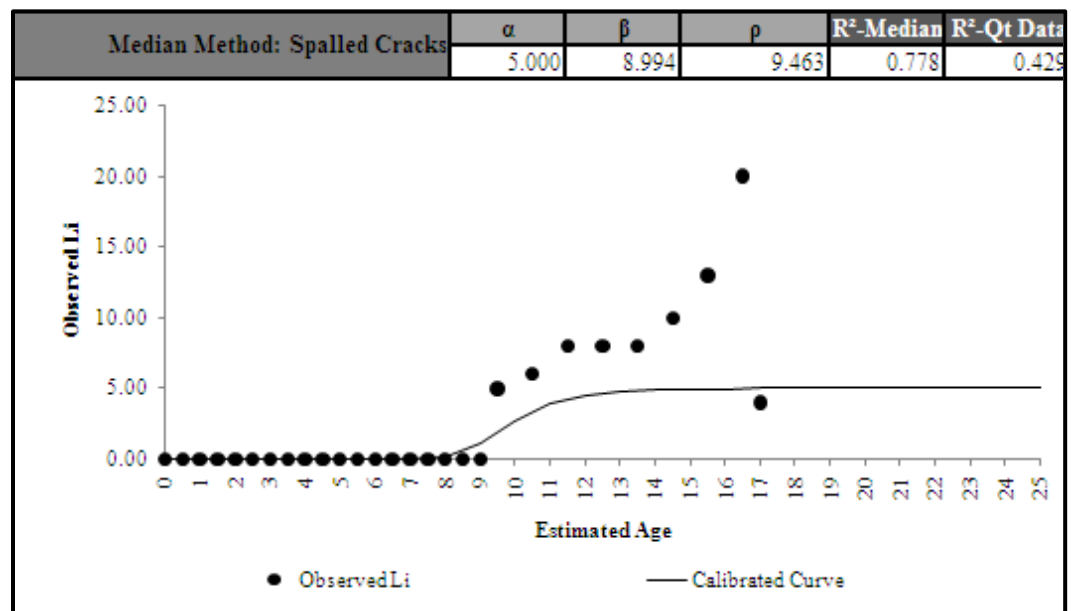


Figure D 5.4. Calibrated Performance Model for Paris District, Li Median Method (Constrained).

Zone 2-Punchouts

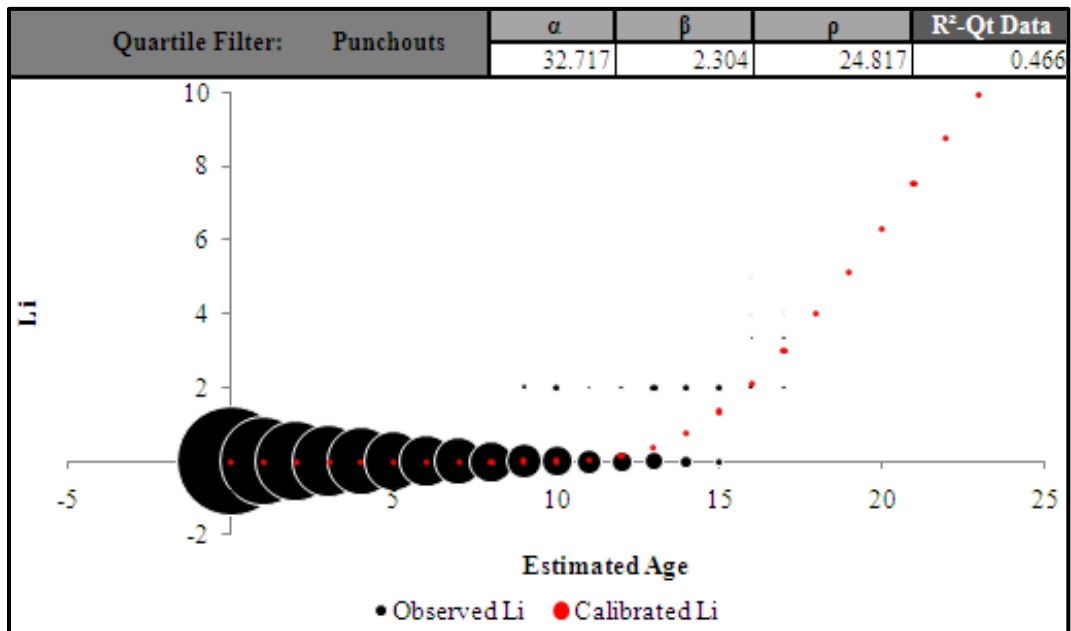


Figure D 6.1. Calibrated Performance Model for Fort Worth District, Li Quartile Method (Unconstrained).

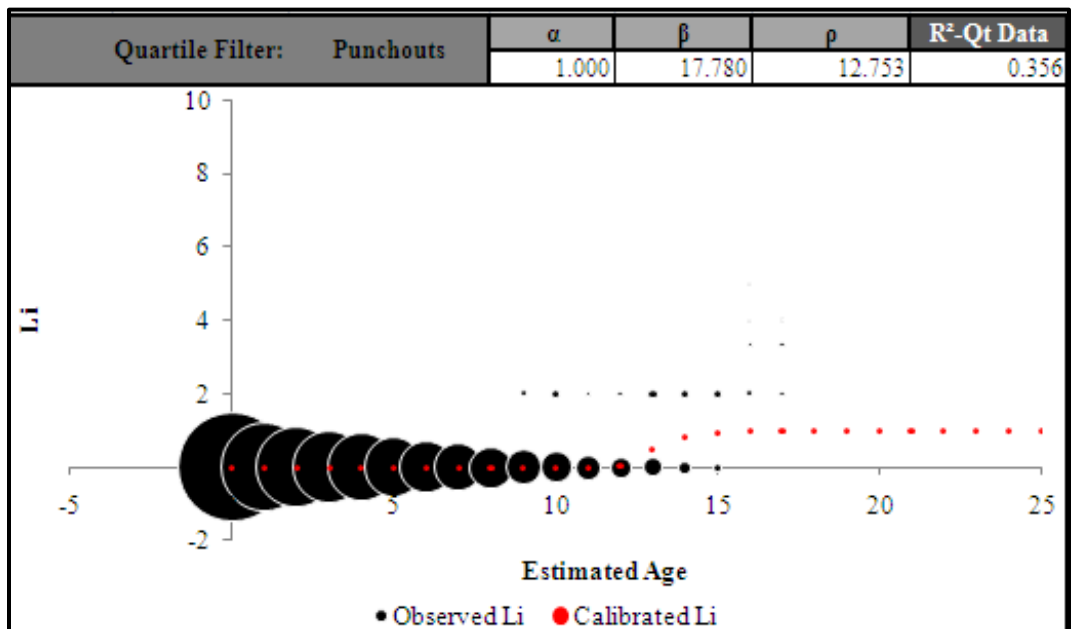


Figure D 6.2. Calibrated Performance Model for Fort Worth District, Li Quartile Method (Constrained).

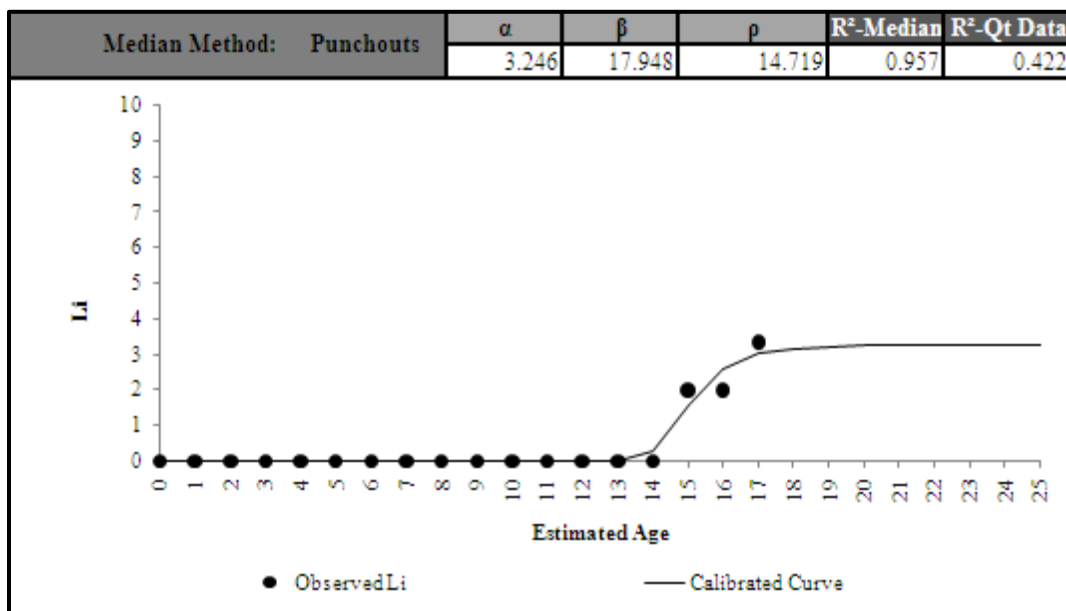


Figure D 6.3. Calibrated Performance Model for Fort Worth District, Li Median Method (Unconstrained).

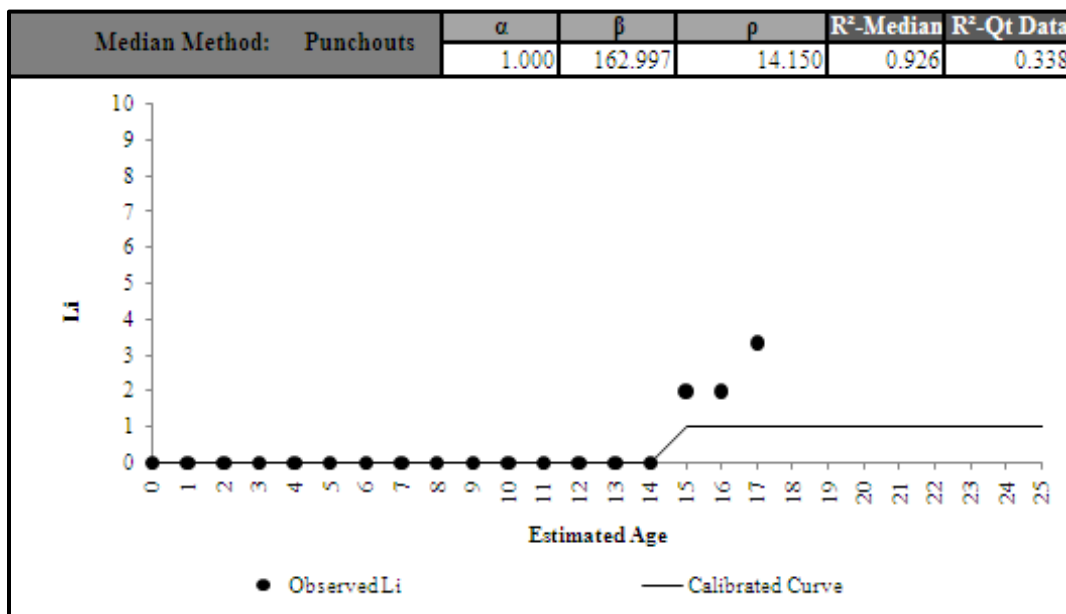


Figure D 6.4. Calibrated Performance Model for Fort Worth District, Li Median Method (Constrained).

Zone 2-ACP Patches

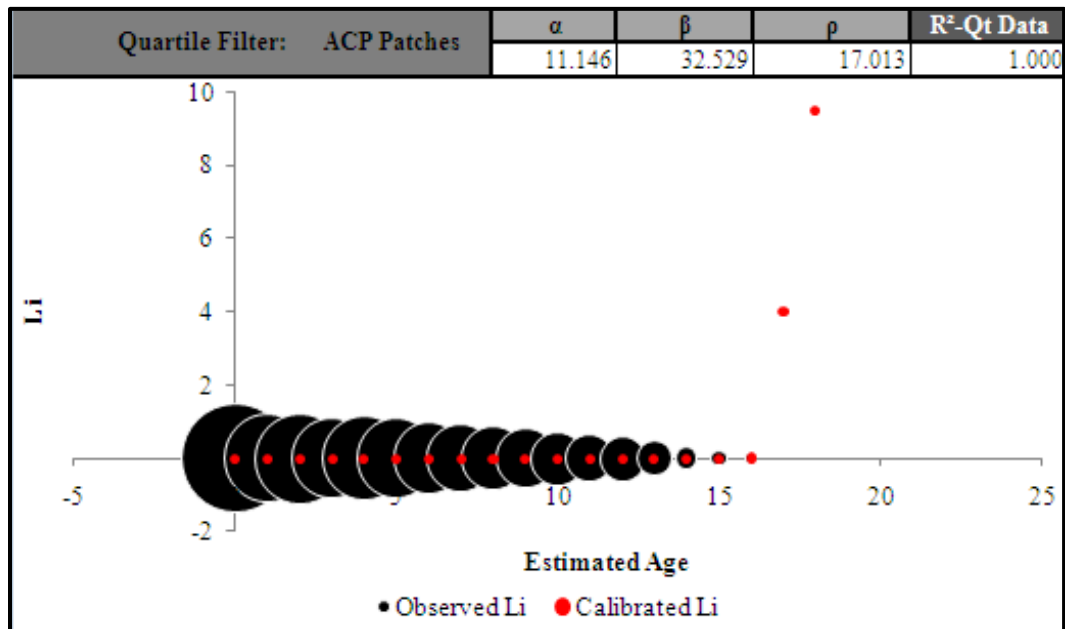


Figure D 7.1. Calibrated Performance Model for Wichita Falls District, Li Quartile Method (Unconstrained).

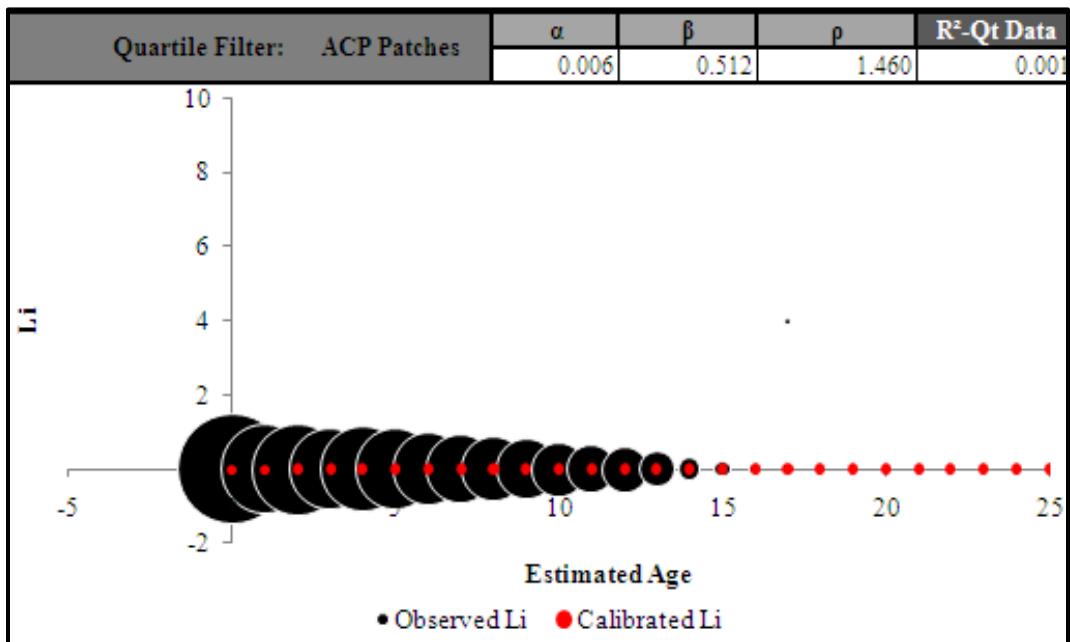


Figure D 7.2. Calibrated Performance Model for Wichita Falls District, Li Quartile Method (Constrained).

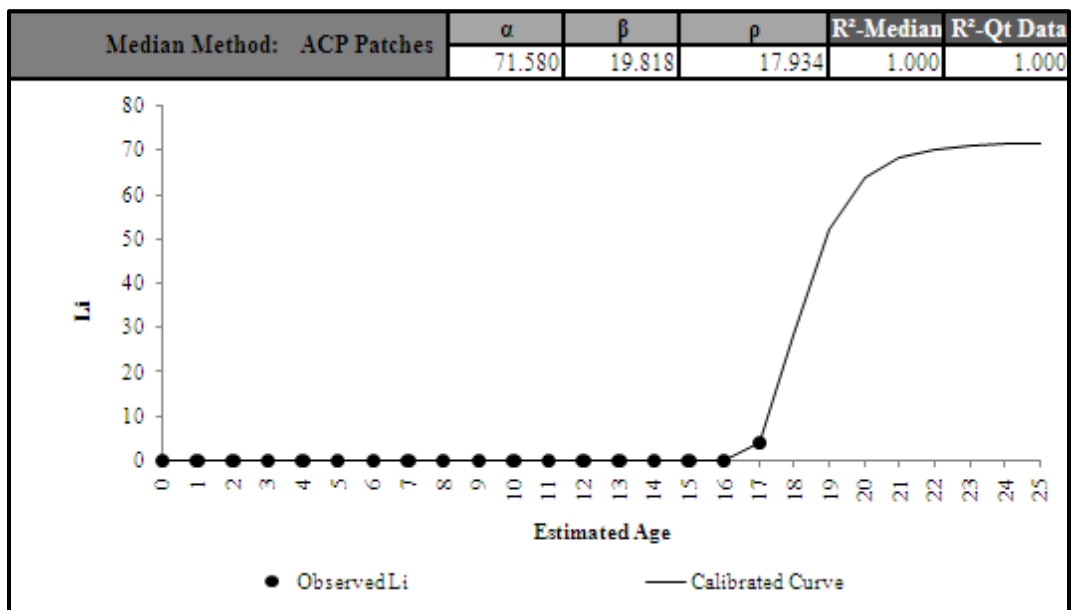


Figure D 7.3. Calibrated Performance Model for Wichita Falls District, Li Median Method (Unconstrained).

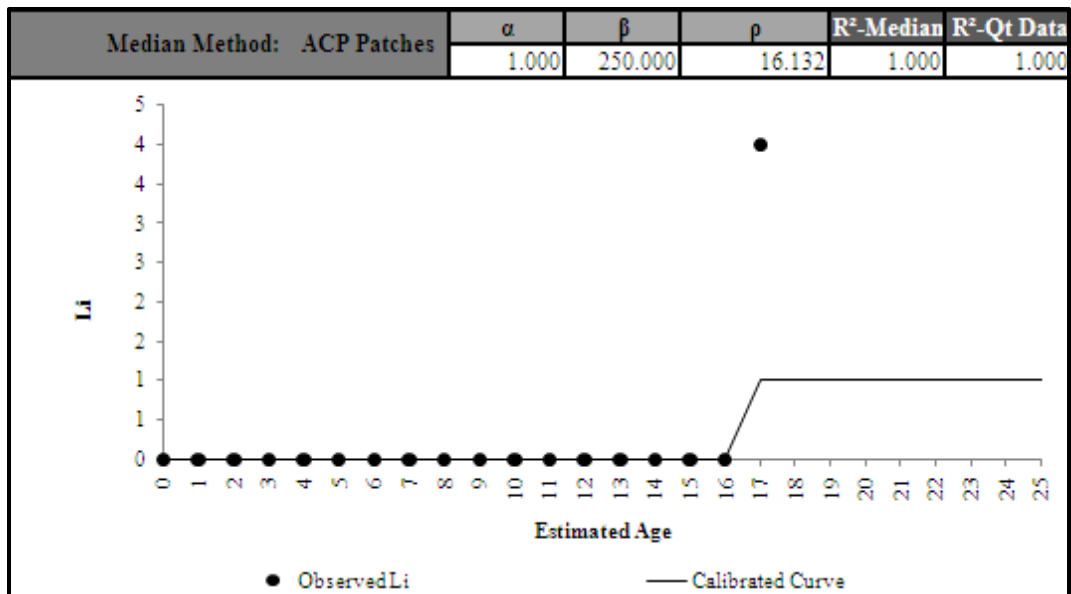


Figure D 7.4. Calibrated Performance Model for Wichita Falls District, Li Median Method (Constrained).

Zone 2-PCC Patches

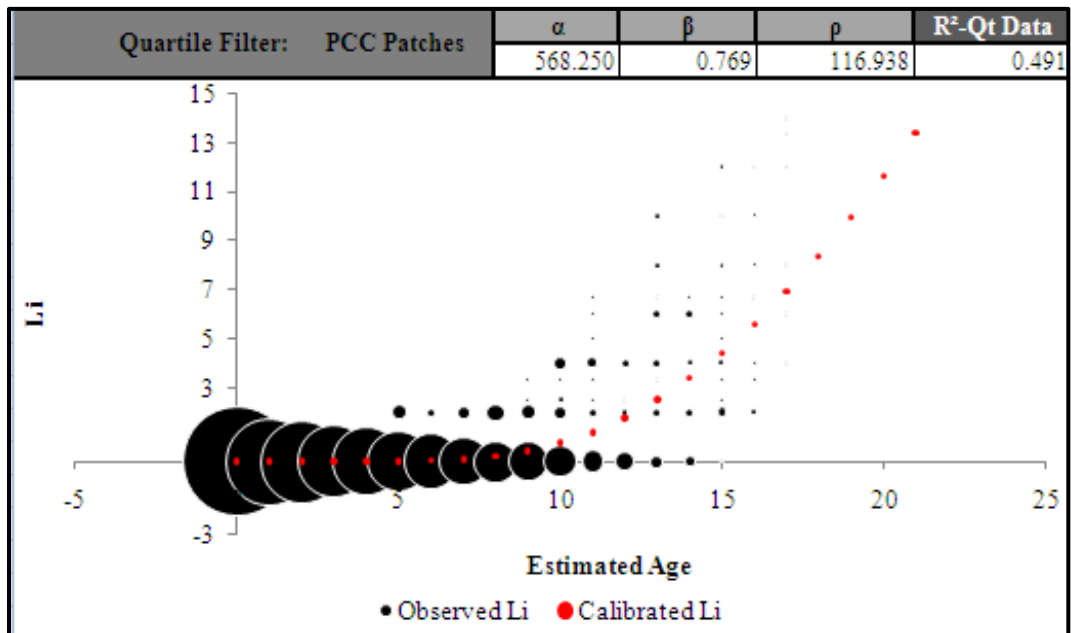


Figure D 8.1. Calibrated Performance Model for Amarillo District, Li Quartile Method (Unconstrained).

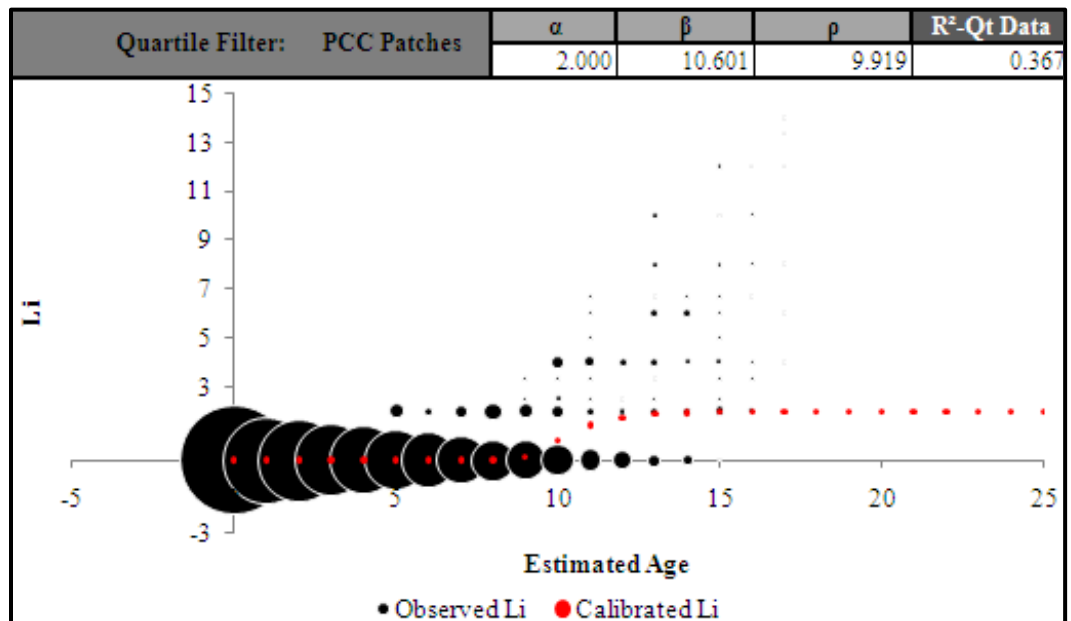


Figure D 8.2. Calibrated Performance Model for Amarillo District, Li Quartile Method (Constrained).

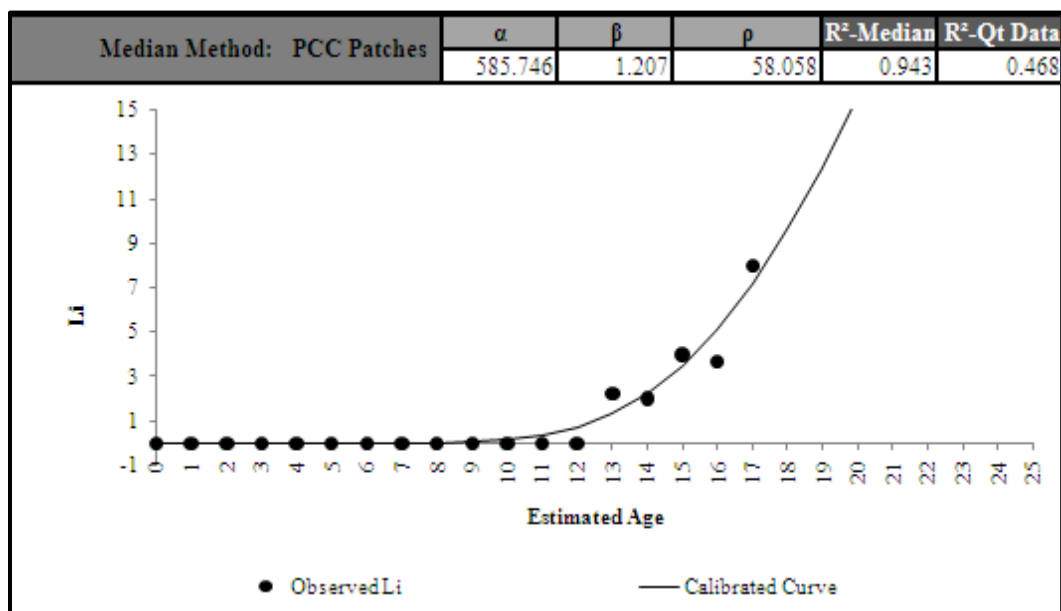


Figure D 8.3. Calibrated Performance Model for Amarillo District, Li Median Method (Unconstrained).

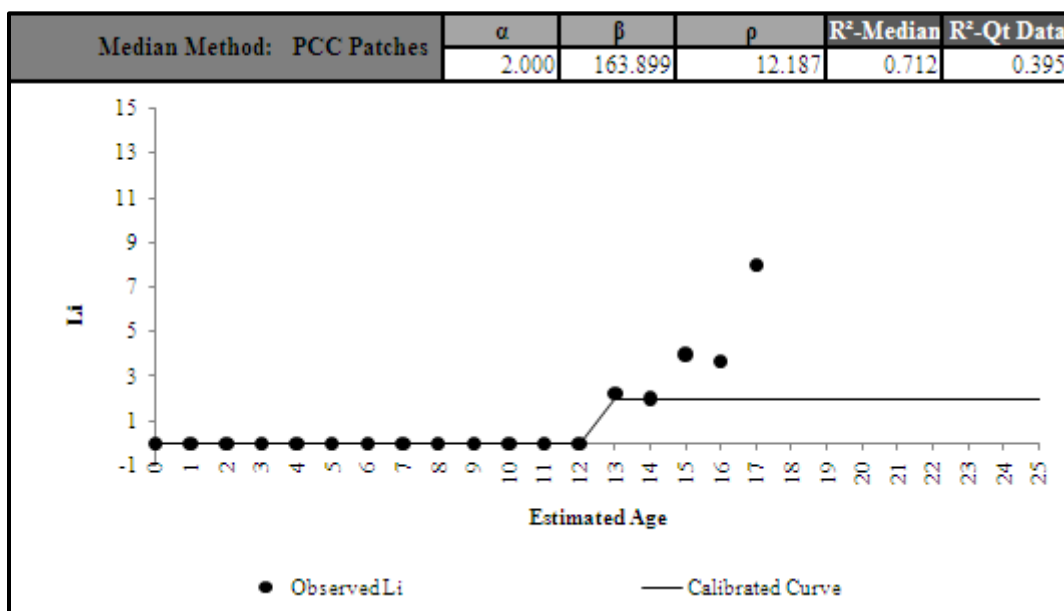


Figure D 8.4. Calibrated Performance Model for Amarillo District, Li Median Method (Constrained).

Zone 3-Spalled Cracks

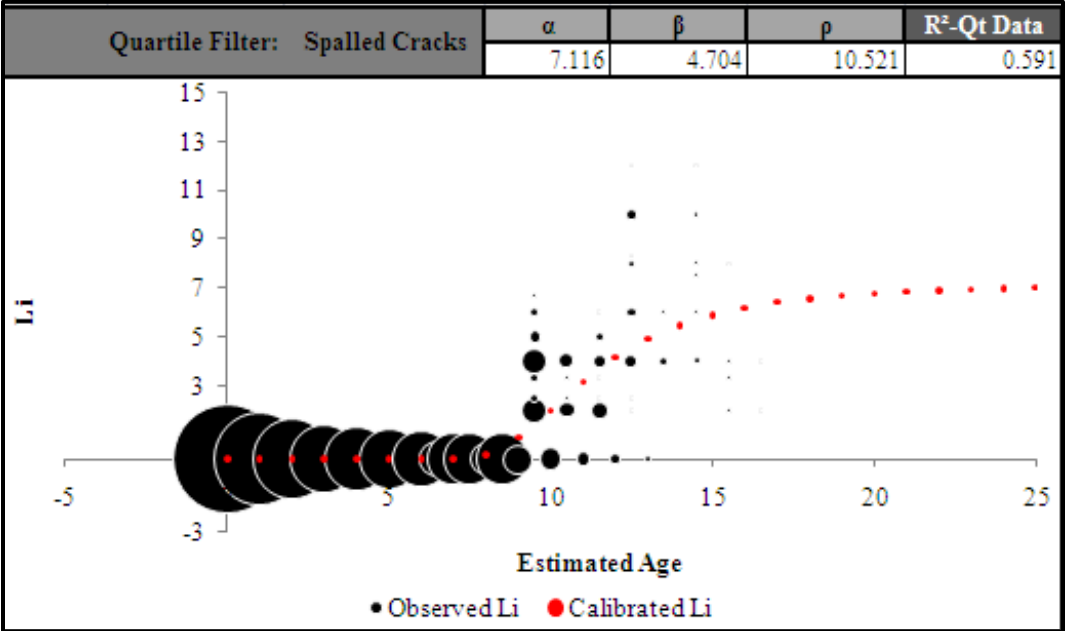


Figure D 9.1. Calibrated Performance Model for Paris District, Li Quartile Method (Unconstrained).

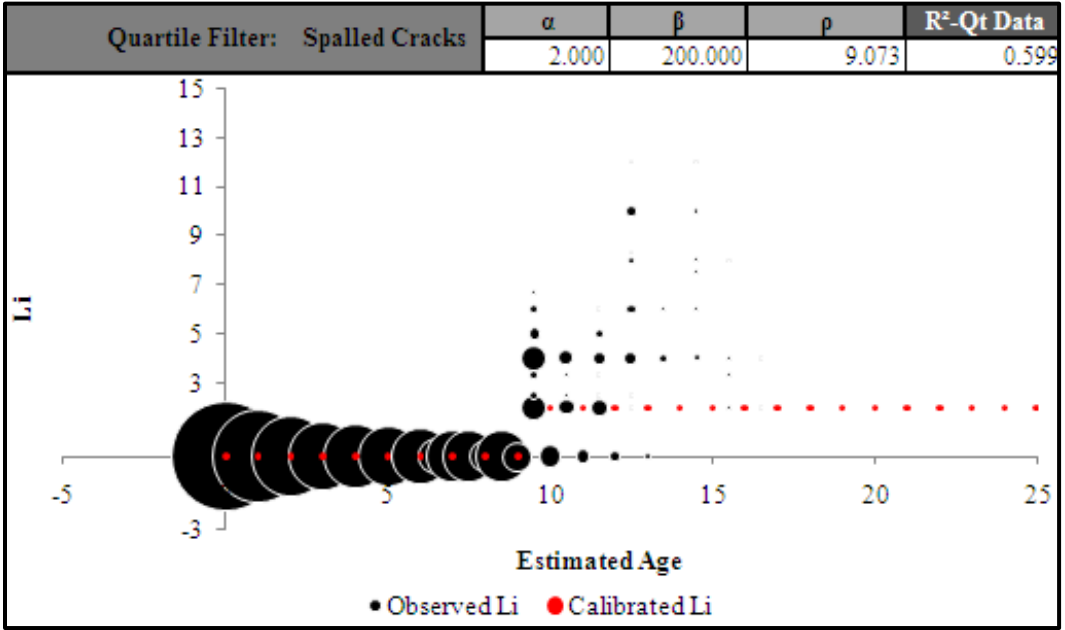


Figure D 9.2. Calibrated Performance Model for Paris District, Li Quartile Method (Constrained).

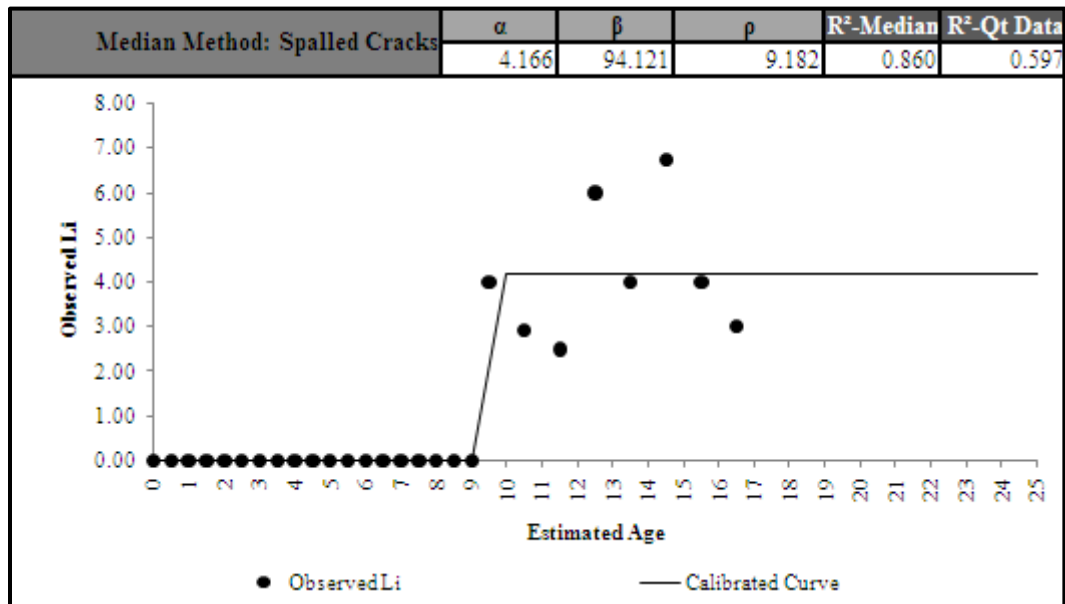


Figure D 9.3. Calibrated Performance Model for Paris District, Li Median Method (Unconstrained).

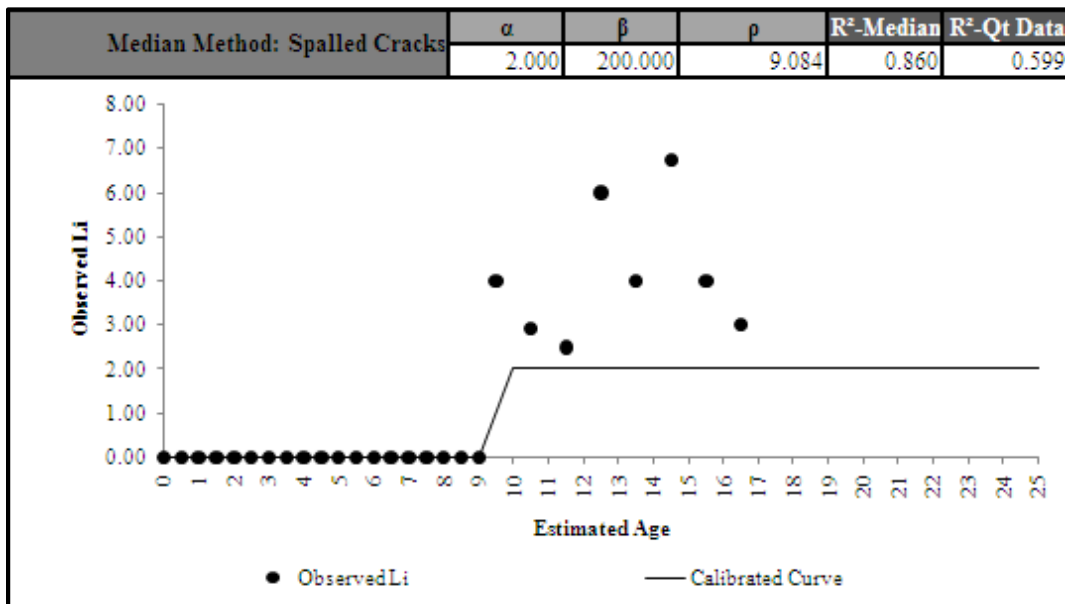


Figure D 9.4. Calibrated Performance Model for Paris District, Li Median Method (Constrained).

Zone 3-Punchouts

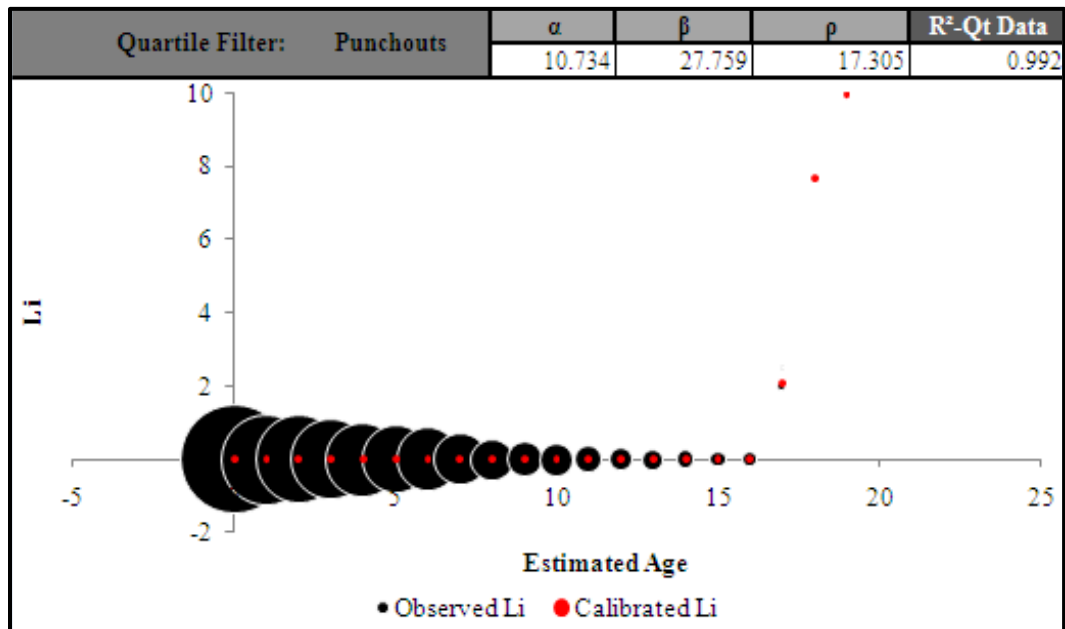


Figure D 10.1. Calibrated Performance Model for Fort Worth District, Li Quartile Method (Unconstrained).

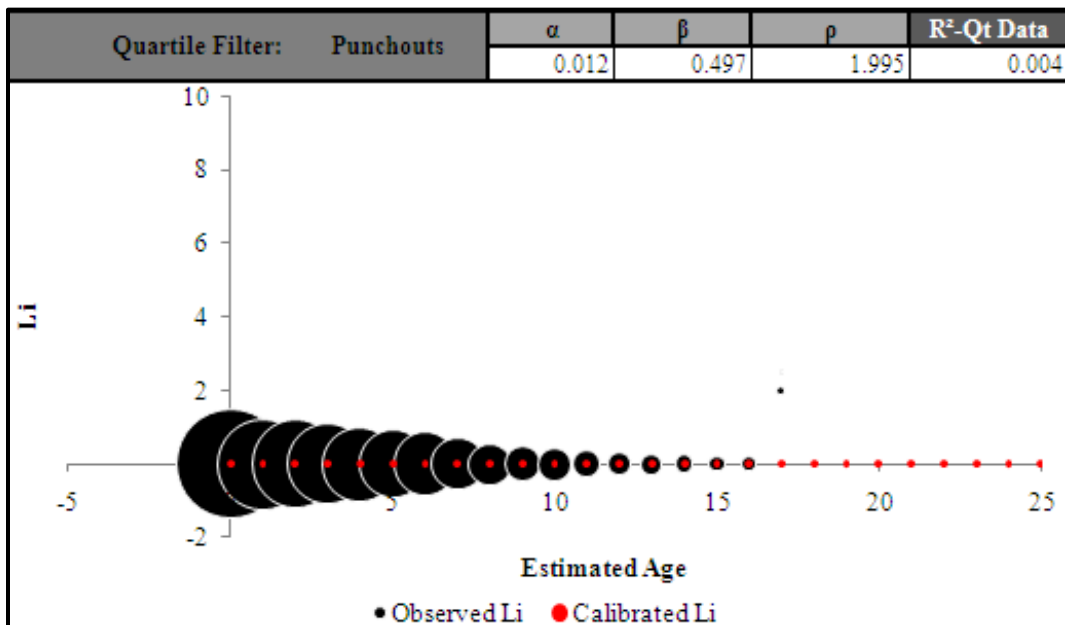


Figure D 10.2. Calibrated Performance Model for Fort Worth District, Li Quartile Method (Constrained).

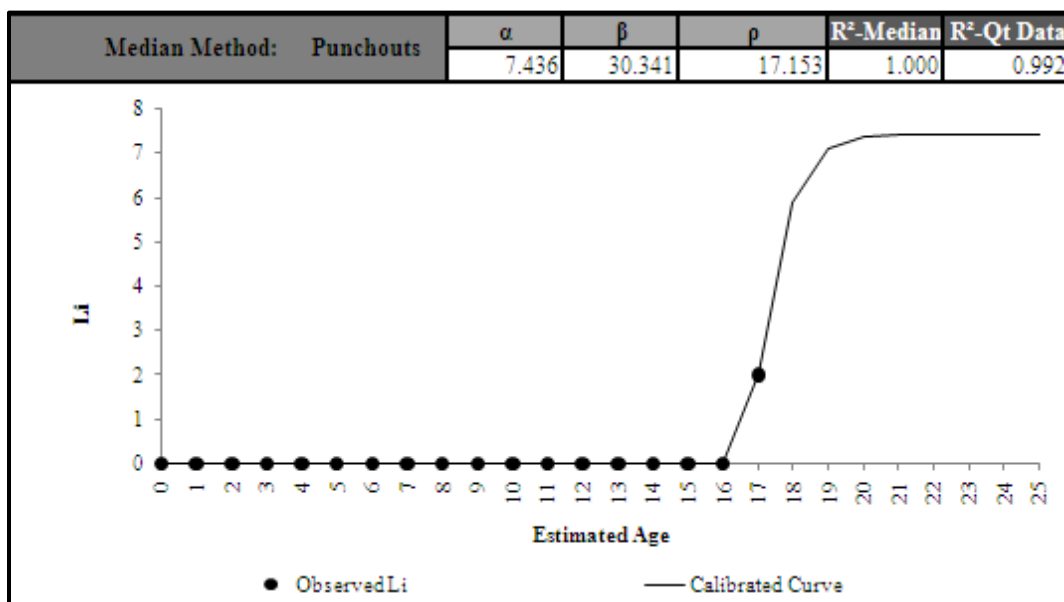


Figure D 10.3. Calibrated Performance Model for Fort Worth District, Li Median Method (Unconstrained).

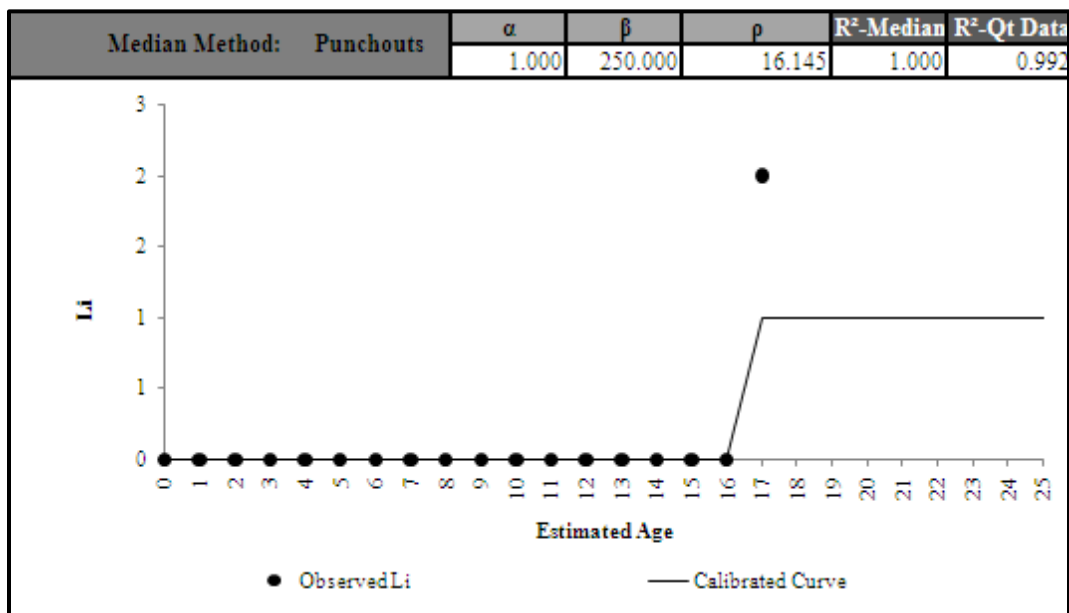


Figure D 10.4. Calibrated Performance Model for Fort Worth District, Li Median Method (Constrained).

Zone 3-ACP Patches

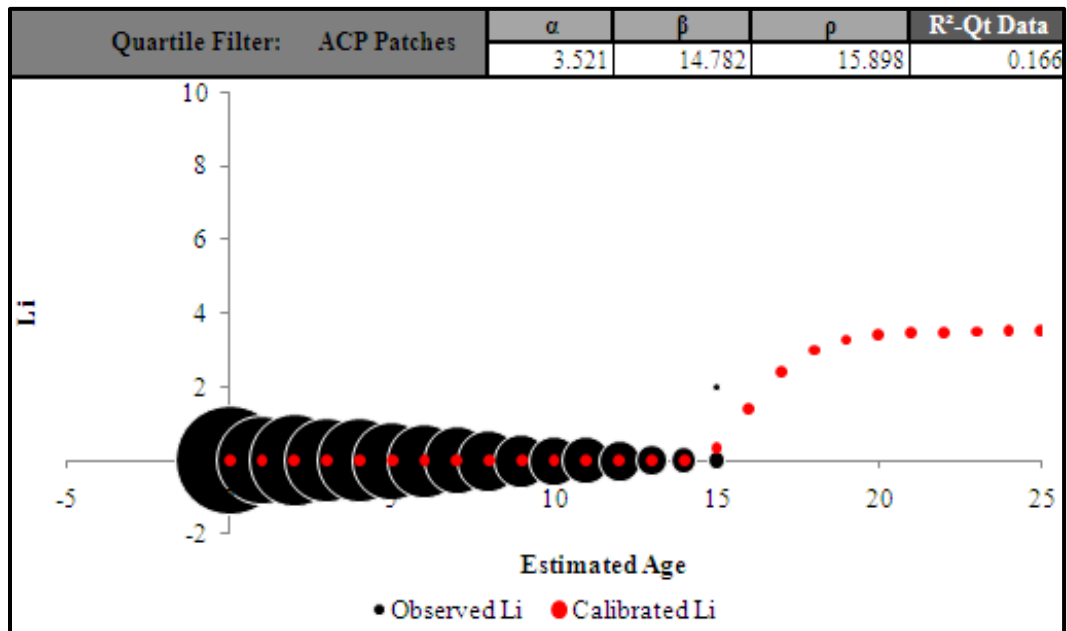


Figure D 11.1. Calibrated Performance Model for Wichita Falls District, Li Quartile Method (Unconstrained).

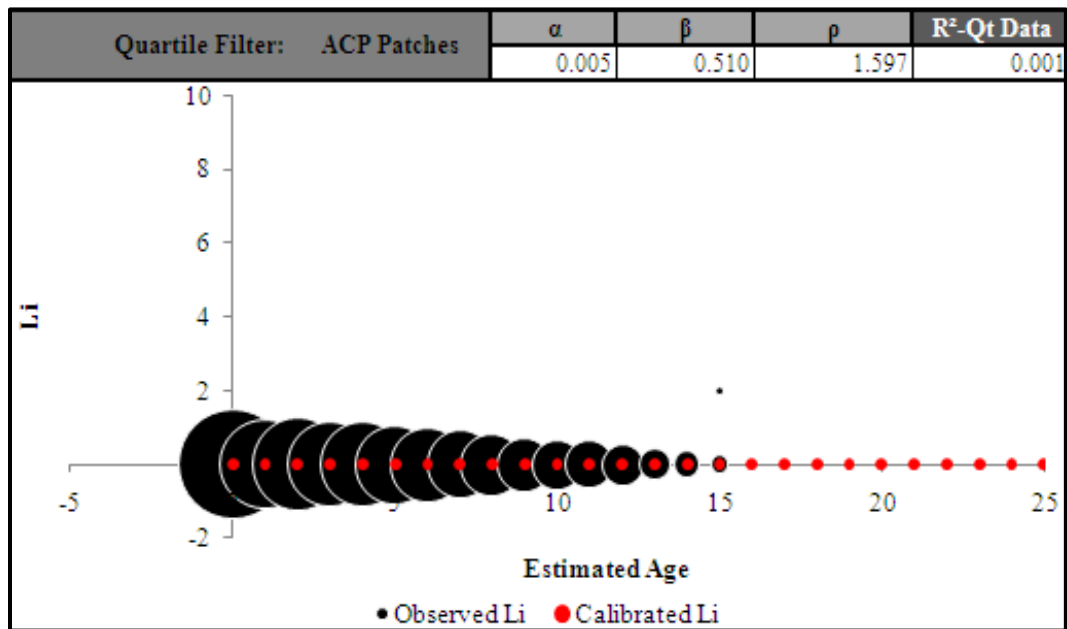


Figure D 11.2. Calibrated Performance Model for Wichita Falls District, Li Quartile Method (Constrained).

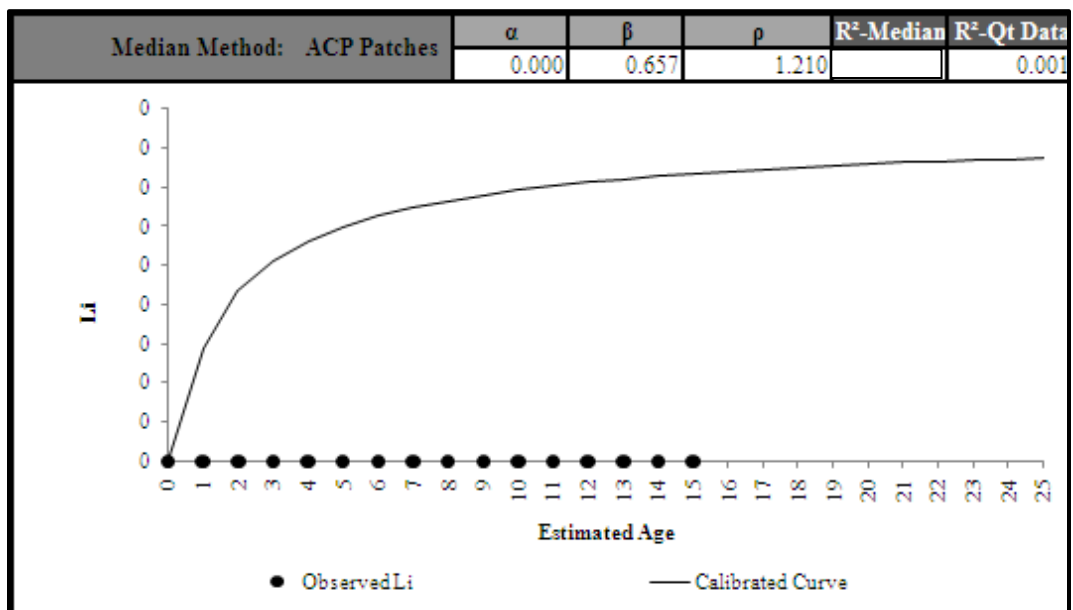


Figure D 11.3. Calibrated Performance Model for Wichita Falls District, Li Median Method (Unconstrained).

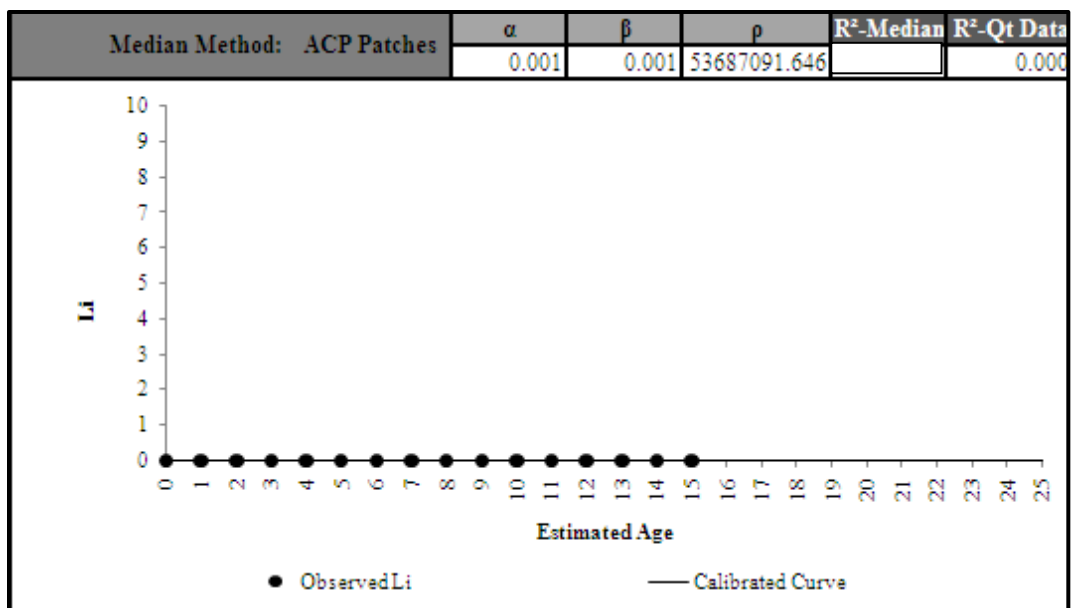


Figure D 11.4. Calibrated Performance Model for Wichita Falls District, Li Median Method (Constrained).

Zone 3-PCC Patches

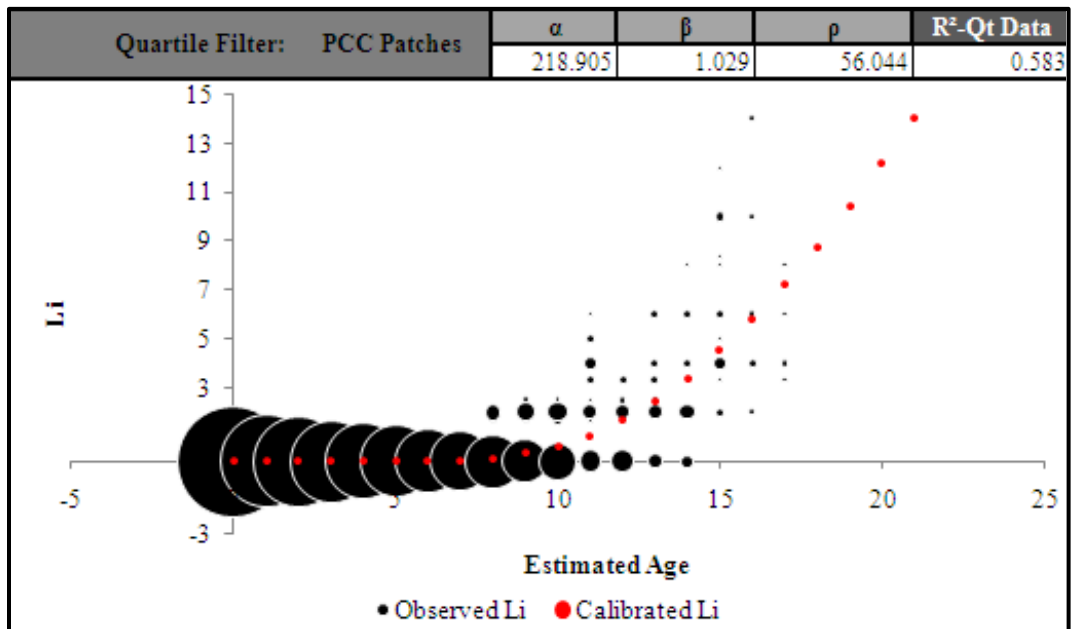


Figure D 12.1. Calibrated Performance Model for Amarillo District, Li Quartile Method (Unconstrained).

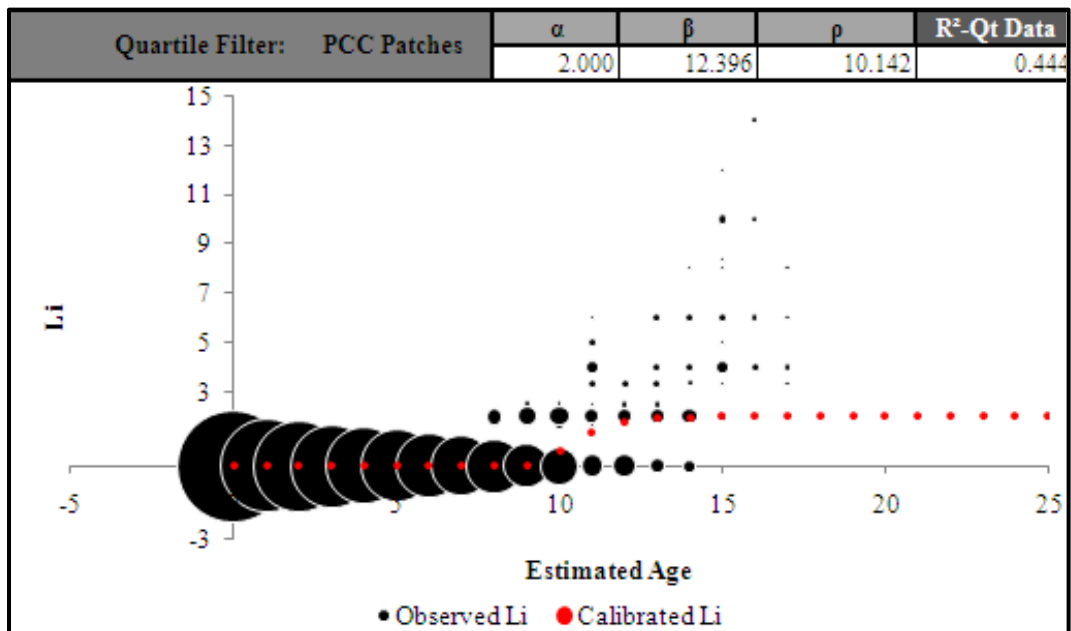


Figure D 12.2. Calibrated Performance Model for Amarillo District, Li Quartile Method (Constrained).

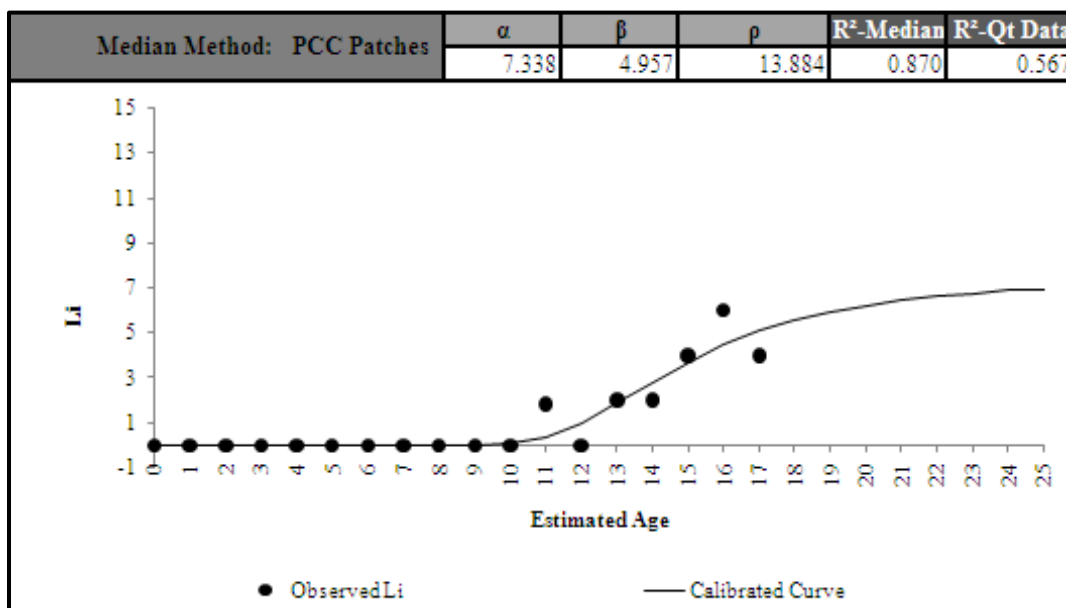


Figure D 12.3. Calibrated Performance Model for Amarillo District, Li Median Method (Unconstrained).

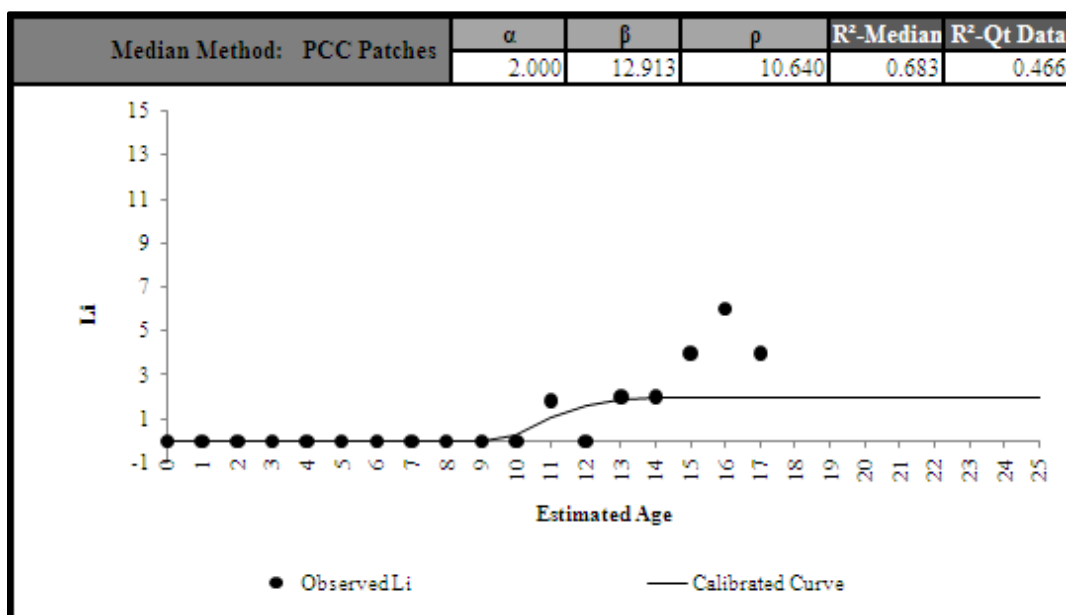


Figure D 4.4. Calibrated Performance Model for Amarillo District, Li Median Method (Constrained).

Zone 4-Spalled Cracks

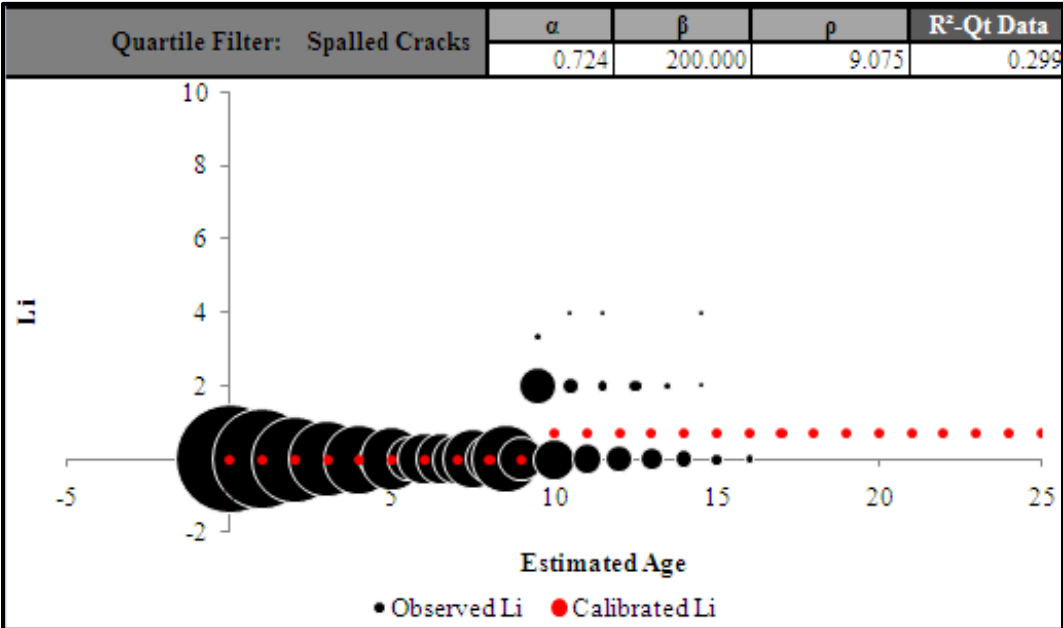


Figure D 13.1. Calibrated Performance Model for Paris District, Li Quartile Method (Unconstrained).

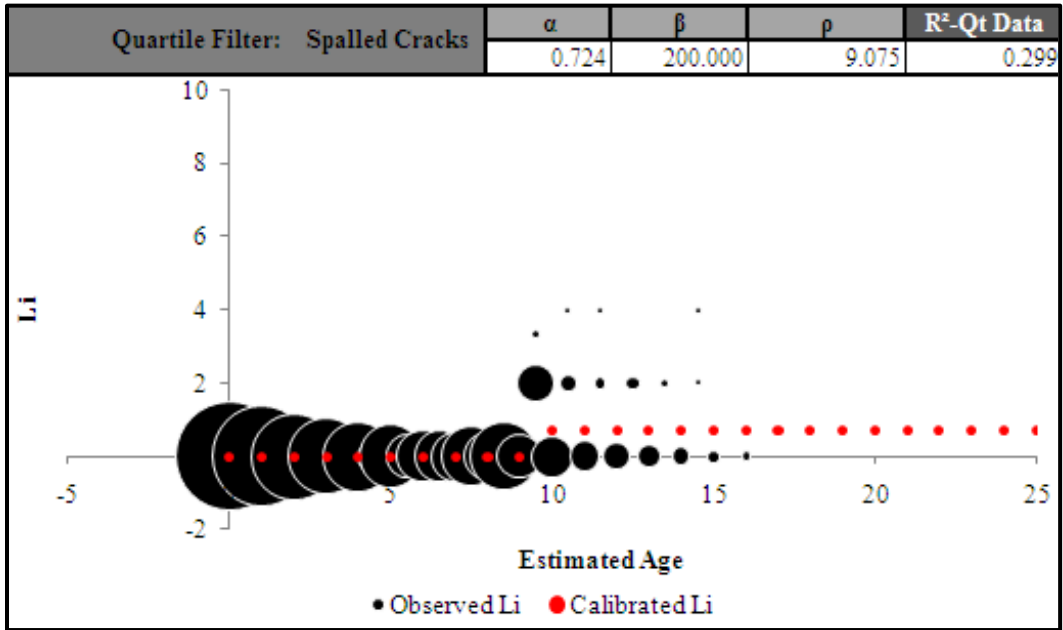


Figure D 13.2. Calibrated Performance Model for Paris District, Li Quartile Method (Constrained).

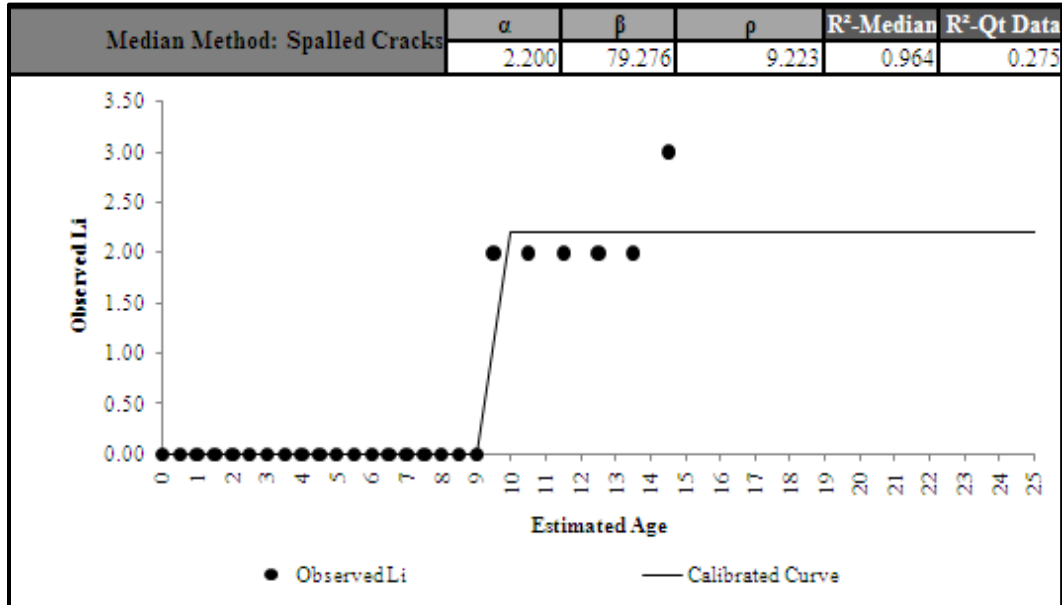


Figure D 13.3. Calibrated Performance Model for Paris District, Li Median Method (Unconstrained).

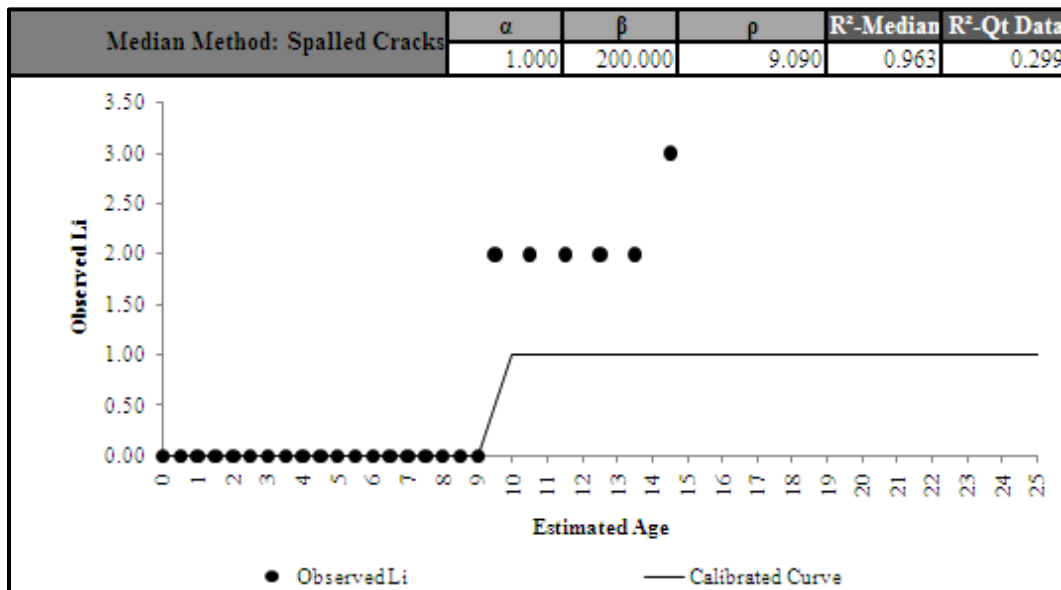


Figure D 13.4. Calibrated Performance Model for Paris District, Li Median Method (Constrained).

Zone 4-Punchouts

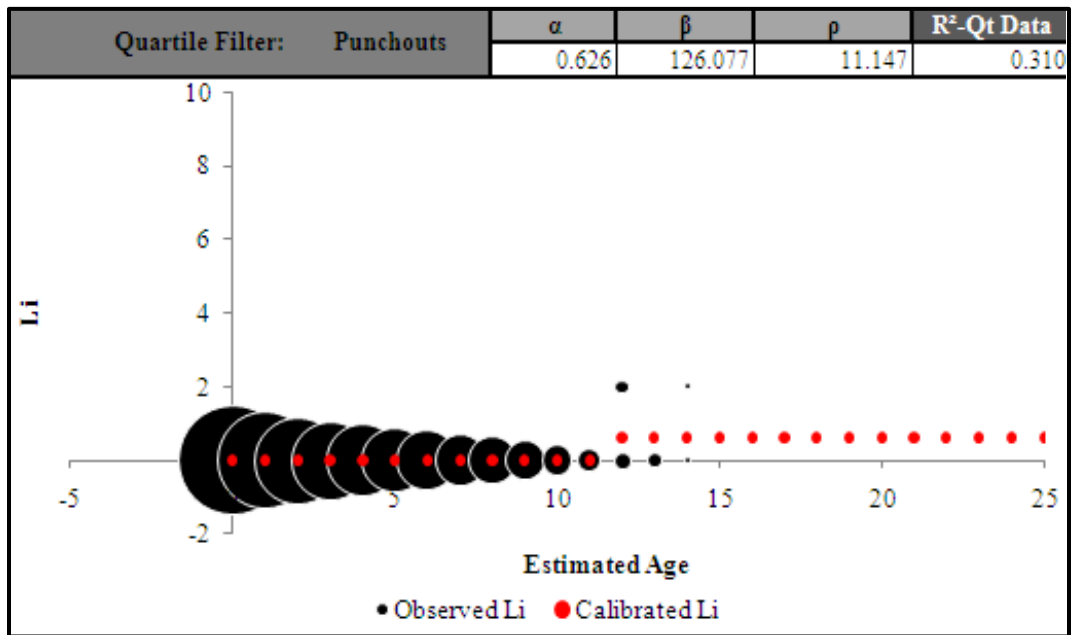


Figure D 14.1. Calibrated Performance Model for Fort Worth District, Li Quartile Method (Unconstrained).

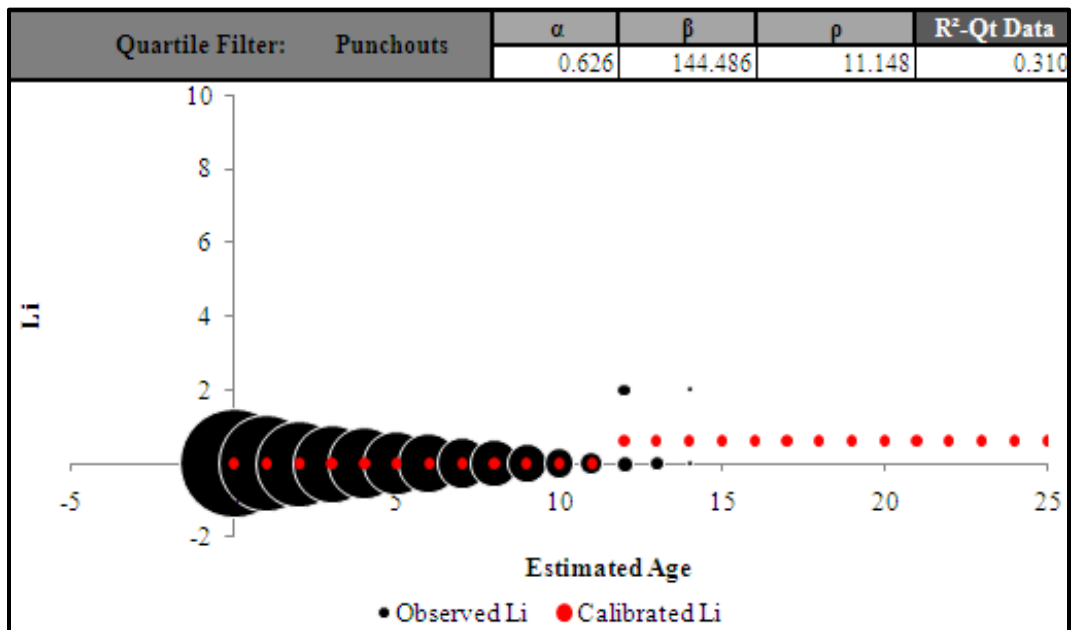


Figure D 14.2. Calibrated Performance Model for Fort Worth District, Li Quartile Method (Constrained).

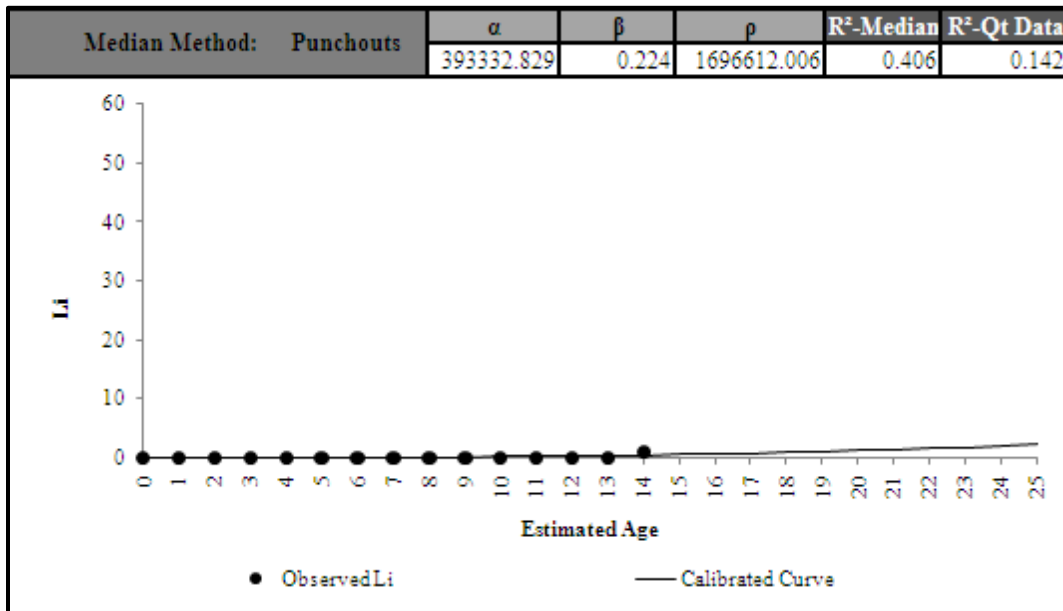


Figure D 14.3. Calibrated Performance Model for Fort Worth District, Li Median Method (Unconstrained).

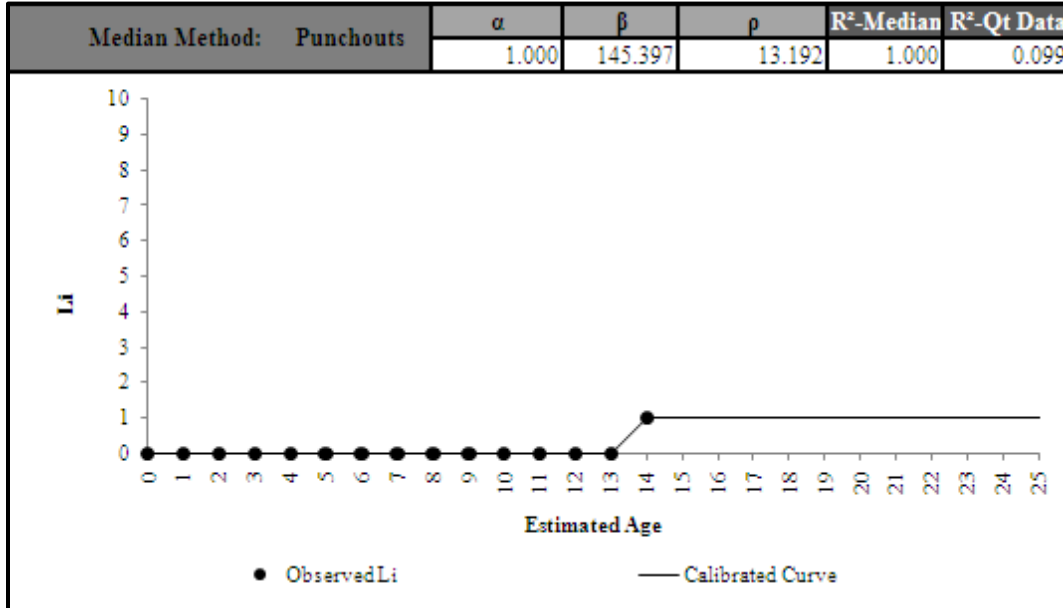


Figure D 14.4. Calibrated Performance Model for Fort Worth District, Li Median Method (Constrained).

Zone 4-PCC Patches

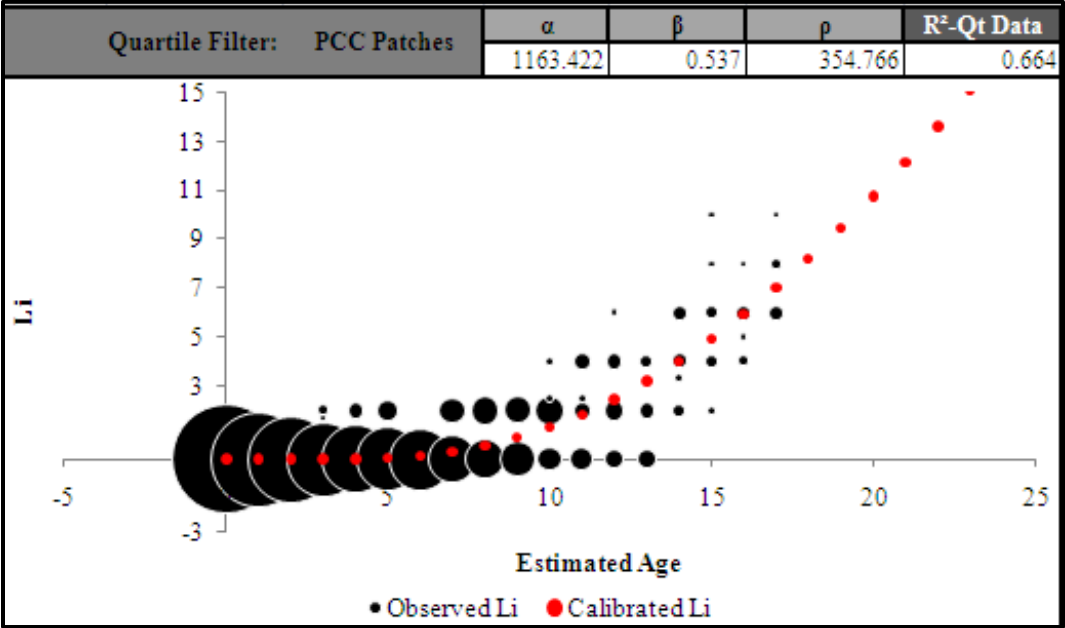


Figure D 16.1. Calibrated Performance Model for Amarillo District, Li Quartile Method (Unconstrained).

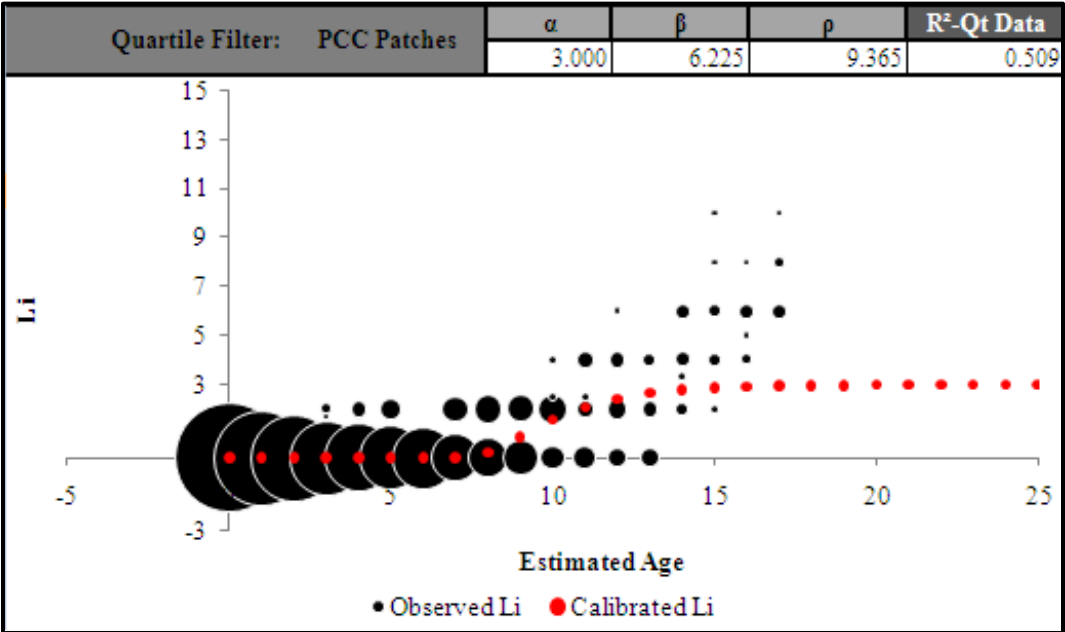


Figure D 16.2. Calibrated Performance Model for Amarillo District, Li Quartile Method (Constrained).

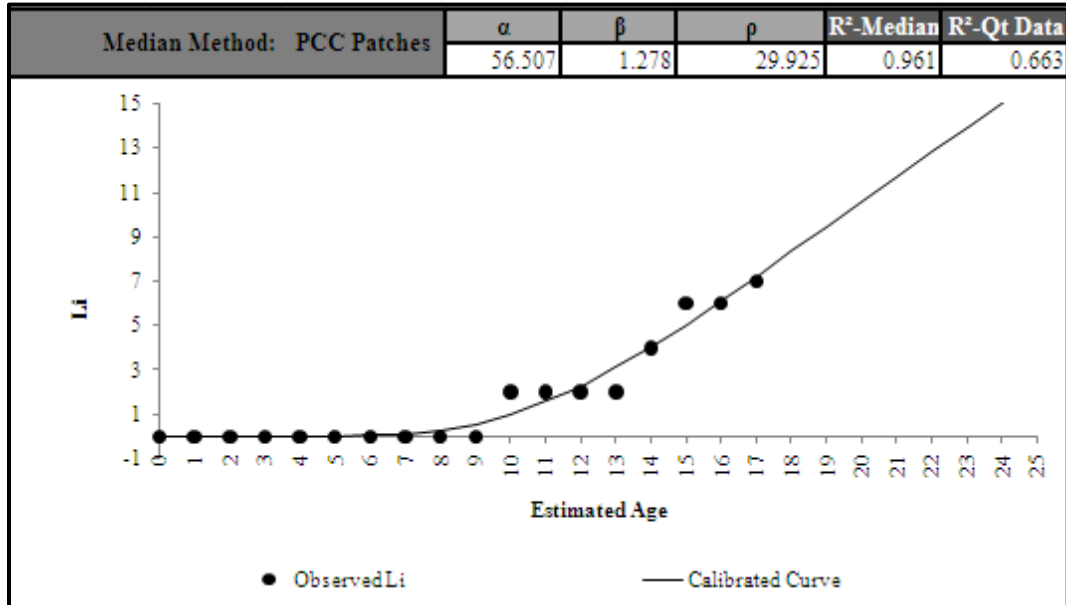


Figure D 16.3. Calibrated Performance Model for Amarillo District, Li Median Method (Unconstrained).

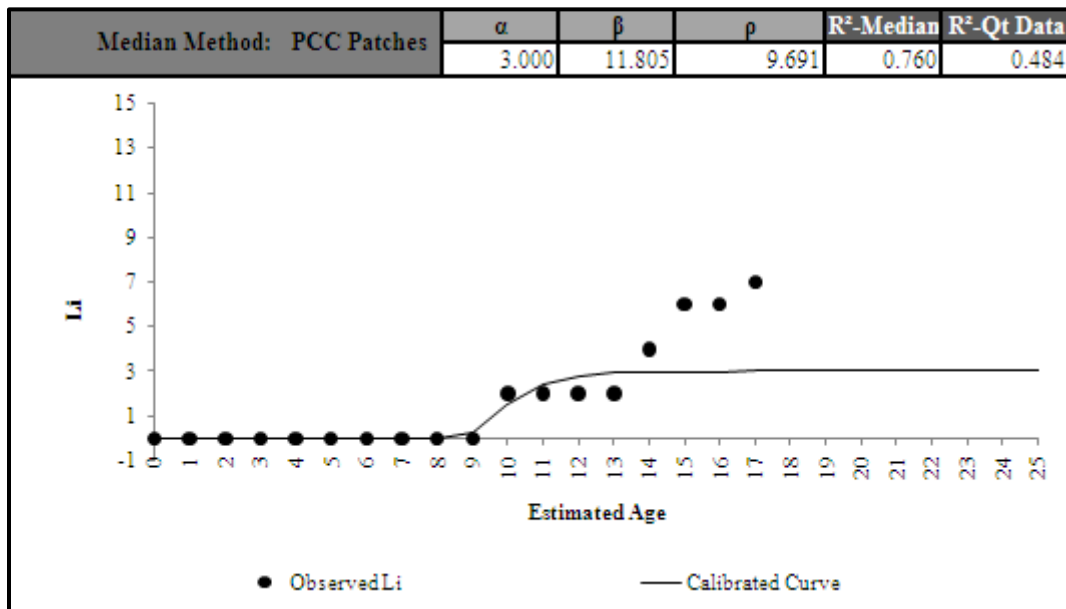


Figure D 16.4. Calibrated Performance Model for Amarillo District, Li Median Method (Constrained).

Appendix E

Calibrated CRCP Ride Quality Performance Models for Texas Districts

Paris District 01

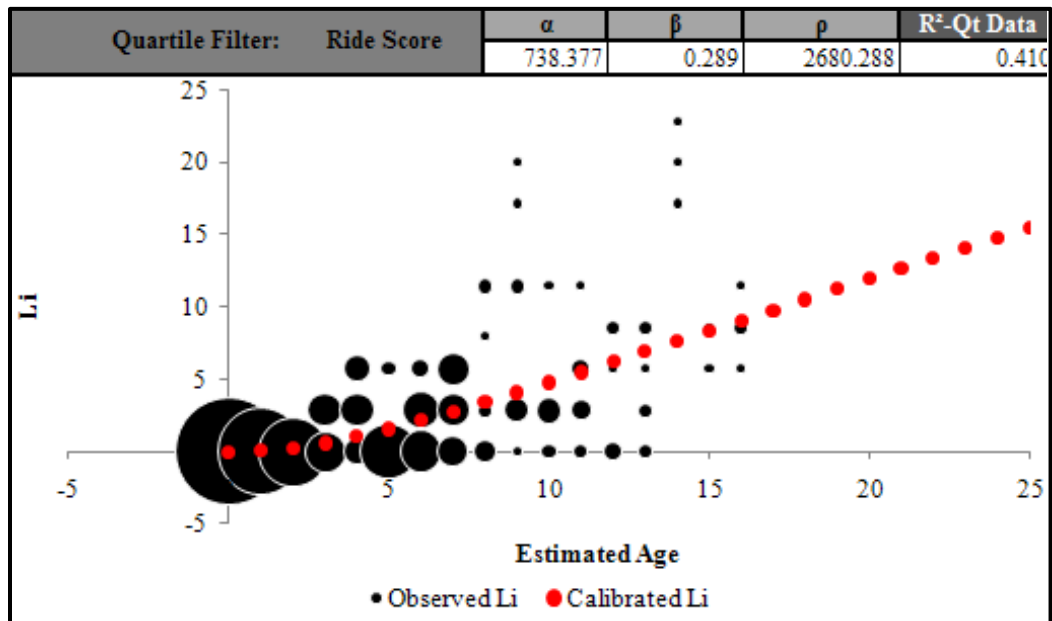


Figure E 1.1. Calibrated Performance Model for Paris District, Li Quartile Method (Unconstrained).

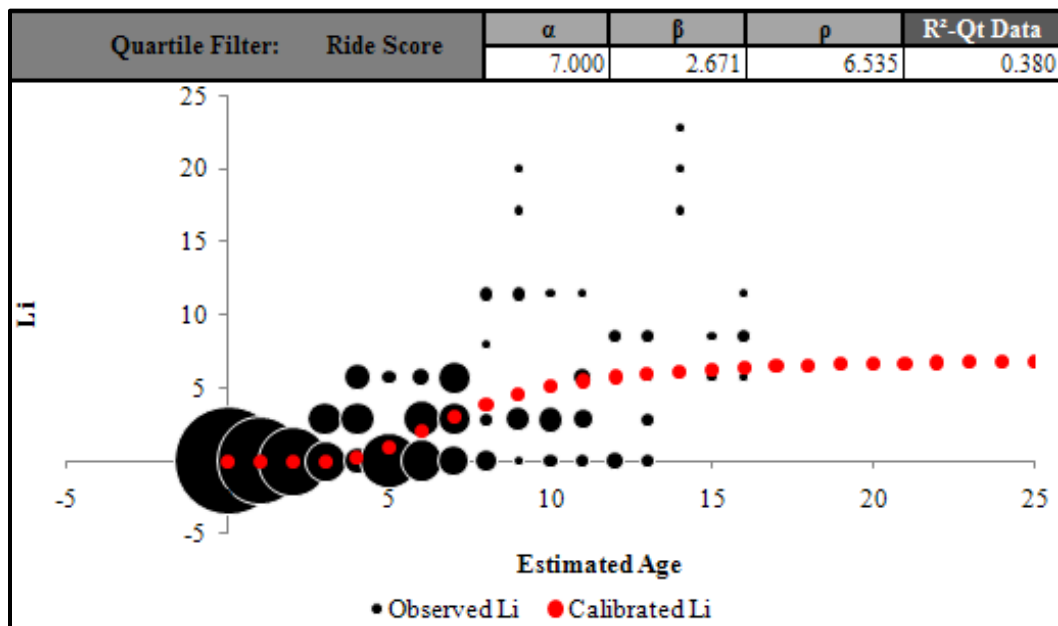


Figure E 1.2. Calibrated Performance Model for Paris District, Li Quartile Method (Constrained).

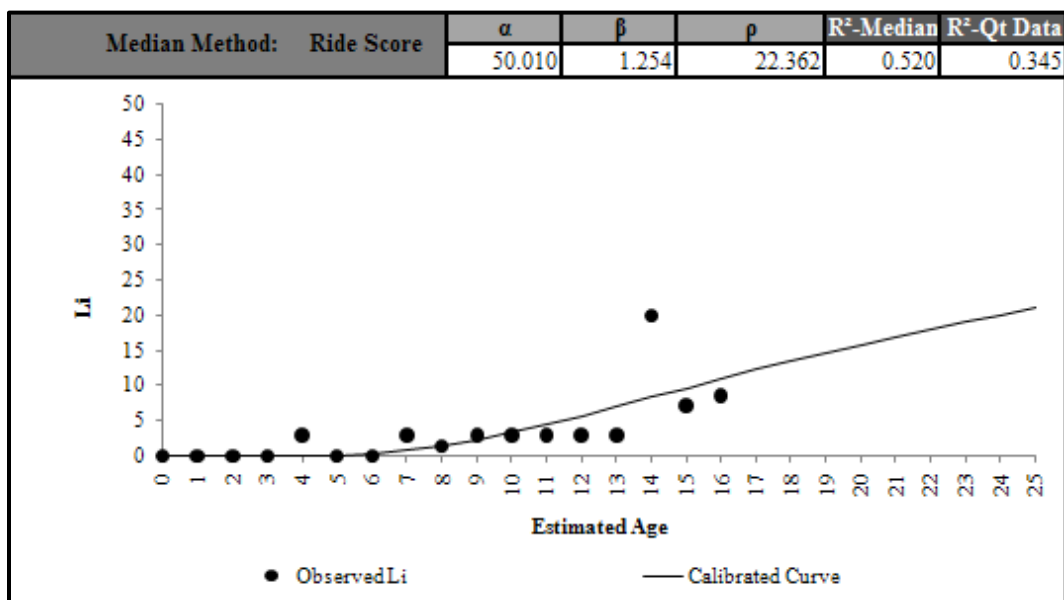


Figure E 1.3. Calibrated Performance Model for Paris District, Li Median Method (Unconstrained).

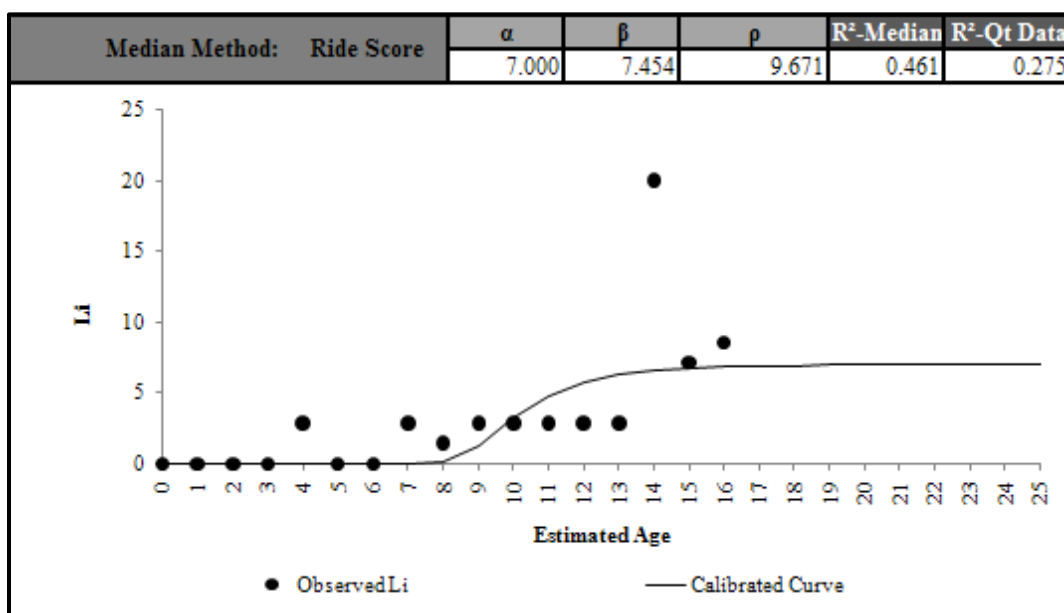


Figure E 1.4. Calibrated Performance Model for Paris District, Li Median Method (Constrained).

Fort Worth District 02

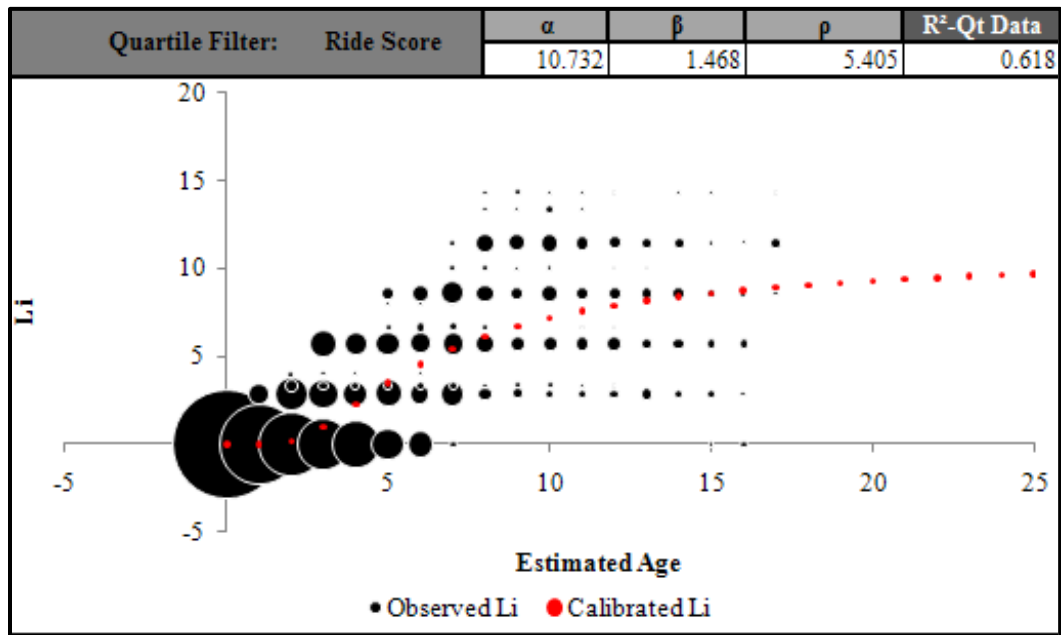


Figure E 2.1. Calibrated Performance Model for Fort Worth District, Li Quartile Method (Unconstrained).

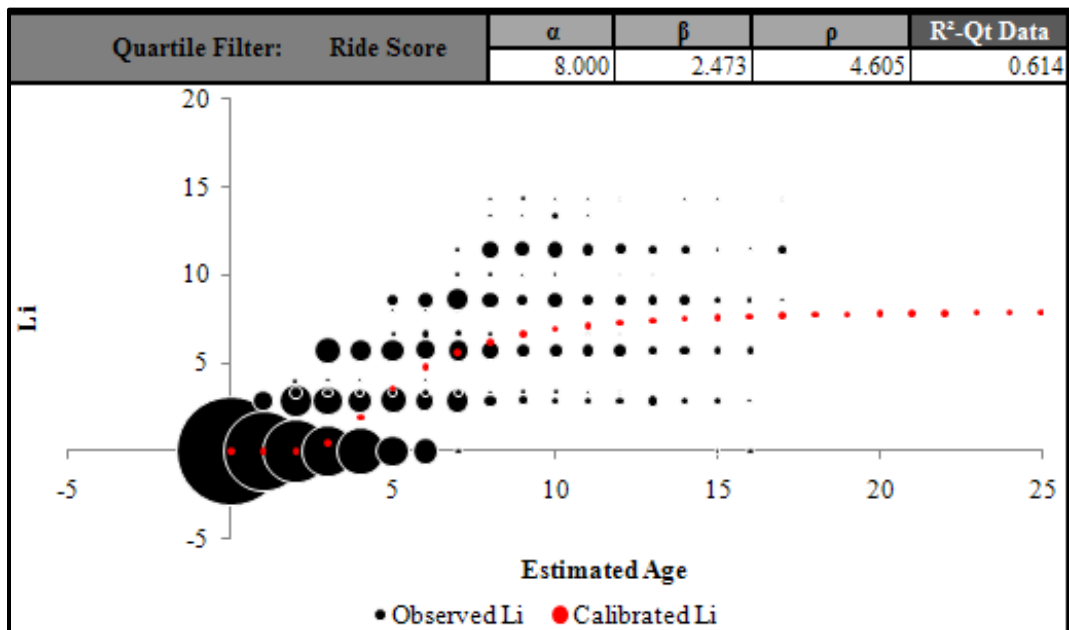


Figure E 2.2. Calibrated Performance Model for Fort Worth District, Li Quartile Method (Constrained).

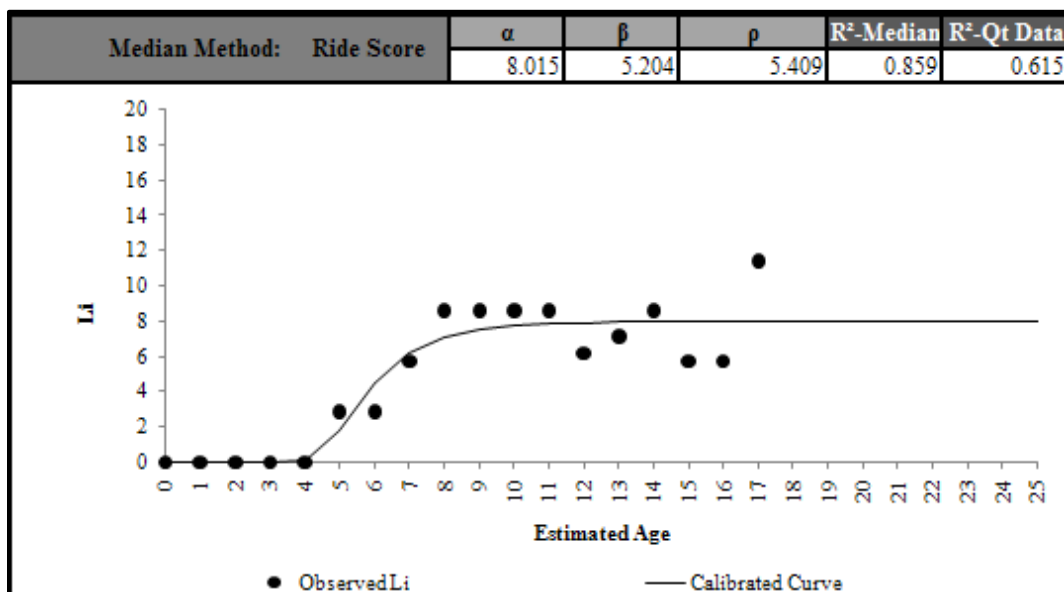


Figure E 2.3. Calibrated Performance Model for Fort Worth District, Li Median Method (Unconstrained).

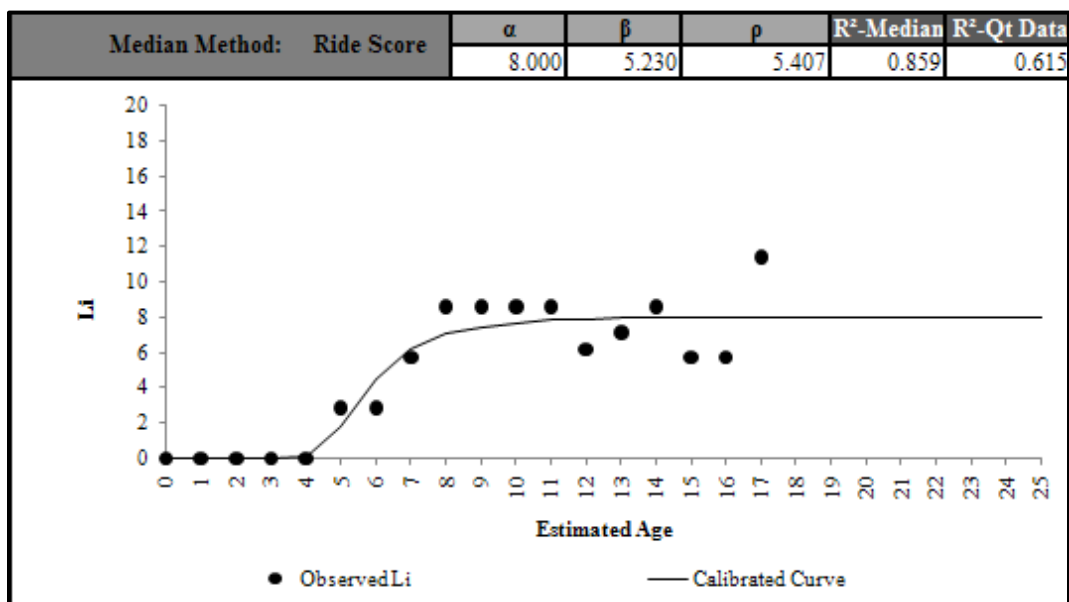


Figure E 2.4. Calibrated Performance Model for Fort Worth District, Li Median Method (Constrained).

Wichita Falls District 03

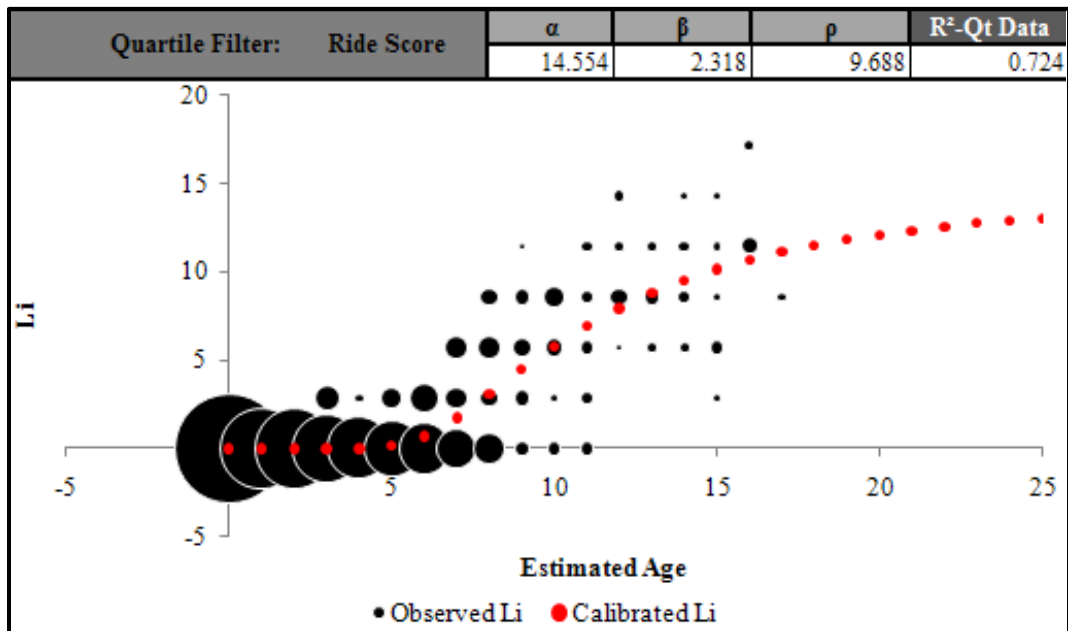


Figure E 3.1. Calibrated Performance Model for Wichita Falls District, Li Quartile Method (Unconstrained).

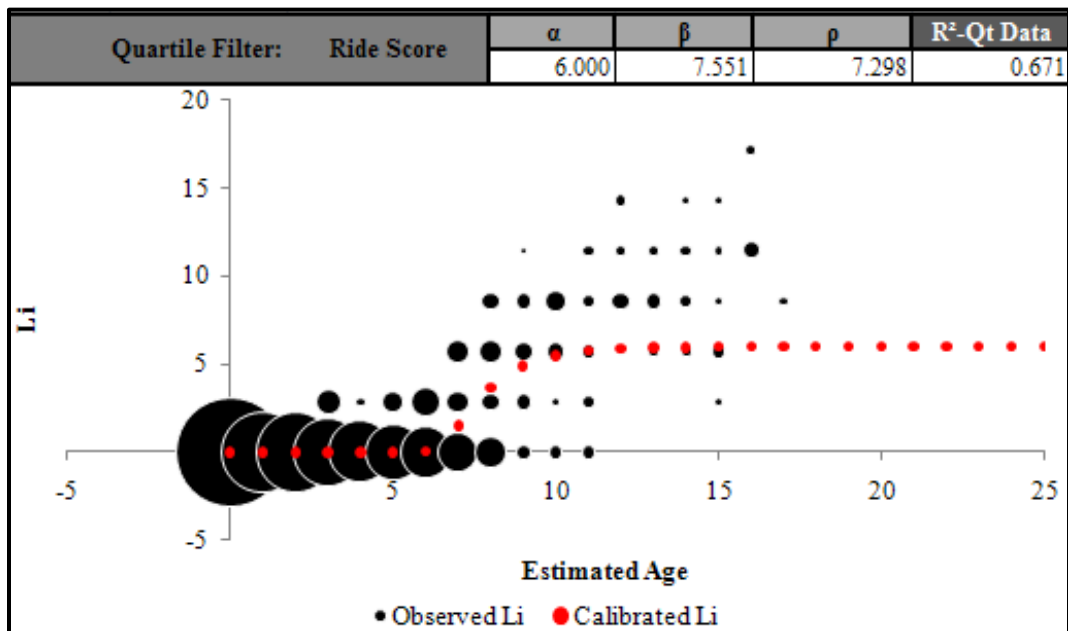


Figure E 3.2. Calibrated Performance Model for Wichita Falls District, Li Quartile Method (Constrained).

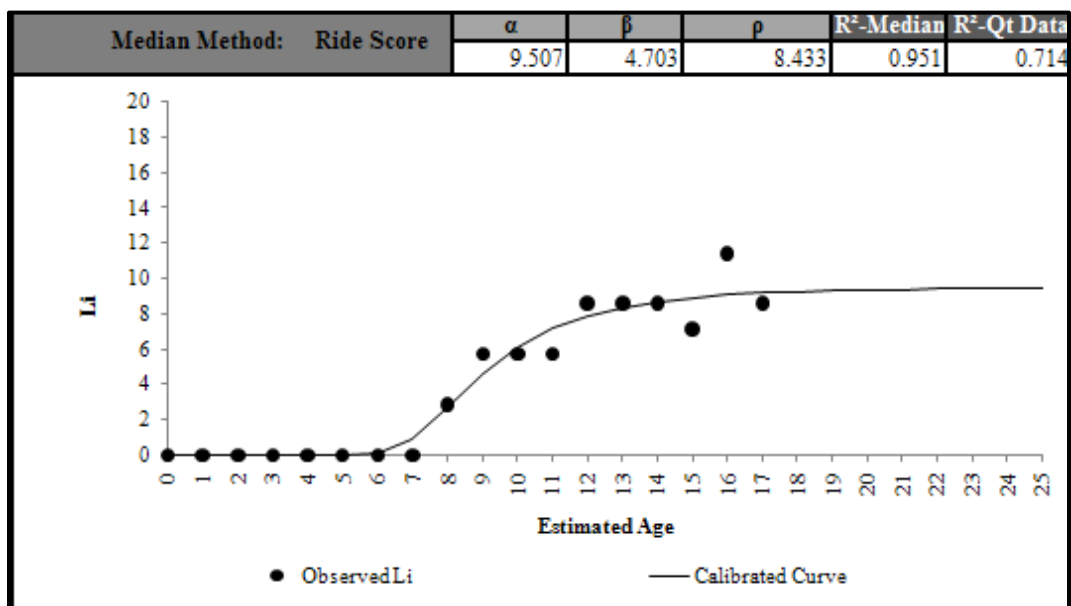


Figure E 3.3. Calibrated Performance Model for Wichita Falls District, Li Median Method (Unconstrained).

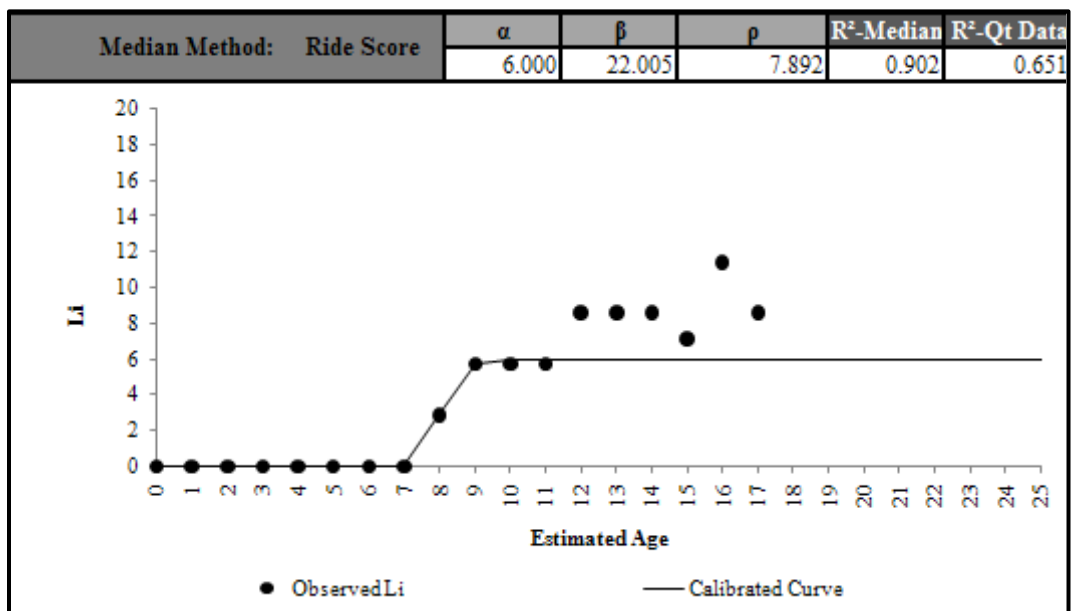


Figure E 3.4. Calibrated Performance Model for Wichita Falls District, Li Median Method (Constrained).

Amarillo District 04

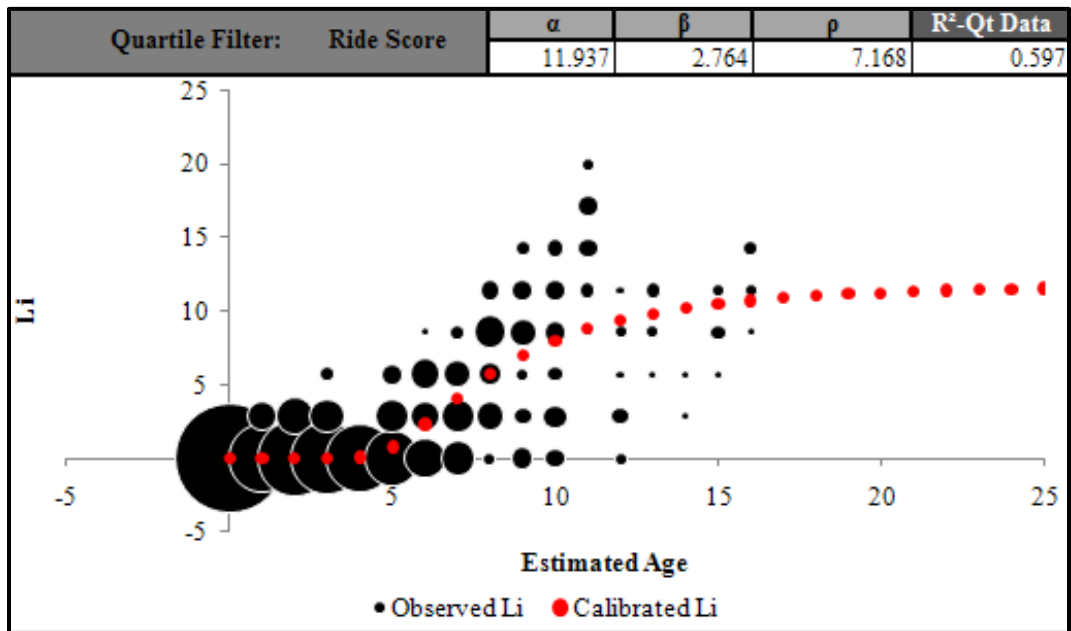


Figure E 4.1. Calibrated Performance Model for Amarillo District, Li Quartile Method (Unconstrained).

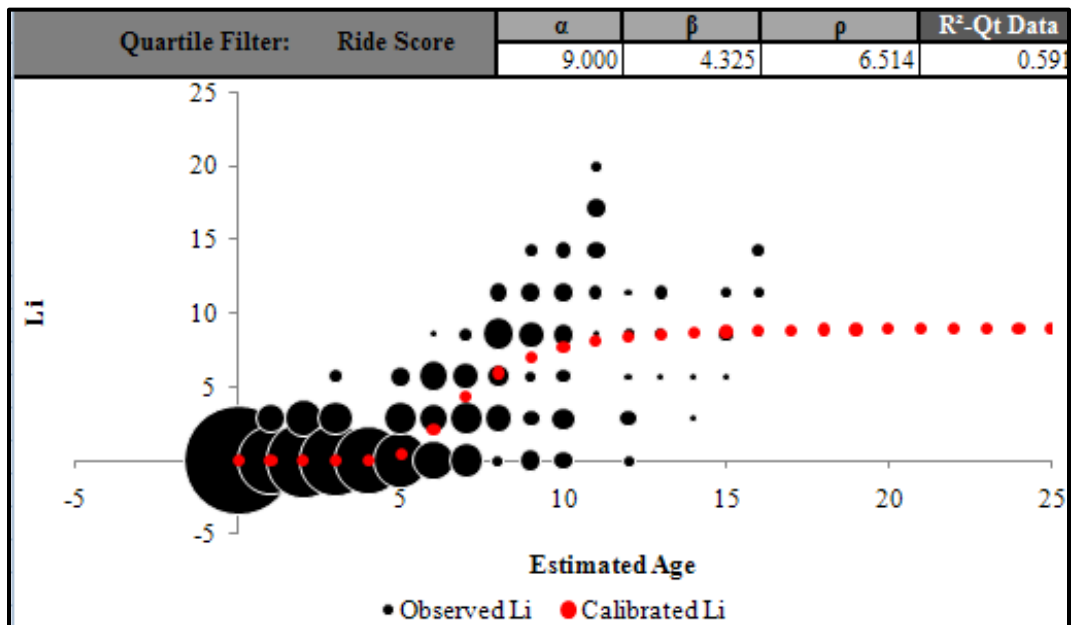


Figure E 4.2. Calibrated Performance Model for Amarillo District, Li Quartile Method (Constrained).

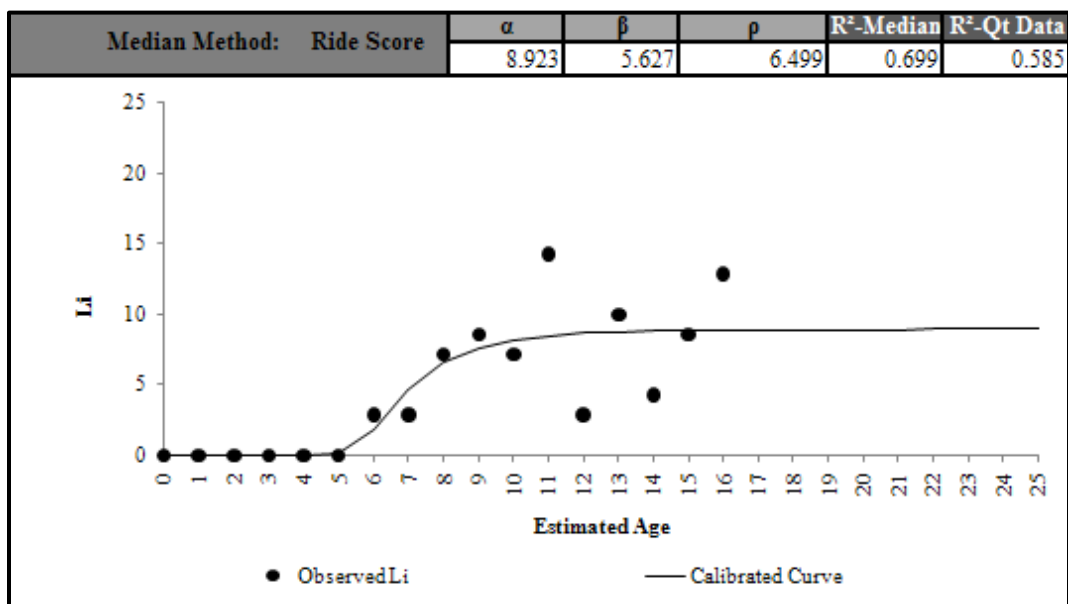


Figure E 4.3. Calibrated Performance Model for Amarillo District, Li Median Method (Unconstrained).

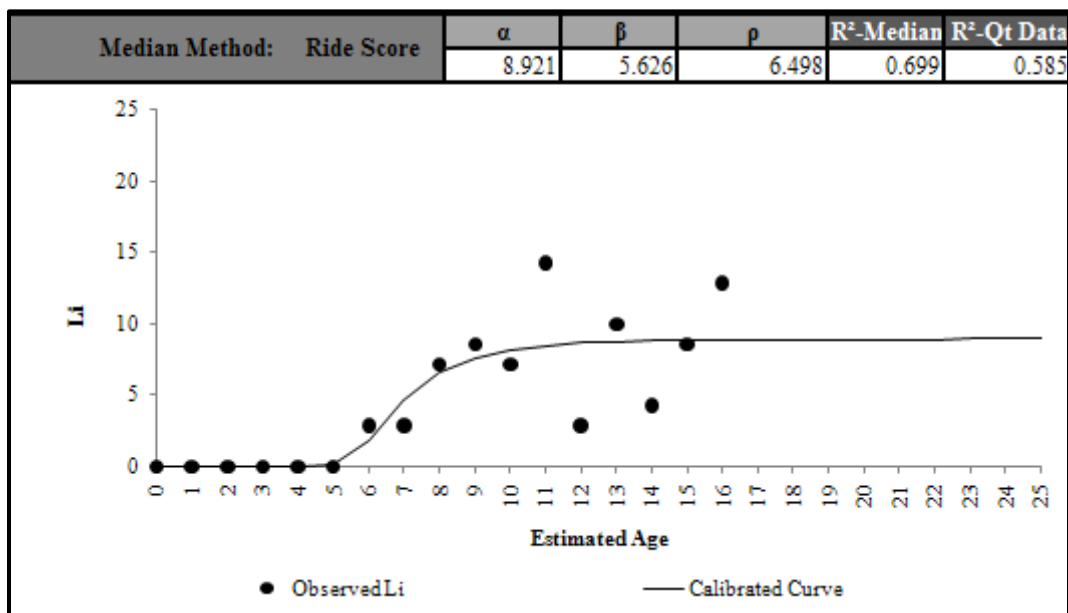


Figure E 4.4. Calibrated Performance Model for Amarillo District, Li Median Method (Constrained).

Lubbock District 05

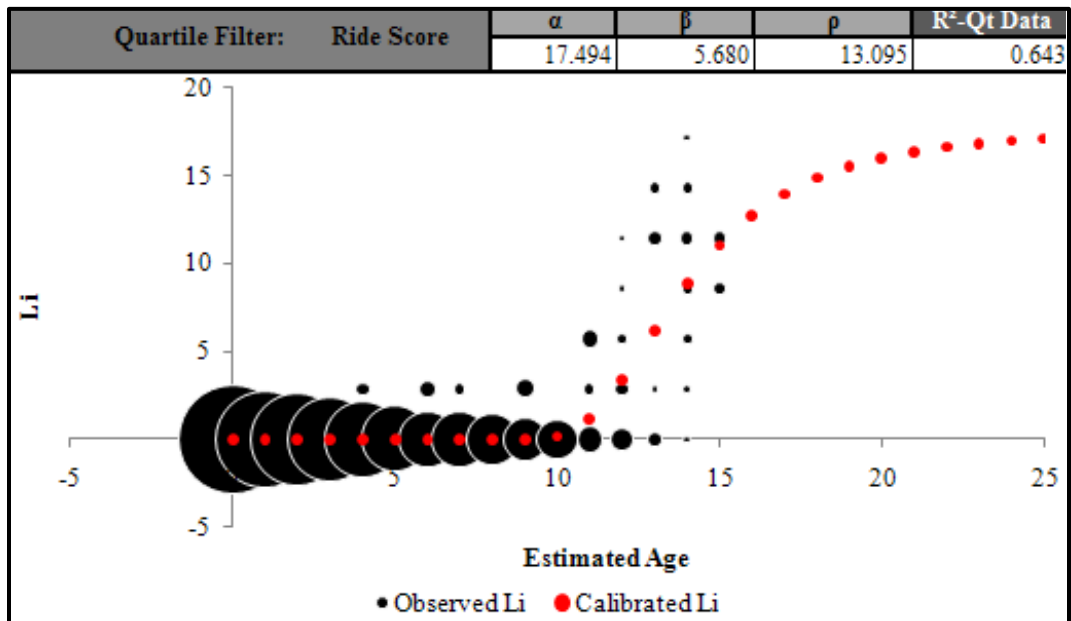


Figure E 5.1. Calibrated Performance Model for Lubbock District, Li Quartile Method (Unconstrained).

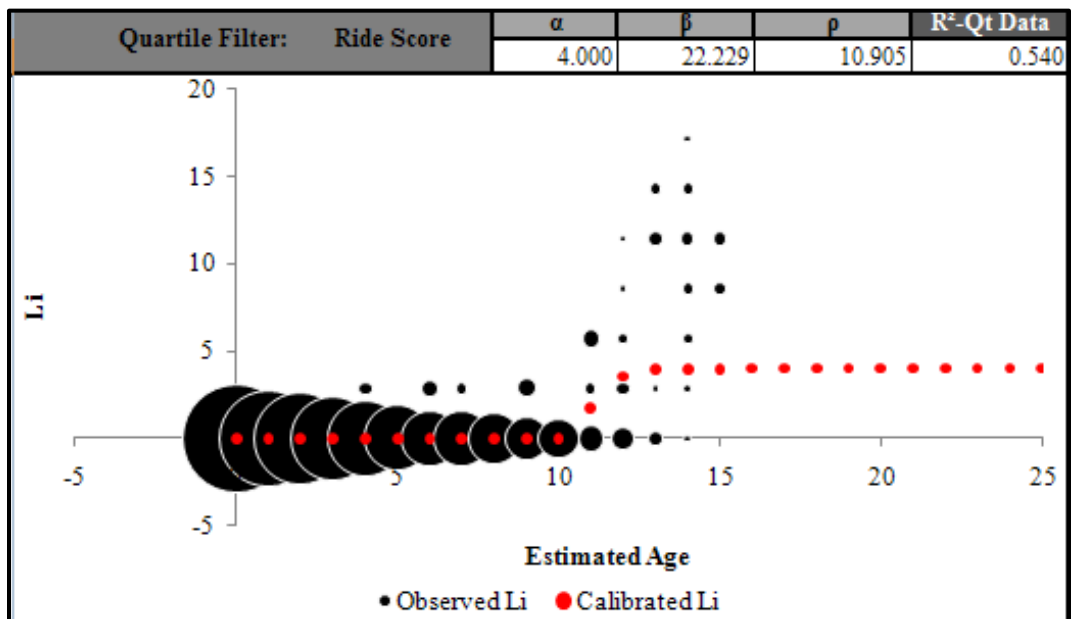


Figure E 5.2. Calibrated Performance Model for Lubbock District, Li Quartile Method (Constrained).

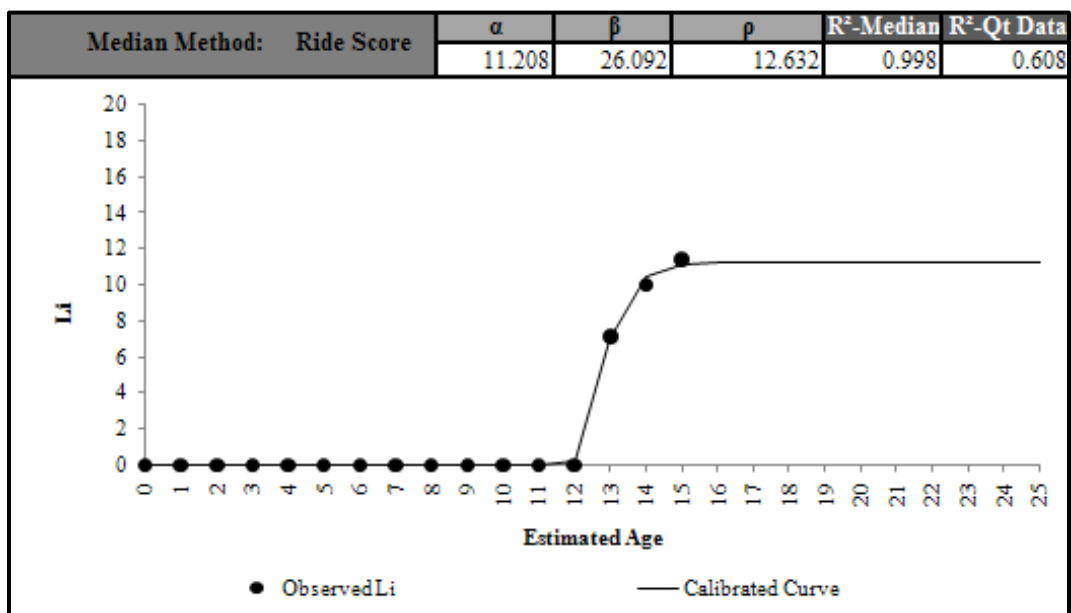


Figure E 5.3. Calibrated Performance Model for Lubbock District, Li Median Method (Unconstrained).

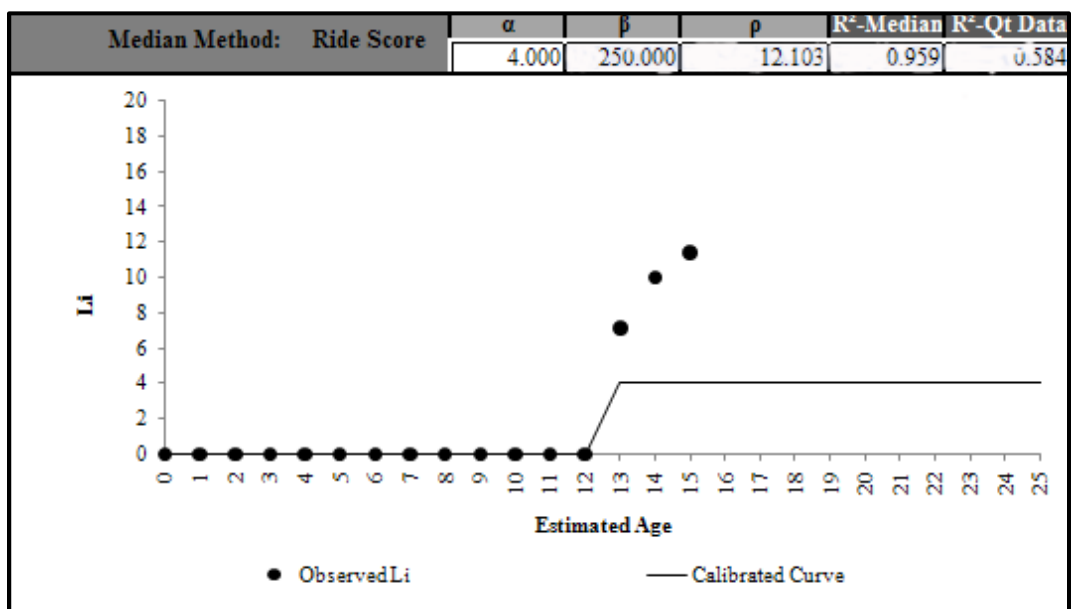


Figure E 5.4. Calibrated Performance Model for Lubbock District, Li Median Method (Constrained).

Odessa District 06

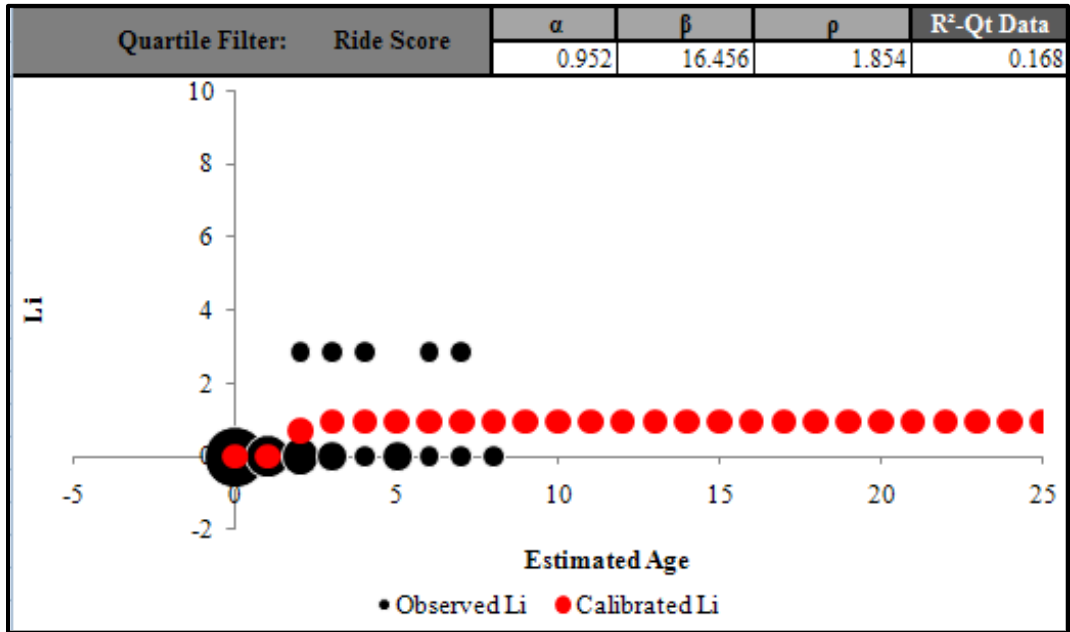


Figure E 6.1. Calibrated Performance Model for Odessa District, Li Quartile Method (Unconstrained).

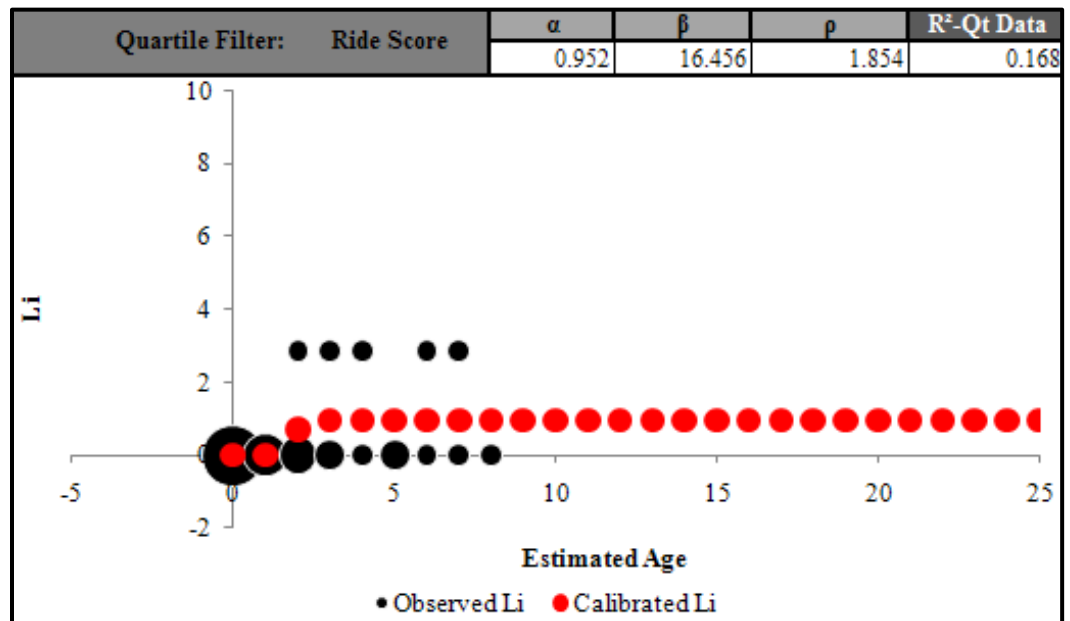


Figure E 6.2. Calibrated Performance Model for Odessa District, Li Quartile Method (Constrained).

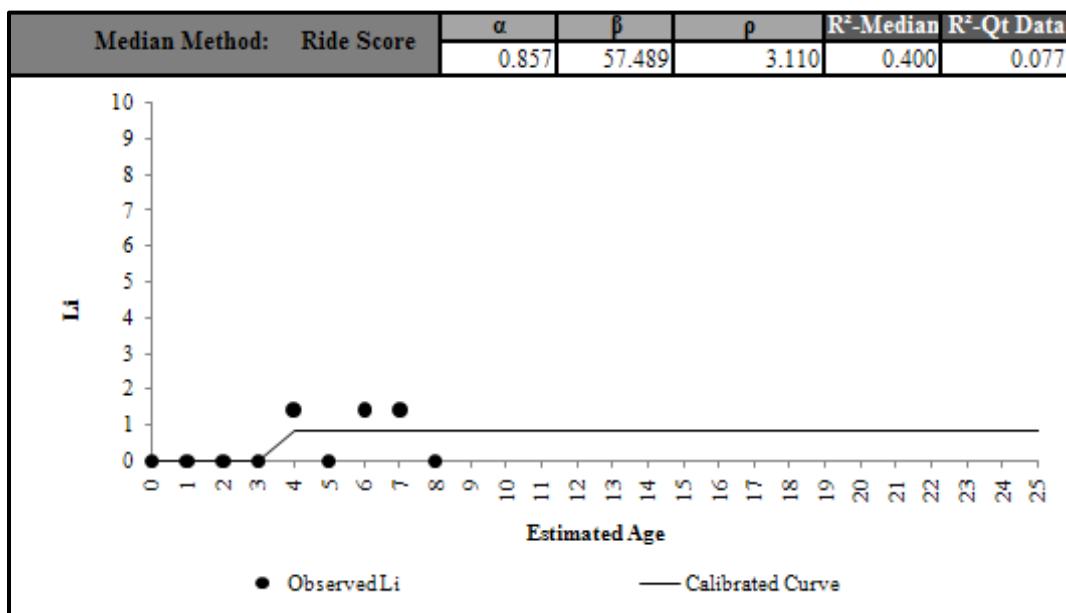


Figure E 6.3. Calibrated Performance Model for Odessa District, Li Median Method (Unconstrained).

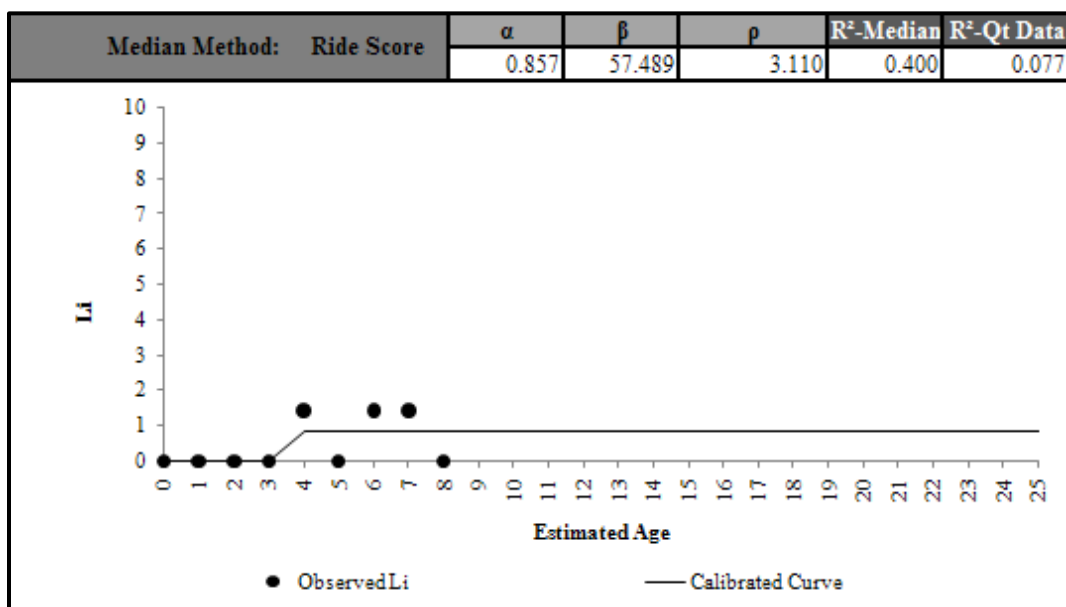


Figure E 6.4. Calibrated Performance Model for Odessa District, Li Median Method (Constrained).

Waco District 09

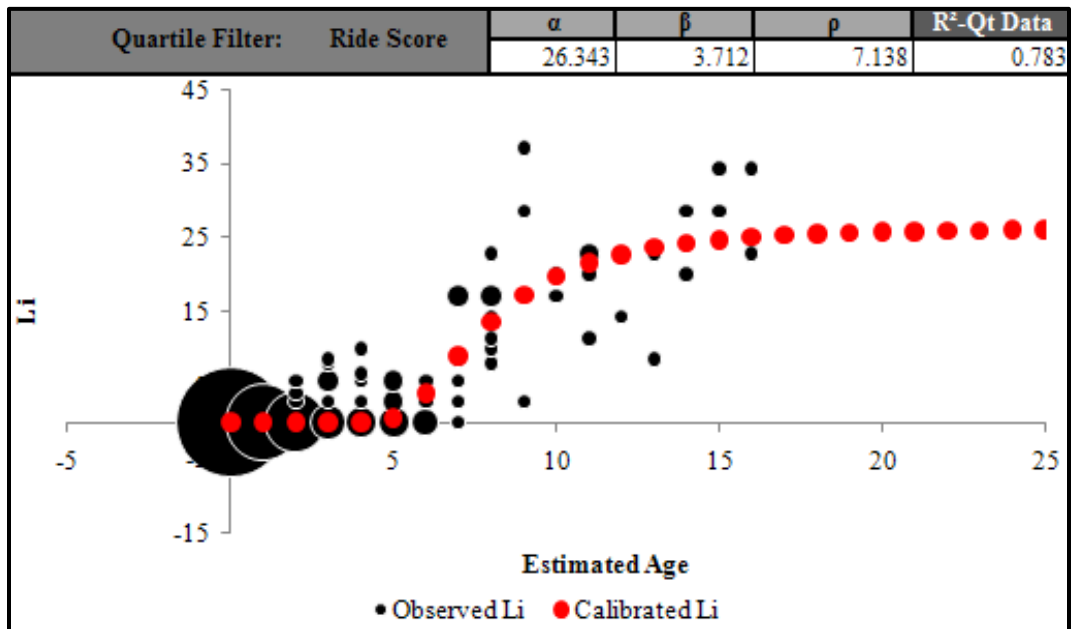


Figure E 9.1. Calibrated Performance Model for Waco District, Li Quartile Method (Unconstrained).

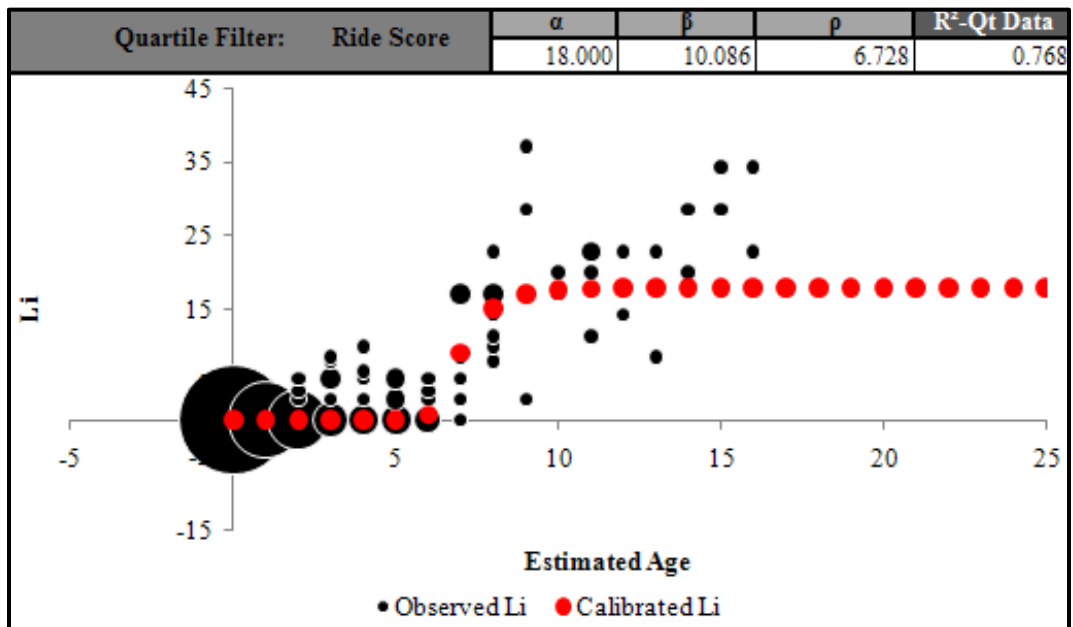


Figure E 9.2. Calibrated Performance Model for Waco District, Li Quartile Method (Constrained).

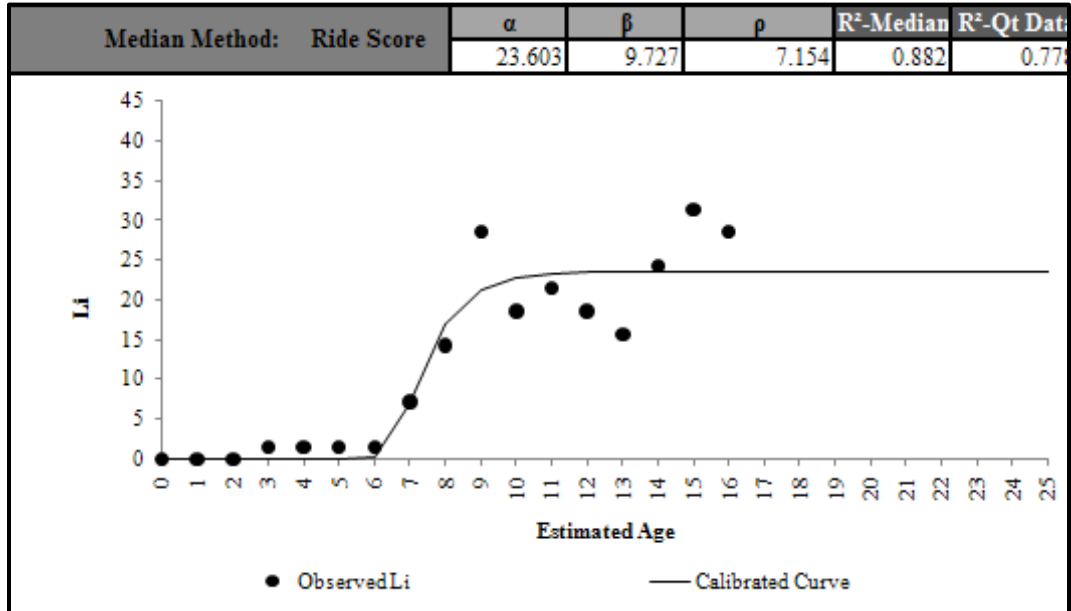


Figure E 9.3. Calibrated Performance Model for Waco District, Li Median Method (Unconstrained).

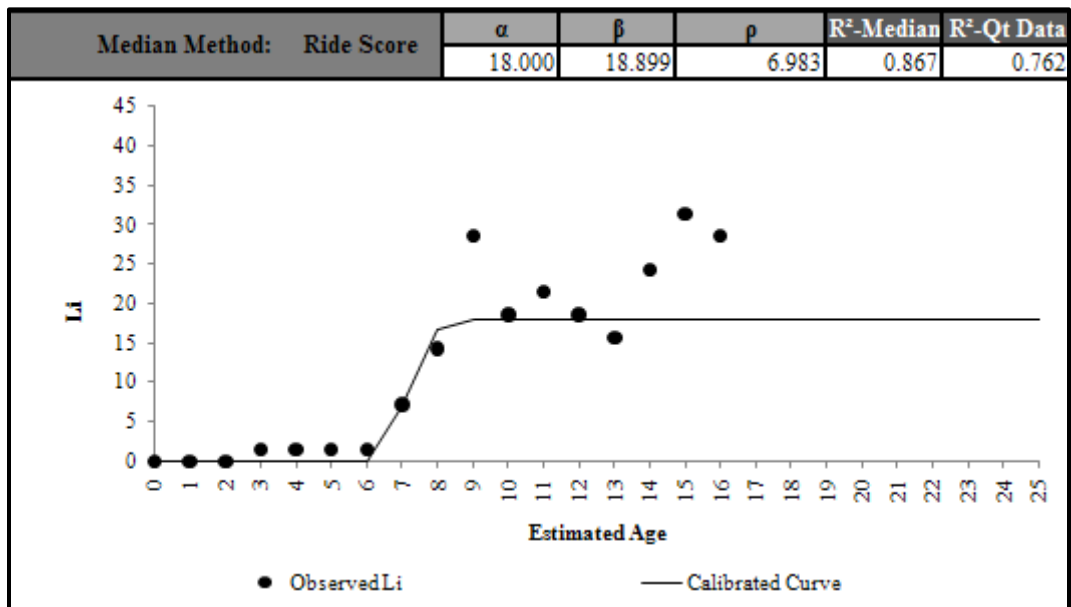


Figure E 9.4. Calibrated Performance Model for Waco District, Li Median Method (Constrained).

Houston District 12

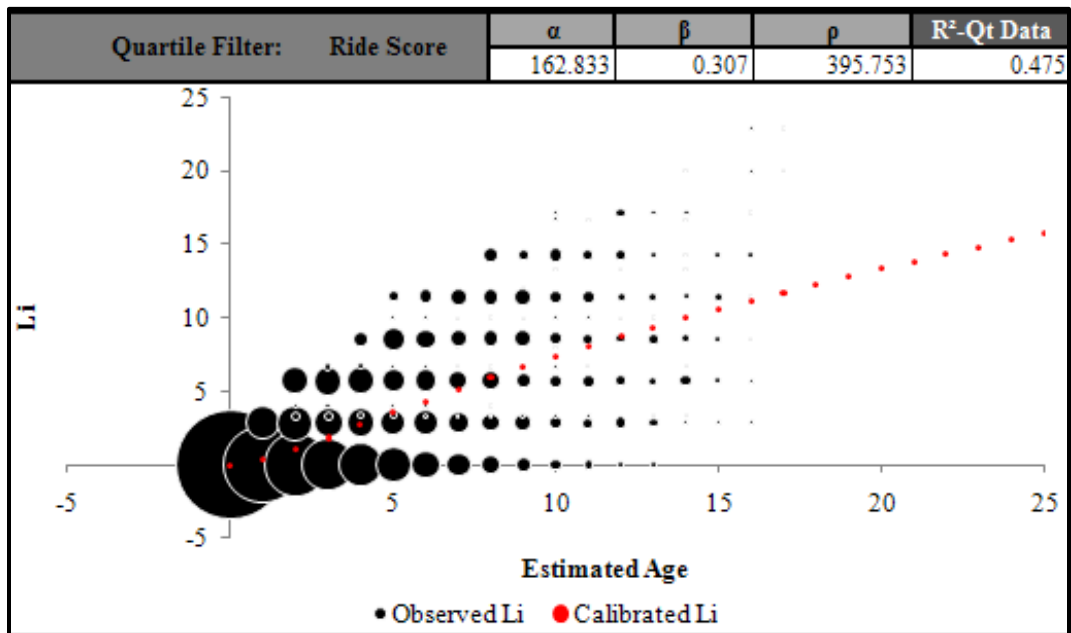


Figure E 12.1. Calibrated Performance Model for Houston District, Li Quartile Method (Unconstrained).

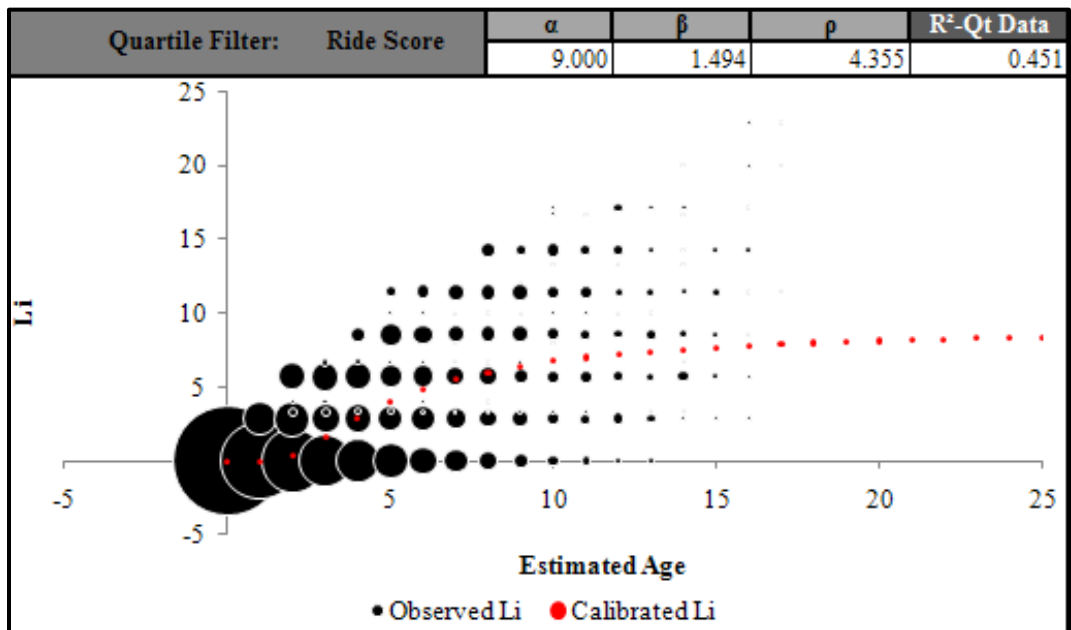


Figure E 12.2. Calibrated Performance Model for Houston District, Li Quartile Method (Constrained).

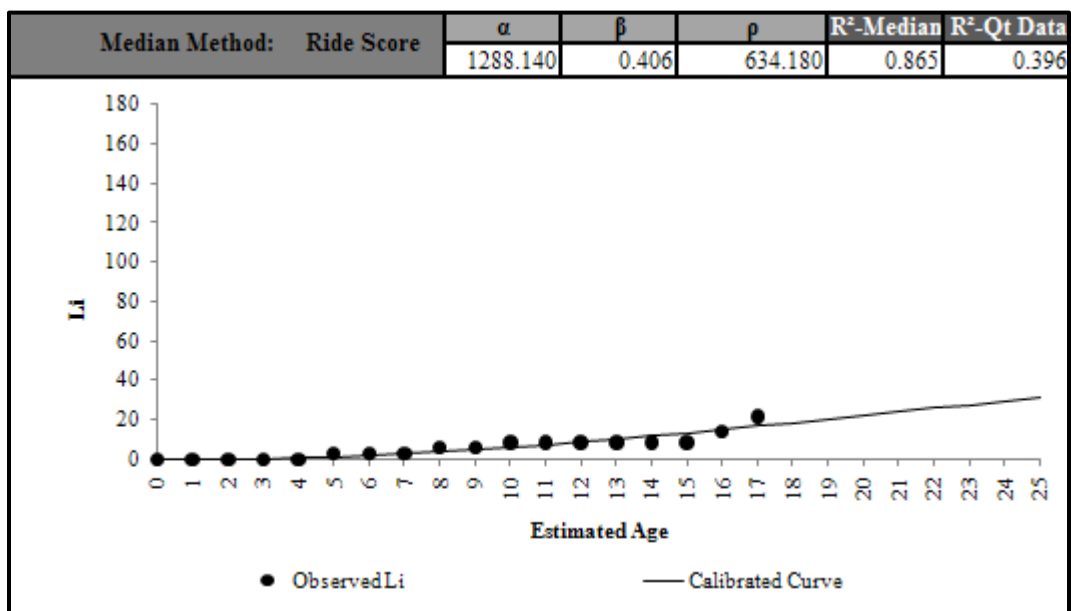


Figure E 12.3. Calibrated Performance Model for Houston District, Li Median Method (Unconstrained).

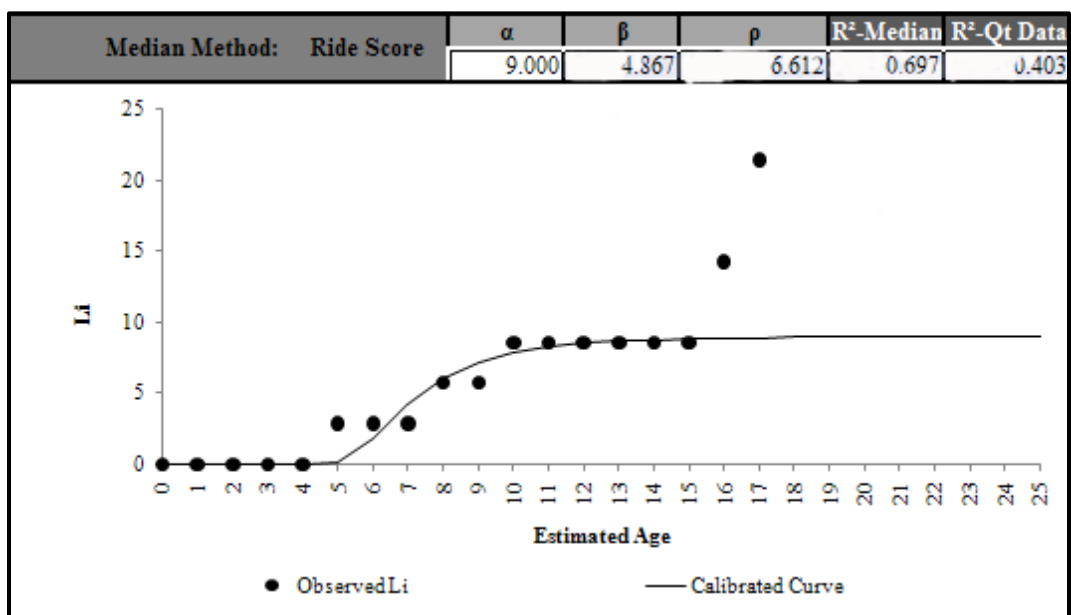


Figure E 12.4. Calibrated Performance Model for Houston District, Li Median Method (Constrained).

Yoakum District 13

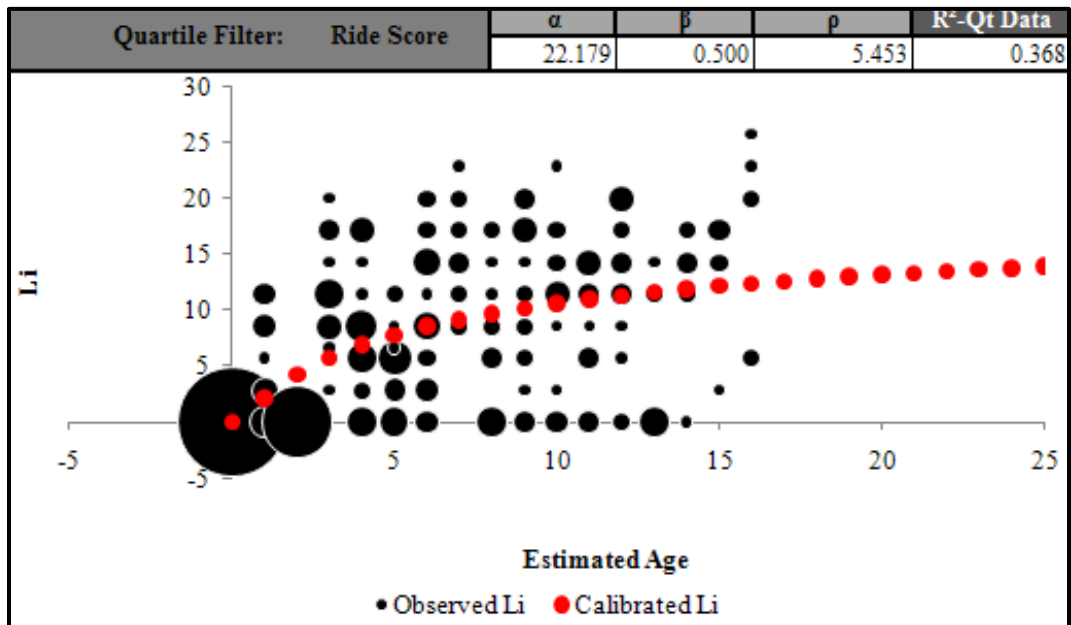


Figure E 13.1. Calibrated Performance Model for Yoakum District, Li Quartile Method (Unconstrained).

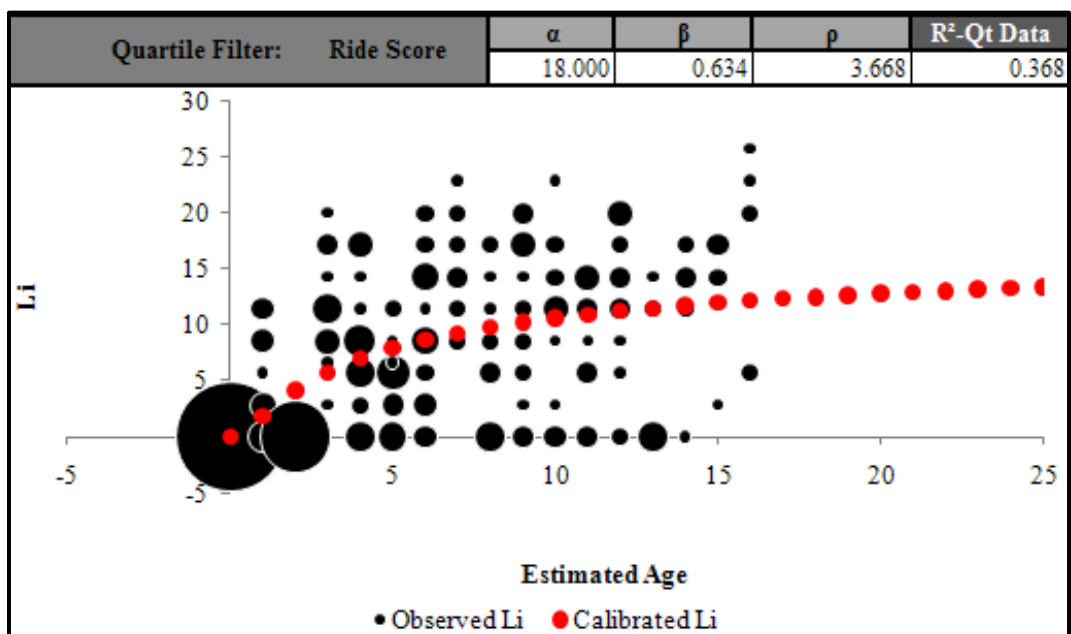


Figure E 13.2. Calibrated Performance Model for Yoakum District, Li Quartile Method (Constrained).

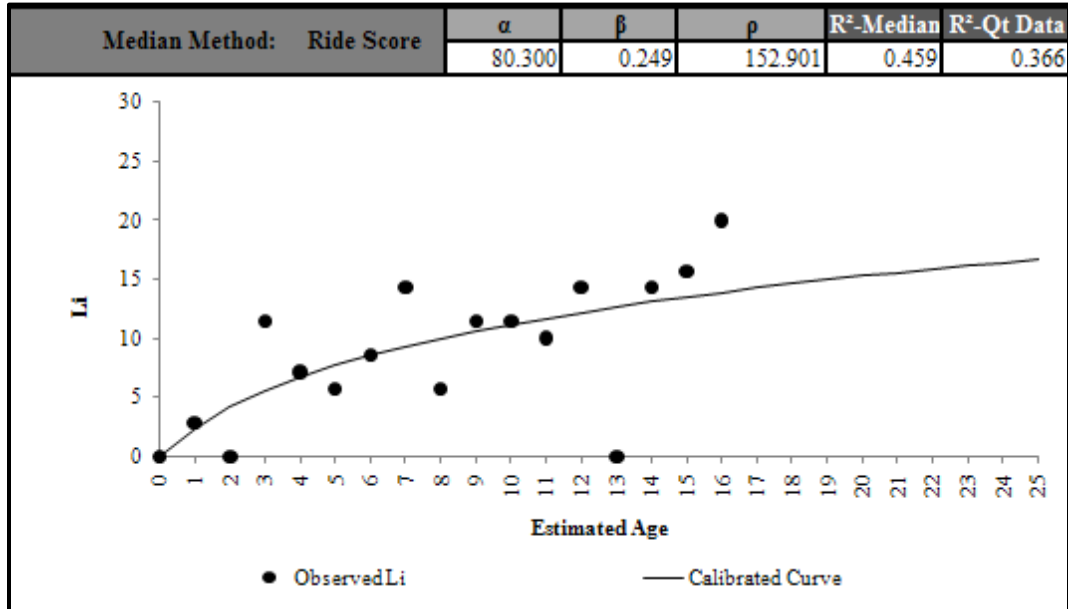


Figure E 13.3. Calibrated Performance Model for Yoakum District, Li Median Method (Unconstrained).

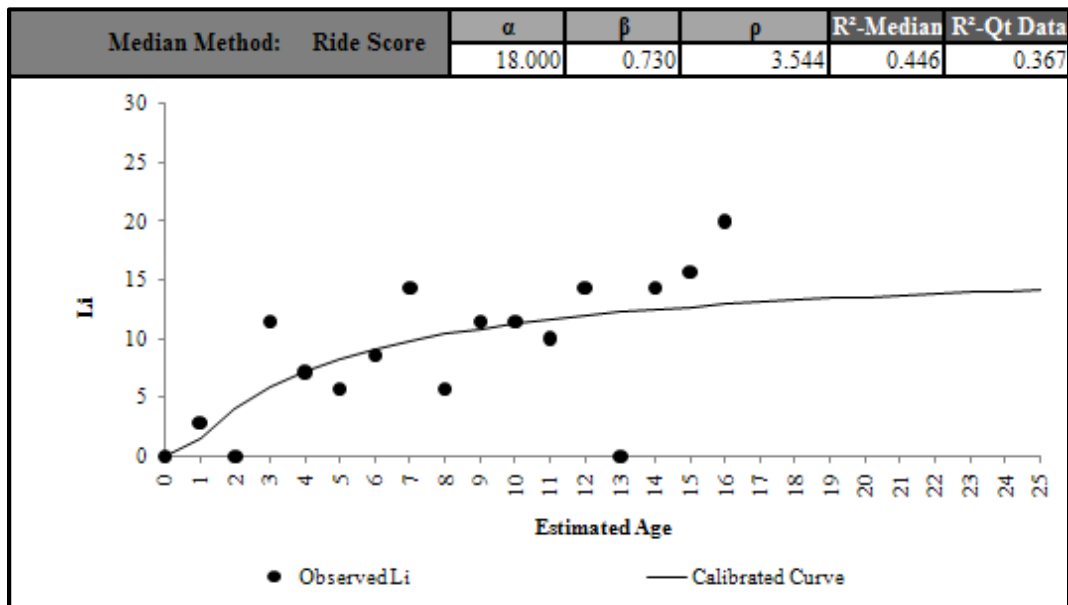


Figure E 13.4. Calibrated Performance Model for Yoakum District, Li Median Method (Constrained).

Austin District 14

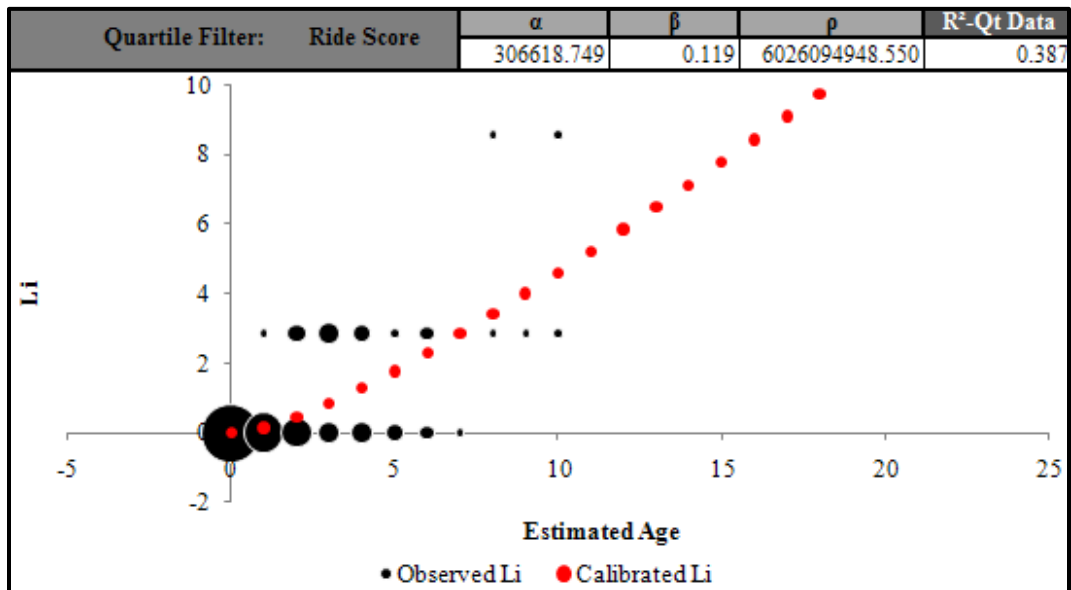


Figure E 14.1. Calibrated Performance Model for Austin District, Li Quartile Method (Unconstrained).

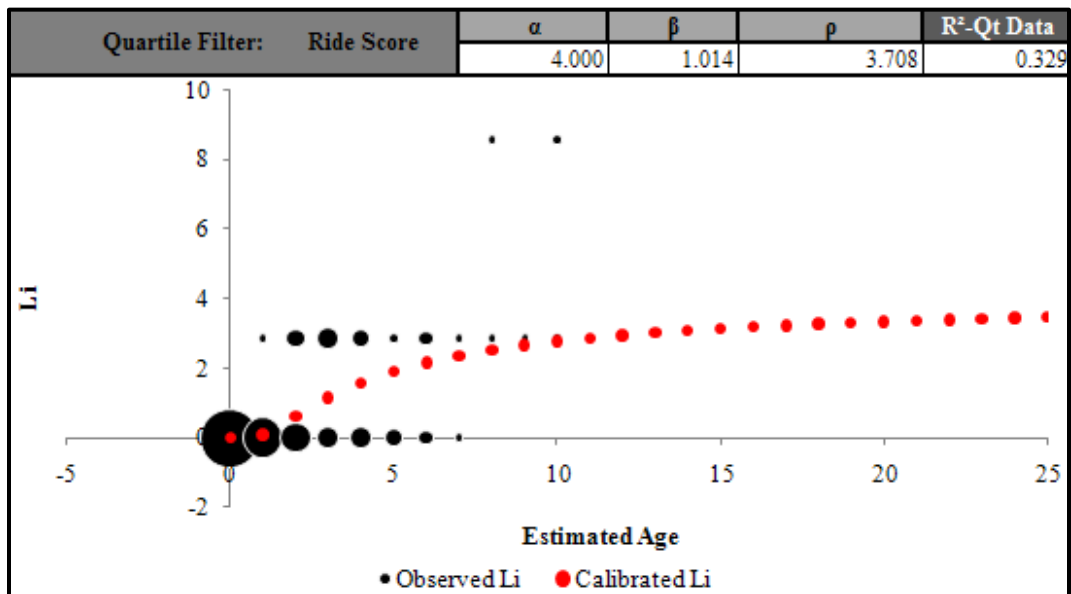


Figure E 14.2. Calibrated Performance Model for Austin District, Li Quartile Method (Constrained).

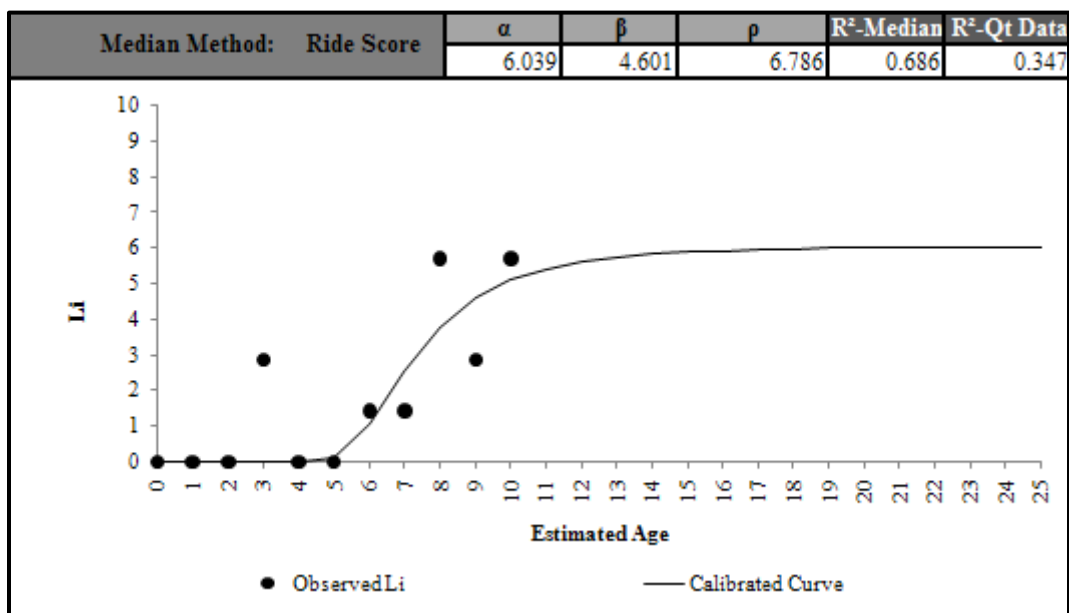


Figure E 14.3. Calibrated Performance Model for Austin District, Li Median Method (Unconstrained).

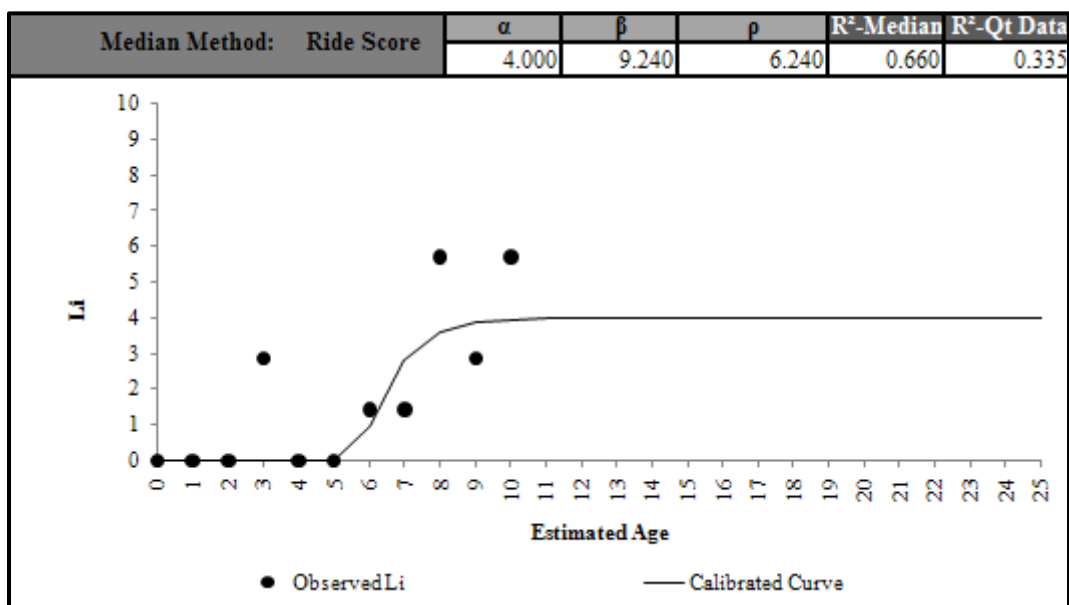


Figure E 14.4. Calibrated Performance Model for Austin District, Li Median Method (Constrained).

San Antonio District 15

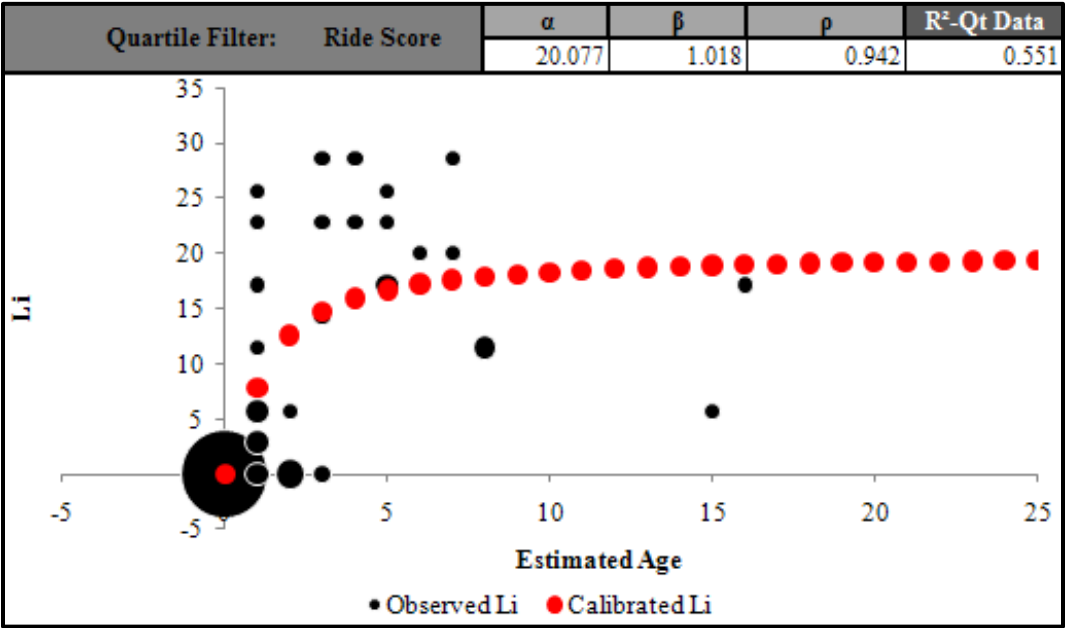


Figure E 15.1. Calibrated Performance Model for San Antonio District, Li Quartile Method (Unconstrained).

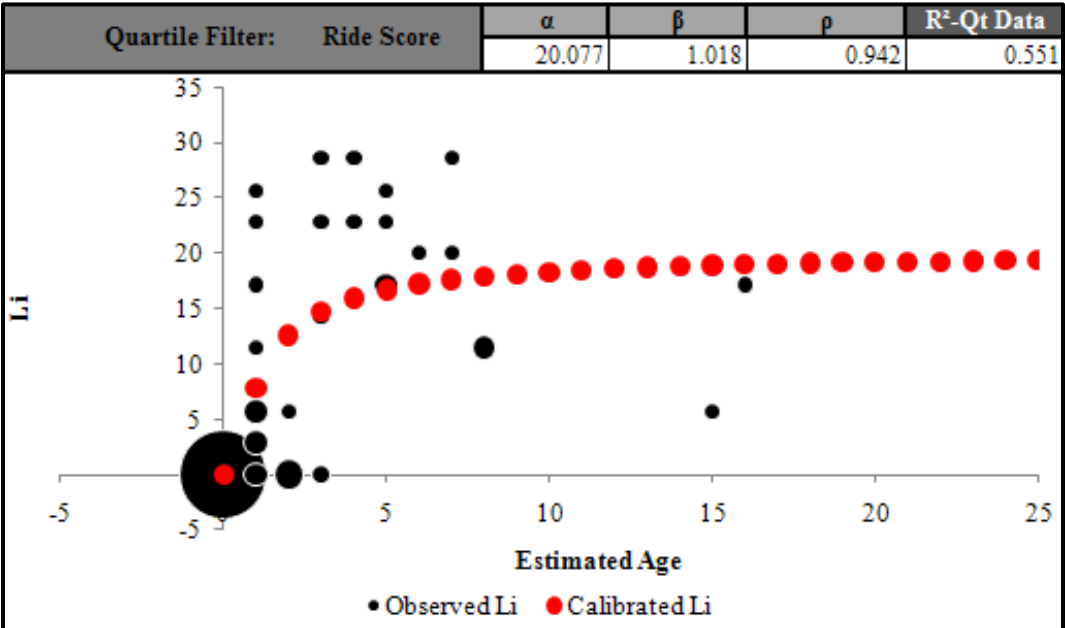


Figure E 15.2. Calibrated Performance Model for San Antonio District, Li Quartile Method (Constrained).

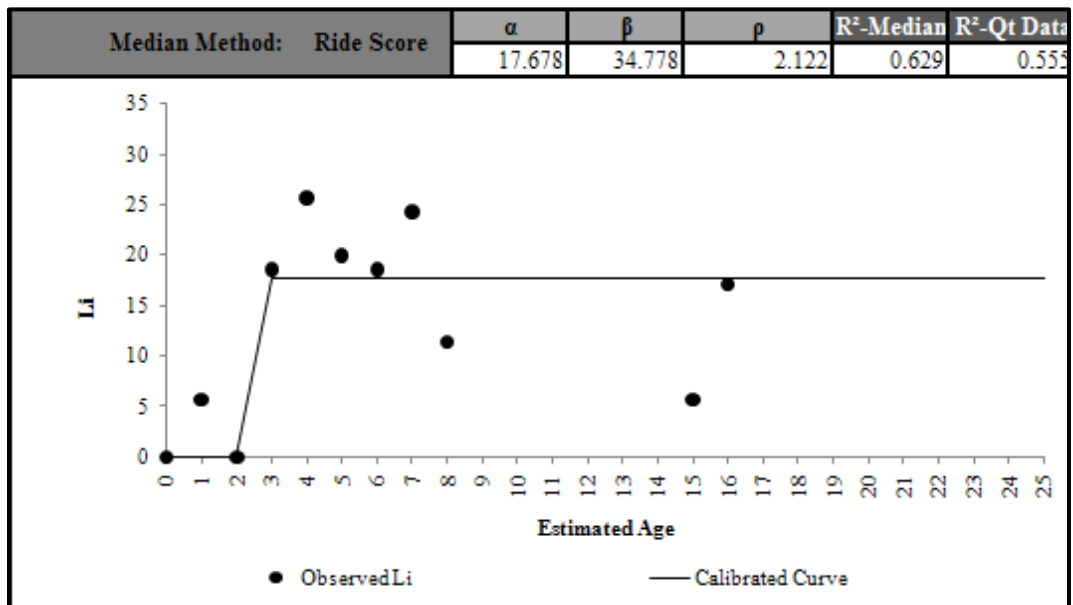


Figure E 15.3. Calibrated Performance Model for San Antonio District, Li Median Method (Unconstrained).

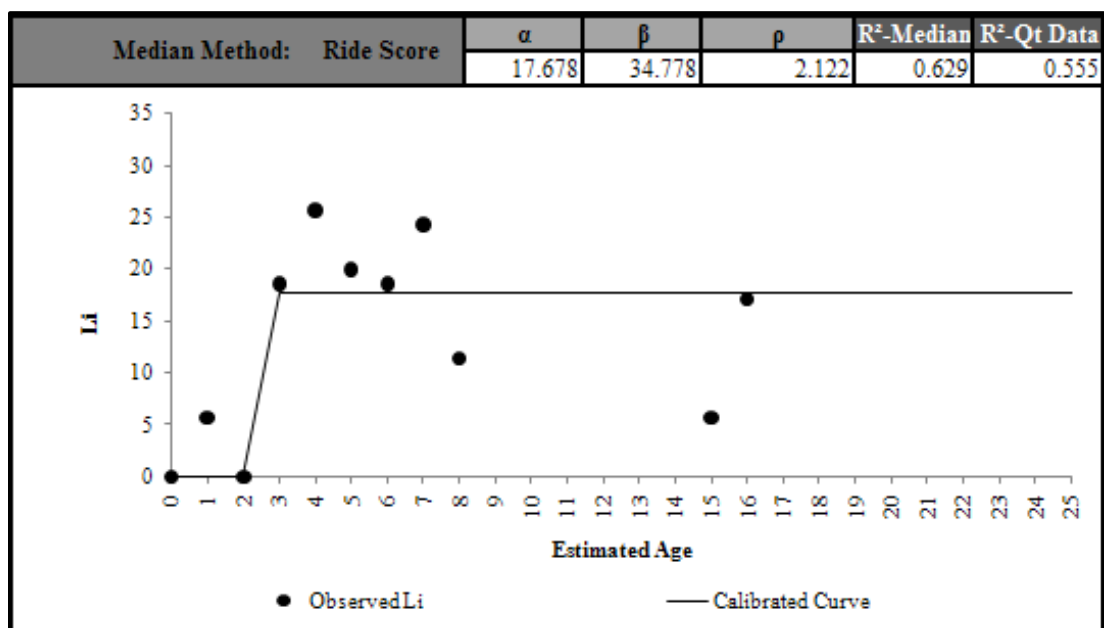


Figure E 15.4. Calibrated Performance Model for San Antonio District, Li Median Method (Constrained).

Bryan District 17

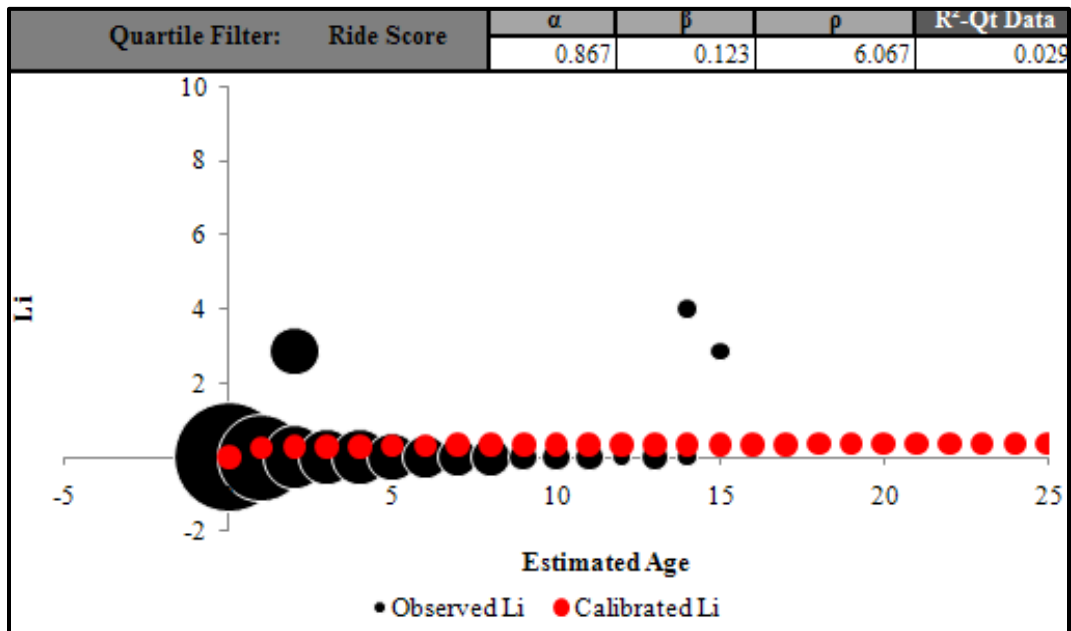


Figure E 17.1. Calibrated Performance Model for Bryan District, Li Quartile Method (Unconstrained).

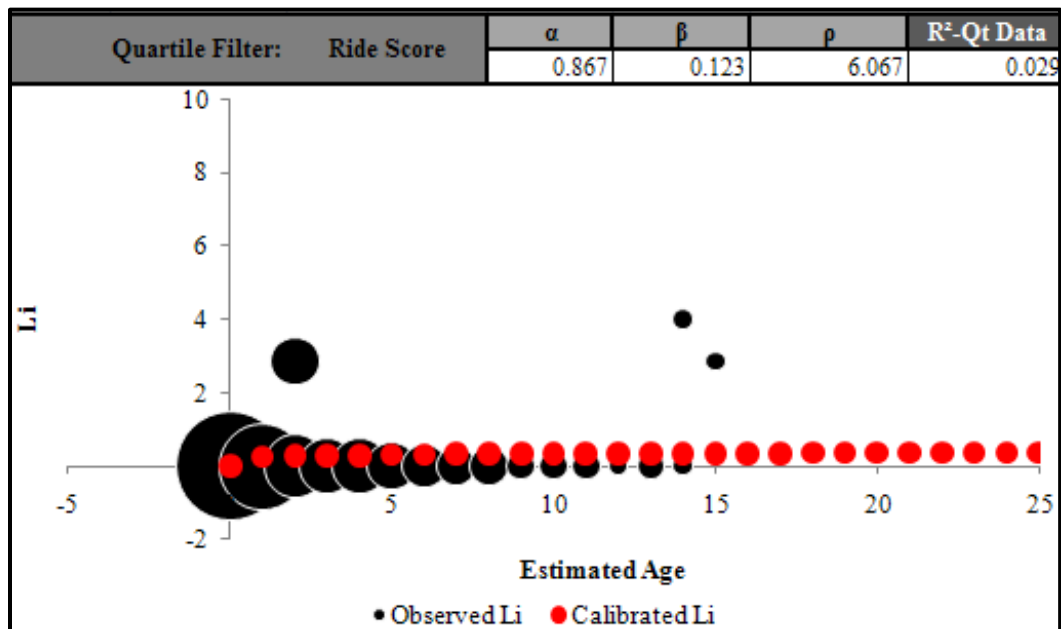


Figure E 17.2. Calibrated Performance Model for Bryan District, Li Quartile Method (Constrained).

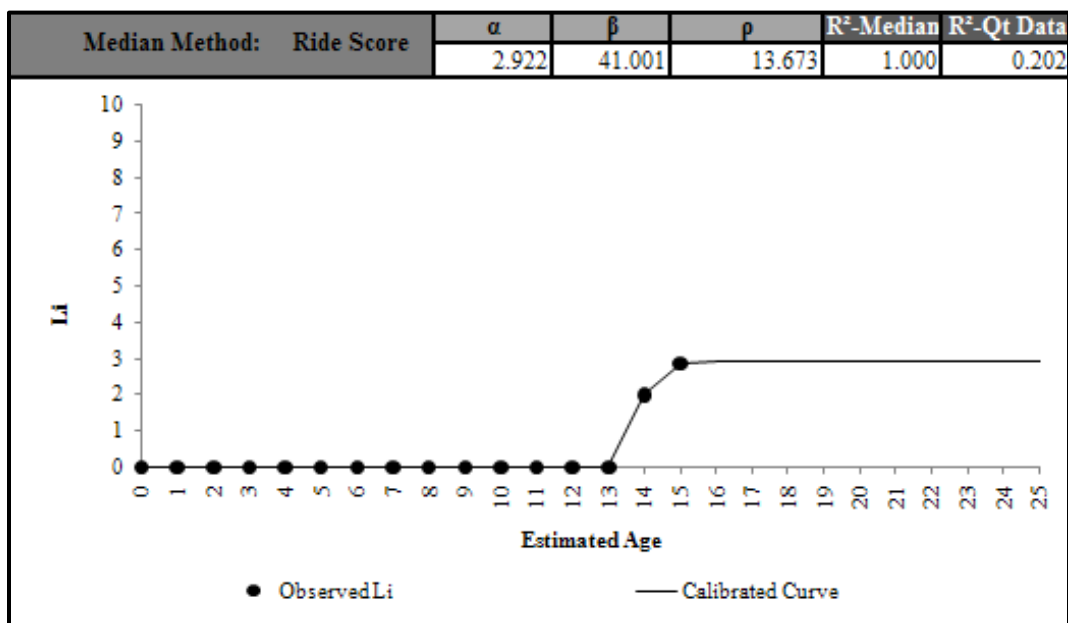


Figure E 17.3. Calibrated Performance Model for Bryan District, Li Median Method (Unconstrained).

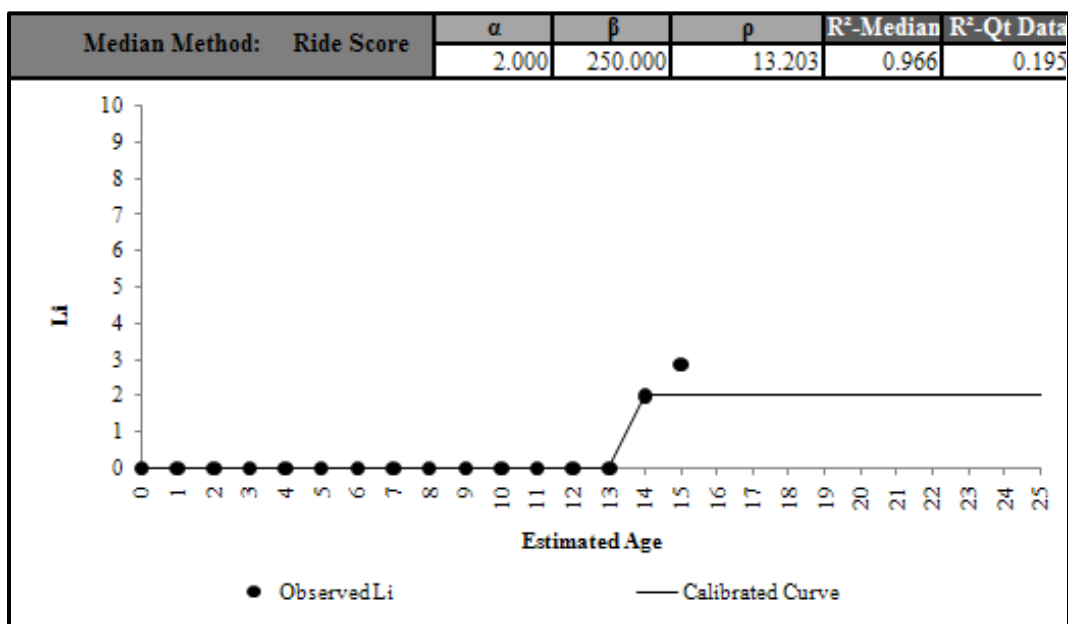


Figure E 17.4. Calibrated Performance Model for Bryan District, Li Median Method (Constrained).

Dallas District 18

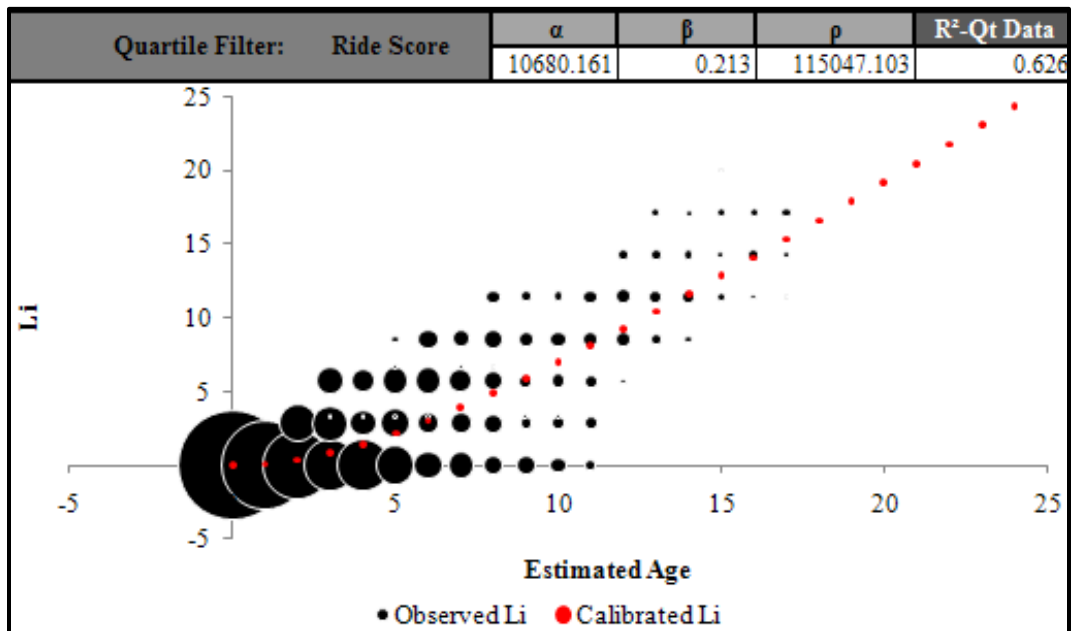


Figure E 18.1. Calibrated Performance Model for Dallas District, Li Quartile Method (Unconstrained).

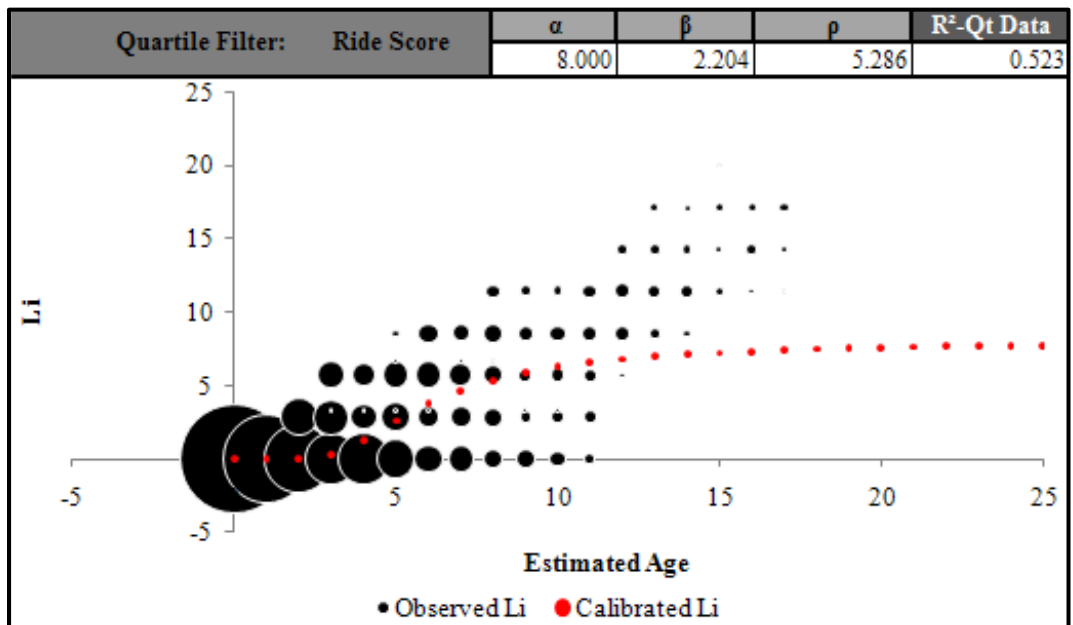


Figure E 18.2. Calibrated Performance Model for Dallas District, Li Quartile Method (Constrained).

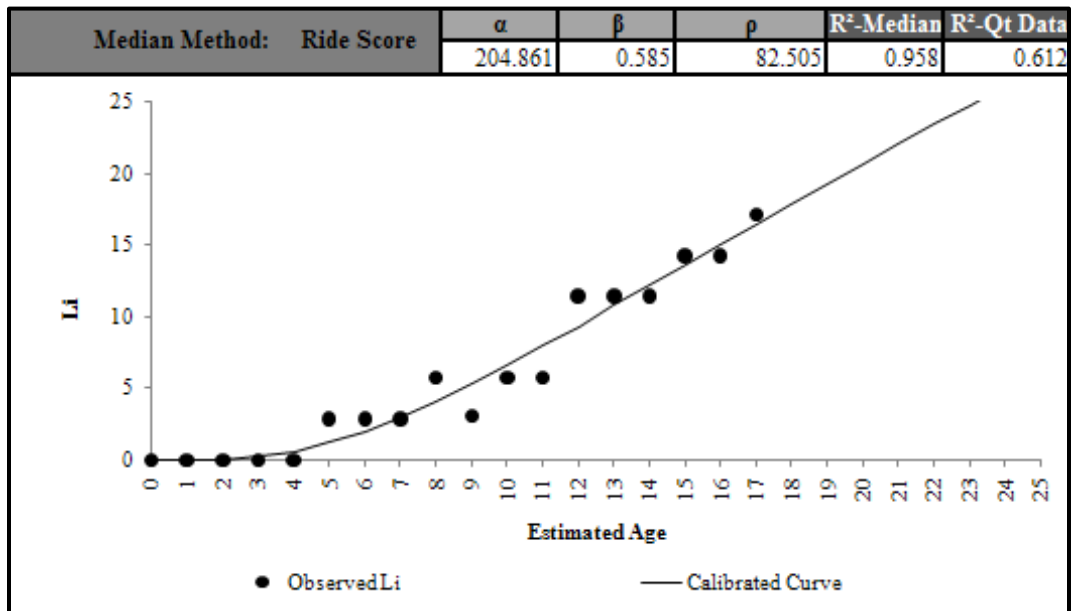


Figure E 18.3. Calibrated Performance Model for Dallas District, Li Median Method (Unconstrained).

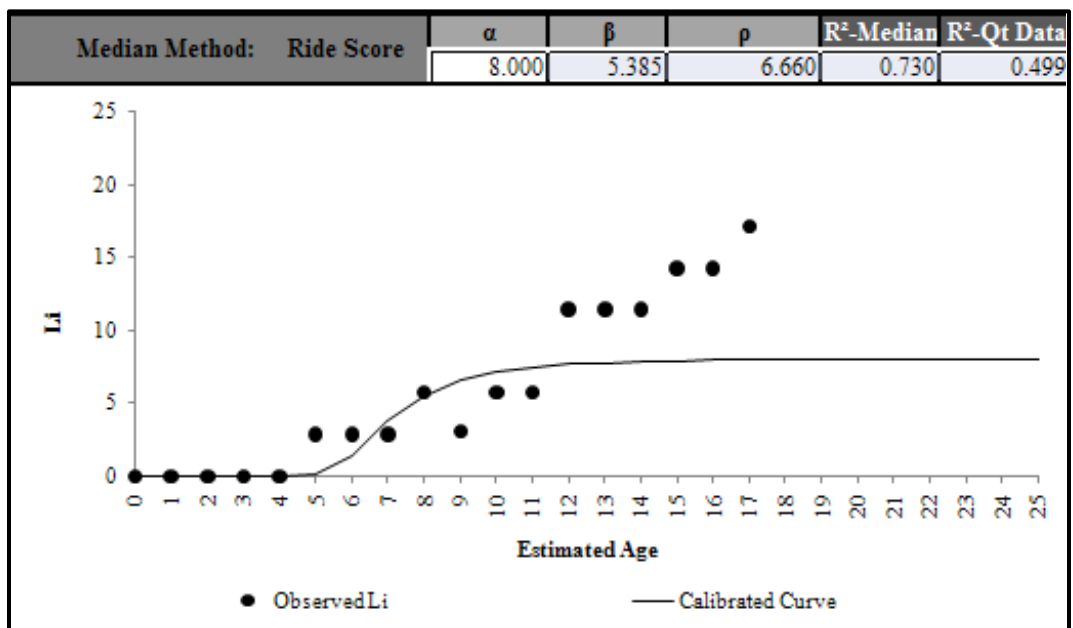


Figure E 18.4. Calibrated Performance Model for Dallas District, Li Median Method (Constrained).

Atlanta District 19

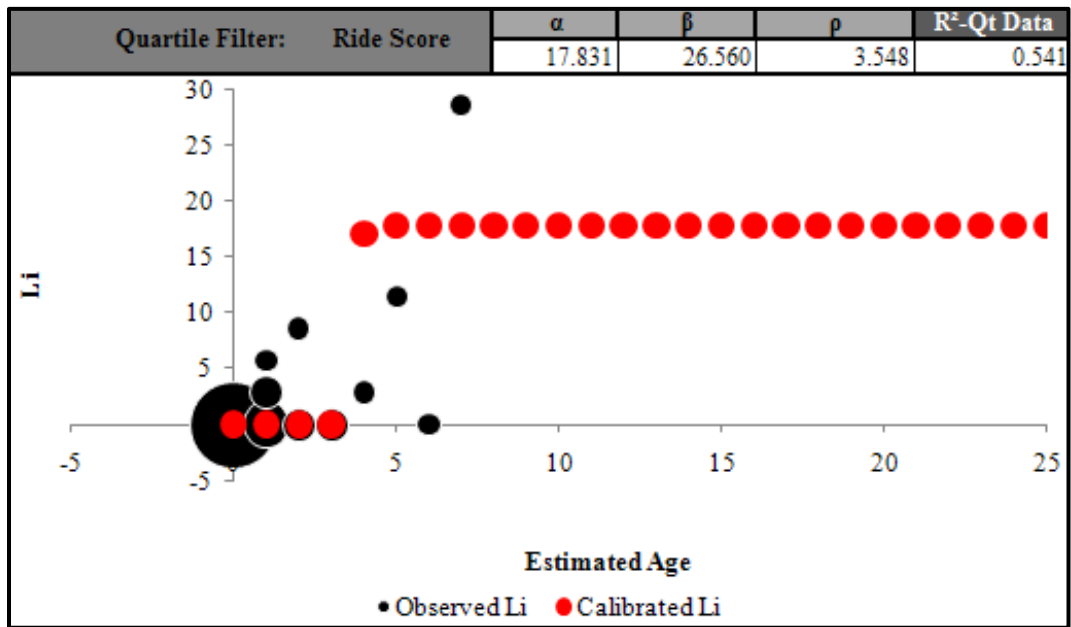


Figure E 19.1. Calibrated Performance Model for Atlanta District, Li Quartile Method (Unconstrained).

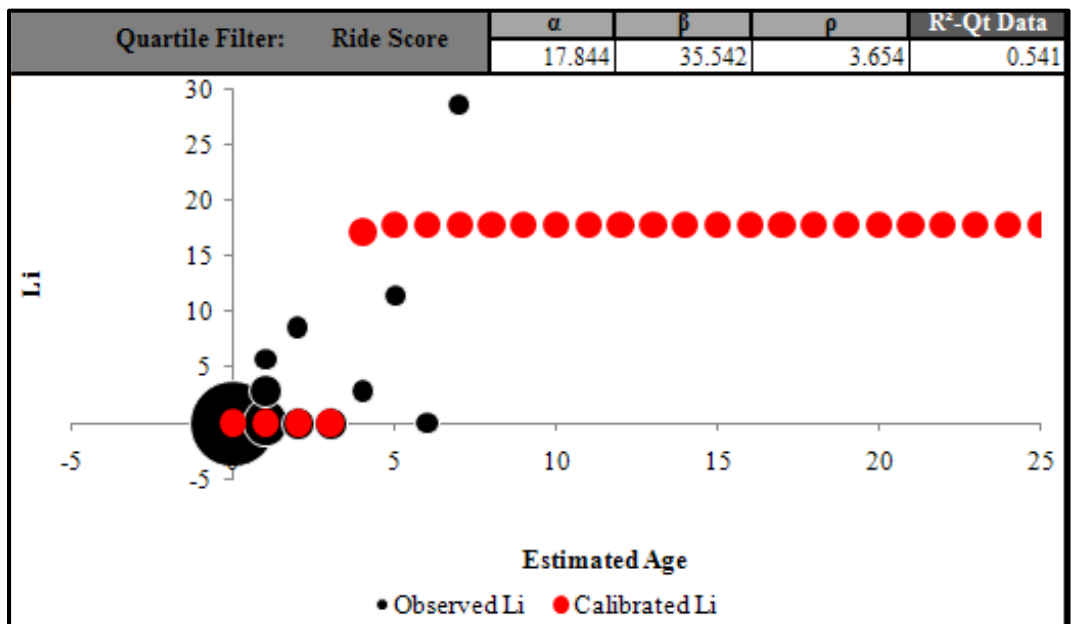


Figure E 19.2. Calibrated Performance Model for Atlanta District, Li Quartile Method (Constrained).

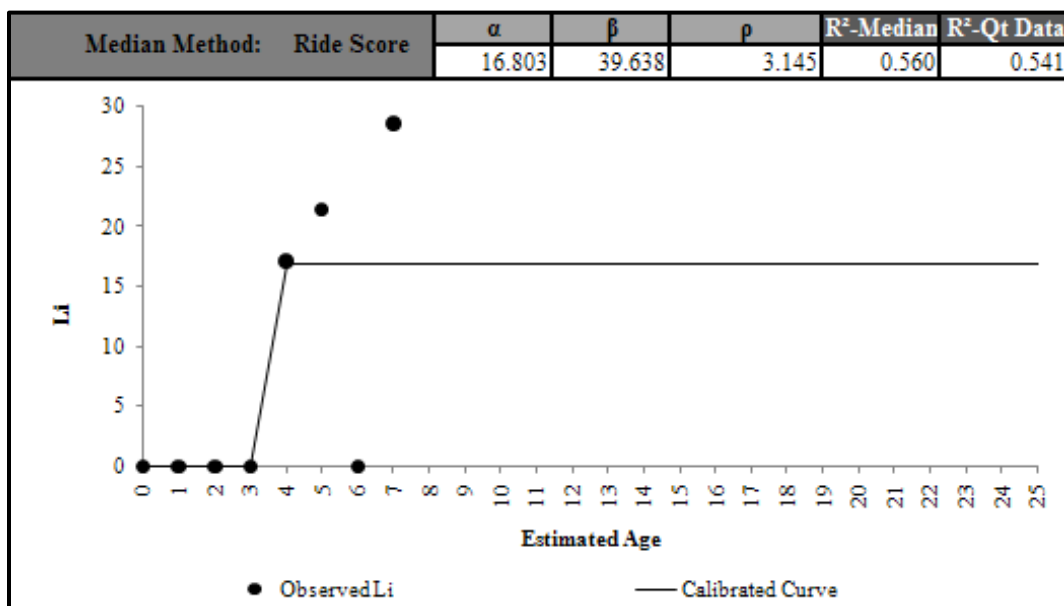


Figure E 19.3. Calibrated Performance Model for Atlanta District, Li Median Method (Unconstrained).

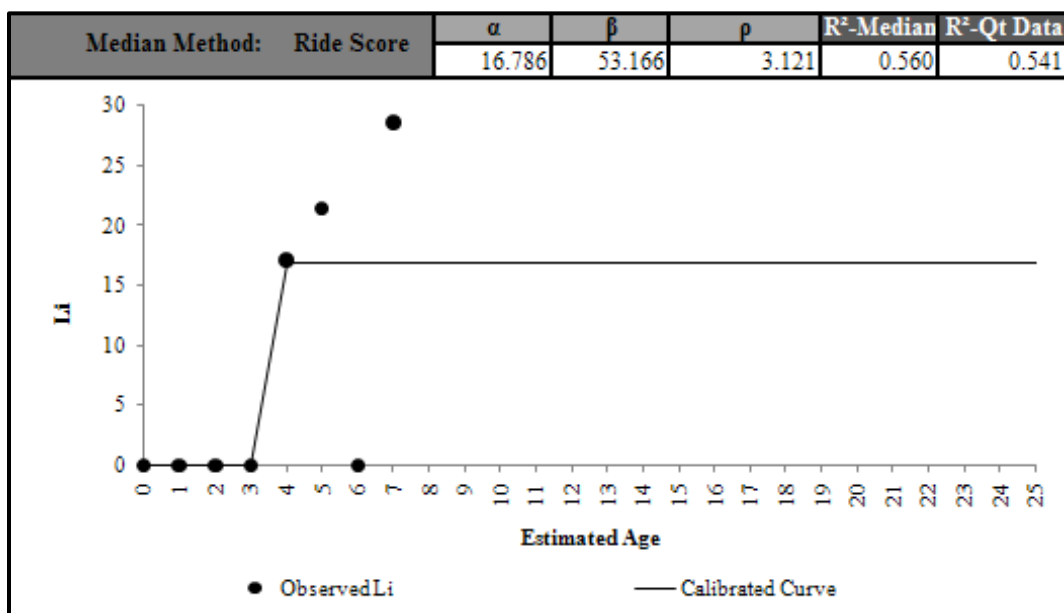


Figure E 19.4. Calibrated Performance Model for Atlanta District, Li Median Method (Constrained).

Beaumont District 20

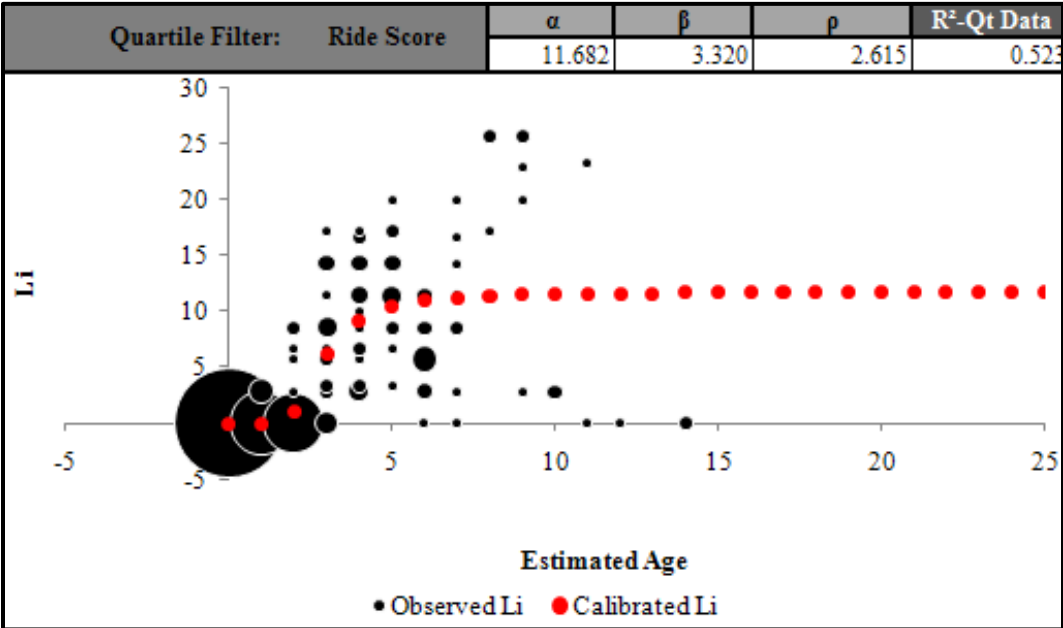


Figure E 20.1. Calibrated Performance Model for Beaumont District, Li Quartile Method (Unconstrained).

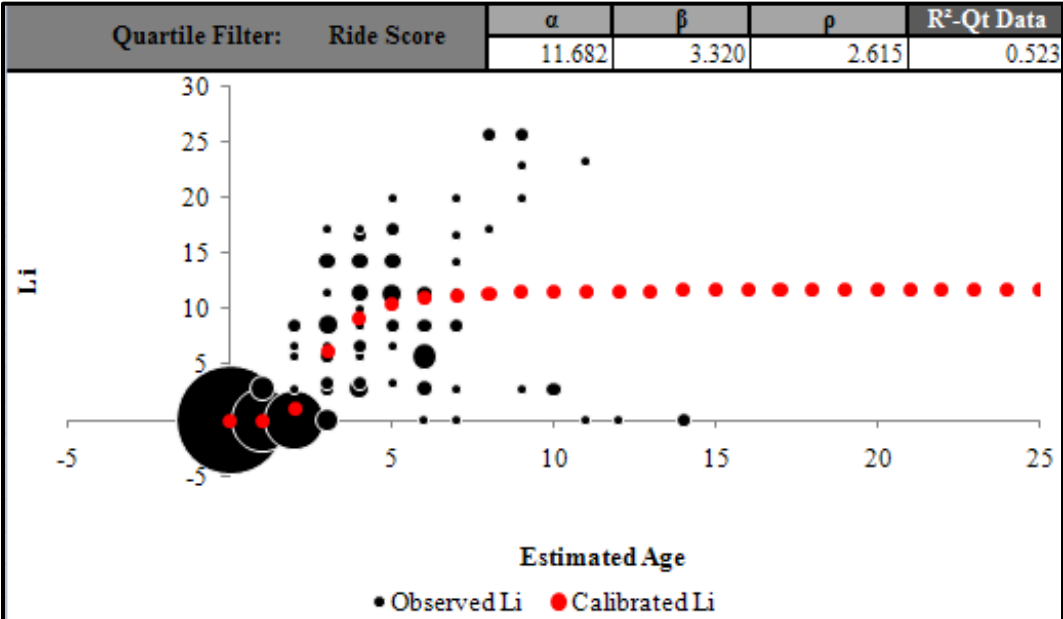


Figure E 20.2. Calibrated Performance Model for Beaumont District, Li Quartile Method (Constrained).

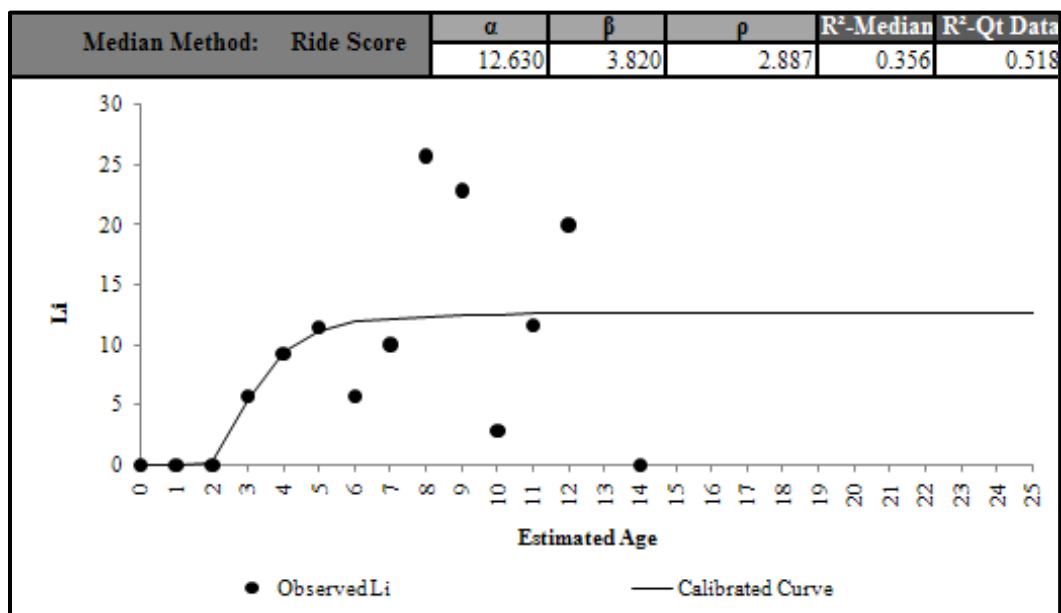


Figure E 20.3. Calibrated Performance Model for Beaumont District, Li Median Method (Unconstrained).

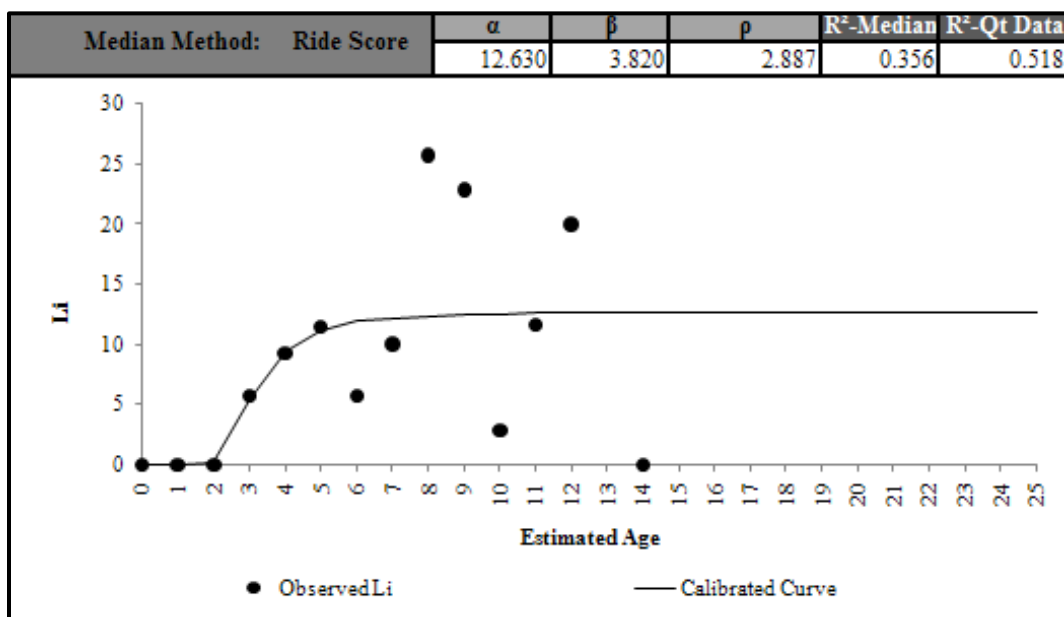


Figure E 20.4. Calibrated Performance Model for Beaumont District, Li Median Method (Constrained).

Laredo District 22

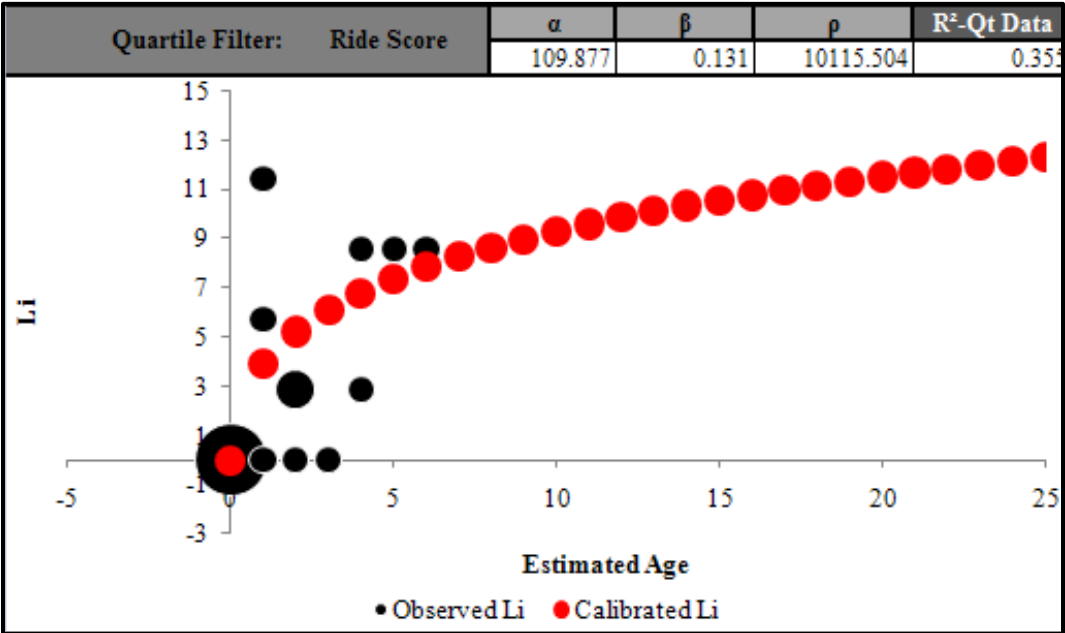


Figure E 22.1. Calibrated Performance Model for Laredo District, Li Quartile Method (Unconstrained).

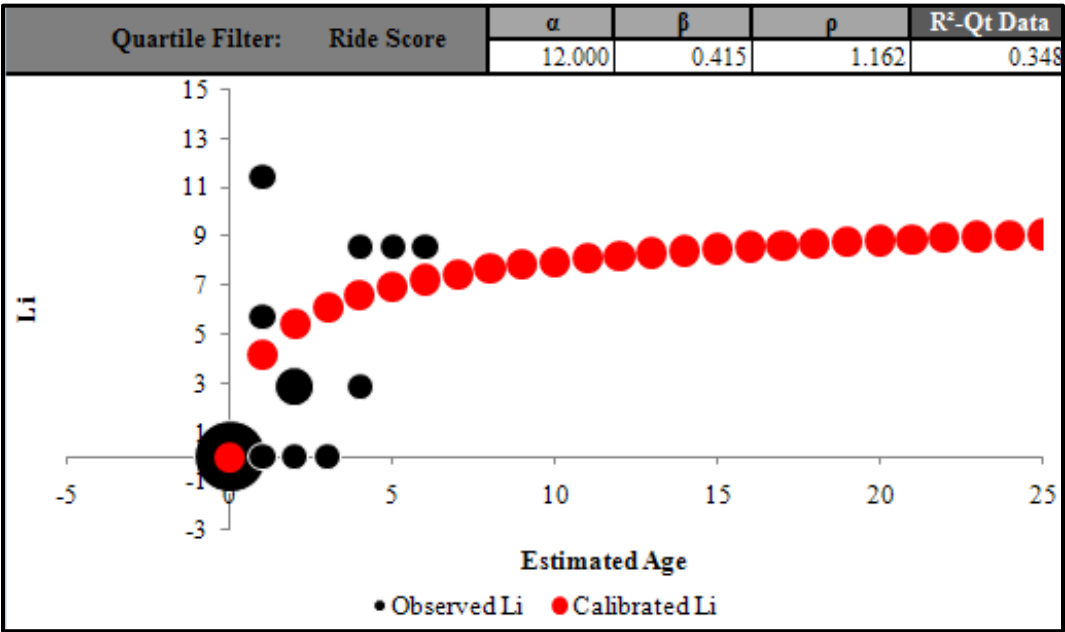


Figure E 22.2. Calibrated Performance Model for Laredo District, Li Quartile Method (Constrained).

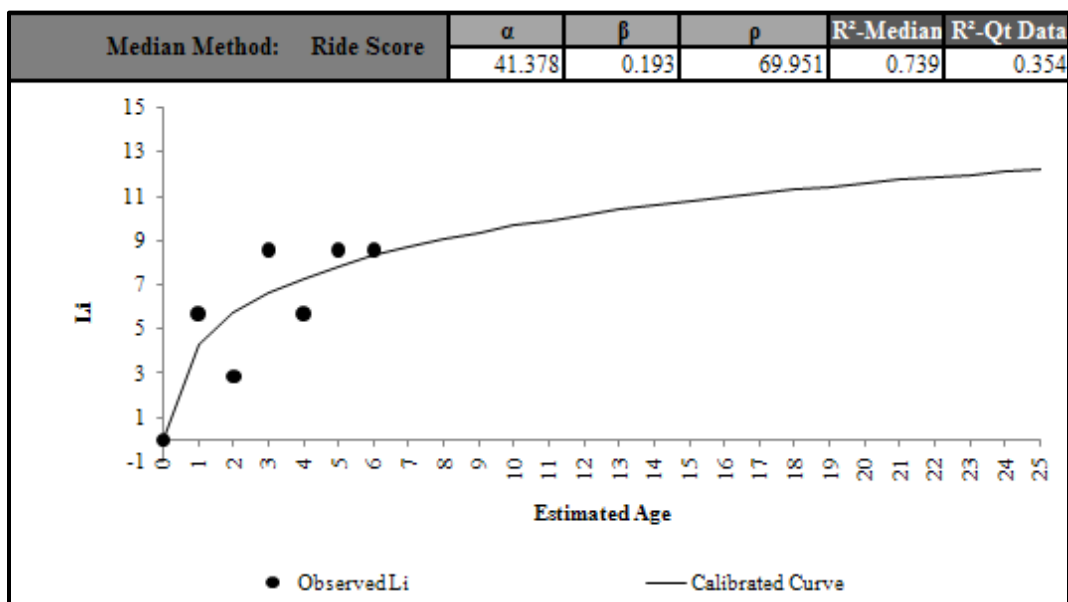


Figure E 22.3. Calibrated Performance Model for Laredo District, Li Median Method (Unconstrained).

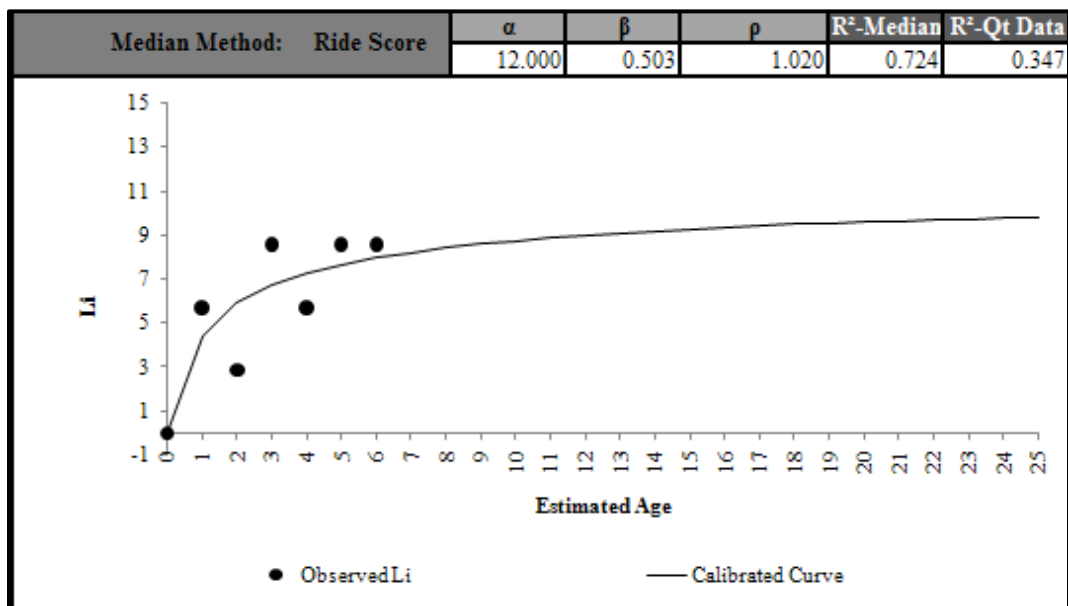


Figure E 22.4. Calibrated Performance Model for Laredo District, Li Median Method (Constrained).

El Paso District 24

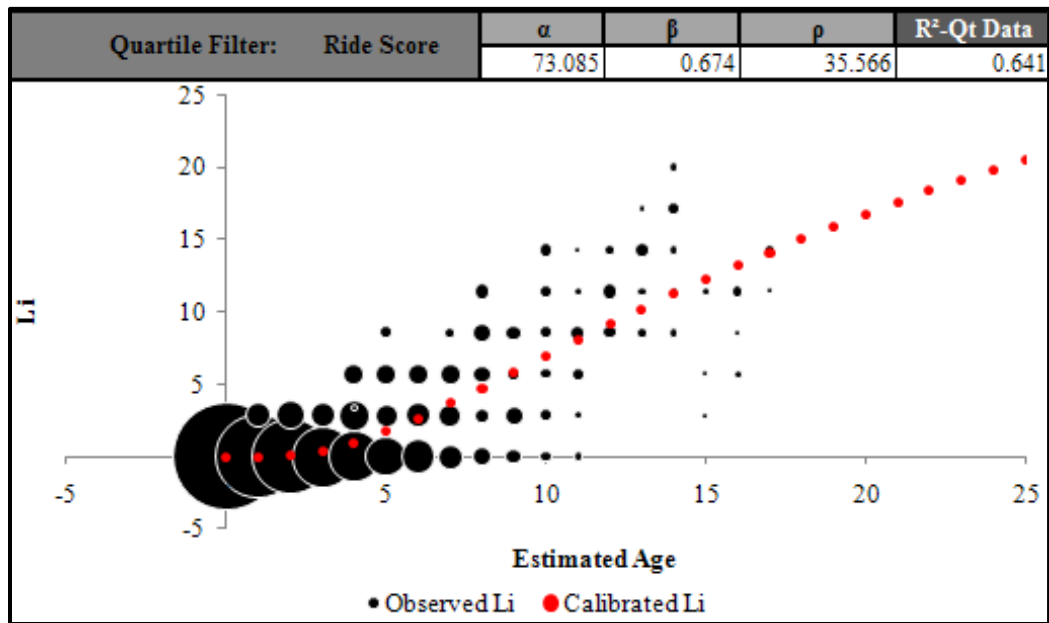


Figure E 24.1. Calibrated Performance Model for El Paso District, Li Quartile Method (Unconstrained).

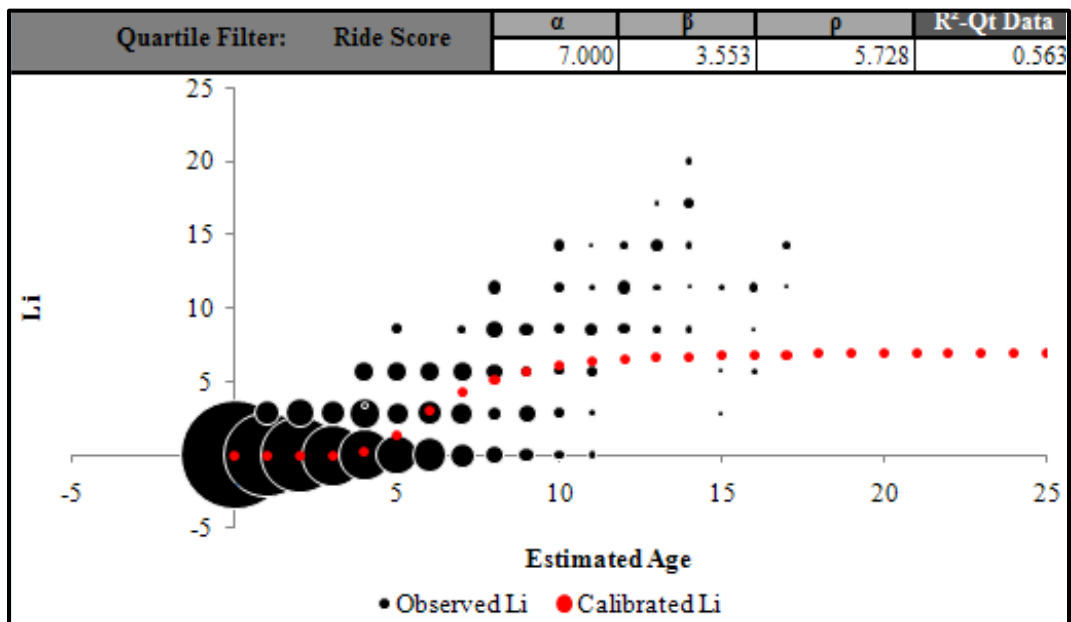


Figure E 24.2. Calibrated Performance Model for El Paso District, Li Quartile Method (Constrained).

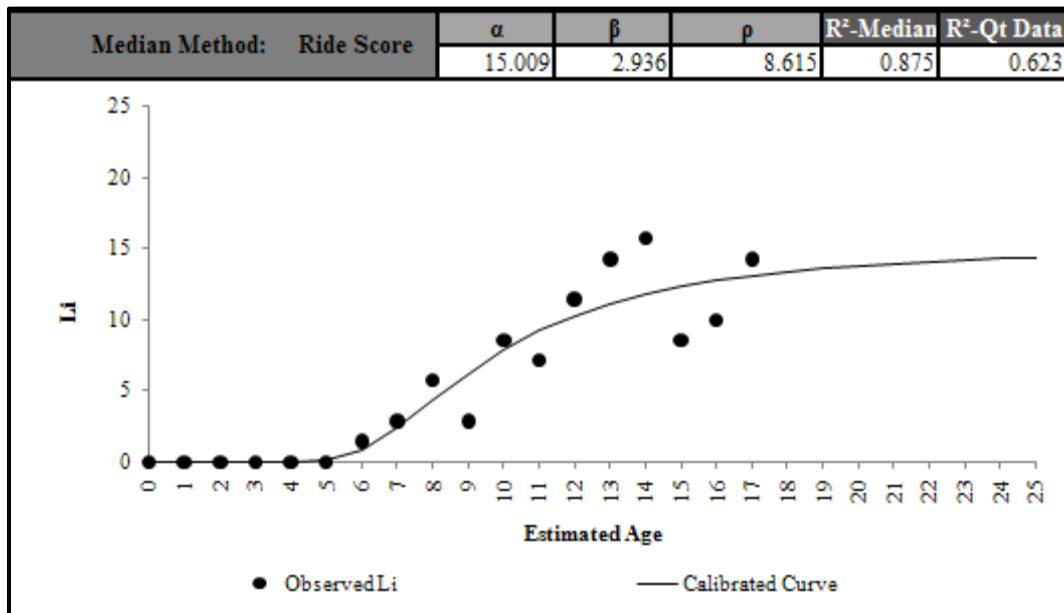


Figure E 24.3. Calibrated Performance Model for El Paso District, Li Median Method (Unconstrained).

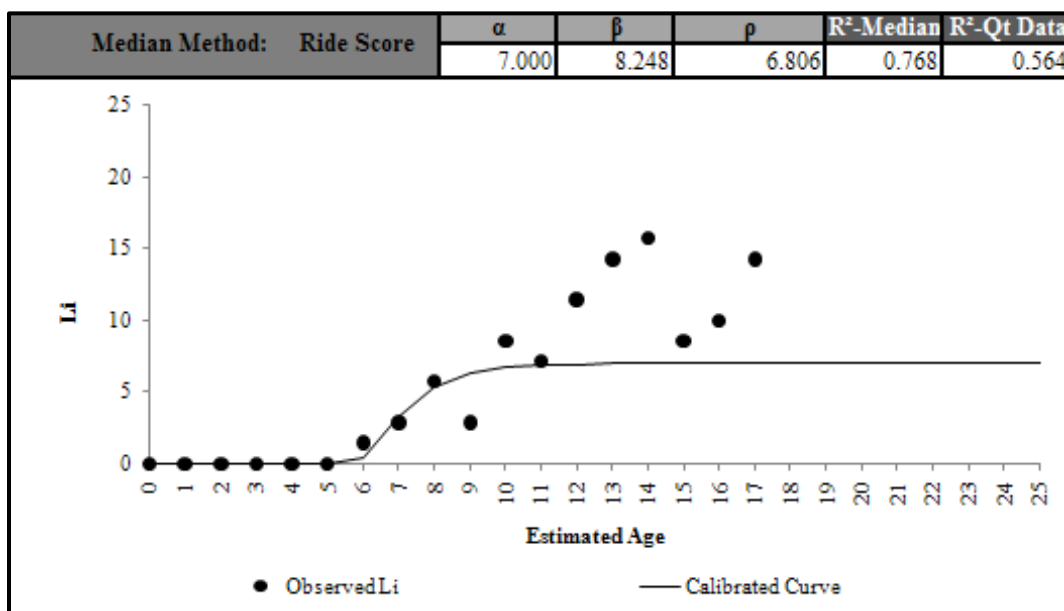


Figure E 24.4. Calibrated Performance Model for El Paso District, Li Median Method (Constrained).

Statewide

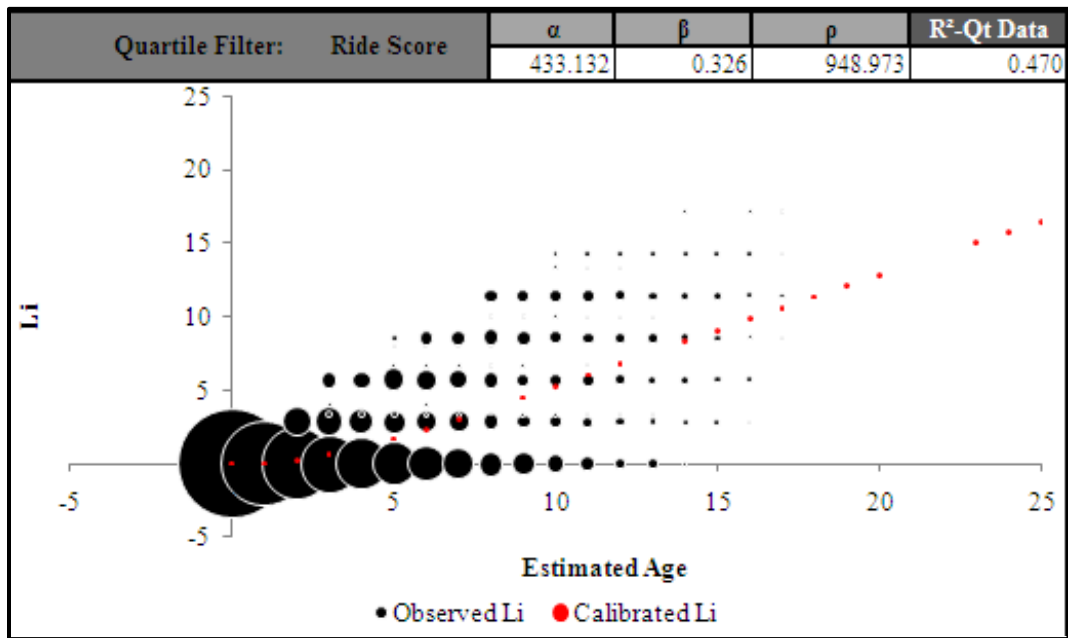


Figure E 25.1. Calibrated Performance Model, Li Quartile Method (Unconstrained).

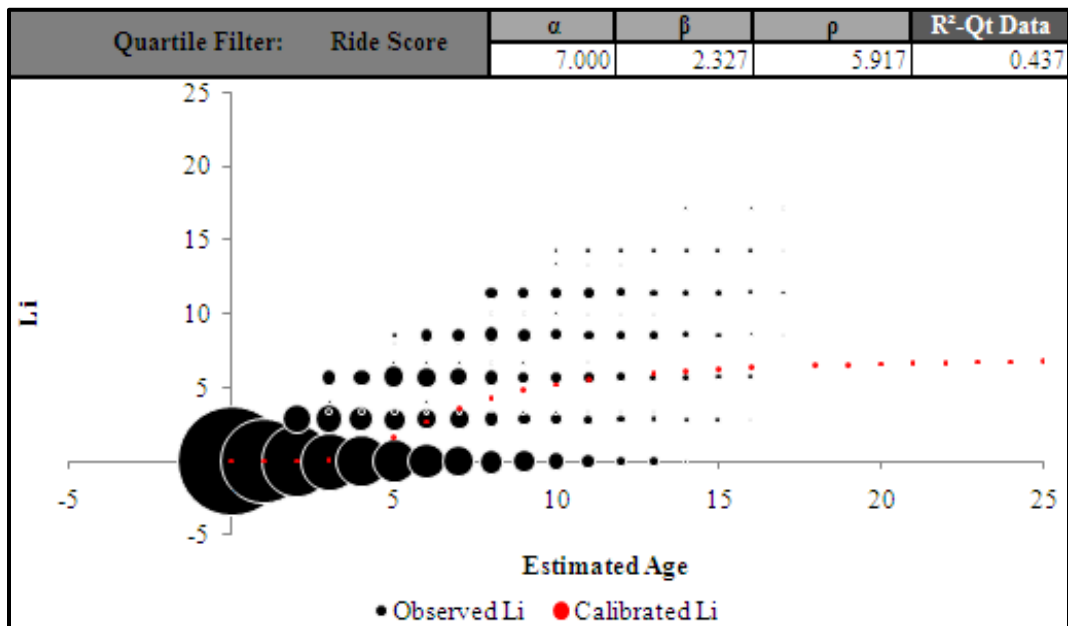


Figure E 25.2. Calibrated Performance Model, Li Quartile Method (Constrained).

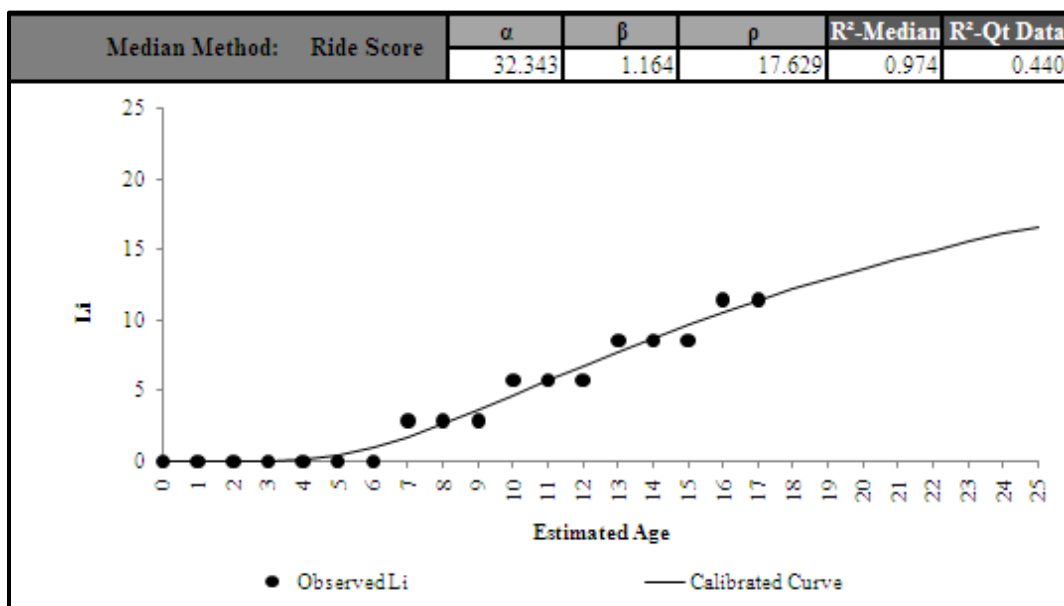


Figure E 25.3. Calibrated Performance Model, Li Median Method (Unconstrained).

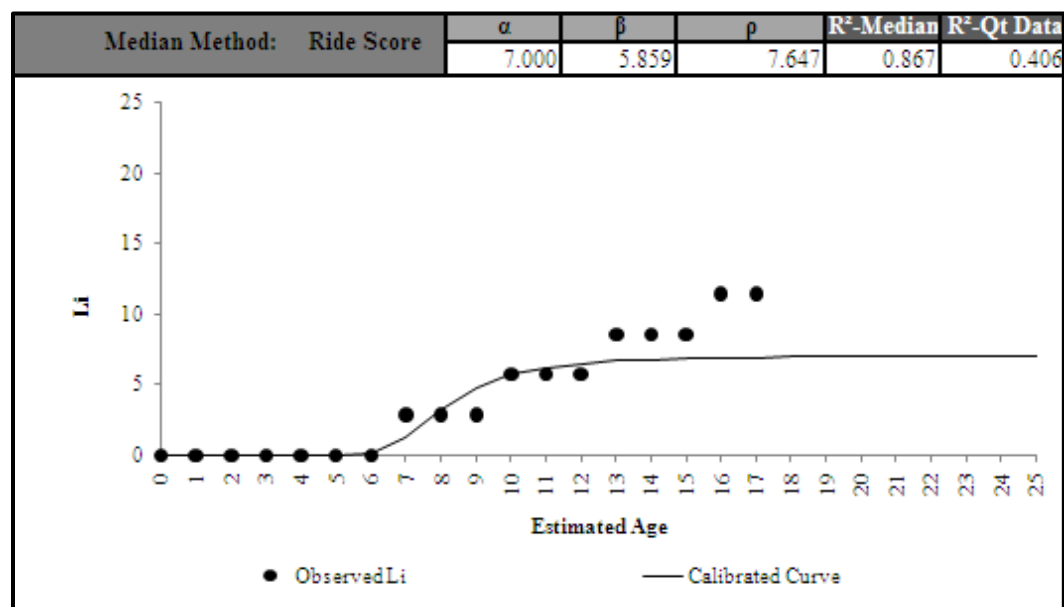


Figure E 25.4. Calibrated Performance Model, Li Median Method (Constrained).

Appendix F: Calibrated CRCP Ride Quality Performance Models for Climate and Subgrade Zones

Zone 1

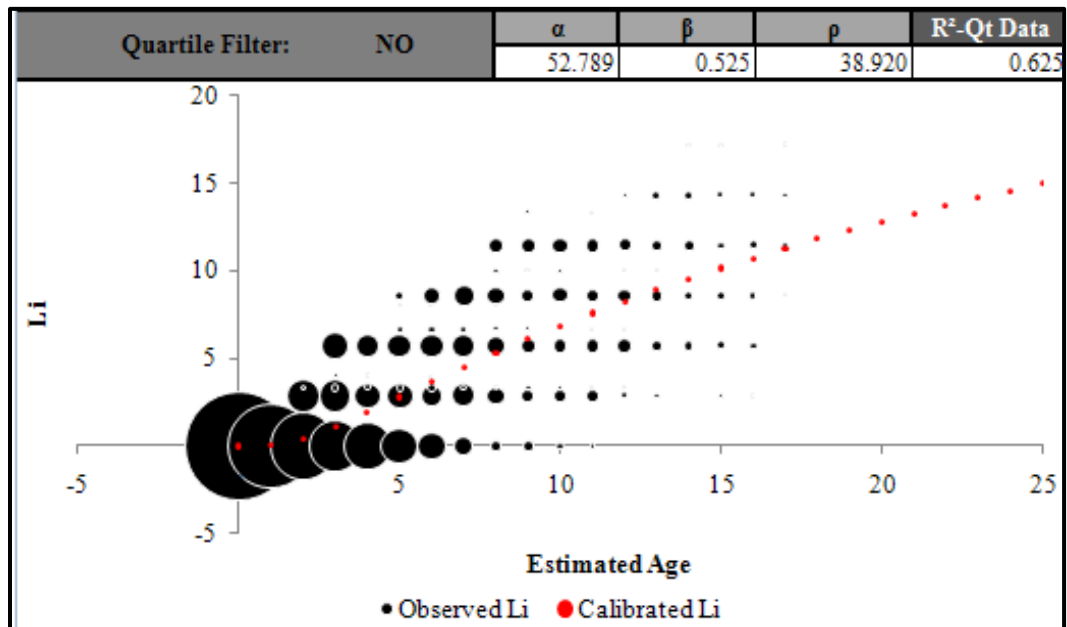


Figure F 1.1. Calibrated Performance Model for Paris District, Li Quartile Method (Unconstrained).

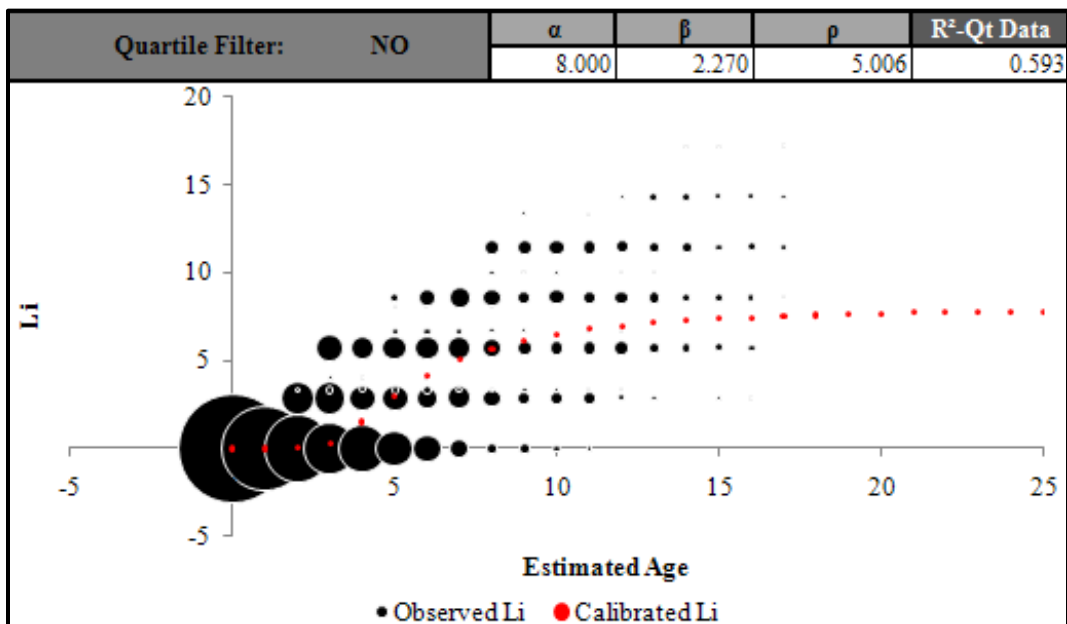


Figure F 1.2. Calibrated Performance Model for Paris District, Li Quartile Method (Constrained).

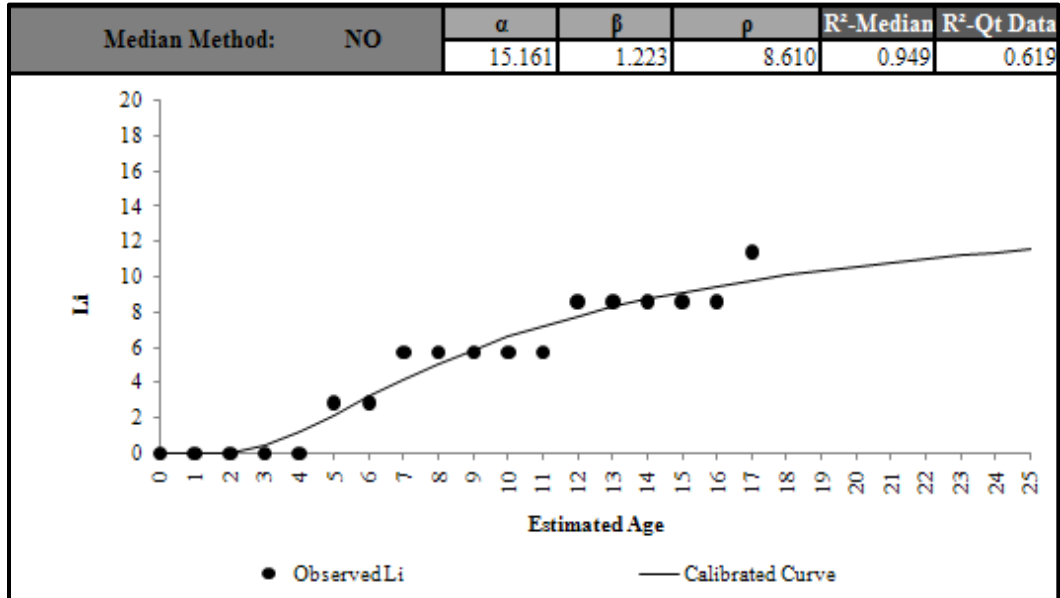


Figure F 1.3. Calibrated Performance Model for Paris District, Li Median Method (Unconstrained).

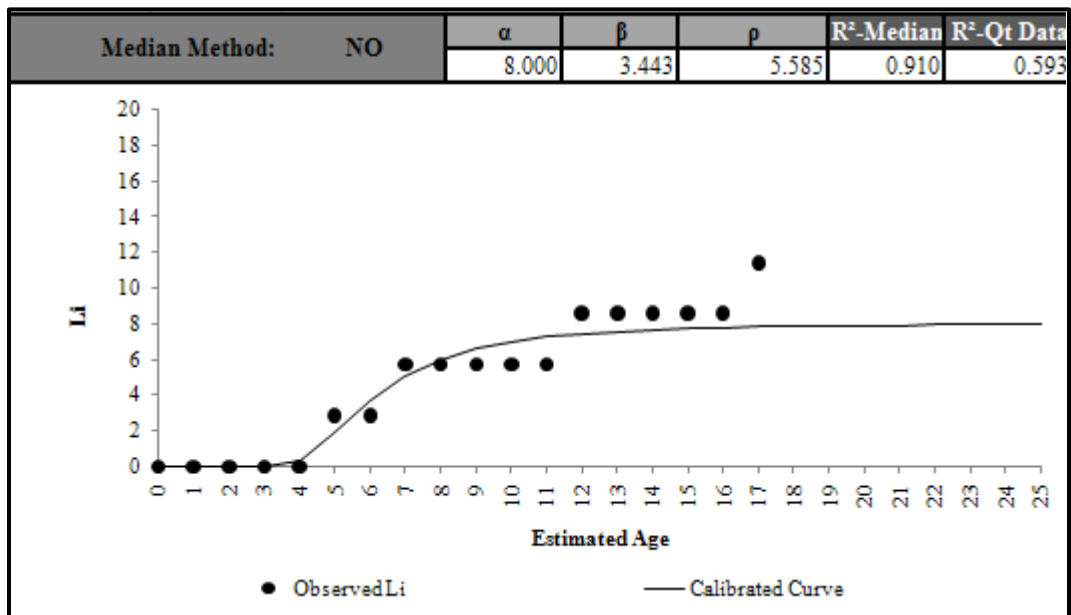


Figure F 1.4. Calibrated Performance Model for Paris District, Li Median Method (Constrained).

Zone 2

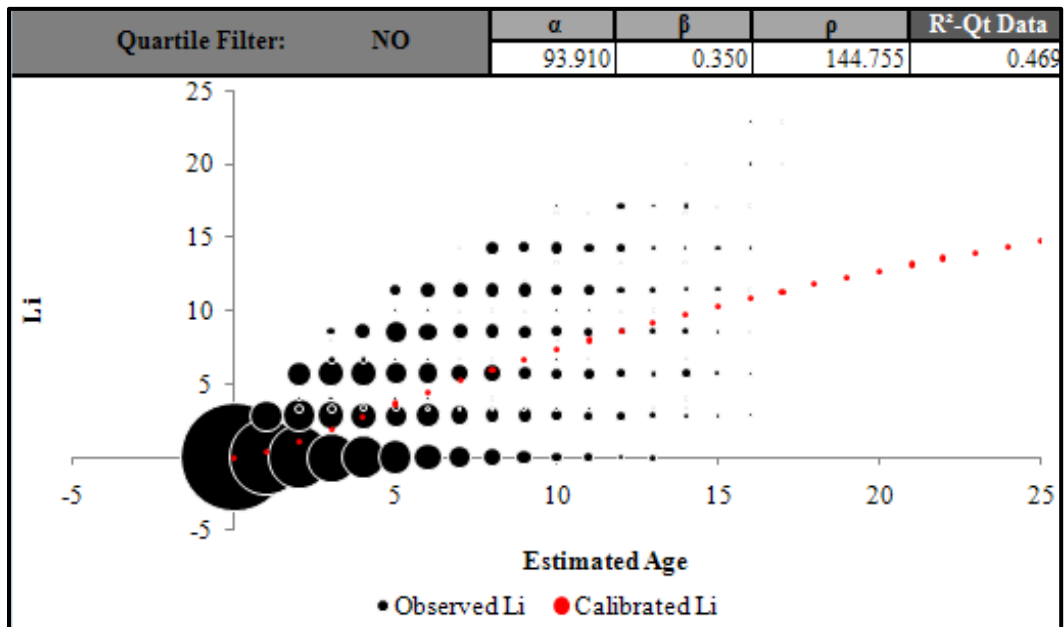


Figure F 2.1. Calibrated Performance Model for Paris District, Li Quartile Method (Unconstrained).

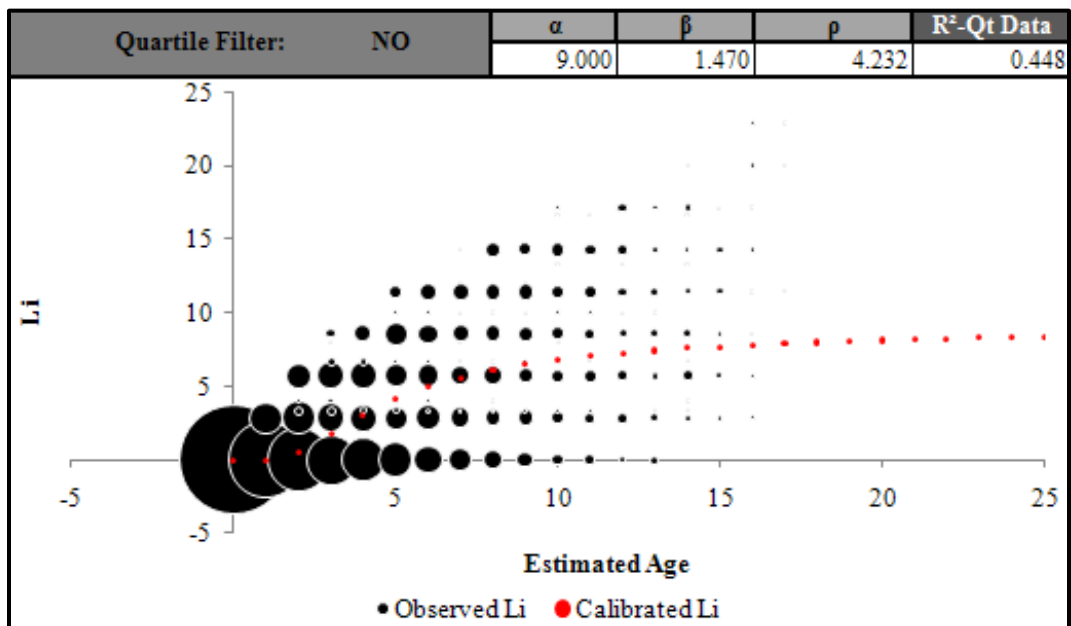


Figure F 2.2. Calibrated Performance Model for Paris District, Li Quartile Method (Constrained).

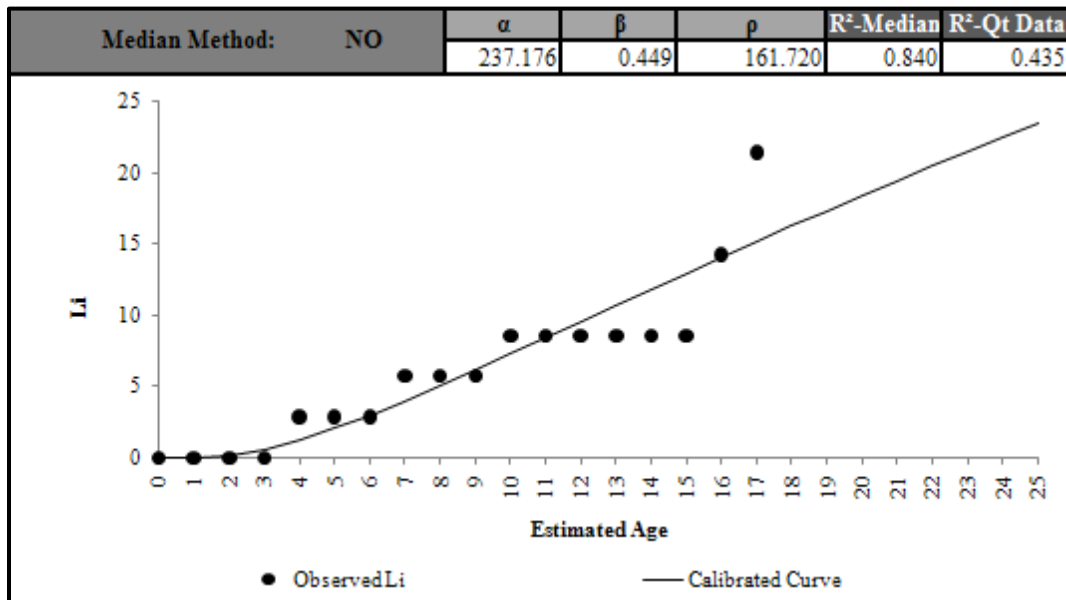


Figure F 2.3. Calibrated Performance Model for Paris District, Li Median Method (Unconstrained).

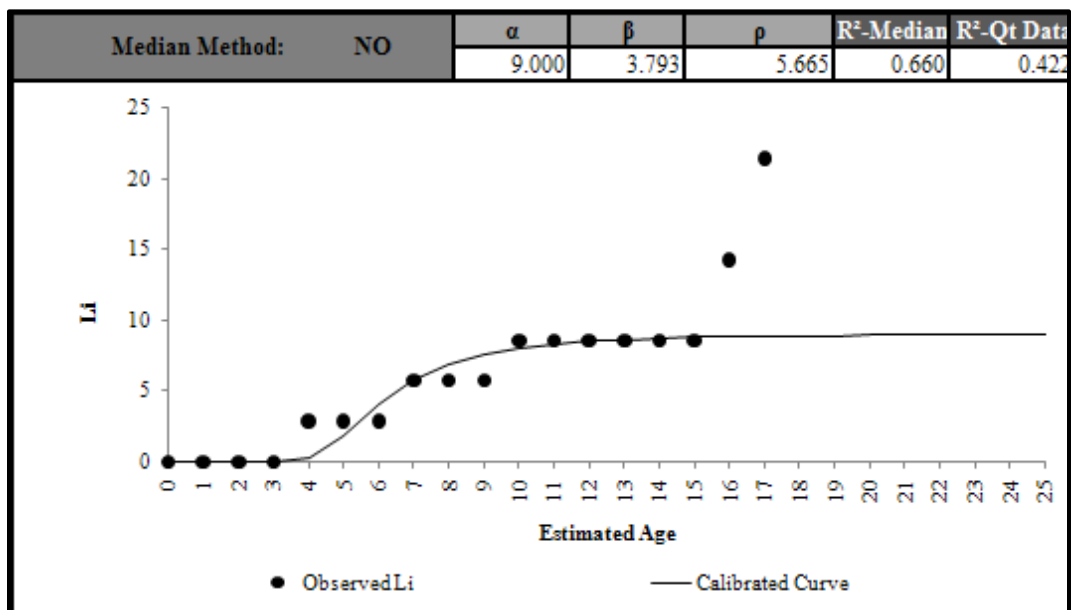


Figure F 2.4. Calibrated Performance Model for Paris District, Li Median Method (Constrained).

Zone 3

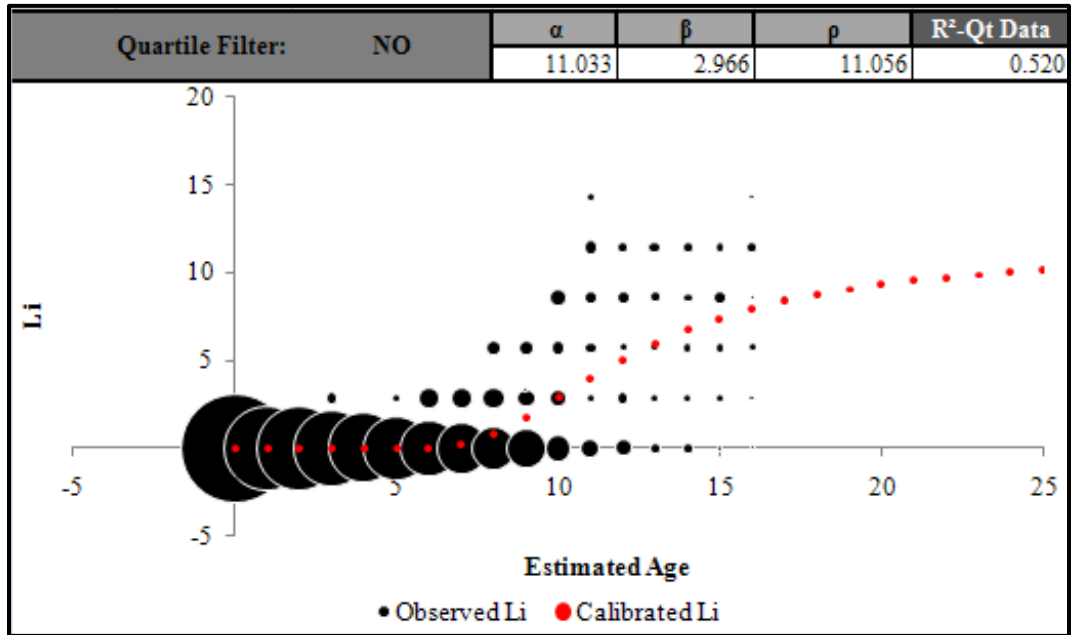


Figure F 3.1. Calibrated Performance Model for Paris District, Li Quartile Method (Unconstrained).

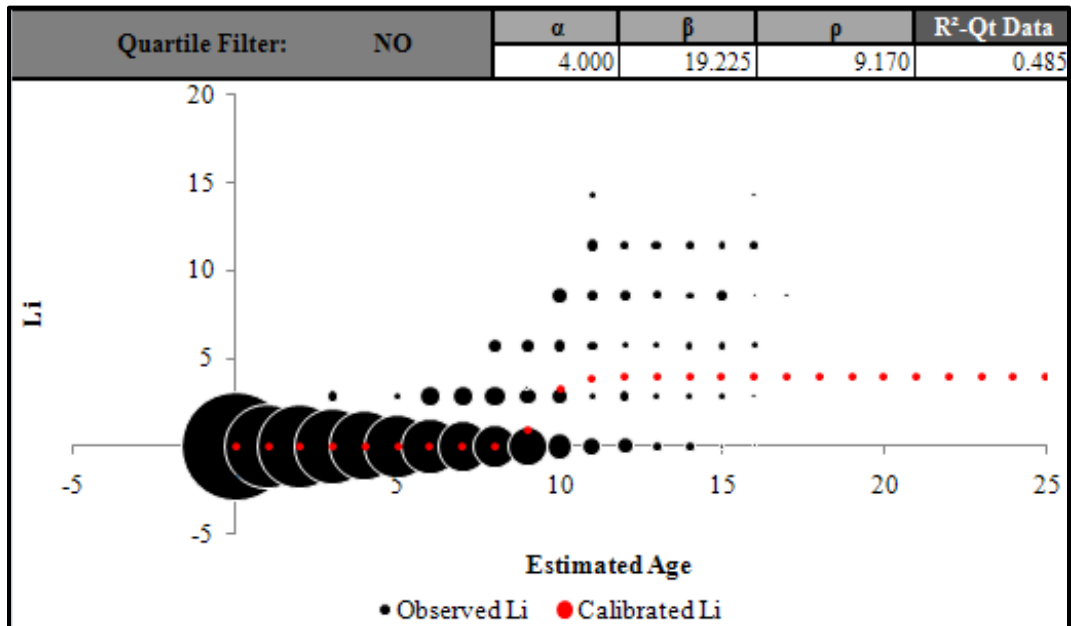


Figure F 3.2. Calibrated Performance Model for Paris District, Li Quartile Method (Constrained).

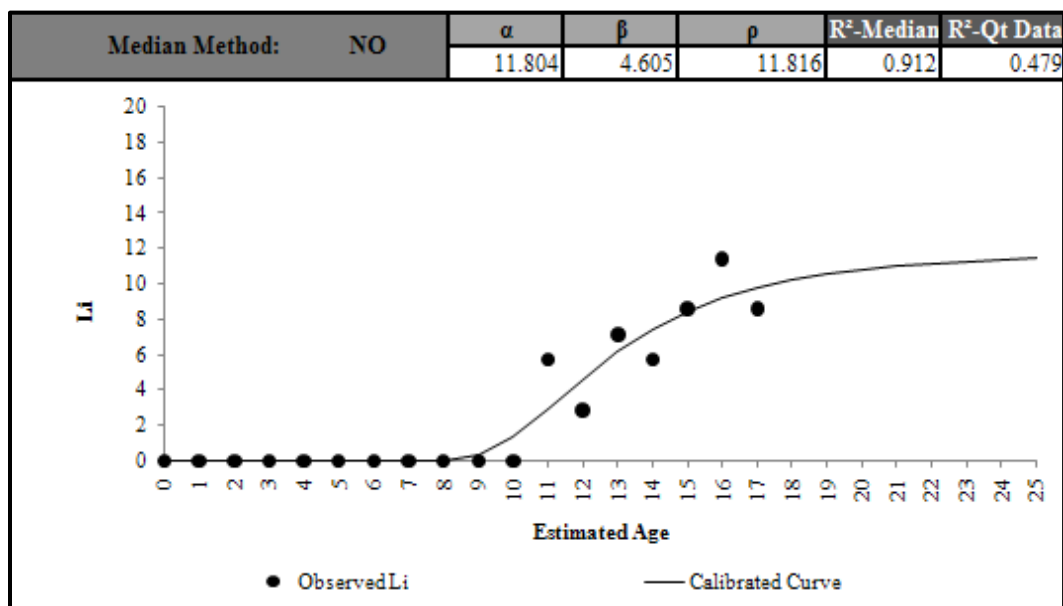


Figure F 3.3. Calibrated Performance Model for Paris District, Li Median Method (Unconstrained).

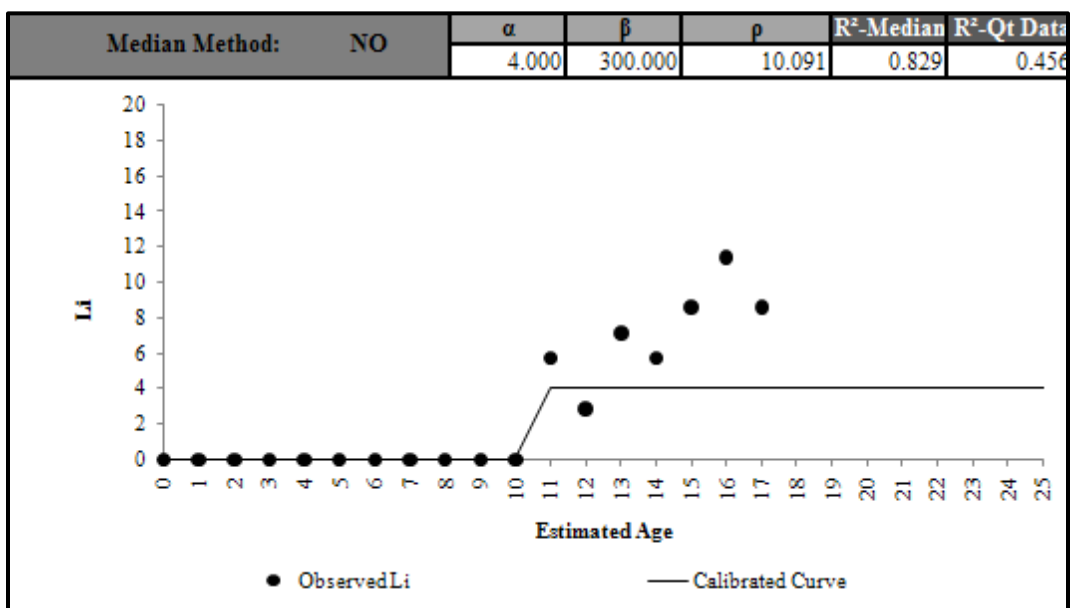


Figure F 3.4. Calibrated Performance Model for Paris District, Li Median Method (Constrained).

Zone 4

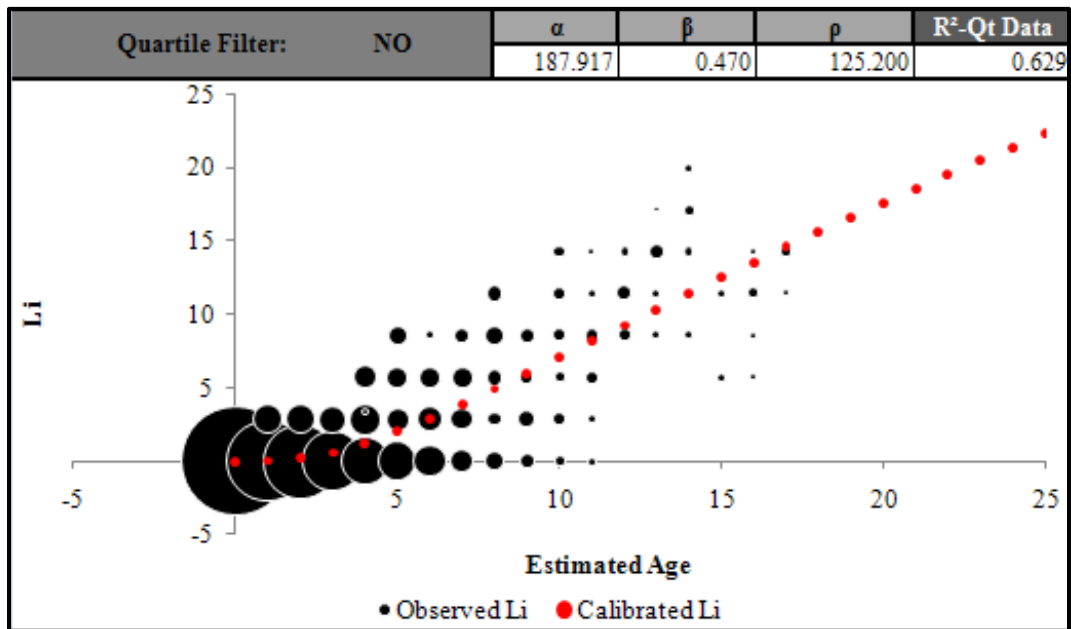


Figure F 4.1. Calibrated Performance Model for Paris District, Li Quartile Method (Unconstrained).

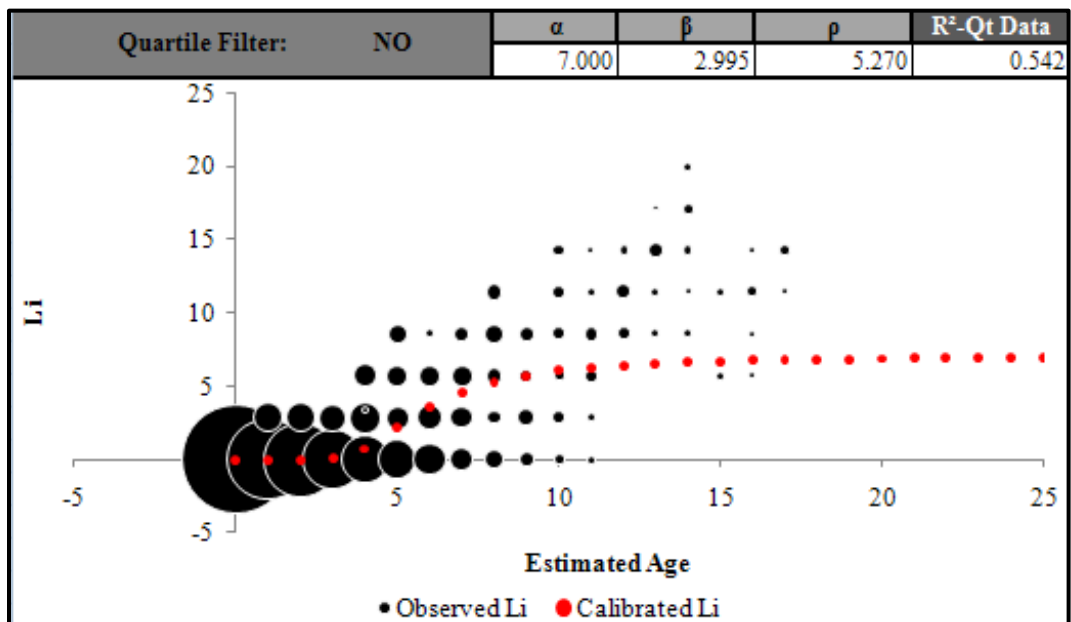


Figure F 4.2. Calibrated Performance Model for Paris District, Li Quartile Method (Constrained).

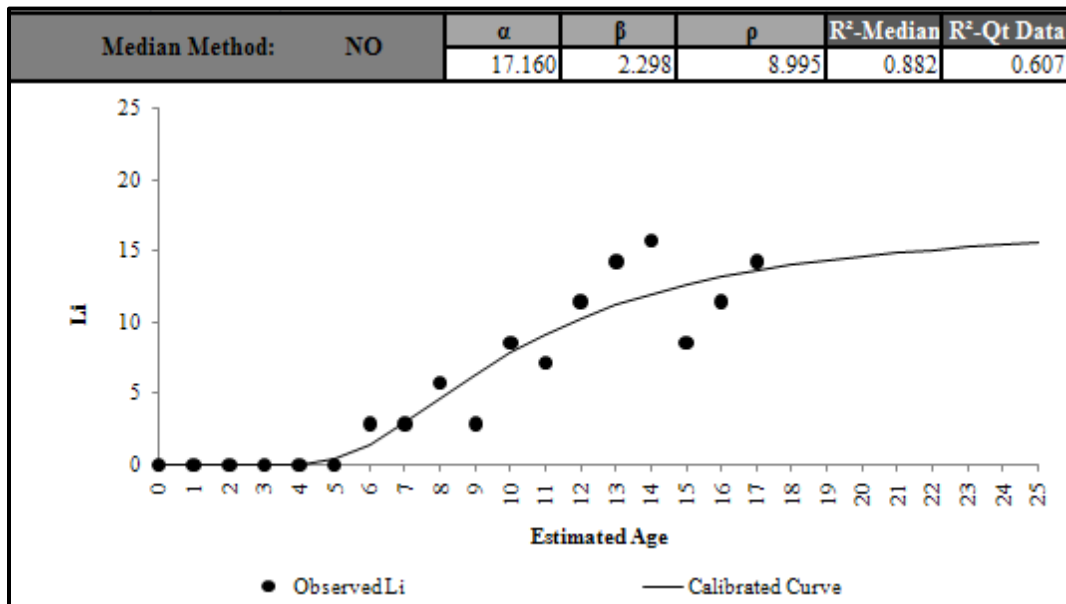


Figure F 4.3. Calibrated Performance Model for Paris District, Li Median Method (Unconstrained).

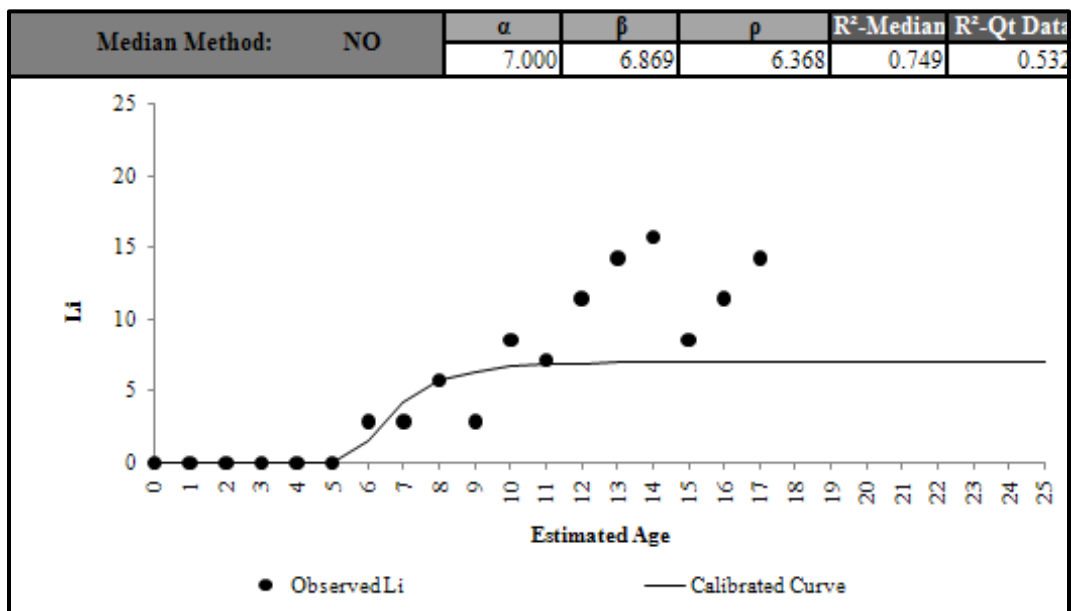


Figure F 4.4. Calibrated Performance Model for Paris District, Li Median Method (Constrained).

Vita

Alejandra Gallegos was born in El Paso, Texas. In the spring of 2010, she earned her Bachelor of Science in Civil Engineering degree at the University of Texas at El Paso (UTEP). She enrolled in the Civil Engineering Master's Program at UTEP in the fall of 2010. In the fall of 2011, Alejandra became the first UTEP student to participate in the Dual Masters Degree Program in Transportation and Logistics Systems at the Czech Technical University in Prague in the Czech Republic and the University of Zilina in Slovakia. During part of her undergraduate and graduate studies, she worked as a research assistant with Dr. Carlos M. Chang-Albitres. Her research includes projects with the Texas Department of Transportation.

Permanent address: 158 Lake Champlain
El Paso, Texas, 79928

This thesis was typed by Alejandra Gallegos.